

# Birla Central Library

PILANI (Jaipur State)  
Engg College Branch

Class No :- 624.151

Book No :- K9735

Accession No :- 32718





# Soil Mechanics

*The quality of the materials used in the manufacture of this book is governed by continued postwar shortages.*



# SOIL MECHANICS

*Its Principles and Structural Applications*

BY

Dimitri P. Krynine

CONSULTING ENGINEER; LECTURER IN CIVIL  
ENGINEERING, YALE UNIVERSITY

*Second Edition*

SECOND IMPRESSION

New York and London

McGRAW-HILL BOOK COMPANY, INC.

1947

SOIL MECHANICS

COPYRIGHT, 1941, 1947, BY THE   
MCGRAW-HILL BOOK COMPANY, INC.

PRINTED IN THE UNITED STATES OF AMERICA

*All rights reserved. This book, or  
parts thereof, may not be reproduced  
in any form without permission of  
the publishers.*

TO THOSE

WHO SEEK THE TRUTH

IN SIMPLICITY AND HUMILITY

THIS BOOK IS DEDICATED



## PREFACE TO THE SECOND EDITION

The unusually rapid development of airport construction during and after the Second World War has made it advisable to add two chapters to this book, namely, Chap. XII, on highway and runway subgrades, and Chap. XI, a part of which is devoted to pipe culverts. By using the theory of the transfer of pressures by shearing stresses it becomes possible to establish an analogy between the study of tunnels and of retaining walls.

Since the art of building airports is still relatively undeveloped, the items concerned with soils in airports are discussed very briefly. All features that may possibly undergo changes in the near future have been abbreviated or omitted.

To further the aim of presenting a discussion of the fundamentals of soil mechanics in a simple and compact form, some details, mostly those referring to laboratory procedures, have been shifted from the main body of the book to the appendixes. The addition of new material, however, makes the book larger than it was in the first edition. Every effort has been made to make the chapters of Part Three (Structural Applications) independent of each other, so that, if time limitations prohibit the use of the entire book for teaching purposes, separate chapters of Part Three may be omitted according to the wishes of the teacher. For practicing engineers, many of whom use this book as a reference, its relative completeness should be an advantage.

The author acknowledges with thanks the interest expressed by readers of the first edition and their many comments, all of which have been considered in the revision of the book.

DIMITRI P. KRYNINE

NEW HAVEN, CONN.,  
*June, 1947.*



## PREFACE TO THE FIRST EDITION

Foundations of structures and structures made of earth material are as old as human civilization itself. Most of the principles controlling their construction and behavior have been known through decades and perhaps centuries, but these principles have been completed, crystallized, and put together only in the past twenty or twenty-five years, to form a branch of engineering knowledge termed "soil mechanics."

An earth mass is visualized in soil mechanics as an actual physical body; hence the necessity of studying its physical properties. This is done in Part One of this book. Behavior under load may be studied theoretically in idealized earth masses only. The discussion of stresses and strains in such masses, together with the establishment of sharp demarcation lines between idealized and actual masses, is taken up in Part Two. Finally, Part Three is dedicated to the discussion of the engineering use of the principles advanced in Parts One and Two.

The principal aim of the author has been to present a discussion of the fundamentals of soil mechanics in a simple and readable form. The book has been written primarily for civil engineering students and for civil engineers in practice—designers and construction and maintenance engineers—who wish to have a general outlook on the present state of this branch of engineering knowledge. Particular attention has been given to answering possible queries, such as what can soil mechanics do for the practicing engineer and particularly what kind of information can be expected from the laboratory. Since the book is not addressed to soil-mechanics specialists and laboratory technicians, the laboratory side of the subject has been described in a concise form. In the discussion of tests an effort has been made, however, to explain clearly why a given test is necessary and to establish its relationship to the fundamentals under consideration.

Very little mathematics has been used throughout the book. The analytical approach to the solution of earth engineering problems, which are based mostly on rough assumptions, has not

proved very successful. In this book mathematics has been considered as a tool in the understanding of fundamentals and has been used only when strictly necessary. On several occasions simple logical reasoning accompanied by a sketch has replaced complicated symbolical operations.

By revising derivations of formulas and proofs of statements it has been possible to present them in very simple forms. Some new graphical procedures have been introduced, and generally all the drawings have been schematized as much as possible to permit the student easily to reproduce most of them on the black-board or in his notebook. A goodly number of problems are designed with the purpose of encouraging the student to work independently on some details purposely omitted in the text. Some of the problems may seem difficult, and it is not expected that an average student will be able to solve all the problems presented without the help of the instructor.

Furthermore, only a comparatively limited number of terms has been used extensively, since it has been observed that new terminology often handicaps an engineer in reading soil-mechanics literature. However, a rather large number of new terms has been presented and briefly explained, either in the text itself or in the problems.

The great value of practical experience in foundation problems has been pointed out. Full advantage has been taken of the principle of continuity of strains, which is practically never used by soil-mechanics writers, and this has permitted the establishment of limitations of theoretical formulas in a very simple manner.

The author has borrowed freely from the published works of different soil-mechanics investigators, especially from those of Professor Terzaghi. Credit has been given to all authors for this borrowed material. In each case the author has tried to present his own views on the subject.

Frequent talks with Professor Hardy Cross on the general aspects of civil engineering have had a definite bearing on the preparation of this book.

The author expresses his appreciation to Kenneth W. Lange and Frederick A. Reickert for proofreading and valuable suggestions.

DIMITRI P. KRYNINE

NEW HAVEN, CONN.,  
March, 1941.

# CONTENTS

	PAGE
PREFACE TO THE SECOND EDITION . . . . .	vii
PREFACE TO THE FIRST EDITION . . . . .	ix
SOIL-MECHANICS NOMENCLATURE . . . . .	xiv
INTRODUCTION . . . . .	1

## PART ONE

### ELEMENTS OF SOIL PHYSICS

#### CHAPTER I

ORIGIN AND GENERAL CHARACTERISTICS OF SOILS . . . . .	8
Soil Formation—Kinds of Soils—Mechanical Analysis—Texture and Structure of Soils.	

#### CHAPTER II

SOIL MOISTURE: SOIL PLASTICITY AND CONSISTENCY . . . . .	29
Varieties of Soil Moisture—Capillary Movement—Drying Out of a Clay Mass—Limits of Consistency—Soil Classification.	

#### CHAPTER III

SEEPAGE PHENOMENA AND FROST ACTION IN SOILS . . . . .	51
Coefficient of Permeability—Darcy Formula—Seepage through Earth Dams and from Canals—Freezing in Soils—Technical Measures.	

## PART TWO

### ELEMENTS OF THE MECHANICS OF EARTH MASSES

#### CHAPTER IV

STRESSES IN EARTH MASSES . . . . .	91
General—Stresses in an Elastic Continuum—Stresses in an Idealized Fragmental Mass—Direct Loading Experiments.	

#### CHAPTER V

SHEARING RESISTANCE AND CONDITIONS OF FAILURE OF AN EARTH MASS . . . . .	131
Equilibrium and Failure of Idealized Fragmental Masses—Friction and Cohesion—Shear Tests—Plastic Flow—Failure Lines.	

	PAGE
CHAPTER VI	
COMPRESSION STRAINS: THEORY OF CONSOLIDATION . . . . .	157
General—Theory of Consolidation—Consolidation Test—General Discussion of the Theory of Consolidation.	
CHAPTER VII	
REVIEW OF PARTS ONE AND TWO; AND INTRODUCTION TO PART THREE . . . . .	186
PART THREE	
STRUCTURAL APPLICATIONS	
CHAPTER VIII	
STABILITY OF FOUNDATIONS . . . . .	199
Spread Foundations—Pile Foundations—Eccentrically Loaded Foundations.	
CHAPTER IX	
STABILITY OF CUTS AND EMBANKMENTS . . . . .	235
Stability of Slopes—General Features of an Earth Dam—Stability of the Body and Foundation of an Embankment—Selection of Materials—Earth Dam Failures.	
CHAPTER X	
STABILITY OF RETAINING WALLS AND COFFERDAMS . . . . .	290
Rankine and Coulomb Formulas—General Wedge Theory— Method of Equivalent Fluid—Flexible Walls—Bulkheads and Coffe- dams.	
CHAPTER XI	
PRESSURE ON TUNNELS AND CONDUITS . . . . .	337
Stability of Circular Tunnels—Pressure on the Roof of a Rectangular Tunnel—Rigid and Flexible Pipe-culverts.	
CHAPTER XII	
HIGHWAY AND RUNWAY SUBGRADES . . . . .	360
Soil Stabilization—Design of a Subgrade—Underdrainage of the Subgrade.	
CHAPTER XIII	
SETTLEMENT OF STRUCTURES. . . . .	388
Settlement Caused by Static Loads and Vibrations—Subsidences Due to Excavations and Tunnels—Observations; Measures; Damage.	

*CONTENTS*

xiii

	<b>PAGE</b>
<b>CHAPTER XIV</b>	
<b>SOIL SAMPLING AND FIELD SOIL TESTING . . . . .</b>	<b>438</b>
General—Sampling—Field Tests.	
<b>APPENDIX A. WET MECHANICAL ANALYSIS OF SOILS . . . . .</b>	<b>475</b>
<b>APPENDIX B. VERTICAL PRESSURE FROM A DISTRIBUTED LOAD . . . . .</b>	<b>482</b>
<b>APPENDIX C. SHEARING TESTS . . . . .</b>	<b>484</b>
<b>APPENDIX D. THEORY OF CONSOLIDATION: CONSOLIDATION TEST . . . . .</b>	<b>490</b>
<b>AUTHOR INDEX . . . . .</b>	<b>497</b>
<b>SUBJECT INDEX . . . . .</b>	<b>503</b>

## SOIL-MECHANICS NOMENCLATURE

The following list of notations may be used *except where a given symbol is explained in the adjacent text.*

- A, a** area
- $A_p$**  pressure area in the theory of consolidation
- $a$**  coefficient of compressibility in the theory of consolidation
- B, b** width (or half width)
- C** coefficient
- $c$**  unit cohesion (*e.g.*, lb. per sq. ft.)
- $c_m$**  mobilized unit cohesion
- $c_v$**  coefficient of consolidation
- D, d** diameter
- E** modulus of elasticity
- $E_1$**  modulus of elasticity from a nonconfined compression test
- $E_2$**  modulus of elasticity from a confined compression test
- $e$**  voids ratio; also base of natural logarithms
- F** lateral pressure against the wall; also safety factor
- $F_a$**  active pressure
- $F_m$**  lifting force of a meniscus
- $F_n$**  natural earth pressure
- $F_p$**  passive pressure
- $F_s$**  pressure on a wall caused by surcharge
- $F_w$**  pressure on the wall caused by water
- H** thickness of a soft layer
- $h$**  height
- $h_c$**  height (length) of capillary movement
- I** impact coefficient
- $i$**  hydraulic gradient; also slope or angle with the horizon
- K** coefficient of pressure at rest; ratio of the horizontal pressure to the vertical pressure above a tunnel
- $K_a$**  active Rankine value
- $K_p$**  passive Rankine value
- $k$**  coefficient of permeability; modulus of subgrade; modulus of foundation; modulus of passive resistance; "soil constant" (in tunnels)
- L** length
- LL** liquid limit
- $n$**  porosity
- P** concentrated load; lateral pressure on a tunnel
- PI** plasticity index
- PL** plastic limit

- $p$  unit load; pressure  
 $\bar{p}$  line load  
 $p_i$  intrinsic pressure  
 $q$  discharge; also compressive strength  
 $q_f$  ultimate bearing value  
 $R, r$  radius ( $R$  may also mean reaction)  
 $R_d$  dynamic resistance of a pile  
 $R_s$  static resistance of a pile  
 $S$  stress  
 SL shrinkage limit  
 SN stability number  
 $s$  density (specific gravity) of soil particles; also unit shearing resistance (shearing strength)  
 $s_0$  specific gravity of water  
 $s_c$  part of the shearing resistance due to cohesion  
 $s_f$  part of the shearing resistance due to friction  
 $s_m$  specific mass gravity (apparent specific gravity)  
 $T$  time factor in Chap. VI; temperature in Chap. III.  
 $t$  time  
 $U$  percentage consolidation  
 $u$  neutral stress; hydrostatic excess  
 $W$  weight  
 $w$  water content in fractions of one unit  
 $x, y, z$  orthogonal coordinates  
 $z$  depth under the ground surface  
 $\alpha$  general designation of an angle; particularly angle of rupture  
 $\beta$  angle of visibility  
 $\gamma$  unit weight of soil  
 $\gamma_0$  unit weight of water  
 $\Delta$  displacement; settlement  
 $\Delta H; \Delta h$  decrease in thickness or in height  
 $\epsilon$  strain  
 $\theta$  polar angle; also angle made by the backface of a wall with the horizontal  
 $\mu$  Poisson's ratio  
 $\rho$  radius (radius vector)  
 $\sigma$  normal stress  
 $\sigma_1; \sigma_2; \sigma_3$  principal stresses  
 $\sigma_z$  vertical pressure  
 $\sigma_x; \sigma_y$  horizontal pressure  
 $\tau$  tangential stress (shear)  
 $\phi$  angle of internal friction  
 $\phi'$  angle of repose; also "weighted" angle of friction in Chap. IX  
 $\phi_1$  angle of friction of earth against a wall  
 $\psi$  angle of obliquity



# SOIL MECHANICS

## INTRODUCTION

**Interaction between Structure and Earth Mass.**—Every engineering structure is in contact with earth or rock. Earth material in this case is either in the natural state or artificially placed. For instance, to construct a building, an excavation is made in natural ground, or piles are driven and a masonry or concrete foundation is built in the excavation. In the same way, the base of a retaining wall touches the natural ground and, in addition, keeps in equilibrium an artificial backfill. A building exerts a pressure on the earth mass with which it is in contact, and in the case of a retaining wall the backfill exerts pressure against the structure. Thus there is an interaction between the structure and the adjacent earth mass; and as a result, stresses develop in both. In turn, stresses produce changes both in the shape and in the size of the structure and of the earth mass. Thus the structure may move somewhat downward, and it is said then that the structure “settles.” Sometimes the structure moves sidewise, also. Usually when the earth mass is resistant enough to withstand the action of the stresses and to move a negligible amount only, this settlement is harmless for the structure. Should, however, the motion of the earth mass be appreciable, cracks may appear in the structure, and it may even collapse.

When planning a structure, an engineer must be able to visualize it and to forecast its behavior at any time. Hence, besides the determination of the stresses caused in the structure by the action of external forces, such as loads, wind, its own weight, and others, it is necessary to determine or at least to estimate (a) the character and the value of stresses in the structure and the adjacent earth mass caused by their interaction, (b) the character and the value of changes in shape and size of the structure and of the earth mass in contact with it. Especially important is the determination of the probable amount of settlement. The process of settlement is

nothing but the downward travel of the structure during which it is exposed to dangers of being cracked or otherwise damaged. The less the amount of settlement and the more uniform the settlement the better.

**Soil Mechanics.**—Stresses and strains are studied in mechanics. General principles of mechanics are the same under all circumstances and for any material. Any material possesses, however, some peculiarities that distinguish it from other materials. Hence methods of computing stresses and strains may be different for different materials. There is a mechanics of metals, a mechanics of fluids; and so far as earth masses are concerned, stresses and strains in them are studied in soil mechanics. This is theoretical soil mechanics, which, when further applied to the analysis and to the design of engineering structures, becomes applied soil mechanics.

Theoretical soil mechanics is discussed in Part Two of this book, and applied soil mechanics (or structural applications of soil mechanics) in Part Three.

**Soil Physics.**—A stress does not always produce the same effect on a given soil. The stress-strain interrelationship depends (a) on the character of the soil itself and (b) on its state at a given time. This is a well-known fact to all who have an opportunity to observe soils in fields and on roads. Clays do not resist stresses in the same way that coarse sands do; clay when wet becomes soft and weak, whereas reasonably dry clay may be very hard. Excessively dry soils do not resist even the superficial action of the wind which in times of drought blows them away from the fields. Many other examples could be quoted. It follows that the study of soil properties is a necessary prerequisite to the study of resistance to the action of stresses. Not all soil properties are interesting to an engineer. Some of them are of purely agricultural value, for instance chemical reactions important in plant nutrition or microbiological processes caused by microorganisms in the upper layers of an earth mass.

The necessary knowledge of properties of soils is the province of soil physics, an outline of which as applied to engineering may be found in Part One of this book.

**Field Investigations.**—In regard to structures, it should be stated that some structures, such as earth dams and railroad and highway embankments, may be composed almost entirely of

earthy material. In the case of such structures an accurate knowledge of soil properties becomes especially important. For instance, a storage earth dam has to hold back water in the reservoir and hence must be adequately impermeable, whereas a highway embankment should be made of coarse, permeable material for the sake of better stability of the road surface. The properties of the material to be used in such structures may be regulated by specifications as in the case of other engineering materials. A sharp difference exists, however, between earth and other materials—metals, for example. Natural earth material from a borrow pit can be improved but slightly if at all; but if refined technological processes are used, metals may be brought to a high grade of perfection so as to satisfy very rigid specifications. In general, as far as borrow-pit material is concerned, one can only select the best material from whatever is available in the locality. For a structure resting at the bottom of an excavation, even such a selection cannot be made, since a foundation must be built on the material available at the site. Methods of soil stabilization for highways and runways are being steadily developed; but the technique of soil improvement as applied to foundations of structures is still in its infancy.

Soil properties cannot be adequately appreciated unless they are studied in a laboratory. For this purpose soil samples should be secured in the field according to certain rules, sometimes from greater depths. In addition to such a sampling, soil testing in the field under natural conditions should be encouraged where possible. Methods of sampling and other field soil investigations are discussed in Part Three of this book.

**Engineering Geology.**—Soil mechanics *is not* a geological science; it is *a branch of engineering knowledge*. Engineering geology in turn is a branch of geology, which discusses in some detail and in an applied way geological matters important and interesting for an engineer. Acquaintance with geology and close contact with geologists, when necessary, are of great importance for a foundation engineer. There are several textbooks on engineering geology, and the reader is advised to consult them.

**Soil Science and Role of Chemistry.**—Soil science is an agricultural science that studies soils from the point of view of plant nutrition. It starts with a study of soil physics and in this respect has much in common with soil mechanics. It then proceeds

toward chemistry, whereas soil mechanics follows the path of physics and applied mechanics (Part Two of this book).

Chemistry is of extreme importance in the problems of soil stabilization (Part Three). Hence a knowledge of chemistry is necessary for a civil engineer working along these lines. It should be noted that the development of soil-stabilization processes is being done in close cooperation with chemists and chemical engineers.

**Historical.**—The study of earth pressure, as applied to fortifications, started in France, perhaps in the sixteenth century. In 1773 the French scientist Coulomb published a discussion of earth pressure. About 1856 Rankine (in Great Britain) developed a theory of equilibrium of earth masses and applied it to some elementary problems of foundation engineering. Both Coulomb and Rankine and their numerous followers considered what is termed in this book “idealized fragmental masses,” consisting of grains like sand and possessing some friction and sometimes cohesion. Their theories are often referred to as “classical theories of soil mechanics.”

A study of American engineering literature for the past 50 years shows that almost all outstanding ideas of soil mechanics were known to the profession years ago. This valuable knowledge was scattered, however, throughout the pages of technical periodicals, and it was necessary to put it together and to correlate it more closely with physics and mechanics. This was done in the past quarter of a century.

The idea of studying the physical properties of soils in actual conditions came to the engineering profession only gradually. In 1913 two committees on soil research were established, one by the Swedish State Railways and another by the American Society of Civil Engineers. But a period of extensive development in this field began between 1925 and 1929, when Dr. Charles Terzaghi was on the faculty in the Massachusetts Institute of Technology. In 1925 this outstanding investigator published a book on soil mechanics<sup>1</sup> followed by a series of papers and articles on the same subject. In June, 1936, an International Conference on Soil Mechanics and Foundation Engineering was held at Harvard University. Numerous papers from various foreign countries where soil-mechanics research is being done (Germany, Holland, Russia, England, Sweden, Japan, and others) were presented, in addition to papers

submitted by research workers of the United States. These papers have been published in the three volumes of the *Proceedings* of the conference.<sup>2</sup>

**Work at the Present Time.**—Before the Second World War (1939–1945) emphasis was laid in the United States on the study of soil-mechanics problems in the fields of earth dams and highway engineering. Important work along the lines of dam research and design was carried on by the U. S. Army Engineers<sup>3</sup> and by the Bureau of Reclamation. Intensive research in the application of soil mechanics to roads and highways was done by the Public Roads Administration (formerly the U. S. Bureau of Public Roads), by the Highway Research Board,<sup>4</sup> and by the state highway departments of Michigan, California, and many other states. This work was slowed down by the war. The unusual development of airport construction made necessary the study of problems of pavement slabs and subgrades to take care of the landing of heavy aircrafts. This was done by both Army and Navy organizations, with participation of civilian specialists. The Bureau of Yards and Docks developed among other things considerable research work on soil problems connected with harbor facilities and shipbuilding.

The postwar activities are still concerned mostly with airports and runways, with revived interest in highways and dams. As in the prewar period, the A. S. C. E. is studying soil problems through its soil mechanics and foundation division. Leading American institutions of higher learning have introduced soil mechanics with laboratory exercises into their curricula. In some of these institutions, research work of importance also is under way.

Analogous work has been carried on abroad, mostly in prewar Germany. There are in that country several excellent soil laboratories working both theoretically and for practical purposes, and there is a special Society for the Study of Soil Mechanics (“Degebo”) which from time to time publishes the results of its work.<sup>6</sup>

The Building Research Station of the English government works on soil mechanics, among other subjects. The British Institution of Civil Engineers often discusses problems along these lines. There is marked interest in soil mechanics in English dominions and in India.

Considerable advanced research work has been also done by the Russian research institutes. In Russia as in the United States the

study of soils started in connection with roads and highways and afterward involved other kinds of foundations.

France has given to the world many original theories of "classical" soil mechanics, but research work began only in about 1935. The research is being done partly by the government, partly by private concerns.

Among the Swedish establishments there are two laboratories: one is at the Technical University of Stockholm, and the other belongs to the Geotechnical Committee of the Swedish Railroads. The Swedish Institute of Public Roads (Svenska Väginstitutet) maintains an active contact with geologists.

A special geotechnical committee exists in Japan and publishes a bulletin. Its work is connected mostly with railroads. In Hungary, soil-mechanics research is carried on by the Technical University of Budapest.

There is no special periodical dedicated to soil mechanics, but many leading civil engineering journals freely open their pages to papers of this kind.

**Trend of Development of Soil Mechanics.**—It cannot be stated that the "classical" theories of soil mechanics are wrong, though sometimes they furnish quite inadequate results. They can be used, but *only within limitations*. This is because every theory is based on certain assumptions and is no better than those assumptions. In Part Two of this book an effort is made to point out most of these limitations.

Since existing theories cannot be applied in all cases, it is often necessary to follow a *semi-empirical method* of study. Experience has shown that small-scale experiments do not always furnish results consistent with those recorded in the case of actual structures. Thus observations on full-sized structures should be *especially emphasized*. Unfortunately, in order to draw decisive conclusions on some points, numerous observations on full-sized structures are needed, and these are not always available. To proceed from a qualitative to a quantitative appreciation of the facts requires long, accurate, and systematic field recordings. The latter cannot be done by the research workers alone. *Nothing worth while* along these lines can be accomplished *without cooperation of practicing engineers* in different branches of foundation engineering, including highways and earth structures such as dams and canals.

## References

1. KARL TERZAGHI: "Erdbaumechanik," Franz Deuticke, Leipzig and Vienna, 1925; also "Theoretical Soil Mechanics," John Wiley & Sons, New York, 1943.
2. *Proc. Intern. Conf. Soil Mech. and Foundation Eng.*, Cambridge, Mass., 1936.
3. *Proc. Soils and Foundation Conf.*, U.S. Engineer Department, Boston, Mass., 1939.
4. Soil Mechanics and Soil Stabilization, *Proc. Eighteenth Ann. Meeting, Highway Research Board*, 1938, pt. II (also *Proc.* of other meetings).
5. *Proc. Purdue Conf. Soil Mech. and Its Applications*, Purdue University, Lafayette, Ind., 1940.
6. Veröffentlichungen des Instituts der deutschen Forschungsgesellschaft für Bodenmechanik (Degebo), Berlin, since 1933.



PART ONE  
ELEMENTS OF SOIL PHYSICS



## CHAPTER I

### ORIGIN AND GENERAL CHARACTERISTICS OF SOILS

**1:1. Definitions.**—The term “soil” as used by engineers usually designates earth material, lying in its original undisturbed state, removed from the earth crust in order to be placed in a structure, or having already been placed there. The terms “soil mass” or “earth mass” in engineering language refer synonymously to natural or artificially laid bodies of earth material. The term “mass,” used in this sense, is purely conventional and has a meaning entirely different from the term as used in physics.

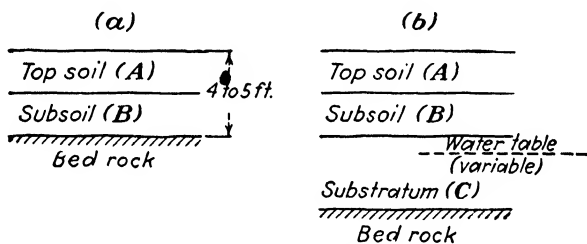


FIG. 1:1.—Soil layers.

In agriculture the term “soil” or “topsoil” refers to the upper part of the earth crust that is generally suitable for the growth of plants. A cross section through the earth crust may be of two types, as shown in Fig. 1:1. In both types there is a layer of *topsoil*, followed by *subsoil* from which it has been formed (total thickness, 4 or 5 ft.). In its turn, the subsoil, as shown in Fig. 1:1a, is formed from the underlying *bedrock* (which in this case may be referred to as the “parent rock” of the soil). Figure 1:1b shows an additional layer between the subsoil and the bedrock, namely, *substratum*. The whole picture shown in Fig. 1:1b suggests that the three upper layers topsoil, subsoil, and substratum are formations brought from elsewhere and deposited on the surface of the bedrock. Another interpretation of Fig. 1:1b is that the sub-

stratum alone has been brought from another locality and that subsoil and topsoil have developed afterward on its surface.

The soil layers, or "horizons," as shown in Fig. 1:1 are designated by agriculturists with letters: *A* means topsoil; *B*, subsoil; and *C*, substratum. Further subdivisions may be shown by indexes; for example, *B*<sub>1</sub>, *B*<sub>2</sub>, *B*<sub>3</sub>, . . . . The upper part of horizon *A* is designated by the symbol *A*<sub>0</sub> and is termed "humus." The latter is of organic origin (decomposed remnants of animals and plants mixed with soil particles) and is important in agriculture but in most cases is removed from the earth surface before a structure is built.

Not all soil horizons are equally interesting to the engineer. For highway purposes, especially for earth road construction, and also for irrigation engineering, horizons *A* and *B* are of importance. In the construction of foundations of heavy buildings, however, it is desirable to reach the ledge- or bedrock if the latter is not very deep or at least to found the structure on a trustworthy layer of substratum.

The designation of soil horizons with the letters *A*, *B*, *C*, and their derivatives is not very popular among engineers, descriptive terms being preferred in general.

**1:2. Soil Formation.**—Atmospheric agents attack the surface of the earth relentlessly, transforming even the hardest rocks into soil. The process of soil formation is always in operation; but since it is very slow, we do not notice it. The attack of the atmosphere upon rocks may be *mechanical* (disintegration) or *chemical* (decomposition). Disintegration processes are due to the action of such agents as the expansive force of freezing water in fissures or sudden changes of temperature. Decomposition processes consist of the combination of minerals either with oxygen (oxidation) or with water (hydration). Thus, a rock may be transformed into soil in place, or, to use the Latin term, "in situ" (Fig. 1:1a). The combined mechanical and chemical action of atmospheric agents is called "weathering." The *climatic factor* is of the greatest importance in the process of soil formation by weathering. The theory of soil formation based on this idea was first advanced by Russian soil scientists (Dokouchaev, Glinka, and others). The same original rock material (parent rock) may yield different types of soil in different climates. For instance, granite, if weathered chemically in a humid northern climate, may produce *podzols*, whereas in humid tropical climate the formation of *laterites* is to be

expected. The term "podzol" is of Russian origin and may be translated as "ashlike," because of the predominant gray color of these soils. In these formations horizon *A* is a leached one, and the products of leaching or "cluviation" are deposited in horizon *B*. In the course of this process *hardpans* or cemented soil layers, so familiar to a builder, may be formed. Incidentally, the term "gley," used by some European writers, means a soil formed under the same conditions as a podzol, but in the presence of a water table at or near the surface. A certain percentage of the podzol particles are scalelike (flakes), while laterite particles are rich in rounded ferruginous concentrations, residual quartz grains, and red ferruginous and aluminous clayey matter.

Reverting to Fig. 1:1b, it should be noticed that *transporting agents* which may be active in soil formation are *running water*, contributing to the formation of "alluvial" soils; *wind* ("aeolian" soils); moving *ice sheets* ("glacial" soils); and the *force of gravity*, when earth masses simply slide down. The effect of these agents on soil formation is discussed in the following three sections.

*Volcanic action* may also be responsible for the formation of soils. Thus bentonite, a natural product of great importance in industry found in Montana, South Dakota, Wyoming, and other places in the United States, has been formed from volcanic ash. The commercial term sometimes used is "volclay." Another example of soil formed mostly from volcanic ash is the treacherous soil of Mexico City, described several times in engineering literature.

**1:3. Sedimentation and Alluvial Soils.**—It may be assumed that soil as defined here (Sec. 1:1) is insoluble in water, and mixtures of soil particles with considerable quantities of water are practically *soil suspensions*, and not soil solutions. The latter term is seldom used by engineers. Only a small amount of salts contained in a soil may form a true chemical solution.

If there is only a limited amount of soil in a quiet basin, for instance in a pond, soil particles will settle to the bottom in the order of their sizes, first the coarser and afterward the finer. The relation between the diameter of a particle and its sinking velocity in quiet water was first given by Stokes in 1845 in the following form:

$$v = \frac{2}{9} g r^2 \frac{s - s_0}{\mu} \quad (1:1)$$

where  $v$  = speed of sinking, cm. per sec.

$g$  = acceleration of gravity, cm. per sec. per sec.

$r$  = radius of the particle, cm.

$s$  = density of the particle (specific gravity), g. per cc.

$s_0$  = density of the liquid, g. per cc.

$\eta$  = coefficient of viscosity of the liquid, poises.\*

Since 1 cc. of water weighs approximately 1 g., the average density of water may be assumed to be  $s_0 = 1$ . Assuming, furthermore, the following averages:  $s = 2.65$ ;  $g = 981$  cm. per sec. per sec.; and  $\eta = 0.01$  for a temperature of 67°F. (about 20°C.), and designating by  $D$  the diameter of the spheroidal particle ( $D = 2r$ ),

$$v = 9,000D^2 \quad (1:1a)$$

It is to be noted that the diameter of the spheroidal particle in formula (1:1a) is expressed in centimeters, and not in millimeters. For example, the speed of sinking of a spheroidal particle  $D = 0.01$  mm. = 0.001 cm. in water at a temperature of 67°F. will be

$$v = 9,000 \times 0.001^2 = 0.009 \text{ cm. per sec.}$$

The Stokes formula has been developed for one particle under the following assumptions: (a) The medium through which the particle sinks is homogeneous and of unlimited extent; (b) the particle itself is a smooth and rigid sphere falling with a very small velocity. The closer the actual conditions to these assumptions the more reliable the results furnished by the Stokes formula, and vice versa. Studies by numerous investigators have shown that the Stokes formula is applicable only within a certain range of coarseness (0.0002 mm. — 0.2 mm., approximately).

In nature the process of gradual settling of soil particles suspended in water, termed "sedimentation," generally takes place in the following way: First, soil is eroded from the earth surface, for instance by rain water (wash), and the suspension is carried to the tributary of a stream or to the stream itself. Sedimentation may take place either in this running water or in the basin into which the stream flows. The size of the particles that remain in suspension varies approximately as a certain high power of the velocity; hence if the velocity of the running water decreases, soil particles

\* The physical dimension of a poise used in the c.g.s. system for measuring the coefficient of viscosity is grams per centimeter per second. For numerical values, see Appendix A.

above a certain size will settle. Such a decrease in velocity takes place, for instance, behind a dam constructed to store the water of a stream; and if the latter carries much soil, serious problems such as "silting" may arise in this connection. Engineering measures taken to eliminate or curb consequences of such sedimentation are of great importance and interest. They have been described with some detail in engineering literature, particularly with reference to sedimentation in the Colorado and Sacramento rivers. In periods of fresh water, streams often overflow their banks; velocity in the overflow portion is generally very small, with the result that part of the load carried by the water is dropped to form a flood plain. Also, a quick decrease in velocity takes place when the stream issues into a sea or lake, and as a consequence delta deposits are formed. In general, deposits left by running water are coarsest near their source of supply, and the finest material is carried farthest away. Hence, as a rule, particles brought by a stream to the sea or a lake are relatively fine-grained and settle slowly to form marine and lacustrine (lake) deposits of fine-grained material. Owing to geological changes in level, these deposits may finally become exposed. Soils formed by the action of running water either in streams or in basins of deposition are referred to as "alluvial," or water-laid, soils.

Sedimentation may be activated by the action of *electrolytes*, such as ammonia, soda, common salt, or lime. The soil particles carry electrical charges of the same sign, this being the reason why they are mutually repulsed. In addition, the fine colloidal soil particles are continually "bombarded" by water molecules which prevent them from settling down regularly (the so-called "Brownian movement"). These circumstances retard the settlement of very fine colloidal particles, which may sometimes remain in suspension almost indefinitely. Addition of an electrolyte decreases the repulsive action of fine particles, they collide and form aggregates or floccules which, upon becoming larger, settle to the bottom. The processes described are termed "coagulation" and "flocculation," with consequent "precipitation." Sea water contains salt which is an electrolyte; hence fine-grained marine deposits are generally formed quicker than lake deposits, other circumstances being equal. Another example of the action of electrolytes on a natural soil suspension is the case of a stream carrying fine-grained dispersed soil (for instance, clay) into a lake if the slopes surround-

ing the latter are of exposed limestone. Rainwash will carry lime, which is an electrolyte, to the lake, and in this way the formation of a deposit will be accelerated.

Nature's principles of sedimentation in the formation of alluvial deposits are taken advantage of in soil testing laboratories, as will be explained in Sec. 1:9.

**1:4. Wind Action and Aeolian Soils.**—Wind may produce practically the same erosive action as running water, as is proved by the great dust storms that in 1935 and 1936 swept up immense areas of topsoil in the Middle West and transported it to varying distances. Of a certain importance in foundation engineering are *loess deposits*, which may be found in the United States, for instance, in the Mississippi Valley, and which occupy considerable areas in China, the Argentine Republic, Russia, and other regions. Loess is composed of particles ranging around 0.05 mm. or somewhat less in diameter. It is very porous and in places possesses cavities several feet long, with remnants of vegetation. The loess mass is quite amorphous; its thickness ranges from a few inches to hundreds of feet. When dry, loess is able to carry considerable loads, but it loses a great part of its resistance if wet. The heterogeneous interlocking structure of loess makes possible the existence of steep slopes and even vertical walls, and there are highway cuts in loess with exceedingly high slopes.

*Dunes*, or migrating hills of sand, represent another type of wind deposit. In some regions the problem of anchoring dunes, which in some cases are known to destroy buildings, is an important one. Vegetation may be of help in this connection.

*Beach or shore deposits* are not to be confused with aeolian soils. These deposits, consisting of fine, frequently rounded grains, are formed by the action of waves which bring the eroded material and move it in both transverse and longitudinal directions with respect to the shore.

**1:5. Glacial Soils.**—Glacial deposits were formed from the debris carried by advancing ice sheets during the glacial epoch. Maps of maximum glaciation are given in textbooks on geology. The ice came close to Philadelphia, Pa., and reached Topeka, Kans., and Spokane, Wash. In contrast to water-laid deposits, glacial soils lack stratification and homogeneity. As a rule, they contain stones and boulders brought by the ice sheets. When the ice melted, the debris carried was released and, if left in place, formed

deposits of glacial drift or till. Glacial gravels make excellent building soils when permeability is required. Coarse sand and gravel pits are widely exploited in glaciated regions for highway embankments and subgrade and for concrete. Clay that was deposited in glacial lakes is glacial clay; as a rule it is stratified (compare end of Sec. 1:10).

**1:6. Size and Shape of Soil Particles; Soil Fractions.**—The soil material may be characterized by its *texture*, *i.e.*, by the size of its constituent particles and their grading—or, what amounts to the same, by distribution of the soil material into groups or fractions (grade sizes). Various soil-research organizations establish the upper and the lower limit of such fractions rather arbitrarily. The classification adopted by the Bureau of Chemistry and Soils, U. S. Department of Agriculture, is the following:

Diameter of Particles, mm.	
Fine gravel (grit) . . . . .	2 to 1
Coarse sand . . . . .	1 to 0.5
Medium sand . . . . .	0.5 to 0.25
Fine sand . . . . .	0.25 to 0.10
Very fine sand . . . . .	0.10 to 0.05
Silt . . . . .	0.05 to 0.005
Clay . . . . .	0.005 and below

A way to memorize this table is to remember that the size of silt particles lies between 0.05 and 0.005 mm. Two figures only, 0 and 5, are necessary to express numerically this size. All soils coarser than silt are sands (or gravels); all finer soils are of clayey nature.

According to the classification of the U. S. Bureau of Public Roads, the items in this table are

Gravel: particles retained on a No. 10 (2-mm.) sieve.

Coarse sand: particles passing a No. 10 sieve and retained on a No. 40 (0.42-mm.) sieve.

Fine sand: particles passing a No. 40 sieve and retained on a No. 270 (0.05-mm.) sieve.

The sieves referred to are U. S. Standard sieves.

Matter in a very fine state of dispersion—namely, particles finer than 0.0001 mm. = 0.1 $\mu$  (micron)—is referred to as *colloidal* in chemistry. It is assumed for soil-research purposes that soil particles finer than 0.002 mm. = 2 $\mu$  already possess colloidal properties. There are two kinds of colloids: (a) *gels*, or jellylike colloids; (b) *sols*, or colloids similar to a liquid. Some gels upon

being vibrated lose their consistency and become liquid (sols). After a period of rest the former state of gel is restored. Such are the so-called *thixotropic* clays.

Sands and gravels are composed of grains and particles that are either *rounded* (bulky) or *angular*; the intermediate shape is termed *subangular*. The average diameter of these grains can be measured with a certain degree of accuracy. A goodly percentage of clay particles are *scalelike* or flaky (compare end of Sec. 1:8); and strictly speaking, the concept "diameter" is not applicable in this case. The term *equivalent* diameter of a soil particle means the diameter of a hypothetical sphere made of the same material and sinking in water with the same speed as that of the given soil particle. The shape of colloidal matter is not exactly known, and some investigators visualize it as being like crumpled paper. In any case, colloidal particles are not spherical and hence possess no diameter. Some investigators propose to drop the concept "diameter" as applied to soil particles and replace it by the concept of speed of fall in water.

**1:7. Principal Kinds of Soils.**—Besides the terms used in Sec. 1:6, a term very often used in practice is "loam," which designates a mixture of sand, silt, and clay, sometimes with organic admixtures.\* According to the proportion of these ingredients, there are sandy loams, silty loams, and clayey loams. To show that there is some admixture of silt or clay to a sand, the terms "silty" and "clayey" sands, respectively, are used. Any soil mixed with a considerable amount of gravel or stone may be classed as "gravelly" or "stony." For instance, there may be stony sandy loams or gravelly clays, etc. Sandy materials are designated as "light-textured" and clays as "heavy-textured" soil. These terms have nothing in common with the weight of the soil.

*Silt* is fine-ground rock flour. As found in borrow pits and excavations, it is usually a light gray or pink, fine-grained material without organic admixtures. In rivers, particularly close to their deltas, there are often deep deposits of organic silt sometimes 100 ft. or more thick, often smelling unpleasantly owing to the pres-

\*The amount of organic matter in a soil is often determined by ignition at very high temperature. Organic matter is practically burned out of the sample in this test. This method may involve oxidation, however, and hence may indicate a wrong weight for the burned material. There are also other methods.

ence of the methane gas. Organic silt is dark in rivers and light gray when dry. Moist organic silt can be rolled in threads between the fingers; *i.e.*, it is plastic, whereas nonorganic silt is not plastic.

*Mud* is a slimy or pasty mixture of soil and organic admixtures at the bottom of a river or a lake. Sometimes organic silt is incorrectly called "mud."

*Gumbo* is a fine-grained soil usually devoid of sand. It is impervious when saturated and waxy in appearance and to the touch.

*Adobe* is a heavy-textured alluvial clay found mainly in the semi-arid regions of the Southwestern United States.

*Caliche* is a term used mostly in the Southwestern United States to designate formations in the shape of cemented clays, sands, and gravels. The cementing material is calcium carbonate, deposited through the evaporation of ground waters during changes in their level.

*Marl* is clay with calcium carbonate (calcareous clay) and is more homogeneous than caliche.

*Hardpan* (compare Sec. 1:2) is a highly compressed and cemented mixture of sand, clay, gravel, and boulders generally located on top of the ledge rock, thus underlying other substratum materials. To designate this material, the term "boulder clay" is also used. The term "hardpan" as used in different localities does not designate exactly the same material.

Organic deposits are formed where there is decay of vegetation. *Peat*, for instance, is partly decayed plant material. Impure peat containing considerable inorganic admixture is known as *muck*. Organic deposits in small vestigial lakes are *peat bogs* or *muskegs*.

Because no written definition can give an accurate idea of a soil, different kinds of soils are only mentioned in this section. To know a soil, an engineer has to observe it under field conditions and as placed in structures. This practical knowledge should be supplemented with laboratory tests of soils.

**1:8. Clay.**—Silica,  $\text{SiO}_2$ , is one of the chief constituents of both common quartz sand and clay. The latter is formed from clay minerals ("clay materials") that chemically are hydrous aluminum silicates, *i.e.*, contain silica,  $\text{SiO}_2$ , often in colloidal form, and sesquioxides, of the general formula  $\text{R}_2\text{O}_3$ . The symbol R stands chiefly for Al and Fe, so that the corresponding sesquioxides will be aluminum oxide,  $\text{Al}_2\text{O}_3$ , and iron or ferric oxide,  $\text{Fe}_2\text{O}_3$ . The ratio

$\text{SiO}_2/\text{R}_2\text{O}_3$ , that of silica to the sum of sesquioxides (by weight), is termed the "silica sesquioxide ratio." As a rough average, clay contains 50 per cent of silica and 25 per cent of sesquioxides, so that the average value of the ratio  $\text{SiO}_2/\text{R}_2\text{O}_3$  is about 2.

There may be organic admixtures to clay, usually in the form of very fine particles.

The two basic groups of clay minerals are (a) the *kaolinite* group, and (b) the *montmorillonite* group. One of the members of the latter

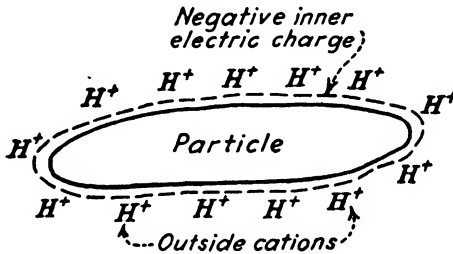


FIG. 1:2.—Schematic representation of a particle of H-clay.

group is bentonite (Sec. 1:2). Besides there are many clay minerals of the *illite*, or micalike, group. Other clay minerals found in few clays or in small amounts are halloysite and allophane. The latter is amorphous, whereas all other clay minerals are *crystalline*. Clays range in color from white to black, including green, red, and brown. Particularly, kaolin,  $\text{Al}_2\text{O}_3 \cdot 2\text{SiO}_2 \cdot 2\text{H}_2\text{O}$ , which belongs to the kaolinite group is white, and so is allophane.

A clay particle is assumed to be covered with a double electric layer: (a) The inner layer is negative and forms a unit with the particle itself, whereas (b) the outside layer consists of positive ions or *cations* which may be detached from the particle. Clays are often designated according to the chemical nature of the outside cation. For instance, there may be H-clay (Fig. 1:2), Mg-clay, and others. If treated with a chemical, the soil may replace its own cations by the cations of the chemical if it has more *affinity* to those cations than to its own. This is the so-called "base exchange" so important in soil stabilization (Chap. XII). As an example, a Mg-clay in suspension treated with sodium silicate,  $\text{Na}_2\text{SiO}_3 \cdot 9\text{H}_2\text{O}$ , loses its Mg-cations and becomes Na-clay easily dispersed in water, whereas Mg-clay is hard to disperse.

A clay particle is able to attract water and, under most circum-

stances, to keep it attracted. This is the so-called *adsorptive* (or simply "sorptive") capacity. Since the base exchange is nothing more than a cation adsorption, it should be concluded that to possess both high sorptive and high exchange capacities, a clay must be able to develop space available for possible storage of attracted water or cations. In both basic clay-minerals groups (kaolinite, montmorillonite) the crystals are arranged in such a way that the *crystal lattices* are alternate flat sheets of silica and alumina. In the case of the montmorillonite, however, the crystal lattices are expandable, whereas in the case of the kaolinite group they are fixed (tight). Hence, the minerals of the montmorillonite group are able to accommodate larger amounts of water molecules and cations; their sorptive and exchange capacities are high. In contrast, the minerals of the kaolinite group can offer but a limited space for attracted water and cations, and their sorptive and exchange capacities are low.

**1:9. Mechanical Analysis and the Size Distribution Curve.**—A soil material may be subdivided into fractions according to the size of its constituent particles. Such a subdivision is known as a *mechanical analysis* of the soil. A good mechanical analysis is not equally valuable in different branches of engineering. The size of the soil grains is of importance in such cases as construction of earth dams or railroad and highway embankments where earth is used as a material that should satisfy definite specifications. In foundations of structures, data from mechanical analysis are generally only illustrative; other soil properties, such as compressibility or shearing resistance, are of more importance. In a mechanical analysis, coarser fractions are separated by the use of sieves; finer particles are separated by methods of wet analysis based principally on the speed of sedimentation—the finer the particle the more time it requires to settle through a certain distance (Sec. 1:3). The method of wet analysis generally used by American engineers is the *hydrometer method* originally proposed in 1926 by Prof. Bouyoucos of Michigan Agricultural College and developed by the U. S. Bureau of Public Roads and Prof. A. Casagrande of Harvard.\* This method depends upon variations in the density of a soil suspension contained in a 1-liter graduate (*i.e.*, with a capacity of about 1,000 cc.). The density of the suspension is measured with the hydrometer at determined time intervals; then,

\* See Appendix A.

the coarsest diameter of particles in suspension at a given time and the percentage of particles "finer than" that coarsest (suspended) diameter are computed.

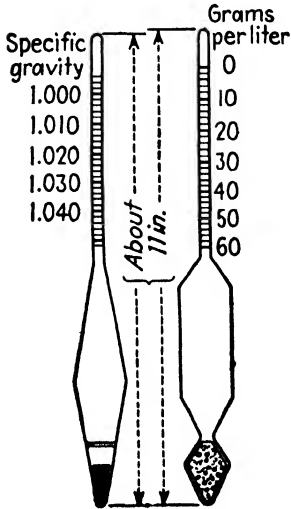


FIG. 1.3.—Hydrometers used in mechanical analysis of soils (new type is at the left).

These computations are based on the Stokes formula (1:1). Figure 1:3 shows the new (streamlined) and the old type of hydrometer. Other methods of wet analysis sometimes used by engineers are the *pipette method* and the *elutriation method*. In the former method a certain volume of the suspension is extracted from a certain depth at predetermined intervals, and the percentage "finer than" a certain diameter is determined directly by drying the extracted fluid and weighing the residue. In the elutriation method, which also is based on the Stokes formula, sedimentation takes place not in quiet water, as in the hydrometer or pipette method, but against an upward flow of liquid. There are many other methods devised along these lines.

Figure 1:4 shows the results of a mechanical analysis graphically represented in the form of a "size distribution curve" or "grading curve." The abscissas of this curve

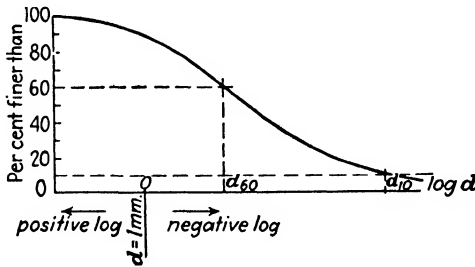


FIG. 1.4.—Size distribution curve.

are diameters of particles plotted on a logarithmic scale, and the corresponding ordinates show the percentage of particles "finer than" a given equivalent diameter. The *effective size* of the given soil is the maximum diameter of the smallest 10 per cent ( $d_{10}$  in

Fig. 1:4), and the uniformity coefficient is the ratio obtained by dividing the maximum size of the smallest 60 per cent ( $d_{60}$ ) by the effective size ( $d_{10}$ ). The uniformity coefficient is much greater in the case of clay than in that of sands. In some writings the uniformity coefficient is designated with the symbol  $c_u$ .

**1:10. Structure of Soil; Voids Ratio.**—The frame or the skeleton of a soil mass is made up of soil particles, and the voids (pores) between the particles are filled with moisture or air or both. The manner of arrangement of the particles forming a soil mass characterizes its *structure*.

Let us designate the total volume of a soil mass and the volume of the voids between its particles by 1 and  $n$ , respectively; admittedly  $n$  is a fraction of a unit. Then the fraction  $1 - n$  will represent the volume of solid particles within the given mass. The fraction  $n$ , upon being multiplied by 100, represents the *porosity* of the given mass as expressed in per cent. The *voids ratio*  $e$  is the ratio of the volume of the pores  $n$  to the volume of soil particles forming the skeleton of the given mass,  $1 - n$ .

$$e = \frac{n}{1 - n} \quad (1:2)$$

According to the degree of compactness, an earth mass may be in its *densest state* (voids ratio,  $e_{\min}$ ), in its *loosest state* (voids ratio,  $e_{\max}$ ), or in some intermediate state (voids ratio,  $e$ ). The *relative density* of the mass is defined as the value of the ratio

$$\frac{e_{\max} - e}{e_{\max} - e_{\min}}$$

In the case of a hypothetical soil consisting of ideal spherical grains, the maximum and the minimum porosities are  $n = 47.6$  and  $n = 26.0$  per cent, respectively. The average porosity of a coarse or medium sand mass is about 33 per cent, which corresponds approximately to a voids ratio of  $e = 0.5$ . Fine sand masses are often looser than coarse or medium sand masses and possess a greater voids ratio. Still greater is the porosity and voids ratio  $e$  of silty and clayey sediments. Such materials settle out of water slowly, since the resistance to their falling is considerably greater than in the case of sands. Two clay particles coming into contact do not roll to the bottom as sands but stay close to the spot of fall, being attracted to each other, and this force of attraction over-

comes the action of gravity. In such cases soils of *honeycomb* or *spongy structure* are formed (Fig. 1:5a). Another kind of structure is the *flocculent* one shown in Fig. 1:5b. If a clay *consolidates*, as

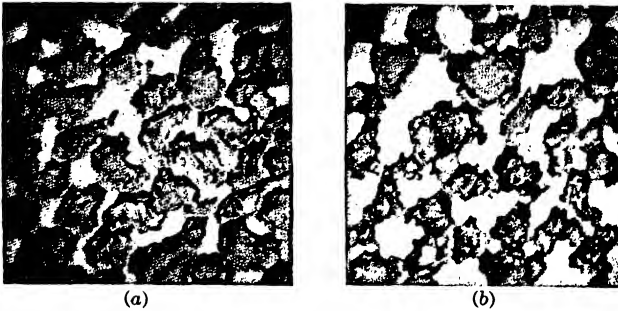


FIG. 1:5.—(a) Honeycomb and, (b) flocculent structure of soil. (After Terzaghi.)

when it is subjected to the action of the weight of a thick overlying deposit, moisture is squeezed out of the pores. Moreover, according to a hypothesis advanced by A. Casagrande, considerable unit pressures develop under and close to silt grains. In Fig. 1:6 the

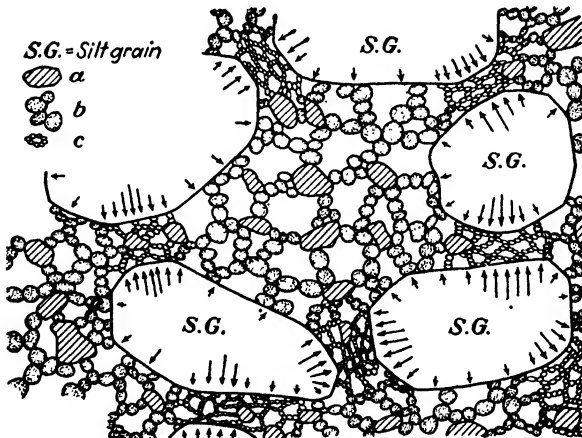


FIG. 1:6.—Hypothesis of bonds between coarser particles in a clay. (After A. Casagrande.)

symbols *a*, *b*, and *c* refer to clay particles, flocculated colloidal particles of low degree of consolidation, and flocculated colloidal particles of high degree of consolidation, respectively. Bonds thus formed between coarser silt grains are responsible for much of the resistance of undisturbed clay samples extracted from the soil

without disturbing its natural structure and moisture content. In a disturbed clay sample, these bonds have been broken and the resistance has been lowered.

If a small slip of paper is dropped from a certain height, it will touch the floor with its flat side. In a similar manner most of the scalelike clay particles are *oriented* parallel to the bottom of the basin where sedimentation took place. Particularly, *varved* (or laminated) clays are formed by alternate bands of fine and coarse materials, such as clay and silt. The bands are of variable thicknesses (a rough average being  $\frac{1}{2}$  in.) and not necessarily of the same color. Apparently, each band corresponds to the sedimentation during one season, though there are other explanations of the origin of varved clays.

If the surface of each soil particle within a mass could be measured and the sum of these surfaces computed, it would equal the "internal surface" of the whole mass. Generally, the internal surface is expressed in square units per unit of weight of the mass. It varies within very wide limits and may be 200 or 300 sq. ft. per lb. of sand; in the case of clays this value may be as high as 20,000 or 30,000 sq. ft. per lb.

**1:11. Specific Gravity and Unit Weight of Soil.**—The heavier the material from which a given soil has been formed the greater the specific gravity of the soil particles. For instance, during the construction of the Alexander Dam in Hawaii, the specific gravity of the particles of a soil that was formed from heavy montmorillonite was about 3.3. On the other hand, organic admixtures such as humus diminish the specific gravity considerably. The average specific gravity of the soil particles to be designated by  $s$  is 2.0 to 2.7 and is somewhat more for finer clay particles. For approximate computations a value  $s = 2.65$  may be used, as has already been done in developing formula 1:1a. The unit weight of soil will be expressed in pounds per cubic foot. Its designation will be  $\gamma$ , and the designation of the unit weight of water will be  $\gamma_0$ . The latter value, as is well known, equals about 62.4 lb. per cu. ft. For the purposes of approximate computations the value of  $\gamma$  may be taken at 100 or 110 lb. per cu. ft. Pure quartz sand may weigh (per cubic foot) approximately 90 to 105 lb. when dry and up to 120 lb. (or even more when moist). The specific mass gravity\* of the soil, to be designated by  $s_m$ , may be determined by dividing the

\* Termed also "apparent specific gravity."

unit weight  $\gamma$  in pounds per cubic foot by  $\gamma_0 = 62.4$  lb. per cu. ft., which is the approximate unit weight of water. Hence the specific mass gravity of a soil weighing 100 lb. per cu. ft. would be  $s_m = 100/62.4 =$  about 1.6.

In metric measures the specific mass gravity of soil particles  $s_m$  is the unit weight of 1 cc. of this soil in grams. Strictly speaking, this is true at the temperature  $+4^\circ\text{C}$ . only. To obtain the weight of 1 cu. m. in kilograms it is necessary to multiply the specific gravity  $s_m$  by 1,000. Sometimes the terms "absolute density" and "bulk density" are used instead of the terms "specific gravity" and "specific mass gravity," respectively. The terms "specific gravity" and "density" are to be considered synonymous.

To determine the specific gravity  $s$  of the soil particles, *picnometers* are used. Picnometers used by physicists have a volume of 50 to 100 ml. (milliliters) at a certain temperature (usually  $+20^\circ\text{C}$ .) and this volume is marked with a line on the neck of the picnometer. Soil investigators use larger flasks, about 500 cc., and soil samples of 25 to 50 g. Designation for the latter weight will be  $W_0$ . The flask is partly filled with distilled water, and the soil sample is introduced. To evacuate the air adhering to the soil particles, the liquid in the flask is boiled for at least 1 hr., or a vacuum is applied. Upon cooling (in the case of boiling) and filling the picnometer with water up to the mark on the neck, the weight "picnometer + sample + water"  $W_s$  is determined. The weight of the picnometer  $W_w$  filled with the distilled water up to the mark on the neck, corresponding to the temperature of the experiment, is taken from a chart that is to be prepared for each flask; otherwise the picnometer with water is to be weighed at every test. The specific gravity  $s$  of the soil is

$$s = \frac{W_0}{W_0 + W_w - W_s} \quad (1:3)$$

The denominator of the fraction, formula (1:3), is the weight of the water displaced, the specific gravity (density) of water being assumed equal to 1. The weight of the sample  $W_0$  to be used in formula (1:3) is generally determined *after the experiment* by drying out the contents of the picnometer in an evaporating dish (without boiling) and weighing the residue.

The specific mass gravity  $s_m$  of a large sample may be deter-

mined by dividing its weight by its volume (in metric measures). The volume of a small soil sample may be determined by weighing mercury displaced by the sample and dividing the result by 13.6, which is the specific gravity of mercury.

### Problems

1. A perfectly dry sand sample completely fills a metallic cylinder. Determine the voids ratio  $e$  of that sand in terms of volume of the cylinder,  $V$ ; specific gravity of grains,  $s$ ; unit weight of water,  $\gamma_0$ ; dry weight (weight in a completely dry state) of the sand enclosed in the cylinder,  $W_s$ . Prepare also a list of tests to be made in the laboratory for this purpose.

$$\text{Ans. } e = \frac{Vs\gamma_0}{W_s} - 1$$

2. A lump of loam, say about 1 cu. ft., containing pebbles and small rocks was extracted close to the earth's surface, immediately covered with hot paraffin, and brought to the laboratory to determine the voids ratio of that soil in natural state. The laboratory operator determined the volume of the paraffin-coated sample by immersing it in water and measuring the volume of displaced water ( $V_1$ ). Afterward, the paraffin coat was carefully peeled off and placed in a large beaker, and the beaker was placed over a flame. As soon as the paraffin melted, it rose to the top, whereas the soil particles adhering to it fell to the bottom. After the completion of this separation, the flame was removed, and the paraffin hardened into a cake. Let its weight be  $W_p$  and its specific gravity  $s_p$ . (The value of  $s_p$  is about 0.9.)

Develop a formula for determining the voids ratio  $e$  in terms of volume of the whole paraffin-coated sample  $V_1$ ; volume of the paraffin coat alone,  $V_p$ ; specific gravity of grains,  $s$ ; dry weight (*i.e.*, weight after drying out) of the soil contained in that lump,  $W_s$ ; unit weight of water,  $\gamma_0$ . Explain also how the specific gravity  $s_p$  of paraffin can be determined.

$$\text{Ans. } e = \frac{(V_1 - V_p)s\gamma_0}{W_s} - 1$$

3. The specific mass gravity (apparent specific gravity)  $s_m$  of a soil equals 1.62. The specific gravity of the grains is 2.68. Determine the voids ratio  $e$  under the assumption that the soil is perfectly dry. Ans. 0.65

4. The porosity  $n$  of a coarse sand is 33 per cent. Determine its voids ratio  $e$ . Ans.  $\frac{1}{4}$ .

5. Determine the maximum value of the voids ratio  $e$  for a sand composed of grains assumed to be perfectly round. (Consult Sec. 1:10.)

### References

1. H. RIES and THOMAS L. WATSON: "Engineering Geology," 5th ed., John Wiley & Sons, Inc., New York, 1936.
2. C. LONGWELL, R. FLINT, and A. KNOPF: "Physical Geology," Part 1, John Wiley & Sons, Inc., New York, 1932.
3. ROBERT F. LEGGETT: "Geology and Engineering," McGraw-Hill Book Company, Inc., New York, 1939.

4. A. SCHEIDIG: "Der Loess und seine geotechnische Eigenschaften," T. Steinkopf, Leipzig, 1934.
5. G. W. ROBINSON: "Soils: Their Origin, Constitution and Classification," T. Murby & Company, London; D. Van Nostrand Company, Inc., New York, 1932.
6. T. L. LYON and H. O. BUCKMAN: "Nature and Property of Soils," The Macmillan Company, New York, 1929.
7. Recent Marine Sediments, *Am. Assoc. Petroleum Geol.*, Tulsa, Okla., 1939.
8. Publications of the Bureau of Chemistry and Soils, U. S. Department of Agriculture, Washington, D. C.

## CHAPTER II

### SOIL MOISTURE: SOIL PLASTICITY AND CONSISTENCY

**2:1. Ground Water.**—Below a certain level, soil layers are saturated with water. Such saturation is shown in Fig. 1:1b. This level is the *water table*, and the subsurface water which lies below the table is *ground water*. Sometimes the water table reaches the earth surface or is close to it, as in swamps or in some meadows. The ground water moves both sidewise and vertically. The sidewise movement is practically in the same direction as the surface runoff; obviously it is slower because of the friction against soil particles. The vertical movement of the ground water consists in the fluctuation of the water table. For instance, the water table rises in times of rain and subsides in times of drought. Also, barometric pressure and the ground-water level are interrelated (Sec. 2:2). Daily fluctuations, apparently due to temperature changes, have been reported. On some occasions, these fluctuations have been also explained by the influence of plants. The water table is not level, and it may or may not follow the irregularities of the surface beneath which it lies.<sup>1</sup> The “infiltration theory” of the origin of the ground water, accepted by the American geologists, postulates that the ground water is derived chiefly from the downward seepage of surface water (from rain, snow, streams, and lakes).

**2:2. Soil Moisture; Soil Air.**—The interstices between soil particles above the water table contain some water that in engineering terms is known as “moisture.” In pores there is also air, which is thought to be saturated fully or partially with water vapor; under some circumstances the latter may condensate. The composition of the soil air may be somewhat different from that of the outside air. The soil air may or may not be in communication with the outside atmosphere. In the latter case small or even microscopic air bubbles are incorporated in soil moisture. This is the so-called *entrapped air*. Soil-mechanics investigators assume, as a rule, that there is no entrapped air in the deeper clay deposits.

Observations on ground-water fluctuations suggest the presence of some entrapped air in the soil below the water table, however. The water table rises when the outside barometric pressure drops, and vice versa (compare Sec. 2:1). This phenomenon has been observed in wells and apparently could be explained by changes in the volume of the entrapped air bubbles.

**2:3. Phases of Matter in the Soil.**—Soil particles constitute the solid phase of a soil mass; water (moisture) represents its liquid phase; and entrapped air and water vapor if any, is its gaseous phase. A moist soil above the water table containing some entrapped air is a *three-phase soil system*. A soil mass under the water table containing no entrapped air is a *two-phase soil system*. Finally, an absolutely dry sand is a *one-phase system*, since the pore air in this case does not constitute an integral part of the mass and practically does not handicap the movement of grains, at least in the upper layers.

**2:4. Moisture Content.**—As a rule, moisture within an earth mass is neither uniformly distributed nor in static equilibrium. This is especially true the closer a given point of an earth mass is to the surface, because of the influence of atmospheric agents such as changes in temperature and air pressure. Apparently, at greater depths soil moisture is more uniformly distributed through the earth mass and is more stable than when close to the surface of a mass.

In taking samples for determining the moisture content of an earth mass, one should be very careful to extract such portions as are true representatives of the whole mass. As a rule, more reliable results are obtained from *large samples*. A large sample is weighed and dried out either in the open air or in a large oven until its weight becomes constant. The moisture content is expressed in per cent of the dry weight (accurate to 0.1 per cent) and is obtained by dividing the difference between the wet and the dry weight by the latter and multiplying the ratio by 100. Sometimes the moisture content is expressed as a fraction  $w$  of the dry weight. For instance, if a moist soil sample weighs  $10\frac{1}{2}$  lb., and the weight of moisture is  $\frac{1}{2}$  lb., the moisture content is 5 per cent by dry weight, or  $w = 0.05$ .

Small samples are put in containers (in small weighing glass bottles with ground-glass covers or between two watch glasses

fastened with clips), weighed, and placed uncovered in an oven at about 110°C. Higher temperature may cause chemical changes of soil ingredients, such as oxidation, and thus influence the weight of the sample. The sample is dried to a constant weight; generally 4 hr. are sufficient for complete drying of a heavy-textured soil; light-textured soils dry out more quickly. A dried sample is placed in a desiccator and weighed when cooled, after which the moisture content may be computed. The weighing bottles or watch glasses referred to must be numbered, and their weight recorded. Analytical balances or in any case balances accurate to 0.01 g. are to be used. Soil samples, both large and small, come to a laboratory in containers generally sealed with melted paraffin to prevent evaporation. When the paraffin is removed, the wet sample must be weighed with the container as soon as possible.

**2:5. Specific Gravity, Voids Ratio, and Moisture Content Interrelated.**

—The value of the specific gravity  $s$  of soil particles, that of the apparent specific gravity  $s_m$ , that of the moisture content expressed as a fraction of dry weight  $w$ , and that of the voids ratio  $e$  are interrelated. The parallelepiped in Fig. 2:1 represents a soil mass containing exactly 1 cc. of solid matter. The volume of voids is then  $e$  cc., and the volume of the whole mass  $(1 + e)$  cc. The full weight of this mass is

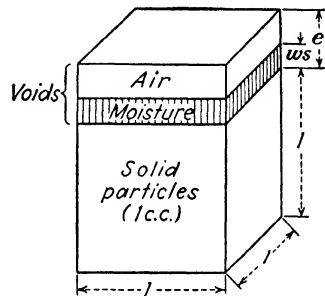


FIG. 2:1.—Meaning of the term "voids ratio."

	Grams
Weight of the soil (1 cc.) . . . . .	$s$
Weight of moisture . . . . .	$ws$
Air . . . . .	Neglected
Total . . . . .	$s(1 + w)$

To obtain the apparent specific gravity  $s_m$  of the mass, the weight of the parallelepiped in Fig. 2:1 is to be divided by its volume:

$$s_m = s \frac{1 + w}{1 + e}, \quad \text{or} \quad \frac{s_m}{s} = \frac{1 + w}{1 + e} \quad (2:1)$$

Formula (2:1) is evidently of a general character and may be applied to any earth mass. It follows from Fig. 2:1 that in the case of a saturated mass (two-phase soil system, Sec. 2:3) which

contains soil particles and moisture but no air, both values,  $e$  and  $ws$ , are equal:

$$e = ws \quad (2:2)$$

Formula (2:2) means that to determine the value of the voids ratio of a fully saturated mass, its moisture content  $w$  is to be multiplied by the specific gravity  $s$  of the particles. Formulas (2:1) and (2:2) hold in the case of both metric and English measures.

**2:6 Example.**—The moisture content of a fully saturated soil mass is 40 per cent, or  $w = 0.4$ ; and the specific gravity  $s$  of the particles is 2.65. The value of the voids ratio  $e$ , according to formula (2:2), is

$$e = ws = 0.4 \times 2.65 = 1.06$$

The apparent specific gravity  $s_m$  of the mass, using formula (2:1) is found thus:

$$s_m = s \frac{1 + w}{1 + e} = 2.65 \times \frac{1.40}{2.06} = 1.8$$

The unit weight of this mass is  $62.4 \times 1.8 =$  about 112 lb. per cu. ft.

**2:7. Varieties of Soil Moisture.**—It is, as a rule, extremely difficult to establish accurate boundaries between different kinds of soil moisture. *Hygroscopic* moisture is attracted from the air by soil particles, as common salt attracts it; *capillary moisture* is that attracted by particles from the level of a liquid. In a general way, moisture attracted by a soil particle and accumulated either at its surface or even in its interior (compare Sec. 1:8) is termed “adsorbed moisture,” though in the latter case the term “absorbed” would be more correct. Ground water is termed “free” or “gravitational” because the action of gravity is prevailing in this case, whereas in other kinds of moisture the action of gravity is negligible in comparison with that of molecular forces and surface tension.

**2:8. Hygroscopic Moisture.**—The greater the internal surface of a soil (see end of Sec. 1:10) the greater the quantity of moisture that may be attracted from the air by that soil, other conditions being equal. The maximum percentage of moisture that may be taken up by a dry soil in contact with an atmosphere saturated with water vapor is its *hygroscopic coefficient* (or hygroscopic capacity) at that temperature. The average value of the hygroscopic coefficient at 16.5°C. varies from 2 or 3 per cent (or even less) by dry weight in the case of light sandy soils to 13 or more

per cent in the case of heavy clays. The actual hygroscopic moisture content is determined by drying out a sample in the oven, as described in Sec. 2:4.

**2:9. Capillary Moisture.**—Engineers are perfectly familiar with the term “capillary movement” of water. In a general case the term “capillary rise,” often used, is inaccurate, because capillary moisture may move in any direction, not only upward. During and after rains, when the surface soil is more moist than the lower layers, the capillary force added to that of gravity drives the water into the ground. When the surface soil has been dried by the action of the sun and the wind, the moisture movement is upward.

In coarse-grained sands, capillary moisture moves only a few inches, but very quickly. It reaches ultimately a greater height in fine-grained soils, but in the latter case the full capillary movement may sometimes last months and even years. Both the speed and the length (height) of the capillary movement are more considerable in wet soils than in dry ones. Warm capillary water moves more quickly than cold, probably because of its lower viscosity. Solutions move slower than pure water; generally the denser the liquid the slower its capillary movement in the given soil. In a general case the moisture content in a soil column moistened by capillarity is largest close to the water table from which moisture is being lifted. Except some special cases, it decreases with the distance from the water table, and this fact is of an extreme importance in engineering applications (compare Sec. 2:14 and Fig. 12:7).

**2:10. Two Hypotheses of Capillary Action in Soils.**—From the theoretical point of view, there is an *older* and a *modern* conception of capillary action. The older and still prevailing conception may be termed the “capillary-tube hypothesis”. The soil is pictured as behaving like a bundle of parallel capillary tubes of different diameters, and the capillary movement is assumed to be caused by the surface tension.

In the other hypothesis (“capillary potential hypothesis”) the capillary action is assumed to be due to attraction of water by the soil, the measure of this attraction being the so-called “capillary potential.”<sup>2,3,4</sup> The simple term “attraction” is used here to cover more complicated concepts of soil-moisture interaction as used in soil physics.

It is assumed in this book that both attraction of water by soil due to *affinity* and the surface tension act simultaneously, since there is no reason to believe that the action of one of these causes of capillary action excludes the other.

**2:11. Capillary-tube Hypothesis.**—If a thin glass tube is introduced into still water, the water in the tube will rise up to a cer-

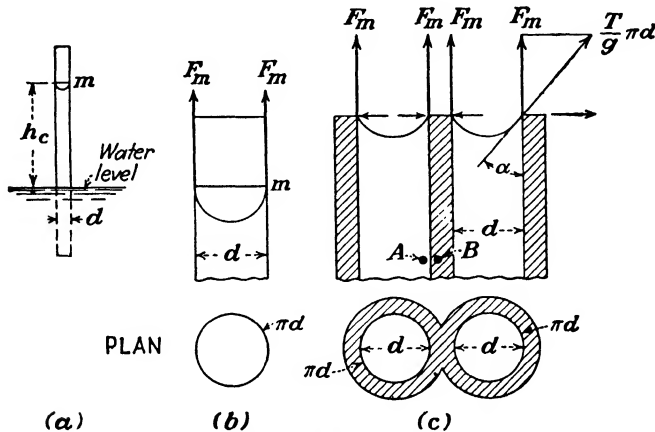


FIG. 2:2.—Meniscus in a capillary tube.

tain level and its surface will form a meniscus  $m$  (Fig. 2:2a). The latter is semispherical if both water and glass are clean (Fig. 2:2b); otherwise its shape approaches a smaller segment (Fig. 2:2c). This phenomenon due to the action of capillary forces is explained in treatises on physics.

Suppose that dry soil powder is placed in thin layers in a container with a bottom provided with numerous very small holes so that soil particles cannot fall out and that this bottom is brought into contact with a water level. The soil would then be gradually moistened from below. The level of the rising moisture is practically horizontal at all times, as if the moisture were moving in parallel thin tubes of equal diameter. This diameter is characteristic of a given soil and may be called the *statistical diameter* of its pores, the latter being imagined to be in the form of vertical tubes. The designation  $d$  is used hereafter for the statistical diameter.

According to the capillary-tube hypothesis, the capillary movement is explained by the *lifting force of the meniscus*, or curved surface, at the top of the column of capillary moisture (Fig. 2:2). A

hypothetical straight line traced at the surface of a liquid is assumed to be extended by the force of surface tension. The latter is measured by units of force (for instance, grams) per unit of length (for instance, centimeter). The value of surface tension for pure water at the room temperature (about 67°F.) is  $T/g$  grams per cm., the value of  $T$  being equal to 72.8 and  $g$  to 981.\* It is assumed that the circumference of the meniscus, as of any other line at the surface of the liquid, is extended by the surface tension. If the meniscus is fully developed as shown in Fig. 2:2*b*, the surface tension at its perimeter acts vertically and upward. When the meniscus is not fully developed (Fig. 2:2*c*), the surface tension at its perimeter acts along the tangents to the surface of the meniscus. The angle  $\alpha$  formed by these tangents with the walls of the tube is the "angle of contact" or "angle of capillarity." Its value may change from 90° (horizontal meniscus) to 0° (semi-spherical meniscus). As already explained, the value of the angle of contact may depend on the state of the liquid and of the walls.

It is seen from Fig. 2:2*c* that the force of surface tension  $(T/g)\pi d$  acting at the circumference of the meniscus may be broken into a vertical force  $F_m = (T/g)\pi d \cos \alpha$  and a horizontal force. The force  $F_m$  is the lifting force of the meniscus, which is supposed to lift a column of water from the surface of the liquid to the level of the meniscus (Fig. 2:2*a*). If the angle of contact  $\alpha$  gradually decreases, the lifting force of the meniscus increases to reach a maximum when the meniscus is fully developed, as in Fig. 2:2*a* and *b*.

The height  $h_c$  of a water column that can be lifted by the meniscus in a capillary tube ("effective length" of capillary movement) can be determined from conditions of equilibrium. Designate with  $a$  the cross section of the tube. Then

$$F_m = h_c a \gamma_0 \quad (2:3)$$

where  $\gamma_0$  is the unit weight of water. Since  $F_m$  is proportional to the diameter of the tube  $d$ , and the area  $a$  is proportional to  $d^2$ ,

$$h_c = \frac{\text{const.}}{d} \quad (2:4)$$

If  $d$  in formula (2:4) is expressed in centimeters, the value of the

\* The value of the surface tension per centimeter is  $T = 72.8$  dynes, and 1 gram equals  $g = 981$  dynes. It should also be remembered (a) that 1,000 grams (or 1 kilogram) equals 2.2046 avoirdupois pounds and (b) that 1 cu. m. of water weighs 1 metric ton.

constant may be taken equal to 0.3. Thus  $h_c$  as expressed in centimeters

$$h_c = \frac{0.3}{d} \quad (2:5)$$

Formula (2:5) has been obtained by placing an average value of the surface tension, as already given for pure water, in the expression of the lifting force  $F_m$  of the meniscus. This formula is quite correct if the tube is completely filled with water as in Fig. 2:2a. This is not the case of soils, however, as explained at the end of Sec. 2:9. Hence formula (2:5) and similar formulas based on the assumption of full capillary saturation are crude approximations only.

**2:12. Capillary Pressure.**—Assuming again that capillary moisture completely fills the bundle of tubes representing the given soil, the average tensile stress acting on the water within a capillary tube may be determined from Eq. (2:6):

$$F_m = a\sigma \quad (2:6)$$

It follows, from comparison of Eqs. (2:3) and (2:6), that

$$\sigma = h_c\gamma_0 \quad (2:7)$$

Consider two points  $A$  and  $B$  (Fig. 2:2c), located on either side of the boundary of the tube wall, and trace a horizontal plane, 1 sq. ft. in area, through those points (not shown in Fig. 2:2c). Since the horizontal plane in question is in equilibrium, the tensile stress in water (point  $A$ ) should be balanced by a compression stress of equal magnitude in soil (point  $B$ ). This means that if an earth mass saturated by capillarity is exposed, it is compressed by a hydrostatic pressure ( $h_c\gamma_0$  lb. per sq. in.). Since in reality a certain part of the pores only is filled by the capillary moisture, both the possible tensile stress in water and the compression stress in soil differ from the value furnished by Eq. (2:7), the latter being an approximation. As an example, consider a semi-infinite mass in the state of capillary saturation, and assume that the effective length (height) of capillary movement equals  $h_c = 12$  ft. According to formula (2:7) the mechanical effect of this saturation is tantamount to a unit load uniformly distributed at the exposed horizontal surface of the given mass, the value of this load being  $12 \times 62.4 =$  about 750 lb. per sq. ft.

**2:13. Length of Capillary Movement.**—The best way to determine the length of capillary movement is to make *field observations* at the given place. There are cases when capillary moisture rises as high as 50 or 60 ft. or more. This fact is sometimes questioned, since a suction pump can lift water to a height equal to atmospheric pressure only (about 34 ft.). The explanation lies in the difference in action between the plunger of a suction pump and a meniscus combined with attraction force. In the former case, water is *pushed up* by the atmospheric pressure, whereas in the latter case it is *pulled up* by a considerable force practically independent of the atmospheric pressure.

*In laboratories* capillary rise is sometimes observed by means of vertical glass or lucite tubes filled with the given soil generally in the form of dry powder. The bottom of the tube is covered by a metallic cover with numerous small holes (or with cheesecloth) and put in contact with distilled water. The diameter of experimental tubes varies from  $\frac{3}{4}$  to 6 in. If the variable length (height)  $h$  of the capillary movement in such a tube is plotted against the time of movement  $t$ , a curve approaching a parabola would be obtained. The equation of this curve is

$$\frac{h^N}{t} = m \text{ (const.)} \quad (2:8)$$

where the value of  $N$  is usually above 2 and the constant  $m$  is different for different soils (Fig. 2:3).

When the capillary movement takes place horizontally, the value of  $N$  equals exactly 2, and the curve shown in Fig. 2:3 is a true parabola. In the case of fine-grained soils, the capillary-tube tests are very slow and require long tubes. Capillary motion in tubes (and presumably in nature) depends on the temperature and humidity of the surrounding air. To obtain consistent results these factors should be kept as constant as possible in a laboratory.

*Capillarimeters.*—The general purpose of a laboratory capillarimeter is to measure the maximum length of a water column that can be safely supported by the menisci and attractive forces.<sup>5</sup>

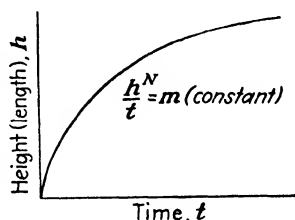


FIG. 2:3.—Relation between time and height (length) of capillary movement.

This can be done in a rather brief time, and no long glass or lucite tubing is required.

Figure 2:4a shows Beskow's capillarimeter. A moist soil sample is placed in a glass container *a*, where it rests on a layer of coarse sand or on a screen covered with filter paper. The container *a* is ground into the neck of the funnel *b*, which is connected by a rubber hose with another funnel *c*. Both funnels and the hose are filled with water to touch the bottom of the sample; then funnel *c* is lowered until the contact between the water and the sample is

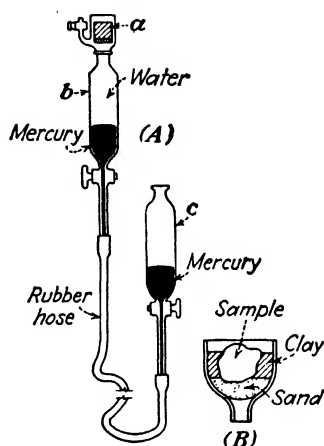


FIG. 2:4.—Beskow's capillarimeter.

broken and air bubbles start to work through the sample. This means that at this moment the lifting force of the sample cannot hold the water column suspended to it from below. Hence the difference between water levels furnishes the length of that column. Mercury may be applied to decrease the difference between levels referred to and hence the size of the apparatus. To test an undisturbed sample (Fig. 2:4b), the latter is packed around with heavy textured clay or similar material. Admittedly, the capillarity of this material must be greater than that of the given sample.

The length of "passive capillarity" as determined by a capillarimeter is smaller than the length of "active capillarity" as determined by a tube test.<sup>13,14</sup> Possible causes of this phenomenon are (a) a capillarimeter measures the length of a soil column in which *all pores* are filled with water [compare formula (2:5)]; and this length is smaller than the actual length of capillary movement; (b) in a capillarimeter test the water column breaks off as soon as the menisci in the widest pores (which are the weakest) are destroyed.

*Tensiometers.*—A particular kind of capillarimeter for field measurements is a tensiometer.<sup>4</sup> A porous ceramic cup filled with water and attached to a manometer is buried in the given earth mass. If the moisture content of that mass is below saturation, water moves out through the walls of the porous cup. The mercury in the manometer follows the moving water. The height of the

moved mercury column multiplied by the specific gravity of mercury (13.6) furnishes an approximate value of the effective length of the capillary movement  $h_c$  [compare formula (2:5)].

**2:14. Distribution of Capillary Moisture.**—If the temperature during a tube test (Sec. 2:13) is kept constant, the moisture content decreases with the height (compare Sec. 2:9). At the horizontal plane of contact of the soil mass with water practically all pores are filled with water, and it may be assumed approximately that at the half effective height  $h_c$  of the capillary movement, between one-third and one-half of all pores available are filled with capillary moisture.

**2:15. Natural Moisture Content and State of Capillary Moisture in the Pores.**—In a general way, in a homogeneous earth mass under constant temperature and humidity and without alimentation, moisture tends to flow from regions of high moisture content to regions of lower moisture content. However, if two different soils are in contact, moisture may flow either way. Study of varved clays (Sec. 1:10) at the bottom of the Connecticut River, Hartford, Conn., has revealed that in intermittent silt and clay layers in equilibrium the moisture contents were 35.5 and 57.0 per cent, respectively, a difference of about 20 per cent.

Moisture contents in sands and gravels are low owing to coarseness of the particles. The average moisture content in such soils above the water table is perhaps 6 or 8 per cent, though it is considerably higher under the water table.

In a boring made in Douglas, Ariz., in a deep valley filled with debris, the average moisture content in the upper layer of adobe 14 ft. thick was 16 per cent, and in a layer of white clay located at a depth of more than 50 ft. it was 34 per cent.

According to Peck,<sup>16</sup> the moisture content in Chicago blue clay at a depth of 10 ft. and more is in many cases close to 20 per cent, though occasionally it reaches 30 or 40 per cent and more.

Due to changes of temperature and other causes there may be occasional condensation of water vapor close to the earth surface. Rainfall or hot dry weather may cause either downward or upward movement of moisture. In a particular case of a shallow water table, insolation and evaporation during the daytime and decrease in the temperature at night may create a continuous upward moisture stream and heavy moisture content in the upper 2 or 3 ft. On muck and peat swamps moisture contents such as 300 per

cent or more (by dry weight, of course; compare Sec. 2:4) are often found.

As to the state of pore moisture in narrow pores it should be realized that it differs from the usual liquid state. Owing to attraction of soil particles, a part of capillary moisture is thought to be solidified (jellylike or even harder). On the other hand, a part of capillary moisture moves in the form of vapor.

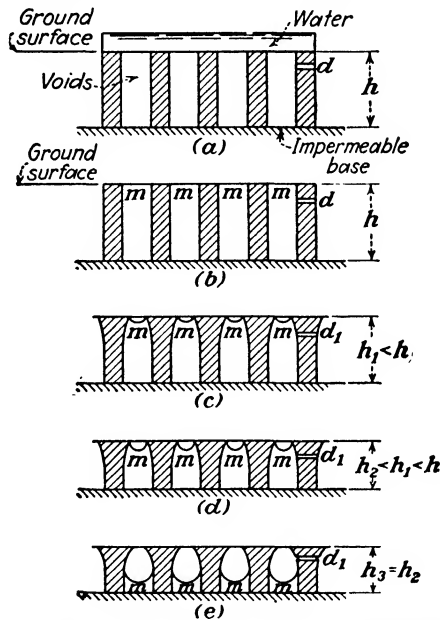


FIG. 2:5.—Gradual evaporation and shrinkage.

**2:16. Shrinkage and Swelling of Clay.**—As already stated, when an earth mass is drying out, there is an upward movement of moisture. Consecutive stages of such a process are shown in Fig. 2:5. The earth mass is schematically represented as walls of tubes (voids) filled with water. In addition, these walls (dashed in Fig. 2:5) are pierced by voids of smaller diameters and hence are able to shrink if compressed. Of these smaller voids *one* only (labeled  $d$ ) is shown in Fig. 2:5a. First, the earth mass is assumed to be covered with water (Fig. 2:5a). At that time surface tension acts at the water surface and does not have any influence on the earth mass. Owing to the action of atmospheric agents, evaporation starts; and at the end of a certain time interval, the water

level becomes flush with the earth surface (Fig. 2:5b). The menisci  $m$  are, then, horizontal and do not yet possess lifting power. Small pores piercing the earth mass, such as  $d_1$ , are still filled with water. Subsequent drying out of the earth mass may be subdivided into two periods, hereafter called the "first period" and "second period."

*a. First Period.*—Under the action of sucking atmospheric agents, menisci acquire concave form to reduce the exposed surface to a minimum. Owing to curvature of the menisci, oblique surface tension  $(T/g)\pi d \cos \alpha$  (Fig. 2:2c) develops. The upward vertical component of this force is balanced by the downward vertical support reaction. This support reaction compresses the walls (dashed in Fig. 2:5) and squeezes out moisture from thin pores  $d$ . Obviously the latter become thinner, and the walls shrink. At the same time, the horizontal component of the surface tension is balanced by the horizontal support reaction which tends to pull the walls together, but larger pores, shown vertical in Fig. 2.5, do not shrink yet. The amount of water evaporated at the meniscus exactly equals the amount of moisture thus removed from the pores. This first period of drying out is characterized by the completion of the vertical shrinkage of the mass, the latter remaining fully saturated. This state of things is shown in Fig. 2.5d.

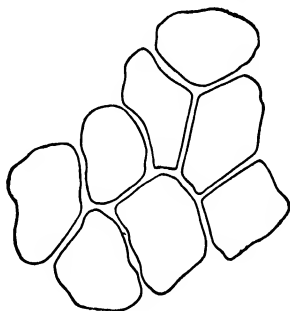


FIG. 2:6.—Cracking of the surface of a clayey mass at drying.

*b. Second Period.*—Only at the end of the first period of the drying-out process is the meniscus fully developed and exerting its full lifting power (Fig. 2:5d). The corresponding compressive stress is not sufficient to cause further vertical deformation of the walls, and vertical shrinkage stops. The meniscus is now being shifted down, and entrances to thin pores  $d_1$  become exposed. Compression stress, exerted by these thin pores, is much greater than that exerted by wider pores. The vertical shrinkage not being possible any longer, the mass shrinks horizontally and cracks (Fig. 2:6). The depth of the cracks may be insignificant, but in some cases it reaches several inches and even several feet, according to the tensile strength of the material.

*c. Flooding of a Drying-out Surface.*—Should an excess of water come from above, it would not be handicapped in filling the pores of an earth mass that is in the process of drying out. In this case the surface tension will be shifted to the free water surface; thus clay particles will be freed from surface tension and hence from compression. Particles will then expand; clay *swells* if placed under water; and if not confined, the mass disintegrates. The *slaking test* used by highway engineers is based on the principle described and consists in immersing a sample in water and in observing its gradual disintegration. It is to be noticed that the so-called *bulking of sand* has nothing in common with the swelling of clay, though it represents an increase in volume due to addition of water. In sands a moisture content of 6 to 8 per cent may cause “bulking” amounting as high as 25 per cent or more by volume. If more water is added to the sand, the bulked volume may be again decreased.

**2:17. Limits of Consistency.**—The first period of the drying-out process (Sec. 2:16) may be subdivided into the following stages: At the beginning the mass represents a more or less uniform dense fluid. It is then said to be in the *liquid state*. Upon further drying, the mass becomes stiffer and at a certain moisture content, termed *liquid limit* (LL), loses its capacity to flow as a liquid but can be readily molded and holds its shape. The mass in question is now in the *plastic state*. Upon further loss of moisture the plastic properties are lost, and at a certain moisture content, termed *plastic limit* (PL), the soil crumbles when worked. This is the *semisolid state*. The second period of the drying-out process corresponds already to the gradual passage to the *solid state*. The limit between the semisolid and solid state is the *shrinkage limit* (SL).

The following table gives an outline of possible states of a clay mass and corresponding limits of consistency:

State of the Clay Mass	Limits between the States
1. Liquid	
	Liquid limit (LL)
2. Plastic	
	Plastic limit (PL)
3. Semisolid	
	Shrinkage limit (SL)
4. Solid	

To determine the moisture contents corresponding to the limits of consistency, soil engineering laboratories use methods designed about 1911 by A. Atterberg, a Swedish scientist.<sup>6,7</sup> To find the *liquid limit* (LL), a soil cake is placed in a dish and divided, with a special grooving tool, into two halves as shown in Fig. 2:7 (top). Ten light blows are then applied to the latter. The experiment is repeated several times, the moisture content being gradually increased until the soil begins to flow as in Fig. 2:7 (bottom).

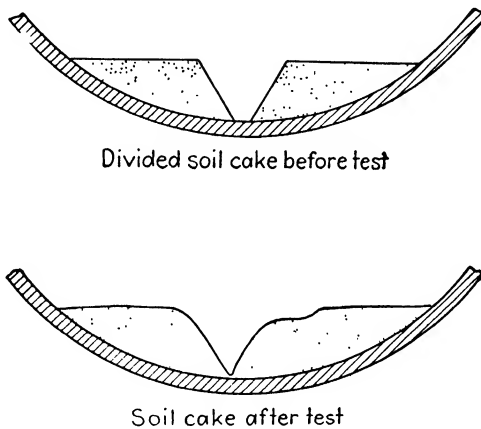


FIG. 2:7.—Diagram illustrating liquid-limit test.

An apparatus designed to eliminate the personal equation in this test is Casagrande's liquid-limit device (Fig. 2:8). It consists of a brass dish and cam mounted on a hard rubber base. The cake is placed and divided as in the hand method, and the shocks are produced by causing the dish to fall through a distance of 1 cm. by turning the crank at an approximate rate of two rotations per second. The experiment is repeated, the moisture content of the sample being varied. Moisture contents (arithmetic scale) are plotted against numbers of blows required to close the groove (logarithmic scale). *Flow lines*, thus obtained, are straight lines for most soils. The ordinate of a flow line corresponding to 25 blows shows the value of the liquid limit. For instance, the liquid limit is about 41.0 per cent in the case of the soil shown in Fig. 2:8 (bottom).

The *plastic limit* (PL) is the lowest moisture content at which

the soil can be rolled into threads  $\frac{1}{8}$  in. in diameter without the threads crumbling or breaking into pieces (Fig. 2:9).

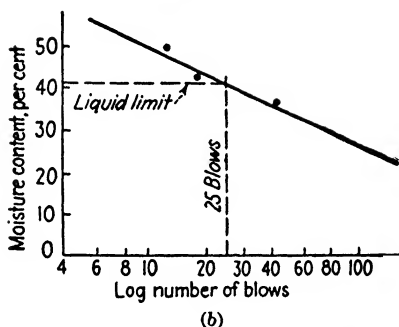
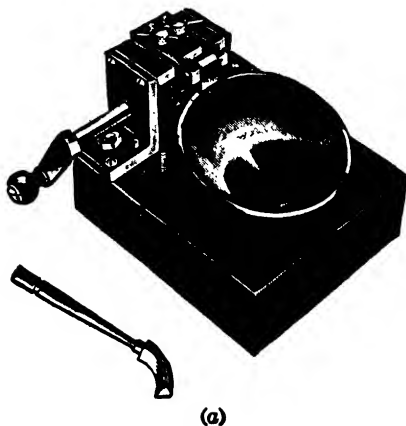


FIG. 2:8.—(a) Casagrande's liquid-limit device—grooving tool at the left; and (b) example of flow curve.

The percentage corresponding to capillary saturation lies in the interval between the plastic limit and the liquid limit. The difference  $LL - PL$  is the *plasticity index* or *plastic number* (PI) of the given soil. It is customary to express the value of the plasticity index as an abstract number, *i. e.*, without adding the words "per cent." The greater the plasticity index the more plastic is the corresponding soil. Regularly plastic clays possess a plasticity index of 15 or more. The plasticity index of coarse and medium sands is close to zero. Organic admixtures increase the plastic limit, sometimes considerably.

It is to be noted that for determining the consistency limits, only finer particles of a given soil are often used, namely, those passing through No. 40 sieve. In such a case, the percentage of such particles in a natural soil sample must be reported together with the results of the consistency tests.

The *shrinkage limit* (SL) of a saturated sample that is being dried out is defined as the moisture content taken when this sample stops losing volume while continuing to lose weight owing to evaporation. Such a sample does not crack, since it can shrink freely in any direction. At the shrinkage limit air invades the pores, and because of this the soil mass changes its color from dark to light. The

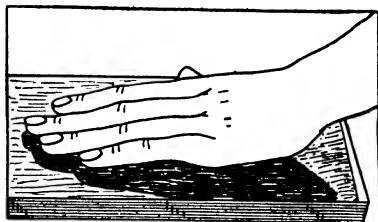


FIG. 2:9.—Plastic-limit test.

shrinkage limit can be determined if the specific gravity  $s$  of particles is known, and if after drying out the given sample, its specific mass gravity  $s_m$  has been determined (see end of Sec. 1:11). The voids ratio  $e$  is the same at the shrinkage limit when the mass is still saturated (compare Sec. 2:5) and when the mass becomes perfectly dry. Hence the value of  $e$  may be found (a) from Eq. (2:2) by placing  $w = \text{SL}$  and (b) from Eq. (2:1) by placing  $w = 0$ . Equalizing both values thus found,

$$e = [\text{SL}] s = \frac{s}{s_m} - 1 \quad (2:9)$$

from which

$$\text{SL} = \frac{s - s_m}{s \cdot s_m} = \frac{1}{s_m} - \frac{1}{s} \quad (2:10)$$

The shrinkage limit as expressed in per cent by dry weight of the sample is

$$\text{SL} = \left( \frac{1}{s_m} - \frac{1}{s} \right) \times 100 \quad (2:11)$$

The fact that in formulas (2:10) and (2:11) the symbol  $s_m$  refers to the sample in a completely dry state cannot be overemphasized. The term "shrinkage ratio," sometimes used, is the ratio of the weight of a dry-soil sample to its volume, or, in other words, the specific mass gravity of the dry sample designated by  $s_m$  in formulas

(2:10) and (2:11). It is advisable to determine the shrinkage limit from both undisturbed and disturbed clay samples because the corresponding results *may be very different*.

The so-called "sticky point" which characterizes the capacity of the given soil to adhere to metallic surfaces lies between the liquid limit and the plastic limit. It is high in soils rich in humus, even in sandy ones. In nature, the sticky point may be observed on earth roads several hours after a heavy rain, when the moisture content has somewhat decreased but the resistance to movement of vehicles has increased.

**2:18. Factors Controlling Plasticity of the Soil.**—Plasticity may be defined as the capacity of a body to flow without change in volume under the action of steady forces if the latter exceed a certain limit and to keep a deformed shape after the total removal of the acting forces. Soil plasticity *differs from the plasticity of metals* in that it is caused by the presence of a certain amount of water or, generally speaking, of a liquid with bipolar molecules. When the soil is mixed with a liquid possessing molecules not distinctly bipolar (for instance, carbon tetrachloride,  $\text{CCl}_4$ ), no plasticity phenomena are observed. Furthermore, another condition for soil plasticity is the presence of scalelike particles (Secs. 1:6 and 1:8). Since clays contain a considerable percentage of scalelike particles (see end of Sec. 1:6), they are plastic, whereas coarse sands with round grains are not plastic. Apparently, there is a strong electric field at the surface of scalelike particles which makes the bipolar water molecules place themselves so that their axes are normal to the surface of these flaky particles. A rough model of this situation would be a great number of automobiles parking not parallel but perpendicular to a sidewalk. It follows that apparently the real cause of plasticity in soils is not the particles themselves but strongly attracted, solidified moisture which probably is plastic in the same way that metals are plastic (compare also end, Sec. 2:15).

**2:19. Water-holding Capacity; Moisture Equivalent.**—The capacity of a soil to hold water under the action of a force that tends to remove it is termed *water-holding capacity*. The latter is due to both the surface tension and attraction of moisture by the soil particles. The *centrifuge moisture equivalent* is the moisture content of a soil that, initially saturated, has been centrifuged for a given time (generally an hour) with a given centrifugal accelera-

tion, generally 1,000 gravity. Most of the water held in coarser interstices of a soil is removed, whereas all the moisture in finer interstices may remain.<sup>6</sup>

The value of the moisture equivalent for very permeable soils is 3 to 4 or less; for standard Ottawa sand this value is practically zero. Sandy loams and other fairly permeable soils generally have a moisture equivalent between 5 and 12. A moisture equivalent above 12 generally indicates that the soil is not very permeable. The moisture equivalent of a clay may be 40, 50, or more. Especially high values for the moisture equivalent have been found in the testing of bentonite (Sec. 1:2). Soils possessing a low moisture equivalent dry out easily, and vice versa. There is a certain relation between the moisture equivalent and the percentage of finer particles in a soil.

To determine the value of the *field moisture equivalent*, a soil paste is prepared, and water is dropped at its surface until the latter becomes shiny and does not absorb any more water. The moisture content is then determined, and in many cases it checks with the centrifuge moisture equivalent.

**2:20. Interrelation of Soil Properties; Soil Classification.**—Light- or coarse-textured soils such as sands generally have but *little affinity* to water. Their moisture equivalent is low; and if wet, they dry out quickly. Such soils generally are but slightly plastic if at all so; their plasticity index is low and sometimes approaches zero. As a rule, heavy- or fine-textured soils possess, on the contrary, *very marked water affinity*. Their moisture equivalent is high; and if wet, they remain so for a relatively long time. Their plasticity index is high, and they actually shrink during the evaporation process—a shrinkage that does not occur with sands, for example. This difference between two kinds of soils suggested the idea that perhaps a “single value,” or a single figure determining quantitatively a certain soil property, could be characteristic for the soil as a whole. No definite results have been attained as yet in developing this idea. At the present time there is no definitely established engineering soil classification. The creation of such a classification is a difficult and lengthy undertaking requiring a great amount of carefully planned research and may be approached but gradually.

There are charts correlating graphically the liquid limit of a soil

with its plasticity index, shrinkage limit, centrifuge moisture equivalent, and field moisture equivalent. These charts have been prepared by the Public Roads Administration,<sup>9</sup> which subdivides all the highway subgrades into eight groups, according to their size and with regard to the characteristics mentioned (groups A-1, A-2, A-3, . . .). This subdivision is tentative, however.

Besides the soil classification of the Bureau of Chemistry and Soils, based on the size of particles (Sec. 1:6), there are two more soil classifications based on the same factor: the so-called "International" classification adopted by the International Soil Congresses (mostly agricultural) and the Massachusetts Institute of Technology classification.<sup>12</sup>

An approach to a soil classification was made during the construction of the Quabbin Dams in Massachusetts<sup>10</sup> and by the Providence, R. I., District, U. S. Engineers.<sup>11</sup> A. Casagrande proposed a soil classification to be used for military airports. This classification is discussed in Chap. XII.

Soil tests so far described and also the permeability tests (Chap. III) are sometimes termed "identification tests" to distinguish them from the purely engineering tests described in Chaps. V and VI.

#### Problems

1. A fully saturated clay sample has a volume of 162 cc. and weighs 290 g. The specific gravity of the particles is 2.79. Determine its voids ratio  $e$ , porosity  $n$  in per cent, moisture content in per cent of dry weight, and the unit weight in pounds per cubic foot. *Ans.* These values are 1.267, 55.9 per cent, 45.5 per cent by dry weight, 112 lb. per cu. ft., respectively.

2. A sample of moist (but not fully saturated) soil had a volume of 42 cc. and weighed 61.1 g. After complete drying out in an oven, its weight was 49.2 g. The specific gravity of the soil particles is 2.65. Compute the degree of saturation in per cent. *Ans.* 50.9 per cent.

*Note:* The degree of saturation is the ratio of the volume of water in pores to the total volume of pores.

3. A sample of fully saturated clay had a moisture content of 40.1 per cent and a specific mass gravity (apparent specific gravity) of 1.85. The latter dropped to 1.76 after the drying out. Determine the shrinkage limit and the specific gravity of grains of this sample. *Ans.* 21.3 per cent; 2.81.

4. The Public Roads Administration (formerly U. S. Bureau of Public Roads) determines the shrinkage limit (SL) of a soil sample from its volume and weight before and after drying. Let  $V_1$  and  $V_2$  be the respective volumes and  $W_1$  and  $W_2$  the respective weights, all values being expressed in metric measures. Express the shrinkage limit in terms of these values.

$$\text{Ans. } SL = \frac{(W_1 - W_2) - (V_1 - V_2)}{W_2}$$

5. In using the Casagrande device, the Harvard Soil Mechanics Laboratory recommends the determination of two groups of points far apart and the connection of the averages for the respective groups with a straight line. The ranges for each group are best chosen between from 6 to 15 blows and from about 23 to 32 blows. The equation of this straight line is

$$w = -F_w \log N + C$$

where  $w$  = moisture content, per cent.

$F_w$  = the so-called "flow index."

$N$  = number of blows.

$C$  = a constant.

Determine the liquid limit and also  $F_w$  and  $C$  for the following test:

Blows	Moisture Content, Per Cent
6.5	52.3
8	51.1
12	47.2
26	38.8
28	37.7
31	36.0

Show on your sketch the geometric meaning of  $F_w$  and  $C$ . In what units are these values expressed? *Ans.* LL = 38.5 per cent.

*Note:* The expression "6.5 blows" means that the sixth blow has closed the groove along a distance of 0.25 in., whereas the seventh blow has brought the two sides together along 0.75 in.

6. Of two soils with equal plasticity indexes (PI), that having the lower plastic limit (PL) is tougher. The "toughness index"  $T_w$  is defined as a ratio:

$$T_w = \frac{PI}{F_w}$$

the symbol  $F_w$  designating the flow index (problem 5). The toughness index generally varies between 0 and 3 and may reach 5.

Determine the plasticity index of the soil of problem 5 if its toughness index is 1. *Ans.* PI = 24.

7. The plasticity index (PI) of a soil is 37, and its shrinkage limit (SL) is 12 per cent. Find its shrinkage index. *Ans.* 25.

*Note:* The term "shrinkage index," used occasionally, means the difference (PI) — (SL).

8. The term "water-plasticity ratio" is occasionally used to designate the percentage

$$B = \frac{w - PL}{PI} \times 100$$

Find the value of the water-plasticity ratio  $B$  when the natural moisture content  $w$  of the sample equals its liquid limit. *Ans.*  $B = 100$  per cent.

## References

1. Information on ground water may be found in "Physics of the Earth," vol. IX, McGraw-Hill Book Company, Inc., New York, 1942 (Chap. X, by O. E. Meinzer and L. K. Wenzel), and in *U. S. Geol. Survey Water Supply Papers*. Fluctuations are discussed in *Papers* 638 and 659. See also C. F. TOLMAN: "Ground Water," McGraw-Hill Book Co., New York, 1937.
2. BERNARD KEEN: "The Physical Properties of Soil," Longmans, Green and Company, London, New York, Toronto, 1931.
3. LEONARD D. BAVER: Retention and Movement of Soil Moisture in "Physics of the Earth" (compare ref. 1); also "Soil Physics," John Wiley & Sons, Inc., New York, 1940.
4. M. B. RUSSELL and M. G. SPANGLER. The Energy Concept of Soil Moisture and the Mechanics of Unsaturated Flow, *Proc. Highway Research Board*, vol. 21, 1941.
5. For a general discussion of capillarimeters, see E. BLANCK: "Handbuch der Bodenlehre," vol. 6, Verlag Julius Springer, Berlin, 1930; also CLEMENT M. JOHNSTON and E. S. BARBER: Compendium on Soil Testing Apparatus, *Proc. Highway Research Board*, vol. 18, 1938.
6. C. A. HOGENTOGLER, SR., C. A. HOGENTOGLER, JR., and others: "Engineering Properties of Soil," McGraw-Hill Book Company, Inc., New York, 1937.
7. A. ATTERBERG: Über die physikalische Bodenuntersuchung und über die Plastizität der Tone, *Intern. Mitt. Bodenk.*, vol. 1, 1911; in English *Public Roads*, 1926 and following years; also ref. 6.
8. A. CASAGRANDE: Research on the Atterberg Limits of Soils, *Public Roads*, vol. 13, 1932.
9. C. A. HOGENTOGLER, SR., and CHARLES TERZAGHI: Interrelationship of Load, Road, and Subgrade, *Public Roads*, vol. 10, 1929; also ref. 4.
10. STANLEY M. DORE: Permeability Determinations, Quabbin Dams, *Trans. A.S.C.E.*, vol. 102, 1937.
11. FRANK E. FAHLQUIST and WALDO J. KENERSON: discussion of the paper on Mechanical Analyses of Soils, *Trans. A.S.C.E.*, vol. 104, 1939.
12. T. T. KNAPPEN and R. R. PHILIPPE: Practical Soil Mechanics at Muskingum, *Eng. News-Record*, vol. 117, 1936.
13. R. VALLE-RODAS: "Experimental Comparison of Passive and Active Capillarity in Sands" (mimeographed), Princeton University, Princeton, N. J., 1944.
14. K. S. LANE, and D. E. WASHBURN: Capillary Tests by Capillarimeters and by Soil Filled Tubes, *Proc. Highway Research Board*, vol. 26, 1946.
15. RALPH B. PECK: Earth-Pressure Measurements in Open Cuts, Chicago Subway, *Trans. A.S.C.E.*, vol. 108, 1943.

## CHAPTER III

### SEEPAGE PHENOMENA AND FROST ACTION IN SOILS

There may be two kinds of flow of moisture in connection with earth masses, namely, (a) viscous flow and (b) plastic flow. Capillary flow as discussed in Chap. II is considered as viscous flow, and so is the movement of moisture from the lower strata to the ground surface during frosts. Plastic flow is discussed in Sec. 5:14.

**3:1. Viscous Flow.**—The simplest case of viscous flow of water in connection with soil is a moving *suspension*. A suspension is not

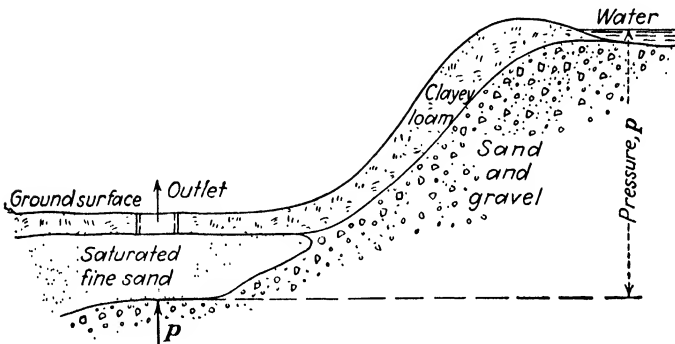


FIG. 3:1.—An example of quicksand action.

necessarily rare. It may be very dense, as are saturated fine sand masses which sometimes act as *quicksands*. Quicksand action as observed in excavations is shown in Fig. 3:1. A weak soil layer at the bottom of an excavation may be broken through by a suspension under pressure. Since in this case sand grains lose weight because of buoyancy, they are very mobile and, upon reaching the surface of the ground, produce a phenomenon known as “boiling.” Thus quicksand is not a particular kind of soil but simply fine suspension sand under pressure.

In a moving suspension soil particles are carried along by water. If, however, the pressure in water is not strong enough to bring

soil particles into motion, the latter stay in their places and water simply percolates through the pores. Such a percolation is usually also visualized as viscous flow. If, for instance, a loaded clay layer is deep and hence confined, moisture is simply *squeezed out* from the pores. This is the case of *consolidation* discussed in Chap. VI. Obviously, squeezing out of moisture cannot take place if the soil skeleton is rigid, as in sands. This is true because, as moisture is squeezed out, the volume of the pores gradually decreases, and a rigid skeleton is not able to decrease in volume considerably. Another case of viscous flow to which the first part of this chapter is devoted is seepage, occurring when water moving under pressure (hydraulic head) is brought into contact with an immovable earth mass. In this case the size and the shape of the pores are assumed constant.

**3:2. Conception of Permeability.**—Obstacles in the way of movement of moisture will be characterized by the degree of permeability of a given soil. Thus soils will be subdivided into permeable, or pervious, soils and impervious soils. The degree of permeability of a soil will be numerically expressed by the *coefficient of permeability*  $k$ , as discussed in Sec. 3:3.

Good permeability of a soil is a favorable factor in the case of (a) foundations, since the settlement of a structure depends on the rate of squeezing out of moisture from underneath a structure; (b) highway and railroad embankments and railroad ballast; and (c) highway subgrades. In the last two instances good permeability ensures the stability of the structure during both rainy weather and thaws. Sometimes poorly permeable soils are desirable, for example, in constructing (d) certain parts of earth dams to keep water in a reservoir and (e) canals to prevent loss of water.

#### A. SEEPAGE

**3:3. The Darcy Formula.**—Moisture moving within an earth mass is under pressure (hydraulic head) which changes from point to point. Thus, on entering the soil sample of a length  $L$  (Fig. 3:2a), moisture is under the pressure  $H_1$ . On leaving the sample, moisture is under the pressure  $H_2$ . The difference between the two pressures  $H = H_1 - H_2$  is spent in traveling through the sample. Suppose that the head  $H$  is subdivided into a great number of equal small increments  $dH$  and the length  $L$  is subdivided into the same number of equal small increments  $dL$ . The

ratio (derivative)  $dH/dL$  is the *hydraulic gradient* at the point of the sample to which the given values of  $dH$  and  $dL$  correspond. It is obvious that in the case of Fig. 3:2a the ratio  $dH/dL$  is constant for all points of the sample and equals  $H/L$ , or the ratio of the head lost in percolation to the distance traveled, which is the length of the sample  $L$ . This is not always so, however. It may happen that in the passage of water through the earth mass, equal increments  $dH$  of the head are spent to pass unequal distances  $dL$ . In such a case, hydraulic gradients  $dH/dL$  will be variable from point to point of the earth mass.

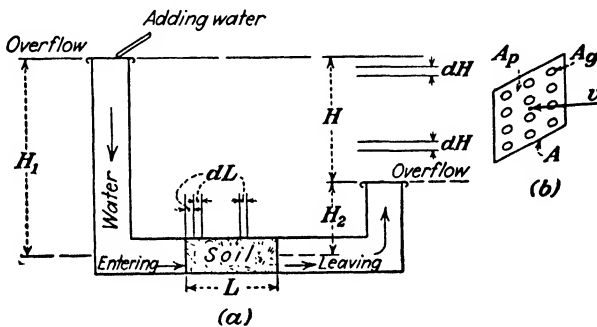


FIG. 3:2.—Percolation through soil.

According to Darcy,\* the discharge velocity  $v$  under the action of a hydraulic gradient  $i$  is

$$v = ki \tag{3:1}$$

where  $k$  is a constant characteristic of the given soil at a given temperature. This formula holds for the case of laminary (and not turbulent) flow, which takes place at slight velocities below a certain critical value. The laminary flow is characterized by a more or less parallel motion of water particles, whereas in turbulent flow water particles move in a rather irregular manner.

The discharge velocity  $v$  in the Darcy formula (3:1) is smaller than the actual velocity of movement  $v_p$  of moisture through the soil pores. In Fig. 3:2b moisture is assumed to pass through an area  $A$ , which is composed of two parts:  $A_o$ , the sum of cross sections of soil grains or particles, and  $A_p$ , the sum of cross sections of the pores. Let  $A_o = 1$ ; then  $A_p = e$  (voids ratio), and

\* A French engineer who proposed formulas (3:1) and (3:4) about 1856.

$A = 1 + e$ . The products  $Av$  and  $A_p v_p$  must be equal, since both represent the total discharge through area  $A$ . Hence

$$v_p = v \frac{1 + e}{e} = \frac{v}{n} \quad (3:2)$$

The symbol  $n$  in formula (3:2) means the porosity of the given earth mass (Formula 1:2).

The constant  $k$  in formula (3:1) is termed by different authors the "coefficient of permeability," "coefficient of conductivity," "transmission coefficient," or "transmission constant." The term "coefficient of permeability" will be used hereafter.

Since the value of the hydraulic gradient  $i$  in formula (3:1) is an abstract number, the coefficient  $k$  has the dimension of velocity. In metric measures it is generally expressed in centimeters per second (designation cm. sec.<sup>-1</sup>), and in English measures in inches per second, in feet per day, or in feet per year.\* Letting  $i = 1$  in formula (3:1),

$$k = (v)_{i=1} \quad (3:3)$$

which means that the coefficient of permeability  $k$  is the velocity of flow under the action of a unit hydraulic gradient ( $i = 1$ ).

The total discharge  $q$  through an area  $A$  during an interval of time  $t$  will be

$$q = Akit \quad (3:4)$$

If  $A$  is expressed in square inches,  $k$  in inches per second, and  $t$  in seconds, the result  $q$  will be in cubic inches. Accordingly, if  $A$  is in square centimeters,  $k$  is in centimeters per minute, and  $t$  in minutes, the discharge  $q$  will be expressed in cubic centimeters.

The Darcy formula (3:1) or (3:4) furnishes very reliable results if the value of the hydraulic gradient  $i$  is small (for instance, for value  $i \leq 1$ ).

**3:4. Principle of Continuity in Seepage.**—Imagine an arbitrary body (for instance, a cube) mentally cut out from the earth mass through which moisture percolates. Moisture enters into that body through some of its sides and leaves through other sides. All theoretical considerations referring to seepage assume a *continuous flow*. This means that the amounts of moisture entering and leaving the cube referred to during a given time interval must

\* The U. S. Geological Survey and some dam builders express the coefficient of permeability as a discharge through a 1-sq. ft. area in gallons per day, at a temperature 60° F. under the action of a hydraulic gradient  $i = 1$ .

be equal. It follows that the discharge  $q$  as determined by formula (3:4) is constant at all cross sections of the earth mass. It follows, furthermore, that areas of the cross sections  $A$  through which moisture percolates are inversely proportional to the corresponding velocities  $v$ , or, which is the same, to the corresponding values of the hydraulic gradient  $i$ .

It should be noted now that the principle of continuity as formulated above does not apply to the phenomenon of the squeezing out of moisture from underneath a load during consolidation. More details on this subject will be given in Chap. VI.

**3:5. Coefficient of Permeability.**—The coefficient of permeability is variable for different soils and may be variable even for one and the same soil. For instance, it commonly occurs that the coefficient of permeability of a soil in a horizontal direction is from two to ten times larger than that in a vertical direction, due to stratification. If plotted against the transverse profile of a locality, coefficients of permeability at various points and at various depths often present a very heterogeneous picture. In a general way the coefficient of permeability depends mostly on the temperature and the voids ratio (degree of packing) and also on the size and shape of the voids. Finally, the value of the coefficient of permeability of a soil is influenced by the air bubbles contained in the moisture. To obtain good experimental results, the use of boiled or deaerated water for percolation tests is advisable.

*Coefficient of Permeability in Metric Measures.*—If the coefficient of permeability is expressed in metric measures (as in the laboratories), it is convenient to represent it as a product of a number by a negative power of 10, for instance  $1.3 \times 10^{-3}$  cm. per sec. Using the fourth negative power of 10 only (as very often done) this value would be  $13.0 \times 10^{-4}$  cm. per sec. Sometimes the coefficient of permeability is expressed in darcies and thousandths of darcy (millidarcies), 1 cm. per sec. being approximately equal to 1,040 darcies.

*Average Values.*—A value of the coefficient of permeability

$$k = 1.0 \times 10^{-6} \text{ cm. per sec.} = 0.01 \times 10^{-4} \text{ cm. per sec.}$$

characterizes soils impervious for all practical purposes. The following numerical data are intended to furnish an approximate idea of the permeability of different soils. Deviations from these values may be very considerable.

Kind of Soil	Coefficient of Permeability, 10 <sup>-4</sup> Cm. per Sec.
Uniform loose sand, sieve 30 to 40.....	3,000
Uniform loose sand, sieve 60 to 70.....	300
Uniform loose sand, sieve 80 to 100.....	100
Fine sands.....	100 to 20
Silts.....	2,000 to 1
Clays.....	10 to practically 0

It should be noticed that 1 cm. per sec. equals 2,822 ft. per day, or, which is the same, the value of  $1.0 \times 10^{-4}$  cm. per sec. equals 0.28 ft. per day. Hence, to convert roughly a value of the coefficient of permeability as expressed in the units  $10^{-4}$  cm. per sec. into feet per day, it is necessary to divide it by 4.

The higher the temperature the less viscous and hence the more fluid is the moisture. It passes more easily through the pores, with the corresponding increase of the coefficient of permeability  $k$ . If the coefficient of permeability  $k_T$  has been determined in a laboratory at a certain temperature  $T$ , this experimental value  $k_T$  should be reduced to a certain standard temperature, which is generally  $20^\circ\text{C.} = 68^\circ\text{F.}$  The coefficients of permeability  $k_T$  and  $k_{20}$ , from which the latter is to be determined, are proportional to the respective coefficients of viscosity  $\eta_T$  and  $\eta_{20}$ .\* Hence

$$k_{20} = k_T \frac{\eta_T}{\eta_{20}} \quad (3.5)$$

**3.6. Laboratory Determination of the Coefficient of Permeability.** *a. Permeameters.*—The general idea of permeameters, or apparatus to determine the coefficient of permeability  $k$  in the laboratory, is (1) to create a flow of water through a sample of a thickness  $L$  and having a definite cross section  $A$  which is practically that of the container in which the sample is placed (Figs. 3:3 and 3:4), (2) to measure the hydraulic gradient  $i$  under the action of which the flow takes place, (3) to measure the discharge  $q$  during a definite interval of time  $t$ . Then all the values in the Darcy formula (3:4) will be known except  $k$ , and the latter can easily be determined.

In the case of the permeameter with constant hydraulic head, constructed by Terzaghi (Fig. 3:3), the water level in the container is kept *constant*. The sample is placed in a metallic container, and the space between the sample and the walls of the

\* For the numerical values of  $\eta$ , see Appendix A.

container is filled with paraffin to prevent leakage. Let  $A$  be the net cross section of the sample in square centimeters. If open tubes p.t. 1 and p.t. 2 (so-called "piezometric tubes") are introduced into the sample, the water level in the container (I) and the water levels in both piezometric tubes (II and III) will be different. This is true because hydraulic head is being spent in percolation.

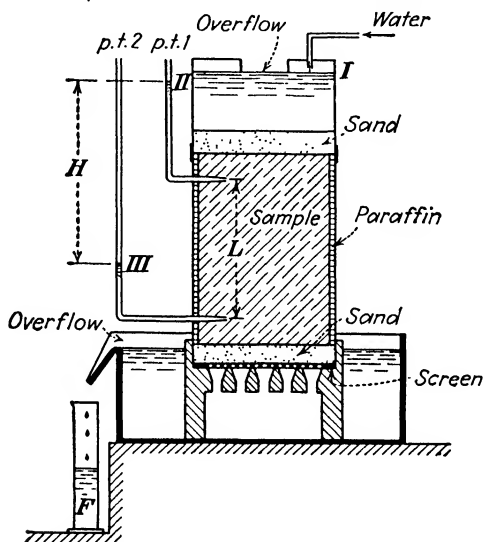


FIG. 3:3.—Constant head permeameter. (After Terzaghi.)

Thus the difference of levels II and III in the two piezometric tubes, designated by  $H$ , expresses the loss of hydraulic head in the percolation through distance  $L$ . Hence the value of the hydraulic gradient is

$$i = \frac{H}{L} \quad (3:6)$$

As soon as percolation starts, percolating water is collected in the measuring flask  $F$ . If percolation lasts  $t$  min., and the whole discharge is  $q$  cc., the value of the coefficient of permeability as expressed in centimeters per minute is

$$k = \frac{1}{At} \frac{q}{i} \quad (3:7)$$

In the *falling head permeameter* (Fig. 3:4), the time  $t$  necessary for the water in the standpipe to drop from a mark  $H_1$  to mark  $H_2$

is observed. The symbols  $H_1$  and  $H_2$  correspond to the heights of the marks in question over an overflow located at the elevation of the bottom of the sample. Thus at the beginning of the test the value  $H_1$  corresponds to the difference in heads  $H$  in Fig. 3:3. In the same way, the value  $H_2$  as observed at the end of the test also

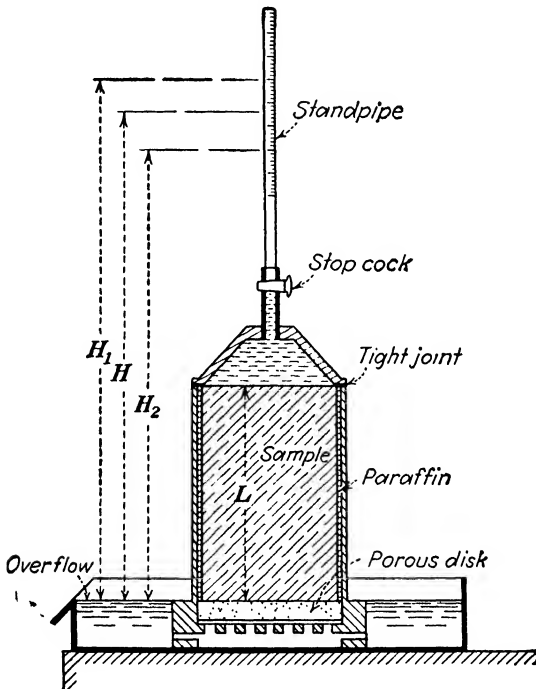


FIG. 3:4.—Falling head permeameter. (After Gilboy.)

corresponds to the difference in heads  $H$  in Fig. 3:3. Hence the hydraulic gradient acting at the beginning of the test is  $i = H_1/L$ , and at the end of the test  $i = H_2/L$ , where  $L$  is the height of the sample.

Let us consider an intermediate situation when the reading on the standpipe  $H$  is between the marks  $H_1$  and  $H_2$ . During a time interval  $dt$ , when the reading drops through a distance  $-dH$ , the discharge through the sample will be  $-a \cdot dH$ , the symbol  $a$  standing for the cross section of the standpipe. The minus sign means that the increment in reading  $-dH$  is negative and that the water level in the standpipe drops. On the other hand, according to the

Darcy formula (3:4) the discharge during the time interval  $dt$  is  $Ak(H/L) \cdot dt$ , the symbol  $A$  standing for the cross section of the sample and  $H/L$  being the hydraulic gradient acting during the given time interval  $dt$ . Equalizing,

$$-a \cdot dH = Ak \frac{H}{L} \cdot dt \quad (3:8)$$

from which

$$dt = -\frac{a}{A} \frac{L}{k} \frac{dH}{H} \quad (3:9)$$

To determine the whole time  $t$  required for the moisture to drop from mark  $H_1$  to mark  $H_2$ , it is necessary to integrate the left side of Eq. (3:9) from  $t = 0$  to  $t = t$  and the right side from  $H = H_1$  to  $H = H_2$ :

$$t = -\frac{a}{A} \frac{L}{k} (\log H_2 - \log H_1) = -\frac{a}{A} \frac{L}{k} \log \frac{H_2}{H_1} \quad (3:10)$$

The symbol "log" in formula (3:10) means "natural logarithm." Remembering now that  $\log H_2/H_1 = -\log H_1/H_2$ , Eq. (3:10) may be rewritten thus:

$$k = \frac{a}{A} \frac{L}{t} \log \frac{H_1}{H_2} \quad (3:11)$$

Formula (3:11) in one form or other is often found in technical literature. Letting for convenience

$$\frac{a}{A} L \log \frac{H_1}{H_2} = c$$

formula (3:11) becomes

$$k = \frac{c}{t} \quad (3:12)$$

In Eq. (3:12),  $c$  is the constant of the given permeameter. It is the same in the case of any soil and may be determined experimentally once for all.

Permeameters with falling hydraulic head have been widely used by Army engineers and other organizations, mostly in connection with dam construction.

Strictly speaking, in using permeameters it is advisable to avoid high values of hydraulic gradients, since the Darcy formula does not hold unconditionally in such cases. In the beginning of a percolation process the value of the coefficient of permeability may

fluctuate owing to "percolational deformations." The finest particles are eroded by the moving moisture, and backfilling also takes place. Fluctuations have been observed not only in the beginning of the process but also when the flow was established. Bubbles of entrapped air incorporated in the sample may completely change the picture of percolation, and efforts should be made to remove them before the test. Also, the results may be quite incorrect owing to the passage of water not through the sample being tested but close to the walls of the container. A paraffin or bentonite jacket between the walls of the container and the sample prevents this.

In permeameter studies it is advisable to use soil samples with undisturbed structure. Disturbed samples may show a degree of

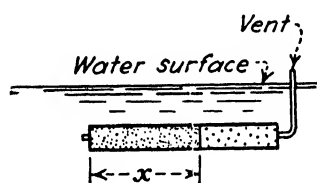


FIG. 3:5.—Determination of the coefficient of permeability by horizontal capillarity. (After A. Casagrande.)

permeability different from that of the natural soil. If the latter is perforated by plant roots and earthworms, as happens close to the surface of the ground, the permeability of the natural soil may be several hundred times higher than that of a disturbed sample. On many other occasions disturbed samples are more permeable than the undisturbed.

*b. Horizontal Capillarity.*—Sometimes the coefficient of permeability  $k$  is determined from observations on the *horizontal capillary movement* as proposed by A. Casagrande.<sup>2</sup> A horizontal tube filled with oven-dry soil and provided with a screen at one side and a vent to evacuate air on the other is placed under water and rotated about its axis to ensure regular motion of moisture (Fig. 3:5). Remembering Eq. (2:8) and placing in it  $N = 2$  for the case of horizontal capillary moisture motion, we have

$$x^2 = mt \quad (3:13)$$

The value of  $m$  is found by plotting the squares of the distances  $x$  against time  $t$  and drawing an average straight line through the points obtained. The coefficient of permeability is found from Eq. (3:14).

$$k = \frac{m^2}{Z} \quad (3:14)$$

where  $Z$  is a constant.

Since the physical dimension of  $k$  is centimeters per second, and that of  $m$  is square centimeters per second, the physical dimension of the constant  $Z$  is cubic centimeters per second. It follows from numerous experiments by A. Casagrande and his coworkers that the values of  $Z = 40$  cc. per sec. may sometimes be acceptable. Formula (3:14) should be considered as a practical way of comparing oven-dried cohesionless soils (mostly fine sands offered for dam construction) with already known soils. To find the value of  $Z$  for a given locality, it is necessary to determine coefficients of permeability for a range of local soils (using permeameters) and then estimate  $Z$  from formula (3:14). The test described cannot be applied to moist cohesive soils as dealt with on construction jobs.

**3:7. Flow Net.**—It will first be assumed that seepage takes place in a homogeneous and isotropic mass. The term “homogeneous” means that the mass is made from one and the same material throughout. The term “isotropic” used in this case means that moisture may move equally well in all directions, obeying the same law. A mass may be isotropic with respect to the propagation of electricity or to distribution of stresses. In the latter case it is called “elastically isotropic,” and this term will be often used hereafter. Seepage in a homogeneous isotropic mass is analogous to the propagation of electricity or to the distribution of stress. Hence, very often if the solution of an electrical or elastic problem is known, the solution of a seepage problem may be found simply *by analogy*. Electrical and elastic analogies of seepage will be discussed in this chapter. To simplify the solution, only two-dimensional or plane flow will be considered. This is, for example, the case when there is water only at one side of a long earth mass (an earth dam or a very wide experimental box). In this instance the movement of moisture in vertical planes perpendicular to the length and at considerable distance from the ends of the mass will be practically the same. Action of piezometric tubes has already been discussed in Sec. 3:6 (designation used in Fig. 3:6 is p.t.). If such a tube is introduced into the mass in question, the water in the tube will rise to a certain level  $h_i$ , according to the pressure within the water at the lower end of the piezometric tube. The value  $h_i$  is different at different points of the mass. Suppose that points  $A$  and  $A'$  in Fig. 3:6 show different heights  $h_i$  and  $h_i'$  of water in the hypothetical piezometric tube but the top of the water

in both tubes is the same. Designate with  $h$  the elevation of the top of this water with respect to an arbitrary horizontal plane  $OO$ . Then the *potential*  $h$  is the same for both points  $A$  and  $A'$ . The location of the horizontal plane  $OO$  is immaterial, since what counts is not the absolute value of the potential but the difference between potentials at two or several points. The locus of points such as  $A$ ,  $A'$ , . . . with equal potentials  $h$  is termed the *equipotential line* (or equipotential surface, in the case of three-dimensional flow). Moisture cannot flow along such a line or surface, but it will flow from point  $A$  to another point with smaller potential. Suppose now that  $BB'$  is the equipotential line, corresponding to a potential

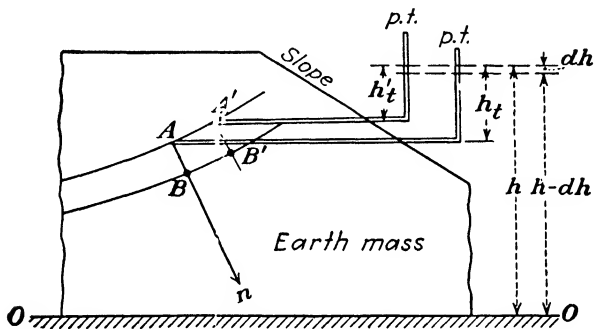


FIG. 3:6.—Flow net: equipotential lines and stream lines.

$h - dh$ . The flow from a point  $A$  of the equipotential line  $AA'$  to a point of the infinitely close equipotential line  $BB'$  may take place if the value of the hydraulic gradient along the distance  $AB$  is at a maximum or, in other words, if the distance  $AB$  is shorter than any other possible distance of flow  $AB'$ . This means that line  $AB$  is normal to both infinitely close equipotential lines  $AA'$  and  $BB'$ . Thus normals to equipotential lines are directions of flow or *streamlines* (termed also *flow lines*). The set of equipotential lines and streamlines that are mutually normal forms what is called flow net. Through each point of a two-dimensional mass both lines forming the flow net can be traced.

**3:8. Electric Analogy of Seepage.**—The electrical apparatus shown in Fig. 3:7 (plan) consists of a shallow trough with plate-glass bottom and sides, filled to a depth of approximately  $\frac{1}{2}$  in. with solution of an electrolyte (for instance, common salt). Two  $\frac{1}{8}$ -in. copper plates are placed at each side of the dam model and connected to a 110-volt alternating current through a lamp bank

which reduces the voltage drop between the terminals to about 18 volts. At the opposite side of the tray, over a scale, is a high-resistance wire, each end of which is connected to one of the terminals by a heavy copper wire. The length  $L$  of this wire is about 3 ft. On the high-resistance wire in question a sliding contact connects through a set of earphones to a probing pencil. When the current passes from one terminal to another, the trajectories described are

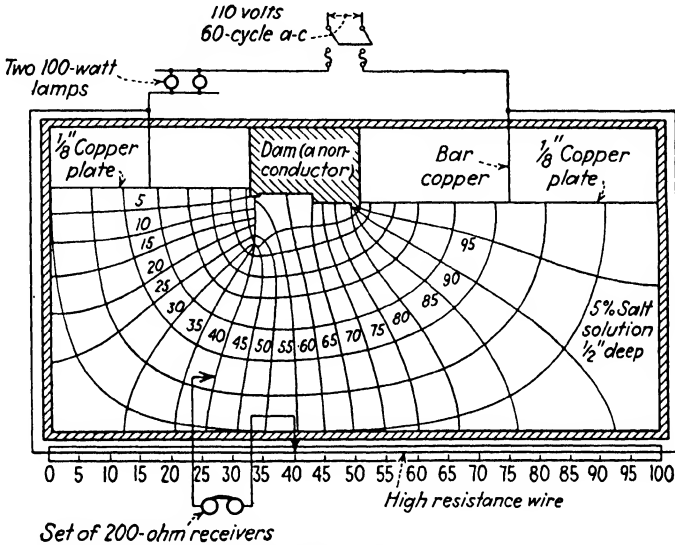


FIG. 3:7.—Electrical analogy of seepage. (From *Civil Engineering*, vol. 4, page 511, October, 1934.)

exactly the same as streamlines in the case of seepage. The purpose of the apparatus is to determine the equipotential lines. As an example, suppose that the equipotential line corresponding to 40 per cent of the total potential drop between the terminals is to be traced. (The drop of potential in this case corresponds to the loss of hydraulic head in the case of seepage.) The sliding contact is then placed at a distance of  $0.4L$  from the left end of the high-resistance wire,  $L$  being the length of the wire. The probing pencil is moved through the tray until the hum in the earphone stops. The point thus found is located on the equipotential line in question.<sup>3</sup>

**3:9. Elastic Analogies of Seepage.**—Consider a semi-infinite, homogeneous, elastically isotropic mass (compare Sec. 3:7). The

term "semi-infinite" means that the mass is bound from above with a horizontal plane and is infinitely deep and infinitely wide. Suppose that this horizontal boundary is loaded with a strip load,  $2b$  wide, like the dam in Fig. 3:8. If this strip load is long enough, it may be considered infinitely long. The strip load in question produces stresses within the mass. If cross sections are drawn normally to this infinitely long strip, the stress distribution will be the same in all these cross sections. Thus stresses in the vertical plane as shown in Fig. 3:8 are the same as in any other vertical plane parallel to it. The stress distribution in this case is two-dimensional or plane, in the same way as there may be two-dimensional or plane flow (Sec. 3:7).

Consider, furthermore, a point  $A$  within the mass. There are pressures at it acting in all directions in the vertical plane (Fig.

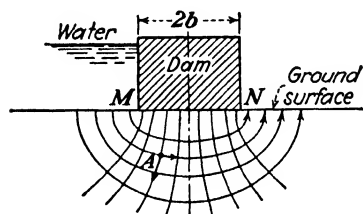


FIG. 3:8.—Flow under a dam.

3:8). One of these pressures, for instance that acting downward, as shown with an arrow, is greater than that acting in any other direction at point  $A$  and is termed the *major* (or maximum) *principal stress*. Pressure normal to the former (acting sidewise, as shown with another arrow) is smaller

than that acting in any other direction at point  $A$  and is termed the *minor* (or minimum) *principal stress*.<sup>\*</sup> Curves can be traced through every point  $A$  of the mass in such a way that the directions of the major and the minor principal stresses will be tangent to them. These curves are termed *trajectories of principal stresses*.

The elastic analogy of seepage in the case of a semi-infinite, homogeneous, permeable mass is the following: Consider the base of the strip load  $MN$  (Fig. 3:8) as impermeable, and assume that there is water at one side of the strip load. Water will then percolate underneath the impermeable base  $MN$ . Streamlines would coincide with trajectories of minor principal stress, and equipotential lines would coincide with trajectories of major principal stresses. Thus, to find the flow net in the case of a semi-infinite, homogeneous, permeable mass, it is necessary to look for the trajec-

<sup>\*</sup> More information on the principal stresses and on the theory of elasticity will be given in Chap. IV.

ories of principal stresses as given by the theory of elasticity. Care should be taken in applying this general statement to finite earth masses.

**3:10. Application of Elastic Analogies.**—The following three cases will be considered:

*a. Flow under a Masonry or Concrete Dam.*—Suppose that the distance  $MN$  represents a dam with head water at the left (Fig. 3:8). Streamlines under this dam are ellipses, and equipotential lines are hyperbolas because these particular curves are trajectories

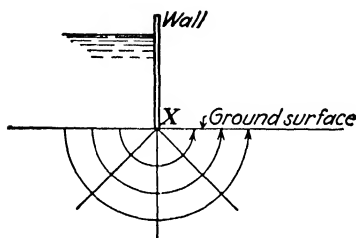


FIG. 3:9.—Flow under a wall.

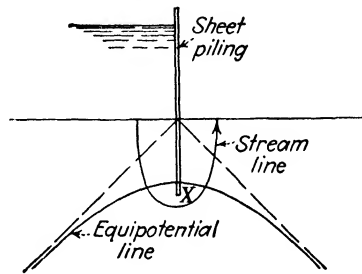


FIG. 3:10.—Flow under sheet piling.

of principal stresses at a point under the action of the uniform strip load  $MN$ . Both systems of curves are confocal, having their foci at the edges of the dam  $MN$ .

*b. Flow under a Wall.*—A wall is analogous to a concentrated force. Trajectories of principal stresses under the latter are radii (major principal stress) and circles (minor principal stress). By analogy, streamlines under a wall without foundation standing at point  $X$  of the mass are semicircles, equipotential lines being radii emanating from point  $X$  (Fig. 3:9). To apply the method of elastic analogies to a more complicated problem, let us consider a sheet-piling wall driven into the ground. The analogy may be found in this case by cutting the mass and the load (Fig. 3:8) along the center line by a vertical plane and turning the drawing  $90^\circ$ . The streamlines are ellipses and the equipotential lines are hyperbolas, with common foci at the tip  $X$  of the sheet piling (Fig. 3:10).

*c. Parabolic Flow.*—The problem is to find the flow net of moisture moving above an impervious infinite horizontal plane which at a certain point  $A$  becomes permeable (Fig. 3:11, top). An analogous elastic problem corresponds to uniform loading of that section of

the boundary which is assumed impervious in the seepage problem (Fig. 3:11, bottom). The lines of principal stresses are confocal parabolas having their foci at point A; hence the flow net in the seepage problem is formed also by confocal parabolas with their foci at point A. This problem has been solved by Kozeny<sup>4</sup> in a more complicated way.

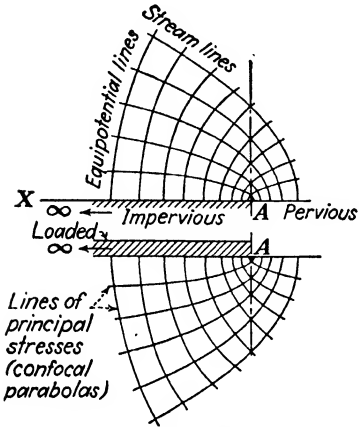


FIG. 3:11.—Parabolic flow.

**3:11. Saturation Line in an Earth Dam.**—The line that bounds a moisture stream from above is termed the “saturation line,” “line of seepage,” or sometimes “phreatic line.” In the case of parabolic flow (Sec. 3:10c) the saturation line is also a parabola. Its equation in polar coordinates (Fig. 3:12) with the origin at the focus is

$$\rho(1 - \cos \theta) = \text{const.} \quad (3:15)$$

where the polar angle  $\theta$  is counted from the horizontal axis clockwise. The value of the constant in Eq. (3:15) is the length of the ordinate  $AA' = y_0$  corresponding to the focus A of the parabola. In fact, make  $\theta = 90^\circ$  in Eq. (3:15). Then

$$\cos \theta = 0 \text{ and } \rho = y_0 = \text{const.}$$

Assume first that the value of the constant  $y_0$  in Eq. (3:15) of a parabola is known. Draw a straight line (horizontal line in Fig. 3:12) which will be the axis of that parabola, point A being its focus. Swing an arc of arbitrary radius from focus A to intersect the axis of the parabola at point E. Plot  $EF = y_0$ . Then point X, that of intersection of the vertical drawn through point F with the arc mentioned, lies on the given parabola. Conversely, if a parabola is given by the position of its axis AE (and its focus A) and a point X, swing arc EX and drop perpendicular XF on the axis. Then  $EF = y_0$ .

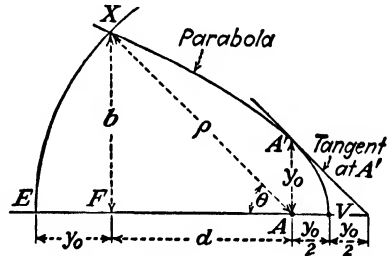


FIG. 3:12.—Parabola in polar coordinates,  $\rho$  and  $\theta$  (origin at focus A).

Designate the horizontal and the vertical distance of point  $X$  from focus  $A$ , with symbols  $d$  and  $b$ , respectively. Since in this case

$$\rho = \sqrt{d^2 + b^2}; \quad \rho \cos \theta = d$$

the value of the constant  $y_0$  is

$$y_0 = \sqrt{d^2 + b^2} - d \tag{3:16}$$

It is known (a) that the focal ordinate  $AA' = y_0$  equals twice the distance from the focus  $A$  to the vertex  $V$  of a parabola and (b) that the vertex of a parabola halves the subtangents. Using these properties and tracing a tangent to the parabola at point  $A'$ , it may be concluded that the slope of this tangent equals a unit. This slope is the hydraulic gradient  $i$  at point  $A'$ . Hence, applying

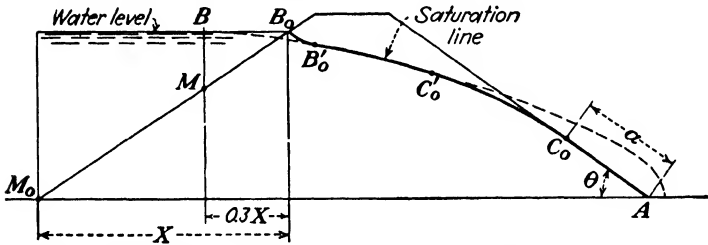


FIG. 3:13.—Saturation line in an earth dam (distances  $B_0B'_0$  and  $C_0C'_0$  are simply sketched).

the Darcy formula to the section  $AA'$ , the discharge through a cross section  $A = y_0 \times 1$ , i.e.,  $y_0$  high and 1 ft. wide, is

$$q = Aki = (y_0 \times 1) (k) (1) = ky_0 \tag{3:17}$$

According to a proposal by A. Casagrande,<sup>5</sup> the saturation line of the parabolic flow (sometimes termed “basic parabola”) is considered as the saturation line in an earth dam (Fig. 3:13). The “basic parabola” is then connected with both the upstream and downstream slopes of the dam to fit the boundary conditions. This is done in the following way: The “basic parabola” is assumed to start at point  $B$  of the upstream water level, which point is determined from the condition that the vertical  $BM$  divides the slope  $B_0M_0$  into two parts, such as

$$B_0M = 0.3B_0M_0$$

Point  $B_0$  is that point where water actually enters the body of the dam. The connecting distance  $B_0B'_0$  is simply sketched to touch

the basic parabola at point  $B_0'$ . The curve  $B_0B_0'$  should be normal to the upstream slope, which is an equipotential line. To connect the "basic parabola" with the downstream slope of the dam, advantage has been taken from the study of numerous flow nets drawn under the supervision of A. Casagrande. His results are given hereafter in a simplified form. Distance  $a$  from the focus  $A$  to the point  $C_0$ , where the saturation line touches the downstream slope, is connected with the radius vector  $\rho$  of the basic parabola by the relation

$$a = \rho(1 - c) \quad (3:18)$$

where  $c$  is a fraction depending in turn on the value of the angle  $\theta$

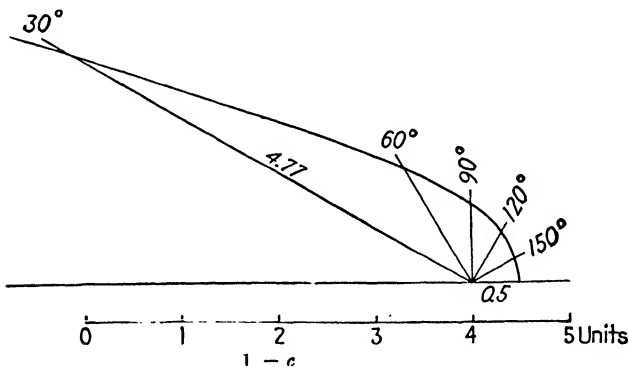


FIG. 3:14.—Graph of the values  $\frac{1-c}{1-\cos\theta}$  to be used in constructing the saturation line in an earth dam [formula (3:19)].

made by the downstream slope with the horizon. Combining Eqs. (3:15) and (3:18),

$$a = y_0 \frac{1-c}{1-\cos\theta} \quad (3:19)$$

To use Eq. (3:19), the value of  $y_0$  is first computed by Eq. (3:16) and afterward multiplied by the ratio  $(1-c)/(1-\cos\theta)$  as read from the graph (Fig. 3:14). It should be always borne in mind that the saturation line does not represent a sharp boundary of the wet soil, since next to this is a strip of soil partly saturated because of the presence of capillary and hygroscopic moisture.

The method of tracing the saturation line in an earth dam furnishes quite satisfactory results without being strictly scientific.

More details along these lines may be found in the *Proceedings* of the Congresses of Large Dams, especially of the Second Congress.

**3:12. Graphical Method of Tracing a Flow Net.**—\*The flow net in a confined space can be constructed by tracing flow lines and equipotentials freehand and gradually improving and correcting them. Figure 3:15 represents a dam built on a pervious soil layer which, in turn, is underlaid with an impervious one. In this case the base of the dam *ABCDEFGH* and the top of the impervious layer are the *boundaries*. Consider now Fig. 3:7 (electrical analogy of seepage). Assume that this figure represents the cross section of a long experimental box filled with soil, with the model of a dam placed on top. In this case the boundaries would be the base of the model and the walls and the bottom of the box. The flow net

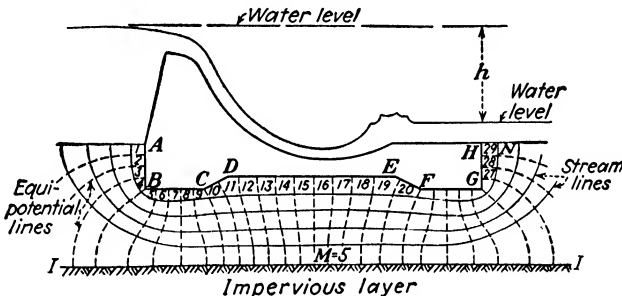


FIG. 3:15.—Graphical method of tracing the flow net in a confined space.

obviously would be as shown in Fig. 3:7. In a confined space the *limit flow lines* are all boundaries and the saturation line (Sec. 3:11) if any. Hence equipotential lines are normal to all boundaries except at the breaks of the boundaries (corners of the box in Fig. 3:7).

The procedure of tracing the flow net is as follows: (a) Trace some equipotentials, and, as a first approximation, divide all of them into equal number of parts; (b) trace flow lines through these division points normally to equipotential; (c) gradually modify the flow net to make the “squares” of the flow net either increase or decrease in a given direction, keeping strict orthogonality (normality) and smoothness of the intersecting curves. The term “square” in this case is purely conventional. Notice that an oblique discharge face, such as the downstream slope of an earth dam, is neither a flow line nor an equipotential, provided that there is no tail water. The upstream face of

\*The method discussed in this section was proposed by Prof. Forchheimer of Germany before 1914. An analogous method of tracing flow nets is used also by electrical engineers in their problems.

an earth dam is an equipotential, however. The equipotential corresponding to the center line of a perfectly symmetrical structure is a straight line. This is not exactly the case of Fig. 3:7, however, since the model shown in it is not symmetrical and is not symmetrically placed.

The discharge of the moisture percolating under the given structure can be computed from the flow net as follows. Let the numbers of the intervals between the equipotentials and between the flow lines be  $N$  and  $M$ , respectively. In Fig. 3:15 these values are  $N = 29$  and  $M = 5$ .

For convenience, assume that both the vertical and the horizontal size of a "square" equal one unit. The difference  $h$  between the levels in the upstream and downstream pools is lost when moisture passes  $N$  squares; hence the loss of hydraulic head corresponding to one square is  $h/N$ . Since the horizontal size of a square is one unit, the hydraulic gradient  $i = h/N:1 = h/N$ . Applying the Darcy formula to any vertical section under the dam and remembering that there are  $M$  intervals between streamlines, the value of the seepage below the dam in a unit of time is

$$q = Aki = (M \times 1)k \left( \frac{h}{N} \right) = kh \frac{M}{N} \quad (3:20)$$

In the case of Fig. 3:15, assuming that  $h = 7$  ft. and  $k = 1$  ft. per day, the amount of seepage through a slice of the mass 1 ft. wide will be

$$q = 1 \times 7 \times \frac{5}{29} \times 1 \text{ ft.} = \text{about } 1.2 \text{ cu. ft. per day}$$

If there is no natural lower boundary confining the flow as in Fig. 3:15, an arbitrary flow line may be considered as the lower boundary, provided the velocity of flow along that flow line is negligible.

**3:13. Flow of Moisture through Aeolotropic Earth Masses.**—An "aeolotropic" earth mass does not conduct moisture equally well in all directions. Another term used to convey this idea is "anisotropic." As stated in Sec. 3:5 the average permeability of a natural soil deposit in a horizontal direction (coefficient of permeability  $k_x$ ) is several times that in the vertical direction  $k_z$ . The graphical method of tracing a flow net (Sec. 3:12) is to be modified in this case.

Samsioe of Sweden proposed to reduce the horizontal dimensions of a structure by the factor  $\sqrt{k_z/k_x}$  and to apply Forchheimer's method (Sec. 3:12) to the transformed cross section. For instance, if  $k_x = 9k_z$ , the value of this factor is  $\frac{1}{3}$ . The flow net is then constructed under the reduced structure (Fig. 3:16b), and vertical ordinates of this flow net are plotted under the corresponding points

of the natural-shaped, nonreduced structure (Fig. 3:16a). As a rule, equipotential lines and streamlines corresponding to this case are not mutually normal. Samsioe's method is an analogy of Wolf's method of determining stresses in aeolotropic masses as explained in Sec. 4:17.

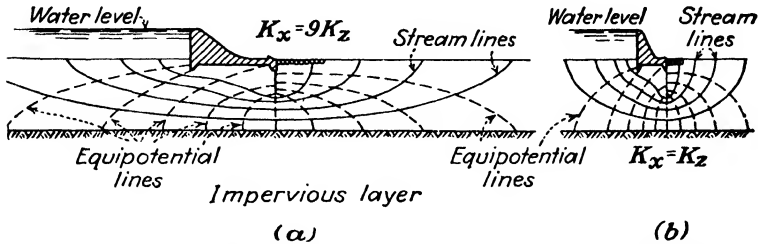


FIG. 3:16.—Samsioe method of tracing the flow net in the case of an aeolotropic mass.

**3:14. Measures against Piping and Internal Erosion in Earth Dams.**—As follows from the inspection of Fig. 3:13, a stream of percolating moisture moves through an earth dam. This stream is bounded by the saturation line, and above that line there is some capillary and hygroscopic moisture. If the percolating moisture moves too fast, excessive pressure may produce “boiling” at the point where moisture leaves the body of the dam. Boiling also

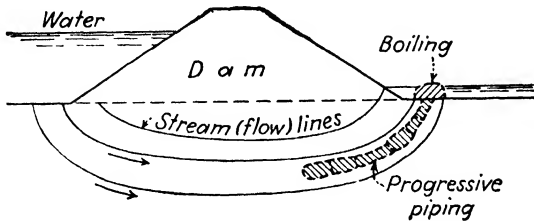


FIG. 3:17.—Gradual formation of a “pipe” within or underneath a dam.

may be produced at the toe of an earth dam if the foundation is more permeable than the body of the dam itself (Fig. 3:17) or at the downstream toe of a masonry or concrete dam. As soon as material becomes unstable at the downstream side of a dam and is partly removed by the flowing water, it is automatically replaced by additional earth from inside the dam or its foundation, as shown in Fig. 3:17. Thus a progressively increasing hollow similar to a pipe is being formed within the dam or its foundation, hence the term *piping* for designating this phenomenon. Fine soil particles,

especially those of colloidal size, are washed out freely within that pipe, and such an internal erosion may cause an ultimate failure of the dam. Piping and internal erosion within a dam were first clearly explained by Terzaghi.

To diminish the destructiveness of a fast-moving moisture stream within a dam or its foundation, it is advisable (a) to

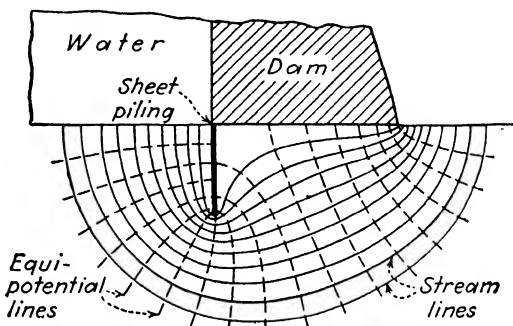


FIG. 3:18.—Flow net under a dam with a cutoff.

decrease the velocity of the percolating water and (b) to decrease the size of the moving stream itself. The corresponding measures are briefly described hereafter.

*a. Decreasing the Velocity of Percolating Moisture.*—It is to be remembered that according to the Darcy formula (3:3), the velocity of percolation is proportional to the hydraulic gradient. Hence to decrease velocity the hydraulic gradient causing the motion of the moisture should be diminished. This can be done, for instance, by developing the *path of percolation*. Imagine that streamlines are real elastic bands like rubber bands; then sheet piling as shown

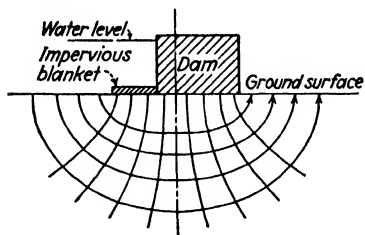


FIG. 3:19.—Action of an impervious upstream blanket.

in Fig. 3:18 would push the streamlines down and contribute to the elongation desired. An impervious blanket covering the earth's surface for some distance upstream from the structure evidently has the same effect (Fig. 3:19). Figure 3:20a and b shows how sheet piling may increase the path of percolation of moisture through a permeable foundation of a rather impermeable earth dam.

Some time ago, dam designers believed that flattening the downstream face develops the path of percolation and may keep the moisture stream within the body of the earth dam. The saturation line was visualized as a straight line staying within the dam (Fig. 3:21). According to Fig. 3:13, the flattening out of the downstream face really can develop the path of percolation, but moisture still will reach the toe of the dam, though in the form of a very shallow stream.

*b. Decreasing the Size of the Percolating Moisture Stream.*—The size of the percolating moisture stream may be decreased by offering it an easy way to leave the dam through highly permeable material introduced for this purpose into the body of the dam. Moisture

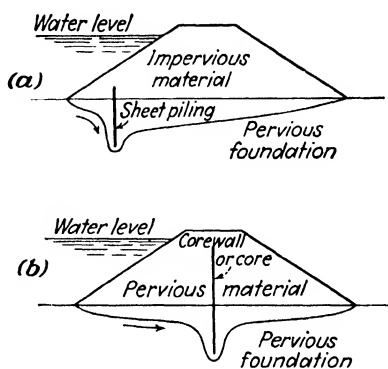


FIG. 3:20.—Path of percolation increased by cutoff wall or sheet piling.

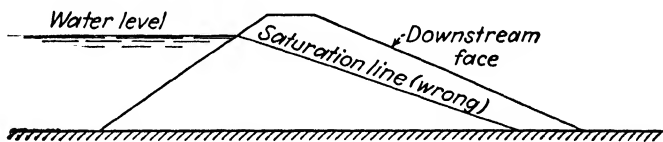


FIG. 3:21.—Flattening the downstream face to keep the saturation line inside (straight-line theory of saturation line is now abandoned).

reaching the surface of such a highly permeable material may be compared to very fine dew. It simply falls down, and the tangent

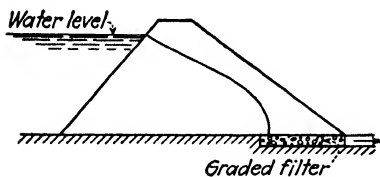


FIG. 3:22.—Saturation line in a dam which is provided with drainage.

to the streamline reaching such a surface is vertical. This can be seen, for instance, in Fig. 3:22, representing a downstream blanket made of graded gravel as proposed by A. Casagrande. Such a blanket, reaching one-third or more of

the width of the dam, draws the streamlines away from the downstream face and has the same effect as the flattening of the latter but is less expensive (compare Fig. 3:21). An inconvenience of these filters is the possibility of silting and, consequently, a pos-

sible loss of stability of the whole structure, since in case of silting the streamlines would return to the downstream face. A downstream rock-fill toe, as shown in Fig. 3:23, also diverts the moisture stream and, besides, contributes to the stability of the dam.

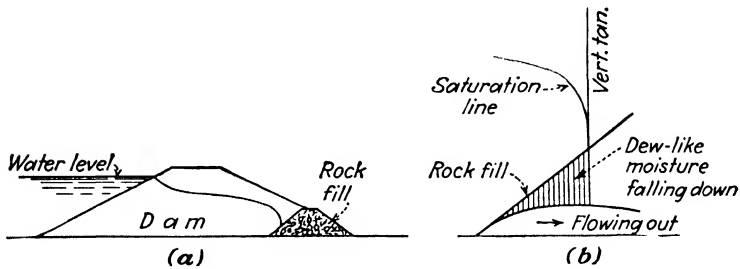


FIG. 3:23.—Action of the downstream rock-fill toe.

**3:15. Action of the Core in an Earth Dam.**—According to L. Casagrande<sup>6</sup> the saturation line, in passing from a less pervious part of a dam into a more pervious part, shifts down; this does not happen when the coefficient of permeability is constant through the

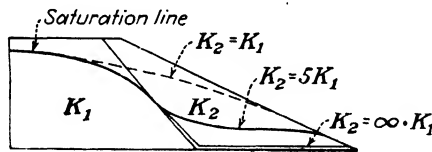


FIG. 3:24.—Transfer of the saturation line from a less permeable to a more permeable medium. (After Leo Casagrande.)

whole section. The saturation line corresponding to the latter case is shown in Fig. 3:24 in dotted lines. With this information in mind, an analysis of core action in an earth dam can be made.

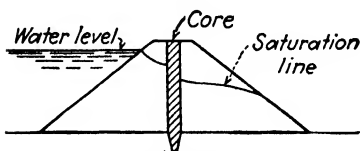


FIG. 3:25.—Influence of the core on the position of the saturation line.

To ensure better impermeability, the central part ("core") of an earth dam is sometimes made of fine impervious material, whereas the outside portions ("shell," "beach," or "shoulder"), which contribute to the stability of the dam rather than to its impermeability, are made of coarse pervious material. The sketch (Fig. 3:25) roughly shows the dropping of the saturation line due to the presence of the core.

**3:16. Seepage from Canals.**—Losses of water from both navigation and irrigation canals are due either to evaporation or to percolation through soil. Percolation takes place either because of the action of gravity, which causes a certain hydraulic head, or because of the action of downward capillary forces, or both. It is to be remembered in this connection that capillary forces may act in any direction, not only upward. The subject of seepage from canals has been studied in recent years only<sup>8</sup>; and solutions of this problem are to be considered as *crude estimations*. The following considerations (Secs. 3:16 and part of 3:17) are based on Terzaghi's work but are presented in a very simplified form.

Moisture that escapes from a canal joins the ground water and afterward moves together with it. Two cases may be distinguished: (a) deep ground water and (b) shallow ground water. When the canal is new, there is no silt on the slopes, and water is lost through them. Afterward, when the slopes are silted, their influence on

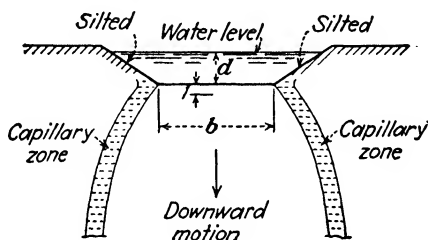


FIG. 3:26.—Downward seepage from a canal in the case of a deep water table.

the amount of seepage may be neglected. Sometimes, to prevent seepage from a canal, the bottom of the slopes is lined. This circumstance also will be disregarded in this discussion.

Losses due to capillary motion of the moisture likewise will not be taken into consideration. In Fig. 3:26, which corresponds to *deep ground water*, the capillary zone is dashed. Referring to this figure, designate with  $b$  the bottom of the canal, with  $d$  the depth of water in it, and consider the flow of water through a prism  $b$  units wide and one unit deep. The corresponding hydraulic gradient

$$i = \frac{d + 1}{1}$$

approximately equals  $d$ , so that the amount of seepage

$$q = bkd \quad (3:21)$$

is practically proportional to the depth of water  $d$  in the canal. If  $b$  and  $d$  are in feet and the coefficient of permeability  $k$  is in feet per year, formula (3:21) furnishes the amount of seepage in cubic feet per year per running foot of length of the canal.

If the ground water is *shallow* and moves toward a near-by brook (Fig. 3:27), it may be very roughly assumed that moisture seeping from the canal also moves toward that brook. Designate with  $i_0$  the natural slope of ground water and with  $i$  the slope of ground water after the construction of the canal. If  $h$  is the elevation of the bottom of the canal over the level of water in the brook, and  $L$  the distance from the canal to the brook, the average

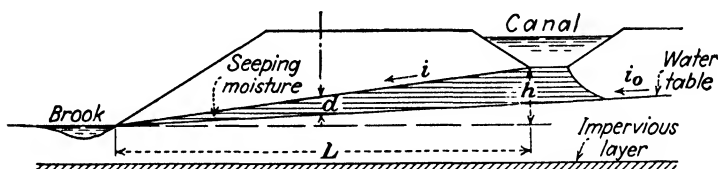


FIG. 3:27.—Seepage from a canal in the case of a shallow water table.

slope  $i$  equals  $h/L$ . Considering also an average cross section in the middle of the distance  $L$ , and designating the excess of depth of ground water due to seepage with  $d$ , the loss  $q$  of water from the canal is

$$q = kd(i - i_0) \quad (3:22)$$

The effective hydraulic gradient of the moisture escaping from the canal is  $i - i_0$  [formula (3:22) and Fig. 3:27], not  $i$ . This is true because this moisture does not move on a horizontal plane but may be visualized as sliding down the water table, with a slope  $i_0$ .

The size of the canal influences the amount of loss of moisture in the case of deep ground water but has no bearing on that amount if the ground water is shallow, at least under the circumstances shown in Fig. 3:27. The amount of water loss from a canal depends also on the nature of the local soil (value of  $k$ ) and on the local hydrological conditions, which in the example of Fig. 3:27 are represented by the values  $h$  and  $L$ .

### 3:17. Field Determination of the Coefficient of Permeability.—

In estimating the loss of moisture from canals and also in other circumstances, it is convenient to determine the value of the coefficient of permeability  $k$  in the field. This can be done, for instance, by observing pumping from a well. The hydraulics of wells has been

known to engineers for a long time and may be found in textbooks on water supply.<sup>6</sup> In a method proposed by Slichter,<sup>7</sup> an upstream well is charged with a strong electrolyte such as ammonium chloride,  $\text{NH}_4\text{Cl}$ , which travels with ground water. On entering one of the downstream wells, the electrolyte forms a short circuit, and a signal is given from which the time of travel is computed. The hydraulic gradient is determined from the difference in levels

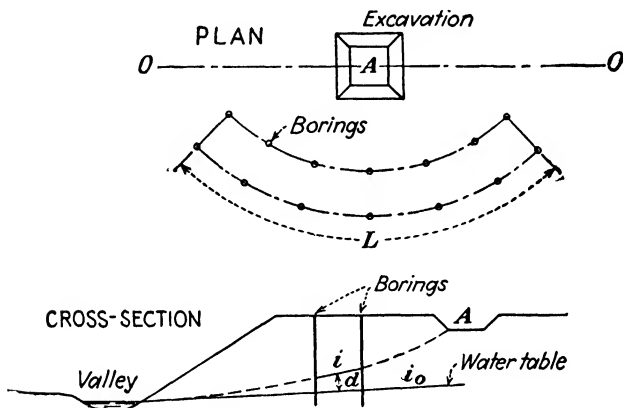


FIG. 3:28.—Field determination of the coefficient of permeability. (After Terzaghi.)

and the distance between the wells, and for computing the coefficient of permeability the Darcy formula is used.

During the soil investigations for the Volga-Don Canal in Russia (Prof. Terzaghi, consulting engineer<sup>8</sup>), fluctuations of water levels in experimental wells were observed. In Fig. 3:28,  $OO$  is the axis of a future canal, and  $A$  is an experimental excavation from which moisture moves to a near-by valley. Borings were made in pairs following a curve of a length  $L$ , and it was assumed that all moisture escaping from the canal passes through that curve. The level of water in the experimental excavation was maintained constant so that the amount of water added per unit of time  $q$  equaled the discharge through curve  $L$ . By observing the difference between levels in the upstream and the downstream borings, the average slope  $i$  of the percolating moisture stream was found. If the depth of the percolating moisture above the original water table is  $d$ , the coefficient of permeability  $k$  may be determined from Eq. (3:23):

$$q = k(i - i_0)Ld \quad (3:23)$$

The symbol  $i_0$  in formula (3:28) again designates the natural slope of the water table.

### B. FROST ACTION IN SOILS

**3:18. General.**—Frost action in soils is closely related to the water properties of a given earth material, particularly to its permeability, since there is a certain flow of moisture when the soil freezes. Thus phenomena accompanying frost represent particular cases of flow of moisture in soils.

Moisture within soil pores freezes (wholly or partly) if the temperature drops to or below the freezing point ( $0^{\circ}\text{C.} = 32^{\circ}\text{F.}$ ). Earth material that is close to the earth surface consists of soil particles, moisture, and air and in freezing becomes a material that may be compared to concrete. This material loses its hardness, however, as soon as it thaws again. The real cause of the hardening of soil in freezing is the passage of the moisture into the solid state. Completely dry sands isolated from any source of water do not freeze. For example, there is dust on earth roads in snowless countries, even during severely cold weather. Again it is relatively easy to open a gravel or sand pit in winter, whereas opening a clay pit in winter presents serious difficulties.

Since the *depth of freezing* depends on local *climatic features*, a construction engineer should be perfectly aware of this depth in a given locality. For instance, the depth of freezing in the central part of the United States is between 3 ft. and 4 ft., whereas in Canada, Alaska, and in certain parts of Siberia and China there are *ever-frozen* (or *perennially frozen*) soils (Sec. 3:25). The term “*permafrost*” is also used.

Frost action consists of the following: (a) in winter and in early spring *frost heaves* in certain places and (b) later in the spring, *back-settling* and *softening* of the ground at the same places. The cause of frost heaves was formerly ascribed to the freezing of pore moisture and the corresponding increase in volume. An average soil, however, does not contain more than 50 per cent of voids, and this should correspond to a maximum heave of  $0.50 \times 0.09 = 0.045$ , or about 5 per cent of the thickness of the frozen layer. The factor 0.09 stands for 9 per cent, which is the difference in volume between ice and water. Heaves corresponding to 20 or 30 per cent of the thickness of the frozen layer are not uncommon, however. This circumstance suggests that some additional water is drawn,

during the freezing process, from some lower layers. Excavations made in frozen soils often show ice lenses within the earth mass. It has also been observed that if there is not sufficient moisture in the freezing clayey or silty soils, the soils may crack in the same way as during the drying process. Observations have revealed also that silty soils suffer most from frost action whereas there are practically no heaves in sands or heavy clays. Highway engineers have observed also that roads do not suffer so much from frosts in the winter as from those early in the spring.

These and similar facts have been known to engineers for a long time, but not until after 1925 had an adequate theoretical explanation of frost phenomena been given.\*

**3:19. Freezing Point; Ice Crystals; Open and Closed Soil System.**—Bouyoucos found that a portion of soil moisture freezes readily at  $0^{\circ}\text{C}$ . ( $32^{\circ}\text{F}$ .); another portion freezes only when a temperature of  $-4^{\circ}\text{C}$ . ( $25^{\circ}\text{F}$ .) is reached; and still another does not freeze even at the extreme low experimental temperature of  $-78^{\circ}\text{C}$ . ( $-108^{\circ}\text{F}$ .).

According to Beskow, the freezing point within narrow pores is below  $0^{\circ}\text{C}$ . ( $32^{\circ}\text{F}$ .). Moreover, within a wider pore the freezing point is lower in the neighborhood of the particle than in the middle of the pore. This means that the *freezing point is variable* throughout the earth mass.

Even the earlier experiments of Taber indicated that the pressure effects accompanying freezing are due to the growth of *ice crystals* and that excessive heaving is to be explained by the segregation of water as it freezes. The success of these investigations is due to the fact that instead of "closed" soil systems Taber dealt with "open" systems. In a closed system no movement of water can take place into or out of the container, whereas in an open system there is both free access and free exit of water to or from the freezing soil. In a system open from below, the heave is greater than in a closed system. This is true because in the latter case the increase in volume is due to the freezing of interstitial water only, whereas in an open system water may be *drawn from below* and thus contribute to the formation of *ice lenses*

\* Most active in the field of frost research have been Stephen Taber<sup>9</sup> of the University of South Carolina, Arthur Casagrande<sup>10</sup> of Harvard University, and Gunnar Beskow,<sup>11</sup> a Swedish geologist working for the Swedish Institute of Public Roads.

within the earth mass. Most soils in the natural state behave as open systems. Taber's apparatus, based on the idea of an open system, is shown in Fig. 3:29. A thick-walled container *K*, filled with the soil to be tested, stands in a vessel containing dry sand *S*. Sand in the smaller vessel *W* is saturated, and moisture

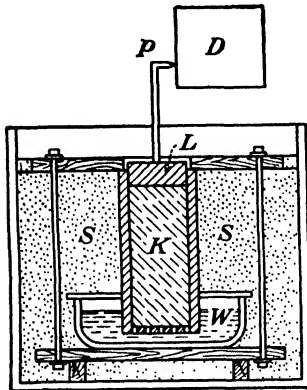


FIG. 3:29.—Taber's device for studying frost heaves.

therefrom may enter (or leave) the container *K* through perforations in its bottom. A heavy lead disk *L* is provided with a recording pen *P*, which traces a continuous line on the revolving drum *D*. Figure 3:30 shows ice lenses in frozen soil cylinders, as obtained in one of Taber's experiments. Ice appears in freezing soil also in the form of thin layers ("fibrous ice").

**3:20. Influence of the Size of Particles.**—Taber found that segregated ice forms easily in materials with a particle size of  $1 \mu$

(micron) or less. Large soil particles prevent ice segregation; for instance, mixtures of Ottawa sand (average diameter about 0.7 mm.) with clay did not show segregated ice upon freezing when the mixtures contained less than 30 per cent of clay. According to A. Casagrande, the critical diameter of particles so far as heave danger is concerned is 0.02 mm. If the amount of these particles is less than 1 per cent, no heave is to be expected, but considerable heaves may take place if this amount is over 3 and over 10 per cent in the case of nonuniform and very uniform soils, respectively.

Heaves in coarse sands, however, have been reported from several sections, among them the state of Michigan. This fact suggests that ice layers may form in all soils including coarse ones, containing moisture in excess.

**3:21. Conditions Necessary for the Frost-heave Formation.**—From Secs. 3:19 and 3:20 the following may be concluded:

A frost heave may occur in any soil provided there is an excess of moisture content either within the mass itself or coming from without. Only in the latter case the heave may be of a considerable size.

Additional moisture required for heave formation may reach the

upper freezing layer at a considerable rate under the following three conditions: (a) there should be a near-by source of water supply from which water may be pulled, in other words, a *shallow water table*; (b) the soil should be able to pull up moisture from that water table; in other words it should contain a certain percentage of *fine particles* (Sec. 3:20) [it is known that coarse soils can pull moisture through a very short distance only (Sec. 2:9)]; (c) the

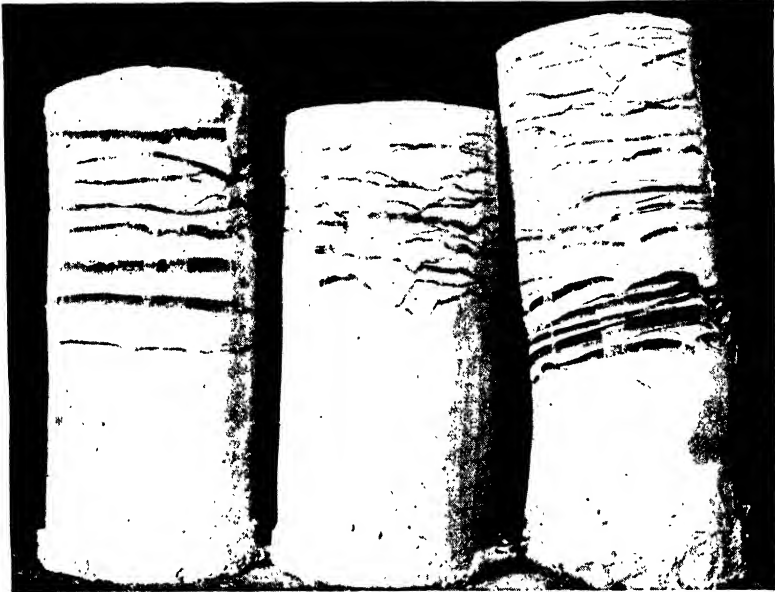


FIG. 3:30.—Ice lenses in frozen soil cylinders. (After Taber.)

way between the water table and the freezing upper layer should be unobstructed; in other words, the soil should possess *good permeability*.

The second and the third conditions are satisfied by both silts and clays; the third condition is better satisfied by silts. Hence, it may be concluded that so far as frost heaves are concerned, *silts are more dangerous than clays*. As already stated (Sec. 3:19) this conclusion is widely corroborated by observations.

It should be noticed that in the majority of cases a shallow water table is accompanied by a saturation of the soil due to capillary rise and condensation (Sec. 2:14). This saturation should still persist when the frost period starts, and to this condition necessary for the heave formation still another must be added, namely,

a gradual dropping of the temperature. In fact, if a sudden heavy frost comes at once, the pores become sealed, thus preventing the further access of moisture and vapor from below. Mild temperatures even somewhat below the freezing point do not stop this access, however (Sec. 3:19).

The volume of a heave obviously depends on the *duration* of that period favorable for the heave formation.

**3:22. Mechanics of the Heave Formation.**—There are two hypotheses explaining the frost-heave formation.

*Crystallization Force Hypothesis.*—From Fig. 3:31, which is a sketch given by Beskow, it may be seen that moisture constituting the adsorbed film is under the action of two forces (neglecting gravity), namely, the attractive force of the growing crystal (“crystallization force”) and the force keeping moisture at the surface of the particles (combined surface tension and molecular attraction due to “affinity,” Sec. 2:10). The fact that the crystal grows shows that the former force overcomes the latter, which still persists and tends to reestablish the thickness of the adsorbed film

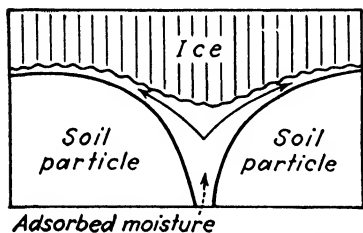


FIG. 3:31.—Growth of ice crystals.  
(After Beskow.)

by pulling water from lower strata. As the freezing isotherm shifts down, the undercooled moisture filling the pores freezes. Where the soil is looser, lenses are being formed. Crystals grow in the direction of cooling, *i. e.*, vertically and tend to lift the soil above. Field and laboratory measurements show that the height of a heave equals the sum of the thicknesses of the ice lenses at the same vertical.

*Condensation Hypothesis.*—The action of the crystallization force is fully recognized by this hypothesis, but it is believed that the freezing moisture is furnished also by the water vapor which moves from the water table upward and condensates *directly* in the form of ice. Formation of thick ice layers directly from air can be observed simply when home refrigerators are left for a certain time without defrosting.

**3:23. Experimental Evidence.**—There are numerous experiments concerned with the redistribution of moisture in a freezing sample. In an experiment by Taber the moisture contents at the

bottom of the sample were 29.0, 23.2, and 9.5 per cent before freezing and 20.8, 18.3, and 7.7 per cent after freezing, respectively. Figure 3:32 shows a redistribution of moisture in a sample with an unfrozen bottom.

**3:24. Technical Measures against Frost Action.**—Moisture accumulated in the upper layers of a frozen soil mass melts in the spring; and because it is prevented from percolating downward, it causes the softening of the mass and a consequent *decrease of shear resistance*. This is a period when many roads suffering from frost heaves cannot furnish adequate support to passing vehicles. Drainage to a reasonable depth may reduce the *frost-boil danger*.

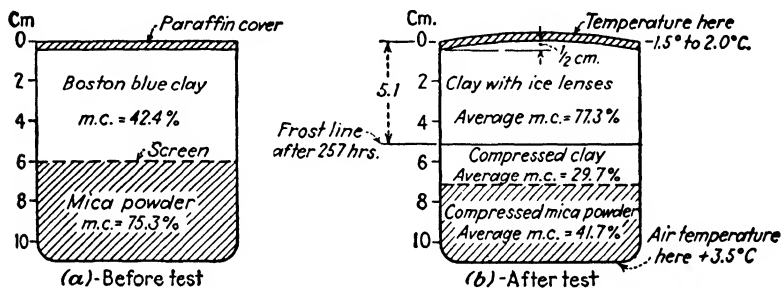


FIG. 3:32.—Redistribution of moisture within a frozen soil sample. (After A. Casagrande.)

It may appear at first glance that the softening in spring of the upper layers is due chiefly to the presence of water proceeding from melting snow. Extensive field investigations made in Sweden have shown that this is not exactly the case. The surface water may contribute somewhat to the softening of the mass, but the real cause of this phenomenon is the excess of moisture in the freezing earth mass itself.

Frost heaves in highway engineering may be relieved by using *insulators*. Sufficiently deep snow is a natural insulator, and sand layers 8 or 10 in. thick, located 12 or 15 in. below the road surface and provided with an outlet above the water level in the adjacent ditch, are considered as good insulators in Sweden. Various other types of insulators are also used. Use of calcium chloride or sodium chloride (common salt) in concentrations of  $\frac{1}{2}$  to 3 per cent by weight of a soil mixture eliminates frost action at temperatures down to  $-10^{\circ}\text{F}$ .<sup>15</sup> Sometimes frost-dangerous soils are removed partly or completely. So far as building construction and struc-

tural engineering are concerned, foundations are generally based *below the frost depth* to avoid possible heave in winter (Sec. 3:18). The force of heaving owing to the adhesion or freezing of the soil to the masonry or concrete of the structure, if any, is only negligible. In some cases, however, when natural frost acts accidentally within the building, there may be harmful consequences. The outside walls of a school building under construction (in West Haven, Conn.) were provided with adequately deep foundations, and the foundations of the inside walls were 14 in. below the basement floor. This depth would be entirely sufficient if the construction took place in summer. But the work started early in the spring, and very soon the inside walls cracked. Inspection revealed that besides the effect of cold weather, the water table was less than 2 ft. deep, and this caused heaving of the ground.

Special attention should be paid to the action of artificial frost within *cold-storage warehouses*. The working temperature in such buildings may be 14°F. or lower almost continuously over a period of years. As a result, the frost depth may reach several feet, and in one occasion a depth of 9½ ft. below the ground surface was reported. The freezing isotherm descends deeper at the center of a cold store than at its perimeter and near open corridors where normal temperature prevails. Lightly loaded floors present small resistance to heaving; hence they heave and crack first, followed by heavier parts of the building. The thawing out of a damaged cold store should be done *very gradually*, since a sudden release of the excess of moisture that was being pulled from deeper strata for years may convert the soil supporting the building into mud in the same way as the roads in the spring (see the beginning of this section). Cork insulation or introduction of a source of heat between the building and the soil during its construction or reconstruction may help the situation. If the water table is close to the floor, as is possibly the case of the basement of a cold-storage warehouse, good drainage around the building should be designed to divert the surface water.<sup>12</sup>

As a general precaution, *careful observations of the water table* and its fluctuations should precede the construction of every important project that may be damaged by natural or artificial frost.

The frost danger should not be overestimated, however, in built-up areas where the frost action is decidedly smaller than in the adjacent open country. Large, well-heated buildings may sub-

stantially modify the temperature regime of the surrounding earth mass.

**3:25. Perennially Frozen Soils.**—Literature on this subject exists in English<sup>13-16</sup> and in Russian.<sup>17</sup> The area occupied by the perennially frozen soils in Russia is larger than the area of the continental United States. A brief information on the Alaskan perennially frozen soils is given hereafter. Throughout most of Alaska, except a coastal zone in the south and southeast, the subsoil is perennially frozen to depths varying from a few inches to 300 ft. and more. The surface soil is subjected to seasonal thawing permitting vegetation but followed by refreezing. The frozen ground contains masses of relatively pure ice, partly in lenses, partly in the form of veins which, in places, merge into overlying ice layers up to 12 ft. in thickness. In some areas ice amounts to 80 per cent of the volume of frozen ground. Heaves up to 7 to 8 ft. high were observed. According to geological data the deep freezing in Alaska occurred apparently in early Pleistocene time, perhaps a million years ago.

**3:26. Lifting of Stones.**—Buried stones, mostly elongated or wedge-shaped downward, are lifted up by the frost action and finally may reach the earth surface. Very little or no uplift of a buried stone occurs during freezing; but during thawing the softened soil tends to settle around the stone which is upheld by the frozen soil below. Taber observed even the downward movement of stones.

### Problems

1. Trace the net of streamlines and equipotential lines under a concrete block (dam model) placed in an experimental box on top of the earth surface. The experimental box is similar to the model flume in Fig. 9:26. Its dimensions are 16 by  $8\frac{1}{2}$  by  $3\frac{1}{2}$  in.; dimensions of the concrete block are 3 by 3 by  $3\frac{1}{2}$  in. Assume two-dimensional (plane) flow.
2. Trace the flow net under the model of a sheet-piling wall driven 10 in. below the earth surface in an experimental box, the dimensions of the latter being 16 by 16 by  $3\frac{1}{2}$  in.
3. The dimensions of a small earth dam are width of the crown, 10 ft.; height, 40 ft. The upstream face is 1 height for  $2\frac{1}{2}$  bases, and the downstream face is 1 height for 2 bases. The freeboard, or the vertical distance from the plane of the crown to the level of the water, is 5 ft. Locate the saturation line, and compute the amount of seepage through that dam. Assume a coefficient of permeability and an impervious foundation.
4. Compute the daily loss from the canal shown in Fig. 3:27, assuming  $L = 400$  ft. and  $h = 10$  ft. Assume the value of the coefficient of perme-

ability  $k$  and the slope of the ground water table  $i_0$ . In this case does the width of the canal influence the amount of loss from it? Why?

5. For constructing a lock on the Mississippi River, at Trempealeau, Wis., the cofferdam shown in Fig. 3:33 was constructed. Curves 1, 2, 3, 4, 5, and 6 are flow lines; the saturation line (perpendicular to the steel sheet piling and tangential to the wood one) is not numbered. The velocities of seepage (see table) were determined by fluorescein dye on a model one twenty-fourth of the prototype in which the same Mississippi River sand was used. Are these velocities the same for the model and the prototype? Why?

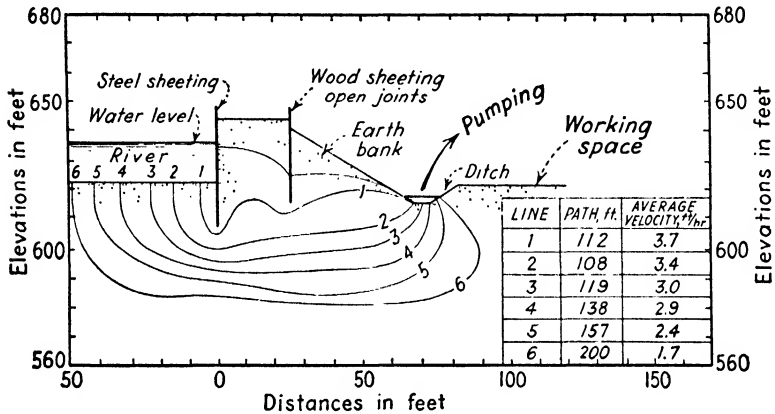


FIG. 3:33.—Trempealeau, Wis., Cofferdam. (From Lazarus White and Edmund A. Prentis, "Cofferdams.")

Increase the scale of Fig. 3:33, and trace a complete flow net. Compute the average coefficient of permeability from the table, and estimate the amount of water reaching the drainage ditch where the pumps were installed. Neglect (a) the seepage beyond flow line 6, (b) the capillary flow above the saturation line. How high, in your opinion, does the capillary water rise above the saturation line (a) in the model and (b) in the prototype?

6. What thickness, in your opinion, should be given to the blankets in Figs. 3:19 and 3:22?

7. Assume reasonable dimensions of the rock fill in Fig. 3:23 for an earth dam 100 ft. high.

#### References

1. M. MUSKAT: "The Flow of Homogeneous Fluids through Porous Media," McGraw-Hill Book Company, Inc., New York, 1937.
2. DONALD W. TAYLOR: "Notes on Soil Mechanics" (lith.), Massachusetts Institute of Technology, Cambridge, Mass., 1938.
3. E. W. LANE, F. B. CAMPBELL, and W. H. PRICE: *Civil Eng.*, New York, vol. 4, 1934.
4. J. KOZENY: *Die Wasserwirtschaft*, vol. 26, 1933.
5. ARTHUR CASAGRANDE: Seepage through Dams, *New Eng. Water Works Assoc.*, vol. 51, 1937. An outstanding paper.

6. F. E. TURNEAURE and H. L. RUSSELL: "Public Water Supplies," John Wiley & Sons, Inc., New York, 1924.
7. U. S. Geol. Survey Water Supply and Irrigation Papers, No. 67, 1902, and No. 140, 1905; see also ref. 6.
8. K. VON TERZAGHI: *Die Wasserwirtschaft*, vol. 23, 1930. Other information on the seepage from canals: J. KOZENY: *ibid.*, vol. 26, 1933; R. DACHLER: "Grundwasserströmung," Verlag Julius Springer, Berlin, 1936; V. V. WEDERNIKOW: *Wasserkraft und Wasserwirtschaft*, vol. 29, 1934, and *Z. angew. Math. Mech.*, vol. 17, 1937; C. G. J. VREEDENBURGH and O. STEVENS: *Proc. First Congr. on Large Dams*, vol. 4, 1933; C. G. J. VREEDENBURGH: *Proc. Intern. Conf. Soil Mech., Paper K-2*, 1936.
9. STEPHEN TABER: *Jour. Geol.*, vol. 37, 1929; vol. 38, 1930; also *Public Roads*, vol. 11, 1930.
10. ARTHUR CASAGRANDE: *Proc. Eleventh Ann. Meeting, Highway Research Board*, vol. 11, 1931; *Eng. News-Record*, vol. 115, 1935; also in German, *Die Strasse*, 1935.
11. GUNNAR BESKOW: *Communications* 30 and 48 of the Swedish Institute of Public Roads (Svenska Väginstitutet); also, in German, a special publication of *Die Strasse*.
12. L. F. COOLING and W. H. WARD (both of the Building Research Station, England): *Damage to Cold Stores Due to Frost Heaving*, a paper read before the Institute of Refrigeration, London, Dec. 14, 1944.
13. STEPHEN TABER: *Perennially Frozen Ground in Alaska: Its Origin and History*, *Geol. Soc. Am. Bull.*, 54, 1943.
14. W. A. JOHNSTON: *Frozen Ground in the Glaciated Parts of Northern Canada*, *Trans. Roy. Soc. Can.*, vol. 24, 1930.
15. H. F. WINN: *Frost Action in Highway Subgrades and Bases*, *Proc. Purdue Conf. Soil Mech.*, 1940.
16. WAR DEPARTMENT *Technical Bulletin* TB5-255-3. *Construction of Runways, Roads, and Buildings on Permanently Frozen Ground*, Washington, D. C., 1945.
17. M. I. SOUMGIN: *Permanently Frozen Soil in the Limits of the U.S.S.R.*, *Acad. Sci. U.S.S.R.*, Moscow, 1937; and a large number of other publications in Russian on the same subject.



PART TWO  
ELEMENTS OF THE  
MECHANICS OF EARTH MASSES



## CHAPTER IV

### STRESSES IN EARTH MASSES

#### A. GENERAL

**4:1. Basic Problem of Soil Mechanics.**—A structure and the earth mass supporting it represent *a unit* and *act together*. This is true for any masonry, timber, or metallic structure and for any structure made of earth (such as an earth dam).

The designer of any structure has to answer the following two questions and in the following order:

*a.* Will the natural earth mass under the proposed structure support the structure and the superimposed loads, or will it fail (*i. e.*, be destroyed in some way)? And the structure itself, if made of earth, will it stand successfully, or will it fail?

*b.* If the earth masses mentioned in the preceding question do not fail, what is the order of magnitude of their deformations (changes in shape, displacements)? Are these deformations harmful for the purpose to be served by the proposed structure?

In a general case, if the earth mass supporting the structure fails, the structure necessarily will fail with it.

The two questions *a* and *b* constitute two parts of the *basic problem* of soil mechanics.

They may be also referred to as two classes of independent problems. In this case they are termed (*a*) *stability problems* and (*b*) *deformation* (or *elasticity*) *problems*.

**4:2. Idealized Earth Masses.**—The basic problem as considered in Sec. 4:1 is essentially a problem of mechanics and involves the determination of stresses and strains. This can be done only if actual earth masses are idealized, *i. e.*, assumed to possess properties that in reality they may or may not possess (for instance, elasticity). It is possible to devise theories of stress distribution in idealized uniform and homogeneous bodies, but it is very difficult to compute stresses in actual heterogeneous and nonuniform earth masses. The usual procedure is to *assume* that stresses in an actual earth mass are the same as in an idealized body loaded in

the same way as the given earth mass. Stresses thus computed are no closer to the reality than the actual earth mass is to the chosen idealized body. Thus stresses in actual earth masses are not computed, but only *estimated*. To be more sure of the result, it is advisable to make different assumptions and to try to determine two limit values of a given stress such that the true value is somewhere between them. The more limited the range of values thus obtained the better.

Idealized bodies as used in soil mechanics are of two kinds: (a) homogeneous, elastically isotropic bodies, termed "elastic continua" hereafter,\* and (b) homogeneous masses made of idealized fragmental material, termed "idealized fragmental masses" hereafter.

An *elastic continuum* has been already characterized in Sec. 3:8. Such a body is made of one material throughout; *i.e.*, it is homogeneous. The stress propagation in all directions obeys the same laws; *i.e.*, the body is isotropic. Furthermore this body is a continuum; in other words, it has no pores at all. It is perfectly elastic; *i.e.*, it obeys Hooke's law as explained hereafter; and if loaded not over a certain limit, it recovers its shape completely as soon as external forces are removed. Since there are no pores in such a body, there are no individual particles and hence there is no friction between them. Matter forming such a body is held together by molecular forces. Igneous rock strata and stiff clays may be considered as elastic continua.

An idealized fragmental mass is assumed to be porous; and owing to a certain roughness of the particles, *friction* occurs between them. On some occasions particles forming an idealized fragmental mass are assumed to be glued to neighboring particles by the force of *cohesion*.

Conditions of stability of idealized fragmental masses (*i.e.*, their safety against destruction) are considered in the *theory of plasticity*, but similar conditions do not deal with deformations. Hence the theory of plasticity may be used in solving the first part of the basic problem ("stability problems") which deals with the ultimate failure of the mass, but not with its deformations.

In contrast, in the *theory of elasticity* deformations (only up to the so-called "elastic limit") are considered, but conditions of

\* "Elastic continua" is a plural. The singular of this expression is "elastic continuum."

failure are not discussed at all. Hence it is convenient to use this theory in solving the second part of the basic problem ("deformation" or "elasticity" problems).

Both the theory of elasticity and the theory of plasticity are used in soil mechanics in an exceedingly simple way.

Notice that both elastic continua and fragmental masses are assumed to be isotropic. It appears at the first glance that a porous

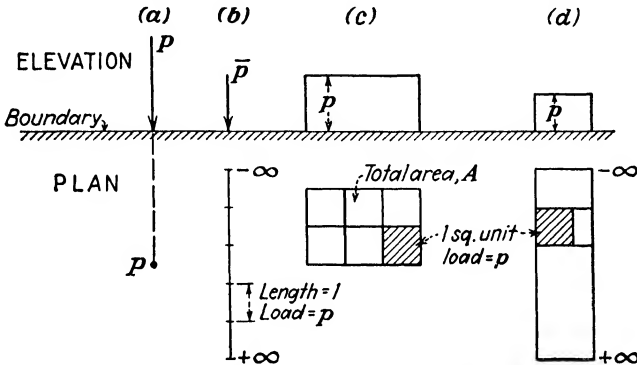


FIG. 4:1.—Superimposed loads: (a) concentrated or point load; (b) line load; (c) uniformly distributed load over area  $A$ ; (d) strip load.

material cannot be isotropic, because the law of stress propagation in a solid particle is not the same as in an adjacent pore. It is assumed, however, that at a certain depth, because of a great number of grains or particles placed at random, stress propagation in an idealized fragmental mass takes place as if that mass were isotropic. This is the so-called "statistical isotropy."

**4:3. Superimposed Loads.**—Loads acting on a semi-infinite earth mass are assumed vertical unless otherwise specified. They act at the boundary of the mass, but not below the boundary. A superimposed force may be (a) a concentrated load or a point load (Fig. 4:1a), (b) a "line load" (Fig. 4:1b) with an intensity of say,  $\bar{p}$  units of weight per unit of length,\* or (c) a uniformly or non-uniformly distributed load along a portion of the surface ( $p$  units of weight per square unit of surface). In a particular case this loaded portion may represent a narrow strip (Fig. 4:1d). If the loaded line or the loaded strip are infinitely long, the stress distribution is the same in all planes perpendicular to the direction of the line or the strip in question. It is said in this case that the problem

\* Note the bar above the letter  $p$  in the symbol  $\bar{p}$  for the line load.

to be solved is not a three-dimensional or space problem as is a general case but only *two-dimensional* or *plane*. In reality, every two-dimensional problem is a particular case of a three-dimensional one. A two-dimensional problem as represented on a drawing must be visualized as being one unit deep (in the direction normal to the drawing). If all dimensions of the drawing are in feet, this depth is 1 ft.

*Example.*—Stress distribution behind long retaining walls at cross sections remote from the ends is computed as if the problem were two-dimensional, and in the case of a long wall this is a satisfactory approximation. Strictly speaking, close to the ends of the wall the stress distribution should be considered again as three-dimensional.

**4:4. Normal and Tangential Stresses.**—Forces acting at the boundary of the semi-infinite earth mass and body forces such as

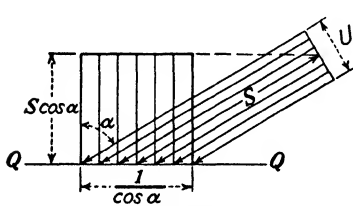


FIG. 4:2.—Projection of a stress.

weight of the mass itself or action of percolating water cause stresses within the mass. The difference between force and stress should be emphasized. A stress is the ratio of the force acting on a small area within the mass to that area when the latter is becoming smaller and smaller. It is expressed in pounds per square inch or in tons per square foot and in kilograms per square centimeter or in tons per square meter in metric measures.\* In other words, what is meant by the term "stress" is in reality "stress intensity."

Again, difference between force and stress may be clearly understood if projections of both are considered. The projection of a force  $P$  on a direction making the angle  $\alpha$  with the direction of that force is  $P \cos \alpha$ , whereas the projection of a stress  $S$  on a direction making the same angle  $\alpha$  with the direction of the stress is  $S \cos^2 \alpha$ . This is true because not only the projection of the force  $S$  constituting the stress is considered but also that of the area on which this force is acting. In Fig. 4:2 a stress  $S$  tons per sq. ft. is acting at an angle  $\alpha$  to the normal to a plane  $QQ$ . The projection of the force  $S$  on the normal is  $S \cos \alpha$  tons; the latter force acts on an area  $1/\cos \alpha$  sq. ft., which gives the stress intensity  $S \cos \alpha \div 1/\cos \alpha = S \cos^2 \alpha$  tons per sq. ft.

\* One kilogram per square centimeter practically equals 1 ton per sq. ft.

It is customary to break stresses acting obliquely to a plane into a component normal to this plane (designation  $\sigma$ ) and another tangential to it (designation  $\tau$ ) (Fig. 4:3). Referring to Fig. 4:3, the projection of the force  $S$  tons, constituting the stress in the plane  $QQ$ , is  $S \sin \alpha$  tons; the latter force acts on an area  $1/\cos \alpha$  sq. ft., which gives the stress intensity of the shear  $S \sin \alpha \div 1/\cos \alpha = S \sin \alpha \cos \alpha$  tons per sq. ft. (see again Fig. 4:3). Thus, *normal* stresses and *tangential* or *shearing* stresses (or simply shears) are considered. Normal stresses, according to their direction with respect to the plane of action, may be *compression* stresses and *tensile* stresses. It follows from the definition of an idealized elastic continuum and of an idealized fragmental mass that the former can resist tensile stresses whereas such stresses are impossible in the case of a fragmental mass if the latter does not possess cohesion that could resist a tensile stress.

*Angle of Obliquity.*—The angle formed by the stress  $S$  with the normal to the plane on which that stress is acting is the *angle of obliquity* ( $\alpha$  in Fig. 4:3; designation  $\psi$  will be used hereafter).

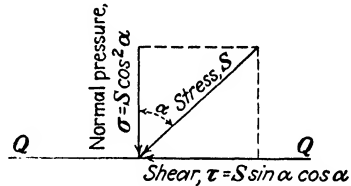


FIG. 4:3.—Normal and tangential stress.

*Sign of the Compression Stress.*—It is customary in mechanics to designate tensile stresses as positive and compression stresses as negative. Since tensile stresses are seldom considered in soil mechanics, compression stresses are generally considered positive, and the plus sign is omitted.

**4:5. Plane Stress; Principal Stresses.**—In Fig. 4:4 a line load  $\bar{p}$  will first be considered. Assuming straight-line stress propagation, the vector corresponding to stress  $S$  at point  $O$  of the mass will be a continuation of the line  $AO$ , which joins point  $A$ , that of application of load  $\bar{p}$ , with point  $O$ . Stress  $S$  is normal to a plane  $QQ$ . It exerts normal pressure on that plane and produces no shear along it. The stressed condition at point  $O$  (Fig. 4:4a) is thus characterized by one vector  $S$  only.

If there are several loads at the boundary or if a portion of the boundary is loaded with distributed load, the situation is different. In Fig. 4:4b four loads  $\bar{p}_1, \bar{p}_2, \bar{p}_3, \bar{p}_4$  produce stresses  $S', S'', S''', S^{IV}$  at point  $O$ . Each of these stresses in striking a plane  $QQ$  drawn

through point  $O$  may be resolved in a pressure on and a shear along that plane, in the way shown in Figs. 4:2 and 4:3. The shears act along plane  $QQ$ , some in one direction and some in an opposite, and a position of plane  $QQ$  may be found such that the shears acting along that plane mutually balance at point  $O$ . Then plane  $QQ$  is the *principal plane*, and the normal to it  $On$  is the direction of the *major* (or maximum) *principal stress*  $\sigma_1$ . The value of the

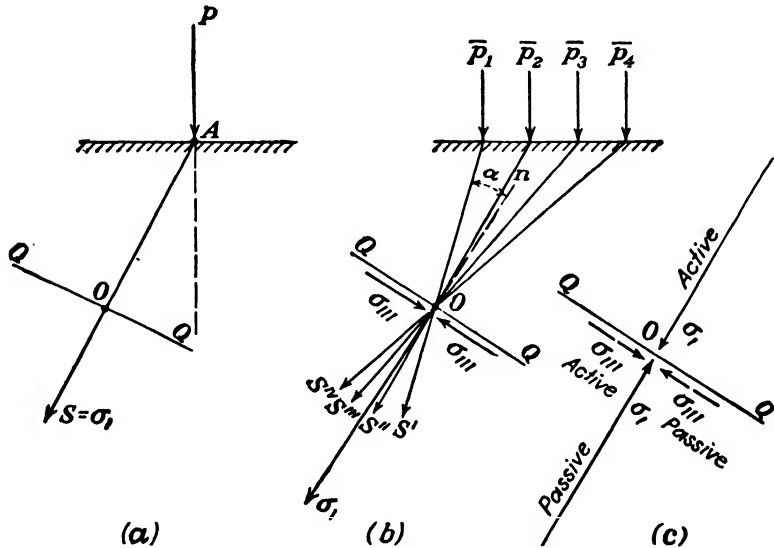


FIG. 4:4.—Principal stress in a plane problem.

major principal stress  $\sigma_1$  is found by projecting all the stresses at point  $O$  on the normal  $On$ . Thus, the projection of the stress  $S'$  on the normal  $On$  is  $S' \cos^2 \alpha$  (Fig. 4:4b).

Consider another plane passing through point  $O$  and normal to plane  $QQ$ . If stresses  $S'$ ,  $S''$ ,  $S'''$ , and  $S^{IV}$  shown in Fig. 4:4 are projected on the normal to that plane which is line  $QQ$ , shears would again mutually balance at point  $O$ . This is *another* principal plane, and the normal to it  $QQ$  is the direction of the *minor* (or minimum) *principal stress*  $\sigma_{III}$ .

Thus in case of several line loads or of a strip load (Fig. 4:4b), the stressed condition is expressed by two vectors  $\sigma_1$  and  $\sigma_{III}$ , which are *pressures* on two mutually normal, principal planes. Extending this statement to the case of one concentrated load

(Fig. 4:4a), it may be said that in that case there are also two principal stresses:

$$\sigma_1 = S; \quad \sigma_{111} = 0$$

In a space or three-dimensional problem there would be *three* and not two principal stresses: the major  $\sigma_1$ , the intermediate  $\sigma_{111}$ , and the minor  $\sigma_{111}$ . In a plane stress distribution the intermediate principal stress  $\sigma_1$ , acts normally to the plane in which the other two principal stresses  $\sigma_1$  and  $\sigma_{111}$  act (plane of drawing, Fig. 4:4) and is not considered.

**4:6. Equilibrium of Stresses.**—If a mass is in equilibrium, the stresses at each and every point of it are in equilibrium. Owing to the *law of equality of action and reaction*, a stress caused by the load (active stress) is balanced by an equal and opposite stress furnished by the mass (passive stress, resistance of the mass). The stressed condition at point *O* (Fig. 4:4c) is represented by two pairs of principal stresses  $\sigma_1$  and  $\sigma_{111}$ . Furthermore, *each and every part* of the mass in equilibrium is in equilibrium under

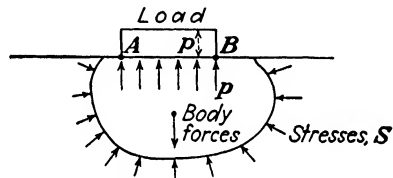


Fig. 4:5.—Stresses must satisfy statics, strains must satisfy geometry.

the action both of the stresses acting at the outside surface of that part and of the superimposed loads applied to that part, including body forces such as gravity (Fig. 4:5). Finally, again due to the *law of equality of action and reaction*, the stress in the mass at each and every point of the boundary *AB* balances the unit load *p* applied at that particular point. If the load in Fig. 4:5 is a loading plate or a structure, the stresses at that plate or structure balance the stresses in the mass at each and every point of the loaded boundary. These are the so-called *boundary conditions*.

**4:7. Mohr's Circle.**—The stressed condition at a point of the mass may be characterized by the stresses acting not only on the principal planes but on *any two mutually normal planes* passing through the given point. Presumably there will be not only normal pressures on but also shears along these new planes. Designate with  $\alpha$  the angle made by the direction of the major principal stress with the normal to the plane that the normal pressure on and the shear along which are to be determined. The following discussion is conducted for a horizontal plane, so that

the angle  $\alpha$  is the angle made by the direction of the major principal stress  $\sigma_1$ , with the vertical. This discussion is valid, however, for any plane passing through the given point.

The following designations will be used hereafter:

$\sigma_z$  = vertical pressure (normal pressure on the horizontal plane).

$\sigma_x$  = horizontal pressure (normal pressure on the vertical plane).

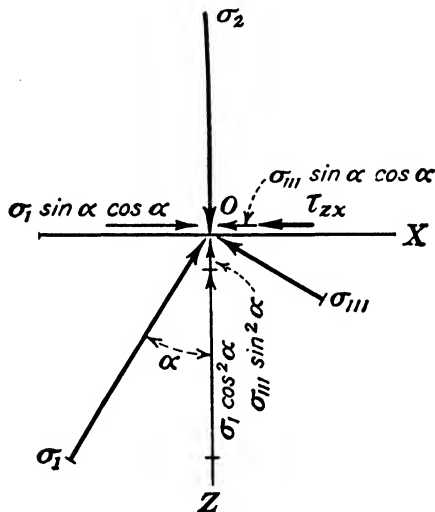


FIG. 4:6.—Vertical pressure and horizontal shear computed from principal stresses.

$\tau_{zx}$  = shear along the horizontal plane.

$\tau_{zx}$  = shear along the vertical plane.

Trace a horizontal plane  $OX$  through point  $O$  in Fig. 4:4c, and replace the principal stresses  $\sigma_1$  and  $\sigma_{33}$  above that plane by a vertical pressure  $\sigma_z$  on and a shear  $\tau_{zx}$  along the horizontal plane (Fig. 4:6). Let point  $O$  be the origin of coordinates, the axis  $OZ$  being directed downward, as usually done in soil mechanics. Since the stresses  $\sigma_z$ ,  $\tau_{zx}$ ,  $\sigma_{11}$ , and  $\sigma_{33}$  (the last two being below the horizontal plane  $OX$ ) are in equilibrium, the sums of their projections on the axes  $OX$  and  $OZ$  equal zero, from which

$$\begin{aligned}\sigma_z &= \sigma_1 \cos^2 \alpha + \sigma_{33} \sin^2 \alpha \\ \tau_{zx} &= (\sigma_1 - \sigma_{33}) \sin \alpha \cos \alpha = \frac{1}{2} (\sigma_1 - \sigma_{33}) \sin 2\alpha \quad (4:1)\end{aligned}$$

To obtain the values of  $\sigma_z$  and  $\tau_{zx}$  graphically, if the principal



In most cases such a confusion is not harmful; but at any rate the difference between the two terms must be clearly understood.

**4:9. Principle of Continuity.**—In a general case, no continuity can be expected from an actual earth mass, and the discussion that follows, refers to idealized masses.

Strains within an idealized mass must be *continuous*; this means that any curve smooth and without breaks, mentally drawn within a mass before deformation, remains *smooth and without breaks* after deformation. In a two-dimensional problem the expression “smooth curve without breaks” means that at any point of such a curve only one tangent, not two, can be drawn. From this standpoint, a straight line should be considered as a smooth curve without breaks. It follows that the horizontal boundary of an idealized semi-infinite mass must be smooth and without breaks when deflected. If in a two-dimensional problem a case of failure of an idealized fragmental mass is considered, the probable line of separation of the two parts of the mass (“failure line”) must also be smooth and without breaks.

Furthermore, the mass itself must be a continuum before, during, and after the deformation. For instance, it cannot break into two or more parts during the deformation. Particles of an idealized cohesionless fragmental mass are assumed to be kept tight together and to have but *very small relative displacements*.

**4:10. Principle of Superposition.**—What is meant by superposition is simple addition at a point of very small strains if displacements corresponding to these strains are along the same direction. If Hooke’s law holds, strains are proportional to stresses; hence in this case (and strictly speaking, *only* in this case) the stresses acting in the same direction may also be simply added.

Other limitations of this principle should be clearly understood: (a) If acting forces produce considerable settlements (deformations) of the surface of the mass, the principle of superposition is not valid any longer. (b) This principle cannot be applied to fragmental masses at shallow depths, because in this case Hooke’s law does not hold.

**4:11. Saint-Venant’s Principle.\***—According to this principle the forces acting on a small portion of a body may be replaced by another statically equivalent system of forces acting on the same

\* Adhémar Barré de Saint-Venant, a French mathematician, civil engineer, and agriculturalist, advanced this principle in 1853.

portion of the surface. In this replacement there is only a negligible effect on the stresses at distances that are large in comparison with the dimensions of the actually loaded portion of the surface. Admittedly, the change in stresses close to the loaded portion is considerable in the case of such a substitution, but this change is purely local. Saint-Venant's principle is of great importance in foundation studies, since it permits the substitution of complicated force systems acting at the boundary of an earth mass with their resultant (a concentrated force) if stresses are to be determined at great depths.

**4:12. Requirements to Be Satisfied by a Stress-distribution Theory.**—A stress-distribution theory in an idealized mass must satisfy the following three conditions:

- a. Stresses must satisfy statics (Sec. 4:6).
- b. Strains must satisfy geometry (Sec. 4:9).
- c. Properties of the material must be considered; in other words, the value of a strain must be expressed in terms of the corresponding stress graphically or analytically. The three conditions mentioned are those commonly accepted in structural engineering. They have been clearly formulated by Cross.<sup>1</sup>

In the theory of elasticity, which is the mechanics of an elastic continuum, these conditions are satisfied so that no checking is needed if formulas of the theory of elasticity (or simply "elastic formulas") are used. If some other theory for the study of deformations in the mass is proposed, careful checking should be made, especially whether or not the principle of continuity is satisfied in that theory.

The stress-strain relationship as used in the theory of elasticity is the direct proportionality between stress and strain. This is the well-known Hooke's law.\*

## B. STRESSES IN AN ELASTIC CONTINUUM

In determining the stresses in an elastic continuum as caused by superimposed load, it is assumed that the elastic continuum in question (idealized earth mass) is *weightless*. If the total stress as caused by both the weight of the continuum and the superimposed loads is required, both kinds of stresses are computed and summed

\* Robert Hooke (1635–1703) was an English experimental philosopher, professor of geometry in Gresham College.

up, since in this case the principle of superposition holds (Sec. 4:10).

**4:13. Elastic Constants.**—Hooke's law may be expressed by Eq. (4:3):

$$S = E\epsilon \quad (4:3)$$

where  $S$  = stress.

$\epsilon$  = strain.

$E$  = modulus of elasticity.

The latter is practically constant for many materials, but not for soils, except some in particular cases. In the theory of elasticity, the modulus of elasticity  $E$  is assumed constant. Hence the first limitation of the formulas of the theory of elasticity (or "elastic formulas," as is often said) is the requirement of an approximately constant modulus of elasticity. Since the strain  $\epsilon$  is an abstract number, the modulus of elasticity is expressed in terms of stress.

When a sample made of a homogeneous elastically isotropic material  $L$  units long and  $B \times B$  units in cross section is subjected to compression, there is a decrease in length  $dL$  and an increase  $dB$  in the length  $B$  of each side of the cross section. Hence, in the case of a compression of the sample in question, there is an axial strain  $dL/L$  and a transversal strain  $dB/B$ . The ratio of the transversal strain  $dB/B$  to the axial strain  $dL/L$  is called Poisson's ratio,\*  $\mu$ :

$$\mu = \frac{dB}{B} \div \frac{dL}{L} \quad (4:4)$$

In technical applications, instead of Poisson's ratio  $\mu$  its reciprocal  $m = 1/\mu$  is often applied. Obviously, Poisson's ratio is expressed by an abstract number.

**4:14. Stresses within an Earth Mass That Are of Importance in the Design of Structures.**—These stresses are:

*a. The vertical pressure  $\sigma_z$*  (designated sometimes by  $p_z$ ). The knowledge of this value is of great importance in the theory of consolidation of soft, deep layers as discussed in Chap. VI.

*b. The maximum shear stress,  $\tau_{\max}$ ,* at different points close to the boundary, especially in the neighborhood of the edges of the structure. This value is especially important in computations

\* S. D. Poisson (1781–1840), a French scientist, was one of the founders of the theory of elasticity.

of stability of foundations, particularly those of earth dams. These two stresses,  $\sigma_z$  and  $\tau_{\max}$ , will be discussed hereafter. The corresponding formulas unless otherwise specified are based on the theory of elasticity.

**4:15. Vertical Pressure.**—*a.*

*Boussinesq Formula.*—A load  $P$  applied at the horizontal boundary of a homogeneous elastically isotropic mass produces at a point  $O$  a vertical pressure  $\sigma_z$  (Fig. 4:8). To determine it, the following formula, known as the “Boussinesq formula,” was published in the Report of a Special Committee on Earths and Foundations of the A.S.C.E.:<sup>2</sup>

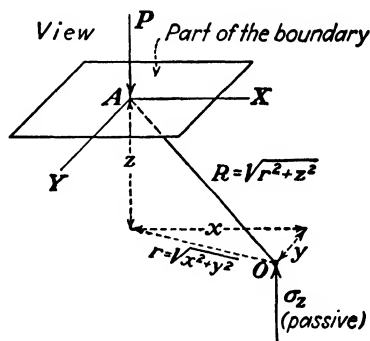


FIG. 4:8.—Vertical pressure within an earth mass.

$$\sigma_z = k \frac{P}{z^2} \tag{4:5}$$

in which

$$k = \frac{3}{2\pi} \frac{1}{\left[1 + \left(\frac{r}{z}\right)^2\right]^{\frac{5}{2}}} \tag{4:6}$$

For designations  $r$  and  $z$ , see Fig. 4:8. If we compute the ratio  $r/z$  from that figure, the corresponding values of the coefficient

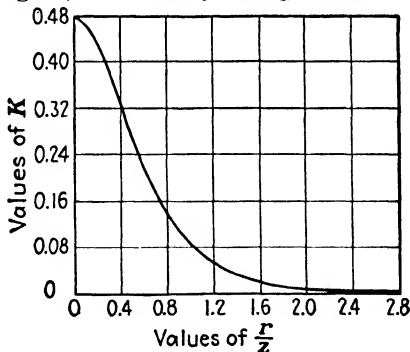


FIG. 4:9.—Values of  $k$  for use in Boussinesq formula.

$k$  [formula (4:6)] may be readily found from the graph, Fig. 4:9. There are also tables<sup>2</sup> to find the value of the coefficient  $k$  from

the ratio  $r/z$ . Formula (4:6) is simple enough to permit direct computations if such tables or graphs are not available. If we designate with  $R$  the value of the radius vector of point  $O$  which equals  $\sqrt{r^2 + z^2}$ , formula (4:5) may be represented thus:

$$\sigma_z = \frac{3P}{2\pi} \frac{z^3}{R^5} \quad (4:7)$$

*Example.*—Assume a load of 4,500 tons applied as a point concentration at the surface. Determine the vertical pressure  $\sigma_z$  at a point 40 ft. below the load and 15 ft. away horizontally. In this case  $z = 40$  ft. and  $r = 15$  ft., so that  $r/z = 0.375$ . The value of the coefficient  $k$  as computed by formula (4:6) is  $k = 0.3436$ , and the vertical pressure  $\sigma_z$  is found thus:

$$\sigma_z = 0.3436 \times \frac{4,500}{40^2} = 0.97 \text{ tons per sq. ft.}$$

If a combination of point loads is given, the stress intensities  $\sigma_z$  at a point from the several loads may be added, since in the case of an elastically isotropic body the principle of superposition holds.

If a loaded portion is given, it may be subdivided into small rectangles, and loads acting at each rectangle may be replaced by concentrated loads, as is done in the example that follows. Another way to compute vertical pressure  $\sigma_z$  from a loaded portion is to apply existing tables, graphs, or methods of graphic integration.\*

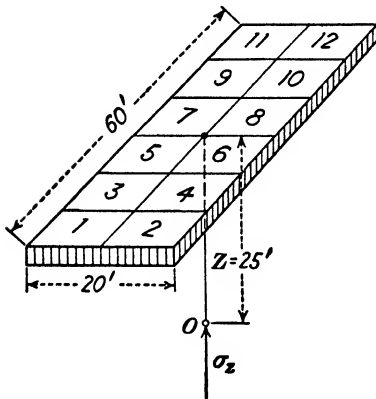


FIG. 4:10.—Vertical pressure,  $\sigma_z$ , under the center of a raft. (From *Proc. A.S.C.E.*, May, 1933, p. 784.)

*Example.*—The vertical pressure is to be computed at a point 25 ft. directly below the center of a nonrigid raft foundation 20 ft. wide and 60 ft. long (Fig. 4:10) carrying a uniform load of 3 tons per sq. ft.

*Solution.*—The raft is subdivided into 12 squares, and the vertical pressure  $\sigma_z$  from three squares only is computed and multiplied by 4, since the system is symmetrical about both center lines. Taking the squares 1, 3, and 5, the respective values of  $r$  (in feet) are  $5\sqrt{26}$ ,  $5\sqrt{10}$ , and  $5\sqrt{2}$ . The ratios  $r/z$  are therefore 1.020, 0.632, and 0.283, respectively. The corresponding coefficients  $k$  furnish a sum  $0.08 + 0.21 + 0.39 = 0.68$ , and the vertical pressure

$$\sigma_z = 4 \times 0.68 \times \frac{300}{25^2} = 1.31 \text{ tons per sq. ft.}$$

\* See Appendix B.

It is to be emphasized that this is the *maximum* unit pressure at the given level.

*b. The 60° and the 2-to-1 Method.*—The Building Code of the City of Boston, Mass., recommends the determination of the vertical pressure  $\sigma_z$  on the assumption that the load is spread uniformly at an angle of 60° with the horizontal. This is a purely empirical rule. In the case of overlapping, pressures from adjacent structures should be added.

Even simpler and at the same time somewhat more conservative is the 2-to-1 method, in which the load is supposed to spread under a slope of two heights to one base. Assume the dimensions of the structure at the level of the ground  $a$  and  $b$ . Then at a depth  $z$  the weight of the structure would spread approximately on a rectangle with the sides  $a + z$  and  $b + z$ . The maximum pressure may be roughly estimated at 150 per cent of the average. In the case of medium-sized structures such as bridge piers, the results obtained by this method and by using the Boussinesq formula are sometimes very close.

*Example.*—Applying the 2-to-1 method to the case of Fig. 4:10, the total pressure on the structure is  $3 \times 20 \times 60 = 3,600$  tons, and the area on which it spreads at the depth  $z = 25$  ft. is  $(20 + 25) \times (60 + 25) = 3,825$  sq. ft. Hence the average (but *not* the maximum) vertical pressure  $\sigma_s$ , at that level

$$\sigma_s = \frac{3,600}{3,825} = 0.94 \text{ tons per sq. ft.}$$

Estimated maximum pressure

$$\sigma_s = 0.94 \times 1.5 = 1.41 \text{ tons per sq. ft.}$$

*c. Vertical Pressure Caused by a Line Load.*—Replace load  $P$  in Fig. 4:8 by an infinitely long line load of intensity  $p$  per unit of length. As before, let  $R = \sqrt{r^2 + z^2}$ . The vertical pressure  $\sigma_s$  at point  $O$  may be then obtained from formulas (4:5) and (4:7) by integration from  $-\infty$  to  $+\infty$ :

$$\sigma_s = \frac{2\bar{p}}{\pi} \frac{z^3}{R^4} \quad (4:8)$$

Formula (4:8) may be called the two-dimensional (plane) analogue of the three-dimensional (space) formula (4:7). Designate with  $\theta$  the angle made by the radius vector of the given point  $O$

(line  $AO$  in Fig. 4:8) with the vertical. Then the two formulas in question will be

$$\sigma_s = \frac{3P}{2\pi R^2} \cos^3\theta \quad (4:7a)$$

$$\sigma_s = \frac{2P}{\pi R} \cos^3\theta \quad (4:8a)$$

Notice that the term  $2\pi R^2$  is the half surface of a sphere of a radius  $R$  whereas  $\pi R$  is the half circumference of the same radius.

*d. Vertical Pressure Caused by a Strip Load.*—It is known from the theory of elasticity that if a portion  $MN$  of the boundary of a

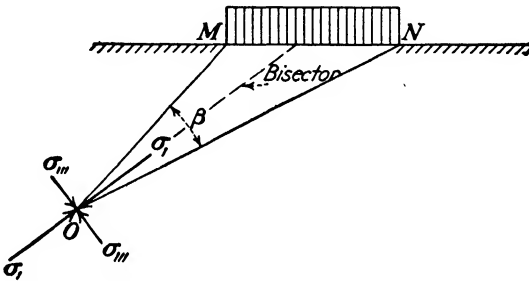


FIG. 4:11.—Principal stresses in the case of a strip load.

semi-infinite elastically isotropic mass is loaded with a strip load of an intensity  $p$  per square unit, the principal stresses (both compressive) at point  $O$  are (Fig. 4:11)

$$\left. \begin{aligned} \sigma_1 &= \frac{p}{\pi} (\beta + \sin \beta) \\ \sigma_3 &= \frac{p}{\pi} (\beta - \sin \beta) \end{aligned} \right\} \quad (4:9)$$

where  $\beta$  is the angle  $MON$ , termed sometimes "angle of visibility" because this is the angle under which the loaded portion  $MN$  is seen from point  $O$ . The direction of the major principal stress  $\sigma_1$  bisects the angle of visibility. Thus the value of the angle  $\alpha$  made by the direction of the principal stress  $\sigma_1$  with the vertical line is known. Hence the value of the vertical pressure  $\sigma_s$  may be determined analytically by formulas (4:1) or, graphically, by Mohr's circle (Sec. 4:7).

**4:16. Maximum Shear.**—The two-dimensional problem of determining the maximum shear  $\tau_{\max}$  will be first considered.

It follows from Mohr's circle (Fig. 4:7) that for any homogeneous

mass, whether elastically isotropic or not, the value of  $\tau_{\max}$  corresponds to  $2\alpha = 90^\circ$ , or  $\alpha = 45^\circ$ . Since  $\alpha$  is the angle made by the normal to a given plane with the direction of the major principal stress, it means that the plane along which the maximum shear develops bisects the angle made by the directions of the principal stresses. The value of  $\tau_{\max}$  may be obtained from the second formula (4:1), placing in it  $\alpha = 45^\circ$ .

$$\tau_{\max} = \frac{1}{2}(\sigma_1 - \sigma_{III}) \quad (4:10)$$

The difference between the principal stresses  $\sigma_1 - \sigma_{III}$  is often termed simply "stress difference." Thus the maximum shear equals half the difference between the principal stresses, or, by formulas (4:9),

$$\tau_{\max} = \frac{p}{\pi} \sin \beta \quad (4:11)$$

Formula (4:11) may be applied to any point of the mass. There are, however, some points within the mass at which the value of  $\tau_{\max}$  is greater than at others. Evidently, these are points where  $\sin \beta = 1$  or  $\beta = 90^\circ$ . The locus of these points is the circumference having the distance  $MN$  for its diameter (Fig. 4:12). The maximum possible value of the shear under a strip load is

$$\text{Max } \tau_{\max} = \frac{p}{\pi} = \text{about } \frac{1}{3}p \quad (4:12)$$

It must be clearly understood that formulas (4:11) and (4:12) are valid for homogeneous elastically isotropic masses only, because formulas (4:9) used in their derivation are formulas of the theory of elasticity.

If the strip load is not uniform, as is the case of highway embankments or earth dams, the maximum shearing stress  $\tau_{\max}$  may be found at a great number of points by more complicated methods. Points with equal values of  $\tau_{\max}$  are joined with curved lines in the same way that contour lines are traced in surveying. Figure 4:13 shows the set of isolines of the maximum shear under a triangular load. If the unit load at the center line of the loaded portion is  $p$ , the value of  $\text{max } \tau_{\max}$  is  $0.256p$ . The corresponding point is located

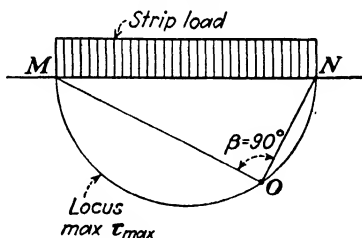


FIG. 4:12.—Maximum shear in the case of a strip load.

at the center line at a depth about one-fourth of the width  $B$  of the loaded strip.

*Three-dimensional Problem.*—The value of the maximum shear in a three-dimensional problem equals half principal stress difference, the same as in the two-dimensional problem [formula (4:10)]. The principal stresses and their difference depend in this case on the value of the Poisson ratio  $\mu$ . The computation of principal stresses in a three-dimensional problem presents, however, serious mathe-

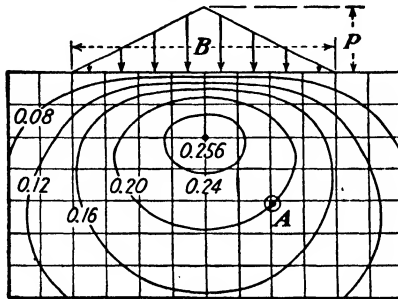


FIG. 4:13.—Shears under a triangular strip (maximum shear at  $A$  is  $0.2p$ ).

matical difficulties. This computation becomes somewhat simpler if the loading possesses planes of symmetry. There are no shears along the planes of symmetry, which consequently are principal planes. Consider the case of a uniformly loaded circular disk (unit load  $p$ ) placed at the boundary of a semi-infinite continuum, the value of the Poisson ratio of the latter being  $\mu = 0.3$ . The point with maximum shear is then located at the center line of the disk approximately at a depth of two-thirds of the radius of the disk (more accurately 0.638 of that radius). The numerical value of  $\tau_{\max}$  in this case is  $\frac{1}{3}p$  [compare formula (4:12)].

**4:17. Vertical Pressure in Aeolotropic and Nonhomogeneous Masses.**—A body or a mass that is not isotropic is called “aeolotropic” (another term is “anisotropic”; compare Sec. 3:13).

*Two-dimensional Problem.*—The simplest case of an aeolotropic mass occurs when the modulus of elasticity in the vertical direction  $E_v$  is smaller than in the horizontal direction  $E_h$ . Let  $k^2 = E_v/E_h$ . Wolf<sup>17</sup> has shown that plane principal stresses at a point in such an aeolotropic mass may be computed by replacing this mass by an isotropic one, vertical ordinates  $z$  being divided by the value of  $k$ . This constitutes an analogy to the Samsioe solution of the problem of seepage in aeolotropic masses (Sec. 3:13).

Designating by  $R$  the radius vector of the given point of the aeolotropic mass (depth  $z$ ) and by  $R_1$  the radius vector of the isotropic mass (depth  $z/k$ ), we have the value of the vertical pressure  $\sigma_z$ :

$$\sigma_z = \frac{2\bar{p}}{\pi} \frac{z^3}{kR^2R_1^2} \quad (4:13)$$

It is advisable to compare this formula with (4:8).

The influence of a rigid base at a certain depth was studied by Carothers.<sup>19</sup> His formulas containing hyperbolic functions are sometimes used by dam designers.

*Three-dimensional Problem.*—Biot<sup>18</sup> computed the vertical pressure  $\sigma_z$  caused by a concentrated load at the boundary of an elastic layer with the underlying base of another material. The point where the pressure  $\sigma_z$  is determined is located exactly at the vertical line of action of the concentrated load. The Poisson ratio of the elastic layer is assumed to be  $\mu = 0.5$ . Taking the result given by the Boussinesq formula (4:5) for unit, Biot's figures are

For a frictionless rigid base, 1.711.

For a rough rigid base, 1.557.

Thus under the given assumptions, the presence of a rigid base increases the vertical pressure through 50 to 70 per cent.

The opposite phenomenon takes place when a hard layer is underlain by a softer one. The hard layer produces in this case the "bridging effect" and redistributes the pressure within the soft layer. Thus in comparison with a homogeneous mass this pressure is decreased at the vertical line of action of the load itself and increased at the points remote from that line.

Finally, it should be mentioned that if a clay layer, otherwise homogeneous, has very thin sand inclusions, the vertical pressure in such a layer is a few per cent less than in a perfectly homogeneous mass. Biot's more accurate figure is 0.942, the Boussinesq vertical pressure being again taken as unity.

Cummings<sup>21</sup> integrated Biot's formulas for the case of a circular uniformly loaded disk resting on an elastic layer (thickness  $d$ ). He found that the vertical pressure  $\sigma_z$  at the intersection of the center line of the disk with the boundary of the underlying rough rigid base may be simply obtained from the Boussinesq formula (4:5), in which the depth  $z$  equals, not  $d$ , but  $0.75d$  only. Cummings' rule is simple and practical and may be recommended for use in approximate estimations.

**4:18. Limitations of Elastic Formulas.**—Formula 4:5 follows directly from the formulas developed by the French mathematician Boussinesq<sup>3</sup> for the case of an elastic continuum loaded *at the boundary* with a point load. Surface loading is also an assumption in the derivation of other formulas of the theory of elasticity so far advanced. In most practical cases the load is applied below the earth surface (for instance, in foundations of buildings). Hence, in such cases formulas so far advanced become an approximation, even in a perfect elastic continuum.

According to the theory of elasticity there is a *stress concentration* under a concentrated load. The edges of a strip,  $M$  and  $N$  (Fig. 4:12) are also points of stress concentration. Therefore, theoretically speaking, if a mass approaches an elastic continuum (as, for instance, many kinds of clay), the shearing stress at the edges of a strip may be larger than  $\frac{1}{3}p$  [formula (4:11)]. Besides, all elastic formulas are based on the assumption that the loaded material possesses the same properties *before and after loading*. In reality material under the structure itself is disturbed or smashed. Hence application of such formulas close to the loaded surface is not advisable.

Stresses in Boussinesq formulas depend on the value of the load, on the position of the point where they are determined, and on elastic properties of the material as expressed by the Poisson ratio  $\mu$  or its reciprocal  $m$ . Strains, in addition, depend also on the value of the modulus of elasticity  $E$ . In the particular case of the vertical pressure  $\sigma_z$ , and in all cases of plane stresses, the value of the stress is independent from  $\mu$ . [Compare formulas (4:5), (4:8), (4:9), and (4:11).] This means that formulas for the vertical pressure  $\sigma_z$  and for all plane stresses are valid for all homogeneous elastically isotropic bodies whatever their elastic constants may be. Other stresses, however, do depend on the value of the Poisson's ratio—as, for instance, horizontal pressure,  $\sigma_x$ , as discussed in Sec. 4:27.

It follows that if close to the ground surface there is, for instance, a clay layer 500 ft. thick and in another place, also close to the ground surface, a sand layer also 500 ft. thick, theoretical vertical pressures  $\sigma_z$  at analogous points of both layers will be exactly the same, provided, of course, that the acting loads are the same in both cases and that the points where the vertical pressure is determined are sufficiently deep. If the point where the vertical pres-

sure  $\sigma_z$  is to be determined is shallow, better results may be expected for clays than for sands.

An actual earth mass is not homogeneous; on the contrary, it is *heterogeneous* and consists of layers of different materials. As a rule these layers are of variable thickness and very often are not horizontal. It is believed, however—and this is very probable—that *at greater depths* vertical pressures  $\sigma_z$  determined by the Boussinesq formula are close to the reality. There is no sufficient experimental or field evidence, however, to prove or to disprove this statement.

**4:19. Pressure of Moisture in Pores.**—Considerable difference between an elastic continuum, as studied in the theory of elasticity, and an actual earth mass is also due to the pressure of moisture in pores.

*Hydrostatic Pressure.*—Moisture in the pores of a saturated natural earth mass stands under the action of the hydrostatic pressure and does not carry the weight of the soil particles (skeleton). The hydrostatic pressure equals the product of the unit weight of water  $\gamma_0$  and the depth of the given point  $z$  below the water table. An increase in hydrostatic pressure beyond the value of the product  $\gamma_0 z$  is termed *excess hydrostatic pressure*. Another term of the same meaning is *neutral pressure* (or “neutral stress”) as caused by external loading. Both terms are used in the literature.

Pressure that is transmitted from one particle of the mass to another through their surfaces of contact is *effective* or *intergranular* pressure. The total pressure intensity across a plane within a saturated mass equals the sum of both the intergranular and neutral pressures. If the vertical pressure determined by the Boussinesq formula (4:5) or otherwise is  $\sigma_z$ , and the neutral pressure is  $u$ , then the value of the intergranular pressure is  $\sigma_z - u$ . A clay particle having several points of contact with an underlying particle but at the rest of its lower surface separated from that particle by a thin moisture film is acted upon by the pressure in that film  $u$  as if the points of contact did not exist at all (Fig. 4:14a). An analogous phenomenon on a large scale takes place in masonry dams when an upward hydrostatic pressure (“hydrostatic uplift”) apparently acts on the full surface of the base of the dam as if there were no points or surfaces of contact between the base of the dam and its foundation (Fig. 4:14b).

*Hydrodynamic Pressure.*—Percolating moisture exerts a pressure that at a given point is proportional to the value of the hydraulic gradient at that point. Actually, imagine that at point *A* of a streamline a small prism, having a cross section *a* and being  $\Delta L$

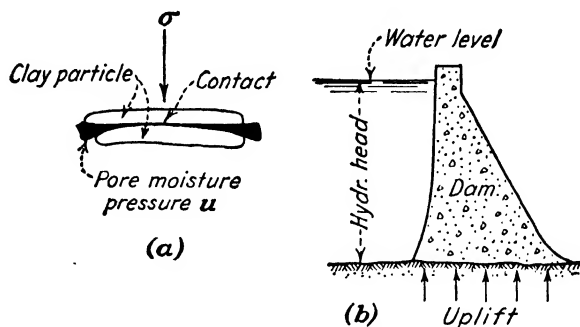


FIG. 4:14.—Analogy between (a) pore pressure in clay and (b) hydraulic uplift in a dam.

in length, has been cut out. Designate by  $p$  the unit pressure acting at the face  $a$  of that body and by  $\gamma_0$  the unit weight of water (Fig. 4:15). It is quite evident that to produce a pressure  $p$  a hydraulic head  $\Delta h = p/\gamma_0$  is needed. It follows therefrom that if pressure  $p$  acts at the face  $a$  of the body in question, the hydraulic gradient at that point is

$$i = \frac{\Delta h}{\Delta L} = \frac{1}{\gamma_0} \frac{p}{\Delta L} \quad (4:14)$$

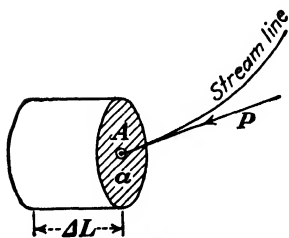


FIG. 4:15.—Pressure due to percolating moisture.

If we multiply both the denominator and the numerator of the fraction  $p/\Delta L$  by  $a$ , it can be seen that this fraction represents the force required to push moisture through the given small body as referred to a unit of volume of that body. Hence this force equals  $\gamma_0 i$  and is measured in the same units as  $\gamma_0$ , since  $i$  is an abstract number.

If the pressure  $p$  acts upward, it diminishes the acting weight of the soil; and at a certain critical value of the hydraulic gradient  $i$ , the whole weight of the soil will be balanced by the action of water. With  $n$  designating the porosity of the given soil,  $\gamma_0$  the unit weight of water, and  $s$  the specific gravity of the grains, the

value of the critical hydraulic gradient may be determined from the condition

$$\gamma_0 i = \gamma_0 s(1 - n) - \gamma_0(1 - n) \quad (4:15)$$

or

$$i = (1 - n)(s - 1) \quad (4:16)$$

In an average case of loose sand, when  $n = 0.5$  and  $s = 2.65$ , the value of  $i$  is practically close to a unit.

It follows that in applying elastic formulas to an earth mass, one must not lose sight of the effect of percolating water. In this connection hydraulic gradients over a unit ( $i > 1$ ) are to be considered as undesirable.

### C. DIRECT LOADING EXPERIMENTS

Formulas developed for idealized earth masses (Secs. 4:13 to 4:19) should be checked against the results of both direct loading experiments and pressures under actual structures.

**4:20. General Trend of a Loading Experiment.**—Direct loading experiments made in the past 50 years were performed on artificial fills made of dry or moist sand. Only on some exceptional occasions were experiments made on clay. It is very difficult both to place clay material in an orderly arrangement in a box and to maintain the same properties of the clay through the whole experiment. The sand fills were made either in large boxes to minimize the influence of the walls or on a firm (concrete) floor. The general method of experimentation was as follows:

*a.* Sand was placed in the box according to a certain routine which was individual for each experiment (for instance, in layers and with tamping).

*b.* Before applying the load, initial pressure at the bottom of the box was recorded. Pressure-measuring apparatus included membranes connected with manometers, small areas cut out from the bottom of the box (plugs) and supported by a scale, pressure-measuring cells (Fig. 4:16), etc.

*c.* The load was placed at the center of the box, and pressures at different points  $a, b, c, \dots$  of the bottom were measured. Initial pressures were subtracted. The same result may be obtained by measuring the pressure at the central point of the bottom and moving the load to different points at the surface of the fill (Fig. 4:17a).

*d.* Experiments were repeated for different depths of fill  $h_1, h_2, h_3, \dots$

e. It was assumed that the pressure at the bottom of the box where a fill of a depth  $h$  was placed is the same as in a semi-infinite earth mass at the same depth.

f. Pressure was plotted against distances from the center, and thus pressure curves were obtained. As the depth  $h$  increases, these curves become flatter but more extended sidewise (Fig. 4:17b). Horizontal lines corresponding to different pressures  $p_1, p_2, p_3, \dots$  were traced, and their points of intersection with particular pressure curves were recorded. Then *isobars*, or curves connecting points of equal vertical pressure, were traced. It is obvious that

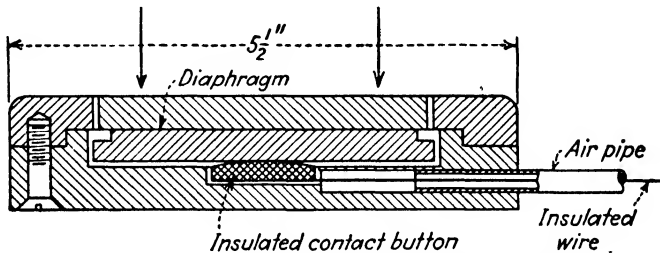


FIG. 4:16.—Goldbeck pressure measurement cell.

isobars (Fig. 4:17c) in this three-dimensional case are surfaces of revolution about the center line of the experimental disk.

From a great number of pressure-measuring cells, the so-called Goldbeck cell will be described as an example. This is a low metallic cylinder or disk, about  $5\frac{1}{2}$  in. in diameter (Fig. 4:16). Compressed air is blown in from a station into the cell buried at the bottom of the fill. As soon as the pressure of the compressed air balances the sand pressure, an electric contact breaks, a light at the station is extinguished, and a reading is taken at the pressure gauge. Goldbeck cells may also be used for measuring pressures under full-sized structures. In such a case a set of cells is buried under the structure in question during the construction period and stays there. The compressed-air station may be placed at the structure itself or even at a certain distance away.

Stresses within a body cannot be measured, and attempts to do so fail. All the measurements made in the soil-loading experiments described here were measurements of small displacements at or close to the rigid boundary of the mass, these displacements being correlated with pressures in the measuring devices.

**4:21. Experiments by Various Investigators.**—*a.* The first experiments of this kind were those by Steiner and Kick in Prague, Czechoslovakia, in 1879. After a certain interval the direct loading experiments were renewed by Strohschneider<sup>7</sup> in Graz, Czechoslovakia, in 1909–1911, on a very small scale.

At approximately the same time a series of important research projects were started in the United States. Enger<sup>8</sup> worked in 1910–1913 in the University of Illinois. His experiments were made on a much larger scale than those of Strohschneider. Enger used sand layers 6, 12, and 18 in. thick and applied loads through

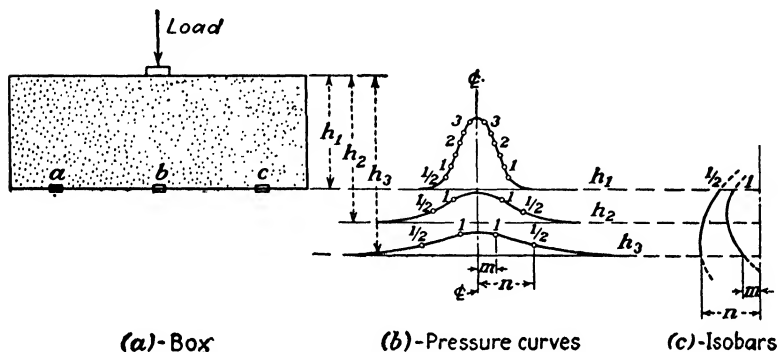


FIG. 4:17.—Direct loading experiment ( $\frac{1}{2}$ ; 1; 2; 3 . . . are pressures).

plates 9 to 21 in. in diameter. According to Enger, pressures below the center of the loaded plate are much greater than the value of the unit load  $p$  acting at the disk. Another observation was that sand particles tend to escape from underneath a rigid loading plate; this was proved by radial scratches at the bottom of the loading plate. Further experiments were made in 1913–1914 at Pennsylvania State College<sup>9</sup> and by Goldbeck,<sup>10</sup> first for the U. S. Bureau of Standards and afterward for the U. S. Bureau of Public Roads, about 1917. Again after an interval, comprehensive experiments were made by Kögler\* and Scheidig<sup>11</sup> in Freiberg *i/S.*, Germany, in 1925–1927. Subsequently, some loading experiments were made in Switzerland (Hugi and Gerber) and in Germany (Press).

Figure 4:18 represents comparatively (1) a set of theoretical isobars constructed under the assumption that the plate is not rigid

\* Franz Kögler (1882–1939), professor of mechanics at Freiberg Mining Academy, Germany, was very active in soil-mechanics research and teaching.

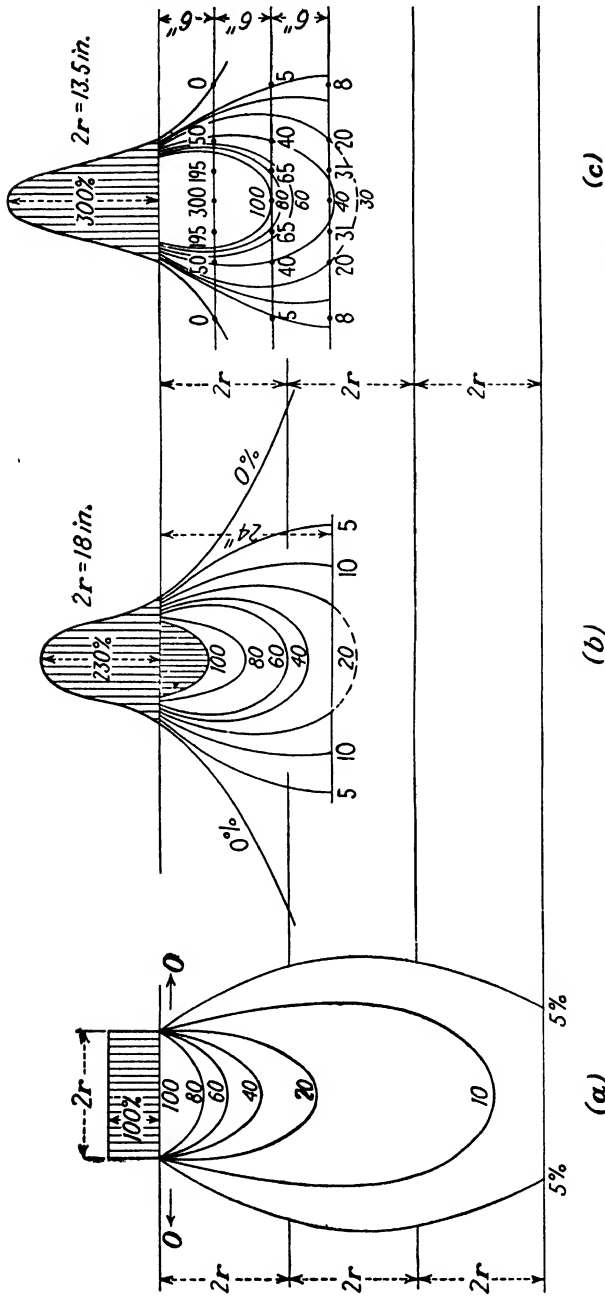


FIG. 4:18.—(a) Isobars under a circular disk placed at the boundary of an elastically isotropic body; (b) Kögler and Scheidig's experimental isobars; (c) Enger's experimental isobars.  
NOTE: Experimental data for (b) and (c) are in solid lines.

and that the sand mass is elastically isotropic, (2) a set of isobars in an experiment by Kögler and Scheidig, and (3) a set of isobars by Enger. The scales of these three drawings are different in order to make the diameter of the disk of the same length in all cases. Kögler and Scheidig found in the "disturbed zone" under the middle of the loading plate smaller pressures than Enger's pres-

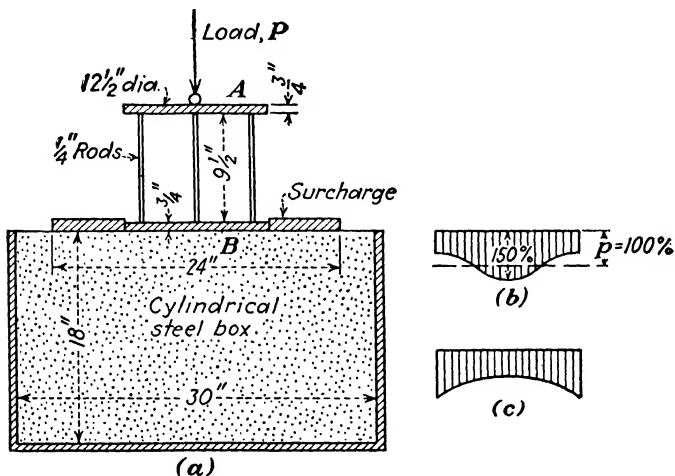


FIG. 4:19.—Faber's loading experiment.

ures [230 per cent as compared with Enger's 300 per cent (Fig. 4:18*b* and *c*, respectively) and with 100 per cent according to elastic formulas (Fig. 4:18*a*)].

*b. Faber's Experiments.*—Practically all the experiments described have been made with fragmental material such as sand. Faber<sup>12</sup> made experiments in England about 1933 with both sands and clays. His results permit the checking of elastic theories, since clay approaches an elastic continuum. Earth material was placed in a cylindrical steel box, 30 in. in diameter and 18 in. high and loaded through a device consisting of two equal parallel and concentric metallic disks *A* and *B*, each about 1 ft. in diameter, connected with each other by 16 vertical metallic rods (Fig. 4:19*a*). The acting load *P* was applied to the upper disk *A*, and contractions of the connecting rods were accurately measured. It may be approximately assumed that the stresses both at the top and the bottom of the lower disk *B* are the same. Furthermore, vertical pressures at the bottom of disk *B* balance with earth reactions,

owing to the law of equality of actions and reactions. Hence it should be concluded that each connecting rod is compressed by a force equal to the pressure exerted by the disk *B* at a point corresponding to the foot of that rod. To prevent the escape of sand particles at the edge of the loading plate, Faber used a circular surcharge around that plate. Faber's results are schematically shown in Fig. 4:19*b* and *c*. In the case of sands confined by the surcharge (Fig. 4:19*a* and *d*) the maximum pressure was about 150 per cent of the average unit load *p*, which qualitatively checks against the experiments already described. In the case of clays (Fig. 4:19*c*) there was an overloading at the edges.

**4:22. Disturbed Zone.**—It follows from experiments described in Sec. 4:21 that sand under the loading disk is exceedingly compact

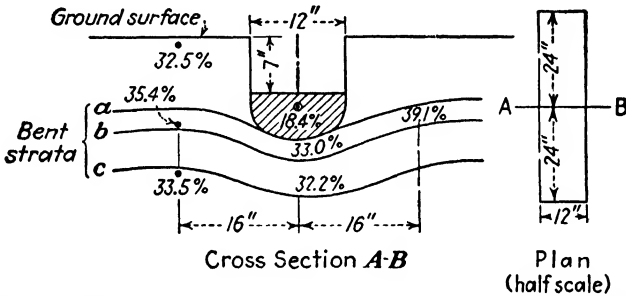


FIG. 4:20.—A loading experiment in East Hartford, Conn. (Percentages show moisture content after experiment.)

and there is a zone which is evidently distinct from the rest of the experimental material. The cause of the formation of the disturbed zone is generally traced to the escaping of sand grains at the edges of a loaded plate. Owing to the lack of support at the edges, the plate thus becomes overloaded at the middle. The chief reason for the formation of a "disturbed zone," however, is apparently the packing in of the particles from underneath the loaded plate into the disturbed zone. This statement can be proved by the following two experiments.

A platform 4 ft. long was loaded with 12 tons of pig iron and settled through 7 in. (Fig. 4:20). The earth material from the rectangle, 7 by 12 in., has been shifted to the disturbed zone (dashed in Fig. 4:20). The moisture content in the disturbed zone proved to be considerably lower than in the rest of the mass.

Two posts, shown in Fig. 4:21, were located at the bottom of a

large excavation and loaded with equal loads. One of them was standing on the floor of the excavation, and the base of the other was placed within a wooden cofferdam 3 ft. below that floor. The ground surface bulged around the former and sank around the latter. This settlement may be explained by the formation of the disturbed zone below the base of the post and by the consequent packing in of the material.

The earth material in the case of Fig. 4:20 was fine silty sand, and in the case of Fig. 4:21, fine sand. There are no examples of the formation of disturbed zones on clay. It may be concluded

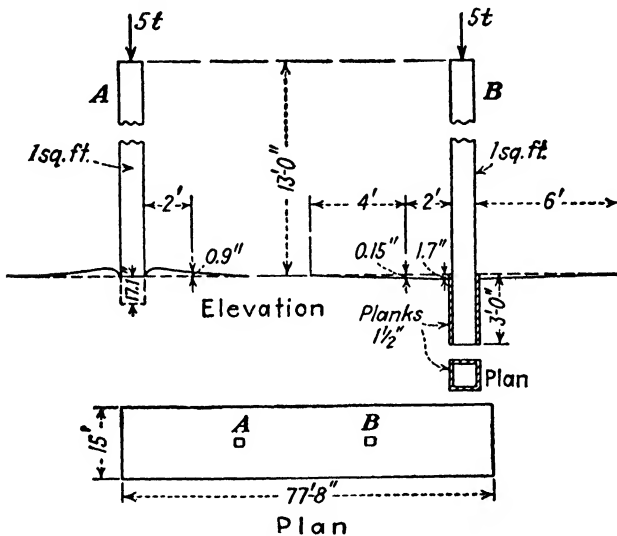


FIG. 4:21.—A loading experiment in Stratford, Conn. (bulging in test 1; sinking in test 2).

by analogy with metals, however, that such a formation is possible. Figure 4:22 represents a thin mild-steel plate deformed plastically by being pressed in (indented) with a rigid punch. In the reheating of the specimen, the grains recrystallize and clearly show the disturbed zone (white in Fig. 4:22).

It would be premature, however, to conclude that a disturbed zone geometrically similar to that obtained in laboratory and field experiments exists under actual structures. Apparently, the structure of earth material at the base of an actual structure is disturbed to a relatively insignificant depth. This disturbance is generally neglected, and the only precaution taken is not to com-

pute stresses too close to the base of the structure, as already explained in Sec. 4:18.

**4:23. Discussion of the Direct Loading Experiments.** *a. Rigid Loading Plates.*—Direct loading experiments as described in Sec. 4:22 were made with rather rigid loading plates. A structure or a loading plate will be termed “absolutely” or “perfectly” rigid if it can be visualized as consisting of thin vertical slices so strongly bound together that they act as a unit. An opposite case would be a “nonrigid” structure or a “nonrigid” loading plate, which can be visualized as consisting of thin vertical slices with no lateral



FIG. 4:22.—An etching of mild steel showing in white circle recrystallized zone under indentation of a punch. (From Nádai, “Plasticity.”)

bonds, so that each of them can settle down individually. The degree of rigidity in actual engineering structures (and also in the experimental loading plates) is some value between these two limits. The experiments described show that if a rigid plate is placed on top of a fragmental mass such as sand, it is overloaded at the middle and, if placed on top of a clay mass, is overloaded at the edges. Clay approaches an elastic continuum; and according to elastic theories, a circular rigid disk placed at the horizontal boundary of a semi-infinite elastic continuum is overloaded at the edges. If the radius of such a rigid disk is  $r$ , the pressure at a point distant  $cr$  from the center of the disk would be

$$\sigma_z = p \frac{1}{2\sqrt{1-c^2}} \quad (4:17)$$

The pressure  $\sigma_z$  equals  $\frac{1}{2}p$  at the center of the disk ( $c = 0$ ) and becomes infinite at the edges ( $c = 1$ ). Since there are no perfectly rigid structures or loading disks, even the slightest settlement at the edge of the loaded disk relieves the stress considerably, so that

practically all stresses at the base of the loaded disk are finite. Figure 4:23 shows in solid lines the pressure distribution according to formula (4:17); dotted lines refer to the probable actual distribution.

There is no mathematical theory that could explain why a rigid disk placed on top of a fragmental mass is overloaded at the center, as revealed by all the experiments described in Sec. 4:21.

Heavy overloading at the middle of the plate in the experiments by Enger and Kögler and Scheidig should be apparently attributed both to the tendency of the sand to escape at the edges of the plate and to the action of the rigid base (floor) under the experimental sand layer. It seems reasonable, however, to believe that in the case of a rigid loading plate on sand, *some* overloading at the middle of the plate still exists as revealed by Faber's experiments.

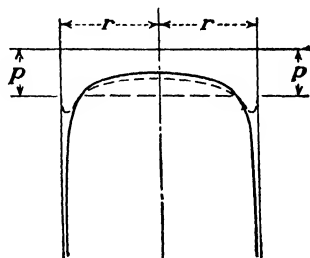


FIG. 4:23.—Theoretical and probable pressure distribution at the base of an absolutely rigid disk at the top of an elastically isotropic mass.

The results obtained in the loading tests described can be obtained by computation changing the Boussinesq formula (4:7a) as follows:<sup>20</sup>

$$\sigma_z = \frac{\nu P}{2\pi R^2} \cos^3\theta \quad (4:18)$$

The symbol  $\nu$  designates the so-called "concentration factor" varying from 3 to 6 for different sands. If  $\nu = 3$ , formula (4:18) becomes the Boussinesq formula (4:7a). The idea of the "concentration factor" is not very much used, however.

*b. Nonrigid Plates.*—According to the theory of elasticity, if a perfectly nonrigid disk is placed at the surface of an elastic continuum, the vertical pressure under its base decreases from its center line toward its edges—exactly opposite to what occurs in the case of rigid plates.

If the horizontal surface of a sand mass is loaded with a circular disk, particles tend to escape at the edges (compare Enger's experiments, Sec. 4:21). If the loading disk is *rigid*, most particles are driven downward to occupy their ultimate positions. In the case of a *nonrigid* loading disk, only a restricted number of grains are confined at the middle of the disk and support it, whereas the edges of the disk settle down. Such a situation has been revealed

in an experiment by Kögler and Scheidig, as shown in Fig. 4:24. It cannot be concluded, however, that in the case of a nonrigid disk on sand the maximum pressure under its base is at the edges. Figure 4:25 shows another pressure experiment by Kögler and Scheidig. In this case the center-line pressure was about three times the unit load ( $3p$ ) under a slightly rigid disk, whereas a more rigid disk

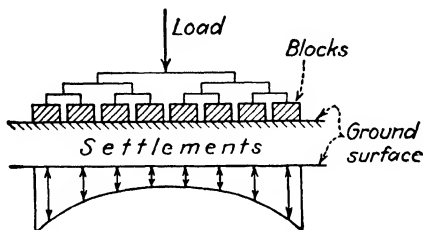


FIG. 4:24.—Settlements of a surface of a sand mass under a nonrigid load. (After Kögler and Scheidig.)

distributed the pressure more uniformly, with a center-line pressure of  $1.6p$ , where  $p$  is the unit load carried by the disk. Apparently strong overloading of the center line in Fig. 4:25a is due to a more concentrated character of the load than in Fig. 4:25b. Since the evidence given by Figs. 4:24 and 4:25 is not conclusive, it may be only stated that in the case of a nonrigid disk on sand, settlements

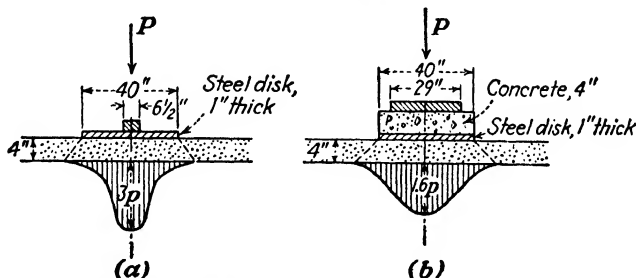


FIG. 4:25.—Influence of the rigidity of the loading plate on the center-line pressure. (After Kögler and Scheidig.)

are likely to produce close to the edges. Building practice (Chap. XIII) confirms this expectation.

*c. Decrease in Pressure with Depth.*—Direct loading experiments show a decrease in vertical pressure  $\sigma_z$  as the depth  $z$  increases. This result is in accordance with elastic formulas available (for instance, with the Boussinesq formula). Some experimental data along these lines are shown in Fig. 4:26. Solid curves in that

figure furnish theoretical pressure at the center line of a disk placed at the top of a semi-infinite elastically isotropic body: curve *a* corresponds to a concentrated load acting directly at the surface of the soil; curve *b* corresponds to a uniform distribution; and curve *c* corresponds to the case of a perfectly rigid disk. At a depth of twice the diameter of the disk ( $4r$ ) all curves practically coincide, and this accounts for the statement that at that depth, a loaded

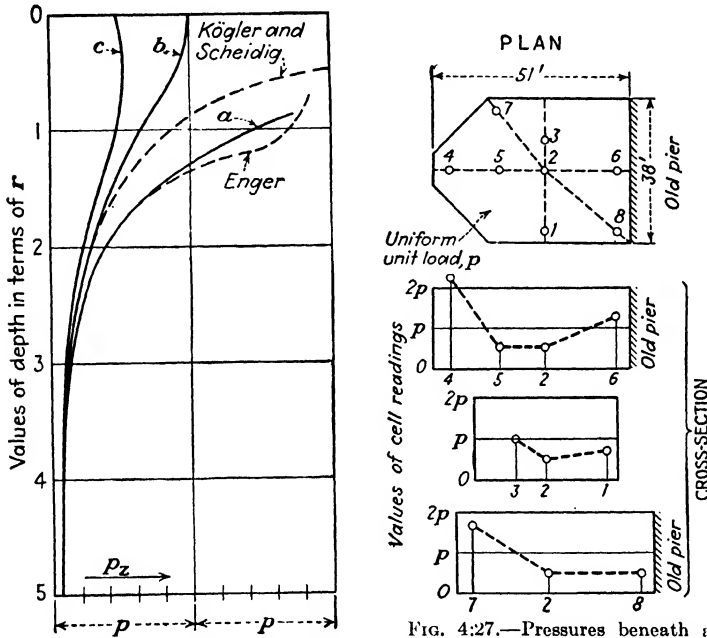


FIG. 4:26.—Decrease of vertical pressure with the depth.

FIG. 4:27.—Pressures beneath a bridge pier over the Rhine River in Germany.

plate acts practically as a concentrated load. At a depth equal to the diameter of the disk ( $2r$ ) curves *c* and *b* are very close to each other; the pressure at the center line of the disk at that depth does not depend on whether the loaded plate is rigid or not.

**4:24. Pressure Distribution under Actual Engineering Structures.**—During the construction over the Rhine River of the new bridge connecting Mannheim and Ludwigshafen, Germany (about 1932), eight Goldbeck cells were placed beneath a pier, and it was discovered that the foundation was overloaded at the edges (Fig. 4:27). The local soil was gravelly, and the result shows that

at a greater depth pressures in any soil approximately follow elastic formulas.<sup>13</sup>

In about 1933 a building was constructed by the Agricultural and Mechanical College of Texas.<sup>14</sup> Six Goldbeck cells were embedded under a footing, as shown in Fig. 4:28. The soil beneath

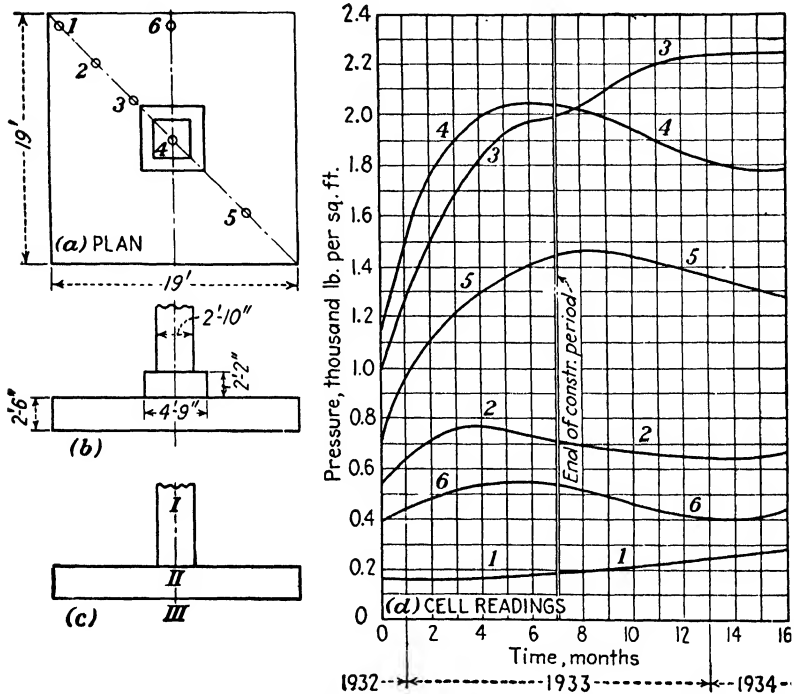


FIG. 4:28.—Pressures beneath a footing of a building at Texas Agricultural and Mechanical College. (After Giesecke and associates.)

the building is clay, with small, varying quantities of sand and coarse material. The maximum pressure during the construction was at the center of the footing (cell 4), but this shifted gradually during a period of about seven months to cell 3. No definite conclusion can be drawn from this example. Attention should be called, however, to the fluctuations of pressure under the footing. Apparently pressure distribution under a structure may be not constant; it may change as time passes.

*Interrelation of Stresses between the Structure and the Earth Mass.*—A structure, particularly a building, is nothing else than an object placed on the bottom of an excavation. Soil reactions

are in equilibrium, not with unit loads acting at the loaded surface, but with stresses within the structure close to the surface of contact with the earth. A structure assumed uniformly loaded by its designer in reality causes nonuniformly distributed soil reactions, with especial disturbances close to the edges of the structure (compare Secs. 8:12 and 8:14).

D. LATERAL PRESSURE

4:25. Lateral Pressure in a Nonloaded Semi-infinite Mass.—

Consider a very small cube (dimensions 1 by 1 by 1) located at a depth  $z$  below the horizontal boundary of an elastic continuum. It is compressed by the vertical pressure  $\sigma_z = \gamma z$ , where  $\gamma$  is the unit weight of the material. Since the prism is confined and there is no lateral displacement, it should be concluded that there are compression stresses  $\sigma_x$  and  $\sigma_y$  which act on the lateral sides of the prism (Fig. 4:29). Owing to the symmetry, these two stresses are equal ( $\sigma_x = \sigma_y$ ). A stress acting on a side of the prism produces a certain strain in its own direction (axial strain) and in the two perpendicular directions strains that equal the axial strain multiplied by Poisson's ratio  $\mu$ . The same effect would be produced if, in addition to each axial stress  $\sigma_x$ ,  $\sigma_y$ , and  $\sigma_z$ , stresses  $\mu\sigma_x$ ,  $\mu\sigma_y$ , and  $\mu\sigma_z$  in the two perpendicular directions are considered, and if no strain due to Poisson's ratio is taken into account. Since there is no lateral displacement, stresses acting along axis  $XX$  (or  $YY$ ) are in equilibrium.

Thus

$$\sigma_x - \mu\sigma_x - \mu\sigma_y = 0$$

from which, remembering that  $\sigma_x = \sigma_y$ ,

$$\frac{\sigma_x}{\sigma_x} = \frac{\mu}{1 - \mu} \tag{4:19}$$

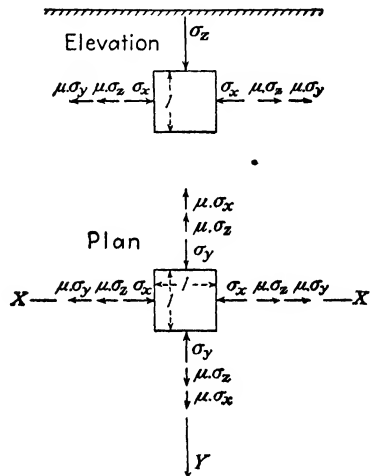


FIG. 4:29.—Lateral pressure within an elastic continuum.

or, replacing the value of Poisson's ratio  $\mu$  with its reciprocal  $m = 1/\mu$ ,

$$\frac{\sigma_x}{\sigma_s} = \frac{1}{m - 1} \quad (4:20)$$

It is evident that in this case the vertical pressure is the major principal stress ( $\sigma_v = \sigma_x$ ) and that the intermediate and the minor principal stresses are equal ( $\sigma_{ii} = \sigma_{iii} = \sigma_x = \sigma_y$ ). Owing to symmetry, lateral pressure at a given depth is constant in any horizontal direction.

The lateral pressure  $\sigma_{iii}$ , in a natural earth mass is visualized as a portion of the vertical pressure  $\sigma_v = \sigma_x$ :

$$\sigma_{iii} = K\sigma_v \quad (4:21)$$

The ratio  $K$  is termed "coefficient of pressure at rest." If instead of the given earth mass a liquid is considered, the ratio  $K$  would equal unity. Thus the value  $K$  is the coefficient by which the lateral pressure in the liquid of a given unit weight (hydrostatic pressure) is to be multiplied to obtain the lateral pressure in the earth mass of the same unit weight. Equation (4:21) seems to be a fair assumption for shallow earth layers, but whether or not it holds for deeper strata is not known.

**4:26. Experimental Determination of Poisson's Ratio in Soils.**—Terzaghi<sup>4</sup> determined the value of the lateral pressure exerted by a soil sample on the walls of a container by pulling out a metallic tape pressed by the earth against that wall. By comparing the pulling force with the vertical pressure, he found the value of the coefficient of pressure at rest  $K$ , which was for dense sand 0.40 to 0.45, for loose sand 0.45 to 0.50, for clay 0.70 to 0.75. The value of Poisson's ratio for a soil may be estimated from the value of  $K$  by formulas (4:20) and (4:22):

$$K = \frac{\mu}{1 - \mu} \quad (4:22)$$

The average values of Poisson's ratio thus computed are for sand about 0.30 and for clay about 0.40 or slightly more.

Another method<sup>5</sup> for determining the coefficient of pressure at rest  $K$ , is to enclose a sample in a rubber envelope and to place it in a container with water. The sample is then subjected to loading, and this causes the increase in pressure in the adjacent liquid. The ratio between the pressure in water and the acting

compression stress furnishes the values of the coefficient of pressure at rest. This method is somewhat similar to the triaxial compression test described in Chap. V. Still another method has been reported.<sup>6</sup>

**4:27. Lateral Pressure in a Loaded Semi-Infinite Mass.**—If a concentrated load acts at the boundary of an *elastic continuum*, then at a point *O* of that continuum there are three normal stresses  $\sigma_x$ ,  $\sigma_x$ , and  $\sigma_y$  and also three shears. These values may be determined by the Boussinesq formulas. The vertical pressure  $\sigma_z$  has been already discussed in Sec. 4:15. The two horizontal normal stresses  $\sigma_x$  and  $\sigma_y$  are shown in Fig. 4:30, in which it is assumed that point *O* is located at the plane *XZ*. The horizontal projection of this plane is shown in the plan (Fig. 4:30, bottom) by the line *AX*. The values of the normal stresses  $\sigma_x$  and  $\sigma_y$  close to the top of the mass are negative (tensions) for any value of Poisson's ratio, except  $\mu = \frac{1}{2}$ . Since a natural earth mass hardly can stand tensile stresses, some advantage may be taken from elastic formulas only by placing  $\mu = \frac{1}{2}$ . In such a case Boussinesq formulas for the horizontal pressures  $\sigma_x$  and  $\sigma_y$  will be

$$\left. \begin{aligned} \sigma_x &= \frac{3P}{2\pi} \frac{x^2z}{R^5} \\ \sigma_y &= 0 \end{aligned} \right\} \quad (4:23)$$

The symbol *R* stands in formula (4:23) for the radius vector, which in this case equals  $\sqrt{x^2 + z^2}$ .

If we place  $z = 0$  in the first of Eqs. (4:23), horizontal pressure  $\sigma_x$  would vanish. It is to be noticed that the horizontal pressure *at the top of an idealized fragmental mass* also vanishes.

Spangler<sup>15</sup> measured horizontal pressure against a concrete retaining wall 7 ft. high and 15 ft. long, the pressure having been caused by the action of a truck placed at the variable distance  $x$  from the wall. The backfill was gravelly, and measurements were

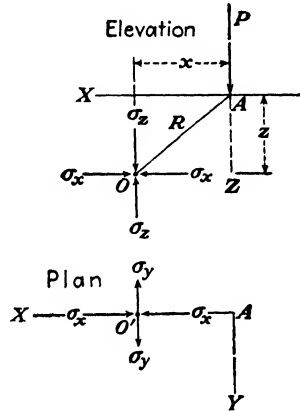


FIG. 4:30.—Horizontal pressure in the case of a concentrated force *P* (normal stresses  $\sigma_x$  and  $\sigma_y$ ).

made under both dry and wet conditions. A comparison of the stresses given by Eq. (4:23) and the pressures measured in Spangler's experiments reveals a similarity in the shapes of the two distribution curves (Fig. 4:31). The measured pressures are greater than those given by Eq. (4:23) and shown in dotted lines. The divergence between the experimental pressures and the Boussinesq pressures was a varying quantity, being relatively greater when the load was close to the wall. Spangler found that in all cases the

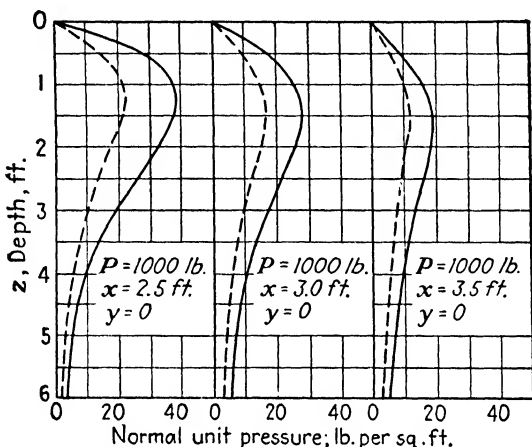


Fig. 4.31.—Horizontal pressure from a concentrated load  $P$ . (After Spangler.)

horizontal pressure at the top of the experimental gravel backfill was zero, and this is theoretically consistent, as already explained. Experiments similar to Spangler's were made in 1929 by Gerber in Switzerland.<sup>16</sup>

### Problems

1. A monument weighing 1,000 tons is to be considered as a concentrated load. Assuming that the earth mass is elastically isotropic, compute the vertical pressure under the monument at a depth of 20 ft. *Ans.* 1.2 tons per sq. ft.
2. A masonry bridge pier is 30 ft. high and 20 ft. wide. It is long enough so that the problem can be considered two-dimensional. Compute the horizontal shearing stress at a point 15 ft. deep and 22 ft. distant from the center line of the pier. Neglect the live load and assume that the earth mass is elastically isotropic. *Ans.*  $\tau_{zx} = 0.31$  tons per sq. ft., assuming the unit weight of masonry at 150 lb. per cu. ft. and uniform pressure distribution at the base of the pier.
3. Compute the vertical pressure at the point specified in problem 2, with

the assumption that the earth mass is elastically isotropic. *Ans.*  $\sigma_z = 0.25$  tons per sq. ft.

4. Two square buildings (75 by 75 ft.) are uniformly loaded with 2 and 3 tons per sq. ft. of the base, respectively. The buildings are separated by an alley 12 ft. wide. Find the vertical pressure  $\sigma_z$  at the center point of the heavier building, at a depth of 60 ft. from the ground surface. Assume that in this case the Boussinesq formula holds and use the Saint-Venant principle.

*Ans.* About 1.8 tons per sq. ft.

5. Compute the vertical pressure at a point located 20 ft. below a corner of a nonrigid raft measuring 22 by 58 ft. and carrying a unit load of 2.5 tons per sq. ft. Compare two methods: (a) subdividing the raft into small rectangles, (b) Prof. Newmark's charts as described in Appendix B.

*Note:* This problem also can be solved by the "reduced-area method" and by using charts proposed by Prof. Burmister (for both methods see *Trans. A.S.C.E.*, vol. 103, 1938).

6. A structure 60 ft. long and 35 ft. wide is loaded with 3 tons per sq. ft. Determine the vertical pressure exactly under the center of this structure, but at a depth of 60 ft. Use for comparison the Boussinesq formula and the 2-to-1 method. In determining stresses by the Boussinesq formula, assume that the structure may be replaced with a concentrated load.

#### References

1. HARDY CROSS: Limitations and Applications of Structural Analysis, *Eng. News-Record*, vol. 115, 1935.
2. Earths and Foundations, progress report of special committee, *Proc. A.S.C.E.*, vol. 59, 1933.
3. J. V. BOUSSINESQ: "Application des potentiels à l'étude de l'équilibre et du mouvement des solides élastiques," Gauthier-Villars et Cie, Paris, 1885.
4. CHARLES TERZAGHI: Principles of Soil Mechanics, *Eng. News-Record*, vol. 95, 1925.
5. N. GERSEVANOFF: Improved Methods of Consolidation Test and of Determination of Capillary Pressure in Soils, *Proc. Intern. Conf. Soil Mech.*, vol. 1, Paper D-4, 1936.
6. Government Railways of Japan, *Geotechnical Committee Bull.* (printed in Japanese), issue 4, 1936.
7. O. STROHSCHNEIDER: Elastic Pressure Distribution and Pressure Excess in Fills (German), *Sitzg. Ber. der k.-kais. Akad. Wiss., Vienna*, vol. 121, section II-a, 1921.
8. M. L. ENGER: High Unit Pressures Found in Experiments on Distribution of Vertical Loading through Sand, *Eng. Record*, vol. 73, 1916.
9. J. A. MOYER: Distribution of Vertical Soil Pressure, *Eng. Record*, vol. 69, 1914, and vol. 71, 1915.
10. A. T. GOLDBECK: Distribution of Pressures through Earthfills, *Proc. A.S.T.M.*, vol. 17, 1917.
11. FRANZ KÖGLER and A. SCHEIDIG: Pressure Distribution in Building Soil (German), *Die Bautechnik*, vol. 5, 1927, vol. 6, 1928, and vol. 7, 1929.

12. O. FABER: Pressure Distribution under Bases and Stability of Foundations, *Structural Eng.*, vol. 11, 1933.
13. F. SCHLEICHER: Distribution of Soil Pressures under Rigid Foundations (German), *Der Bauingenieur*, vol. 14, 1933.
14. F. E. GIESECKE and associates: The Distribution of Soil Pressure beneath a Footing, *Tex. Eng. Exp. Sta. Bull.* 43, 1933.
15. M. G. SPANGLER: Horizontal Pressures on Retaining Walls Due to Concentrated Surface Loads, *Iowa Eng. Exp. Sta. Bull.* 140, Iowa State College, 1938; also *Proc. Intern. Conf. Soil Mech.*, vol. I, Paper J-1, 1936; *Proc. Eighteenth Ann. Meeting, Highway Research Board*, part II, 1938.
16. EMIL GERBER: "Investigations on the Pressure Distribution in Locally Loaded Sand" (dissertation in German), Zürich, 1929.
17. K. WOLF: Ausbreitung der Kraft in der Halbebene und in Halbraum bei anisotropem Material, *Z. angew. Math. Mech.*, vol. 15, 1935.
18. M. A. BIOT: Effect of Certain Discontinuities on the Pressure Distribution in a Loaded Soil, *Physics*, vol. 6, 1935.
19. S. D. CAROTHERS: Direct Determination of Stresses, *Proc. Roy. Soc. (London)*, series A, vol. 47; also two papers in *Proc. Intern. Math. Congr.*, Toronto, Canada, part II.
20. O. K. FRÖHLICH: "Druckverteilung im Baugrunde," Julius Springer, Vienna, 1934; also A. E. CUMMINGS, Distribution of Stresses under a Foundation, *Trans. A.S.C.E.*, vol. 101, 1936.
21. A. E. CUMMINGS: Foundation Stresses in an Elastic Solid with a Rigid Underlying Boundary, *Civil Engineering*, New York, vol. 11, 1941.

## CHAPTER V

### SHEARING RESISTANCE AND CONDITIONS OF FAILURE OF AN EARTH MASS

In this chapter conditions of failure of earth masses will be considered. This is an approach to the solution of the first part of the basic problem of soil mechanics as formulated in Sec. 4:1 ("stability problems"). Failure of an earth mass will be defined as loss of continuity due to the action of a shearing stress. In the case of cohesive soils the term "rupture" may be used.

**5:1. Conception of Shearing Resistance.**—A shearing stress tends to displace isolated particles of an earth mass with respect to each other or to displace a part of the mass with respect to the remainder. There is *slip of particles* if they are displaced with respect to each other. If a part of the mass is displaced with respect to the remainder, it is said that the mass *disintegrates* along certain failure lines; or if the mass is plastic, the phenomenon of *plastic flow* takes place. This mutual displacement of particles or parts of an earth mass is *opposed by its shearing resistance*. Shearing resistance is a passive stress and develops (or is "mobilized") only if there is a shearing stress. The value of the shearing resistance equals the value of the shearing stress at any time; and if the shearing stress increases, the shearing resistance increases accordingly. This may continue *only up to a certain limit s*, which is termed *shearing value* (also shearing strength, ultimate shearing resistance, or yielding value). At that point the resistance of the earth mass may be considered as exhausted, and failure, as already described, occurs. Shearing resistance of an earth mass is due to complicated physicochemical phenomena within the earth mass. To simplify its study, the source of shearing resistance in an idealized fragmental mass is traced to friction and cohesion between particles. In an actual earth mass, especially in clay, such a simplification is purely *conventional*. Shearing resistance and both its components, friction and cohesion, are to be expressed in terms of stress, for instance, in tons per square foot. The shearing strain

or the deformation produced by the shearing stress in an earth mass consists of an inelastic (irreversible) and an elastic (reversible) part. The latter disappears as soon as the shearing stress is removed.

#### A. EQUILIBRIUM AND FAILURE OF IDEALIZED FRAGMENTAL MASSES

**5:2. Equilibrium of an Idealized Cohesionless Fragmental Mass.**—Consider the surface of contact of two grains or fragments of a cohesionless fragmental mass (Fig. 5:1) and a small area of one square unit at this surface. The stress transmitted from one

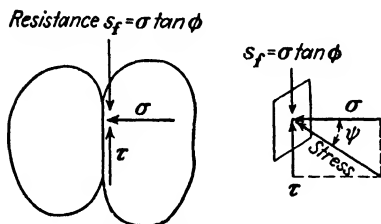


FIG. 5:1.—Equilibrium of an idealized cohesionless fragmental mass.

grain or fragment of the mass to the other will be broken into a normal stress  $\sigma$  and a tangential  $\tau$ . There will be no slip if the ratio  $\tau/\sigma$  is less than the coefficient of friction of one grain with respect to the other. In its turn, this coefficient of friction equals  $\tan \phi$ , where  $\phi$  is the *angle of internal friction*

(or simply the angle of friction) of the mass. Hence there will be no slip of the particles shown in Fig. 5:1 if

$$\frac{\tau}{\sigma} < \tan \phi \quad (5:1)$$

The mass will be in the state of “limit equilibrium” or “plastic equilibrium” if the ratio  $\tau/\sigma$  *exactly* equals  $\tan \phi$  at any point of the mass. A slip will then start at this particular point. The condition

$$\frac{\tau}{\sigma} = \tan \phi \quad (5:2)$$

is the “condition of failure” or “condition of plasticity” of the mass. Notice that the term “plasticity” is used here in a sense quite different from that in Sec. 2:18. What is termed “friction” or “internal friction” in this discussion is termed in mechanics “static friction,” or friction at the start of motion.

It should be clearly understood that the idealized fragmental mass is *not* assumed to be in the state of limit equilibrium *throughout*, as often believed. Though it is idealized, it possesses friction;

and if at some part of the mass equilibrium is lost, the mass may be in perfect equilibrium at a certain distance from that part. In an actual earth mass there is some difference between the angle of internal friction  $\phi$  and the angle of repose  $\phi'$ , the latter being generally smaller than the former. The value of the angle of repose may be found by pouring grains or particles through a funnel, practically without impact. The cone thus formed (Fig. 5:2) possesses *natural slopes* making angles  $\phi'$  with the horizon.\* Thus in an actual earth mass the angle of friction  $\phi$  is not to be confused with the angle of repose  $\phi'$ .

The two-dimensional problem to be solved is as follows: Given a point of the mass in the state of limit (or plastic) equilibrium, find the ratio of the principal stresses  $\sigma_{III}$  and  $\sigma_I$  at that point.

Should the impending failure at the given point take place along a plane identified by point  $D'$  (stresses  $\sigma$  and  $\tau$ , Fig. 5:3), this point  $D'$  necessarily lies on a tangent to the Mohr circle. Otherwise the ratio  $\tau/\sigma$  would be less than  $\tan \phi$ , and the plane in question would not be at the state of limit equilibrium.

**5:3. Rankine Formula.**—As is well known, distances  $OC$  and  $OH$  in Mohr's circle (Fig. 5:3) represent the major principal stress  $\sigma_I$  and the minor principal stress  $\sigma_{III}$ , respectively. Let  $OA = 1$ ; then  $AC = \sin \phi$ . The relationship between the major and the minor principal stress, which corresponds to the state of limit equilibrium, may be defined thus:

$$\begin{aligned}\sigma_{III} &= 1 - \sin \phi \\ \sigma_I &= 1 + \sin \phi\end{aligned}$$

or

$$\frac{\sigma_{III}}{\sigma_I} = \frac{1 - \sin \phi}{1 + \sin \phi} \quad (5:3)$$

Simple trigonometric transformations would lead to formula (5:4):

$$\frac{\sigma_{III}}{\sigma_I} = \tan^2 \left( 45^\circ - \frac{\phi}{2} \right) \quad (5:4)$$

\* If the experiment is carefully done, there are small roundings at the vertex and at the base of the cone, explained by the boundary conditions.

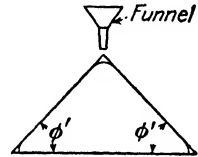


FIG. 5:2.—Angle of repose.



though the value of the maximum shear still corresponds to these bisectors.

**5:5. Active and Passive Pressure.**—Principal stresses in a semi-infinite mass run vertically (major principal stress,  $\sigma_1 = \gamma z$ ) and horizontally (minor principal stress,  $\sigma_{111} = K\sigma_1$ ). Designations are as follows:

- $K$  = coefficient of pressure at rest.
- $\gamma$  = unit weight of earth.
- $z$  = depth.

If a part of the semi-infinite mass is removed and replaced by an immovable, undeformable, and *frictionless vertical plane AB* (Fig.

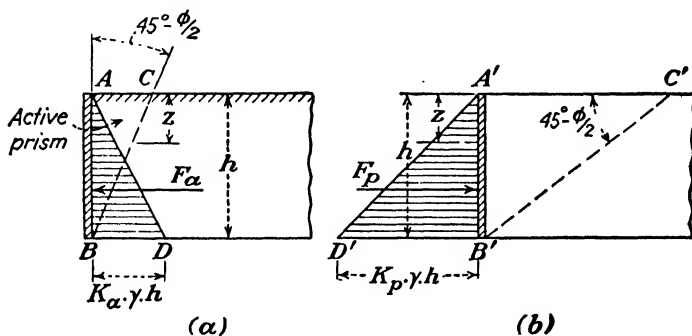


FIG. 5:4.—Active and passive pressure.

5:4a), the unit horizontal pressure on that plane will not change, still equaling  $\sigma_{111} = K\gamma z$ . If, however, the vertical plane *AB* moves from the mass, the unit horizontal pressure decreases to reach a minimum value  $\sigma_{111} = K_a\gamma z$ . In the case of further movement there will be no continuity of strains, and failure will occur along line *BC*, making the angle of rupture  $45^\circ - (\phi/2)$  with the direction of the major principal stress. In this connection the latter is assumed to be still vertical, which is an approximation; hence straight line *BC* is also an approximation.

In Fig. 5:4b vertical plane *AB* is assumed to be moved against the mass. To produce failure, the pushing force should be considerable and greater than the weight of the mass close to the wall. Hence the major principal stress may be assumed horizontal and the minor one vertical. The plane in the state of limit equilibrium along which slips occur forms an angle of  $45^\circ - (\phi/2)$  with the horizon or  $45^\circ + (\phi/2)$  with the vertical line. If we apply formula

(5:3) to this case, a value of  $K_p = \tan^2 [45^\circ + (\phi/2)]$  would be obtained. It may be termed the *passive Rankine value*. It is evidently the reciprocal of the active Rankine value  $K_a$  (compare Sec. 5:3):

$$K_p = \frac{1}{K_a} \quad (5:6)$$

Failure line  $BC$  separates the active prism  $ABC$  from the rest of the mass. In the same way, the passive prism  $A'B'C'$  is separated from the rest of the mass by failure line  $B'C'$ . Obviously, straight line  $B'C'$  is an approximation.

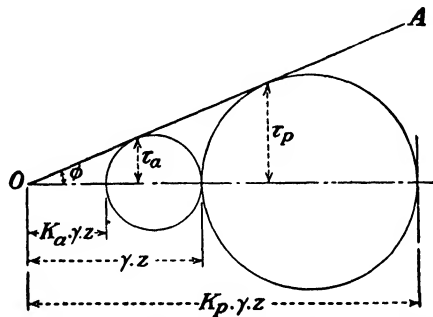


FIG. 5:5.—Active and passive pressures in terms of a Mohr's circle.

In the computation of the active pressure  $F_a$  against plane  $AB$  (height  $h$ , Fig. 5:4a), it is to be remembered that unit active pressure  $K_a \gamma z$  is proportional to the depth  $z$  and hence may be represented by a straight line ( $AD$  in Fig. 5:4a). Pressure  $F_a$  equals the area of triangle  $ABD$ :

$$F_a = \frac{1}{2} \gamma h^2 K_a \quad (5:7)$$

In the same way, passive pressure  $F_p$  equals the area of triangle  $A'B'D'$ :

$$F_p = \frac{1}{2} \gamma h^2 K_p \quad (5:8)$$

Figure 5:5 shows how both the active and the passive pressure may be represented in terms of Mohr's circle. For the left circle, vertical pressure  $\gamma z$  is the major principal stress, and unit active pressure  $K_a \gamma z$  is the minor principal stress. For the right circle, vertical pressure  $\gamma z$  is the minor principal stress, and unit passive pressure  $K_p \gamma z$  is the major principal stress. Active pressure is the minimum pressure that the mass exerts on a movable but undeformable vertical plane just before failure occurs, and passive

pressure is the maximum pressure that the mass may withstand without failure. Passive pressure is several times as great as the active. Both active and passive pressures are compression stresses.

The values of unit shearing stresses causing failure are  $\tau_a$  in the case of active pressure and  $\tau_p$  in the case of passive pressure (Fig. 5:5).

Between the start of motion of the plane  $A'B'$  against the mass (Fig. 5:4b) and the moment of failure, lateral (horizontal), pressure in the mass close to that plane may acquire different values. The range of these values is between the natural lateral pressure, as controlled by the value of the coefficient of pressure at rest  $K$ , and the passive pressure, as controlled by the Rankine passive value  $K_p$ .

It is to be noticed that instead of the terms "active pressure" and "passive pressure," the terms "earth pressure" and "earth resistance" are also used.

**5:6. Coulomb Formula.\***—If an idealized cohesionless fragmental mass is in the state of limit equilibrium, condition (5:2) furnishes

$$\tau = \sigma \tan \phi \quad (5:9)$$

Since the mass is in the state of limit equilibrium, it has developed as much frictional resistance  $s_f$  as it can. It is obvious that

$$s_f = \tau = \sigma \tan \phi \quad (5:10)$$

This means that the frictional resistance which a fragmental mass can develop *depends on the acting normal stress*  $\sigma$ .

The idealized fragmental mass may possess cohesion, *i. e.*, its particles may be glued to each other. Cohesion is visualized as a passive stress that together with friction may be "mobilized" to oppose the shearing stress acting in any direction. Designate by  $c$  the maximum value of unit cohesion that a mass can develop. Assuming first that the mass does not possess any frictional resistance at all, the maximum cohesive resistance  $s_c$  is

$$s_c = c$$

Assuming, furthermore, that the mass can develop both frictional and cohesive resistance, its full shearing value  $s$  would be

$$s = s_f + s_c = \sigma \tan \phi + c \quad (5:11)$$

\* Charles Auguste de Coulomb (1736–1806), famous French physicist, also a military engineer.



This ordinate expresses at the same time the shearing value of the mass  $s$ . It consists of two parts: frictional resistance  $DJ = \sigma \tan \phi$  and cohesive resistance  $JF = GK = p_i \tan \phi = c$ . Thus Fig. 5:6 is the Coulomb formula graphically represented.

It follows also from Fig. 5:6 that the condition of plastic equilibrium of a cohesive fragmental mass may be written under the form of a generalized Rankine formula (5:13):

$$\frac{\sigma_{III} + p_i}{\sigma_I + p_i} = \frac{1 - \sin \phi}{1 + \sin \phi} = \tan^2 \left( 45^\circ - \frac{\phi}{2} \right) = K_a \quad (5:13)$$

It is noteworthy that the value of the angle of rupture in this case is again  $45 - (\phi/2)$ . In other words, in an idealized fragmental mass *cohesion does not influence the value of the angle of rupture*.

**5:8. Zones of Discontinuity in a Two-dimensional Problem.**—When a shear failure occurs, the fragmental mass is subdivided

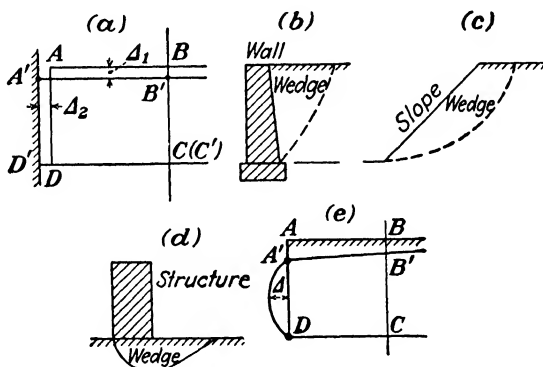


FIG. 5:7.—Zones of discontinuity.

into small, approximately rectangular areas by a pattern of *failure lines*, termed also “slip lines,” “shearing surfaces,” and “sliding surfaces.” In some cases a part of the mass is separated from the rest of it by a *crack* that, after all, follows one of those failure lines. It should be borne in mind that in the state of limit or plastic equilibrium there are no failure lines as yet and only *possible* failure lines are considered. Hence, if there are cracks or fissures in an earth mass, meaning a failure, theoretical formulas cannot be applied. Furthermore, conditions of failure developed for mass  $A'B'C'D'$  (Fig. 5:7a), which is in the state of limit equilibrium, in reality are used in studying the stability of mass  $ABCD$ , which is

in the natural (or original) state. If mass  $A'B'C'D'$  is to be substituted for mass  $ABCD$ , displacements  $\Delta_1$  and  $\Delta_2$  must be small.

Zones or sections of a mass with cracks and fissures and also with considerable displacements of particles, will be termed "zones of discontinuity." If separated from the rest of the mass by a crack, a zone of discontinuity is often termed a *wedge*. There may be no definite crack or failure line if discontinuity is due to considerable displacements or to plastic flow. It is obvious that the conception of "zone of discontinuity" is broader than that of "wedge."

In the case of an elastic continuum, it will be assumed that a zone of discontinuity is that zone of the body where the shearing resistance of the material has been overcome by the shearing stress. A few examples of zones of discontinuity are also shown in Fig. 5:7. They are a wedge behind a moving retaining wall (Fig. 5:7*b*), a sliding wedge of an unstable slope (Fig. 5:7*c*), and a prism pushed out from underneath a structure (Fig. 5:7*d*). A zone of discontinuity due to considerable displacements  $\Delta$  of a part of a flexible lateral support is shown in Fig. 5:7*e*.

Generally an assumption is made that the shearing stress in an idealized fragmental mass is *uniformly distributed* along a failure line and that failure occurs simultaneously along its whole length. This assumption is completely unwarranted in the case of actual earth masses; since both the shearing stress and the shearing strength of the earth material are not constant along a failure line, equilibrium will only be broken at one or more points of that line. Then this part of the failure line will be inactive, and the mass under consideration will be transformed into a different condition of stress. Hence, it is impossible to establish analytically the equation of a failure line for an actual earth mass. There are, however, theoretical considerations for determining the shape of the failure line for idealized masses, as discussed hereafter.

**5:9. Failure Lines in a Fragmental Mass.**—Theoretical failure lines along which a fragmental mass disintegrates may be found from the condition that the tangent to the failure line intersects the direction of the major principal stress under the angle of rupture  $45^\circ - \phi/2$  (Sec. 5:4).

*a. Case of a Line Load.*—For the case of a line load  $\bar{p}$  applied at the boundary failure lines are *logarithmic spirals*, since tangents to this curve make a constant angle with the radius vectors. The point of application of the load  $\bar{p}$  is the origin of the spiral. Radius

vectors of the curve, or straight lines emanating from the origin, are directions of major principal stresses. At each point  $B$  of the boundary and at each point of the mass, there are two logarithmic spirals 1 and 2 which intersect the boundary under the angle of rupture  $45^\circ - \phi/2$  and each other under  $90^\circ - \phi$ . Their equations are

$$\rho = \rho_0 e^{\pm a\theta} \tag{5:14}$$

where  $\rho$  = a radius vector of the spiral.

$\rho_0$  = distance from the origin

to points  $B$  where the spirals intersect the horizontal boundary.

$\theta$  = polar angle counted clockwise at the right half of Fig. 5:8 (and counterclockwise at the left half).

$a$  = cotangent of the constant angle of intersection of the spiral with the radius vectors:

$$a = \cot\left(45^\circ - \frac{\phi}{2}\right) = \tan\left(45^\circ + \frac{\phi}{2}\right) = \sqrt{K_p} \tag{5:15}$$

The sign "plus" in Eq. (5:14) refers to curve 2 in Fig. 5:8, and the sign "minus" to curve 1.

*b. Case of a Uniformly Loaded Strip.*—The procedure to be followed in this case would be essentially the same as in the case of a line load. Since, however, the determination of the directions of principal stresses in a fragmental mass (not in an elastic continuum, Sec. 4:15*d*) presents some difficulties, the

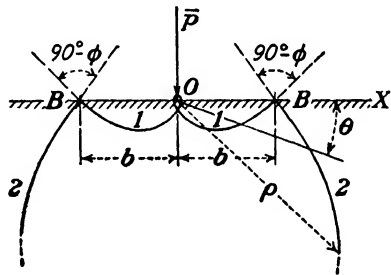


FIG. 5:8.—Failure lines in a fragmental mass are logarithmic spirals.

shape of the failure line, instead of being found theoretically, is simply assumed: (1) An active prism  $A$  is formed under the strip; (2) a passive prism  $P$  has to be pushed out; (3) both prisms are connected with a smooth curve, generally a logarithmic spiral  $A_1P_1$  (Fig. 5:9), the origin of the spiral being at point  $O$ . There are also other assumptions in the soil-mechanics literature; but whatever the assumed failure lines might be, they must satisfy the condition of continuity (Sec. 4:9), *i.e.*, be smooth curves without breaks.

Referring to Fig. 5:4 and taking into account that the direction



Hence, using the table,

$$\begin{aligned}\rho_2 &= 20.9 \times 1.77 = 37.0 \text{ ft.} \\ R &= 20.9 \times 1.48 = 30.9 \text{ ft.}\end{aligned}$$

Referring to Fig. 5:9, plot  $OA' = 20.9$  ft. and  $OP' = 37.0$  ft. To find the center of the circle replacing the logarithmic spiral, swing arcs of a radius  $R = 30.9$  ft. from both points  $A'$  and  $P'$ . The replacing circle is not exactly tangent to the sides of the prisms, the difference being small, however.

The radius vectors emanating from the origin of the logarithmic spiral in Fig. 5:9 are *not* the directions of major principal stresses as in Fig. 5:8 but a *fan of failure lines*, which, of course, intersect the logarithmic spiral under an angle of  $90^\circ - \phi$ . Hence the value of  $a$  as in Eq. (5:14) would be

$$a = \cot(90^\circ - \phi) = \tan \phi \quad (5:17)$$

and the equation of the spiral in the given case.

$$\rho = \rho_0 e^{\theta \tan \phi} \quad (5:18)$$

The zone between the active and the passive prisms is called sometimes "zone of radial shear" (Fig. 5:9).

Remembering that lines  $OA$  and  $OP$  (Fig. 5:9) make an angle of  $90^\circ$ , we have

$$\rho_2 = \rho_1 e^{\frac{\pi}{2} \tan \phi} \quad (5:19)$$

The radius of the replacing circle  $R$  may be taken equal to the average of the radii of curvature at points  $A_1$  and  $P_1$  as done in Eq. (5:16).

**5:10. Failure Lines in an Elastic Continuum.**—Failure lines under a uniformly loaded strip on the horizontal boundary of an elastic continuum are constructed as trajectories of maximum shearing stresses  $\tau_{\max}$ . The maximum shearing stress  $\tau_{\max}$  at a point of an elastic continuum acts on the planes bisecting the angles between the principal stresses. In the case of a semi-infinite elastic continuum loaded with a strip load, trajectories of principal stresses are confocal ellipses and hyperbolas (Figs. 5:9a and 3:8). To trace the direction of the trajectory of maximum shearing stress  $\tau_{\max}$  at point  $A$ , a tangent  $T'$  either to the ellipse or to the hyperbola intersecting at that point is to be drawn. The tangent  $T'$  to the trajectory of maximum shearing stress makes an angle  $\alpha = 45^\circ$  with the tangent  $T$ . There are two trajectories of maximum shearing stress at each point of the mass; they are orthogonal, *i.e.*, they intersect each other at a right angle. In Fig. 5:10b a set of such trajectories is shown. If a solid approaching an elastic continuum is overloaded, "slip lines," or "Lüders lines," appear on its surface. As observed in the case of metals, they have a shape

close to that of trajectories of maximum shearing stress, at least in

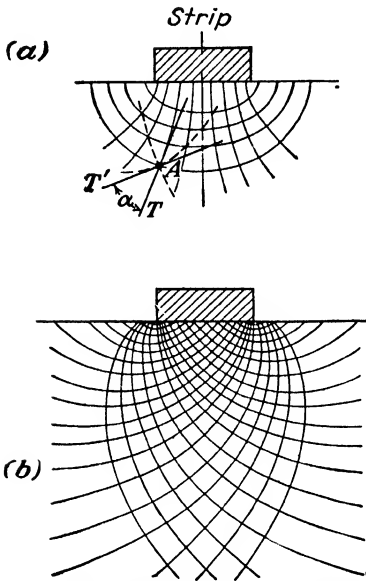


FIG. 5:10.—Trajectories of maximum shear.

the most highly stressed portion under the concentrated load. It is generally thought that failure (or, more accurately, disintegration combined with plastic flow) of an elastic continuum occurs along the trajectories of maximum shearing stress which obviously are *smooth lines without breaks*. After all, failure lines in an elastic continuum are nothing more than failure lines in an idealized fragmental mass with the angle of internal friction  $\phi = 0$ .

To obtain experimentally an idea of the pattern of failure lines under a strip load, it is sufficient to extend a layer of moist cohesive soil approximately  $\frac{3}{4}$  in. thick and to apply carefully, but strongly a rigid metallic punch to its upper boundary AA (Fig. 5:11).

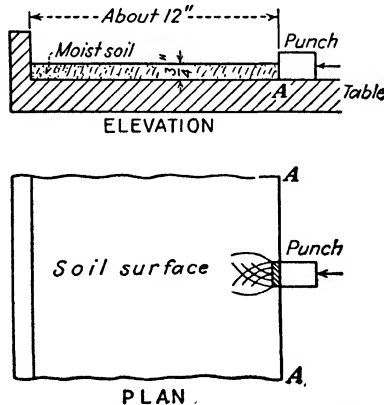


FIG. 5:11.—A simple way of securing failure lines in the laboratory.

Housel<sup>7</sup> placed a cohesive soil mass between two glasses, loaded it from above, and subjected it to a prolonged photographic exposure.

Marks made on the visible surface of the mass moved along shear lines which could be seen on the photograph in the form of short curves.

### B. FRICTION AND COHESION IN ACTUAL EARTH MASSES

In the development of conditions of equilibrium and failure of idealized fragmental masses, the conceptions of "friction" and "cohesion" have been presented in a very simplified way, and it is convenient at the present stage of the discussion to clarify these two conceptions as applied to actual earth masses.

**5:11. Angle of Internal Friction in Actual Earth Masses.**—Condition (5:2) presupposes that the angle of friction for a given material is *constant throughout the whole mass*. This is not true, however, in the case of actual fragmental masses such as sand masses, in which the angle of friction changes from point to point of the mass. The value of the angle of friction  $\phi$  depends on the normal pressure  $\sigma$ , on the density of the given sand, on the grain size, on the shape of the grains, and on the uniformity of the material. Average values of  $\phi$  as used in design should be considered merely as "design conventionalities" introduced for the sake of simplicity. For medium and coarse dry sands, the value of the angle of friction may be estimated at from 30 to 35°, and somewhat less if the material is under water; the angle of friction of both dry and wet medium and coarse sand is practically the same. The angle of repose of these materials may be different, however.

The angle of internal friction of clays is much smaller than that of sands; it ranges in clays from a practically zero value (soft plastic clays) to 15° or perhaps 20°. Strictly speaking there is no angle of internal friction in clays and also in some sands (Sec. 5:1). What is called "the angle of internal friction" of a soil is the value of  $\phi$  found in a shearing test, which in reality is nothing more than an *apparent*, or conventional, value. Sometimes the value of  $\phi$  obtained from a shearing test is called "angle of shearing resistance."

**5:12. Cohesion in Actual Earth Masses.**—There are two kinds of cohesion in soils: (a) true cohesion, caused by the mutual attraction of particles due to molecular forces; (b) apparent cohesion, due to the action of moisture films. For instance, dry sand, especially fine sand, becomes cohesive when moist. This is so because the surface tension in this case acts at the surface of the film and holds

the sand grains together. In a general case true cohesion in soils is small and may be disregarded. Some exceptions, however, are (a) dense gravels composed of both coarse and fine particles, the latter acting as a "binder" which cements the whole mass, and (b) compact sands and a few other soils.

In the following discussion apparent cohesion *only* will be considered. To make a soil mass cohesive, the moisture content should be adequately but not exceedingly high. If, for instance, a given soil is very cohesive when containing 15 per cent of moisture by dry weight, it may be less cohesive when containing 5 or 25 per cent of moisture. In the former case there may not be moisture enough to form films on all particles of the mass, and in the latter case the surface tension may be removed by the excess of water. The "optimum" value of moisture content, corresponding to maximum cohesion, should be determined for each soil experimentally. It is assumed that cohesion in idealized fragmental masses *does not* depend on the value of the normal stress. This may be true in the case of metals or rocks but is an approximation in soils, since in this case the normal stress controls the moisture content and the latter controls cohesion. Cohesion may be developed in any direction within the body.

As already stated, the value of the ultimate cohesive resistance that may be "mobilized" within the body is designated by the symbol  $c$ . Some average values are

	c, lb. per sq. ft.
1. Almost liquid clay . . . . .	100
2. Very soft clay . . . . .	200
3. Soft clay . . . . .	400
4. Medium clay . . . . .	1,000
5. Muddy sand . . . . .	400
6. Very dense sand and gravel . . . . .	1,000

The fact that these values are *average values* and that cohesion in soils *may* depend on the normal stress cannot be overemphasized.

### C. SHEAR FAILURE IN AN ACTUAL EARTH MASS

**5:13. Progressive Failure.**—As stated in Sec. 5:7 a shear failure in an actual earth mass occurs gradually. When the stresses and strains are small, the mass is said to be in an *elastic state*. When the limit equilibrium has been destroyed by the shearing stress, the mass either disintegrates or flows plastically. In both of these cases

the mass is said to be in a *plastic state*. It is sometimes believed that the soil material first becomes plastic in the disturbed zone (Sec. 4:22). Afterward the plastic state propagates to the adjacent zones, thus bringing the material to an intermediate *elasto-plastic state*. Finally failure occurs more or less according to Fig. 5:9.

At the present state of our knowledge (1947) it is not known how to correlate the shearing stress and the shearing strain in actual earth masses, though deformations may be observed in the laboratory shear devices described hereafter (division D of this chapter). It is obvious, however, that under the action of the shearing stress a loaded plate or a structure moves down, this movement being accompanied by a slow gradual *motion of the mass along shearing surfaces*.

Another phenomenon that may contribute to progressive failure of an earth mass is *changes in its shear resistance*. Owing to fluctuations of the water table or saturation of the mass by rain followed by drought, the shearing resistance of the soil may decrease and increase cyclically, thus causing movement of the mass by jerks.

**5:14. Plastic Flow.**—Plastic flow is caused by a shearing stress and may occur only in a mass that possesses a very small angle of internal friction and considerable cohesion. Thus sands cannot flow plastically. As already explained (Sec. 5:13), sand and other soils are said to be in a “plastic state” when the limit equilibrium is overcome. Hence this expression, if met in the literature, should be given correct interpretation. In plastic clay, particles are surrounded by attracted solidified moisture, so that the whole represents a peculiar suspension of clay particles in a plastic medium. If such a clay layer is located close to an overloaded earth surface, plastic moisture flows from underneath the load, and clay particles suspended in it move in such a way that both soil particles and moisture form a whole. Such a movement is very much like the plastic flow of metals, or creep.

It is assumed that the shearing stress in the flowing zone is constant and equals the ultimate cohesion value of the material:

$$\tau = s_c = c \quad (5:20)$$

The latter assumption has been introduced into mechanics by Saint-Venant (compare Sec. 4:11). It has been observed on many occasions that plastic flow stops, whereas according to condition

(5:20) there is no reason for it. It should be concluded, therefore, that at a certain stage of plastic flow the shearing stress  $\tau$  decreases or the shearing strength  $s_c$  increases or both phenomena occur simultaneously. The decrease in the shearing stress  $\tau$  would mean that deformation relieves stress, and the increase in shearing strength would mean that the flowing mass changes its properties. Apparently both phenomena occur simultaneously, and the mass recovers a part of its cohesion lost owing to the action of an excessive shearing stress after the latter has decreased.

Since plastic flow is a movement, equations describing it should contain a time element  $t$ . Owing to some assumptions, however, equations of plasticity, like elastic formulas, do not contain the time factor  $t$ .

During the plastic flow the volume of the moving mass does not change; hence the value of Poisson's ratio corresponding to the plastic flow should be  $\mu = \frac{1}{2}$ , as for incompressible bodies.

**5:15. Flow Failures.**—An earth mass, particularly a sand mass, may be in its *densest state*; the opposite, then, would be the *loosest state*. A sand mass in its loosest state is simply an agglomeration of individual sand particles in which there is no continuity of strains (Sec. 4:9). Hereafter such an agglomeration will be termed conventionally "loose mass" or "loose-sand mass."

*a. Causes of a Flow Failure.*—A loose-sand mass may be dry, moist, or saturated with water. Imagine two soil particles placed one on top of the other and held in place by a normal stress  $\sigma$  (Fig. 4:14a). The frictional resistance preventing their mutual motion is expressed by formula (5:10). Two cases will be considered: (1) Owing to vibrations (earthquakes, explosions, blasting, or pile-driving), the upper particle may jump up. Consequently, the normal stress  $\sigma$  will vanish; and before the upper particle resumes its position, the lower one may move. Since this happens throughout the mass, the latter flows as a liquid. Or (2) in a saturated loose mass the pore moisture  $u$  may increase to balance the normal stress  $\sigma$ , and if the pore moisture cannot flow out quickly to relieve  $u$  (such is the case of silts and fine sands), a sudden liquefaction of the mass takes place. The *flow failure* as described is a particular case of shear failure, since, after all, shear is a change in shape and so is a flow failure.

*b. Particular Cases.*—Settlements of embankments and flattening of slopes during earthquakes have been observed. Sudden

liquefaction of saturated deposits of chemical wastes and of saturated silt hills at the shore of a river or a lake has been reported. Real causes of such liquefaction may be quite insignificant in themselves. Formation of cracks at the surface of the mass and subsequent gradual filling of these cracks with rain water may be one of the causes of a sudden liquefaction of the mass, which will take place suddenly as soon as water in the crack reaches a certain level and the pore moisture pressure increases accordingly. A displacement within the mass due to a sudden application of even a small load may increase the pore moisture pressure and cause a failure. To prove this, Casagrande<sup>3</sup> deposited fine quartz sand in a loose saturated state into a small tank with free water standing at its surface, then thrust a stick into the sand, and suddenly the weight sank.

**5:16. Some Cases of Change in Shearing Resistance.**—*a. Thixotropic Clays.*—Flow failures in loose fine sands and silts (Sec. 5:15) should not be confused with flow failures in thixotropic clays (Sec. 1:6), which are also caused by vibrations. As is known, gels of such clays, if vibrated, become liquid sols without addition of water. In this connection, the given clay loses its shearing resistance, since liquids possess none or practically none. After a period of rest, however, sols become gels again, and the clay rehardens.

*b. Confinement of a Loose-sand Mass.*—A loose-sand mass, if acted upon by a load, may flow (Sec. 5:15) only if it is offered a possibility to flow in some direction. But if it is confined either by adjacent huge portions of the same mass or by a substantial container, its voids ratio will decrease under load, and finally a certain increased value of shearing resistance will be reached. Compaction of earth fills is based on this property of loose masses. Figure 5:12 also illustrates this point. Very loose sand is placed in a channel *a* and pushed forward with a vertical plank *A*, and it is evident that the regular motion of the mass as a whole will take place only when all the grains gather together to form a mass.

The phenomenon shown in Fig. 5:12 may be termed "adjustment" of particles to each other (known to petrographers as "mutual accommodation of particles"). It constitutes the initial step of practically every deformation of a mass under load (compare also Sec. 6:1).

*c. Reynolds' Experiment.*—To prove that if a sand mass cannot expand, it acts practically as a rock, the experiment made by

Reynolds (Cambridge, England) should be remembered. A watertight bag filled with dry sand may be deformed easily, but the bag becomes exceedingly rigid if all the pores are filled with water.

This experiment may be performed in another way by connecting a rubber bag filled with sand with a vacuum apparatus. The outside atmospheric pressure acts then as a load, and the

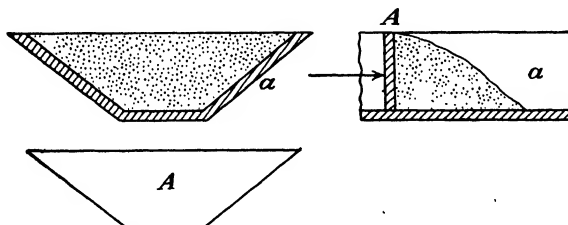


FIG. 5:12.—Model showing "adjustment" of sand particles.

loose sand acquires properties of a sand layer located at a great depth and compressed by the overburden.

#### D. SHEAR TESTS\*

**5:17. Classification of Shear Tests.**—The objective of a shear test is to find experimentally the values of  $\phi$  (and hence of  $\tan \phi$ ) and  $c$  to be used in the Coulomb formula (5:11). A shear test is a test to failure.

Consider again Fig. 5:6. It is obvious that this figure furnishes the value of the shearing strength in the Coulomb formula graphically. In fact, distance  $DF = s$ . Since the unit cohesion  $c$  of an idealized cohesive mass is assumed to be constant, the shearing strength of that mass  $s$  may be changed only by changing the value of the normal stress  $\sigma$  acting on the failure line. In Fig. 5:6 this stress is represented by the distance  $ED$ . Consider now Fig. 5:13, representing a compressed specimen just before failure along failure line  $AB$ , *i.e.*, at the state of plastic equilibrium. The symbol  $\sigma$  then denotes the normal pressure on plane  $AB$  at that state. In reality, the changing of the normal stress  $\sigma$  in the laboratory is done by placing the soil sample between two boxes (Fig. 5:14), one  $X$  movable and the other  $Y$  fixed, that are pressed together by a variable normal load  $N$  and the box  $X$  is pulled laterally. What in Fig. 5:13 is the failure line  $AB$ , in the shear boxes (Fig.

\* For more details see Appendix C.

5:14) is the horizontal plane between the boxes *X* and *P*, the normal unit pressure  $\sigma$  on it being built up by the variable load *N*. The test shown in Fig. 5:14 is the *direct shear test*.

Another way to vary the normal stress  $\sigma$  is to control the principal stresses  $\sigma$ , and  $\sigma_{III}$ . These stresses are clearly seen in Fig.

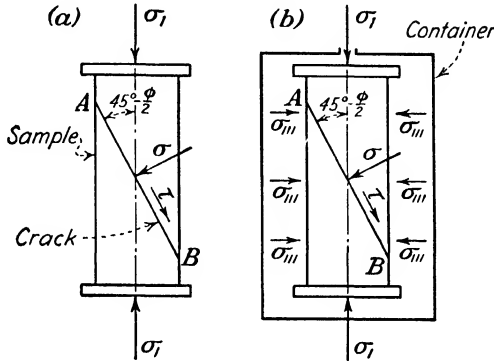


FIG. 5:13.—(a) Nonconfined compression test; (b) triaxial compression test (cylinder test).

5:6, and on the specimen shown in Fig. 5:13a the major principal stress  $\sigma$ , acting along the vertical axis of the sample is built up by the vertical load compressing the sample. The minor principal stress  $\sigma_{III}$ , in Fig. 5:13b is due to the pressure of the liquid in a closed container in which the sample is placed; in Fig. 5:13a the minor principal stress  $\sigma_{III} = 0$  owing to boundary conditions, since at the surface of the specimen no horizontal force is applied except atmospheric pressure. The tests shown in Fig. 5:13a and b are the *nonconfined compression test* and *triaxial compression test* (termed also “cylinder test”), respectively.

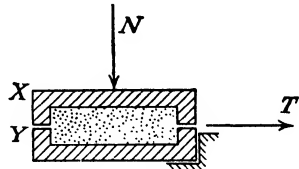


FIG. 5:14.—Direct shear test.

Besides the three basic shear tests there are other interesting shear tests which, however, are not so often applied.<sup>11, 12</sup>

**5:18. Basic Shear Tests. a. Nonconfined Compression Test.**—A cohesive sample is compressed between two rigid plates (Fig. 5:13a). Obviously, the value of the major principal stress  $\sigma$ , equals the compression load divided by the area of the cross section of the sample. Usually the cross section of the sample is square (about 1.0 by 1.0 in. or more); the height of the sample being

from two and one-half to three times the side of the cross section. At the state of plastic equilibrium or a little later, the crack  $AB$  (failure line) appears, making a theoretical angle of  $45^\circ - \phi/2$  with the vertical. This angle could be measured on the failed sample.

Such a procedure does not furnish accurate results, however, and the use of the nonconfined compression test may be recommended only if the value of the angle of friction is known or can be esti-

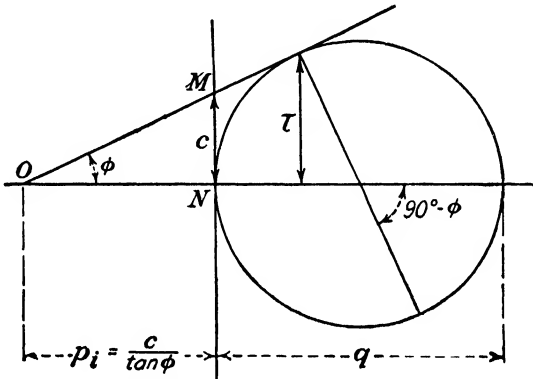


FIG. 5:15.—Mohr's circle for a nonconfined compression test.

ated. Figure 5:15 represents the Mohr circle for the nonconfined compression test obtained from Fig. 5:6 by making  $\sigma_{III} = 0$ . If the angle of friction is practically zero, as is the case of natural deposits of saturated soft plastic clays, the value of the cohesion equals approximately half compressive strength (Sec. 6:19a):

$$c = \frac{1}{2}q \quad (5:21)$$

Instead of failing completely, the sample in this test may bulge like a barrel. In such a case a certain decrease in height of the sample, for instance, by 20 per cent, is considered as a failure.

*b. Triaxial Test; Direct Shearing Test.*—If a series of triaxial tests with different values of  $\sigma_{III}$  is available, the envelope of corresponding Mohr's circles is a curve characteristic for a given material (Fig. 5:16). It is termed "line of rupture" or "Mohr's envelope." The use of the term "line of rupture" is not encouraged in this book in order to avoid confusion with the term "failure line," used to designate a surface (or a line in a two-dimensional representation) along which an overstressed mass disintegrates. So

far as cohesive soils are concerned, this envelope is a curve that approaches a straight line as the value of the compression stress increases. For an idealized fragmental material, this envelope is a straight line (compare also line  $OA$  in Fig. 5:5). Mohr's envelope is also often assumed to be approximately straight for actual earth masses, though it may be slightly curved even in the case of sands.

From different theories of failure of structural materials the so-called "Mohr's hypothesis" has been adopted in soil mechanics. Mohr assumed that in an actual three-dimensional case the value of the intermediate principal stress  $\sigma_{ii}$  has no influence on the

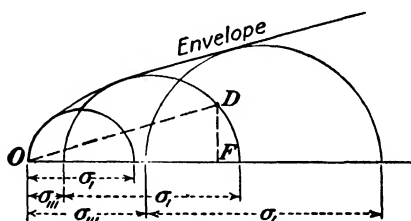


FIG. 5:16.—Mohr's envelope.

position of the "envelope," this assumption being an approximation.

To obtain a Mohr's envelope for a *cohesive soil* (both  $\phi$  and  $c$  required), at least *two* triaxial tests should be available. For checking purposes it is advisable to make more than two tests and to trace an average envelope. Figure 5:17 shows a straight-line envelope obtained from two triaxial tests. Experimental values from one of these tests are encircled in the figure. Instead of plotting the experimental values of  $\sigma_i$  and  $\sigma_{iii}$  from the triaxial tests and drawing Mohr circles, experimental values of  $\sigma$  and  $\tau = s$  [Eq. (5:11)] from two direct shear tests can be plotted (see the upper part of Fig. 5:17). The envelope and hence the values of  $\phi$  and  $c$  theoretically should be the same in both cases. It is advisable to compare Figs. 5:15 and 5:17, the letters  $O$ ,  $M$ , and  $N$  being at analogous places in both figures.

For the case of *cohesionless sand* ( $\phi$  only required) points  $O$  and  $N$  in Fig. 5:17 coincide. The envelope passes through point  $N$  which becomes the origin instead of  $O$ . Theoretically in this case *only one* (either triaxial or direct shearing) test is required. It is advisable, however, to make more than one test for checking purposes.

**5:19. Quick and Slow Shearing Tests on Cohesive Soils.**—  
*a. Direct Shearing Test.*—In a “quick test” the pulling force  $T$  (Fig. 5:14) is applied immediately after application of the normal force  $N$ , in order to prevent the sample from consolidating and decreasing its voids ratio.

Another way of conducting the direct shearing test on cohesive soils is to make the sample consolidate fully under a given normal load  $N$ . In this case the sample is placed between porous gratings,

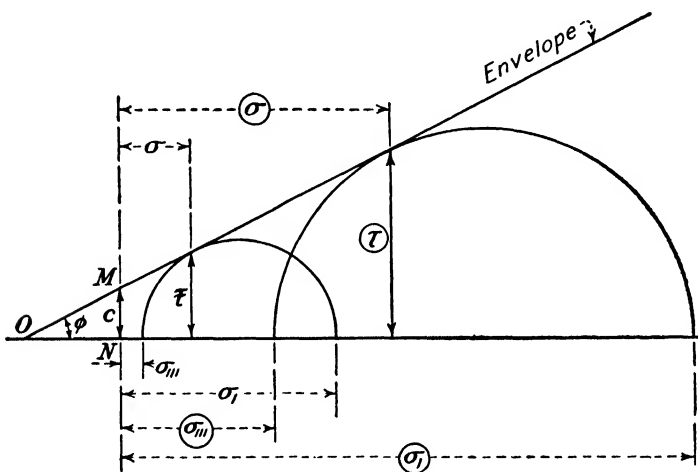


FIG. 5:17.—Graphical determination of  $\phi$  and  $c$  from two triaxial compression tests (or from two direct shearing tests).

whereas for a quick test impervious gratings are preferable. After consolidation is completed (in about 24 hr.), the pulling force  $T$  is applied either quickly or at a slow rate. These are the “consolidated quick test” and the “consolidated slow test,” respectively.

*b. Triaxial Compression Test.*—This test may also be performed in a “quick” and a “slow” manner so far as application of the axial load  $\sigma_1$  (Sec. 5:17) is concerned. Before application of the axial load the sample is generally permitted to consolidate under the hydrostatic pressure  $\sigma_{111}$ .

*c. Selection of Test for a Cohesive Soil.*—The subject of shear test on cohesive soils is controversial at the present time (1947). Preconsolidation of the sample increases its shearing resistance, and the more complete that preconsolidation the stronger the

sample. The neutral stress  $u$  in a quick test is larger than in the case of a slow one. The Coulomb formula (5:11) in this case is

$$s = (\sigma - u) \tan \phi + c \quad (5:22)$$

from which it follows that quick tests furnish smaller shearing resistance than the slow ones. The choice between a quick and a slow test is controlled by the nature of forces and stresses tending to destroy the prototype earth mass. As to the choice between a direct shearing and a triaxial test,<sup>9</sup> it is claimed that the stress distribution in the former test is rather obscure and hence the results are uncertain. Instead, the technique of a triaxial test is involved, and in the hands of an insufficiently trained man the test furnishes erratic data. Besides, triaxial tests are very sensitive to the disturbance of samples used.

**5:20. Critical Density.**—The term “critical density” (or critical porosity, critical voids ratio) of a sand mass has been introduced by A. Casagrande.<sup>3</sup> In a triaxial test the saturated sand sample is packed into a thin rubber membrane between two porous stones and connected with a vertical glass pipette. The changes of the volume of the sample can be determined from the fluctuations of the water level in that pipette. Casagrande observed that in this connection *dense sands expand and very loose sands decrease their volume*. The boundary between the range of porosities in which expansion or volume decrease occurs is the *critical density*. A flow failure (Sec. 5:15) may occur if the mass is looser than the critical density for a given load. To find the critical density several tests with different porosities of the samples should be made.

**5:21. Selection of a Shear Test for Sand.**—The concept of critical density may be important when *fine sand* is used for the construction of a dam. In this case the triaxial test contributes information for determining the necessary degree of sand compaction and is preferable to the direct shear test. The latter, however, should be used in other occasions of sand testing because of its simplicity. *Shear tests on sands should not be overdone*, however. On many occasions they are not essential at all, for instance, as in the design and analysis of foundations on thick sand deposits. In fact, for a constant value of the normal stress  $\sigma$  the shearing resistance of two sands with the angles of internal friction  $\phi = 30^\circ$  and  $\phi = 35^\circ$  (which is the range of  $\phi$ ; compare Sec. 5:11) differs by about 18 per cent only.

## Problems

1. The compressive strength of a soft clay sample in a nonconfined compression test is 1.0 kg. per sq. cm. Estimate roughly its shearing value in tons per square foot. *Ans.* 0.5.

2. Determine the Rankine values for a sand with an angle of internal friction  $\phi = 35^\circ$ . *Ans.*  $K_a = 0.27$ .

3. The cross section  $a$  of the sample in a compression test gradually increases because of the decrease in height of the sample. Hence the unit compressive stress decreases. Suppose that the height  $h$  of a clay sample has thus decreased through  $\Delta h$ . Assume that the clay in question is elastically isotropic, its Poisson's ratio being  $\mu = \frac{1}{2}$ , and that the load which broke the sample was  $P$ . The values  $a$ ,  $h$ , and  $\Delta h$  are given in inches or square inches,  $P$  in pounds. Develop a formula for the shearing value.

$$\text{Ans. } c = \frac{1}{2} \cdot \frac{P}{a} \frac{h - \Delta h}{h} \text{ lb. per sq. in.}$$

4. Trace the logarithmic spirals as determined by Eq. (5:18) for a value of  $\rho_0 = 1$  and  $\phi = 32^\circ$ .

5. Complete Fig. 5:8 by freehand-drawn logarithmic spirals 1 and 2, to make it somewhat similar to Fig. 5:10b.

## References

1. KARL TERZAGHI: "Theoretical Soil Mechanics," John Wiley & Sons, Inc., New York, 1943.
2. A. CASAGRANDE: The Shearing Resistance of Soils, etc., *Proc. Soils Foundation Conf.*, U. S. Engineer Department, Boston, 1939.
3. A. CASAGRANDE: Characteristics of Cohesionless Soils Affecting the Stability of Slopes and Earth Fills, *Jour. Boston Soc. Civil Eng.*, vol. 23, 1936.
4. A. CASAGRANDE and R. E. FADUM: "Notes on Soil Testing for Engineering Purposes" (lith.), publication of the Graduate School of Engineering, Harvard University, 1940.
5. W. S. HOUSEL: Internal Stability of Granular Materials, *Proc. A.S.T.M.*, 1936.
6. W. S. HOUSEL: Shearing Resistance of Soil, Department of Engineering Research, University of Michigan, 1940.
7. W. S. HOUSEL: a discussion in *Eng. News-Record*, vol. 109, 1932.
8. A. NÁDAI, "Plasticity" (especially Chap. 33), McGraw-Hill Book Company, Inc., New York, 1931.
9. Symposium on Shear Testing of Soils, *Proc. A.S.T.M.*, vol. 39, 1939.
10. Technique of Determining Shearing Strength of Soils (a committee report), *Proc. A.S.C.E.*, February, 1942.
11. M. J. HVORSLEV: A Ring Shearing Apparatus, *Proc. Intern. Conf. Soil Mech.*, vol. 2, 1936.
12. A. E. CUMMINGS: a discussion in *Trans. A.S.C.E.*, vol. 108, 1943.

## CHAPTER VI

### COMPRESSION STRAINS; THEORY OF CONSOLIDATION

#### A. GENERAL

In this chapter an approach to the solution of the second part of the basic problem of soil mechanics is given (Sec. 4:1). It will be assumed that the earth mass under consideration does not fail under given loading conditions. The point now is to find *its deformations*, which are mostly caused by compression stresses.

**6:1. Compressed Idealized and Actual Earth Masses.**—To determine the value of a deformation in a compressed mass it is necessary to know (a) the value of the stress causing the given deformation (mostly the vertical pressure  $\sigma_z$ ) and (b) the stress-strain relationship. For the determination of stresses in an earth mass, elastic formulas as discussed in Chap. IV will be used. As to strains, it will be assumed that a compressed idealized fragmental mass (and an actual earth mass as well) changes its volume only because of the decrease in volume of its pores. Individual particles of such a mass are considered as small, incompressible bodies which, under the action of a stress, may come into closer contact with each other.

**6:2. Compression of Sands.**—If a body closely resembling an elastic continuum (such as a piece of steel) is compressed and the stress produced in the material is below the elastic limit, there are only elastic (reversible) deformations within that body. They disappear upon removal of the acting load. If the stress is above the elastic limit, only a part of the deformation disappears upon removal of the acting load; another part remains. The latter part is *irreversible* or *plastic* deformation.

The behavior of a compressed earth mass is *different* from that of metals. For instance, a rigid loaded plate when placed on the surface of a previously unloaded sand mass settles down, and this primary settlement *always* consists of a reversible and an irreversible part. The reversible part of the settlement (termed “elastic rebound” upon removal of the load) may constitute only a small

portion of the whole settlement, for instance, 15 or 20 per cent in the case of a rather loose sand mass. If consecutive cycles of loading and unloading occur with the same load, which is transmitted through a more or less rigid loading plate, the irreversible part of the settlement gradually decreases after each of the cycles ( $a, b, c$ , in Fig. 6:1), whereas the reversible part remains practically constant. Loading-unloading curves (Fig. 6:1) form "hysteresis loops" by intersecting. As the loading-unloading progresses, the

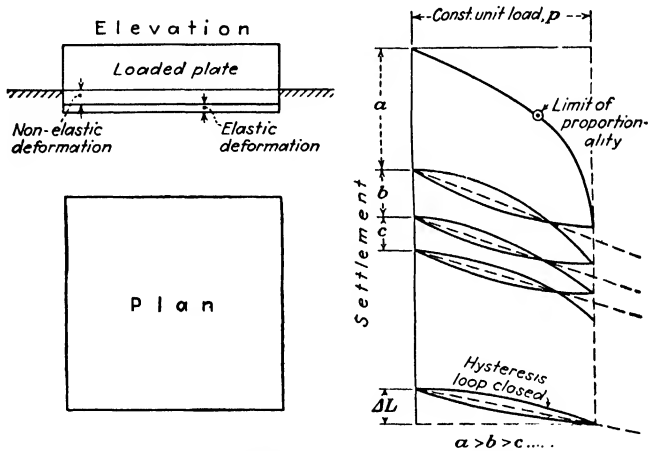


FIG. 6:1.—Elastic and nonelastic deformations of a loaded sand mass.

hysteresis loops become longer and narrower. Finally, after a considerable number of loading-unloading cycles (sometimes over one hundred), the hysteresis loop becomes closed as shown at the bottom in Fig. 6:1. This means that the sand mass *has acquired elasticity*, though strains may not be proportional to stresses, and hence Hooke's law may not be valid. Should a greater load be applied to such an apparently elastic sand mass, there would be irreversible deformations again. It follows that sandy or similar foundation beds under structures subjected to repeated loads (for instance, in the case of pavements or steam hammers) are elastic *up to a given load* but may become inelastic if a larger load is applied. This is the reason why a single very heavy truck may destroy an earth road that has become elastic and stable under the action of moderate traffic. To summarize: Particles of a compressed sand mass first adjust to each other to form a single mass instead of a system of isolated small bodies. This process is known to petro-

raphers as "mutual accommodation of grains." Another source of deformation of a compressed sand mass is the elastic action (change in shape) of particles. Obviously, both adjustment and elastic action contribute to the decrease in voids.

It follows from the preceding discussion that *for uncompactedsands* a modulus of elasticity is valid for *one application* of the load *only*, because after that application it will change its value. For *compact sands* there is a definite value of the modulus of elasticity, provided the load applied does not exceed a certain value.

**6:3. Compression of Clays.**—It should be remembered that the term "saturated clay" means clay with pores completely filled with moisture (Sec. 2:5), no matter what the percentage of pores is. For nonsaturated clays and similar soils, a modulus of elasticity is valid *for one application of the load only* as for uncompactedsands. In the case of saturated clays the following three consecutive steps or stages of deformation occur under a steady load: (a) first an instantaneous but rather small compression of the clay layer in the same way as in the case of nonsaturated clays or uncompactedsands, (b) flowing out (squeezing out) of moisture from the pores and consequently a decrease in porosity and a delayed settlement called "consolidation" (already mentioned in Sec. 1:10). The term "primary compression" is also used to distinguish this stage from the next, which is (c) a continued long-time settlement termed "secondary compression" or "secondary time effect."

**6:4. Modulus of Elasticity of a Soil.**—The concept of modulus of elasticity of a soil should be used with great care, since in this case this modulus is not constant as in elastic continua.

*a. Modulus of Elasticity from a Nonconfined Compression Test.*—A sample ( $L$  units long) made of cohesive soil material is subjected to compression as shown in Fig. 6:2*a*. In Fig. 6:2*b* the stress-strain diagram corresponding to this test is represented, strains (contractions) being plotted against unit pressures. A part of this curve corresponding to the range of unit pressures between some  $\sigma'_2$  and  $\sigma'_1$  values may be assumed straight. Supposing that the range of pressures  $p = \sigma'_2 - \sigma'_1$  is that to be used in the design of the given structure and that the corresponding decrease in height is  $\Delta_1 L$  it can be stated that the modulus of elasticity  $E_1$  for this particular range is derived thus:

$$E_1 = p \div \frac{\Delta_1 L}{L} \quad (6:1)$$

If both vertical and horizontal scales of the drawing are equal, *i.e.*, if one unit of length represents  $\Delta_1 L/L = 1$  and  $p = 1$ , then  $E_1 = \cot \alpha$  (see Fig. 6:2), or the modulus of elasticity is the slope of the straight line replacing the stress-strain relationship curve in the given range of stresses. If the scales of the drawing are not the same, correction is to be introduced.

Sometimes the value of the angle  $\alpha$  is found by tracing a tangent line to the stress-strain curve at its origin  $O$ .

*b. Modulus of Elasticity from a Confined Compression Test.*—The modulus of elasticity of the sand could be found from the closed

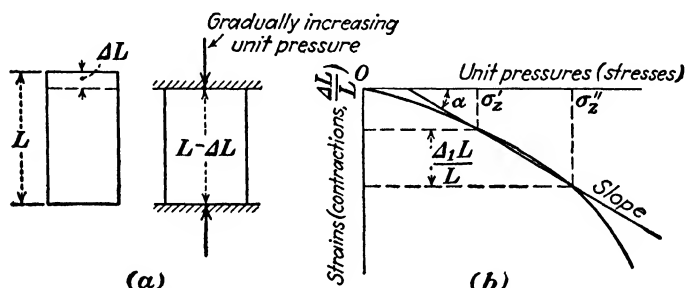


FIG. 6:2.—Nonconfined compression test.

hysteresis loop in Fig. 6:1 if the height of the tested sample were known. Suppose that this field test is duplicated in the laboratory, a metallic cylinder ( $L$  units long) being filled with sand and the unit load  $\sigma_z$  being applied through a piston to bring the sand to an elastic state corresponding to the pressure with an elastic rebound  $\Delta_2 L$ . Then

$$\sigma_z = E_2 \frac{\Delta_2 L}{L} \quad (6:2)$$

In order to avoid the effect of friction of sand against the walls of the experimental cylinder, the latter should not be excessively high.

The modulus of elasticity  $E_2$  of clay during the process of consolidation may be found from the "consolidation test" as described hereafter. The "consolidation test" is a particular case of the confined compression test. A loaded clay mass possesses two moduli of elasticity:  $E_1$  at the time moment of application of the load and  $E_2$  as soon as consolidation starts.

## B. THEORY OF CONSOLIDATION

The term "consolidation," referring to the process described in the preceding sections, has been in use among engineers for some

time. This process was first explained in mathematical form by Terzaghi.<sup>1</sup> Later the theory of consolidation was completed by Terzaghi in cooperation with Fröhlich.<sup>2</sup> In the following discussion this theory is presented in the most elementary form possible; analytical procedures have been simplified, and graphical methods introduced.

**6.5. Mechanical Model of the Consolidation Process.**—A piston  $P$ , provided with holes and supported by elastic springs, may move up and down within a cylinder  $C$  (Fig. 6:3a). The space under the piston is filled with water. Should a load be applied to the piston, the latter will tend to move downward.

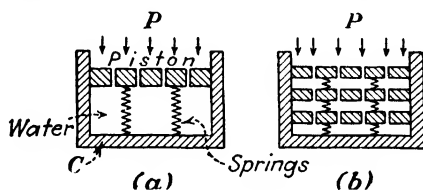


FIG. 6.3.—Mechanical model of consolidation. (After Terzaghi.)

But as this happens, and before the springs start to contract, a part of the water will be squeezed out from underneath the piston. As this squeezing proceeds, the springs contract more and more, and finally the downward movement of the piston stops. It follows that upon application of the load, the whole pressure is taken up by water and is gradually transmitted to the springs. Thus at the beginning of the downward movement of the piston, the water is stressed, but the springs are not. At the end of the movement the situation is reversed, and the whole load is carried by the springs, but there is no stress in the water. A more elaborate model is shown in Fig. 6:3b.

It may be assumed that in both models the springs and the water under the piston correspond to clay particles and pore moisture, respectively. When a saturated clay mass is loaded, the whole stress is first taken up by the pore moisture, which gradually transmits it to the soil particles (skeleton of the mass). During the consolidation process the pore moisture is under the action of a gradually decreasing stress called "hydrostatic excess." It is evident that the trend of consolidation depends on the permeability of the given soil; in the case of very permeable soils, such as sands, there is practically no consolidation process at all in the sense described, though adjustment of particles still exists.

**6:6. Limitations.**—Materials considered in the theory of consolidation are clays or other soft soils with *flexible skeleton*. These materials are assumed to be *saturated*, i.e., their pores are assumed to be completely filled with moisture. During the process of consolidation moisture is gradually *squeezed out* of the pores but still fills all the pores available.

All loads are first assumed to be applied *suddenly*, but without impact. Afterward a correction for the gradual application of the load is introduced.

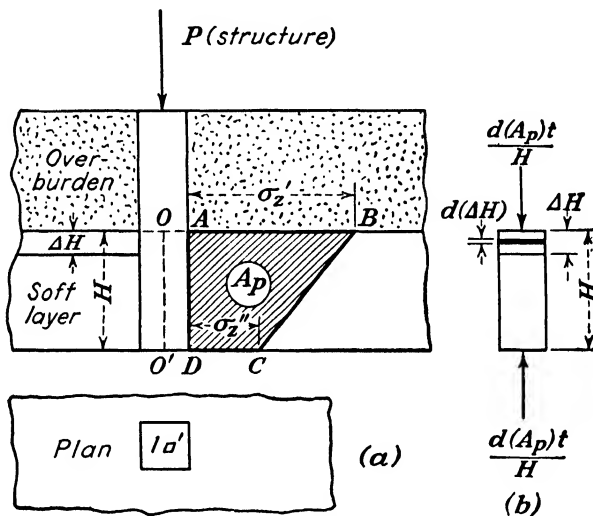


FIG. 6:4.—Pressure area and total settlement.

**6:7. Consolidation Problem.**—Two typical consolidation problems are (a) settlement of a structure  $P$  due to consolidation of a deep soft layer as in Fig. 6:4, (b) settlement of an embankment, for instance of a hydraulic fill. In the former case the deformations (decrease in thickness) of the overburden (see Fig. 6:4) are disregarded, since they are small in comparison with the deformations of the soft layer itself.

The consolidation problem consists of two parts: (a) determination of the *total settlement* due to a given loading, (b) determination of *progressive* settlement or of the distribution of the total settlement in time. The rate of settlement, which is largest immediately after construction, decreases as the time goes.

**6:8. Total Settlement.**—Assume that the soft layer shown in Fig. 6:4a had been formed by sedimentation in a basin such as a lake. First the layer was very thin but gradually grew up to its full thickness and subsequently was covered by an overburden. During this process the layer was steadily consolidating and finally reached the state of *full consolidation* such that there was no further settlement.

The straight line *I* in the diagram Fig. 6:5, termed “virgin compression line” (or “virgin compression curve”), shows that the voids ratio of the layer in question, which initially, perhaps thousands of years ago, was  $e_1$ , became  $e_2$  at the state of full consolidation. The corresponding unit pressure that caused this consolidation is termed “preconsolidation unit load” or simply “preconsolidation load” (designation  $p_c$ , sometimes  $p_p$ ). This load may equal the weight of the actual overburden combined with the weight of the layer itself, or it may even exceed it if erosion had removed a part of the overburden. At the present stage of the discussion it will be assumed that the position of the virgin compression line and the value of the preconsolidation load  $p_c$  are known.

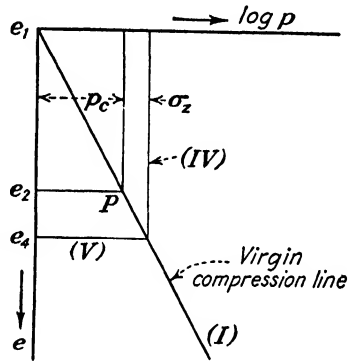


FIG. 6:5.—Decrease of the voids ratio of a consolidating natural clay layer.

Let  $\sigma_z$  be the *average* vertical pressure exerted by the proposed structure on the given layer along a vertical line  $OO'$  (Fig. 6:4a), point  $O$  being at the top of the given layer and point  $O'$  at its bottom. Under the action of this additional load the consolidation process will resume, the relationship between voids ratios and pressures being again expressed by the continuation of the virgin compression line *I*. Hence the voids ratio  $e_4$ , corresponding to the end of the consolidation under the action of the proposed structure, may be found by tracing lines *IV* and *V* as in Fig. 6:5.

The thickness of the soft layer in Fig. 6:4 is  $H$  ft., the amount of the settlement being  $\Delta H$ . There are two ways to compute the latter value: either (a) from the voids ratios  $e_2$  and  $e_4$  (before and after consolidation, respectively) if they are known or may be

estimated or (b) by applying Hooke's law, in which case the average vertical pressure  $\sigma_z$  and the value of the modulus of elasticity  $E_2$  of the soil are to be known (compare end, Sec. 6:4). In case (a) refer to Fig. 2:1 from which it may be concluded that if, owing to a compression stress, the voids ratio  $e_2$  of a sample  $(1 + e_2)$  ft. thick decreases to  $e_4$ , the decrease in thickness of the sample will be  $e_2 - e_4$ . Proportionately, if the thickness of the sample is not  $(1 + e_2)$  ft., but  $H$  ft., the decrease in thickness will be

$$\Delta H = \frac{H}{1 + e_2} (e_2 - e_4) \quad (6:3)$$

Applying approximately Hooke's law to the compression of the soil mass by the unit stress  $\sigma_z$  (case b) as specified above, we have

$$\sigma_z = E_2 \cdot \frac{\Delta H}{H} \text{ or } \Delta H = \frac{H\sigma_z}{E_2} \quad (6:4)$$

where  $E_2$  is the modulus of elasticity of the soil (compare end, Sec. 6:4).

Introduce a designation

$$\frac{1 + e_2}{E_2} = a$$

from which

$$E_2 = \frac{1 + e_2}{a} \quad (6:5)$$

Place this value of  $E_2$  into the second equation (6:4). Then

$$\Delta H = H\sigma_z \frac{a}{1 + e_2} \quad (6:6)$$

The value of  $a$  is often termed "coefficient of compressibility." Its physical dimension is reciprocal of stress

Emphasis should be laid on the fact that in Fig. 6:5 the voids ratios  $e$  are plotted against the *logarithms* of the unit pressures  $p$ , not of unit pressures themselves. For constructing diagrams as in Fig. 6:5, the use of semilogarithmic paper is convenient. The straight-line relationship referred to line  $I$  in Fig. 6:5 has been suggested by Terzaghi as a result of his experimental work (ref. 1, Chap. I).

**6:9. Pressure Area.**—Consider again Fig. 6:4. Compute vertical pressures caused by the load  $P$  along vertical line  $OO'$  which, as specified, may be under the load  $P$  or at some other place of the soft layer. For computing the vertical pressures the Boussinesq

formula or some other method (Sec. 4:15) can be used. Plot these vertical pressures horizontally, and join the ends of the ordinates with a curve (Fig. 6:4). Designate area  $ABCD$  with  $A_p$ , and term it "pressure area." Then the average value of the vertical pressure  $\sigma_z$  acting on the soft layer is the average ordinate of area  $A_p$ :

$$\sigma_z = \frac{A_p}{H} \quad (6:7)$$

Place this value in Eq. (6:6); then the value of the total settlement would be

$$\Delta H = A_p \frac{a}{1 + e_2} \quad (6:8)$$

The curve limiting the pressure area may be replaced by a straight line  $BC$  (Fig. 6:4). In this case the value of the vertical pressure  $\sigma_z$  is simply an arithmetical average of vertical pressures  $AB = \sigma'_z$  at the top of the layer and  $DC = \sigma''_z$  at its bottom.

**6:10. Time Moment; Time Interval.**—The *time moment* is a time at which a certain event happens (for instance, the time moment of a sudden application of a load). The *time interval* is a portion of time between two time moments. Symbol  $t$  with or without subscripts will be used for both time moments and time intervals. Very small time intervals will be designated with the symbol  $dt$ . Time intervals in settlement computations are expressed in years; laboratories measure time intervals mostly in minutes or seconds.

**6:11. Isochrones and "Effective" Pressure Areas.**—At any time moment  $t$  the full vertical pressure at a point of the earth mass  $\sigma_z$  is balanced by the sum of both the hydrostatic excess  $u$ , at that point and at that time moment, and the pressure carried by the skeleton ( $\sigma_s - u$ ).

$$\sigma_s = u + (\sigma_s - u) \quad (6:9)$$

Formula (6:9) is simply an equation of statics. Using terms given in Sec. 4:19, the value of  $(\sigma_s - u)$  is the effective or intergranular pressure, whereas  $u$  is the neutral pressure at the given point of the mass and at the given time moment.

If the values of the neutral pressure  $u$  at different points of the vertical  $OO'$  (Fig. 6:4) were known and plotted horizontally, the ends of the corresponding ordinates would form a curve  $AM$  (Fig. 6:6), which will be termed "isochrone" or "moisture-pressure curve" at the time moment  $t$ . At the top of the layer (point  $A$ )



the procedure of solving the consolidation problem is as follows:

*First Step.*—Determine the elementary discharge  $q$  during the time interval  $dt$  that follows a time moment  $t$ .

*Second Step.*—Determine the elementary settlement  $d(\Delta H)_t$  due to the increase in intergranular pressure during that time interval  $dt$ .

*Third Step.*—Equalize  $q$  and  $d(\Delta H)_t$ . This will furnish the value of the time interval  $dt$  during which the settlement  $(\Delta H)_t$  of the given layer increases on a value of  $d(\Delta H)_t$ .

**6:13. Elementary Discharge.**—The Darcy formula (Sec. 3:3) will be used for computing the elementary discharge. Since the cross section of the prism under consideration (Fig. 6:4) equals 1 sq. ft., the discharge  $q$  during a very small interval of time  $dt$  is

$$q = ki \cdot dt \quad (6:10)$$

In formula (6:10) the symbol  $k$  stands for the coefficient of permeability of the given soil which will be assumed known and constant, and  $i$  is the hydraulic gradient. Consider an elementary layer  $dz$  thick, located at a depth  $z$ . In passing through this elementary layer, moisture loses an amount  $du$  in pressure. Figure 6:7 shows that to produce a pressure  $du$  at a point, the hydraulic head  $du/\gamma_0$  is needed, the symbol  $\gamma_0$  standing for the unit weight of water. Hence, the loss in hydraulic head required to make moisture percolate through the given elementary layer  $dz$  thick is  $du/\gamma_0$ , from which the value of the hydraulic gradient  $i$  is

$$i = \frac{1}{\gamma_0} \cdot \frac{du}{dz} \quad (6:11)$$

It follows from inspection of Fig. 6:6 that the value of  $du/dz$  equals  $\cot \alpha$ , the symbol  $\alpha$  standing for the angle made by the tangent to curve  $AM$  at point  $N$  (or at point  $N'$ , since both points are infinitely close) with the horizontal. Furthermore, since there is no flow at the bottom of the layer (plane  $CD$ , Fig. 6:6), the corresponding hydraulic gradient is zero, which means that curves  $AM$  and  $AM'$  have vertical tangents in intersecting the bottom

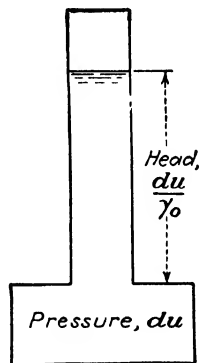


FIG. 6:7.—Pressure and hydraulic head interrelated.

*CD* of the layer. The value of angle  $\alpha$  corresponding to the tangent to the isochrone at point *A* will be designated with  $\alpha_0$ . Thus the hydraulic gradient  $i_0$ , which drives moisture out of the layer through plane *AB*, is

$$i_0 = \frac{1}{\gamma_0} \cot \alpha_0. \quad (6:12)$$

Using formula (6:10), the discharge  $q$  from the given prism during an interval of time  $dt$  would be

$$q = \frac{k}{\gamma_0} \cot \alpha_0 \cdot dt \quad (6:13)$$

**6:14. Elementary Settlement.**—Refer to formula (6:7). Applying it to a part  $d(\Delta H)_t$  of the total settlement  $\Delta H$ , we will have

$$d(\Delta H)_t = d(A_p)_t \frac{a}{1 + e_2} \quad (6:14)$$

where  $d(A_p)_t$  means the increase in effective pressure area  $(A_p)_t$  during a time interval  $dt$ , in other words, from the time moment  $t$  to which the pressure area  $(A_p)_t$  corresponds to the time moment  $t + dt$ . As stated in Sec. 6:11 this increase is expressed graphically by the area  $AMM'$  between the two isochrones corresponding to time moments  $t$  and  $t + dt$ , respectively (Fig. 6:6).

**6:15. Time of Settlement.**—Equalizing the right sides of Eq. (6:13) and (6:14),

$$\frac{k}{\gamma_0} \cot \alpha_0 \cdot dt = d(A_p)_t \frac{a}{1 + e_2} \quad (6:15)$$

from which

$$dt = \frac{a \gamma_0}{k(1 + e_2)} \cdot d(A_p)_t \tan \alpha_0 \quad (6:16)$$

Introducing a designation

$$c_v = \frac{k(1 + e_2)}{a \gamma_0} \quad (6:17)$$

Equation (6:17) becomes

$$c_v \cdot dt = d(A_p)_t \tan \alpha_0 \quad (6:18)$$

the value of  $c_v$  being termed "coefficient of consolidation" (not to be confused with the coefficient of compressibility  $a$ ).

**6:16. Coefficient of Consolidation; Percentage Consolidation.**—The physical dimension of the coefficient of consolidation  $c_v$  is

square feet per year (or square centimeters per minute). This is true because the physical dimensions of other values in Eq. (6:17) are

Coefficient of permeability  $k$ , ft. per year.

Unit weight of water  $\gamma_0$ , tons per cu. ft.

Coefficient of compressibility  $a$  (reciprocal of stress), sq. ft. per ton. To pass to the dimension square feet per year, it is necessary to multiply the laboratory value given in square centimeters per minute by 564.

“Percentage consolidation” (or degree of consolidation, symbol  $U$ ) at the given time moment  $t$ , will be defined as the ratio of the settlement at that time moment to the total settlement, either in fractions of one unit or in per cent.

$$U = \frac{(\Delta H)_t}{\Delta H}, \text{ or } U \% = \frac{(\Delta H)_t}{\Delta H} \times 100 \quad (6:19)$$

By analogy with formula for  $\Delta H$  (6:8)

$$(\Delta H)_t = (A_p)_t \frac{a}{1 + e_2} \quad (6:20)$$

where  $(A_p)_t$  is the “effective” pressure area (Sec. 6:11) corresponding to the time moment at which the gradually increasing settlement reaches a value of  $(\Delta H)_t$ . From Eq. (6:8), (6:19), and (6:20)

$$U = \frac{(A_p)_t}{A_p}, \text{ or } U \% = \frac{(A_p)_t}{A_p} \times 100 \quad (6:21)$$

**6:17. Graphical Procedure.**—If the given clay layer is located on an *impervious base*, the following graphical procedure may be used:

Trace the pressure area  $A_p$  as shown in Fig. 6:8a, placing the thickness of the layer  $AD$  horizontally and its pervious top  $AB$  vertically. Trace several isochrones  $t_1, t_2, t_3, \dots$  and measure “effective” pressure areas bounded by them as explained hereafter (Sec. 6:18). Measure the total pressure area  $(A_p)$  and “effective” pressure areas  $(A_p)_t$  corresponding to various isochrones  $t_1, t_2, t_3, \dots$  in square feet, using the horizontal scale of distances both horizontally and vertically in Fig. 6:8a. The areas thus obtained are plotted to an *arbitrary* scale on vertical line  $P$  in Fig. 6:8b. The ends of line segments corresponding to various pressure areas are shown in Fig. 6:8b with encircled numerals. For example, the



isochrones marked  $\bar{1}, \bar{2}, \bar{3}, \dots$  in Fig. 6:8a to intersect horizontal lines passing through encircled points 1, 2, 3, . . . on vertical line  $P$ . Then a horizontal ordinate of this polygon (for instance, that passing through the encircled point 3, its length being conventionally designated with symbol  $m$ ) represents the sum of the products  $d(A_p)t \tan \alpha_0$  up to the given time moment ( $t_3$  in the case of the ordinate  $m$ ). Since the physical dimension of the coefficient of consolidation  $c_v$  is square feet per year (Sec. 6:16), the physical dimension of the product  $c_v \cdot dt$  in Eq. (6:18) is square feet, and so is the sum of products  $d(A_p)t \tan \alpha_0$  at the right side of Eq. (6:18). Hence ordinate  $m$  can be measured in square feet using the scale of the vertical line  $P$  (Fig. 6:8b). To measure ordinate  $m$  in terms of years, sum up both sides of Eq. (6:18) from the zero time moment (application of the loading) to a given time moment, for instance,  $t_3$ :

$$c_v t_3 = m \quad (6:22)$$

If  $t_3 = 1$  year, then  $m = c_v$ . This means that ordinate  $m$  and all other horizontal ordinates in Fig. 6:8b can be measured in terms of years, using  $c_v$  as a unit. For instance if  $c_v = 45$  sq. ft. per year, this unit is 45 sq. ft. on the scale used to plot distances on line  $P$  (Fig. 6:8b).

The more numerous the isochrones in Fig. 6:8a the closer the polygon in Fig. 6:8b approaches the theoretical *time-settlement* curve (or simply "time curve") for this case. This curve tends to touch asymptotically the horizontal line passing through point 7 on line  $P$ . This means that the *theoretical* time of full consolidation is infinitely long.

The procedure described above is applicable if the vertical and horizontal scales of the pressure area *are equal*, for instance, if one unit of length, say 1 in., equals horizontally  $n_1$  ft. and vertically  $n_1$  tons per sq. ft. (Fig. 6:8). But if the vertical scale is 1 in. equals  $n_2$  tons per sq. ft., the abscissas of the time-settlement curve increase  $n_1/n_2$  times, and to find year divisions on the axis of abscissas a value of  $(n_1/n_2) \cdot c_v$ , and not  $c_v$ , is to be used.

It should be noticed that the change in the vertical scale of a trapezoidal pressure area modifies the size of the abscissas but does not affect the general shape of its time curve, which depends solely on the ratio of the parallel sides of the trapezoid. Notice that a triangle is a trapezoid with the ratio of parallel sides equal to

infinity, a rectangle being a trapezoid with equal parallel sides (ratio = 1). Hence a single time curve corresponds to all triangular pressure areas with the vertex at the bottom, another to all triangular pressure areas with the vertex at the top, and still another one to all rectangular pressure areas. It should be recalled that in the preceding discussion pressure areas with a pervious and an impervious boundary are considered.

Time-settlement curves are often drawn on semilogarithmic

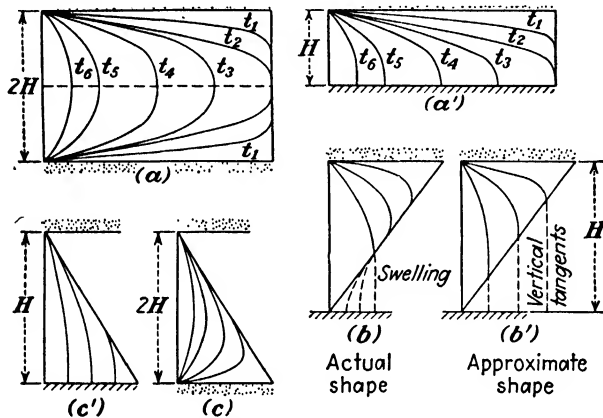


FIG. 6.9.—Pressure areas and moisture-pressure curves, termed also “isochrones.”  
(After Terzaghi-Fröhlich.)

paper plotting logarithms of time horizontally and settlements vertically.

*Examples:* 1. To find the percentage consolidation 3 years after application of the load for a given pressure area and a given coefficient of consolidation  $c_v$  (Fig. 6:8) draw a vertical 3-X to intersect the time curve. The horizontal line XY determines the value of the percentage consolidation  $U$  (64 per cent in Fig. 6:8). Equality of horizontal and vertical scales of the pressure area is assumed in this example.

2. The scale on line  $P$  (Fig. 6:8) is 1 in. = 200 sq. ft., the scale of the pressure area being 1 in. equals 25 ft. horizontally and 5 tons per sq. ft. vertically. If coefficient of consolidation  $c_v = 40$  sq. ft. per year, each year division on the axis of abscissas would be

$$\frac{40}{200} \times \frac{25}{5} = 1 \text{ in.}$$

**6:18. Some Types of Pressure Areas and Isochrones.**—Some types of pressure areas and isochrones are shown in Fig. 6:9. Particularly in the case of a rectangular pressure area with pervious material at both top and bottom of the given layer (Fig. 6:9a),





horizontal and vertical scales in measuring the pressure area  $A_p$  (in square feet) and plot it vertically as on line  $P$  in Fig. 6:8. Plot along the axis of abscissas a distance  $c_v = 1$  sq. ft. on the scale used for plotting  $A_p$ . The point thus obtained corresponds to  $t = 1$  year [compare text after Eq. (6:22)] and defines the position of the abscissa  $T = 1$ , all other abscissas such as  $T/2$  or  $T/4$  being found proportionately. Thus a  $U$ - $T$  graph, or time-factor graph, is simply a time curve for the pressure area of a given shape, which may be plotted either on an arithmetical or a logarithmic scale (Fig. 6:11a and b, respectively). Curves 1, 2, and 3 in Fig. 6:11 may be obtained either using the graphical procedure (Sec. 6:17) or from analytical computations by various investigators (see Appendix D). Curves 4 and 5 in Fig. 6:11 have been traced by interpolation between curves 1 and 3, breaking the trapezoidal pressure area into a rectangle and a triangle. Notice that curve 1 is applicable to any rectangular pressure area independently of the character of its boundaries.

A diagonal of a rectangular pressure area with two pervious boundaries subdivides this area into two triangles, with identical patterns of isochrones (such as in Fig. 6:9c) located in perfect symmetry with respect to the two pervious boundaries. Hence the consolidation processes caused by either of these pressure areas acting separately are identical; and since both areas together form the rectangular pressure area, the consolidation process caused by a triangular pressure area is identical with that caused by a rectangular pressure area provided that the boundaries of these areas are pervious. Since any polygon may be subdivided into triangles, it may be stated that curve 1 in Fig. 6:11 constructed for rectangular pressure areas is to be used for all pressure areas possessing two pervious boundaries and bounded by straight lines. For example, the consolidation of a hydraulic fill built on a pervious base (triangular pressure area, for isochrones see Fig. 6:9c) proceeds according to curve 1, neglecting possible effects of evaporation at the top.

*Example.* For a trapezoidal area of type 5 (top, Fig. 6:11), the percentage consolidation corresponding to  $T = 0.5$  is 0.81. Assuming the value of the coefficient of consolidation  $c_v = 45$  sq. ft. per year and the thickness of the layer  $H = 20$  ft., the time required to reach that degree of consolidation is

$$t = 0.5 \times \frac{20^2}{45} = \text{about 4.5 years.}$$

**6:20. Comparative Time of Settlement.**—When reaching a certain percentage consolidation  $U$ , two soil layers of different thickness  $H_1$  and  $H_2$ , but made of the same material (same value of  $c_v$ ), have the same value of the time factor. Designating the time intervals required to reach that percentage consolidation with  $t_1$  and  $t_2$ , respectively and using formula (6:23)

$$\frac{c_v t_1}{H_1^2} = \frac{c_v t_2}{H_2^2}$$

from which

$$\frac{t_1}{t_2} = \frac{H_1^2}{H_2^2} \quad (6:24)$$

Formula (6:24) means that the times required to reach a certain

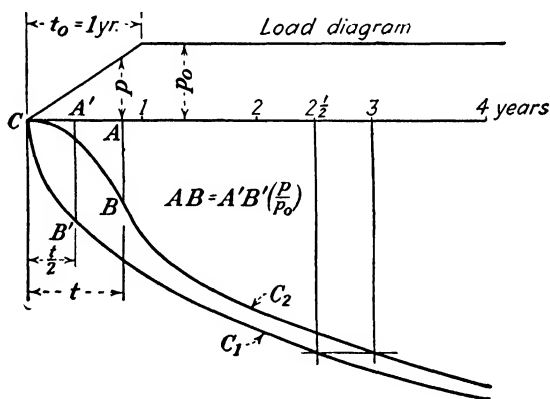


FIG. 6:12.—Time-settlement curve ( $C_2$ ) if the load increases gradually.  
(After Terzaghi and Fröhlich).

percentage consolidation relate as the squares of the thicknesses of the corresponding layers. Formula (6:24) is accurate if the pressure areas of the given layers correspond to the same curve on the diagram (Fig. 6:11); otherwise it is an approximation.

**6:21. Consolidation under Increasing Load.**—Vertical pressure at a point within a soil mass does not appear suddenly as assumed hitherto but increases gradually from zero to a certain value during a certain time. Such is, for instance, the increase in pressure due to the progress of construction during the building period, which may be estimated, as an average, at 1 year. In Fig. 6:12 curve  $C_1$  is the time-settlement curve for the case when the acting load is

applied suddenly but without impact at the initial time moment  $t = 0$ . Curve  $C_2$  corresponds to the gradual application of the load during 1 year ( $t = t_0 = 1$  year), as shown at the top of Fig. 6:12. It is assumed that during the period of construction, the percentage consolidation at any time moment  $t$  (acting unit load  $p$ ) equals the percentage consolidation at a time moment  $t/2$  in the case of sudden application of the load  $p$ . For instance, to find point  $B$  of curve  $C_2$ , halve distance  $CA$ , draw the vertical  $A'B'$  to intersect curve  $C_1$ , and plot  $AB = A'B' (p/p_0)$ . For all points of curve  $C_2$  beyond  $t_0 = 1$  year, the ordinates equal the ordinates of curve  $C_1$ ,  $t_0/2$  years before. For instance, the settlement at 3 years, as shown by curve  $C_2$ , is the settlement at  $2\frac{1}{2}$  years, as shown by curve  $C_1$ .

**6:22. Secondary Compression.**—If settlements observed during a certain time interval are plotted against time, a time curve is obtained. If the settlement process follows the theory of consolidation, there should be proportionality (approximate, of course) between the observed settlement values and those given by theoretical time-settlement curves (Secs. 6:17 and 6:19). In reality both field and laboratory time curves are in agreement with the theory of consolidation generally up to the value of consolidation  $U = 50$  or  $60$  per cent, after which the so-called secondary compression (secondary time effect) starts. If plotted on semilogarithmic paper, (Fig. 6:15) the part of the time curve corresponding to the secondary compression generally appears as a straight line (though in some cases curves have been reported).

Soil conditions under the base of the footings of the Chicago Auditorium, built about 1888, are in round figures: 15 ft. of artificial fill, 15 ft. of sand, 60 ft. of plastic blue clay, and 20 ft. of hardpan underlain by rock (Niagaran limestone). The seat of settlement being in the plastic clay, observations on one of the tower piers based on top of the sand layer have shown that the part of the settlement which obeyed the theory of consolidation (1.5 ft) lasted till 1896, *i.e.*, for about 8 years. The secondary compression, totaling about 0.8 ft., was noticeable 50 years after construction.

### C. CONSOLIDATION TEST

**6:23. Objective of a Consolidation Test.**—A consolidation test is not a test to failure, as the shearing tests are, but simply a *model test* in which the deformations of a sample (model of the given clay layer) are generalized to the prototype, obviously with certain limitations. According to Sec. 6:7 there are two questions

to answer from the study of that model: (a) What is the total settlement of the layer for which, as in any other compression test, a *stress-strain diagram* should be drawn; (b) what is the rate of settlement under a given steady load, for which an experimental *time-settlement curve* should be drawn?

To answer these questions the laboratory must determine for the given clay layer (a) the values of the voids ratios  $e_2$  and  $e_4$ , those before construction and after complete consolidation, respectively; (b) the value of the coefficient of consolidation  $c_v$ . A thick

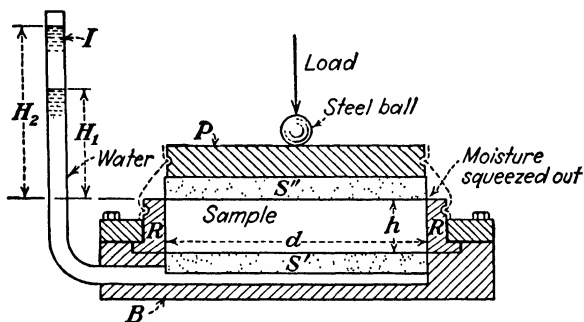


FIG. 6:13.—Standard consolidation device. (After A. Casagrande.)

layer may be subdivided in several thinner ones, and investigation carried on separately for each of these. Admittedly, in such a case clay samples from each thin layer are to be available.

**6:24. Consolidation Apparatus.**—As in the case of a nonconfined compression test (Fig. 5:12), “undisturbed” soil samples are used in the consolidation test. They are extracted from different depths in such a way that their natural structure and moisture content are conserved and are cut carefully to fit within a metallic ring  $R$  which may be from  $\frac{1}{2}$  to  $1\frac{1}{2}$  in. high and from about  $2\frac{1}{2}$  to 4 in. in diameter (Fig. 6:13). The cutting is generally made in a humid room in order to maintain the natural moisture content. The ring  $R$  rests on a metallic base  $B$  with a porous stone  $S'$  under which there is a space for water connected with the water inlet  $I$ . The sample is covered with another porous stone  $S''$  and a piston  $P$ . Pressure may be applied to the piston through a hard steel ball to ensure centric action. Porous stones permit the moisture to be squeezed out of the sample; and to avoid evaporation and create a saturated atmosphere, the upper edge of the ring  $R$  is protected with thin rubber cloth (“rubber dam,” dotted lines in Fig. 6:13).

Sometimes a removable metallic tank which may be filled with water replaces that rubber dam. The downward movement of the piston  $P$ —or, in other words, the compression of the sample—is measured with a dial gauge (accurate to  $1/10,000$  in).

The unit pressure acting on the piston is applied gradually, in predetermined increments (for instance, 0.40, 0.80, 1.50, 3.00, 6.00 kg. per sq. cm.). In the case of very soft soils, it is advisable to subdivide the first increment into smaller ones. In all cases, before applying the next increment, the sample is permitted to consolidate; this may require 24 hr. or more of application. The unloading, which, in a general case, is optional, is also made by gradual decrements (for instance, 1.50, 0.40, 0.00 kg. per sq. cm.). The voids ratio  $e$  is determined in the laboratory before starting the test and is afterward computed for all stages of loading and unloading. To check the value of  $e$  computed for the last unloading stage, the sample is taken out at the end of the test and its moisture content determined in the usual way. From this moisture content the final value of the voids ratio  $e$  may be checked.\* Notice that the pressure area of the sample in the consolidation device is a rectangle with two pervious boundaries (compare Sec. 6:19).

**6:25. Voids-ratio-pressure Curves.**—By plotting voids ratio against unit pressure as applied to the piston, voids-ratio-pressure curves (termed also “ $e$ - $p$  curves” and “recompression curves”) are obtained. These curves represent the stress-strain relationship of the given sample. An example of such a curve is given in Fig. 6:14, which has to be considered together with Fig. 6:5. From various loadings and unloadings the position of the experimental virgin compression line is established, and using a conventional procedure a point  $P$  is fixed on it.† This point corresponds to what in nature is the “preconsolidation unit load”  $p_c$  (Sec. 6:8). The voids ratio of the sample  $e_3$  at which the test starts is larger than the natural voids ratio  $e_2$  in the earth mass, because the sample expands upon being extracted from the earth and relieved from the pressure that acted on it. A computed value of the unit vertical pressure  $\sigma_z$ , exerted by the structure on the clay layer is added to

\* This apparatus, designed by A. Casagrande and sometimes termed “consolidometer,” is a further improvement of the original Terzaghi “odometer.”

† For more information on the consolidation test see Appendix D.

the unit preconsolidation load  $p_c$ , and the final value of the voids ratio  $e_4$  is found. Finally formula (6.3) is applied.

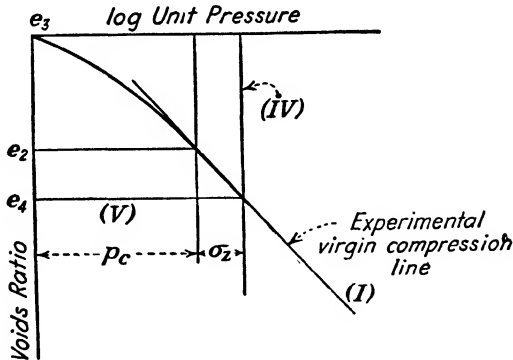


FIG. 6:14.—Experimental voids-ratio pressure curve. (Compare Fig. 6:5.)

**6:26. Experimental Time-settlement Curve.**—A typical experimental time curve is shown in Fig. 6:15. The three stages of clay compression (Sec. 6:3), namely, (a) the initial stage, (b) the primary compression, and (c) the secondary compression, are clearly seen. The boundary between stages (b) and (c) is established using a conventional procedure.

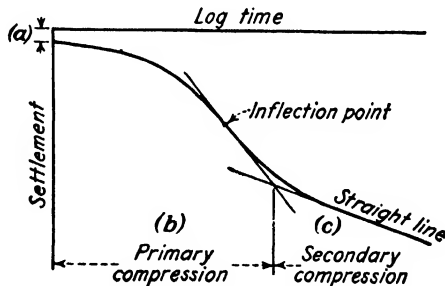


FIG. 6:15.—Laboratory time-curve. (See also Appendix "D.")

From a set of experimental time curves the value of the coefficient of consolidation  $c_v$  is determined. This is done using again a conventional procedure. The value of  $c_v$  is then used either in the graphical procedure (described in Sec. 6:17) or for computing the value of the time factor  $T$  and using the corresponding graph (Sec. 6:19).

**D. GENERAL DISCUSSION OF THE THEORY OF CONSOLIDATION**

**6:27. Basic Assumptions Discussed.**—According to the theory of consolidation, moisture that is squeezed out from the pores flows according to Darcy's formula with a constant coefficient of permeability  $k$ , as in seepage (Chap. III). Besides this generally accepted assumption proposed by Terzaghi, there may be other assumptions. One of them is as follows: In a completely consolidated saturated clay mass there is practically no free (gravitational) water; otherwise it would be squeezed out by the weight of the mass, because free moisture has no shearing strength at all. All the pore moisture is attracted, and the closer a moisture film to the particle the stronger the attraction. Moisture is squeezed out from a loaded mass when the shearing resistance mobilized between the moisture and the pore walls is overcome. Resistance to the squeezing out of moisture increases, however, from the middle of a pore toward a particle, hence a decrease in amount of moisture squeezed out as time goes. As soon as the shearing stress, which tends to separate the moisture from the pore walls, and the shearing resistance are balanced, the consolidation process stops. According to this assumption, the whole process may be characterized as plastic flow of moisture with decreasing velocity.

**6:28. Discussion of Different Features of the Theory of Consolidation.**—*a. Secondary Time Effect.*—The only mathematical theory on secondary compression is that by Taylor and Merchant.<sup>9</sup> According to their explanation, "primary compression causes shearing stresses which constitute a small degree of remolding or destroying of structure of the sample and this breakdown of structure is the cause of secondary compression." Since the secondary compression is supposed to take place without squeezing out of moisture and there is still some settlement, it must be admitted that either moisture or soil particles are compressible (probably the latter). The fact of compressibility of soil particles during the secondary compression is, however, contradictory to the assumption of soil incompressibility during the primary compression.

*b. Upward Percolation.*—The upward percolation of moisture is not vertical ("one-dimensional process of consolidation") but oblique, in all directions from underneath a structure.

*c. Downward Percolation.*—If there is pervious material on both sides of the compressed soft layer, and the surcharge covers the

whole surface of the semi-infinite earth mass, as in the basic case of the theory of consolidation, a downward percolation into the saturated sand layer is physically impossible.

*d. Infinite Time of Consolidation.*—Of course, “infinity” in this case is a conventional concept only, and the consolidation process necessarily has to stop sometime. According to the theory of consolidation, the slightest load applied to the earth surface causes an infinitely long consolidation process in a deep clay layer. It is sometimes assumed that the process of consolidation is practically completed at reaching 90 per cent of the total settlement.

*f. Partly Saturated Soils.*—The theory of consolidation has been designed for soft saturated soils only. In the case of a partly saturated soil this theory should be used with great care and, at any rate, with due corrections.

*g. Grain-to-grain Pressure and Validity of the Consolidation Test.*—As consolidation progresses, soil grains are assumed to come in contact with each other, and in this connection “intergranular,” or “grain-to-grain,” pressure develops. The shape of clay particles is, however, too complicated to visualize it in the form of spheres covered with moisture films. Moreover, a situation can be easily realized when a considerable part of the moisture has been already squeezed out but grains have not yet come into contact with each other.

In one of his papers Terzaghi<sup>3</sup> states that completely consolidated clay (clay in “solid state”) consists of grains mutually touching each other. Sudden application of a heavy load brings the clay into a “lubricated” state, in which the soil mass is highly compressible. This is the case of laboratory consolidation tests as described above. In nature, however, loads are applied at a very slow rate, without considerable increase in compressibility. Hence the virgin compression line as determined in the laboratory (curve I, Fig. 6:15) is *too steep*. To prove his opinion Terzaghi quotes several cases of clay deposits in water basins in which the moisture content does not decrease with the depth but practically remains constant through the deposit. Casagrande and Fadum,<sup>4</sup> however, present opposite evidence.

*h. Relative Motion of the Skeleton.*—No friction between moisture and skeleton is considered; also, inertia forces during the consolidation process itself are not taken into account. Being very small, all these forces may be neglected, however.

**6:29. Historical.**—In one of his works Terzaghi<sup>2</sup> states that as early as in 1856 Tyndall discussed “partially consolidated mud” in his “Fragments of Science.” Furthermore, in 1920, Allen Hazen spoke of “consolidation” in his paper on the hydraulic fill dams in *Trans. A.S.C.E.* The differential equation of consolidation analogous to that used in the theory of heat transfer was established by Terzaghi in 1923 and published in his “Erdbaumechanik” in 1925. Independently of Terzaghi, Lederer developed a similar equation in studying the process of drying out of soaps (*Z. angew. Chem.*, 1924).

To these data as furnished by Terzaghi himself it should be added that fairly satisfactory information on the consolidation process in soft clays existed among American engineers more than fifty years ago. In 1891 Collingwood\* stated:

In most cases it is sufficient to reach sound undisturbed earth of a known quality. But this should always be penetrated to a sufficient depth to insure that it is not underlain by semifluid or compressible material which may in time yield and cause trouble and danger.<sup>5</sup> . . .

In 1892, from actual observations on the settlement of an embankment on a soft foundation, Carter<sup>6</sup> found that the time curve is a rectangular hyperbola and that by using its equation “it is possible to determine the maximum settlement which will occur in an infinite time.” In 1898, from settlement observations in Chicago, Sooy Smith<sup>7</sup> gave an accurate description not only of the squeezing out of moisture from the consolidating clay but also of what is now termed “secondary compression.”

The mathematical theory of consolidation as developed by Terzaghi has been so far unique along these lines. Its publication revived the interest of the engineering profession in the causes of settlement and in earth engineering in general. Terzaghi’s work has had repercussions in all countries.<sup>8</sup>

#### Problems

All clay layers in problems 1 to 7 are assumed to be saturated.

1. A clay layer 28 ft. thick is underlain with impervious rock and covered with pervious overburden. A structure wide enough to be considered infinite in any horizontal direction has been constructed close to the top of the overburden and loaded with a uniform load, which is 2 tons per sq. ft. of the

\* Francis Collingwood (1834–1911), a well-known American earth and sanitary engineer. Established Collingwood prize for juniors, American Society of Civil Engineers.

surface. In the consolidation test made on a sample  $\frac{1}{2}$  in. thick, the initial voids ratio was 0.876 and the final one was 0.863. Determine the values (a) of the final settlement, (b) of the settlement at 50 per cent consolidation.

*Ans.* (a) 2.3 in. (b) 1.2 in.

2. A building has been constructed on a sand layer underlain with a 50-ft.-thick fully consolidated clay deposit located on rock. The vertical pressure at a point at the top of this deposit has been estimated at 2 tons per sq. ft., whereas that at its bottom has been found to be negligible. Draw (freehand) the set of isochrones for this case, and locate the isochrone corresponding to 50 per cent consolidation.

*Suggestion:* The curve in question halves the "pressure area" and can be found by trial and error.

3. The consolidation test in the case of the layer in problem 2 furnished the value of the coefficient of consolidation:  $c_v = 0.005$  sq. cm. per min. Using the graph (Fig. 6:11), determine the time necessary to reach 35 per cent consolidation. Disregard secondary compression. *Ans.* About 30 years.

4. There is a fully consolidated clay layer 25 ft. thick with the drainage at the top and rock at the bottom. A new building has been constructed, and vertical pressures  $\sigma_z$ , below the center of this building are 2.5 tons per sq. ft. at the top and 1.0 tons per sq. ft. at the bottom of the given layer. The total settlement expected is 3 in. Draw a set of isochrones and a time-settlement curve, assuming the value of the coefficient of consolidation  $c_v = 0.027$  sq. cm. per min. Disregard secondary compression.

5. How will the time-settlement curve of the preceding problem change if the load is applied gradually and uniformly during a one-year construction period?

6. A hydraulic fill 20 ft. high is built on an impervious base. The total settlement expected is 5 in., the coefficient of consolidation of the material being  $c_v = 0.088$  sq. cm. per min. Use the time-factor graph (Fig. 6:11), and compute the settlement one year after construction. Disregard secondary compression and consider sudden application of the load. *Ans.* About  $1\frac{1}{4}$  in.

7. Assume the same conditions as in the preceding problem except the base which is pervious. Compute again the settlement one year after construction.

*Ans.* About  $3\frac{1}{2}$  in.

#### References

1. KARL TERZAGHI: "Erdbaumechanik auf bodenphysikalischer Grundlage," Franz Deuticke, Leipzig and Vienna, 1925; also "Theoretical Soil Mechanics," John Wiley & Sons, Inc., New York, 1943.
2. TERZAGHI and FRÖHLICH: "Theorie der Setzungen von Tonschichten," Julius Springer, Leipzig and Vienna, 1936.
3. KARL TERZAGHI: Undisturbed Clay Samples and Undisturbed Clays, *Jour. Boston Soc. Civil Eng.*, vol. 28, 1941.
4. A. CASAGRANDE and R. E. FADUM: Applications of Soil Mechanics in Designing Building Foundations, *Trans. A.S.C.E.*, vol. 109, 1944.
5. F. COLLINGWOOD: Foundations (a lecture at the Rensselaer Polytechnic Institute), *Eng. News*, vols. 25-26, Feb. 14, 1891.
6. HENRY H. CARTER: Settlement of the Embankment, etc., *Jour. Assoc.*

- Eng. Soc.*, vol. 11, 1892; also FRANK M. BARON: The Study of Earths: An American Tradition, *Civil Eng.*, vol. 11, 1941.
7. WILLIAM SOOY SMITH: The Foundations for the U. S. Government Post Office and Custom Building at Chicago, *Jour. Western Soc. Eng.*, 1898.
  8. N. M. GERSEVANOFF: "Principles of the Dynamics of Earth Masses" (official publication, printed in Russian), Moscow, 1933.
  9. DONALD W. TAYLOR and WILFRED MERCHANT: A Theory of Clay Consolidation Accounting for Secondary Compression, *Jour. Math. Phys.*, vol. 19, July, 1940.

See also references at the end of Appendix D.

## CHAPTER VII

### REVIEW OF PARTS ONE AND TWO; AND INTRODUCTION TO PART THREE

Part One of this book is dedicated to the discussion of what physics can furnish for the better understanding of the behavior of soils. In Part Two, stresses and strains in idealized masses are discussed, and the difference between the idealized masses and actual earth masses is pointed out. It is deemed convenient to begin with a brief review of the two parts in order to draw some conclusions and to formulate some statements that may be useful in the study of the structural applications of soil mechanics outlined in Part Three.

**7:1. Continuity and Discontinuities.**—Theories concerning stresses and strains may be developed for idealized materials only. Earth masses, however, are complex aggregations of soil particles and moisture and sometimes of gases and substances dissolved in the moisture contained in the pores. To determine stresses and strains in an actual earth mass, the latter is to be visualized either (*a*) as a homogeneous elastically isotropic body obeying Hooke's law or (*b*) as an idealized fragmental mass possessing friction and sometimes cohesion. The essential difference between the two kinds of idealized masses is that a fragmental mass is porous and close to its surface does not obey Hooke's law, for the simple reason that it cannot resist tensile stresses which may develop there if elastic theories are valid in this case. The term "elastic continuum" is used in this book as an equivalent of the expression "homogeneous elastically isotropic mass obeying Hooke's law."

It is obvious that all actual earth masses, being porous and not obeying Hooke's law, are more similar to idealized fragmental masses than to elastic continua. The reason that soil investigators nevertheless make use of the theory of elasticity is very simple: The theory of elasticity is the only branch of mechanics that enables us to determine stresses and strains produced within a body by superimposed loads. Mechanics, however, does not give us

any information as to the magnitude of the stresses produced within a fragmental mass by a superimposed load. However, stresses due to the weight of the semi-infinite fragmental mass itself may be computed.

Hence, the first meaning of the term "continuity" as used in this book is to designate an elastic mass without pores. Such a mass may be nonhomogeneous, however; *i.e.*, it may be composed of two or more different materials. A similar case is an elastic clay layer underlain by rock at a shallow depth. Such a situation is sometimes characterized by the term "discontinuity." The use of this term in the given sense is discouraged in this book. The term "discontinuity" is reserved for "zones of discontinuity" where conditions of failure are already operative or where displacements are exceedingly great.

In this connection there is another use of the term "continuity," namely, in the term "the principle of continuity of strains." All theories of idealized deformable masses have been developed on the basis of this principle. Particles of a mass should not move with respect to each other as rigid bodies, and displacements should be very small. The deflected horizontal boundary of a semi-infinite mass should be smooth and without breaks, and at each point thereof there should be only one tangent. Two tangents at one point mean a break. The same requirements should be satisfied by failure lines, which should also be smooth and without breaks (compare Secs. 5:9 and 5:10). Obviously, the presence of breaks or points with two tangents at the boundary of a *finite mass* does not contradict continuity if the number of these breaks is the same and they are at the same places *before and after deformation*.

Finally, the term "continuity" has been used in the study of seepage. The amount of liquid leaving a certain volume of the mass during a certain time interval must be equal to the amount of moisture that enters that volume.

**7:2. Straight-line Formulas.**—Stresses within actual earth masses cannot be computed, but only *estimated* from comparison with stressed condition in corresponding idealized masses. In turn, for computing stresses in idealized masses, mathematical formulas as simple as possible are used. The simplest shape of a mathematical formula is a first-degree equation expressed geometrically in the form of a straight line. There are three formulas of that kind as used in previous sections, namely,

a. Hooke's law:

$$S = E\epsilon \quad (4:3)$$

where  $S$  = stress.

$\epsilon$  = strain.

$E$  = modulus of elasticity.

b. Darcy formula:

$$v = ki \quad (3:1)$$

where  $v$  = velocity of flow.

$i$  = hydraulic gradient.

$k$  = coefficient of permeability.

A complete analogy between the two formulas has permitted development of the method of elastic analogies in seepage, as explained in Sec. 3:9. Some seepage problems have been solved by borrowing ready solutions from the theory of elasticity.

c. Still another straight-line formula is the Coulomb formula:

$$s = \sigma \tan \phi + c \quad (5:11)$$

where  $s$  = shearing resistance (shearing strength, shearing value) of the soil.

$\sigma$  = normal stress.

$\phi$  = angle of friction.

$c$  = ultimate unit cohesion.

This formula differs from the other two formulas by the presence of a constant member  $c$  and if plotted graphically does not pass through the origin. Formulas discussed in this section do not express any strict laws of nature. They are simply conventional statements introduced into engineering for convenience in computations.

**7:3. Thermodynamic Analogy.**—Besides the method of elastic analogies as mentioned in Sec. 7:2, one of the most important problems of soil mechanics, the consolidation problem, has been originally solved by analogy. The author of the mathematical theory of consolidation, Terzaghi, established a differential equation that is analogous to one used in the theory of heat transfer. Thus it became possible to use a ready solution which already existed in that theory.

**7:4. Plasticity and Plastic Equilibrium.**—The meaning of the term "plasticity" as used in soil mechanics is twofold:

a. Plasticity is a property of a soil that causes it to hold the deformed shape upon the removal of the force which has caused

that deformation (Sec. 2:18). The "plastic flow" is a flow of a soil mass without change in volume (Sec. 5:14), maintaining the value of the Poisson's ratio  $\mu = 0.5$ .

b. An earth mass is said to be in the state of "plastic equilibrium" if the slightest increase of the shearing stress or the slightest decrease in shearing strength would cause a failure of the mass either by disintegration along "failure lines" or by plastic flow (Secs. 5:9, 5:10, 5:14). As a rule, a failure of an earth mass is caused by a *shearing stress*. A mathematical expression defining the value of the shearing stress when the mass is at the state of plastic equilibrium is the "condition of plasticity" (or of failure). The best way to express a condition of plasticity is to do it graphically by drawing a *Mohr's circle* corresponding to the state of plastic equilibrium (for example, Figs. 5:3 and 5:6). The Mohr's circle is a simple but powerful tool for the study of soil mechanics, and every student of this branch of engineering knowledge must know how to use it perfectly. It should not be forgotten that the idea of the Mohr's circle is based on *simple statics* (Sec. 4:7).

**7:5. Infinite Solutions.**—There are two infinite solutions in soil mechanics that need to be clarified: (a) According to the Boussinesq formula, the slightest load applied at the boundary of a semi-infinite elastic continuum causes stresses and strains at any point of that continuum; (b) according to the theory of consolidation, the slightest load applied at the boundary of a semi-infinite mass possessing a deep soft layer causes an infinitely long consolidation process of that layer.

It should be remembered that such a thing as a semi-infinite body does not exist at all. The conception of the semi-infinite mass presumes infinite space subdivided by a horizontal plane into two halves, one of these halves being filled with earth material and another being empty. It is quite evident that only a small part of the actual ground surface around the load can be considered as plane, and the greater the distance of a point of the earth mass from the load the more considerable is the divergence between the theoretical and actual displacements. An analogy of the situation is plane surveying, in which a part of the earth surface if small enough may be considered plane, otherwise not.

Furthermore, in an actual *physical* body which is finite, all phenomena are also *finite*, *i.e.*, they have a beginning and an end. Obviously this statement is true for an earth mass, too. If it were

possible to solve a problem concerning an earth mass directly, infinite solutions possibly would not come. They do come as answers to mathematical problems which are substituted for actual physical ones. Particularly, in the case of the Boussinesq formula, it is assumed that at any distance from the point of application of the load, the earth mass responds with a strain obeying Hooke's law. In the squeezing out of moisture from a consolidating layer, it is assumed that the Darcy formula, which is analogous to Hooke's law (Sec. 7:2), holds at all times, including the end of the consolidation process. With these assumptions, mathematical problems furnishing infinite solutions are created.

Reverting to the Boussinesq formula, it is interesting to notice that Boussinesq himself was of the opinion that at a considerable distance from the load there are no strains at all. The following is a quotation from one of the Boussinesq books:<sup>1</sup>

... besides it is evident that the sections of the body located at infinity, or rather beyond a certain distance from the loaded portion (contact area), keep their shape and their dimensions.

Thus, what conventionally is meant by "infinity" may be a rather short distance, according to the properties of the soil and the value of the load.

**7:6. Time Element.**—A fresh sand embankment, if made without compaction, decreases in height or settles. In an analogous way, sand placed in a container—for instance, in large beaker—also decreases in volume. The process in question obviously is not consolidation as described in Chap. VI but a gradual adjustment of sand particles (for example, Fig. 5:12). Time is required for this settlement to be produced. The fact of such settlement has been known to practical engineers for years and perhaps for centuries.

Chambers<sup>2</sup> in 1921 described the influence of the time element in these terms:

When the shores were first installed, after the lapse of some hours the jacks\* were found to be comparatively loose. The jacks were then tightened and again the yielding of the soil was observed. This action continued for a week or more, depending upon the character of the soil before the jacks remained tight during a considerable period of time. It would appear from this that the time element must be taken into

\* These jacks supported a building which was being underpinned.

account in foundation work, and the determination of the bearing capacity of a pile or a footing must be obtained by a series of tests extending over a considerable period of time.

The phenomenon observed by Chambers was either adjustment or adjustment combined with consolidation. In any event, the role of the time element is very clearly described in this early statement.

**7:7. Additional Methods of Study: Freehand Drawing.**—Problems of soil mechanics are studied in this book in the following way. Interpretation of field observations and laboratory experiments is furnished, and attempts are made to express the relationship between different factors mathematically, in analytical form. Graphical solutions are also used. As an addition to graphical methods, freehand drawing of curves and families of curves is recommended: (a) In the study of seepage, flow-net lines may be drawn freehand (for example, Fig. 3:15), and (b) the isochrones that are used in the theory of consolidation may be also drawn freehand (Sec. 6:17). This method is used not only in soil mechanics but also in other branches of civil engineering and is very promising.\* It permits solution of the most complicated problems which cannot be approached otherwise.

Still another method of study—namely, the use of models—is discussed in Sec. 7:8.

**7:8. Models.** *a. Disturbed Zone.*—There are apparently convincing experiments on the disturbed zone under heavily loaded plates. Figures 4:18 and 4:20 show disturbed zones representing half a circle or more in cross section. The results of these experiments may be applied to full-sized structures only *with great caution*. However, since there are no field observations to prove or disprove the existence of such a disturbed zone under full-sized structures. Apparently the disturbed zone does not form under reasonably loaded structures. The earth mass under such structures is at a state intermediate between the natural state at rest and the state of limit equilibrium; in other words, it has not reached the latter state as yet.

*b. Lack of Similitude.*—Special care is recommended in the application of the results of small-scale experiments to full-sized

\* Prof. Hardy Cross of Yale University uses this method extensively in the study of deflected structures. It may be applied also in the theory of elasticity, in the study of stress surfaces.

structures, because of the lack of similitude in some cases. As an example, take two boxes as shown in Fig. 7:1. One of these boxes is twice as large as the other. Both carry a concentrated load at the center of the upper surface. Assuming the boxes to be wide and long enough, and hence neglecting the effect of the walls of the boxes, the vertical pressure at the center of the bottom

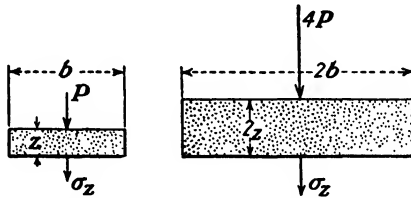


Fig. 7:1.—Caution is recommended in the use of models.

of the small box  $\sigma_z$  may be found by applying the Boussinesq formula and adding the pressure due to the weight of the soil:

$$\sigma_z = \frac{3P}{2\pi z^2} + \gamma z$$

It is evident that in order to obtain a pressure  $\sigma_z$  at the center of the large box, the concentrated load should be  $4P$ , not  $2P$  as may be supposed at the first glance, and in addition the pressure due to the weight of the earth is not the same in both cases. Another example is the height (thickness) of the capillary zone above the saturation line in an earth dam. This thickness is exactly the same in the model and in the full-sized structure, since it depends only on the height of capillary rise  $h_c$ , not on the size of the model.

Models are very good for demonstration purposes; for instance, models showing percolation under and within dams and under walls furnish excellent results. Yet the solution of numerical problems by the use of models is not a promising field.

*c. Photoelastic Experiments.*—Results of these experiments, discussed in Part Three, should also be carefully examined before they are applied to full-sized structures.

**7:9. Pore Moisture.**—An earth mass is termed “saturated” if all its pores are filled with moisture no matter what their volume. If such a mass contains a small amount of bubbles of entrapped air, it is still termed “saturated.” A saturated earth mass is said to be fully “consolidated” if at each and every point of that mass, pressure in pore water and pressure that the soil particles exert on the

moisture are balanced. If owing to external loading or some other circumstance the pore pressure of such a mass increases ("hydrostatic pressure excess" or "neutral stress"), the stresses within the mass are unbalanced, and a movement starts in the form of outflow of the moisture from the pores ("consolidation" of the mass). At a given time moment the pore moisture exerts a pressure equal to that excess of hydrostatic pressure in all directions and thus decreases the shearing strength of the material [formula (5:11) and the explanatory text]. As the consolidation process progresses, the shearing strength of the mass increases. This is the reason why earth dams should not be constructed hastily (see Chap. IX). In fact, the fresh earth material placed in a dam does not possess due shearing strength as yet and, if overloaded, may yield.

The theory of consolidation (Chap. VI) refers to saturated masses *only*. A loaded nonsaturated mass settles down owing to decrease of the pore volume accompanied by the removal of the air. Progressive removal of the air may, however, convert a nonsaturated into a saturated mass.

Artesian water and quicksand are related phenomena explained also by the pore moisture pressure. In the former case pore water under high pressure, if liberated by the drilling of a well, rushes upward, practically without destroying the skeleton of the earth mass. In the latter case, mixture of fine sand and water liberated by an excavation (Fig. 3:1) also moves up, but in the form of a flowing suspension.

**7:10. Theoretical Formulas: Their Applicability and Limitations.**—There are pessimistic views on the theoretical formulas as used for determining stresses and strains and conditions of failure in earth masses. It is often said that in most cases formulas do not fit actual conditions. It should be very clearly stated that all formulas advanced are excellent and furnish satisfactory results *when properly used*. Condition of the actual earth mass to be studied should correspond, however, with the assumptions that have served as a basis for establishing a given formula. Otherwise a formula cannot be applied. Particularly, there cannot be a slightest doubt as to the validity of the original Rankine formula which determines the ratio of the two principal stresses just before a shear failure occurs [formula (5:3)]. As applied to semi-infinite homogeneous masses the Rankine formula means that the lateral pressure in such masses is expressed by a triangular diagram formed

by a vertical and an oblique line ( $AB$  and  $AD$ , also  $A'B'$  and  $A'D'$  in Fig. 5:4). But if the earth mass is disturbed in some way, for instance, by the construction of a tunnel or a retaining wall ("discontinuities"), the oblique line of the diagram  $AD$  or  $A'D'$  becomes wavy, still following general directions  $AD$  or  $A'D'$ , however. In such cases, the Rankine formula should be applied with care, as explained in Part Three.

**7:11. Sketch to Be Used in the Study of Stability of Masses and Structures.**—The weight of an earth mass combined with that of the structure  $W$  should be balanced by the vertical reaction of the

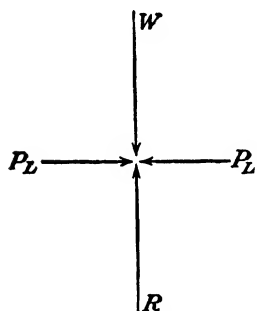


FIG. 7:2.—Sketch to be used in the study of stability of foundations and earth masses.

earth mass  $R$ . The lateral pressure  $P_L$  should be large enough to maintain the mass in equilibrium. These statements are graphically represented in a sketch (Fig. 7:2). This sketch refers to static loads only.

If the weight of the mass  $W$  is increased, for instance by building a structure on top of it, and the vertical reaction  $R$  cannot be developed in accordance, the mass will settle vertically to a considerable extent (example: consolidation in deeper strata). If the vertical reaction can be developed to balance the increased value  $W$  and the lateral support as represented by the value  $P_L$  is strong enough, the settlement will be very small (example: foundations on compact sand).

If the weight  $W$  of the mass remains constant but the vertical reaction  $R$  decreases, there will be a downward settlement of the mass (example: disturbance of the mass by mining operations or by shallow tunneling).

If the weight  $W$  of the mass increases and the lateral support  $P_L$  is insufficient, the mass will fail laterally (example: Fig. 5:7*d*). If the lateral support is weakened or removed, there will be also a lateral failure. Such is the case of excessive movement of the wall when the failure is sometimes manifested in the form of a crack behind the retaining wall (Fig. 5:7*b*). Another example is the sliding of the slope as shown in Fig. 5:7*c*. A part of the mass, representing the lateral support (at the left of the slope, Fig. 5:7*c*), is removed. Its place is taken by the shearing resistance (both friction and cohesion) along the eventual failure line. If this

shearing resistance is insufficient or is decreased in the lapse of time—for instance, because of excessive moisture content—the mass would fail as shown in Fig. 5:7c.

There are cases when the upward pressure  $R$  becomes greater than the weight  $W$  of the mass. In such exceptional cases there will be an upward movement of the mass (example: upward movement due to frost).

**7:12. Examples.**—Two examples of failure of huge earth masses are given here. Both failures are large-scale slides, and both are due to the activities of man.

*Case 1.*—In October, 1881, a great slide—termed “northslide” hereafter—occurred in the valley of the Thompson River, about 200 miles from Vancouver, B.C.<sup>3</sup> This was one of the series of slides which damaged the Canadian Pacific Railroad passing through that region. The geological formation is glacial drift underlain by boulder clay. The causes of all the slides in that region are excessive irrigation and lubrication of the boundary between two strata. Particularly, the immediate cause of the “north slide,” which amounted to 100,000,000 tons of earth, was the bursting of a reservoir about two miles from the river. The upper soil layer slid

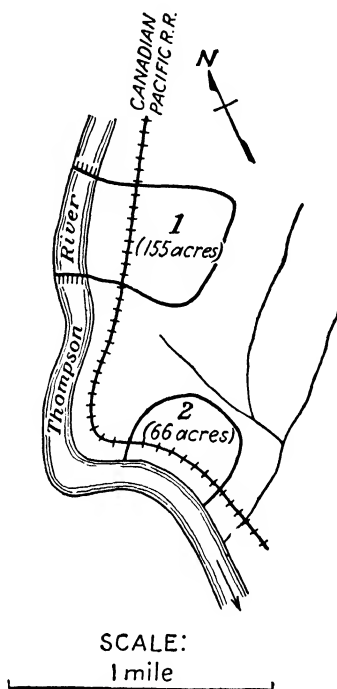


FIG. 7:3.—Slides in the zone of Canadian Pacific R. R. (1, north zone; 2, south zone).

down toward the river and formed a kind of dam in it (Fig. 7:3). Referring to the sketch (Fig. 7:2), note that this failure was due to the weakening of the lateral support  $P_L$  because of the lubrication and decrease in shearing resistance along the boundary of the two strata (compare also Fig. 5:7c).

*Case 2.*—Figure 7:4 shows subsidence due to the extraction of sulphur from deeper strata at Freeport, Tex. Water heated to 320°F. was forced through holes to reach sulphur-carrying gypsum. Sulphur was washed out and lifted up through holes not shown in

the profile. Subsidence of the whole locality was accompanied by cracks of the ground surface.<sup>4</sup>

In terms of the sketch (Fig. 7:2) this case is the decrease in vertical reaction  $R$ .

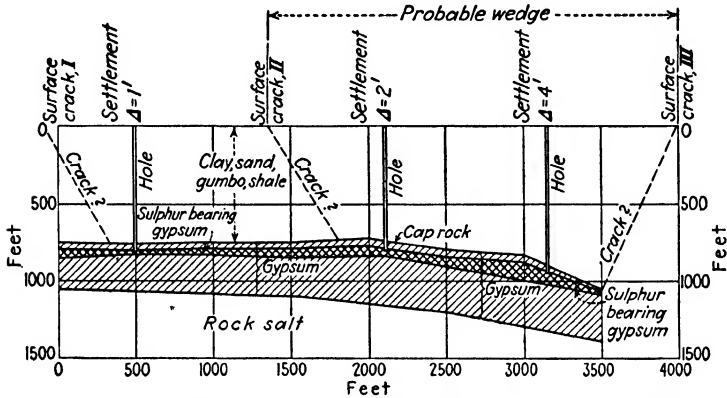


FIG. 7:4.—Settlement due to sulphur extraction at Freeport, Texas.

#### References

1. J. V. BOUSSINESQ: "Application des potentiels à l'étude de l'équilibre et du mouvement des solides élastiques," Gauthier-Villars & Cie, Paris, 1885, p. 51, lines 8-11.
2. RALPH H. CHAMBERS: Foundation Problems in Erecting Standard Oil Building, *Eng. News-Record*, vol. 87, Nov. 3, 1921.
3. R. B. STANTON: The Great Landslides on the Canadian Pacific Railway in British Columbia, *Minutes Inst. Civil Eng.*, vol. 132, 1897.
4. A personal communication from Mr. Edwin J. Beugler, consulting engineer, Cheshire, Conn.

**PART THREE**  
**STRUCTURAL APPLICATIONS**



## CHAPTER VIII

### STABILITY OF FOUNDATIONS

#### A. SPREAD FOUNDATIONS

The term "foundation" as used in engineering practice has a twofold meaning. It may designate either the lower part of a structure in contact with the earth or the upper part of the earth mass in contact with the structure. No sharp distinction between these two meanings has been made in this book.

The term "spread foundations" first refers to *isolated* footings under a structure. Isolated footings may be connected to form continuous or *strip* footings. Sometimes a footing extends under the whole area occupied by the structure and then represents the so-called *raft (mat) foundation*.\*

**8:1. Depth and Width of a Foundation.**—The depth of a foundation of a building is controlled by several factors, for instance by use of the subsurface space for the basement. Sometimes the presence of neighboring structures has an influence on that depth. If a structure is adjacent to flowing water, as in the case of dams and bridges, fear of erosion may have a certain bearing on the design. According to a tentative rule given by Terzaghi,<sup>1</sup> if the water rises in the river through a certain vertical distance, the scour may deepen the bed through three or four times that distance. Finally, the depth of a foundation is controlled by the *frost depth* in the given locality. As already stated (Sec. 3:18), the frost depth in the central part of the United States is between 3 and 4 ft. The New York Building Code establishes it at 4 ft.

The width of a foundation or, more accurately, its area of contact with the earth is controlled by two factors: (a) the purpose of the structure and (b) the bearing value of the soil. To determine the area of contact referred to, the total load acting on the base of the structure is divided by a conventional value termed

\* For construction details of spread and pile foundations, see the book "Foundations of Bridges and Buildings" by Jacoby and Davis, 3d. ed., McGraw-Hill Book Company, Inc., New York, 1941.

“bearing value” or “bearing power” of the soil. The discussion following hereafter tends to establish limitations of this method.

**8:2. Stress-strain Condition of the Earth Mass Next to a Spread Foundation.**—As soon as the designer has established (largely from experience) the size of the base of the structure and the depth of the foundation, the safety of the latter must be checked from the following two considerations:

- a. The surrounding earth mass must be safe against failure produced by shear.
- b. The structure must be safe against movements or settlements that may be due to the displacements in the earth mass.

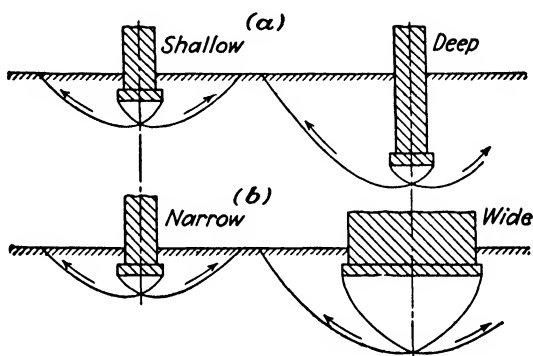


FIG. 8:1.—Shear danger is decreased by using deep or wide foundations.

a. *Shear Danger.*—Figure 8:1a shows possible failure lines under a shallow and a deep foundation. The deeper the foundation the less is the shear danger. The shearing resistance  $s = \sigma \tan \phi + c$  of the underlying layer, which depends on the normal stress  $\sigma$ , rapidly increases with the depth owing to the weight of the overburden, whereas the shearing stress  $\tau$  caused by the structure decreases. Hence the value of the safety factor  $s/\tau$  increases with the depth of the foundation.

Figure 8:1b shows possible failure lines under a wide and a narrow foundation. The wider the foundation the less is the shear danger. In this case, because of repartition of the acting load on a larger area, the shearing stress  $\tau$  decreases, whereas the shearing resistance  $s$  increases for the reasons already explained. Overloaded narrow foundations are often dangerous from the point of view of shear, and corresponding structures may tip.

More details along these lines will be given in Chap. XIII, dealing with settlement of structures.

It follows from Fig. 8:1 that shear failures may be *avoided by deepening or widening a foundation* or both. Economic considerations are, however, against deep or exceedingly wide foundations, and the task of the designer is to reconcile in the most rational way both the technical and the economic considerations mentioned.

*b. Settlements.*—A foundation must be so designed as to avoid considerable vertical or horizontal displacements which may produce cracks in the structure or distortion of its parts or both. There may be lateral displacements of the mass along the failure lines even if failure itself does not occur (Sec. 5:13). These displacements may be accompanied by bulging of earth around the structure. To decrease such displacements, the deepening or the widening of a foundation may be again recommended. Besides, compressibility of the material at a greater depth is much less than that of shallow strata, which may have an influence on the vertical settlement of the structure.

If there is a soft layer which would excessively consolidate under the structure, the best way to have smaller settlement is to relieve the total load of the structure. Little can be accomplished by widening the foundation, except in the case where the layer in question is shallow. This is so because the widening of a foundation diminishes vertical pressures  $\sigma_z$ , which control the settlement; and for a deep layer where the whole structure practically acts as a concentrated load, this decrease is negligible, whereas it may be of some importance for a shallow layer. The deepening of a foundation brings its base near the layer under consolidation and hence increases the acting vertical pressures  $\sigma_z$ . Hence, under such circumstances, such a deepening is not advisable.

**8:3. Bearing Value of the Soil.**—The terms “bearing value,” “bearing power,” and “bearing capacity” are synonymous.

*a. Ultimate Bearing Power.*—The minimum unit load that causes failure of the earth mass when acting at the base of a structure may be termed “ultimate bearing power” of the given soil. Strictly speaking, in specifying the value of the ultimate bearing power of the soil, the value of the loaded area and the depth at which this area is located should be indicated.

*b. Safe Bearing Power.*—The safe bearing power of the soil equals the ultimate bearing power divided by the safety factor (for instance,  $1\frac{1}{2}$  or 2). Sometimes the safe bearing power of a soil is defined as the unit load that would cause a predetermined settlement of the given structure. In some official regulations the term “presumptive” bearing power (instead of “safe” bearing power) is used.

**8:4. Sources of Information on the Bearing Value.**—The sources of information concerning the bearing value of a soil are (a) official regulations, particularly building codes of different cities; (b) loading (or load) tests; (c) theoretical formulas.

Building codes generally establish how many tons per square foot can be placed on the horizontal surface of a given soil. For instance, the New York Building Code regulates the bearing power of the soil in the following way.\*

	Tons per Sq. Ft.
Rock . . . . .	25 to 40
Hardpan overlying rock . . . . .	10
Gravel . . . . .	6
Coarse sand . . . . .	4
Firm clay . . . . .	2
Soft clay . . . . .	1

Building codes sometimes provide for *increase* of the safe bearing value for deep foundations (compare Fig. 8:1). The safe bearing value may be also officially *decreased* for vibrations, for seismicity, for consolidation in deep soft layers (compare Chap. VI), and for inward and outward flow of water. Sometimes cities require a settlement analysis to be made (compare Chap. XIII).

In using the figures of the safe bearing value as given by a building code, there may be three possibilities: (a) The designer *accepts* the official figure; (b) the designer *decreases* that figure (Sec. 8:5) according to the boring data or other considerations; (c) the designer *applies for increase* of the official figure. In this case he possibly will be required to prove his application by a loading test.

**8:5. Considerations for the Decrease of the Safe Bearing Value.**—In choosing the value of the bearing power, the designer must have in view the two considerations concerning the safety of the foundation, as already explained in the beginning of Sec. 8:2.

\* A shortened excerpt from the code.

In such structures as bridge piers on shallow foundations, earth dams, or high narrow monuments, where there is danger of lateral displacement due to a shear failure, a laboratory test must furnish the shearing value  $s$  of the soil at that spot (Sec. 5:6), and this value is to be compared with that of the maximum shearing stress  $\tau$  (Sec. 4:16). If the value of the safety factor thus obtained is unsatisfactory, the bearing value assumed in the design must be decreased proportionately.

If the factor controlling the design of the foundation is settlement due to consolidation in deeper strata, the bearing value should be so chosen as to produce a settlement not exceeding a certain maximum. Any structure may be in such a situation, but mostly these are heavy city buildings, factories, and sometimes bridge supports. Suppose that a building is to be erected on a thick layer of sand underlain by a soft clay layer. Suppose likewise that the consolidation test in the laboratory has shown that in order not to pass a certain maximum of settlement, the unit pressure on the base of the structure should not exceed 2 tons per sq. ft. The latter value is then the bearing value of the given sand on which the building is to be erected. As seen from the preceding table, 4 tons per sq. ft. could be allowed for the given sand foundation, but this load would produce a settlement larger than the maximum referred to.

Unit loads at the base of *light buildings in a city* are simply determined *from experience*, and in this case regulations of a building code are of great value. Very often, in the construction of *new railroads* or in *state highway departments*, excavations for culverts and small bridges are opened and the value of the bearing power is determined simply by *visual inspection*. This expeditive procedure is a success in most cases, admittedly, if the resident engineer has a certain knowledge of the soils of a given locality. In a few instances, however, it may be the cause of complications during the erection of the structure, when it is discovered that the soil is much less resistant than it seemed to be at first inspection.

**8:6. Two Kinds of Loading Tests.\***—*a. Loading Test as Regulated by a Building Code.*—In this kind of test *settlements* of a wooden platform (generally 1 by 1 ft. or 2 by 2 ft.) under the unit load to be used in the design of the structure *must not exceed a predetermined value*. The platform is placed either at the ground

\* Consult also Sec. 14:19c.

surface, previously cleared of grass and humus, or at the bottom of excavation at the elevation of the base of the structure. The following figures are given merely as an example. The design unit load remains on the platform until the settlement is completed, but not for less than 24 hr. Observations of settlement are made at least every 24 hr. After completion of settlement an additional 50 per cent load is applied, and additional settlement observed in the same way as described. The settlement under the design

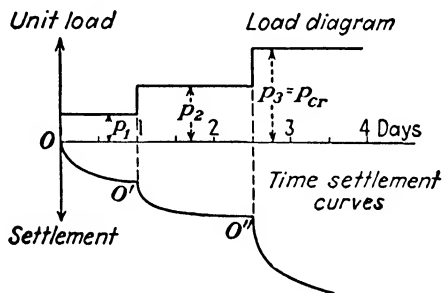


FIG. 8:2.—Results of a load test.

load should not be more than  $\frac{3}{4}$  in., and additional settlement under the 50 per cent load should not be over 60 per cent of the settlement under the design load. As explained hereafter (Sec. 8:7), an experimental settlement of a certain value *does not mean* that the actual settlement of the structure will be of that value; probably it will be larger.

*b. Loading Test in a Locality without Official Building Regulations.*—In this case the loading test is made *to failure*. Load is applied by increments, and settlements are observed. A new load increment is not applied before the settlement from the previous increment is completed, and this may last, for instance, 24 hr. or even more. At first, settlements are more or less proportional to the loads; but in the application of a certain load increment, the limit of proportionality is exceeded. The corresponding load is called the “critical load” and may be considered equal to the “ultimate bearing value” already discussed. The bearing value of the soil in question to be used in the design should be, hence, a fraction of the critical load, according to the assumed value of the safety factor. Figure 8:2 illustrates this kind of test. The time-settlement curves in loading tests are similar to theoretical curves as discussed in Chap. VI.

*c. Double Load Tests.*—It is the belief of some engineers that the bearing value of a soil under a loaded area is made up of two separate strength factors, one of which depends on the perimeter of the area (“perimeter shear”) and the other on the compression resistance of the soil mass. The relative size of the area may be expressed by the perimeter-area ratio  $x = P/A$ , where  $P$  is the perimeter of the plate in feet, and  $A$  is its area in square feet. Housel<sup>2</sup> uses the following straight-line formula for the bearing value  $q$  of the soil under a loaded plate:

$$q = mx + n \quad (8:1)$$

He assumes that the values of  $m$  and  $n$  are constant for any plate loaded with the critical load; then for two plates with values of the perimeter-area ratio  $x_1$  and  $x_2$ , the corresponding unit values of the bearing capacity  $q_1$  and  $q_2$  would be

$$\begin{aligned} q_1 &= mx_1 + n \\ q_2 &= mx_2 + n \end{aligned} \quad (8:2)$$

Thus,  $m$  and  $n$  may be easily determined from Eqs. (8:2). If the perimeter-area ratio of the actual structure is  $x_3$ , the bearing capacity of the soil under it may be determined by using formula (8:1), making  $x = x_3$ . It is to be noticed that in many actual structures the perimeter-area ratio is exceedingly small, so that the product  $mx$  may be neglected, and thus  $q = n$ . The term “perimeter shear” should not be confused with the term “radial shear” (Sec. 5:9).

**8:7. Analysis of the Results of a Loading Test.**—Whatever a loading test may be, its results should be interpreted in conjunction with accurate soil profiles showing stratification and variation in thickness of the layers.

If Hooke's law approximately holds, the value of the shearing stress  $\tau$  is proportional to the unit load of the foundation [Sec. 4:16 and particularly formula (4:11)]. Hence the values of the shearing stress  $\tau$  under the loading platform and of that under the actual structure are equal. The shearing resistance  $s$  under the loading platform is smaller than that under the actual structure, as may be concluded from a mere inspection of Fig. 8:1*b*. It follows that the ultimate bearing value as determined by the loading test is on the safe side.

It is hopeless to attempt to determine the value of the eventual

settlement of a structure from a loading test, however. As a rule, a larger loaded area should produce larger settlement than a smaller. According to the theory of elasticity, the ratio of the settlements produced by the two areas  $A$  and  $a$ , loaded with equal unit loads, equals  $\sqrt{A/a}$ . In reality the settlement under the structure is less than that maximum. For instance, the settlement in a loading test that was made in 1922 for a Standard Oil Company building in San Francisco, Calif., was 0.1 in. under a platform of 1 sq. ft. The actual building (area: 218 by 152 ft.) settled 2 in.<sup>3</sup>

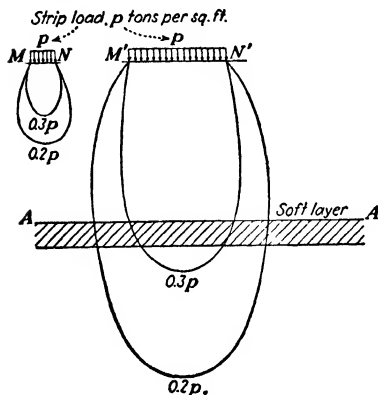


FIG. 8.3.—Comparison of isobars under a narrow and under a wide structure (compare FIG. 4:16).

The situation is even worse if there is a deep, soft layer under consolidation. In Fig. 8:3, plane isobars for a narrow and for a wide structure are shown. It may be seen that in the case of the narrow structure stresses  $0.2p$  and  $0.3p$ , to which these isobars correspond, do not reach the soft layer at all. Hence total settlements under the structures shown in Fig. 8:3 as caused by the consolidation of the soft layer are by no means equal. Besides, short duration

of a loading test (perhaps a week or 10 days) does not permit the full development of the process of the squeezing out of moisture from the pores, which, as is known, requires a considerable time.

Irregular lateral flow of earth, if any, from underneath a loaded plate may completely change the picture of settlement, and a smaller plate may sometimes settle more than a large one.

Places for loading tests should be selected in such a way as to be true representatives of the properties of the whole mass. The greater the area to be loaded the better. A very clear understanding of the real value of small loading tests has existed in American engineering circles for more than 50 years, as the following statement by Collingwood, made in 1891 (Chap. VI, ref. 5), indicates:

. . . and it is insisted upon by experimenters that absolutely certain

results can only be reached when the area tested is approximately the same as that to be built upon.

**8:8. Theoretical Determination of the Ultimate Bearing Power.**—The ultimate bearing power in the case of a two-dimensional problem may be determined theoretically using the concept advanced in Sec. 5:9. An active prism *A* formed under the structure tends to cause the shear failure of the mass by pushing out the resisting passive prism *P*, both prisms and the earth body connecting them being in the state of plastic equilibrium.

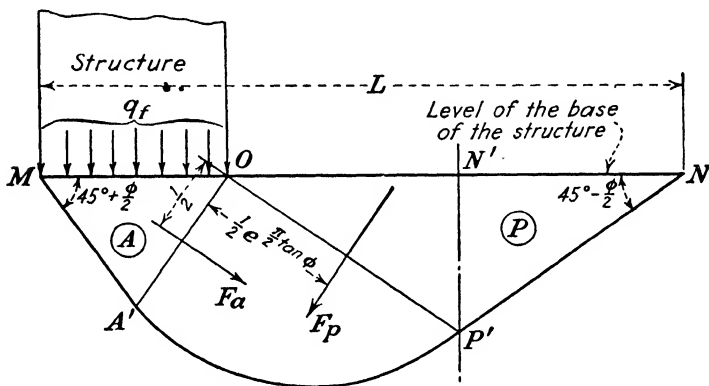


FIG. 8:4.—Ultimate bearing value by Prandtl formula.

*a. Prandtl Formula.*—Consider Fig. 8:4 in conjunction with Fig. 5:9, the letters *A'*, *O*, and *P'* being at analogous places in both figures. Place  $OA' = 1$ ; then according to formula (5:18)

$$OP' = e^{\frac{\pi}{2} \tan \phi} \tag{8:3}$$

In the state of limit or plastic equilibrium the active prism *A* presses on the zone of "radial shear"  $A'OP'$  with a force  $F_a$ ; the passive prism *P* resists the pushing out with a force  $F_p$ . Taking moments of both forces about point *O*

$$F_a \left( \frac{1}{2} \right) = F_p \left( \frac{1}{2} e^{\frac{\pi}{2} \tan \phi} \right) \tag{8:4}$$

It may be assumed, furthermore, that at the state of plastic equilibrium the pressure in the active prism *A* is hydrostatic, *i.e.*, acts equally in all directions. If the value of the ultimate bearing power of the foundation  $OM$  is  $q_f$ , the hydrostatic pressure in the active prism is  $q_f + p_i$ , where  $p_i = c/\tan \phi$  (Sec. 5:7). Hence

$$F_a = q_f + p_i \tag{8:5}$$

The passive prism *P* would cease to resist when its full compressive strength

$q + p_i$  is overcome (for the designation  $q$  refer to Sec. 5:18). According to Fig. 5:15

$$\frac{p_i}{q + p_i} = K_a \quad (8:6)$$

from which

$$q + p_i = \frac{p_i}{K_a} = p_i K_p \quad (8:7)$$

$K_a$  and  $K_p$  being the active and the passive Rankine values (Sec. 5:5). Hence

$$F_p = p_i K_p e^{\frac{\pi}{2} \tan \phi} \quad (8:8)$$

Introducing the values of  $F_a$  and  $F_p$  as given by Eqs. (8:5) and (8:8), respectively, into Eq. (8:4), the final formula is obtained.

The formula derived by Prandtl for the case of action of a tool on an even metallic surface (neglecting the weight of that metallic medium) is

$$q_f = \frac{c}{\tan \phi} \left[ e^{\pi \tan \phi} \tan^2 \left( 45^\circ + \frac{\phi}{2} \right) - 1 \right] \quad (8:9)$$

where  $q_f$  is the safe unit load applied. Notice that (a) the factor of safety in this case is 1 and (b) the value of  $q_f$  does not depend on the width of the loaded area (of the foundation). In the case of soft plastic clay the value of  $\phi$  is close to zero as in metals, and  $q_f = (\pi + 2) c = 5.14c$ .

Designate with  $A$  the area of the zone bounded by the horizontal line  $MON$  and the failure line  $MA'P'N$ , with  $L$  its length, and with  $h$  its average depth:

$$h = \frac{A}{L} \quad (8:10)$$

For a cohesionless mass ( $c = 0$ ;  $\phi > 0$ ) Prandtl's formula furnishes  $q = 0$ . This is because the mass below the base of the structure is assumed weightless. Terzaghi proposed to improve Prandtl's results by replacing  $c$  in formula (8:9) with  $c + c'$ , where

$$c' = h\gamma \tan \phi \quad (8:11)$$

$\gamma$  being the unit weight of soil.

The so-called "modified Prandtl formula" used sometimes is

$$q_f = \left[ \frac{c}{\tan \phi} + \gamma b \tan \left( 45^\circ + \frac{\phi}{2} \right) \right] \left[ \tan^2 \left( 45^\circ + \frac{\phi}{2} \right) e^{\pi \tan \phi} - 1 \right] \quad (8:12)$$

The symbol  $b$  in formula (8:12) means half width of the foundation (half of distance  $MO$  in Fig. 8:4).

b. *Caquot Formula*.<sup>5</sup>—Refer to Fig. 8:4; load the foundation  $MO$  with a unit load  $q_f$  equal to the ultimate bearing power, and load the top of the passive prism  $ON^1$  with a unit load  $\gamma z$ , equal to the unit weight of the earth above the base of the structure  $MO$ . Then, taking moments about point  $O$

$$q_f = \gamma z K_p e^{\pi \tan \phi} \tag{8:13}$$

**8:9. Krey Method.**—Krey\*<sup>6</sup> replaces the theoretical failure lines as shown in Fig. 8:4 by arcs of a circle having its center at

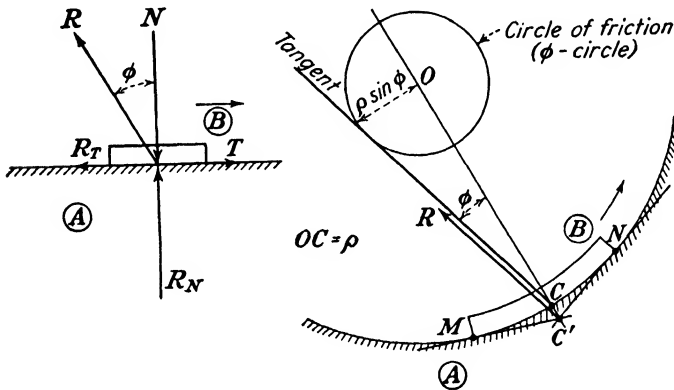


FIG. 8:5.—Circle of friction.

the horizontal plane of the base of the structure  $AB$  (Fig. 8:6). The depth  $z$  and the width of the two-dimensional structure should be assumed.

Before discussing the Krey method, it is necessary to introduce the concept of “circle of friction,” which also will be used in the discussion of stability of slopes (Chap. IX). If body  $B$  is pulled along the plane surface of body  $A$  in the direction shown by the arrow (Fig. 8:5a), the reaction  $R$ , composed of a normal reaction  $R_N = N$  and a tangential reaction  $R_T = T$  is directed against the movement and in the state of limit equilibrium makes an angle  $\phi$  with the normal to the surface of a body  $A$ . Symbols

\* Hans Krey (1866–1928), chief of the German Research Institution for Hydraulic Engineering.

$N$  and  $T$  designate the normal and the tangential force. Should the surface of body  $A$  be cylindrical, of a radius  $\rho$  having its center at  $O$ , the reaction  $R$  at each point of contact of the two bodies  $A$  and  $B$  would touch a circle of a radius  $\rho \sin \phi$  having its center at the same point  $O$ . This circle is termed "circle of friction" or " $\phi$ -circle." It is assumed that the resultant reaction also touches

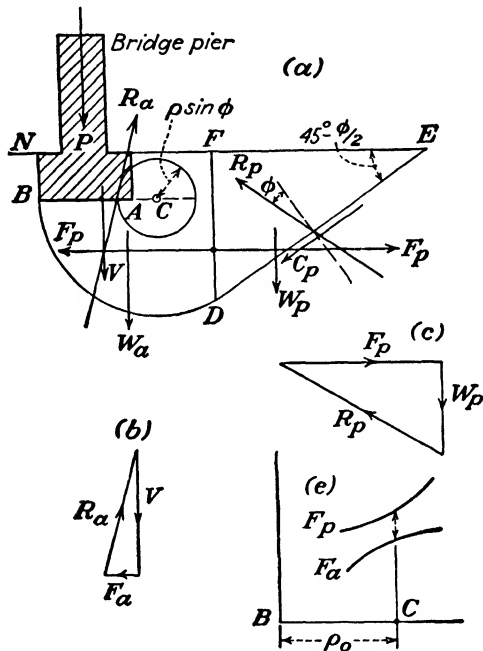


FIG. 8:6.—Krey's method.

the circle of friction. This is not quite correct, since reaction  $R$  passes through point  $C'$  outside arc  $MN$  (body  $B$ ) rather than through its midpoint  $C$ . The error, however, is negligible.

The center of the circular failure line is first chosen at an arbitrary point  $C$  (Fig. 8:6) located at the continuation of the horizontal line  $BA$ , and a circle is traced through point  $B$  (radius  $CB = \rho$ ). A tangent to this circle making an angle  $45^\circ - (\phi/2)$  with the horizontal determines the passive prism  $FDE$ , the area  $NDF$  being the cross section of the active prism. Owing to the action of the weight  $P$  of the structure and that of the active prism  $W_a$ , an active thrust  $F_a$  is developed, its point of application

being the third point of the face  $FD$ . There are three forces acting at the active prism  $NBDF$ , keeping it in equilibrium: (a) the resultant  $V$  of weight  $P$  of the structure and of the weight  $W_a$  of the active prism itself, (b) the reaction of the passive prism equal to  $F_a$  but directed in an opposite direction (from right to left in Fig. 8:6a), and (c) the reaction  $R_a$  of the curved failure line  $BD$ , making an angle  $\phi$ , that of friction, with that failure line. Since the three forces  $V$ ,  $F_a$ , and  $R_a$  must intersect at a point, the direction of the reaction  $R_a$  may be found by tracing a circle of friction of a radius  $\rho \sin \phi$  at point  $C$  and drawing a tangent to it through the point of intersection of the forces  $V$  and  $F_a$ . The value of the forces  $F_a$  and  $R_a$  may be found from a force polygon (Fig. 8:6b).

At any time the passive prism develops a reaction equal and opposite to the active thrust  $F_a$ . The ultimate value  $F_p$  of this reaction may be found by considering the equilibrium of the passive prism under the action of the three forces: (a) weight  $W_p$  of that prism, (b) reaction  $F_p$  passing through the third point of the face  $FD$ , (c) reaction  $R_p$  of the face  $DE$ , making an angle  $\phi$  with the latter. The value of the forces  $F_p$  and  $R_p$  may be found from a force polygon (Fig. 8:6c). The ratio  $F_p/F_a$  is the safety factor for the case when the failure line has its center at point  $C$ . This construction should be repeated for various points  $C'$ ,  $C''$ , . . . located at the continuation of the line  $AB$  (not shown in Fig. 8:6), and values  $F_p$  and  $F_a$  should be plotted against distances  $BC$ ,  $BC'$ ,  $BC''$  or for different values of the radius  $\rho$  (Fig. 8:6c). The value  $BC$ , for which the distance between curves  $F_p$  and  $F_a$  is a minimum, corresponds to the minimum of the ratio  $F_p/F_a$ . Point  $C$  thus determined is the center of the possible failure line (Fig. 8:6e). If the minimum ratio  $F_p/F_a$  is less than the required safety factor (for instance, 1.5), the depth of the foundation is to be increased.

This graphical method may be extended to consider cohesion along the shearing surfaces, either of both prisms or of only the passive prism ( $C_p$  in Fig. 8:6a). To be sure of the result, points  $C$ ,  $C'$ ,  $C''$ , . . . may also be chosen outside the continuation of the line  $AB$ .

**8:10. Rankine Formula for the Depth of a Foundation; Terzaghi Method.**—*a. Rankine Formula.*—This formula should not be confused with formula (5:3). Load the top of both active and passive

prisms ( $ACB$  and  $BCD$  in Fig. 8:7) with the loads  $q_f$  and  $\gamma z$ , respectively (see the Caquot formula). Rankine expresses the value of  $q_f$  as the weight of an equivalent sand column  $H$  ft. high, so that  $q_f = H\gamma$ . Take moments about point  $C$  (Fig. 8:7):

$$q_f = \gamma z K_p^2 \quad (8:14)$$

The failure line has a break (point  $B$  in Fig. 8:7) and does not satisfy the condition of continuity.

*b. Terzaghi's Original Formula.*<sup>7</sup>—Rankine did not consider either the weight of the earth mass below the base of the structure or the size of the foundation. Terzaghi<sup>1</sup> did so and considered equilibrium of prisms I, II, III in Fig. 8:7. He gave the follow-

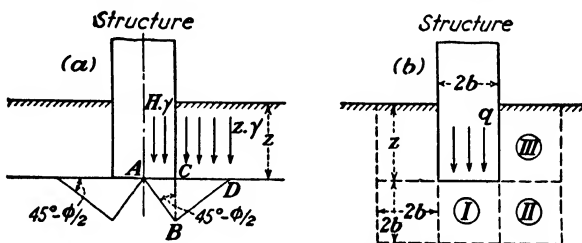


FIG. 8:7.—Semi-empirical determination of the bearing value of a soil. [(a) After Rankine; (b) after Terzaghi.]

ing formula for the ultimate bearing value  $q_f$  in the case of a strip foundation  $2b$  wide:

$$q_f = b\gamma K_p^2 \left[ 1 + \frac{z}{b} + (\text{const.}) \left( \frac{z}{b} \right)^2 \right] \quad (8:15)$$

The value of the constant that accompanies the quadratic member  $z/b$  is generally under  $\frac{1}{4}$ . Thus for the case of shallow foundations or wide structures, when the value of  $z/b$  is small, the quadratic member in formula (8:15) may be neglected:

$$q_f = b\gamma K_p^2 \left( 1 + \frac{z}{b} \right) = \gamma K_p^2 (b + z) \quad (8:16)$$

Rankine bearing values [formula (8:14)] are more conservative than those computed by formula (8:6). At greater depths the quadratic term in formula (8:15) cannot be neglected any longer. It rapidly increases with the depth and furnishes too large bearing values.

*c. Terzaghi's Studies of Passive Resistance.*—The passive pressure (or "passive resistance") has been discussed in Sec. 5:5; and its

unit value  $K_p$  has been established. This value corresponds to a horizontal backfill and a horizontal pushing force acting against a vertical plane. According to Terzaghi<sup>8</sup> if the pushing force makes an angle to the horizontal of  $30^\circ$ , the actual value of the unit passive resistance in this case may be more than 30 per cent smaller than the value of  $K_p$  (Sec. 5:5). Since the theoretical analysis of foundations depends on the passive resistance of soils, Terzaghi's suggestion should be given serious consideration. Accurate computations of the passive resistance using Terzaghi's methods are involved, however. It could be recommended therefore, using not more than two-thirds of the value  $K_p$  (Sec. 5:5) in computations if, of course, the pushing force is not horizontal.

*d. Terzaghi's Method of Determining the Ultimate Bearing Value.*<sup>8</sup>—The failure lines  $A'M$  and  $A'O$  in Fig. 8:4 make angles of  $45^\circ + \phi/2$  with the horizontal. Since a "rough" base of the structure  $OM$  (Fig. 8:4) settles vertically, it is assumed by Terzaghi that the failure line at points  $M$  and  $O$  in this case is vertical. Since at each point of the mass there are two failure lines (shearing surfaces), making an angle of  $90^\circ - \phi$ , the angles made by lines  $A'O$  and  $A'M$  with the horizon would be  $\phi$ . The rest of the Terzaghi's construction is as in Fig. 8:4. Different possibilities of failure (variable lengths  $OP'$  of the side of the passive prism) are discussed. The ultimate bearing value

$$q_f = cN_c + \gamma zN_q + \gamma BN \quad (8:17)^*$$

$N_c$ ,  $N_q$ , and  $N$  being "bearing capacity factors," depending on the angle of friction  $\phi$ . Terzaghi furnishes graphs and formulas for their determination.<sup>8</sup> The symbol  $B$  means half of the width of the two-dimensional foundation  $OM$ . The surcharge on the top of passive prism  $ON$  is  $\gamma z$  (Fig. 8:4).

Apparently formula 8:17 is supposed to be valid for a "rough" base whereas Prandtl formula (Sec. 8:8) should be applied in the case of a "smooth" base. If  $\phi = 0$ , these formulas furnish the values of  $q_f$  equal to  $5.7c$  and  $5.14c$  (Sec. 8:8), respectively. The difference of about 10 per cent is negligible in this kind of estimation.

**8:11. Modulus of the Foundation.**—It is sometimes assumed that the unit soil reaction  $p$  under a uniformly loaded beam resting on the earth surface and the settlement  $\Delta$  of this beam are proportional:

$$p = k_f \Delta \quad (8:18)$$

The value of  $k_f$  is called the "modulus of the foundation" (also "coefficient of the foundation," "foundation number"). Formula (8:18) is correct only in the case of a beam infinitely wide and infinitely long. Otherwise, there are breaks in the deflected earth surface, corresponding to the ends of the beam; this contradicts

the principle of continuity. Formula 8:18 was used in the study of the behavior of railroad ties and highway pavements on compacted subgrade and has furnished satisfactory results; but as a rule, its use is not advisable. The physical dimension of the modulus of the foundation is stress divided by length or, in English measures, pounds per sq. in. per in.

**8:12. Shearing Stresses at the Base of a Structure.**—The pressure distribution at the base of an infinitely wide structure (visualized two-dimensional and uniformly loaded) should be uniform; it cannot be otherwise. Since the structure cannot move because it is infinite, there is no friction (horizontal shearing stresses) at its base. If an infinitely wide structure becomes finite, there may be a tendency to lateral motion. This tendency, if any, is opposed by friction (horizontal shearing stresses) at the base. Another source of horizontal shears at the base of a structure is its settlement. The earth material under a structure moves down and laterally, and the latter motion is opposed by horizontal shears at the base of the structure.

Since at each point of the mass there are two mutually normal shears, vertical shears appearing in conjunction with the horizontal ones may redistribute the pressure of the structure on its base. In analyzing a rigid metallic or masonry structure the shears at its base *are neglected*, however, since they are small, though they may be of importance in the case of an earth dam (Sec. 9:21).

**8:13. Relief of Vertical Pressure by Deep Excavation.**—If the weight of the structure exactly equals the weight of the excavation made for it, the stress distribution in the earth mass supporting this structure will be practically the same as before the construction. In any case, in computing pressures at deeper strata, the weight of the excavation (for instance, for a deep basement) should be deducted from the weight of the structure.

The bottom of an excavation for a structure moves up owing to (a) the relief of pressure (elastic rebound of sand or swelling of clay) and, if any, (b) plastic flow of the material of the surrounding mass. The same phenomenon may be observed in quarries in plastic rock (granite, basalt). In a general case, this upward motion and the subsequent settlement due to recompression of the mass by the structure may or may not be equal.

**8:14. Conclusions from the Theory of Spread Foundations.**—Rules for the design of footings are published by engineering

societies. Examples are the regulations elaborated by the Joint Committee on Reinforced Concrete\* (June 1940) or by the American Concrete Institute (February 1936). Both the A.C.I. Code and the Joint Committee Specifications assume a uniformly distributed soil reaction at the base of a footing. In most engineering offices this assumption is made generally in the design of footings and spread foundations. Let us investigate, in the light of the theoretical considerations, to what extent this practice is justified.

*a. Foundations Large in Plan.*—As explained in Sec. 8:12, pressure distribution under uniformly loaded wide structures is probably more or less uniform, with some slight disturbances at the edges. Examples of such structures are dry docks or large water and oil tanks resting on the earth surface. In such a case rigidity of the structure is not required, except, perhaps, at the edges and except for taking care of weak spots in the soil which accidentally may be present under the structure.

Nonuniformly loaded wide structures do not belong in this category. It has been thought, however, that by making the base of a structure rigid, the load may be thrown uniformly to all parts of the foundation. Apparently, in the case of a wide rigid structure uniformly loaded, soil reactions are more or less uniform at the middle, and there are disturbances at the edges. A design of this kind was made in 1939 for the new office building of the New England Mutual Life Insurance Company in Boston's Back Bay district (A. Casagrande, consulting engineer). Soil conditions are as follows: ground surface, 18 ft. above sea level; rock, more than 150 ft. deep and overlain by 30 ft. of hardpan, 70 ft. or more of glacial clay, and about 20 ft. of silt with 20 ft. of man-made fill above it. The plan of the building is shown in Fig. 8:8. The building comprises an integral box substructure 40 ft. high, with four longitudinal and six cross walls of  $3\frac{1}{2}$  ft.

\* The Joint Committee on Reinforced Concrete is composed of representatives of various engineering societies and organizations.

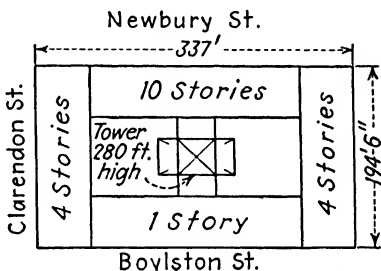


FIG. 8:8.—Plan of a building in Boston, Mass. (From *Eng. News-Rec.*, Nov. 23, 1939.)

minimum thickness, each wall resting on a full-length footing slab 15 to 18 ft. wide and 8 to 10 ft. thick. The average pressure under the wall footings is about 4 tons per sq. ft., without taking account of the buoyancy, or 3 tons per sq. ft. after deducting uplift.<sup>9</sup>

Another example of similar design is the Telephone Building in Albany, N. Y. Both buildings will be taken up again in the discussion of the settlement of structures (Sec. 13:29).

*b. Small Footings.*—Very few failures of footings have been reported in technical literature. An explanation would be that these parts of a structure are hidden in the earth and hence out of sight; and should there be some settlement, it is readily attributed to other causes. Another explanation, perhaps more probable, is that footings are unduly strong. Computed moments and shears in some sections of a footing may be too low, but the factor of safety covers abundantly all underestimations and leaves enough margin for safety. In this case the uniform pressure distribution is a good "design conventionality" which results in safe structures.

Since the design of small footings is an everyday task in engineering offices, and since uniform pressure distribution has proved to furnish rather safe results, it seems good practice to follow the present routine until soil mechanics furnishes more definite suggestions which could lead to more economical solutions.

*c. Spread Foundations of Medium Size.*—Such foundations as supports of large bridges, spread foundations under monuments and public buildings of moderate size, and similar structures belong in this category. It seems adequate to design these foundations under different assumptions, such as uniform pressure distribution and both overloaded and relieved edges. The necessity of further observations on the pressure distribution at the base of full-sized structures of this kind cannot be overemphasized.

## B. PILE FOUNDATIONS

**8:15. Purpose of Pile Driving\***—Piles under structures are driven in the following cases:

- a.* To reach a solid soil layer.
- b.* To support the structure by the friction of the piles against earth.

\* For a detailed description of different types of piles and for pile-driving formulas, see refs. 10, 11, and 30.

c. To consolidate a loose sandy layer.

d. To serve as anchors to the structure (for instance, if a structure is subjected to upward forces, such as hydrostatic uplift).

If considerable scour and consequent failure of a bridge pier may be expected, piles under that pier may contribute to its safety. In any case a pile is nothing more than a *link* between the structure and the soil. The latter carries the full weight of the structure and the super-imposed loads.

Case *a* is illustrated in Fig. 8:9 which represents a *soft upper layer underlain by a solid layer* such as bedrock. Such a solid layer may also be of compact sand extending to a considerable depth, of hardpan, or of other reliable *noncohesive*

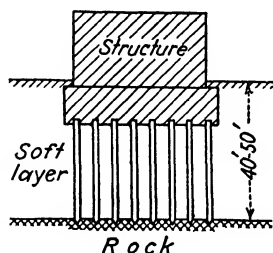


FIG. 8:9.—End-bearing piles.

material. If the thickness of the soft upper layer is less than the maximum permissible length of the piles, the piles are driven through it to transmit the weight of the structure to the lower layer. Piles as shown in Fig. 8:9 behave as columns (“point” or “end-bearing” action) and should be designed as such, entirely regardless of their possible friction against the soil.

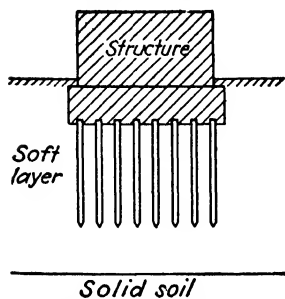


FIG. 8:10.—Floating pile foundation.

Figure 8:10 shows the situation (case *b*) when the upper soft soil layer is *very thick*. Piles driven in this case are “friction piles” (or “floating piles”) and should be designed with regard to the friction of the pile against the soil (Sec. 8:16).

Again, piles may be driven to consolidate *loose sandy deposits* (case *c*). Cohesive soils *cannot* be consolidated in this way, because they are very slightly compressible at the impact; and as a rule, if piles are driven into such a soil, the ground surface between the piles rises. On the contrary, piles, both driven or cast in place, may cause subsidence of a saturated fine sand deposit and decrease its voids. Figure 8:11 shows that piles driven to reach a soft plastic layer cannot be relied upon and must

be extended to become friction piles, whereas they can be made shorter in the case of a compact sand deposit (Fig. 8:11*b*).

There is an idea that pile driving is never harmful and always contributes to the reinforcement of the natural earth material. In reality, the piles *may sometimes be harmful or without value*. For instance, before piles are driven deep into stiff clay, approximate comparative study of the "bearing power" of that clay with and without piles should be made. It may happen that in this case

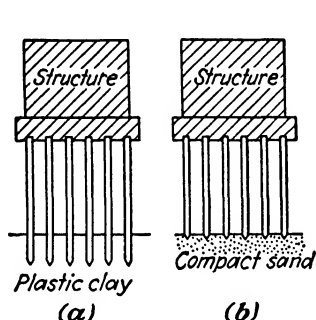


FIG. 8:11.—(a) Friction piles; (b) End-bearing piles.

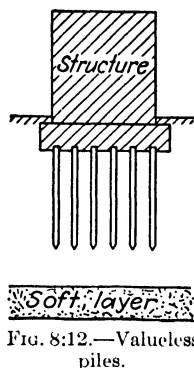


FIG. 8:12.—Valueless piles.

piles would knead the layer, break the natural structure of the clay, and thus weaken the natural resistance of the material. An example of valueless piles is shown in Fig. 8:12. The structure represented in this figure will inevitably settle with the piles because of the presence of a deep soft layer which will consolidate under the weight of the structure.

**8:16. Static and Dynamic Resistance of a Pile.**—A pile under a structure carries a certain load which is rather constant and *static in character*, although in some circumstances this load may fluctuate owing to the live load or vibrations (earthquakes, impact). The soil mass into which the pile has been driven develops a *static resistance*  $R_s$  equal and opposite in direction to the acting load. Owing to the impact of the hammer, a pile that is being driven may be visualized as loaded with a certain load opposed by the *dynamic resistance*  $R_d$  of the soil; as a rule, this dynamic resistance  $R_d$  does not equal the static resistance  $R_s$ . Either of these two resistances consists of two parts: (a) *point resistance*, or a vertical force acting upward at the tip of the pile, and (b) *skin friction*, distributed along the surface of the pile and generally acting

upward also (Fig. 8:13). Experiments in driving a model of a pile into a sand mass with thin horizontal layers of sand of a different color suggest that there is a bearing body (Fig. 8:14) around the pile and that apparently the point resistance acts at that body. The concept of the bearing body is not shared by all investigators, however, and the generally accepted view of the resistance of a pile is that shown in Fig. 8:13.

If a pile is being driven into an *impervious* soil mass, the point resistance under the blow is *considerable*, because water is confined in the pores of the soil mass and cannot be removed suddenly. On the other hand, moisture under a static load is being squeezed out gradually and the point resistance is *smaller* than under a dynamic load.

If a pile is being driven into a *pervious* soil, there is *no considerable difference* between the point resistance under a static and under a dynamic load.

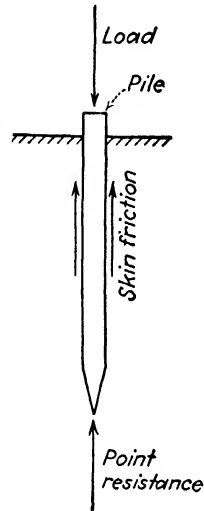


FIG. 8:13.—Skin friction and point resistance of a pile.

**8:17. Skin Friction of a Pile.**—It has been stated in Sec. 8:16 that generally the skin friction at the surface of the pile acts upward. More precisely, the *direction of the skin friction* is that of the *movement of the adjacent soil mass with respect to the pile*. If the pile moves downward under the action of the load, this means that the relative motion of the earth mass is upward and the skin friction develops upward also. This happens, for instance, in incompressible soil (Sec. 8:15). If the earth mass consolidates, the direction of the skin friction is downward (so-called "negative friction"). Thus the point of the pile has to carry not only the static load but also a part of the weight of the soil around the pile, that soil is, so to say, hanging onto the pile.<sup>12,13</sup> As a rule, negative friction is a dangerous factor, since it increases the acting

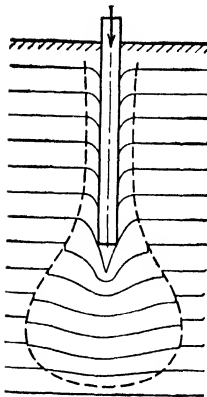


FIG. 8:14.—Bearing body around a pile.

load and may cause an unexpected settlement of the structure.

Negative friction may develop at a part of the pile only, and in some cases it may cause undesirable secondary stresses in the structure. That is true of the concrete pile in Fig. 8:15 if the soft layer shown in that figure consolidates. Figure 8:16a shows a pile under a static load, the frictional resistance being directed upward.

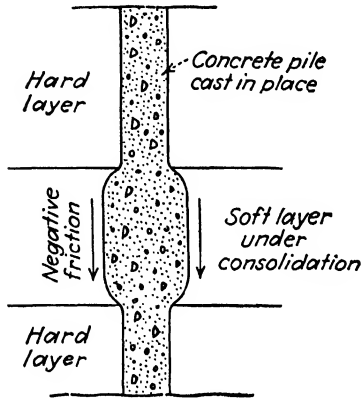


FIG. 8:15.—Negative friction at a part of the pile.

If the pile is pulled out (Fig. 8:16b), the frictional resistance obviously acts downward; the same is true if the adjacent soil mass consolidates (Fig. 8:16c).

The law of distribution of the frictional resistance along the surface of a pile is *unknown*, and in most cases it is assumed that this distribution is uniform. To estimate the total amount of frictional resistance of piles of a given material, diameter, and length driven into a given soil, the force required to extract this pile is measured. It is assumed

in this connection that the force required to extract the pile (dynamic friction) is the maximum value of static friction that may be relied on in the design of the structure.

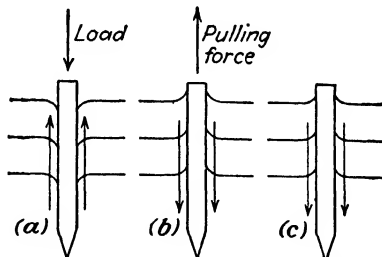


FIG. 8:16.—Frictional resistance, positive and negative.

The total force required to extract a pile, divided by its surface, furnishes the average value of friction expressed in pounds or in tons per square foot. As a rule, this value is applied to piles of the same material but of different diameter and length. Strictly speaking, this practice is justified only if the distribution of

friction along the surface of a pile is really uniform, and such uniformity is, as stated above, uncertain.

Frictional resistance of a pile may be also estimated from a pile-loading test (Sec. 8:20). Data on the frictional pile resistance as published in the technical literature should be considered as partial evidence only, and in using them a good safety factor should be applied. According to some of these data, the average skin friction values are 0.15 to 0.25 ton per sq. ft. for timber piles and 0.3 to 0.6 ton for concrete piles. Metallic piles have friction varying from 0.2 to 0.4 (and somewhat more) ton per sq. ft. of the surface. The lower figures refer to loose sands and sandy clays; the higher ones to rather heavy clays and compact sands. Friction in swampy and silty soils is insignificant.

When a pile is driven into an impervious soil (compare end of Sec. 8:16), skin friction is rather small because of lubrication by moisture that cannot be easily squeezed out. After a *certain period of rest*, sometimes even less than one day, clay that has been disturbed around the pile by shaking apparently has its properties restored and adheres again to the pile. Particularly, soils consisting of disturbed thixotropic clays return to their original state of gels (compare Sec. 1:6). The skin friction of the pile driven into *impervious soil thus increases after rest*. Practical builders are well acquainted with this phenomenon, and it is also well known that if after a period of rest the pile driving is resumed, the pile resistance is high at the first few blows but drops again quickly. There is also an opinion<sup>14</sup> that this increase in resistance is due to the progressive heave of the clay, which may last as long as 30 days, during which period the skin friction gradually increases and thus increases the total pile resistance. For the same reason, the skin friction of a pile driven into a loose sand that consolidates should gradually decrease. Cases were reported when losses in resistance of a pile driven into a saturated pervious soil reached 40 per cent during the subsequent 24 hr.<sup>14</sup>

**8:18. Formulas for Determining the Resistance of a Pile.**— Although building codes prescribe a maximum load to be carried by a pile, designers try to obtain information on the pile resistance by using a number of different formulas.

There are *two principal groups* of such formulas: (a) *static* formulas and (b) *dynamic*, or *pile-driving*, formulas. Static formulas developed from conditions of equilibrium of a pile driven into

soil without disturbing it contain such values as the angle of internal friction  $\phi$ , or unit friction per square foot of the pile. Since such values are rather hard to establish, one cannot expect to obtain reliable results from these formulas. Pile-driving formulas tend to establish the value of resistance of a pile from the dynamic resistance  $R_d$ . As shown in Secs. 8:16 and 8:17, this dynamic resistance is far from being identical with the static resistance. Only in the case of pervious soils, which do not consolidate appreciably during the pile driving, may more or less reliable results be expected from the use of pile-driving formulas.

The so-called "rational pile-driving formula" is developed on the assumption that kinetic energy produced by the fall of the hammer is split into three parts: (a) in the driving of the pile, (b) in the production of some elastic deformations of the pile, and (c) in the production of some plastic (irreversible) deformations. In addition, the energy is partially transformed into vibrations and heat. The value of the dynamic resistance  $R_d$  is expressed through the weight  $W$  of the hammer, its height of fall  $h$ , the weight  $G$  of the pile, the coefficient of restitution  $e$  at the blow, the average penetration  $s$  of the pile at the last 10 blows, and a length  $k$ :

$$R_d = \frac{Wh}{s + k} \frac{W + Ge^2}{W + G} \quad (8:19)$$

Values of  $h$ ,  $s$ , and  $k$  should be expressed in the same units of length. The coefficient of restitution averages 0.2, though in the case of metallic piles it may reach 0.5 and more. For a perfectly elastic blow,  $e = 1$ ; for a perfectly inelastic blow,  $e = 0$ . The pile-driving formula generally used in the United States is the so-called "*Engineering News* formula" proposed by Wellington, the *News's* editor, in about 1888. According to this formula the safe load on the pile (but not the dynamic resistance  $R_d$ ) is found thus:

$$\text{Safe load} = \frac{2Wh}{s + k} \quad (8:20)$$

The value of  $h$  is expressed in feet, and those of  $s$  and  $k$  in inches. The latter value is 1 in. in the case of simple drop and 0.1 in. (or 0.1  $G/W$  in.) in the case of a steam hammer. Formula (8:20) may be obtained from the rational formula (8:19) by assuming arbitrarily a weightless pile ( $G = 0$ ) and a safety factor of 6. In the Hiley formula, which is often mentioned in the literature, the value of  $Wh$  is replaced by  $0.75Wh$  for the usual drop and by

0.9Wh for a single-acting steam hammer. The value of  $k$  is determined in the field by a special method.<sup>15</sup>

**8:19. Discussion of the Pile-driving Formulas.**—Cummings<sup>16</sup> has found that all existing pile-driving formulas are deficient from the theoretical point of view. Particularly, the elastic deformations of a pile under a static load are not the same as under impact, and this difference is not considered in the formulas. The elastic deformation of the soil is not taken into consideration. The losses of energy are computed using Newton's theory of impact (advanced in 1726) notwithstanding Newton's warning that "bodies . . . which suffer some extension as occurs under the strokes of a hammer" should be excluded from this theory..

A special Committee on Pile-driving Formulas of the A. S. C. E. published its report in *Proceedings*, May 1941, after which a thorough discussion followed. The results may be formulated thus: To design a pile foundation, borings should be made, a soil profile (geological section) of the locality prepared to a depth about one and one-half times the width of the structure and studied for the most adequate type of the foundation. The bearing power of a pile should be determined from (a) building codes, (b) pile-loading tests, and (c) experience. The bearing power thus found may be checked against a simple pile-driving formula (such as the *Engineering-News* formula) rather than a complicated one.

It should be added to these conclusions that in some cases simple comparison of the planned structure with safely standing neighboring ones may be of help. Such comparison combined with the use of conservative pile-driving formulas in some cases constitutes the only way to determine the bearing value of piles on small projects where the cost of tests is prohibitive.

A discussion of pile-driving formulas as well as other important data referring to the design and construction of pile foundations may be found in ref.<sup>30</sup>

**8:20. Groups of Piles.**—If a group of piles can be considered as point bearing (Sec. 8:15), they may be spaced as close together as driving conditions permit, usually 2.5 or 3 ft., center to center. However, cast-in-place concrete piles require different construction procedure if the local soil is incompressible clay. As shown already in Sec. 8:15, earth material between such piles may be lifted, thus causing tensile stresses and cracks in adjacent fresh piles. To avoid this, the piles should be either spaced more widely or driven

in alternate rows, the missing row to be completed after sufficient time has elapsed.

Friction piles present a quite different situation. According to Fig. 8:14, the static resistance of such piles is due to soil reactions at the surface of a "bearing body"; and if piles are closely spaced, bearing bodies overlap, and the total static resistance decreases. Apparently, spacing of friction piles 3.5 ft. center to center or somewhat more furnishes the most practical solution.

It follows that, as a rule, the static resistance of a group of friction piles is *less* than the static resistance of a single pile multiplied by the number of piles in that group (cluster).

It is interesting to notice that this simple but very important rule, which on many occasions has been forgotten, was known to American engineers over 40 years ago. In fact, Charles Sooy Smith\* remarked in 1896:

There are many cases where it is certainly a great mistake to take the aggregate bearing capacity of a pile foundation to be the sum of the safe loads on the individual piles composing it.

**8:21. Pile-loading Tests.**—Individual piles or groups of piles may be loaded, and corresponding settlement may be observed. A load that produces a settlement equal to or less than a pre-determined value may be considered as admissible. It is sometimes required that the settlement *after removal of the load* should not exceed 0.01 in. per ton of experimental load, the latter being 150 per cent of the design load. It should be especially emphasized, however, that no categorical conclusions can be drawn from a loading test referring to an individual pile. The larger the group of piles that are tested the closer the results are to the behavior of the pile foundation of which that group of piles will form a part.

Piles may be loaded by means of hydraulic jacks, with auxiliary adjacent piles taking up the pull (Fig 8:17). Anchor piles should be as far as practicable from the tested pile (not closer than 5 or better 10 ft.). The best way to test a group of piles is to apply a dead load by increments of 5 to 10 tons (Fig. 8:18). The full design load and the 150 per cent design load should be allowed to

\* Charles Sooy Smith was the son of General William Sooy Smith (1830–1916), an outstanding foundation engineer of his epoch who, with some others, introduced pneumatic caissons in the United States. In turn, Charles Sooy Smith was a well-known foundation builder. For the quotation given above, see *Trans. A.S.C.E.*, vol. 35, p. 459, 1896.

remain until there is no settlement for a 24-hr. period.<sup>30</sup> For reference purposes two solid bench marks should be established. A loading test may be combined with a pulling test, both tests being made alternately. A pile can be pulled out, for instance, by jacking from two adjacent piles with a suitable cross member

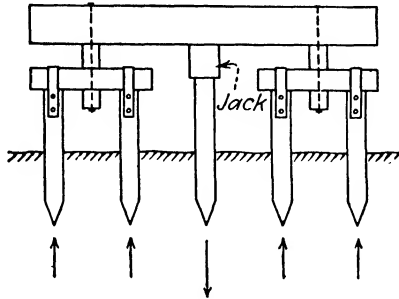


FIG. 8:17.—A pile-loading test (using jack).

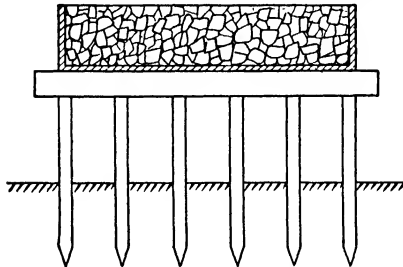


FIG. 8:18.—A pile-loading test (using dead load).

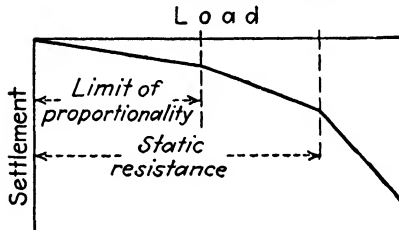


FIG. 8:19.—Diagram of a pile-loading test.

secured to the pile in question. Under no circumstances should loading and pulling tests be made immediately after the piles are driven; they should be made later, for instance, in 30 days. This caution is advisable because of fluctuations in pile resistance, described in Secs. 8:16 and 8:17.

As the acting load increases, the settlement of the loaded pile

also increases. Settlements are *first more or less proportional* to the load but soon begin to increase *more rapidly*, and finally the pile *sinks*. This sinking may be from a fraction of an inch to 3 or 4 ft. To determine the skin friction (compare Sec. 8:17) from a pile-loading test, the point resistance should be neglected or assumed.

**8:22. Pretested Piles.**—Piles of this type were introduced by White.<sup>17</sup> Upon being driven, they are loaded one by one to the full load to be carried in the structure and even more. In this way nonelastic deformations of the soil take place not under the structure but before it is erected. It can be seen that this method will not work if the piles rest on clay, in which consolidation is unavoidable. Pretest piles are mainly used in underpinning, and the load is generally applied by means of hydraulic jacks, the building being used as a counterweight.

According to a general principle advanced in Sec. 6:1, an earth mass may be made elastic by successive loading and unloading. Examination of Fig. 6:1 shows that when a pretested pile is loaded, it settles through the first nonelastic settlement plus the elastic settlement.

Pretesting may be practiced not only with piles but with spread foundations, too, in order to eliminate nonelastic deformations of the soil under the foundation.

**8:23. Stresses in and around a Pile.**—*a. Stresses in the Pile Prior to Loading.*—This subject will be discussed in regard to reinforced concrete piles. Stresses in the pile before loading are due primarily to handling: to both lifting and transportation and to pitching (putting the pile in the driver). In determining stresses, a pile is visualized as a beam, and moments and shears are computed in a general way. Pile manufacturers are interested in this subject, and information along these lines may be found in corresponding catalogues and publications.<sup>18</sup>

Another source of stresses in the pile is the driving itself. At the present time the general approach to the design of a pile is static; the pile is assumed to be compressed by the dynamic resistance  $R_d$  (Sec. 8:16), so that the stress is the same everywhere along the pile. In reality, on impact, waves are set up in the hammer and in the pile. Figures that follow should be considered as crude approximations. The compressive stress due to the blow travels from the head at a velocity of about 12,000 ft. per sec. and is reflected from the foot as a compression or a tension accord-

ing to whether driving is hard or easy. "Hard" driving is that when penetration per blow is small; "easy" driving corresponds to large sets. The stress at any point of the pile is the sum of the stresses due to the down- and up-traveling waves. Under conditions of hard driving, compressive stresses may exceed 3,000 lb. per sq. in.

According to some interesting information from British research workers,<sup>19,20,21</sup> under very easy driving conditions the compressive stress at the toe is very low at first, and the reflected stress wave

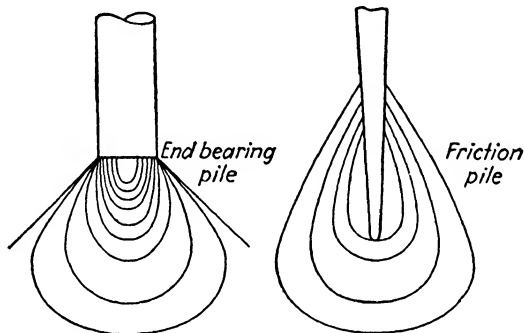


FIG. 8:20.—Approximate shape of isobars under a pile.

is that of tension. Upon combining with the down-coming compression wave, it produces a resultant tensile stress increasing from zero at the toe to a maximum toward the middle of the pile. No failures due to these tensile stresses have been observed, however. The tension at the toe gradually turns to compression as resistance increases and may reach 200 per cent of the head stress. This value is theoretical, but such values as 150 per cent have been recorded.

*b. Stresses around a Pile.*—Figure 8:20 shows how engineers sometimes visualize sets of isobars under an end-bearing pile and under a friction pile. There have also been several attempts to describe mathematically the stress condition in the earth mass around the pile. These attempts were mostly based on the Boussinesq formula applied to the case of a load acting at a point within a semi-infinite body,<sup>22</sup> and such applications involve a crude approximation. In fact, the Boussinesq formula is applicable to surface loading only, a condition that is not satisfied in the case of piles. A solution of the problem of a force acting in the interior

of a semi-infinite solid has been given by Mindlin<sup>23</sup> and should be applied in the case of pile foundations. If a metallic plate is punched through, failure lines (slip lines) approximating logarithmic spirals develop (Fig. 8:21; compare also Fig. 5:8). This means that pressure from the punch is acting radially. This analogy could be applied to piles by considering that pressure from a pile is transmitted to the earth mass horizontally, uniformly in all directions.

Vibrations in the adjacent earth mass caused by pile driving have been studied in restricted numbers by the use of seismometers.<sup>24</sup> The effect of pile driving on adjacent structures is especially harmful if the foundation soil is saturated fine sand.

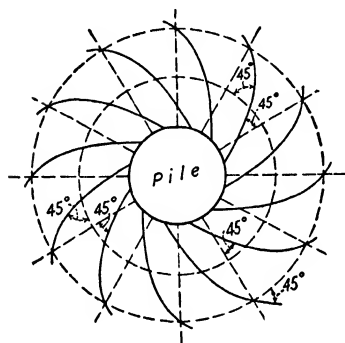


FIG. 8:21.—Probable failure lines around a pile are logarithmic spirals.

*c. Buckling of Piles.*—If a slender pile is driven into a very soft deposit, there may be a danger of failure of the pile by buckling. Cummings<sup>29</sup> assumed the pile to be hinged at both the surface and the bottom of the soft layer and derived a formula for the critical load. The numerical examples in Cummings' paper show that the buckling danger is very remote unless the soil is exceedingly soft.

**8:24. Length of Piles Driven into Deep Deposits.**—The value of the piles driven into a deep deposit depends on the ratio between the length of the pile and the width of the structure; and according to Terzaghi,<sup>25</sup> these two values must be more or less equal. Figure 8:22 shows both a narrow and a wide foundation, each of them either without piles (left side of each sketch) or on 20-ft.-long piles (right side of the sketch). Curves shown in Fig. 8:22 are isobars traced by the Boussinesq formula. These isobars are correct only (a) if the earth approaches the conditions of an elastically isotropic body and (b) if, in addition, the Boussinesq formula may be used in computing stresses under piles; the latter use of this formula is merely an approximation (Sec. 8:23). Suppose, however, that the sketches in Fig. 8:22 reflect reality more or less correctly; it should be first concluded that *in the case of a narrow foundation, short piles are beneficial*, since the pressure is shifted

from the upper, weak layers into deeper, more resistant ones. If the width of a foundation is considerably greater than the length of the piles, longer piles are required to shift an isobar down through a more or less considerable distance, and shorter piles may represent only an unwarranted expenditure.

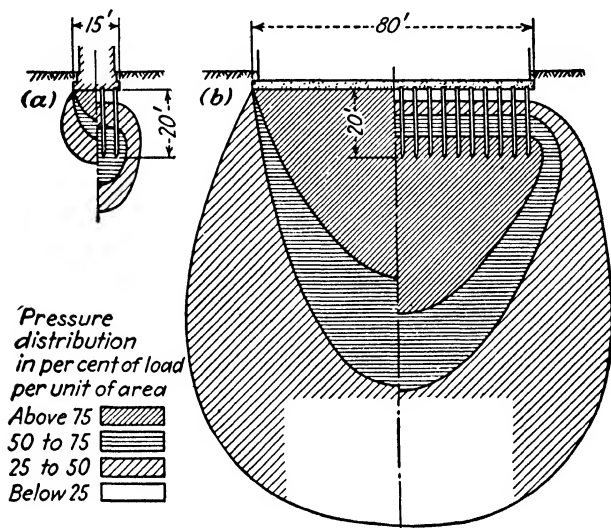


FIG. 8:22.—Piles under (a) a narrow and (b) a wide foundation. (After Terzaghi.)

### C. ECCENTRICALLY LOADED FOUNDATIONS

It will be assumed hereafter that the vertical component of the forces acting on a structure does not pass through the centroid of its foundation. This may happen, for instance, if there are both vertical and horizontal forces acting on the structure.

**8:25. Eccentrically Loaded Spread Foundations.**—*a. Three-dimensional Case.*—The analysis of an eccentrically loaded three-dimensional symmetrical spread foundation will be given here. Let  $a$  be the area of the foundation and  $P$  the total load acting on it. The origin of coordinates will be located at the centroid  $O$  of the cross section of the foundation (Fig. 8:23). The axes of coordinates  $XX$  and  $YY$  are the principal axes of inertia of that cross section. The symbols  $I_x$  and  $I_y$  designate moments of inertia of the cross section with respect to the axes  $YY$  and  $XX$ . The resultant of the acting forces is applied at a point with coordinates  $x_0, y_0$ .

Applying the flexural formulas to the given analysis, the intercepts  $OA'$  and  $OB'$  of the neutral axis would be

$$OA' = -\frac{I_x}{ay_0}; \quad OB' = -\frac{I_y}{ax_0}$$

These simple formulas permit location of the neutral axis  $A'B'$ . Vertical pressure at all points of the neutral axis is zero. All lines parallel to the neutral axis are loci of equal vertical pressures. Particularly, vertical pressures at all points of line  $AB$ , parallel to the neutral axis  $A'B'$  and passing through origin  $O$ , are  $P/a$ .

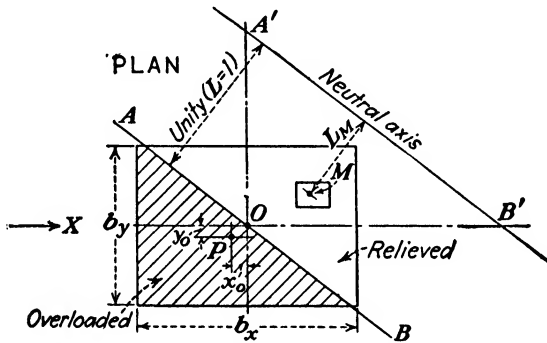


FIG. 8:23.—Analysis of a spread or of a pile foundation (vertical piles only).

Distances to the neutral axis,  $L$  from the origin  $O$  and  $L_M$  from points  $M$  where vertical pressure is to be determined, are measured graphically. Vertical pressure  $\sigma_z$  at point  $M$  is proportional to the ratio  $L_M/L$ :

$$\text{Pressure at point } M = \frac{P}{a} \frac{L_M}{L} \quad (8:21)$$

If the foundation is rectangular, as in Fig. 8:23,

$$OA' = -\frac{b_y^2}{12y_0}; \quad OB' = -\frac{b_x^2}{12x_0}$$

*b. Two-dimensional Case.*—If we look at the foundation from the side as shown with an arrow in Fig. 8:23, left, a two-dimensional case may be conceived if the given foundation is sufficiently long in the direction of the axis  $XX$ . The flexural formulas being applied again, it may be seen that if the resultant of the acting

forces is within the middle third of the base (Fig. 8:24a) the edge pressures are

$$\text{Pressure at the edge} = \frac{P}{a} \left( 1 \pm \frac{6y_0}{b_y} \right) \quad (8:22)$$

If the resultant is applied outside the middle third of the base, distance  $m = (b_y/2) - y_0$  from the resultant to the edge of the

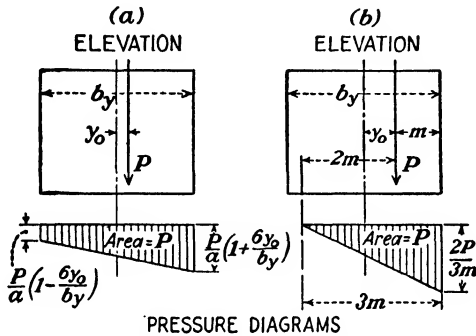


FIG. 8:24.—Eccentrically loaded foundations (two-dimensional case).

foundation is computed, and it is assumed that the vertical load is uniformly distributed over an area  $3m$  long (Fig. 8:24b). The method shown in Fig. 8:24 is that often used in the offices.

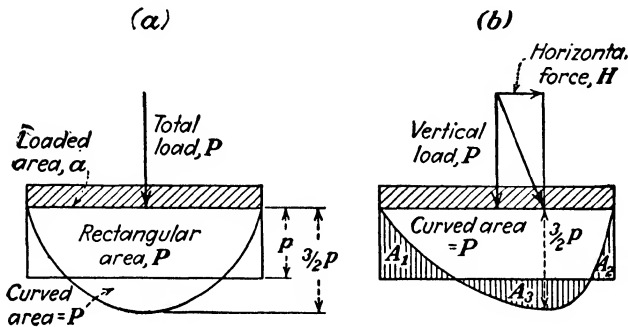


FIG. 8:25.—Distribution of vertical pressure under an eccentrically loaded foundation (a suggestion).

A suggestion as to the shape of the diagram of vertical pressures under an eccentrically loaded sand foundation is given in Fig. 8:25. If there is no horizontal force acting on the foundation (Fig. 8:25a), the pressure diagram should be a curve similar to that revealed by loading experiments (Fig. 4:16). Its largest ordinate may be

assumed to be equal to  $\frac{2}{3}$  of the average pressure on the foundation, or  $(\frac{2}{3})(P/a) = (\frac{2}{3})p$ . The action of the horizontal force consists in distorting the shape of the pressure diagram without changing its area, which still equals the total load  $P$  acting on the foundation. The maximum ordinate of the pressure diagram is shifted to the point of application of the resultant, and a skew parabola is traced freehand to satisfy the condition

$$\text{Area } A_1 + \text{area } A_2 = \text{area } A_3$$

In the case of a clay foundation, the pressure diagram (Fig. 4:21) should be somewhat distorted by the horizontal force, so that one edge is overloaded and the other edge of the foundation is relieved.

If the foundation is wide, eccentricity has but slight influence on the pressure diagram.

**8:26. Eccentrically Loaded Pile Foundations.**—*a. Foundations with Vertical Piles Only.*—When there are vertical piles only in the foundation, methods advanced in Figs. 8:23 and 8:24 may work. Areas corresponding to individual piles ( $M$  in Fig. 8:23) are determined, and unit pressures at the centroid of that area are computed by formula (8:21). If the neutral axis  $A'B'$  intersects the foundation, there may be tensions instead of pressures on the piles. In the case of a two-dimensional foundation, the total trapezoidal area shown in Fig. 8:24a is subdivided into smaller trapezoids, each of them equaling the bearing value of a pile. Thus the location of the piles in the plan may be found.

*b. Foundations with Both Vertical and Battered Piles.*—There are several methods for the analysis of pile foundations with both vertical and battered piles. An extensive bibliography may be found in the references.<sup>26,27</sup> A very simple and efficient method has been proposed by Westergaard.<sup>11,28</sup> Vetter's method<sup>27</sup> is similar to Westergaard's. These and similar methods of analysis however, *cannot give conclusive results* to the designer, because the assumptions adopted in establishing these methods do not correspond exactly to those in actual practice. However, their use for comparison or checking purposes should be encouraged.

#### Problems

1. A long bridge pier is 20 ft. wide and carries a load of 240,000 lb. per lin. ft. of length. The bottom of the base is 20 ft. below the ground surface ( $z = 20$  ft). The angle of friction  $\phi$  of the soil is  $14^\circ 30'$ ; the unit cohesion,  $c = 1,000$  lb. per sq. ft.; unit weight, 100 lb. per cu. ft. Is this pier stable or not? If it is, estimate the safety factor.

2. What is the value of the unit pressure at the overloaded edge of the foundation (Fig. 8:24a) corresponding to the case when the pressure diagram becomes a triangle?

3. What is the most rational way to produce mechanical energy  $Wh$  [see formula (8:19)]: by heavy hammers and small drops or light hammers and high drops?

*Suggestion:* By heavy hammers. Consult Cummings' paper.<sup>16</sup>

4. The bottom of a river is made of fine sand layer, 12 ft. thick, underlain by a compact gravel slab 20 ft. thick. Medium sand (17 ft.) and rock follow. Would you found a highway bridge pier on that gravel, or would you go to rock by using metallic piles to break through the gravel?

*Suggestion:* It is necessary to make additional borings to see whether or not the gravel slab is wide and thick enough around the pier. A possibility of shifting the axis of the bridge may be considered also

#### References

1. KARL TERZAGHI: The Failure of Bridge Piers Due to Scour, *Proc. Intern. Conf. Soil Mech.*, vol. 2, Paper N-6, 1936.
2. WILLIAM S. HOUSEL: A Practical Method for the Selection of Foundations, *Univ. Mich. Eng. Research Bull.*, October, 1929; also *Eng. News-Record*, vol. 110, 1933.
3. L. PRANDTL: Ueber die Härte plastischer Körper, *Nachr. Ges. Wiss. Göttingen, Phys.-math. Klasse*, 1920.
4. L. PRANDTL: Spannungsverteilung in plastischen Körpern, *Proc. First Intern. Congr. Applied Mech.*, 1924; also articles in *Z. angew. Math. Mech.*, vol. 1, 1921; vol. 3, 1923.
5. ALBERT CAQUOT: "Equilibre des massifs à frottement interne," Gauthier-Villars & Cie, Paris, 1934.
6. KREY-EHRENBURG: "Erddruck, Erdwiderstand und Tragfähigkeit des Baugrundes," 3d ed., Wilhelm Ernst und Sohn, Berlin, 1932.
7. KARL TERZAGHI: "Erdbaumechanik auf bodenphysikalischer Grundlage," Franz Deuticke, Vienna and Leipzig, 1925.
8. KARL TERZAGHI: "Theoretical Soil Mechanics," John Wiley & Sons, Inc., New York, 1945.
9. A. CASAGRANDE and R. E. FADUM: Application of Soil Mechanics in Designing Building Foundations, *Trans. A.S.C.E.*, vol. 109, 1944.
10. ROBERT D. CHELLIS: "Pile-driving Handbook," Pitman Publishing Corporation, New York, 1944.
11. A. C. DEAN: "Piles and Pile Driving," C. Lockwood and Sons, London, 1935.
12. TERZAGHI and FRÖHLICH: "Theorie der Setzungen von Tonschichten." Franz Deuticke, Leipzig and Vienna, 1936.
13. C. FRAUX: *Proc. Intern. Conf. Soil Mech.*, vol. 1, Paper H-3, 1936.
14. R. W. MILLER: Soil Reactions in Relation to Foundation on Piles, *Trans. A.S.C.E.*, vol. 103, 1938.
15. A. HILEY: A Rational Pile Driving Formula, *Engineering*, vol. 119, 1925.
16. A. E. CUMMINGS: Dynamic Pile-driving Formulas, *Jour. Boston Soc. Civil Eng.*, vol. 27, 1940.

17. EDMUND ASTLEY PRENTIS and LAZARUS WHITE: "Underpinning," Columbia University Press, New York, 1931.
18. "Concrete Piles," a pamphlet published by the Portland Cement Association.
19. E. N. FOX: Stress Phenomena Occurring in Pile Driving, *Engineering*, vol. 134, 1932; also vol. 137, 1934.
20. W. H. GLANVILLE, G. GRIME, and W. W. DAVIES: The Behaviour of Reinforced Concrete Piles during Driving, *Jour. Inst. Civil Eng.* (London), no. 2, 1935; also *Intern. Assoc. Bridge and Structural Eng., Second Congr.*, 1936.
21. Joint Subcommittee on Pile Driving: Notes and Practical Suggestions on Pile Driving, *Jour. Inst. Civil Eng. (London)*, April, 1936.
22. F. E. RELTON: The Stress Distribution around a Pile, *Proc. Intern. Conf. Soil Mech.*, vol. 1, *Paper E-2*, 1936.
23. RAYMOND D. MINDLIN: Force at a Point in the Interior of a Semi-infinite Solid, *Physics*, vol. 7, 1936; also *Proc. Intern. Conf. Soil Mech.*, vol. 3, *Paper E-13*, 1936.
24. L. BENDELL: Bestimmung der Grösse und Art der Erschütterungen beim Rammen von Pfählen, *Schweiz. Bauzeitung*, vol. 105, 1935.
25. CHARLES TERZAGHI: The Science of Foundations, Its Present and Future, *Trans. A.S.C.E.*, vol. 93, 1929.
26. A. AGATZ: "Der Kampf des Ingenieurs gegen Erde und Wasser im Grundbau," Verlag Julius Springer, Berlin, 1936.
27. C. P. VETTER: Design of Pile Foundations, *Trans. A.S.C.E.*, vol. 104, 1939.
28. H. M. WESTERGAARD: The Resistance of a Group of Piles, *Eng. and Contr.*, vol. 49, 1918; also *Jour. Western Soc. Eng.*, vol. 22, 1917.
29. A. E. CUMMINGS: The Stability of Foundation Piles against Buckling under Axial Load, *Proc. Highway Research Board*, vol. 18, part 2, 1938.
30. Pile Foundations and Pile Structures, *A.S.C.E., Manuals of Engineering Practice*, No. 27, New York, 1946.

## CHAPTER IX

### STABILITY OF CUTS AND EMBANKMENTS

#### A. STABILITY OF SLOPES

Artificial slopes only, *i.e.*, those constructed by the engineer in cuts and embankments, will be considered in this chapter. Inadequate slope in any material may fail; hence it is necessary to correlate physical properties of a given earth material and the steepness of the slope to be constructed. Stability of natural slopes is also of great importance for the engineer. Since corresponding phenomena are discussed in textbooks on geology, they will be only mentioned here.

**9:1. Landslides and Related Phenomena.**—A very detailed classification of landslides and related types of mass movement was presented in 1925 by Terzaghi (Chap. IV, ref. 1) who divided these movements into (a) dry movements with static friction fully effective and (b) mush movements with static friction wholly or partly eliminated. A further very comprehensive subdivision has also been given.

In a work by Sharpe<sup>1</sup> earth mass movements have been divided into four groups: (a) slow flowage, (b) rapid flowing, (c) sliding, and (d) subsidence or sinking of ground over mines and caves. *Slow flowage* is characteristic in a slow downslope movement of superficial soil or rock debris (only a few feet deep). Slow flowage from higher to lower ground of masses of waste saturated with water is sometimes termed *solifluction*.\* Rapid flowing is chiefly due to oversaturation of earth or mud masses, accompanied or not accompanied by a sliding motion. Such are earthflows and mudflows. Finally, a *landslide* is the perceptible downward sliding or falling of a relatively dry mass of earth, rock, or a mixture of both. Figure 9:1 represents different types of landslides.

Ladd<sup>2</sup> subdivides all natural slope failures into two groups only: (a) *landslides* and (b) *subsidences*. In terms of the sketch (Fig.

\* From Latin *solum*, "soil," and *fluere*, "to flow."

7:2), landslides occur when the lateral support is removed or weakened, whereas subsidences correspond to the decrease in

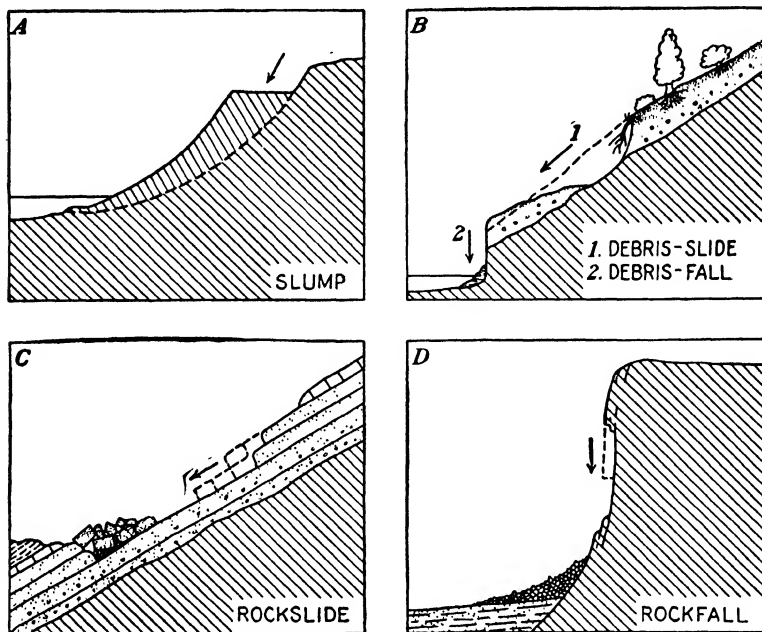


FIG. 9:1.—Types of landslides. (After Sharpe.)

vertical reaction. According to Ladd, accidental *rockfalls* should be considered separately.

**9:2. Slope Rule in Noncohesive Soils.**—In the design of a safe slope in a cohesionless soil mass (for instance, in a sandy mass), the angle made by the slope with the horizon should be smaller than the angle of repose  $\phi'$  (Fig. 9:2):

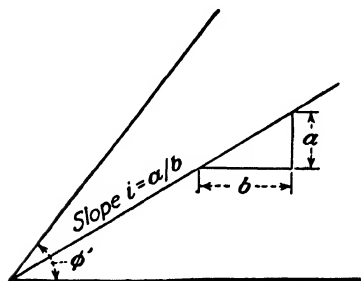


FIG. 9:2.—Slope rule for non-cohesive soils.

$$i < \tan \phi' \quad (9:1)$$

A slope of a noncohesive soil may be of *indefinite height*, provided it satisfies Eq. (9:1), whereas in the case of *cohesive soils* the *height* of a slope is *limited* according to the physical properties of the given earth material.

**9:3. Types of Slope Failures in Cohesive Soils.**—Figure 9:3*a* shows a type of failure that often takes place in trenches, such as those excavated for water supply or sewers. Down to a certain elevation the vertical slope is safe; but when a critical depth is reached, slides start. As a rule, such slides are not general but only local and intermittent, a fact that is explained by the non-uniformity of the shearing value through the material. Figure 9:3*b* shows a partial sliding of the slope. Such small slides may

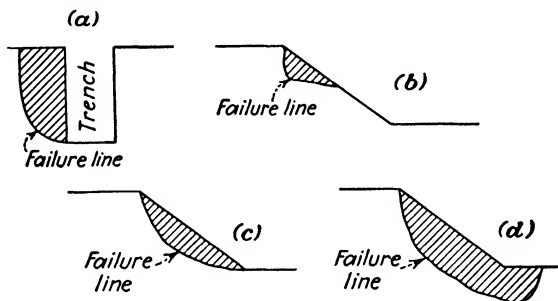


FIG. 9:3.—Types of slope failures in cohesive soils.

often be found early in the spring on the slopes of highway or railroad cuts and may be explained by the oversaturation of the material. This may occur if the soil is silty and the ground-water table is shallow (compare Sec. 3:21). Figure 9:3*c* and *d* show slides of the entire slope. Noteworthy is case *d*, termed “base failure” or “Swedish break,” since failures of this kind were first described by Swedish engineers.

**9:4. Conventional Manner of Slope Design.**—In the designing of a slope a wedge about to separate from the slope is considered. It is assumed to be in the state of limit equilibrium. The shape of the probable failure line that bounds the wedge is *assumed*. To simplify computations, the Swedish engineer Petterson proposed to consider the failure line as *an arc of circle*—a proposal that, as a rule, is in sufficient agreement with experience. There are also attempts to represent the failure lines as a logarithmic spiral or a cycloid.<sup>3</sup> Since the arc of the circle is the only shape of failure line used by American engineers in slope design, the discussion that follows will be based on this assumption unless otherwise specified.

Furthermore, the *average* shearing stress  $\tau$  acting along the failure line is found and compared with the *average* value of the shearing resistance  $s$  along the failure line. Progressive failure is

not considered, and it is assumed that the failure occurs at once along the whole failure line; this is *not correct*, as already indicated in Chap. V.

In the discussion that follows, slope design will be considered as a two-dimensional (plane) problem.

**9:5. Swedish Method of Checking Stability of a Slope.**—Pettersson's assumption (Sec. 9:4) referring to the shape of the failure line is equivalent to the assumption that the wedge  $ABCD$ , located above the circular failure line  $ABC$ , in sliding down rotates about the center  $O$  of that arc (Fig. 9:4).

The *three steps* to be taken to check the stability of a slope according to the Swedish method follow:

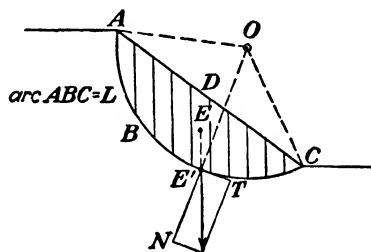


FIG. 9:4.—Swedish method of analyzing stability of slopes.

a. The approximate position of the center of rotation for the failure line is assumed; it will be explained hereafter how this is done.

b. The sliding wedge  $ABCD$  is divided by vertical lines into a number of segments, perhaps 10 or 12.

c. The weight of each segment is determined and is assumed to act at the projection  $E'$  of the center of gravity  $E$  of the segment on the failure line, where this weight is broken into a normal force  $N$ , passing through the center of rotation, and a tangential force  $T$ , acting in a direction normal to  $N$ . In computing the weight of the wedge  $ABCD$ , the latter is assumed to be "one unit" wide as measured normally to the plane of the drawing.

The force tending to produce the displacement of the given segment (or shearing force) at point  $E'$  is  $T$ . The resisting force is due partly to friction and partly to cohesion. The former part equals  $N \tan \phi$ , where  $\phi$  is the angle of friction, and the latter equals the unit cohesion resistance  $c$  as obtained in a shearing test multiplied by the area of contact of the given element with the failure line. Summing all the displacing or shearing forces for all elements of the sliding wedge, the total would be  $\Sigma T$ ; and summing the resisting forces, the total would be  $\tan \phi \Sigma N + cL$ ,

where  $L$  is the total length of the failure line ( $ABC$  in Fig. 9:4). Hence the "true" safety factor:

$$\text{Safety factor} = \frac{\tan \phi \Sigma N + cL}{\Sigma T} \tag{9:2}$$

The same result may be obtained by equalizing the moments of the displacing and the resisting forces about the center of rotation.

As already explained in Sec. 9:4, the Swedish method considers the *average shearing stress* along a predetermined trajectory, and this shearing stress is compared to the *average shearing resistance* along the same trajectory. Since the Swedish method is only a design conventionality, the safety factor computed by formula (9:2) cannot be considered as something absolute. It has been reported, for instance, that in the construction of levees in the lower Mississippi Valley, slopes with a safety factor between 0.75 and 1.00 were sometimes stable.<sup>4</sup> Similar inconsistencies may be explained in some cases by the inaccuracy in estimating the value of the safety factor as specified hereafter.

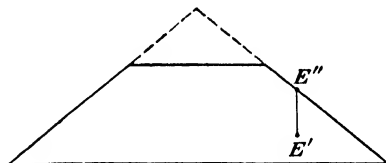


FIG. 9:5.—Vertical pressure at a point as assumed in the Swedish method.

Another objection to the Swedish method (termed also the "slice method") is the assumption that interaction between slices may be neglected. Thus point  $E'$  within the earth mass (Fig. 9:5) is assumed to be loaded by the weight of the earth material above it (ordinate  $E'E''$ ). This point would carry exactly the same amount of load if additional earth were placed on top of the given mass, as shown in dotted lines in Fig. 9:5, and this is obviously illogical.

Instead of subdividing the sliding wedge into a number of slices of finite width, the following construction may be applied: Ordinate  $E'E''$  in Fig. 9:6a is proportional to the weight of an infinitely thin slice supported by the failure line at point  $E'$ . Hence, when we drop the perpendicular  $E''F$  from point  $E''$  on the radius  $OE'$ , the distances  $E''F$  and  $E'F$  will be proportional to the components  $T$  and  $N$ , respectively, of the weight of that infinitely thin slice. Plotting distances  $E''F$  and  $E'F$  vertically from point  $E'$ , and repeating this construction for several points

$E'$  of the failure line, we obtain two areas proportional to  $\Sigma T$  and  $\Sigma N$ , respectively. An area proportional to  $\Sigma T$  is shown in Fig. 9:6b with vertical dashing, whereas horizontal dashing represents an area proportional to  $\Sigma N$ . Values of  $\Sigma T$  and  $\Sigma N$  to be introduced into formula (9:2) may be obtained by multiplying areas shown in Fig. 9:6b by the unit weight of the given earth material.

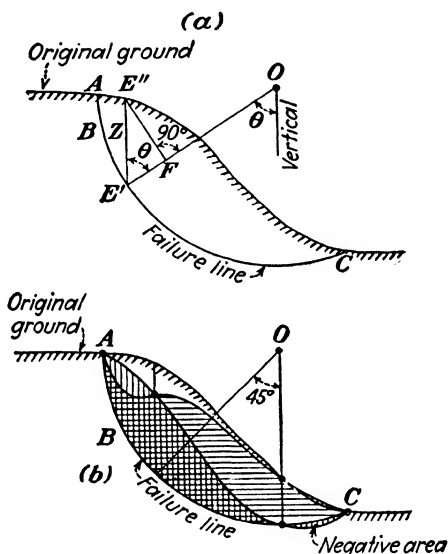


FIG. 9.6.—Graphs of shearing and resisting forces in the Swedish method.

The areas in question may be measured with a planimeter or as in Sec. 6:17. The construction shown in Fig. 9:6 may be very useful if the given slope is not a straight line but is of a rather irregular shape.

*Safety Factor.*—The generally accepted method of computing the safety factor against sliding is as in formula (9:2). The inaccuracy of this method has been shown by Burmister.<sup>37</sup> In fact the “negative area” in Fig. 9:6b is proportional to that part of the tangential force  $\Sigma T$  acting in favor of stability, *i.e.*, against sliding. This part should be subtracted from the denominator and added to the numerator of the fraction in Eq. (9:2), which would furnish a larger value of safety factor.

*Center of Rotation.*—To locate approximately the center of rotation, angles  $\alpha$  and  $\beta$ , taken from the following table, are con-

structed at the top and at the bottom of the slope, respectively. The intersection of the corresponding lines determines point  $O$ , the center of rotation (Fig. 9:7).

Slope	Angle made with the horizon, $A$	$\alpha$	$\beta$
1:0.58	60°	40°	29°
1:1	45°	37°	28°
1:1½	33°47'	35°	26°
1:2	26°34'	35°	25°
1:3	18°26'	35°	25°
1:5	11°19'	37°	25°

This approximate method has been proposed by Fellenius.<sup>5</sup> The procedure described in this section is repeated for other centers of rotation, located more or less arbitrarily, until the center of rotation and radius of curvature give a minimum value of the safety factor. The corresponding arc may then be accepted as the *critical* one along which failure is most likely to occur.

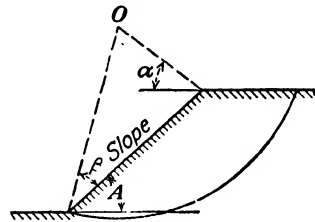


FIG. 9:7.—Center of rotation. (After Fellenius.)

**9:6.  $\phi$ -Circle Method: General Discussion.**—The  $\phi$ -circle method is based on the assumption that the resultant reaction of

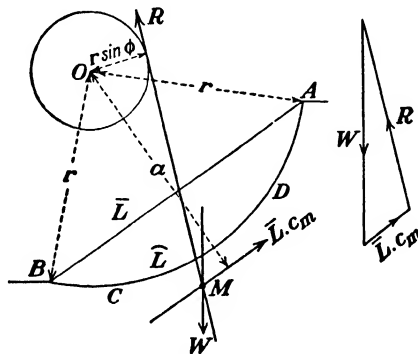


FIG. 9:8.— $\phi$ -circle method.

the circular failure line touches a circle of a radius  $r \sin \phi$  having the center of rotation  $O$  of the failure line (Fig. 9:8) for its center.

In the expression  $r \sin \phi$ , the symbol  $r$  corresponds to the radius of curvature of the circular failure line, and  $\phi$  is the value of the angle of friction. This assumption was used when the Krey method was described (Sec. 8:9). The  $\phi$ -circle method, widely used by Fellenius,<sup>5</sup> has been simplified and thoroughly studied by Taylor<sup>6</sup> in the United States. The discussion that follows is based principally on Taylor's work.

It will be assumed that unit cohesion  $c_m$  required to keep the sliding wedge in equilibrium is constant along the failure line  $AB$  (Fig. 9:8). In a general way, if a shearing stress  $c_m$  is constant along a sliding arc  $AB = \hat{L}$ , its resultant equals  $\bar{L}c_m$  where  $\bar{L}$  is the length of the chord  $AB$  and is parallel to that chord. This statement may be proved easily by constructing a plan of forces and the corresponding string polygon. The arm  $a$  of the resultant  $\bar{L}c_m$  may be determined by taking the moment of all forces acting along the arc  $AB = \hat{L}$  about the center of rotation  $O$  and equalizing the result to the moment of the resultant  $\bar{L}c_m$  about the same point:

$$\hat{L}c_m r = \bar{L}c_m a$$

from which

$$a = r \frac{\hat{L}}{\bar{L}} \quad (9:3)$$

In other words, the value of the arm  $a$  of the resultant does not depend on the value of the stress  $c_m$ , provided the latter is constant along the failure line. It follows that by Eq. (9:3), the location of the resultant of the cohesive resistance  $\bar{L}c_m$  may be easily found, whether the unit cohesion  $c_m$  is known or unknown.

The wedge  $ABCD$  shown in Fig. 9:8 is in equilibrium under the action of the following forces:

- a. Its weight  $W$ .
- b. Cohesional resistance  $\bar{L}c_m$  acting parallel to the chord  $AB$ , as stated.
- c. Frictional resistance  $R$ , or reaction of the circular failure line, tangent to the  $\phi$ -circle which has a radius  $r \sin \phi$ .

From the condition of equilibrium of these three forces, the total value of the cohesive resistance  $\bar{L}c_m$  required to keep the wedge  $ABCD$  in equilibrium may be found. The corresponding unit cohesion  $c_m$  would be obtained simply by dividing the total value  $\bar{L}c_m$  by  $\bar{L}$ , the length of the chord  $AB$ . If the value of  $c_m$

thus found in less than the maximum cohesion  $c$  which may be developed by the given soil in shearing test, there will be no sliding; otherwise the wedge  $ABCD$  will slide down. The meaning of the index  $m$  in the expression  $c_m$  is "mobilized."

To find the value of the weight  $W$ , area  $ABCD$  (Fig. 9:8) is to be measured and multiplied by the unit weight of the given material. It must be born in mind that the problem is being solved as a two-dimensional one, the dimension normal to the

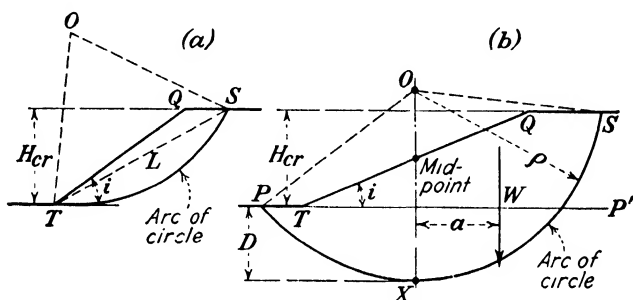


FIG. 9:9.—Critical height of a slope (compare FIG. 9:3 c and d).

plane of the drawing (Fig. 9:8) being one unit. Furthermore, the centroid of area  $ABCD$  is to be located, and a vertical line through it is drawn to intersect the line of action of the resultant cohesion at point  $M$ . This resultant, as stated, is parallel to the chord  $AB$ , and its distance from the center of rotation  $O$  equals  $a$  [Eq. (9:3)]. The reaction  $R$  passes through point  $M$  and is tangent to the  $\phi$ -circle. The values of the cohesion resistance  $\bar{L}c_m$  and the frictional resistance  $R$  may be read on the plan of forces (Fig. 9:8, right).

Results in both methods described (Swedish method and  $\phi$ -circle method) are practically the same.

**9:7. Critical Height of a Slope.**—In Fig. 9:9 two cases of slope failure are shown, the problem being to determine the maximum possible height (critical height)  $H_{cr}$  of a slope that makes an angle  $i$  with the horizon if the angle of internal friction  $\phi$ , the unit cohesion  $c$ , and the unit weight  $\gamma$  of the earth material are given. First, the case of Fig. 9:9a will be studied, when the failure line passes through the toe  $T$  of the slope ("toe circle").

The unit cohesion  $c$  and gravity as expressed by the unit weight  $\gamma$  are body forces uniformly distributed throughout the earth mass. At each point of the slope, cohesion  $c$  prevents failure,

whereas the weight  $\gamma$  tends to produce it. Hence it may be stated *a priori* that the critical height  $H_{cr}$  should be proportional to the unit cohesion  $c$  and inversely proportional to the unit weight  $\gamma$ . At the same time the critical height depends on the

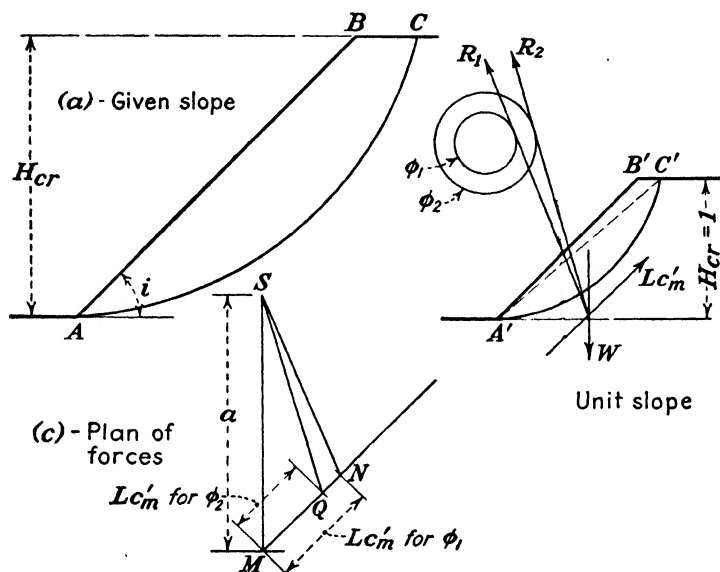


FIG. 9:10.—Determination of the stability number.

angle of internal friction  $\phi$  and on the angle of slope  $i$ . Expressing these statements mathematically

$$H_{cr} = \frac{c}{\gamma} f(\phi, i) \quad (9:4)$$

where  $f(\phi, i)$  is a function of both  $\phi$  and  $i$ . Since the dimension of the ratio  $c/\gamma$  is length (feet), function  $f(\phi, i)$  defines a dimensionless quantity (abstract number), which in Taylor's nomenclature is a reciprocal of a certain "stability number" (SN). Thus

$$H_{cr} = \frac{c}{\gamma} \frac{1}{SN} \quad (9:5)$$

Terzaghi's term "stability factor" (ref. 8, Chap. VIII) refers to the function  $f(\phi, i)$  itself as in Eq. (9:4), and not to its reciprocal. Hereafter Taylor's nomenclature will be maintained.

Figure 9:10 represents a "given slope"  $AB$  and a geometrically similar "unit slope"  $A'B'$ , the critical heights of these slopes being  $H_{cr}$  and 1 ft., respectively. In addition the material of the unit slope is assumed to weigh 1 ton per cu. ft. To hold the given slope  $AB$  in the state of limit (plastic) equilibrium it is required to mobilize along arc  $AC$  (Fig. 9:10a) a unit cohesion  $c$ ; and in order that the unit slope  $A'B'$  be in the state of limit (plastic)

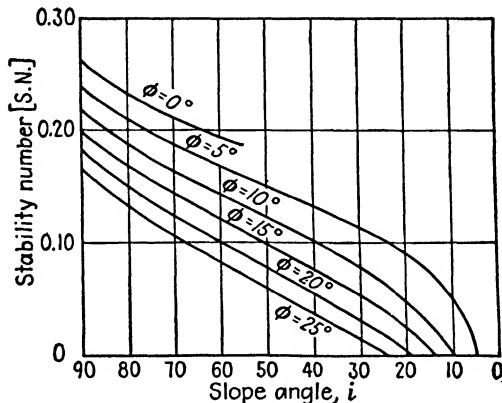


FIG. 9:11.—Values of the stability number. (After Taylor.)

equilibrium, some other unit cohesion  $c'_m$  must be mobilized along arc  $A'C'$  (Fig. 9:10b). Consider the latter case and introduce the values of  $H_{cr} = 1$  and  $\gamma = 1$  into Eq. (9:5). Then

$$1 = \frac{c'_m}{1} \frac{1}{SN} \quad (9:6)$$

or

$$SN = c'_m \quad (9:7)$$

The numerically equal values of  $SN$  and  $c'_m$  [Eqs. (9:6) and (9:7)] do not depend on what measures of length and weight are used in their determination.

As seen from Fig. 9:10b and  $c$  the value of  $c'_m$  (and hence  $SN$ ) may be determined applying the  $\phi$  circle to the case of the unit slope for all possible combinations of  $\phi$  and  $i$ . Figure 9:10c shows that the larger the angle of internal friction  $\phi$  and the smaller the slope angle  $i$  the smaller is the stability number  $SN$ . To determine the value of the stability number Taylor<sup>6</sup> used the  $\phi$ -circle method combined with an analytical procedure. His chart (Fig. 9:11) is valid for all cases of the toe-circle failure except  $\phi = 0$  and  $i < 53^\circ$  (see Sec. 9:12).

**9:8. Safety Factor in the Case of a Toe Circle.**—The height  $H$  of a slope to be built equals the critical height divided by some safety factor  $F$ :

$$H = \frac{H_{cr}}{F} = \frac{1}{F} \frac{c}{\gamma} \frac{1}{SN} \quad (9:8)$$

In other words in building a slope  $H$  ft. high, only a part of the cohesion available  $c_m$  is mobilized:

$$c_m = \frac{c}{F} \text{ or } F = \frac{c}{c_m} \quad (9:9)$$

The value of  $F$  as determined by Eq. (9:9) is the factor of safety "with respect to cohesion," a term introduced into American technical literature by Taylor. It is implicitly assumed in writing Eq. (9:8) that advantage is taken fully of the friction and only partly of the cohesion. In reality, both friction and cohesion do not contribute to the building up of the shearing resistance to their fullest extent, except in the state of plastic (limit) equilibrium.

According to the Coulomb formula (Sec. 5:6) the shearing resistance at a point of failure line is

$$s = \sigma \tan \phi + c \quad (9:10)$$

and if the shearing stress is  $\tau$ , the true factor of safety at that point is

$$F_t = \frac{s}{\tau} \quad (9:11)$$

which, taken as an average for the whole failure line, may furnish a value different from that determined by Eq. (9:9).

**9:9. Example.**—Find the maximum possible height of an unsupported vertical bank (as in a trench) in a purely cohesive material ( $\phi = 0$ ).

*Solution.*—Use formula (9:5) and the chart of Fig. 9:11 for  $i = 90^\circ$  and  $\phi = 0$ . The stability number is 0.25, and

$$H_{cr} = 4 \frac{c}{\gamma} \quad (9:12)$$

In a particular case a safety factor is to be used.

**9:10. Base Failure (Swedish Break).**—For this case shown in Fig. 9:9b the following two limitations will be used:

a. Fellenius<sup>5</sup> has shown that the vertical line drawn through the midpoint of the slope either passes through the center of the circular failure line (arc of failure) if  $\phi = 0$  or touches the circle

of friction if  $\phi > 0$ . According to the limitation  $b$  that follows, the latter case will not be considered at all.

*b.* Since base failures occur mostly in soils with small values of the angle of internal friction  $\phi$ ,\* it will be assumed hereafter that the earth material in which the given base failure occurs possesses no friction ( $\phi = 0$ ).

In the case of a base failure in homogeneous material, the moment of rotation about the center  $O$  of that part of the wedge below the horizontal plane  $PP'$  equals zero. The reaction of the support (arc  $PXS$ ) analogous to the reaction  $R$  in Fig. 9:8 passes through the center  $O$ ; hence its moment about that point is also zero. Thus the overturning moment to be considered is caused by the weight of that part of the wedge above plane  $PP'$ , the resisting moment being due to cohesion along arc  $PXS$ . Designate the length of arc  $PXS$  with  $\hat{L}$  and its radius with  $\rho$ . Then the condition of equilibrium of the wedge is

$$Wa = \hat{L}c\rho \tag{9:13}$$

In a general case the material of the wedge is not homogeneous, and there may be structures or other additional loads within the sliding range. The wedge should be then subdivided into layers with different values of cohesion  $c_1, c_2, c_3, \dots$ ; and in computing moments the weight of additional loads, if any, should be considered.

Very often at a certain depth  $D$  (Fig. 9:9*b*) there is a rigid boundary such as hardpan or rock. Then it may be expected that the failure line would touch that rigid boundary.

**9:11. Examples.** *a. Retaining Wall on Pile Foundation.*—Figure 9:12*a* represents a quay wall on a pile foundation. The total weight of the wedge including the wall is  $W$ , its arm about the point of rotation  $O$  being  $a$ . The weight of water above the prospective failure line is  $W_w$ , and its arm about point  $O$  is  $b$ . The moment of the cohesive resistance may be computed by measuring the length of the arc  $PS = \hat{L}$  with a small opening of a pair of dividers. The cohesive resistance along the arc is  $\hat{L}c$ , and its arm about point  $O$  is the radius of the failure line  $\rho$ . The condition of limit equilibrium is

$$Wa = W_wb + \hat{L}c\rho \tag{9:14}$$

The center of the failure line is located on the vertical line passing through the midpoint of slope  $PQ$ , and the failure line should clear the tips of the piles. If the earth mass consists of different layers with different unit cohesions, the procedure is as explained at the end of Sec. 9:10.

*b. Göteborg Failure.*—The slide that took place on Mar. 5, 1916, in the

\* Or "angle of shearing resistance" (see Sec. 5:12).

harbor of Göteborg, Sweden, was one of the largest in the world. This and some other slides have given Swedish engineers (particularly Fellenius) an opportunity to develop and check their views on the stability of slopes. The concrete harbor pier slid from position 1 into position 2 shown in Fig. 9:12b, and the bottom of the sea, at a distance of about 300 ft. from the shore (letter A in Fig. 9:12b), rose. The failure was probably caused by the excessive weight of the gravel fill.

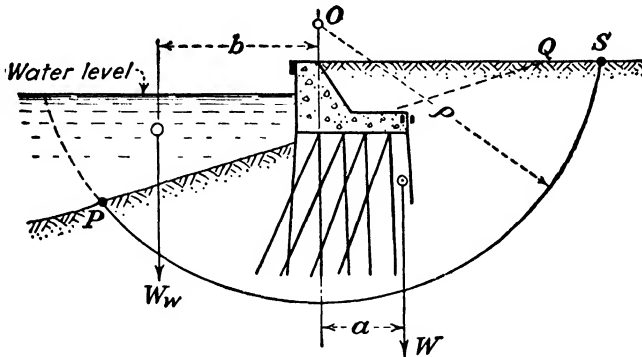


FIG. 9:12a.—Base failure of a retaining wall on pile foundation.

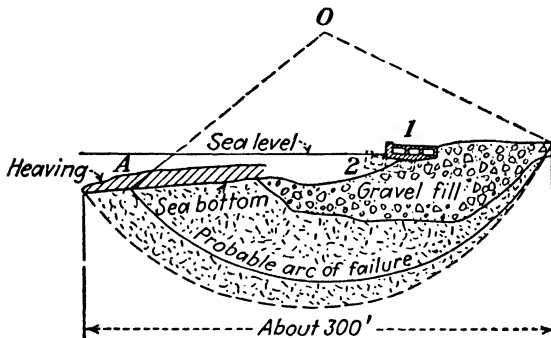


FIG. 9:12b.—Göteborg harbor failure.

**9:12. Toe-circle vs. Base Failure.**—Fellenius<sup>5</sup> and afterward Taylor<sup>6</sup> called attention to the fact that for  $\phi = 0$  and slopes flatter than  $53^\circ$ , the base failure is possible. Referring to Fig. 9:11 the minimum value of the stability number for  $\phi = 0$  is  $SN = 0.181$ , and the corresponding critical height

$$H_{cr} = 5.52 \frac{c}{\gamma} \quad (9:15)$$

Formula (9:15) gives a preliminary idea as to the critical height of a slope when there is a possibility of a base failure.

It is also obvious that any additional natural or artificial loading close to the toe of the slope (to the left of point  $T$ , Fig. 9:9b) decreases the danger of a base failure and any unloading (for instance, an excavation) increases it. The contrary is true so far as the top of the slope (point  $Q$ ) is concerned.

**9:13. Sudden Drawdown.**—Revert to Fig. 9:9a, and assume that the whole space (reservoir) to the left of slope  $QT$  is filled with water that may suddenly drop (“sudden drawdown”). Notice that the shearing resistance (resistance to sliding) along arc  $TS$  does not depend on whether or not there is water to the left of slope  $QT$  in Fig. 9:9a, provided, however, that *water is not permitted to flow out* from the wedge  $TQS$  through slope  $QT$ . Such is the situation just at the very moment of drawdown (but not afterward). Assume for simplicity that the volume of wedge  $TQS$  equals 1 cu. ft. Then the weight  $\gamma_s$  of the wedge  $TQS$  causing “effective” normal stresses  $\sigma$  acting on arc  $TS$  equals the weight of the soil particles within the wedge minus buoyancy on them

$$\gamma_s = \frac{\gamma_0 s}{1 + e} - \frac{\gamma_w}{1 + e} = \frac{s - 1}{1 + e} \gamma_0 \text{ lb. per cu. ft.} \quad (9:16)$$

If the wedge  $TQS$  is in the state of limit equilibrium, both the average shearing resistance and the average shearing stress along arc  $TS$  have the same numerical values.

$$\tau_1 = c + \sigma \tan \phi = c + k \gamma_s \tan \phi \quad (9:17)$$

where  $k$  is a coefficient of proportionality. At the moment of the sudden drawdown the average shearing resistance along arc  $TS$  still equals  $\tau_1$  whereas the shearing stress increases to  $\tau_2$ :

$$\tau_2 = c + k (\gamma_s + \gamma_0) \tan \phi \quad (9:18)$$

This is because in this case the weight of the wedge  $TQS$  is suddenly increased by a value of  $\gamma_0$  that of the vanishing buoyancy. In order to keep the wedge  $TQS$  in equilibrium its critical height  $H_{cr}$  (Fig. 9:9a) can be computed using a smaller value of  $\phi$ , or the so-called “weighted” angle of friction  $\phi'$ . The latter may be found from Eq. (9:17) and (9:18) by making  $\tau_1 = \tau_2$  and as an

approximation replacing the tangents of the angles by the angles themselves:

$$\phi' = \phi \cdot \frac{\gamma_s}{\gamma_s + \gamma_0} \quad (9:19)$$

The use of the "weighted" angle of friction  $\phi'$  has been proposed by Taylor.<sup>6</sup> In the case of a sudden drawdown, Taylor's graph in Sec. 9:11 can be used simply replacing  $\phi$  with  $\phi'$ .

The derivation as above may be easily extended to the case when instead considering the limit equilibrium at the immersion a safety factor is introduced. The procedure described is valid when the whole length of slope  $QT$  is immersed, which in dam engineering is practically always a fair approximation. The shearing stress  $\tau_2$  [Eq. (9:18)] is the greatest just at the moment of drawdown and gradually decreases as water flows out from the wedge  $TQS$ . Hence the most dangerous time moment, so far as a shear failure is concerned, is the moment of drawdown itself. In the case of dams their stability must always be analyzed assuming both full and empty reservoir.

In a particular case when the value of the unit cohesion  $c$  is negligible and the true safety factor  $F_t$  is used, the value of  $\phi$  in formula (9:19) must be divided by  $F_t$ . This follows from Eqs. (9:10) and (9:11) by placing  $c=0$  and substituting  $\phi$  for  $\tan \phi$ . The value of  $\tan \phi'$  is then the safe slope of the given material (problem 4, page 252).

**9:14. Considering Surface Cracking.**—The upper part of the earth mass bounded by a slope is pushed toward that slope by the lateral pressure acting within the mass. If the weight of the earth above a certain horizontal plane is not considerable enough to build up a shearing resistance so as to balance that pushing force, vertical cracks may be formed. Since the weight of the mass increases with the depth, cracks, if any, cannot be of indefinite depth, though they may be deep enough. The probable maximum depth of cracks that may be of progressive nature should be estimated, good judgment being used; and for the analysis purposes, only that part of the eventual failure line which is below the zone of possible cracking should be considered.

**9:15. Other Methods of Checking Stability of Slopes.**—There are many other methods of checking stability of slopes besides the Swedish method and the  $\phi$ -circle method. In all these methods

the earth mass is assumed to be homogeneous, the angle of friction  $\phi$  constant, and shearing resistance obeying the Coulomb formula. According to Résal,<sup>7</sup> if  $i$  denotes the angle made by a given slope with the horizon, and  $\gamma$  is the unit weight of the given earth material, the critical height  $H_{cr}$  of a slope is

$$H_{cr} = \frac{c}{\gamma} \frac{\sin i \cos \phi}{\sin^2 \left( \frac{i - \phi}{2} \right)} \quad (9:20)$$

Résal's function of  $i$  and  $\phi$  corresponds to the reciprocal of the stability number in Eq. (9:5), with some difference in numerical value. Apparently, the first attempt to develop a formula similar to (9:20) was made by Français over 100 years ago.\*

Frontard,<sup>3</sup> using the conjugate stress relationship, developed equations for the failure line. According to this author the upper part of the slope is in tension which checks actual conditions. Interesting analysis methods have been developed by Jáky<sup>8</sup> and Hennes.<sup>29</sup> The so-called "spiral method" as proposed by Rendulic<sup>9</sup> is based on the use of the logarithmic spiral. Culmann's method published as early as 1866, is of historical interest only.<sup>10</sup>

**9:16. Panama Canal Slides.**—The largest slope failures in a cut were those during the construction of the Panama Canal.<sup>11</sup> Slides caused trouble in 1887 to the French who started the work and to the Americans who continued it, starting in 1907. In the Culebra Cut 31 slides occupied a distance of about nine miles. Not all the slides were active simultaneously. At a given time some of them were temporarily quiet, and others already dead. The Cucuracha slide was moving up to May 1911, and was quiet from that time to December 1912. On Jan. 16, 1913, it caught several dirt cars and covered the whole channel. The volume of the Culebra Cut is about 95,000,000 cu. yd., and about, 5,000,000 cu. yd. have been spent "to kill" the slides.<sup>11</sup> During the Second World War (1941–1945) considerable reconstruction work was done in the Panama Canal Zone.

#### Problems

1. A trench with vertical walls for placing sewer pipes is to be made in a clay with the following characteristics:  $\gamma = 110$  lb. per cu. ft.;  $\phi = 9^\circ$ ;  $c =$

\* For the paper of this author, printed in 1820, see an old periodical entitled *Mémoire de l'officier du génie*, which was published at Paris from 1803 to 1892.

300 lb. per sq. ft. Determine the maximum depth of such a trench, assuming the safety factor with respect to cohesion slightly above 1, in view of the temporary character of the excavation. *Ans.* About 12'.

2. A canal 20 ft. deep and having 1:1 slopes is to be excavated in a soil with specific gravity of particles  $s = 2.65$  and a voids ratio  $e = 0.90$ . The angle of internal friction of the earth material is  $\phi = 15^\circ$ . Determine the value of cohesion required to keep the slopes in equilibrium (a) when the canal is completely filled with water (safety factor,  $1\frac{1}{2}$ ) and (b) when the canal is suddenly emptied (safety factor,  $1\frac{1}{2}$ ). *Ans.* (a) 140, (b) 360 lb. per sq. ft.

3. A highway cut 20 ft. deep is to be constructed in a clay deposit cracked to a depth of 6 ft. A shearing test of a sample taken below the cracked zone has furnished  $c = 350$  lb. per sq. ft. and  $\phi = 16^\circ$ . The unit weight of this clay in the state of capillary saturation is 115 lb. per cu. ft.; it may be assumed that there is no seepage. Is a slope  $1\frac{1}{2}$  base to 1 height ( $1\frac{1}{2}:1$ ) safe in these circumstances? *Ans.* Yes.

4. A rolled-fill dam is to be constructed of an earth material possessing an average angle of friction  $\phi = 32^\circ$  and practically no cohesion; its unit weight in the dry state is 110 lb. per cu. ft. and its voids ratio  $e = 0.5$ . Assume no freeboard (distance from the water level in the reservoir to the top of the dam). What side slopes are to be used to make the factor of safety equal to  $1\frac{1}{2}$  under the conditions of sudden drawdown?

*Ans.* 5:1. (Use true safety factor  $F_t$  and formula 9:19.)

## B. GENERAL FEATURES OF AN EARTH DAM

Embankments to be discussed in this chapter are mostly earth dams, though general rules established in this discussion may be applied also to railroad and highway embankments. Comprehensive information on dams of all kinds may be found in ref. 30.

**9:17. Cross Section of an Earth Dam.**—*a. Height.*—As in the case of any other dam, the height of the earth dam is determined from detailed reservoir and site investigations. The hydrology of the region should be thoroughly studied, and both yield of water (rainfalls, watersheds, brooks, rivers, streams, etc.) and loss of water (for instance, by evaporation) should be estimated. A detailed contour-line plan is used to locate the balance of water in the reservoir and to determine the height of the dam.

The described procedure refers to *storage dams*. For *flood-control dams* more detailed data on the volume and duration of fresh water should be available.

There are quite a few earth dams in the United States with a height of over 200 ft. Such are the Cobble Mountain Dam, Massachusetts (255 ft.); the Fort Peck Dam, on the Missouri River, Montana (242 ft.); the Calaveras Dam, California (240 ft.); and the El Capitan Dam, San Diego, California (217 ft.). On

the other hand, a very great number of earth dams are low dams, 15 or 20 ft. high and even less.\* Possible settlement of an earth dam may be estimated at 2 per cent of its height.

*b. Freeboard.*—The distance from the upstream water level to the top of the dam is termed “freeboard” (Fig. 9:13). In most large dams freeboard is of 20 ft., though it reaches sometimes 30 ft. In smaller dams there are freeboards of 4 or 5 ft., and all intermediate values may be found. The principal factor influencing the value of the freeboard is the height of the waves in the reservoir. In this connection the “fetch,” or the length of the reservoir exposed to the prevailing wind, should be determined.

*c. Top Width.*—When a highway is to be located at the crest of a large dam, the top width of the dam is made from 30 to 40 ft. Smaller dams have a top width of about 12 ft. or more.

*d. Upstream Face.*—The steepness of the upstream face is controlled by the value of the angle of repose  $\phi'$  of the earth material, under water. For sand and gravel, slopes 1 height on  $2\frac{1}{2}$  or 3 bases may be recommended. Above the water level 1:2 slopes may be used.

There should be adequate pro-

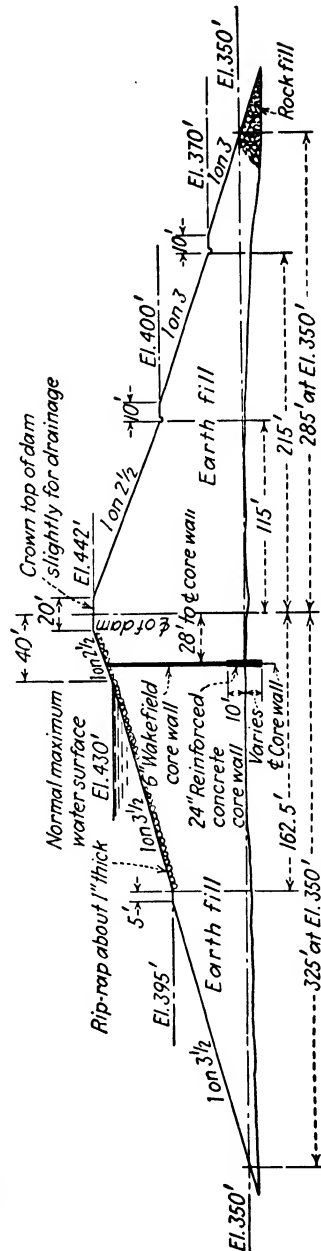


FIG. 9:13.—Rocky River Dam. (Connecticut Light and Power Co.)

\* A special manual entitled *Low Dams* was published by the National Resources Committee, Washington, D. C., in 1938.

tection of the upstream face against wave wash and ice action. In the case of smaller dams, light riprap (stones placed at random) or crushed stone is used; whereas upstream faces of larger dams are protected with heavy riprap, heavy pavement, or monoliths or blocks of Portland cement or bituminous concrete. The thickness of such blocks may reach 10 or 12 in.

If there is no wave-wash protection, slopes should be flatter than specified.

*e. Downstream Face.*—The downstream face should be protected against erosion due to percolation and to the action of rain and other climatic factors. Downstream faces are seldom steeper than 1:2; and they are treated with crushed stone or screened gravel or simply with topsoil to encourage vegetation. Downstream faces are provided with berms 30 or 40 ft. apart vertically. Berms slope slightly toward the dam to collect water in the gutters, which take it to catch basins; therefrom water is conducted to the stream.

It is to be noticed that berms are sometimes made both at the downstream and at the upstream face of a dam.

*f. Cores and Diaphragms.*—In the storage dam, in which impermeability is especially important, impervious central cores of fine impervious material are often made (Fig. 9:13). A diaphragm of reinforced concrete or steel or wooden sheet-piling walls are also placed at the middle of the dam or eccentrically. A full diaphragm may extend from the level of the impounded water down to a reasonably impervious earth stratum to stop the percolating moisture stream. *Cutoffs* are partial diaphragms that do not reach the water level in the reservoir. In Fig. 9:13 the trench under the core is a cutoff trench. Action of sheet-piling cutoffs has been shown in Figs. 3:19 and 3:22.

*g. Rock-fill Toes.*—These are rock-fill prisms placed at the downstream toes of earth dams to deviate the saturation line and thus prevent erosion of the downstream face (compare Fig. 3:23a). Sometimes such rock-fill toes are made both at the downstream and the upstream toes of a dam to increase stability.

At this stage of the discussion it is advisable to read again Secs. 3:11 to 3:15 and to examine Fig. 9:13.

No blankets are shown in Fig. 9:13, but their role should be recalled from Figs. 3:22 and 3:19.

*h. Spillway Arrangements.*—The excess of water should be removed from the reservoir to avoid the danger of overtopping. For this purpose an adequate *spillway* is constructed, and the capacity of the spillway weir should be designed to take care of maximum possible floods. The spillway is provided with both an approach and a discharge channel, and these arrangements may be independent of the dam proper. The spillway capacity is measured in cubic feet per second.\* For instance, the spillway capacity of El Capitan Dam (Sec. 9:16) is 75,000 cu. ft. per sec. and that of the Fort Peck Dam is 254,000 cu. ft. per sec.

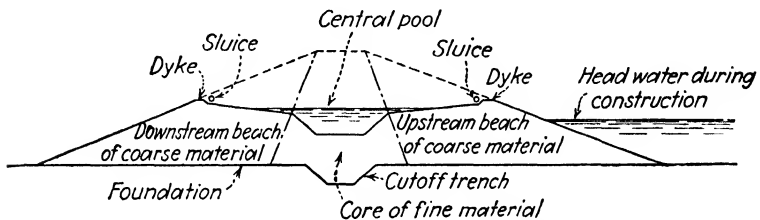


FIG. 9:14.—A hydraulic fill dam under construction.

**9:18. Types of Earth Dams.**—The basic types of earth dams are (a) *hydraulic-fill* dams, where the material flows from the borrow pit to the construction job in the form of a suspension; (b) *rolled-fill* dams, where the material is excavated in a near-by borrow pit and compacted by rolling; and (c) *semihydraulic-fill* dams, the method of construction being a combination of those labeled (a) and (b). Besides that, there are *rock-fill* dams built mostly of rock spoil or of quarried rock.

**9:19. Hydraulicking.**—Streams of water under high pressure are directed through nozzles (“hydraulic giants” or “monitors”) against the exposed face of a borrow pit, and the suspension thus formed flows to a collecting basin where it is guided into pipes or channels (sluiceways) leading to the construction job. The grade of the pipes is about 0.75 per cent. Sluiceways are formed by driving two rows of vertical planks into earth; the grade required for the movement of the suspension is  $2\frac{1}{2}$  or 3 per cent, sometimes more. The place where the pipes or sluiceways are discharged is marked in Fig. 9:14 with the word “sluice.” A temporary dike prevents the suspension from flowing down the slope. In running toward the central pool, coarser particles are

\* The abbreviation “sec.-ft.” is often used for this term.

deposited on the way and from the "beaches," both the downstream and the upstream one. Finer material reaches the central pool to form the impermeable central core.

Instead of the washing of the material from the exposed face of a borrow pit, flooded material may be dredged and pumped directly into the pipes going to the dam. Sandy and silty material is very appropriate for this work.

Still another way of hydraulicking is to excavate the material and transport it to a "hog box" (a boxlike structure of timber and concrete) for mixing. Boulders and large cobbles are separated, and a uniform suspension is directed to the dam. This operation can be done by gravity if the hog box is located high enough; otherwise a dredge pump may be used.

Suspension reaching the dam carries an average of about 10 per cent of solids.

**9:20. Rock-fill Dams.**—A rock-fill dam usually consists of three elements: (a) a loose rock fill constituting the mass of the dam, (b) an impervious facing on the upstream side (for instance, of reinforced concrete or of steel), and (c) rubble masonry between these two. Rock-fill dams are thought to be more stable than masonry dams in earthquake regions. The average height of a rock-fill dam is about 100 ft., though there are much higher rock-fill dams, such as the Salt Springs in California (328 ft.) or the Dix in Kentucky (270 ft.). The base of the structure must be wide enough to withstand the horizontal water pressure. The ratio of height to base of a slope may change from 1:2.5 to 1:3, though there are *considerably steeper slopes*. The crest width of 15 ft. should be considered satisfactory. The water pressure not only causes the vertical settlement of a dam but also moves the structure downstream. For instance, at the Dix dam quoted above the vertical settlement three years after completion was 1.75 ft., whereas the horizontal amounted to 1.5 ft.<sup>12</sup>

There are also mixed structures: rock-fill dams with earth cores or reinforced-concrete core walls and partly rock-fill, partly masonry dams.

An attempt to use rock-fill embankments without culverts instead of earth embankments with culverts has been made on some Russian railroads. This promising idea is still in its experimental stage. Apparently such embankments may be success-

fully applied on temporary routes such as military roads, unless there is danger of eventual silting.

Figure 9:15 shows the cross section of the Oneonta Dam in Alabama.

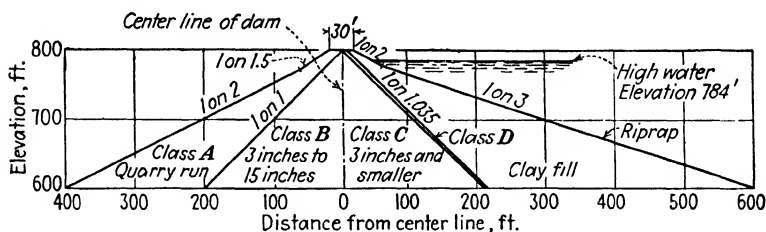


FIG. 9:15.—Oneonta Dam. (After Galloway, *Trans.*, A.S.C.E., vol. 104.)

**9:21. Dikes and Levees.**—Dams are normal, and embankments termed *dikes* (or *dykes*) and *levees* are parallel or oblique to a river or a valley, on one or both shores. Both dikes and levees are constructed mostly for flood control and current regulation purposes. Dikes generally are shorter but higher than levees. Well known is the system of levees in the lower Mississippi Valley,

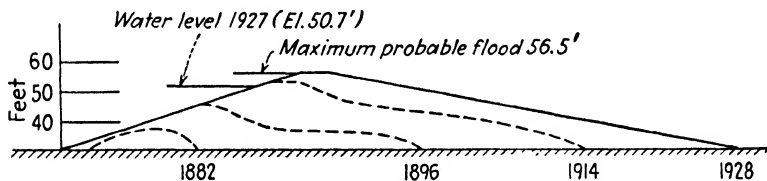


FIG. 9:16.—Gradual increase of Mississippi levees. (After Buchanan, *Trans.*, A.S.C.E., vol. 103.)

involving approximately 761,000,000 cu. yd. of earth material throughout a distance of 1,615 miles. Figure 9:16 shows the gradual increase of the levees' cross sections since 1882. The actual cross section of a levee calls for a top width of 10 or 12 ft., riverside slopes from 1:3 to 1:5, landside slopes from 1:6 to 1:8. Hence a levee is an earth dam with flat slopes, and it should be added that the freeboard of a levee is usually 1 ft. above the level of superflood anticipated.

### C. STABILITY OF THE BODY OF AN EMBANKMENT

The term "stability" as used in dam design has a twofold meaning. Forces acting on the embankment must be in equilibrium, and there should be a certain safety factor which is

characteristic of the purely static conditions of the given embankment. On the other hand, the term "stability" is referred to the material of the dam. The material in question should be such that its shearing resistance  $s$  is greater than the shearing stress  $\tau$  tending to cause the failure of the structure. Hence the problem of stability is also twofold. In the divisions C and D of this chapter the static stability of the embankment will be investigated, and in division E proper selection of the materials will be discussed.

**9:22. Consolidation of the Core of a Hydraulic-fill Dam.**—Figure 9:17 represents the core of a hydraulic-fill dam. It is under

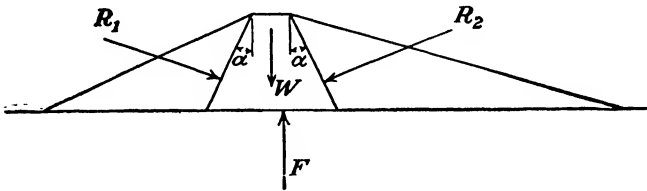


FIG. 9:17.—Forces acting on the core of a dam.

the action of four forces: weight  $W$  of the core, reactions  $R_1$  and  $R_2$  of the shell, and the reaction  $F$  of the foundation. The slope of a hydraulic-fill core is rather steep ( $\tan \alpha$  is about  $\frac{1}{2}$ ; see Fig. 9:17) to prevent danger of sliding. As soon as earth material is placed in the core, the process of consolidation begins, exactly as described in Chap. VI. Moisture is squeezed out from the voids, and soil particles come into closer contact with each other. A part of the pressure initially carried by the pore moisture of the freshly placed material is gradually transmitted to the skeleton, and this *increases the shearing resistance of the material* of which the embankment is made. Obviously this is also true in respect to the foundation of an embankment (see further, division D). It follows that *the greatest danger of sliding* of the core is either *during the construction or soon after it*—a statement confirmed by practice. The speed of construction, or rather the rate at which the height of a dam is increased, influences stability during this period; a dam *should not be constructed too hastily*. Undisturbed samples periodically extracted from the core and tested in the laboratory furnish information as to the path of consolidation which, generally speaking, is very slow. In some occasions pressure cells (Fig. 4:15) have been used to measure actual pressure within an earth dam under consolidation.

In Fig. 9:18 a typical cross section of a narrow-core hydraulic-fill dam in the Miami Conservancy district<sup>13</sup> is shown. Tongues of core material generally filled with moisture extend into the shell. The general tendency of these tongues is to be curved up, and they resemble, perhaps, the trajectories of minor principal stresses within the dam.

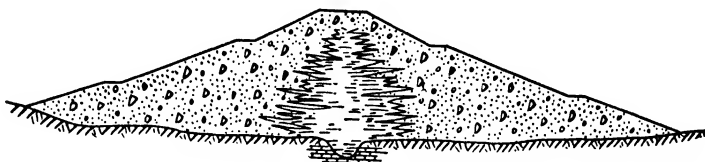


FIG. 9:18.—Tongues of core material extending into beach. (After Paul.)

**9:23. Methods of Analysis of an Earth Dam.**—The existing methods of analyzing earth structures may be subdivided into two main classes: (a) methods by which stability is checked without computing stresses at all individual points of the embankment and its foundation and (b) methods by which such stresses are computed. In both cases a soil profile (geological section) of the locality is traced, and the cross section of the earth structure located on it. For this purpose the general dimensions of the earth structure are first chosen, mostly from experience. For an earth dam as for any other engineering structure the following is demanded (a) design and structural dimensioning, (b) analysis of the structure and checking of chosen dimensions, (c) correction of the design according to the results of the analysis.

**9:24. Separation of a Wedge.**—The most general case of the analysis methods of class a (Sec. 9:23) would be considering con-

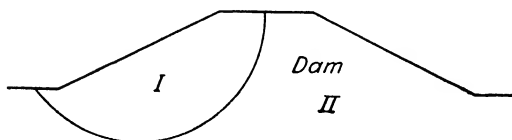


FIG. 9:19.—Separation of a wedge.

ditions of limit equilibrium of the wedge I which tends to separate from the rest of the mass II (Fig. 9:19). Such analyses have been actually made after failure of important earth structures with the purpose of investigating the causes of failure, particularly of determining friction and cohesion which were opposing the motion of the wedge I (compare example b, Sec. 9:11). In the case of

such a failure the position of the failure line may be exactly determined in the field, for instance by borings. In the design of a dam the location of the possible failure line requires considerable trial-and-error work, and tedious arithmetical operations are needed for the rest of the analysis. Therefore, in the dam analysis, simplified methods are used, as explained hereafter (Secs. 9:25, 9:26).

**9:25. Gilboy's Method.**—To simplify the analysis, the cross section of a hydraulic dam will be assumed to be triangular, as

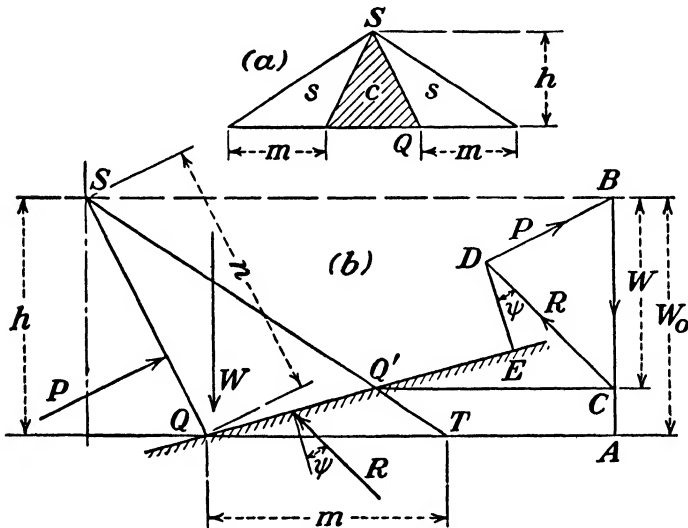


FIG. 9:20.—Gilboy's method of analyzing stability of the core.

shown in Fig. 9:20a, in which  $C$  is the core and  $S$  the shell of the dam. Besides this, the following three assumptions will be made.<sup>14</sup>

- The shell is cohesionless.
- The core acts as a liquid.
- Failure takes place along a plane.

The problem is to investigate stability of the shell against possible blowout of the core. The width of the shell along the horizontal plane of the base and the length of the oblique face of the core  $SQ$  will be designated by  $m$  and  $n$ , respectively. The height of the dam is  $h$ . The problem being two-dimensional, the dimension normal to the cross section is unity. Generally the unit weight of the earth material is not the same in the core and

in the shell. Let  $\gamma_1$  and  $\gamma_2$  be the respective unit weights. Then pressure exerted by the core against the shell is

$$P = \frac{1}{2}nh\gamma_1 \tag{9:21}$$

and the weight of the shell

$$W_0 = \frac{1}{2}mh\gamma_2 \tag{9:22}$$

Sliding along an arbitrary plane  $QQ'$  may take place under the action of the pressure  $P$  if the weight  $W$  of the part of the shell above the plane  $QQ'$  is not sufficient. A vertical  $AB$ , representing the weight  $W$  of the shell to such a scale as to make  $AB = h$ , is drawn. Then the vertical  $BC$  represents the weight  $W$  of the shell above the plane  $QQ'$ , because the height of the small triangle  $QQ'T$  is  $W_0 - W$ . Tracing  $BD$  parallel and equal to the pressure  $P$ , we find the resultant  $R = CD$ . The angle of obliquity  $\psi$  that it makes with the normal to the plane  $QQ'$  should be smaller than the angle of friction  $\phi$  of the material of the shell. This construction should be repeated for various planes  $QQ'$ . Since the basic assumptions of this

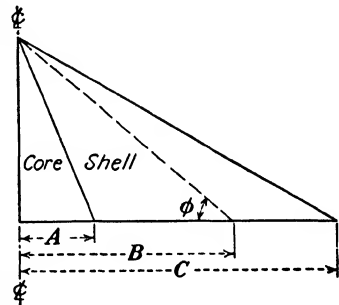


FIG. 9:21.—Notations for formula (9:19).

method are approximations, the method furnishes approximate results only. The analytical solution of the same problem has been given by Gilboy in the following form:

$$\sqrt{R} = \frac{(C - A) \sqrt{1 + B^2} + \sqrt{C - A} \sqrt{C - B} \sqrt{1 + A^2}}{(1 + C^2) - (C - A)(C - B)} \tag{9:23}$$

The notation used is (Fig. 9:21)

- $A$  = cotangent of angle of core slope with horizontal.
- $B$  = cotangent of angle of internal friction of shell material.
- $C$  = cotangent of angle of outer slope with horizontal.
- $R$  = ratio of unit weight of core to unit weight of shell.

Values of  $A$  and  $C$  are the slope constants, representing the ratio of horizontal run to vertical rise. Thus an outer slope of 1 height to 2.5 bases (1:2.5) corresponds to a value of  $C = 2.5$ . Since

all the values entering into formula (9:23) are abstract numbers, the result furnished by that formula is valid for any system of units. A further application of formula (9:23) in the case of dry-placed cores has been developed by Knappen.<sup>16</sup>

**9:26. Shearing Stresses at the Base of an Embankment.**—In studying stresses caused in a semi-infinite mass by external forces (Chap. IV), we have assumed that these forces act vertically at the horizontal boundary of the mass. In such a case there are no shear stresses at that boundary. If, however, the external

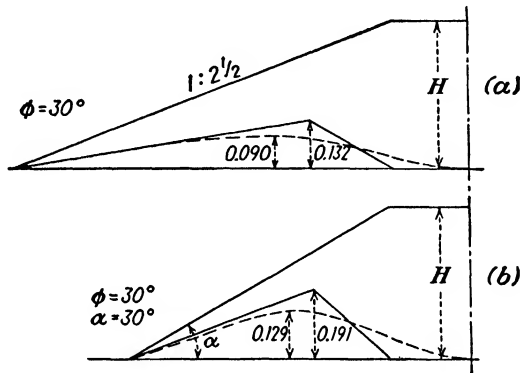


FIG. 9:22.—Comparative values of shearing stresses at the base of an embankment.

force in question is the weight of an embankment, there *are* shearing stresses at the base of the latter. Rendulic<sup>16</sup> approached this problem by considering the embankment as an idealized fragmental mass in the state of limit equilibrium, and he derived formulas that in graphic representation are shown in Fig. 9:22. In this figure, shearing stresses  $\tau$  at different points of the base are plotted vertically, and thus corresponding loci in the form of smooth curves are obtained. A simplified method will be given that can be considered satisfactory in view of the approximate character of the whole problem.

To simplify the reasoning, consider first an embankment of triangular cross section (Fig. 9:23a). Let its height be  $H$  ft., and suppose that the slope in question is defined by the ratio  $n$  bases on one height. Imagine that the embankment is cut into two halves along its center line, and consider conditions of equilibrium of one half only, for instance, of the left (Fig. 9:23b). Because of the symmetry, the left half pushes the right one horizontally,

and vice versa, and there cannot be any vertical component at the center line. Hence the right part can be removed and replaced by the horizontal thrust  $F_0$  that it exerts on the left half. The value of this thrust approximately equals the active pressure of a semi-infinite mass on a vertical plane  $H$  ft. high:

$$F_0 = \frac{\gamma H^2}{2} K_a \quad (9:24)$$

This thrust is resisted by the adherence of the embankment to its base, so that the average shearing stress  $\tau$  at the base will be obtained by dividing the value of the thrust  $F_0$  by the half width of the embankment, which equals  $Hn$ . Hence, the value of the average shearing stress  $\tau$  at the base of a triangular embankment is

$$\tau_{av} = \frac{F_0}{Hn} = \frac{K_a}{2n} \gamma H \quad (9:25)$$

Formula (9:25) furnishes the solution of the problem proposed. To find where the shearing stress reaches its maximum, draw a line through the top point of the dam  $N$  to make an angle  $45^\circ - \phi/2$  with the vertical. The maximum shearing stress  $\tau_{max}$  is thus obtained (Fig. 9:23b) at point  $P$ , and the value of the maximum shearing stress is

$$\tau_{max} = 2\tau_{av} \quad (9:26)$$

It has been assumed in writing formula (9:26) that the shearing stress  $\tau$  vanishes at the toe of the dam because there is no load and at the center line of the dam because of the symmetry. It has been assumed also that the shearing stress increases from both the toe of the dam and its center line toward point  $P$ , following the straight-line law. The final diagram is shown in Fig. 9:23c.

In the case of a wide trapezoidal embankment, as in highways, the shear under the crown is insignificant and can be neglected.

Some results obtained by the method described are shown in Fig. 9:22 in solid lines. They are about 50 per cent in excess of Rendulic's data shown in dotted lines. The point where the shearing stress  $\tau$  is at a maximum checks closely enough in both methods.

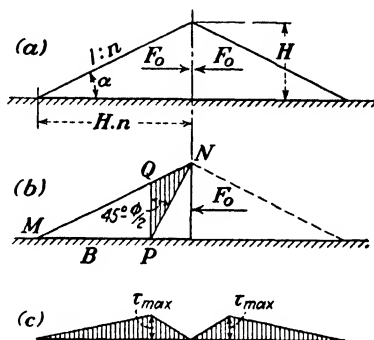


FIG. 9:23.—Shears at the base of a triangular embankment.

Shearing stresses at the base of an embankment may be dangerously increased by overrolling during construction. The overrolled material tends to expand, and this causes such lateral sliding as occurred at the Tappan Dam, Muskingum River Project, Ohio.<sup>15</sup>

**9:27. Shear at the Base of a Dam by Another Method.**—The designer of a dam may find many useful suggestions in the comprehensive work on dams by Creager, Justin, and Hinds.<sup>30</sup> So far as shears at the base of an earth dam are concerned, these authors determine shearing stresses acting from the center of the dam (*a*) toward the downstream toe and (*b*) toward the upstream toe of the dam, considering sudden drawdown in the latter case. The average and the maximum shearing stresses are found (designations  $\tau_{\text{ave}}$  and  $\tau_{\text{max}}$ ). The value of  $\tau_{\text{max}}$  is twice that of  $\tau_{\text{ave}}$ ; the point of application of the maximum shear is located at two-fifths of the half-width of the dam, counting from the center line. In determining the weight of the material, its full or partial saturation, respectively, is considered. It should be noticed, however, that the method in question refers to cohesionless materials (such as sand) only.

**9:28. Computation of Stresses in an Earth Dam.**—There are two methods of computing stresses within an earth dam (methods of class *b*, Sec. 9:23). Both have been elaborated by the engineers of the Bureau of Reclamation. In both cases, the theory of elasticity is used, with or without modifications.

*a. Brahtz's Proposal.*—Brahtz<sup>17</sup> made an attempt to determine stresses within an embankment caused by its own weight. His approach is to start from some basic equilibrium and superimpose systems of reasonable *self-balancing* correction stresses. The basic stressed state is that given by the Swedish method: (*a*) The vertical normal stress  $\sigma_z$  equals the weight of the material above the given point; (*b*) there is no shear either in the vertical or in the horizontal direction. In other words, the vertical pressure  $\sigma_z$  is the major principal stress. To take care of the horizontal normal stress  $\sigma_x$ , a constant "compaction factor"  $K$  is introduced:

$$K = \frac{\sigma_x}{\sigma_z} \quad (9:27)$$

The value of  $K$  as given by formula (9:27) for a *finite* mass should not be confused with the value of the natural hydrostatic-pressure ratio or coefficient of pressure at rest  $K$  within a *semi-infinite* mass (compare Fig. 4:27 and the explanatory text). In the latter case *only* can the value of  $K$  be constant. In the case of a finite mass, however, the value of  $K$  vanishes at the unloaded slopes, owing to boundary conditions. Thus in reality the compaction factor  $K$  as defined by formula (9:27) is *not* constant. According to Brahtz, in a properly consolidated dam  $K$  should not be less than  $50/\gamma$ , where  $\gamma$  is the weight

in pounds per cubic foot of saturated soil. The systems of correction stresses have the purpose of removing stresses from the unloaded surfaces to satisfy boundary conditions. Brahtz's final solution is *not unique*, as are solutions given in the theory of elasticity. Actually, taking another basic stress system, it is possible to find still other correction stresses to satisfy boundary conditions, and the new solution will be different from the initial. Brahtz's work is commendable, however, since it furnishes a solution that apparently will yield results on the side of safety.

b. *Subdivision of the Earth Dam into Elastic and Plastic Regions.*—Glover and Cornwell<sup>31</sup> subdivide the dam and its foundation into alternate plastic and elastic regions (Fig. 9:24). The plastic regions are assumed to be in the state of plastic equilibrium, whereas shearing stresses  $\tau$  in relieved elastic

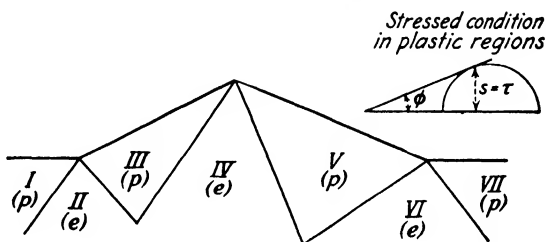


FIG. 9:24.—Conventional subdivision of an earth dam into elastic and plastic regions.

zones are smaller than the shearing strength of the material  $s$ . The difference between the two ( $s - \tau$ ) extended on the whole dam is the *reserve of strength* of the dam.

#### D. STABILITY OF EMBANKMENT FOUNDATIONS.

**9:29. Maximum Shearing Stress in an Elastically Isotropic Foundation.**—Under the action of the weight of an embankment, stresses develop in the foundation, *i.e.*, in the soil mass on which the embankment is built. It is often assumed that (a) the foundation is a semi-infinite elastically isotropic body and (b) at each point of contact of the embankment and the foundation a vertical force acts equal to the weight of the earth column above that point. Obviously the latter assumption means that the embankment is considered as being nonrigid (compare Sec. 9:26) and representing a completely strange body with respect to the foundation. In reality, a large embankment such as a dam, together with its foundation, forms a *new earth body* to be studied.

It is known how to determine the maximum shear stress at a point of a semi-infinite elastically isotropic mass. If points with equal values of the maximum shearing stress are joined, a pattern

similar to that shown in Fig. 4:13 is obtained. It is to be recalled that in the particular case shown in that figure the maximum shearing stress equals 0.256 times the maximum pressure and occurs at a depth of one-fourth the breadth of the load (compare also end of Sec. 4:16). The usual design procedure is to compare the maximum shearing stress with the shearing value that the material can develop. As stated already in Sec. 9:26, the foundation *undergoes consolidation* in the same way as the body of the embankment, so that its shearing value increases to a certain maximum value as time passes up.

It is very questionable, however, if such a shearing stress as that shown in Fig. 4:13 may be operative. It seems that in reality, material located at the center line of a rather wide embankment is confined and compressed by the action of the principal stress and cannot be pushed out (compare also end of Sec. 9:27). The shearing stress may cause failure closer to the edges of the dam, where shearing surfaces are more likely to develop, and earth material may be pushed out. Its value at those points is smaller than along the center line, so that the method of analysis described is on the safe side.

**9:30. Case of a Rigid Boundary at a Depth.**—Another case that may occur in practice is the existence of a hard layer (“rigid boundary”) at a certain depth.

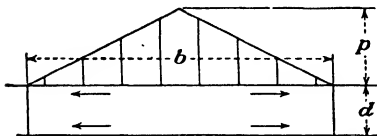


FIG. 9:25.—Checking stability of an embankment foundation.

In such a case a base failure may take place (Sec. 9:10). If the material between the embankment and the rigid boundary is very soft, it may be squeezed out from underneath

the embankment. Some idea of the shearing stress that develops in the soft material may be obtained from Hencky's formula.<sup>32</sup>

$$\tau = p \frac{d}{b} \quad (9:28)$$

in which  $p$  is the unit pressure at the center of the dam, and  $b$  and  $d$  dimensions shown in Fig. 9:25. Formula (9:28) may be used for rough preliminary computations.

**9:31. Photoelastic Studies of the Embankment Foundation.**—Figure 9:26 shows a simple polariscope used in the study of foundations represented by a weak pour of gelatin, the model of the

dam being made of lead shot.<sup>18</sup> Polarized light is obtained by reflection from the polarizer (a mirror or a glass painted black on the reverse side), and the stress bands may be seen in the

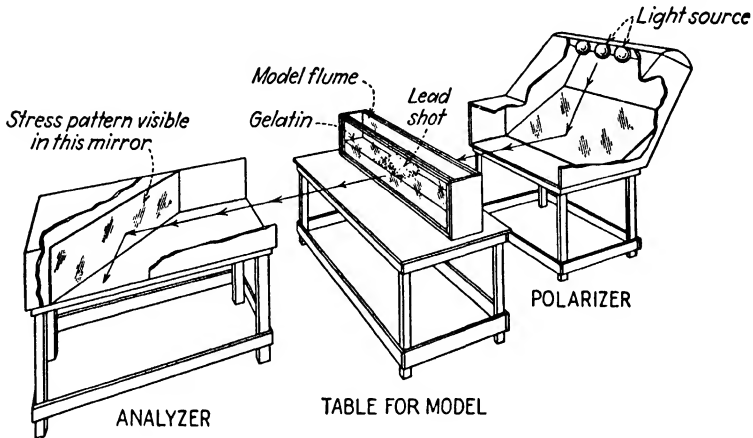


FIG. 9:26.—Photoelastic study of a dam foundation.

analyzer, which is of the same construction as the polarizer. Settlement of the embankment is in this case not at its center line but at points on either side of the center line, about halfway

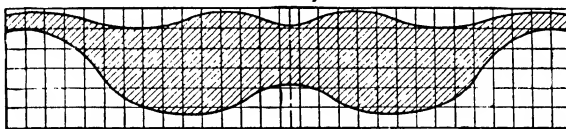


FIG. 9:27.—Settlement of a model dam on gelatin.

toward the toes (Fig. 9:27). This kind of settlement is sometimes termed “heart-shaped,” owing to its resemblance to the lower part of an inverted heart. Some field observations on actual structures

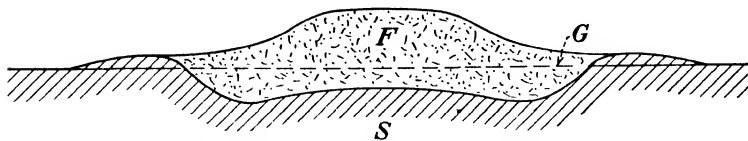


FIG. 9:28.—Actual case of an embankment settlement. (After Gilboy.)

have also shown similar settlement. For instance, Fig. 9:28 shows a section through a highway embankment as reported by Gilboy.<sup>14</sup> *F* is fill; *S*, silt foundation; and *G*, original ground surface. It

cannot be stated in a general way, however, that such materials as gelatin or lead shot, which are far from being soils, *always* duplicate the stressed condition in an earth mass as in Fig. 9:26.

Though in this particular case the results of photoelastic studies and field observations may mutually check, certain *limitations of photoelasticity* in the province of earth-dam design *should be*

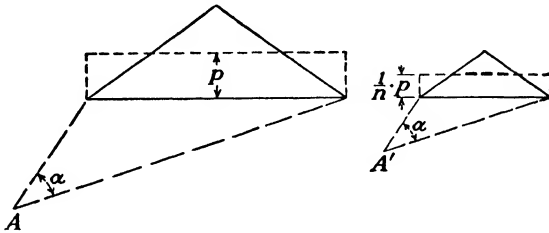


FIG. 9:29.—Stresses under a prototype and the model of a dam.

*emphasized.* First of all, models, including photoelastic ones, do not truly represent the action of a dam on its foundation. In Fig. 9:29 the prototype and a model of a dam are shown; both are of the same material, the model being  $n$  times smaller than the prototype. If we consider the problem as plane and replace the

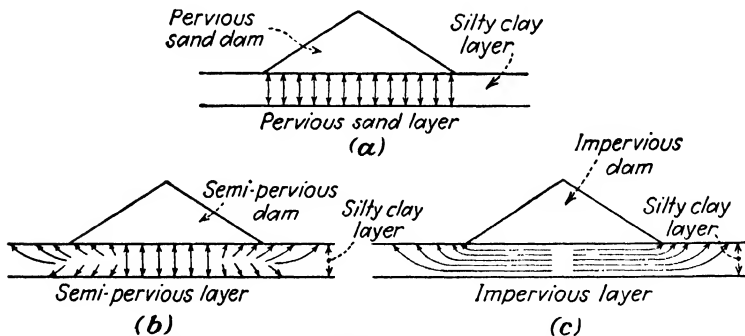


FIG. 9:30.—Fallacies of the photoelastic analysis of a dam foundation. (After Creager, *Trans. A.S.C.E.*, vol. 103.)

triangular load by a uniformly distributed load, for instance,  $p$  in the case of the prototype and  $(1/n)p$  in the case of the model, it may easily be seen that the stresses at point  $A$  of the prototype are  $n$  times greater than those at an analogous point  $A'$  of the model. This inconvenience is sometimes obviated by making the height of the model disproportionately great. Furthermore, a part

of the load of the dam is carried by the moisture of the foundation soil and is transferred to the foundation not vertically, as simulated by the photoelastic method, but possibly in an infinite number of directions (Creager<sup>18</sup>). In the case of Fig. 9:30*a*, the photoelastic investigation may furnish reliable results, whereas it is not so in the case of Fig. 9:30*b* and *c*, where drainage is not vertical. Finally, the photoelastic method cannot take care of the residual shearing stresses in the body of a dam which may develop as a result of heavy rolling, as in rolled-fill dams.

**9:32. Centrifuge Method of Checking Stability of an Embankment.**—As stated in Sec. 9:31, gravity forces are not correctly reproduced in models. Substitution of the forces of inertia for the force of gravity was first (about 1931) suggested by Bucky,<sup>28</sup> who, with some other members of the faculty of Columbia University, utilized a rather small centrifuge. A special centrifuge was constructed by Pokrowski, of Russia, in 1933. The radius of rotation of this centrifuge is about 44 in., as against the 6 to 8 in. generally used. The total number of revolutions per unit of time should be so calculated as to make the centrifugal acceleration  $n$  times gravity, where  $1/n$  is the scale of the model. A two-dimensional model traced in cylindrical coordinates is suspended vertically but during the centrifuging becomes practically horizontal with the center of coordinates coinciding with the center of rotation.

**9:33. General Discussion of the Methods of Checking Stability of Embankment Foundations.**—The purely elastic method of checking stability of an embankment foundation (Sec. 9:29) and the photoelastic method (Sec. 9:31) assume vertical loading, whereas at the base of an embankment there are horizontal stress components, as already explained in Sec. 9:28. Obviously, a correction may be introduced into the elastic method of Sec. 9:29, adding horizontal forces and considering their effect, but this is quite impossible in the case of the photoelastic method. As a rule, the results furnished by the photoelastic method are *qualitative* rather than quantitative; and even so, they should be interpreted with great care.

Concerning the purely elastic method (Sec. 9:29), it is necessary to emphasize that all objections that have been formulated in Chap. IV against the theory of elasticity as applied to soil problems are valid in the present case. However, if earth material is fairly

homogeneous to a considerable depth, the elastic method (Sec. 9:29) is to be applied, since there is no other more adequate method.

Hencky's formula as discussed in Sec. 9:30 assumes that there are vertical cuts at the toes, whereas in reality the layer is continuous. Formula (9:28) is a rough approximation only.

**9:34. "True" Safety Factor in Dam Design.**—Refer to the end of Sec. 9:8. As in the computations of the stability of slope, the "true safety factor" (designation  $F_t$ ) in the computations of stability of earth dams is the ratio of the shearing strength  $s$  to the acting shear stress  $\tau$  [compare formula (9:11)].

$$F_t = \frac{s}{\tau} \quad (9:11)$$

In turn, the shearing resistance  $s$  consists of the frictional resistance  $\sigma \tan \phi$  and the cohesion resistance  $c$ . The latter may vary according to weather conditions and fluctuations of the ground-water level, whereas the former is practically invariable. It is true that as the work progresses, both factors,  $\sigma \tan \phi$  and  $c$ , increase; but the frictional resistance  $\sigma \tan \phi$  increases immediately as soon as the load is applied, whereas the cohesion resistance  $c$  requires time for consolidation. The factor of safety  $F_t$  thus may be broken into two parts:

$$F_1 = \frac{\sigma \tan \phi}{\tau} \quad (9:29)$$

$$F_2 = \frac{c}{\tau} \quad (9:30)$$

From the two dams or dam foundations with equal factors of safety  $F_t$ , that possessing the larger values of  $F_1$  is preferable.

#### E. SELECTION OF MATERIALS FOR EMBANKMENTS

As soon as the cross section of a dam is established, material in prospective borrow pits is analyzed, and, if necessary, measures to improve it are developed. Obviously, absence of suitable earth material on the site or close to it suggests using a concrete or rock fill dam.

**9:35. Earth Material for Hydraulic Fills.**—Suspension delivered to the job by pipes or sluiceways must not contain too many fines; otherwise the core, which is being formed rather automa-

tically from the central pool, will be disproportionately large. The excess of fines may be removed, however, by siphoning off the fines from the pool. If, on the contrary, the borrow-pit materials contain a deficiency of fines, an additional borrow pit with a good content of fines must be located, and a convenient mixture of both materials prepared in the hog box. If this is not done, the core will

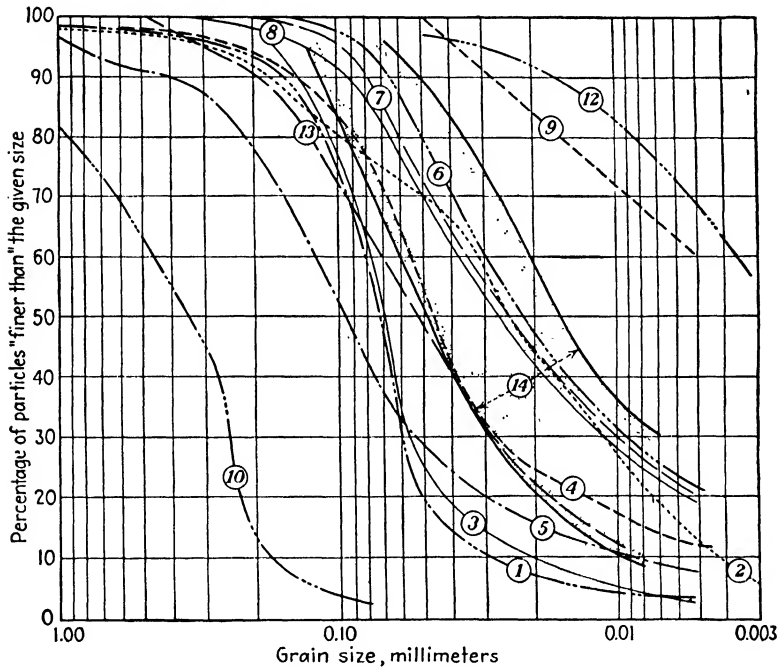


FIG. 9:31.—Core material of several dams. (After Dore, *Trans., A.S.C.E.*, vol. 102.)

become too pervious. Shoulders must contain a reasonable percentage of stones and cobbles, which should be added if missing.

Comprehensive information on the methods of selecting materials for hydraulic and semihydraulic dams may be found in a paper by Dore<sup>19</sup> on the Quabbin Dike in Massachusetts. The locality from which earth material was to be taken was investigated by 2½-in. bore holes and by test pits, 6 to 10 ft. deep, dug by hand. In addition, several large cuts were made by a steam shovel. The samples were tested in the soil laboratory for grain size, permeability, and porosity. Supposing that the eventual

borrow pits will be of the same material as the samples, the problem is to determine the percentage suitable for the core construction. For this purpose materials from the experimental cuts were tested in the "sluicing bin" (length about 40 ft., cross section 15 by 2 ft.) to imitate the action of water in the actual transportation of the material. By measuring the quantity of the material sluiced and the quantities deposited in sections of the sluicing bin corresponding to the beach and core sections of the dam, estimates of the yield of beach and core material can be made. Burmister<sup>20</sup> suggests estimating the yield of core material by the simple analysis of the grading curves of borrow-pit materials; apparently there is a fairly definite separation by the hydraulic process at about No. 100 sieve (0.149 mm.). Figure 9:31 represents the sizes of the core material of 14 hydraulic- and semihydraulic-fill dams. Curves 9 and 12 correspond to Calaveras Dam, California, and Alexander Dam, Hawaii, which failed during construction but were repaired (Sec. 9:43). Curve 13 corresponds to Cobble Mountain Dam, Massachusetts. Curves 14 show the range of materials used in the Quabbin Dike.

**9:36. Design of a Rolled-fill Dam to Suit Available Materials.**—Practically *any available earth material* may be used for a rolled-fill dam. However, proper *location* of the material at different parts of the dam and proper *pretreatment*, such as mixing and compaction, are to be considered. Locating material at different parts of the dam depends on whether the foundation of the dam is pervious or not and to what depth.

*Example 1.*—Coarse sand only is available, but some sandy clay or clayey silt may be imported at a considerable cost. The foundation is pervious to 50 ft. A solution would be to design a core of impervious material as a narrow vertical wall (for instance, 15 ft. wide) to reach the impervious layer. It is more convenient, however, to design a trapezoidal core with a cutoff trench or sheet piling wall. The width of the trench should not be less than about 10 ft. for machine excavation and 4 to 5 ft. for handwork (Fig. 9:32*a*).

*Example 2.*—There are adequate quantities of coarse sand, rather soft silty clay, or clayey silt, and stiff consolidated clay on the site. Particularly, the foundation of the eventual dam is made of the last material. In this case economic considerations prevail. Stiff clay if used for the dam would be probably more expensive in excavating than the two other materials. Hence either the whole dam or only its core (Fig. 9:32*b*) is to be made from silty clay.

*Example 3.*—The situation is as in Example 1, but the foundation is pervious to an indefinite depth. In this case the use of an impervious blanket, at least

2 ft. thick, is advisable (Fig. 9:32c). Some builders make this blanket rather long in the upstream direction (for instance 1,000 or 1,500 ft. long).

**9:37. Earth Material for Rolled-fill Dams.**—There have been attempts to establish limiting size-distribution curves for impervious sections of a rolled-fill earth dam. Such are Lee's limiting

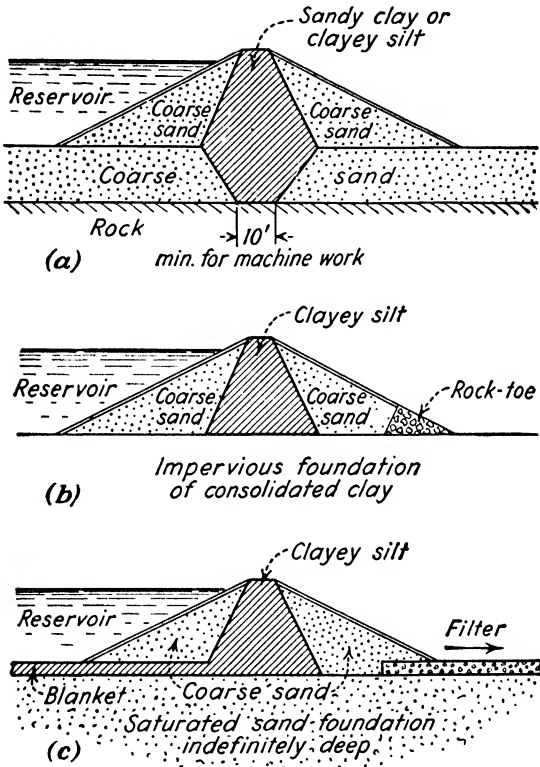


FIG. 9:32.—Examples of design of a rolled-fill dam. (Sketched from "Engineering for Dams," by Creager, Justin, and Hinds.)

curves<sup>21</sup> or Kendorko "classes."<sup>22</sup> It is to be borne in mind that there are only a few earth materials which are not suitable for a rolled-fill earth dam. In a general way, earth material for a rolled-fill dam must satisfy the following requirements:<sup>21</sup>

a. *High shearing value.* This is very often designated in technical literature as "stability" (compare beginning of division C of this chapter).

b. *Watertightness (impermeability),* if the service conditions of

a given dam require it. As already stated, this is the case with water-conservation dams. Dams built for hydroelectrical purposes do not need to be that tight, and considerable leakage may be tolerated in flood-control structures, particularly in levees.

*c. Workability*, or capacity to be compacted readily into a fill of uniform texture and high density, by the use of mechanical equipment.

*d. Adjustability*, or capacity to adjust itself by gradual settlement without cracking or formation of planes of lessened resistance to percolation. In flood-control reservoirs, especially in arid regions, a dam may be not used for years; and if during this dry period cracks develop, they may become a menace when floods fill the reservoir.

*e. Insolubility* of soil particles in water.

*f. Low cost* of handling, such as excavation, transportation, spreading, and rolling. The use of *local materials* is always *preferable*, and the possibilities of opening local borrow pits are to be thoroughly investigated (compare Sec. 9:36).

For preliminary selection of a material a *size distribution curve* is very useful. But to make a final decision, it is often necessary to fall back on *direct measurements* of permeability, porosity, limits of consistency, and shearing value and to make compaction tests as well. To satisfy the basic requirements listed above as (a), (b), and (c), the material must be *graded*, *i.e.*, must contain different fractions, from cobbles and pebbles to clay and colloids, and this fact should be seen on a size distribution curve. It is obvious that the latter must be complete and must represent all fractions of the given material, not only those passed through No. 10 sieve as in Fig. 1:4. Coarse aggregate held on No. 10 sieve (gravel, pebbles) is necessary for that part of shearing strength acquired by friction (the value of the coefficient of friction may be assumed to be 0.25 to 0.50). Sometimes coarse aggregate is crushed rock, 5 or 6 in. in size. Fine sand represents a binder or bedding for the coarse aggregate, and silt and clay are fillers for the voids.

There is an *analogy* between the proportioning of soil mixtures and the *proportioning of concrete*. However, soil mixtures are much lighter than concrete. The average unit weight of concrete is about 155 lb. per cu. ft. or, deducting 6 per cent for water, about 147 lb. per cu. ft., whereas the average unit weight of a dry soil

mixture is 115 lb.—a difference of about one-fourth. These figures, computed by Jacobs,<sup>21</sup> (discussion) are approximate but still characteristic of the situation. Since the weight of a dam contributes to its stability, heavy mixtures of high density are preferable. At the same time, the denser a mixture the greater its watertightness.

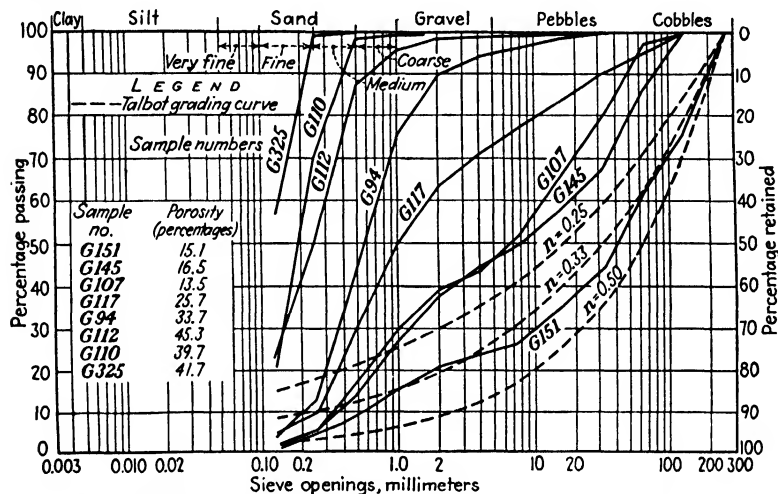


FIG. 9:33.—Relation of porosity to grading. (After Lee, *Trans. A.S.C.E.*, vol. 103.)

The ideal grading for maximum density has been investigated by experiments in concrete engineering. As a result of these experiments the well-known *Talbot formula*<sup>23</sup> was developed:

$$p = \left(\frac{d}{D}\right)^n \tag{9:31}$$

in which  $p$  = proportion by weight passing a given screen or sieve opening.

$d$  = size of opening.

$D$  = maximum particle size.

$n$  = an exponent varying from 0.24 to 1.20.

The value of  $n$  for soil mixtures fluctuates between 0.25 and 0.40. Obviously for  $n = 0.5$  the curve of Eq. (9:31) is a parabola. Figure 9:33 shows several size distribution curves of soils studied by Lee,<sup>21</sup> there are also three Talbot curves plotted (for  $n = 0.25$ , 0.33, and 0.50, respectively). Samples G-151, G-145, and G-107

contain all sizes from large cobbles to fine sand, with a preponderance of coarse sizes and regular graduation of fine particles. In turn, the porosity of these three samples averages 15 per cent, whereas the porosity of other, nongraded samples is much higher.

According to Lee,<sup>21</sup> regularly graded material having a degree of fineness sufficient to include 3 per cent of clay or ungraded material containing at least 25 per cent of clay when thoroughly compacted is practically watertight. Such material may permit leakage of 0.1 gal. per sq. ft. per day (hydraulic gradient = 1; temperature = 60°F.). This is equivalent to a coefficient of permeability  $k = 4.86$  ft. per year. In reality, a greater amount of leakage may be permitted. As a matter of fact, in flood-control structures a leakage of 100 gal. per sq. ft. per day may be permitted if structural measures are taken to allow this leakage to pass without damaging the structure. This involves *proper drainage* of the downstream section of the dam and other measures stipulated in Chap. III.

As to the *impervious diaphragm* (core) within a rolled-fill dam, it is advisable to make it from an ideally graded watertight material. Impermeability of the core does not necessarily require that the core have hardness or even stability if considered separately from the shell. It is to be noticed that glacial flour or the slimes from stamp mills are quite as impermeable as clay; also adobe and similar soils mixed with sand and gravel may be used in the impervious core section.

**9:38. Compaction of Earth Material.**—The purpose of the compaction of earth material is to increase its stability and particularly

- a. To increase *mechanical bonds* (interlocking) of particles.
- b. To decrease the thickness of water films and thus to *increase cohesion*.
- c. To *expel air* from the pores.

The presence of air in the pores of an embankment placed wholly or partly under water is very harmful, since as time passes, air is dissolved in water, which thus gradually fills the pores. Moisture films thus become thicker; cohesion decreases; and material, even if granular, becomes softer.

Compaction is accomplished by *rolling* earth material spread in thin layers (for example, 6 in. thick) with trucks and heavy, flat rollers. Sheepfoot rollers are very popular in dam construction. *Vibration processes* are sometimes used, and in restricted areas

*tamping* is done. To ensure the required moisture content, the earth material may be *sprinkled*.

The immediate result of compaction is the *reduction of porosity*. As an example, an original porosity of 40 per cent may become as low as 15 per cent after compaction. According to data obtained during the construction of the new German super-highways,<sup>24</sup> the maximum compaction is not at the surface of a fill but at a certain depth (for instance, 18 in. or more) below which compaction decreases again. On some occasions, soils resist compaction. As reported in the literature, such soils are (a) soils containing large quantities of ungraded silt and a small amount (for instance, 5 per cent) of organic matter; (b) Hawaiian laterites, in which porosity could not be decreased below 64.8 per cent, even with the most careful packing; (c) porous volcanic ash beds. On the other hand, such a porous material as loess may easily be reduced to a compact state by heavy rolling.

*Optimum Moisture Content*.—Soil particles are surrounded by moisture films which are pressed to the particles both by attraction and surface tension (compare Sec. 2:10): the closer to the soil particles the stronger is that pressure. If during compaction the moisture content is deficient, the films are thin, hence tight and rigid. When compacted, such a material is too hard. Additional moisture, however, would decrease or even destroy its stability. If the moisture content is excessive, the films are thick and hence loose, and the soil particles are movable. For each earth material there is a certain *optimum moisture content* for compaction which can be found experimentally. At the optimum moisture content the films are rigid enough to ensure stability but also flexible enough to permit the particles to adjust to each other, thus forming the *densest possible mass*. As a crude preliminary approximation, the optimum moisture content may be estimated at 20 per cent for fine-grained soils and at 10 per cent for well-graded aggregate with binder. In each particular case, however, the optimum moisture content should be found experimentally (Sec. 9:39).

**9:39. Proctor's Plasticity Needle.**—An original approach to the question of rational compaction of earth material in dams may be found in four articles by Proctor,<sup>25</sup> of the Bureau of Waterworks of the City of Los Angeles, Calif.

Proctor's plasticity needle (Fig. 9:35) is a rod with an enlarged

tip which is forced into the soil at a rate of about  $\frac{1}{2}$  in. per sec. The tip is exchangeable, and tips of different sizes from 0.01 to 1 sq. in., giving readings in pounds per square inch, are used, according to the degree of softness of the soil. The method of testing follows: The soil is passed through a No. 4 sieve and is compacted in three layers within a cylinder 4 in. in diameter and 5 in. high. This cylinder has a removable base plate and a loose collar at the top. Twenty-five firm 12-in. strokes of a special rammer weighing 5.5 lb. are applied to each layer. This can be

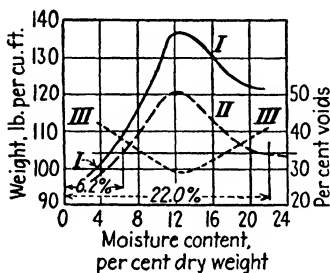


Fig. 9:34.—Compaction and moisture content. (After Proctor.)

done by hand or by mechanical devices developed in some laboratories.\* Afterward, the collar is taken off and the soil is cut off even to the dimensions of the remaining cylinder. According to Proctor, plasticity-needle reading at the optimum moisture content should be 300 lb. per sq. in. or more, but in practice such readings as 200 lb. per sq. in. prove satisfactory in many cases.

The soil on the job that has been compacted, starting at the optimum moisture content, should furnish the same plasticity-needle reading as in the laboratory. The following three data should be obtained at each test:

a. The average needle reading obtained from forcing the needle into earth in the cylinder at three different points.

b. The weight of earth in the cylinder and, since the volume of the latter is known (generally  $\frac{1}{30}$  cu. ft.), the unit weight of tested material in pounds per cubic foot.

c. The moisture content of the earth in the cylinder which is found in a general way by drying out the tested material or a part of it in the oven. The test is repeated for various moisture contents, and both the wet and dry unit weight of the material computed. If the former is  $\gamma$  and the latter  $\gamma_1$

$$\gamma_1 = \frac{\gamma}{1 + w} \quad (9:32)$$

where  $w$  is the moisture content of the earth material at a given

\* Changes introduced by Army Engineers: compaction in five layers, 10-lb. rammer, 18-in. strokes.

test expressed in fractions of one unit. The curves I and II in Fig. 9:34 show the unit weights  $\gamma$  and  $\gamma_1$ , respectively. The point where curve II reaches a maximum corresponds to the optimum moisture content (about 12 per cent in Fig. 9:34). Curve III shows porosity in per cent of volume. It may be seen from this curve that the given earth material, when compacted at 6.2 and

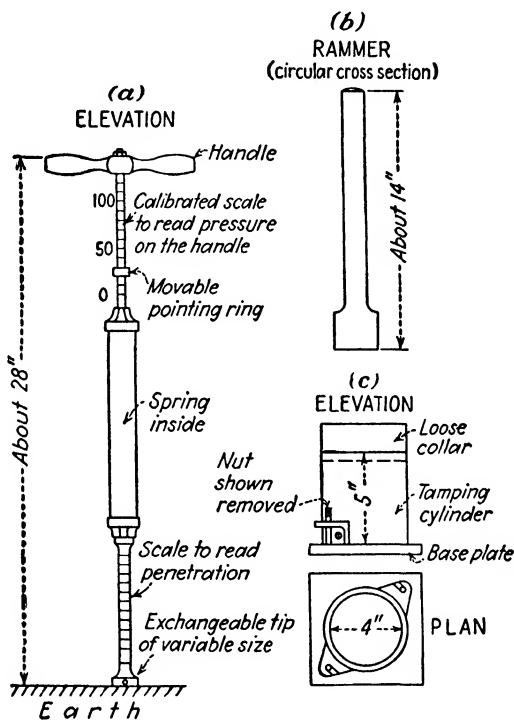


FIG. 9:35.—Proctor's plasticity needle.

22.0 per cent moisture content, furnishes the same dry weight and percentage of voids. In the former case the mass is hard; in the latter the particles may be movable (compare end, Sec. 9:38). It is obvious that in practice curve II only is needed. In many cases the optimum moisture content is not far from the plasticity limit (PL).

**9:40. Yield of a Borrow Pit.**—In the design of a large embankment it is necessary to establish beforehand the quantity of material that every borrow pit may yield and to prepare a plan

of attack as far as equipment and transportation means are concerned. This is important not only for prospective contractors but also for both design and construction engineers, since the factors mentioned influence unit prices and hence the total cost of the project.

In computing the yield of a borrow pit, it is necessary to establish the ratio of the volume of the excavation to the volume of the prospective embankment. This can be done experimentally only by comparing the volume of a small experimental excavation with the volume of the fill made from it. In glacial zones, natural soil is not at its densest state and, when placed in the fill under compaction, may decrease in volume ("shrink"). For instance, most Connecticut sandy and gravelly soils "shrink" 12 to 15 per cent in the fill. On some occasions this is not a decrease but an increase in volume as compared with the borrow pit. Such a phenomenon happens, for instance, when material is extracted early in the spring from a borrow pit with a considerable silt content and when the local water table is shallow. The reason for this phenomenon is the pumping of moisture from the underlying strata during the frost hours (compare end of Sec. 3:21). Thus this moisture is transported in trucks together with earth and contributes to the increase in volume of the fill. The latter will settle as it dries out.

**9:41. Preparing Soil Mixtures from Different Borrow Pits.**— In this section principles for the preparation of soil mixtures as used in highway engineering will be explained.

In such soil mixtures three kinds of materials are used:

- a. *Coarse aggregate* retained on a No. 10 sieve and consisting of gravel or crushed stone.
- b. *Fine aggregate* passing a No. 10 sieve but retained on a No. 200 sieve (stone dust, sand).
- c. *Binder*, passing sieve No. 200 (silt and clay).

As an example, a mixture containing 45 per cent of coarse aggregate, 43 per cent of fine aggregate, and 12 per cent of silt or clay is to be made. Suppose that none of the three local borrow pits X, Y, Z satisfies these specifications, so that material from different borrow pits is to be mixed to obtain the proper proportion. Let the characteristics of the three borrow pits be as shown in the opposite table.

An equilateral triangle is constructed as shown in Fig. 9:36. This is a peculiar system of coordinates, each side of the triangle

Content of sample	X, per cent	Y, per cent	Z, per cent
Coarse aggregate.....	20	100	10
Fine aggregate.....	70	0	40
Silt and clay.....	10	0	50
Total.....	100	100	100

representing the percentage of one of the three aggregates referred to. Points X, Y, and Z, representing the three local borrow pits, and also point A, corresponding to the mixture to be prepared, are plotted in this system of coordinates. It is to be noticed that each point on a line joining two points within the triangle (Fig. 9:36) represents a mixture of the two samples, corresponding to the ends of that line. Thus a point B on line XY is the mixture

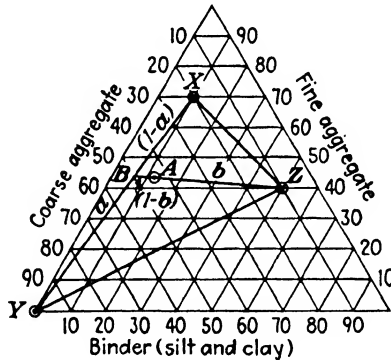


Fig. 9:36.—Proportioning a soil mixture.

of samples X and Y, made in proportion  $BY:BX = a:(1 - a)$ . Hence the given problem is easily solved simply by drawing a straight line through Z and A to intersect line XY. Introduce designations  $AZ = b$  and  $AB = 1 - b$ . Then the proportion of the materials to be taken from the borrow pits X, Y, Z is

X.....	$ab \times 100$
Y.....	$(1 - a)b \times 100$
Z.....	$(1 - b) \times 100$
Total.....	100%

It is often required that the plasticity index (PI) of the mixture be below a certain value, for instance, 6 per cent of that part of the sample passing No. 40 sieve (compare Sec. 2:17). In order to keep the plasticity index of the mixture below the standard referred to, the designer is sometimes obliged to modify the proportion obtained by the method shown in Fig. 9:36.

**9:42. Control of Materials during the Construction of an Embankment.**—Since the design of an embankment is based on the ratio between different kinds of earth materials, it is of extreme importance to maintain this ratio more or less constant during the construction. For this purpose, when a large embankment such as an earth dam is being constructed, a field soil laboratory is established. It checks incessantly both the arriving materials and those already placed into the fill, in the same way that checking is done in metallurgical or chemical factories.

Samples for analysis are taken both in the borrow pit and on the dam. The examination of the borrow pits consists usually of visual inspection and of occasional mechanical analysis. In the case of a hydraulic fill, periodic tests are made on the hog-box samples to check whether or not mixing is being done properly, mostly so far as grain size is concerned. Furthermore, core samples are extracted and tested for grain-size distribution and water content; this furnishes an indication of the trend of consolidation. Voids ratios and permeability are also determined; occasionally shear tests are made. Inspectors on the job make soundings with metallic rods or pipes. The purpose of these soundings is to give indications regarding the process of consolidation and also to discover intrusions or tongues as shown in Fig. 9:18.

In the case of a rolled-fill dam, mechanical analysis and permeability tests are undertaken. Voids ratios are determined, and Proctor needle tests are made both in the laboratory and in the field.<sup>26</sup>

## F. EARTH-DAM FAILURES

**9:43. Kinds of Earth-dam Failures.**—According to Justin,<sup>13d</sup> failures of earth dams are due mostly to overtopping (39 per cent of cases). This means that spillways of the dams that failed were too economically designed. A considerable percentage of failures is due to leakages of all kinds, and slides as such cause only about 5 per cent of all failures.

Hydraulic-fill dams sometimes fail because of the bursting of

liquid cores. Rapid drawdown of the water in the reservoir may be the cause of an upstream failure. Downstream failures may be due to percolation and erosion. If the dam is not compacted enough, internal lubrication and consequent sliding may happen. Defective and weak foundations may cause both upstream and downstream failures.

**9:44. Earth-dam Failures.**—*a. Calaveras Dam Failure.*—This California dam was still under construction when the slip occurred on Mar. 24, 1918. The height of the dam was 185 ft. out of a total designed height of 240 ft. The upstream face was 1:3, faced with  $3\frac{1}{2}$  in. of concrete. The hydraulically placed core occupied about one-fourth of the total width of the dam as measured at the base, the latter being 1,312 ft. wide. Gradual movings in the upstream face, reaching about 4 ft., were noticed before failure, which occurred rather suddenly. The upstream face slid into the reservoir by moving some distance upstream and rotating about an end. The core material, which contained up to 65 per cent of water by volume, flowed out. It scoured a path through the underlying sluiced gravel to the bottom of the valley. All the fill material, placed by cart in the downstream part of the embankment, remained standing.

It seems that clay layers underlying the upstream toe may have had considerable to do with the slip, since they lubricated the surface of the slide. The basic cause of the failure was internal pressure in the core; in addition, the core was too wide. For further details, see ref. 13a.

*b. Fort Peck Failure.*—The Fort Peck Dam is located on the Missouri River in northeastern Montana. Actual construction of the dam was nearly completed when the slide occurred. Both upstream and downstream toes of the dam are fills of  $\frac{1}{2}$ - to 6-in. gravel. Bedrock consists of Bear Paw shale, a firm shale interspersed with thin layers of bentonite. Practically the entire base of the dam was covered with a clay blanket, underlain by a pervious and stable sand. The clay blanket was stripped off; this operation involved the removal of over 4,000,000 cu. yd. of material.

The construction of the fill had been effected by the hydraulic method, with four electrically operated dredge units built at the site of the work. In the construction of hydraulic-fill dams there is always a possibility of a loss of the core pool (compare Fig. 9:14) due to its overtopping or breaking through the shell—as, by

the way, happened at the Calaveras Dam. To minimize the possibility of such a loss at Fort Peck, an alarm system was installed along the entire upstream face of the dam. Its purpose was to stop the work of the dredges and hence the flow of the liquid to the pool in case of danger. In the morning of the day of failure, Sept. 22, 1938, a settlement of the fill at a certain place of the upstream face was observed; the failure itself happened in the afternoon. An official description of the failure follows.<sup>27</sup>

The core pool began to settle, slowly at first and then rapidly. Immediately following this, or simultaneously, cracks generally parallel to the axis were observed on the upstream face about 30 ft. below the crest. Then portions of the upstream shell nearest the pool began to slide into the sinking core pool. In a lesser degree, similar cracks and sliding and slumping were taking place on the upstream portion of the downstream beach. Simultaneously with this development, the main mass of the upstream shell, almost intact, was moving out into the reservoir, in a swing similar to that of a gate hinged at the east abutment.

According to a statement of the board of consulting engineers retained for this occasion, the failure occurred because the shearing resistance of the weathered shale and bentonite seams in the foundation was insufficient to withstand the shearing stress to which the foundation was subjected. Thus the Fort Peck failure is to be considered as an upstream failure that took place because of a defective foundation. The slide lasted about 10 min. It involved a movement of about 5,000,000 cu. yd. and caused the death of eight men. The dam has been reconstructed, taking advantage of the natural slopes of the material after the slide. Thus the slopes of both the upstream and the downstream faces are variable, fluctuating from 1:3.3 to 1:50.

*c. The Belle Fourche Failure.*—The Belle Fourche Dam in South Dakota failed in 1933, following two very dry seasons during which the water level in the reservoir was considerably lowered to provide water for irrigation purposes. Immediately preceding the slide, the rate of drawdown was 25 ft. in 60 days (“sudden drawdown”). Consequently, a 600-ft. length of the upstream face slumped into the reservoir. (For more details, see *Engineering News-Record*, vol. 111, 1933.)

*d. San Gabriel Dam Settlement.*—The dam in question is one of the two similar San Gabriel Dams labeled Dam No. 2. This is a rock-fill dam 265 ft. high, and the rock was placed in it in 25-ft.

lifts. In order to facilitate the movement of the trucks, about 6 in. of earth material was laid down and compacted. The upstream slope of the dam was faced with a placed rock slab overlain by a concrete slab and gunite facing. After severe rains at the end of 1933 and the beginning of 1934, the dam settled very seriously, mostly in the upstream part, and the facing cracked. It was replaced by a flexible wooden slab, and the dam itself was thoroughly jetted; this prevented further settlement. It is to be noticed that jetting of embankments to prevent settlement is also practiced in highway work. (The long and interesting story of the San Gabriel dams may be found in different volumes of *Engineering News-Record*, between the years 1915 and 1938.)

*e. Alexander Dam Failure.*—This dam was built in 1928–1930 on the island of Kanai, Hawaiian Islands, to create a water reservoir for irrigation purposes. Its height is 125 ft., top width 20 ft., upstream slope 1:3, downstream slope 1:2. The dam was constructed by the hydraulic-fill method. The material used was a thoroughly decomposed volcanic ash of considerable specific gravity (compare Sec. 1:11). Analyses indicated that the core material was quite fine (70 per cent finer than 0.005 mm.), indeed finer than in most dams of this type. When the dam under construction reached a height of about 95 ft., a sudden failure took place. The downstream face bulged out, moved forward, and released a gush of liquid mud. The core pool settled following the downstream face, which slumped out, removing about 250,000 cu. yd. of earth. Failure was thought to be due to the pressure of the semiliquid core, which broke the downstream shell. For further details see ref. 13a.

From the point of view of the sketch (Fig. 7:2) all failures described in Sec. 9:44 are due to insufficiency of the lateral support  $P_L$ , with the exception of the San Gabriel Dam settlement (insufficient vertical force  $R$ ).

**9:45. Dikes and Levees Failures.**—*a. Connecticut River Front Dike.*—The flood-control dike, a rolled earth fill parallel to the Connecticut River in Hartford, Conn., had been practically completed two weeks before the slide, which occurred on July 24, 1941. During this time sand from the river was sluiced into a highway fill between the new dike and the old one behind it, belonging to the Colt Arm plant. The height of the dike proper is variable, the average being around 30 ft. The soil conditions are (a) city

dump and silty sand, total thickness about 18 ft.; (b) varved clay, 45 ft.; (c) glacial till, 17 ft.; (d) rock. Apparently, owing to excess of water, the layer (a) and a part of layer (b) were weakened, and under the weight of the highway fill a rather shallow foundation failure took place. In this connection the sheet-piling cutoff at the toe of the dike was shifted 52 ft. toward the river, and a city sewer under the dike destroyed.<sup>33,34</sup>

*b. Pendleton Levee.*—In the fall of 1939 the Vicksburg Engineer District constructed a setback levee along the south bank of the Arkansas River, Pendleton, Ark.<sup>35</sup> The levee, 32 ft. high, was underlain by 4 to 9 ft. of fine sand, followed by a 12 ft. thick clay layer which rests on deep sand. At one point the proposed levee crossed Lake Lenox, the clay material at this crossing being very soft. The most rational way to ensure stability of the structure was to displace the clay. In view of this fact, construction of the levee on that foundation offered an opportunity to study the physics of the failure. Piezometric tubes to measure pore pressure were installed. The failure line started at the top of the levee and was practically tangent to the bottom of the clay layer. The failure itself was apparently caused by building up of pore pressure in the clay stratum near the toes of the structure in excess of the opposing forces, such as the weight of the overburden and its shearing strength. A similar failure took place approximately at the same time at Chingford, Essex, England.<sup>36</sup>

**9:46. Conclusions from Dam Failures.**—With exception of the Belle-Fourche Dam (case *c*, Sec. 9:44) which failed because of a rather sudden drawdown, all failures of earth dams described in the preceding sections occurred *during construction*. The material that is being placed into the dam is, so to speak, *an earth mass in the making* and does not possess due strength; but as the time passes, the earth material consolidates and becomes stronger (Secs. 9:22 and 9:29). In analyzing a proposed dam or studying a failure (Sec. 9:24) one should be very careful in assuming that the full shearing strength is mobilized all along the possible failure line. Also any overloading or eccentric loading of the foundation during construction should be avoided. In fact, a dam foundation sometimes may be overturned as easily as a bowl in the kitchen.

In constructing a hydraulic-fill dam exclusive use of very fine materials should be avoided, since they consolidate very slow

(Alexander Dam, Sec. 9:44). The slopes of the core must be rather steep.

Attention should be paid to possible weakening of the foundation by an excess of water used in sluicing (Hartford Dike, Sec. 9:45).

The example of the Pendleton levee illustrates the possibility of a failure according to Fig. 9:25. Either clay material may be squeezed out bodily from underneath the structure,<sup>35</sup> or excessive pore pressure may be built up at the toes, as stated in Sec. 9:45. Imagine a rubber bag in the form of a sausage filled with water. If pressed heavily at the middle, it possibly will fail not under the pressing hand but at the ends, which in a dam or in a levee corresponds to a toe failure.

Finally, rock dams so attractive at the first glance because of their apparent stability may become a source of permanent trouble due to continuous settlement (San Gabriel dams, Sec. 9:44).

**Problems**

1. Consider the triangular cross section of an earth dam with a base of 297.5 ft. and a height of 50 ft. Determine the ratio in which the maximum shearing stress in the foundation would change if the height of the dam were 55 ft., the base remaining the same. Consider the foundation as a semi-infinite elastically isotropic body. Ans. 1.1.

2. Consider the failure of the Marshall Creek Dam in Kansas (*Eng. News-Record*, Sept. 30, 1937, p. 532). Read this article, and assume that the failure is due to the plastic flow of the layer of blue clay, 30 ft. thick, and that this layer reposes on a "rigid boundary." Make your own assumption as to the depth of the loess layer overlying the clay, and estimate roughly the shearing value of the clay material.

3. For the design of a levee in the lower Mississippi Valley (see ref. 4, p. 1391), the following data were used:

Height at the center . . . . .	34.5 ft.
Thickness of plastic layer in foundation (this layer reposes on "rigid bound- ary") . . . . .	23 ft.
Shearing value of plastic layer . . . . .	0.155 tons per sq. ft.

Allow for a crown width of 10 ft., and design the slopes of the levee from the condition of stability of the plastic layer with a factor of safety 1½. *Ans.* About 4½ : 1, assuming the unit weight of earth material  $\gamma = 100$  lb. per cu. ft.

4. To compute the shearing stress at a rigid boundary at a depth  $h$  under the ground surface, the stress being caused by a uniform load  $p$  acting at an infinitely long strip  $2b$  wide, the Carothers formulas are used:

$$\tau_{xz} = \frac{1}{2}p \left( \operatorname{sech} \frac{\pi}{2} \frac{x+b}{h} - \operatorname{sech} \frac{\pi}{2} \frac{x-b}{h} \right)$$

Distances  $x$  are measured from the center of the strip. Determine the value of the shearing stress under the toe of an embankment 200 ft. wide ( $2b = 200$  ft.) and, as an average, 20 ft. high, if the thickness of the plastic layer is 20 ft. Assume the unit weight of the earth material  $\gamma = 100$  lb. per cu. ft. Use tables of hyperbolic functions, remembering that sech is the reciprocal of cosh.

*Ans.* Approximately  $\frac{1}{2}$  ton per sq. ft.

5. Explain why the solutions of the problems offered in this chapter must be considered as very rough approximations only.

#### References

1. C. F. STEWART SHARPE: "Landslides and Related Phenomena," Columbia University Press, New York, 1938.
2. G. E. LADD: Landslides, Subsidences and Rock Falls, *Am. Ry. Eng. Assoc. Bull.*, vol. 36, p. 377, 1935.
3. M. FRONTARD: Cycloïdes de glissement des terres, *Compt.-rend. acad. sci.*, Paris, 1922; also a paper, *Second Congr. of Large Dams*, Washington, D. C., 1936.
4. SPENCER J. BUCHANAN: Levees in the Lower Mississippi Valley, *Trans. A.S.C.E.*, vol. 103, 1938.
5. W. FELLENIUS: "Erdstatische Berechnungen mit Reibung und Kohäsion (Adhäsion)," Wilhelm Ernst und Sohn, Berlin, 1927.
6. DONALD W. TAYLOR: Stability of Earth Slopes, *Jour. Boston Soc. Civil Eng.*, vol. 24, 1937.
7. JEAN RÉSAL: "Poussée des terres," C. Béranger, Paris, 1904-1911.
8. JOSEPH JÁKY: Stability of Earth Slopes, *Proc. Intern. Conf. Soil Mech.*, vol. 2, Paper G-9, 1936.
9. L. RENDULIC: Ein Beitrag zur Bestimmung der Gleitsicherheit, *Der Bauingenieur*, vol. 16, 1933.
10. K. CULMAN: "Die graphische Statik," Meyer and Zeller, Zürich, 1866.
11. Report of the Committee of the National Academy of Sciences on Panama Canal Slides, *Mem. Nat. Acad. Sci.*, vol. 18, 1924; also R. F. MACDONALD: Some Engineering Problems of the Panama Canal, *Bur. Mines, Bull.* 86, 1915; also A. S. ZINN: The Truth about Culebra Cut Slides, *Eng. News*, vol. 70, 1913.
12. J. D. GALLOWAY: The Design of Rock-fill Dams, *Trans. A.S.C.E.*, vol. 104, 1939.
13. CHARLES S. PAUL: Core Studies in Hydraulic Fill Dams in the Miami Conservancy District, *Trans. A.S.C.E.*, vol. 85, 1920; also ref. 13a.
- 13a. JOEL D. JUSTIN: "Earth Dam Projects," John Wiley & Sons, Inc., New York, 1932.
14. GLENNON GILBOY: Hydraulic Fill Dams, *First Congr. of Large Dams*, Stockholm, 1933; also *Jour. Boston Soc. Civil Eng.*, vol. 21, 1934.
15. THEODORE T. KNAPPEN: Calculation of the Stability of Earth Dams, *Second Congr. of Large Dams*, Washington, D. C., 1936.
16. LEO RENDULIC: "Der Erddruck im Strassenbau und Brückenbau," Volks Verlag, Berlin, 1938.
17. D. R. MAY and J. H. A. BRAHTZ: Proposed Methods of Calculating the

- Stability of Earth Dams, *Second Congr. of Large Dams*, Washington, D. C., 1936.
18. B. K. HOUGH: Stability of Embankment Foundations, *Trans. A.S.C.E.*, vol. 103, 1938.
  19. STANLEY M. DORE: Quabbin Dike Built by Hydraulic-fill Methods, *Trans. A.S.C.E.*, vol. 103, 1938.
  20. DONALD M. BURMISTER: A Study of the Physical Characteristics of Soils with Special Reference to Earth Structures, *Columbia Univ. Dept. Civil Eng. Bull.* 6, June, 1938.
  21. CHARLES H. LEE: Selection of Materials for Rolled-fill Earth Dams, *Trans. A.S.C.E.*, vol. 103, 1938.
  22. For the "Kendorko" soil classification see STANLEY M. DORE: Permeability Determinations, Quabbin Dams, *Trans. A.S.C.E.*, vol. 102, 1937.
  23. *Univ. Ill. Eng. Exp. Sta. Bull.* 137, Oct. 15, 1923.
  24. WILHELM LOOS: Comparative Studies of the Effectiveness of Different Methods for Compacting Cohesionless Soils, *Proc. Intern. Conf. Soil Mech.*, vol. 3, Paper M-5, 1936.
  25. R. R. PROCTOR: Four articles on Soil Compaction, *Eng. News-Record*, vol. 59, 1933.
  26. C. M. WESTON: Earth Embankments for the Pickwick Landing Dam, *Proc. Intern. Conf. Soil Mech.*, vol. 1, Paper M-2, 1936.
  27. Report on the Slide of a Portion of the Upstream Face of the Fort Peck Dam, Corps. of Engineers, U. S. Army, Washington, D. C., 1939.
  28. P. B. BUCKY and others: Centrifugal Method of Testing Models, *Civil Eng.*, vol. 5, 1935.
  29. R. G. HENNES: Analysis and Control of Landslides, *Univ. Wash. Eng. Exp. Sta., Bull.* 91, 1936.
  30. W. P. CREAGER, J. D. JUSTIN, and JULIAN HINDS: "Engineering for Dams," 3 vols., John Wiley & Sons, Inc., New York, 1945.
  31. R. E. GLOVER and F. E. CORNWELL: Stability of Granular Materials, *Trans. A.S.C.E.*, vol. 108, 1943.
  32. H. HENCKY: Article in *Z. angew. Math. Mech.*, vol. 3, 1923.
  33. Foundation Failure Causes Slump in Big Dike, Hartford, Conn., *Eng. News-Record*, vol. 127, 1941.
  34. "The Influence of Drain Wells on the Consolidation of Fine-grained Soils," U. S. Engineer Office, Providence, R. I., July, 1944.
  35. K. E. FIELDS and W. L. WELLS: Pendleton Levee Failure, *Trans. A.S.C.E.*, vol. 109, 1944.
  36. L. F. COOLING and H. W. GOLDER: The Analysis of the Failure of an Earth Dam during Construction, *Jour. Inst. Civil Eng.*, November, 1942.
  37. D. M. BURMISTER: Factor of Safety in Stability Analyses, *Civil Eng.*, vol. 16, 1946.

## CHAPTER X

### STABILITY OF RETAINING WALLS AND COFFERDAMS

The theory of retaining walls is the original chapter of soil mechanics from which this whole branch of engineering knowledge has been developed. Initial theories of retaining walls were formulated by Coulomb<sup>3</sup> in 1773, Poncelet<sup>6</sup> in 1840, and Rankine<sup>7</sup> in 1856 and were extended by other investigators, including Müller-Breslau.<sup>31</sup> In the past two or three decades most of the contributions to the theory of retaining walls have been made by Terzaghi,<sup>1,2,12</sup> besides him, the names of Parsons,<sup>13</sup> Jacob Feld,<sup>14</sup> Jenkin,<sup>15</sup> and others are to be mentioned. Many important papers and articles on construction and behavior of retaining walls are available in technical literature, including some old ones, as for example the outstanding paper by Benjamin Baker.<sup>4</sup>

**10:1. Lateral Pressure on the Wall.**—In all the discussions that follow, a retaining wall will be visualized as a two-dimensional structure. The backfill behind the retaining wall produces a lateral pressure (thrust) on the wall (designation  $F$ ). The thrust  $F$ , like any other force, is characterized by (a) magnitude, (b) direction, and (c) point of application (“center of pressure”). That part of the thrust which is caused by dry cohesionless soil will be designated with  $F_a$ ; that caused by water pressure—with  $F_w$ ; and that caused by the surcharge with  $F_s$ .

The determination of the thrust  $F$  is the chief problem in the analysis and design of a retaining wall. The value of the thrust acting on a retaining wall in the field is *variable* and depends mainly on the properties and moisture content of the backfill. However, a specific value for the thrust to be used in the design must be selected by the designer. In doing so, the designer uses as sources of information

a. Theoretical formulas.

b. Empirical knowledge from tests and observations on large models and full-sized structures.

c. Engineering experience and judgment of the designer himself and of the rest of the profession.

In establishing the value of the thrust, the designer tries to make the retaining wall, like any other structure, both *safe* and *economical*. The term "economical" in this sense means that the cost of erection plus the capitalized cost of maintenance of the structure, including both labor and material, should be a minimum.

There are two classes of retaining walls, namely, (a) *nonflexible* or *rigid* retaining walls such as masonry or concrete walls in which deflections may be neglected and (b) *flexible* walls made mostly of flexible sheet piles.

**10:2. Two Methods of Attack.**—Retaining walls are analyzed using either the Rankine formula (Sec. 5:7) or the Coulomb formula. The latter should not be confused with the other formula of the same author as discussed in Chap. V [formulas (5:9) and (5:11)]. The Rankine formula assumes that the direction of the thrust is *horizontal*, whereas the Coulomb formula takes into consideration also the vertical component of the thrust or, in other words, in a general case considers an *oblique* thrust. As a matter of fact, if the wall tends to move away from the backfill, the latter tends to slide down. This tendency is opposed by friction which develops at the backface of the wall, and this friction causes the vertical component of the thrust and makes the latter oblique.

**10:3. Source of Active Pressure.**—The lateral pressure on a perfectly immovable, indeformable, and frictionless wall obviously would be the same as the horizontal pressure within a natural earth mass made of the same material as the backfill. But little is known about the lateral pressure  $F_n$  in a natural earth mass. The reason is obvious: stresses within a body cannot be measured, and attempts to do so fail. Displacements *could* be measured, however, and stresses estimated from them. But in a natural earth mass these displacements have already been completed long ago and cannot be measured. It may be assumed that the value of the lateral earth pressure  $F_n$  differs but little from that computed using the Rankine or Coulomb formulas and that its distribution is triangular, *i.e.*, that it increases proportionately to the depth computed from the earth surface downward. Note that in reality both Rankine and Coulomb formulas correspond to the

state of plastic equilibrium, which takes place just before the failure of the mass by cracking or plastic flow, and the values computed using these formulas are somewhat smaller than the value of  $F_n$ . This is because to reach the state of plastic equilibrium the wall has to move somewhat from the backfill, and the shearing stresses (friction) opposing this motion decrease the value of  $F_n$ .

Since the horizontal pressure in an earth mass is the only source of the lateral pressure on the wall, it should be admitted that the total lateral pressure on the wall equals the corresponding value computed using the Rankine or Coulomb formula. But if the wall moves from the backfill within some reasonable limits or deflects too much, this pressure, still keeping its *total* value, may be *redistributed* along the height of the wall (compare division E of this chapter).

It is obvious that the natural earth pressure  $F_n$  itself (or the values replacing it as stated above) may grow larger if the weight of the backfill is increased either by a surcharge at its surface or by water filling its pores. Cohesion of the material or buoyancy due to submerged condition may decrease this value.

#### A. RANKINE FORMULA

The active pressure on a nonflexible (rigid) retaining wall from a horizontal backfill computed according to the Rankine formula is represented in Fig. 5:4a by the triangle  $ABD$  (triangular or hydrostatic pressure distribution). The point of application of its resultant (center of pressure) is located "at the third point" of the height of the wall ( $\frac{1}{3} h$  above base  $BD$ ).

Besides formula (5:7), the lateral pressure on a retaining wall is computed in engineering offices by the method of equivalent fluid.

**10:4. Method of Equivalent Fluid.**—Represent the Rankine formula (5:7) in the following form:

$$F = \frac{1}{2}wh^2 \quad (10:1)$$

where  $w = \gamma K_a$ . Since  $K_a$  is an abstract number,  $w$  has the same physical dimension as  $\gamma$ , *i.e.*, unit weight. The value of  $w$  is the unit weight of an "equivalent" fluid that, for computation purposes, is assumed to replace the earth behind the wall. As to the numerical value of  $w$ , it is often assumed in engineering offices at 30 lb. per cu. ft. or somewhat more. In general the U. S.

Engineer Department (Army Engineers) uses 33 lb. above water and 83 lb. below water level. It is evident that from the condition

$$w = \gamma K_a = \gamma \tan^2 \left( 45^\circ - \frac{\phi}{2} \right) \quad (10:2)$$

the value of the angle of friction  $\phi$  may be computed, and, vice versa  $w$  may be found if  $\phi$  is known.

It is obvious that the method of equivalent fluid, which is a slight modification of the Rankine formula, presupposes an idealized cohesionless fragmental material, a horizontal backfill, and the condition that friction of the backfill against the wall is neglected. In other words, the thrust  $F$  is assumed to be horizontal. In the case of a rather dry sandy or gravelly backfill, and if the value of  $w$  satisfies condition (10:2), this method may furnish quite satisfactory results.

**10:5. Lateral Pressure from a Surcharge.**—Lateral pressure from a surcharge  $p$  tons per sq. ft. at the horizontal surface of the backfill will be determined under the assumption that the pressure from the backfill as such is known (Secs. 10:3 and 10:4). Hence the backfill may be assumed weightless. The lateral pressure from the surcharge determined under this assumption should be then added to the lateral pressure from the backfill.

The surcharge  $p$  tons per sq. ft. evidently causes at each point of the backfill, independently of the depth, a vertical pressure  $p$  tons per sq. ft. Hence the lateral pressure at any point of the wall is  $K_a p$  (Fig. 10:1), and the resultant of this pressure  $F_s$  is

$$F_s = K_a p h \quad (10:3)$$

Its point of application is located at the middle of the height of the wall. The lateral pressure from the backfill as such being

$$F_a = \frac{1}{2} K_a \gamma h^2 \quad (10:4)$$

the value of the full thrust is

$$F_a + F_s = \frac{1}{2} K_a \gamma h^2 + K_a p h = \frac{1}{2} K_a \gamma h^2 \left( 1 + \frac{2p}{\gamma h} \right) \quad (10:5)$$

Its point of application can be easily found by equalizing the sum of the moments of the forces  $F_a$  and  $F_s$  to the moment of their sum  $F_a + F_s$ , about the top or the bottom of the wall. Evidently,

this point of application is located above the third point. The larger the surcharge the higher that point of application.

**10:6. Lateral Pressure from a Cohesive Backfill.**—If the cohesive backfill did not possess cohesive properties, the lateral pressure exerted by it on the wall would be expressed by formula (5:7) or (10:4). Graphically this is area  $ABC$  (Fig. 10:2). Cohesion decreases this pressure. To determine this decrease, it should be

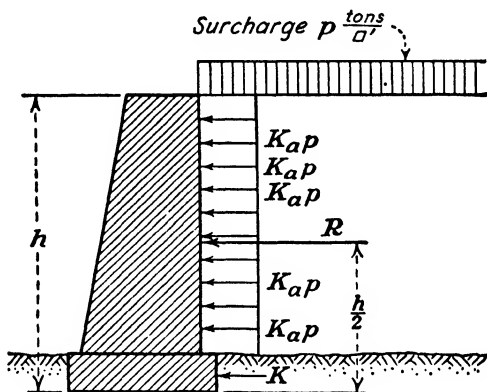


FIG. 10:1.—Lateral pressure from a surcharge.

realized that to withstand the crushing tendency of the weight of the backfill, at each point of it a uniformly distributed ultimate compressive strength  $-q$  is available. The sign "minus" means that the stress  $-q$  is directed upward, *i.e.*, against gravity. The stressed condition thus created is analogous to that which would be caused by a hypothetical *negative* surcharge  $-q$  at the horizontal surface of the backfill. Hence the lateral pressure from a cohesive backfill may be directly obtained from formula (10:5) by substituting  $-q$  for  $p$ :

$$F = F_a - F_s = \frac{1}{2} K_a \gamma h^2 \left( 1 - \frac{2q}{\gamma h} \right) \quad (10:6)$$

Symbol  $F_s$  in formula (10:6) corresponds to the decrease of pressure  $F_a$  due to cohesion. Graphically  $F_s$  is expressed by area  $A E F B$  in Fig. 10:2.

Obviously a cohesive backfill exerts no pressure on the retaining wall if

$$1 - \frac{2q}{\gamma h} = 0 \quad (10:7)$$



Combining Eq. (10:6) and (10:9) and designating with  $F$  the lateral pressure from a cohesive backfill, its value would be represented under the form well known to many engineers:

$$F = \frac{1}{2}\gamma h^2 \tan^2 \left( 45^\circ - \frac{\phi}{2} \right) - 2ch \tan \left( 45^\circ - \frac{\phi}{2} \right) \quad (10:6a)$$

When, under some given circumstances, the lateral pressure on a retaining wall is determined, using formula (10:6a) or some other formula containing the values of  $\phi$  and  $c$ , these values should exactly correspond to the given circumstances. Good judgment should be exercised in using the values of  $\phi$  and  $c$  as determined by shearing tests.

**10:7. Corrections to Formula (10:6).**—Refer to Fig. 10:2. In reality the compressive strength available above point  $D$  is not fully utilized. It is assumed, however, that the excess of compressive strength above point  $D$  is used to compensate its deficiency below that point. In other words, it is assumed that the whole bank  $AB$  behaves as a unit.

A formula identical with (10:6) was originally proposed by Peck on the basis of his work on the Chicago subway.<sup>32</sup> Peck states that the value of  $q$  from a series of nonconfined compression tests in a laboratory is higher than the average of that strength at different points of the sliding surface. This is because a small laboratory sample behaves as a unit and all points of it reach its maximum resistance under load simultaneously whereas in the field this is not the case. Hence, instead of the value  $q$  a corrected value  $nq$  should be used. For Chicago subway conditions the correction factor  $n$  equals 0.75. Besides this, the use of an overall correction factor 1.2 is recommended so that the final shape of formula (10:6) will be

$$\begin{aligned} F &= 1.2\frac{1}{2}\gamma h^2 K_a \left( 1 - \frac{2nq}{\gamma h} \right) \\ &= 0.6\gamma h^2 \tan^2 \left( 45^\circ - \frac{\phi}{2} \right) \left( 1 - \frac{2nq}{\gamma h} \right) \end{aligned} \quad (10:12)$$

If  $\phi$  is close to zero, as in the case of nonconsolidated plastic clays, formula (10:12) becomes

$$F = 0.6 \gamma h^2 \left( 1 - \frac{2nq}{\gamma h} \right) \quad (10:12a)$$

With exception of formulas (10:12) and (10:12a) there is no more or less reliable way, at least at the present time (1947), to estimate wall pressure exerted by a cohesive backfill on a wall other than to deduce conclusions from large-scale experiments and especially from observations on full-sized structures.

**10:8. Lateral Pressure from a Submerged Backfill.**—If the backfill is placed hydraulically or is otherwise fully saturated or submerged, three thrusts should be superimposed:

a. *Full hydrostatic pressure*  $F_w$  exerted on the wall by pore water. It acts as if there were no soil at all in the backfill. Designating

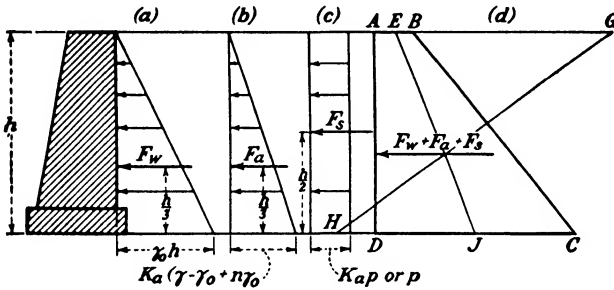


FIG. 10:3.—Lateral pressure from a submerged backfill.

the unit weight of water by  $\gamma_0$  the value of the hydrostatic pressure is (Fig. 10:3a)

$$F_w = \frac{1}{2} \gamma_0 h^2 \tag{10:13}$$

b. *Lateral pressure*  $F_a$  exerted on the wall by the *earth material*, the weight of the latter being relieved by buoyancy. The weight of perfectly dry soil is  $\gamma$  lb. per cu. ft. If the porosity of the soil is  $n$ , the volume occupied by soil grains is  $(1 - n)$  cu. ft. per cu. ft. of material. Buoyancy acts on this volume only so that the unit weight of the earth material relieved by buoyancy is  $\gamma - (1 - n) \gamma_0 = \gamma - \gamma_0 + n\gamma_0$ . For approximate computations the value of  $n$  may be assumed at  $\frac{1}{3}$  for sands and  $\frac{1}{2}$  for clays. The weight of water in the pores is taken care of by formula (10:13). The lateral pressure from the earth material (Fig. 10:3b) is

$$F_a = \frac{1}{2} K_a h^2 (\gamma - \gamma_0 + n\gamma_0) \tag{10:14}$$

It goes without saying that if the backfill is not submerged, but wet with capillary moisture, no allowance for buoyancy should be made.

c. *Lateral pressure*  $F_s$  caused by the *surcharge* ( $p$  tons per sq. ft.). If the backfill is cohesionless, such as sand, the unit pressure from the surcharge is  $K_a p$  (Sec. 10:5). In this case the lateral pressure from the surcharge is transmitted to the wall by the rigid skeleton of the soil. If, however, the skeleton of the backfill is flexible as in the case of clay, the full value of the surcharge  $p$  is transmitted to the wall by the pore water (Sec. 6:5). The lateral pressure from the surcharge will be for rigid and flexible soil skeleton, respectively (Fig. 10:3c):

$$F_s = K_a p h$$

or

$$F_s = p h \quad (10:15)$$

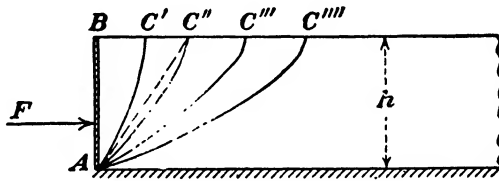


Fig. 10:4.—Coulomb's problem

The full thrust on the wall equals the sum  $F_w + F_a + F_s$  and is represented graphically by the trapezoidal area  $ABCD$  (Fig. 10:3d). The position of its point of application may be found graphically by plotting  $BG = DC$  and  $DH = AB$  and finding the point of intersection of line  $GH$  with line  $EJ$  joining the mid-points of the sides  $AB$  and  $DC$  of the trapezoid. The point of application in question is located above the third point (compare also end, Sec. 10:5).

## B. COULOMB FORMULA

**10:9. Statement of the Problem.**—In a paper presented to the French Academy of Sciences in 1773, Coulomb<sup>3</sup> considered the backfill as an undeformable (but breakable) body; hence in his discussion the conception of "strain" is not used at all.

Coulomb's problem is tantamount to the following: Given an indefinitely long supported body (Fig. 10:4), its unit weight, its angle of internal friction  $\phi$ , and the unit cohesion  $c$ , determine force  $F$  to be applied to this body through a weightless plane  $AB$  in order to keep the body in question in equilibrium. If no force  $F$  is applied, failure will happen along one of the curved lines  $AC'$ ,  $AC''$ ,  $AC'''$ , . . . , for instance, along  $AC''$ . In such a case the

horizontal component  $F'$  of all forces acting on the wedge  $ABC''$  should be computed, and this will be the answer to the problem.

**10:10. Derivation of the Coulomb Formula.**—Coulomb understood perfectly that the failure line is a curve but, for the sake of convenience, assumed it straight (dotted line  $AC''$  in Fig. 10:4).

Figure 10:5 shows a case of horizontal backfill, with no friction between the wall and the backfill. The wedge  $ABC$  is separated from the rest of the mass by the failure line  $AC$ , forming an unknown angle  $x$  with the horizon. Just before this failure line is formed, the wedge  $ABC$  is in the state of limit equilibrium

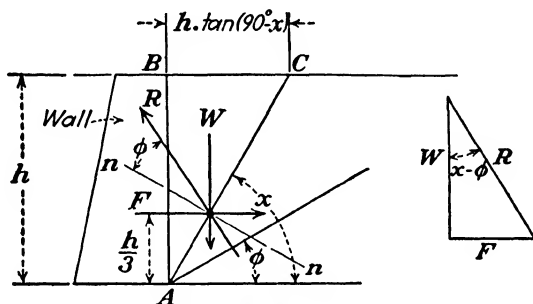


FIG. 10:5.—Equilibrium of the wedge in the case of a horizontal backfill.

under the action of the following forces: (a) its weight  $W$ ; (b) reaction  $F$  of the wall equal and opposite to the thrust  $F$ , acting normally to the backside of the retaining wall; and (c) reaction  $R$  of the rest of the earth mass, this reaction making an angle  $\phi$  with the normal to the side  $AC$ . The three forces  $W$ ,  $F$ , and  $R$  are concurrent. It follows from the plan of forces (Fig. 10:5, at the right) that

$$F = W \tan (x - \phi) \tag{10:16}$$

The weight of the wedge  $ABC$  is

$$\begin{aligned} W &= \frac{1}{2} \gamma h^2 \tan (90^\circ - x) \\ &= \frac{1}{2} \gamma h^2 \cot x \end{aligned} \tag{10:17}$$

where  $\gamma$  is the unit weight of the given material. From Eqs. (10:16) and (10:17)

$$F = \frac{1}{2} \gamma h^2 \cot x \tan (x - \phi) \tag{10:18}$$

Since the  $\frac{1}{2} \gamma h^2$  is a constant, thrust  $F$  is greatest when the product  $\cot x \tan (x - \phi)$  is at a maximum, and this happens when

$$x = 45^\circ + \frac{\phi}{2} \tag{10:19}$$

Taking the value of  $x$  from Eq. (10:19) for Eq. (10:18),

$$F = \frac{\gamma h^2}{2} \tan^2 \left( 45^\circ - \frac{\phi}{2} \right) \quad (10:20)$$

which *exactly coincides with the Rankine formula* for the case of horizontal cohesionless backfill.

The foregoing is a simplified presentation of the Coulomb formula in which friction at the backface of the wall and cohesion in the mass are neglected. In reality, Coulomb considered also cohesion along the failure line. This circumstance *does not influence the position of the failure line*, however, but diminishes the value of the thrust [compare formula (10:6a) which follows formula (10:11)].

In all cases the point of application of the resultant of the thrust  $F$ , computed according to the Coulomb formula, is assumed to be at the third point of the height of the wall, and the distribution of pressure is assumed to follow a triangular (hydrostatic) law. Coulomb's purely geometrical approach to the solution of this problem provoked a series of geometric constructions both in France and in Germany, whereas engineers in the English-speaking countries mostly made use of the Rankine formula.

**10:11. Lateral Pressure in the Case of an Irregularly Surfaced Backfill.**—Coulomb also considered the angle of friction  $\phi_1$  between earth and wall.\* Generally the back face of the wall makes an angle  $\theta$  with the horizon. In Fig. 10:6a the thrust  $F$  is determined graphically for the general case when  $\phi_1 > 0$  and  $\theta \geq 90^\circ$ . The value of the angle made by the probable failure line (crack)  $AC$ , with the horizon, is designated by  $x$ . The surface of the backfill may be assumed to be arbitrary. In Fig. 10:6b line  $AD$  is traced to make an angle  $\phi$ , that of friction, with the horizon. Furthermore, line  $CD$  makes an angle  $\theta + \phi_1$  with line  $AD$ . Triangle  $ACD$  in Fig. 10:6b and plan of forces  $A'C'D'$  in Fig. 10:6a are similar, since the respective angles of these triangles are equal. Hence ratio  $CD/AD$  equals ratio  $C'D'/A'D' = F/W$ . In other words, to determine the value of the oblique lateral pressure  $F$  corresponding to crack  $AC$ , it is necessary to measure the area of wedge  $ABC$  and to multiply it by the product  $\gamma \overline{CD}/\overline{AD}$ , where  $\gamma$

\* Notice the difference in designations between  $\phi_1$  and  $\phi'$ , the latter being that of the angle of repose.

is the unit weight of the soil. The position of crack  $AC$  furnishing the maximum value of  $F$  may be found by successive approximation.

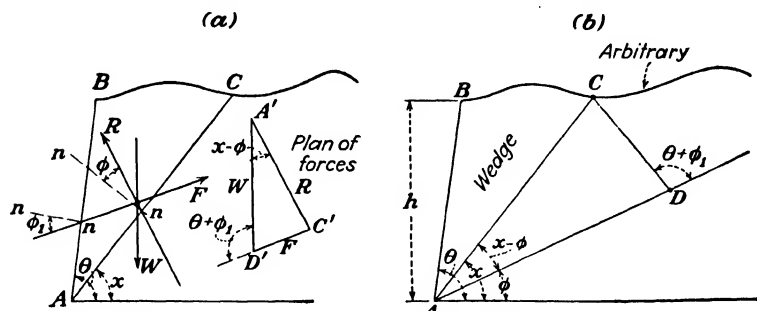


FIG. 10.6.—Lateral pressure in the case of irregularly surfaced backfill.

Should the surface of the backfill be a plane making an angle  $i$  with the horizon, the position of the crack corresponding to the maximum lateral pressure  $F$  would be found by trial and error, making areas  $ABC = A_1$  and  $ACD = A_2$  equal (Fig. 10.7a).

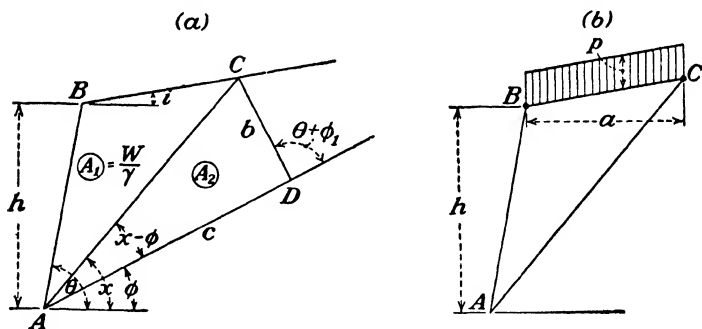


FIG. 10.7.—Rebhann's theorem.

Introduce, for convenience, the designations  $\overline{CD} = b$  and  $\overline{AD} = c$ . Then the value of the lateral pressure

$$\frac{\overline{CD}}{\overline{AD}} W = \frac{\overline{CD}}{\overline{AD}} A_1 \gamma = \frac{b}{c} A_1 \gamma \quad (10.21)$$

On the other hand,

$$A_2 = \frac{1}{2} bc \sin(\theta + \phi_1) \quad (10.22)$$

Combining Eqs. (10.21) and (10.22),

$$F = \frac{A_1}{c} \times \frac{A_2}{c} \times (\text{const.}) \quad (10.23)$$

It may be shown that in this particular case the product  $F$  is at a maximum if both variable factors  $A_1/c$  and  $A_2/c$  are equal, and this means that

$$\text{Area } A_1 = \text{area } A_2 \quad (10:24)$$

Statement (10:24) is termed *Rebhann's theorem*.<sup>5</sup> It may be generalized for the case of an arbitrary ground surface and also for the case when there is a uniformly distributed surcharge of  $p$  tons per sq. ft. of the surface of the backfill. If we designate the width of the wedge  $BC$  by  $a$ , the total surcharge is  $pa$  (Fig. 10:7b). The wedge carries a load  $\gamma'$  per square foot of area  $A_1$ ,

$$\gamma' = \gamma + \frac{pa}{A_1}$$

and the generalized statement (10:24) would be

$$A_1\gamma' = A_2\gamma \quad (10:25)$$

In this connection it is convenient to remember that the lateral pressure on the wall caused by a concentrated load has been already discussed in Sec. 4:27.

Rebhann's theorem was published in Germany in 1871; but about 30 years before, Poncelet<sup>6</sup> in France had come to similar conclusions. Besides a graphical construction, Poncelet derived an analytical formula, which is given here as a matter of information:

$$F = \frac{\gamma h^2}{2} \left[ \frac{\sin^2(\theta - \phi)}{\sin^2 \theta \times \sin(\theta + \phi_1) \left( 1 + \sqrt{\frac{\sin(\phi + \phi_1) \sin(\phi - i)}{\sin(\theta - i) \sin(\theta + \phi_1)}} \right)^2} \right] \quad (10:26)$$

Symbol  $h$  in formula (10:26) means the height of the wall;  $\gamma$  is the unit weight of the material; and  $i$  is the slope of the backfill as in Fig. 10:7a. Formula (10:26) is sometimes called the "Coulomb formula."

**10:12. Comparison of Numerical Results.**—The expression in brackets shown in formula (10:26) will be designated by the symbol  $(K_a)_c$ . For a vertical wall ( $\theta = 90^\circ$ ), a horizontal backfill ( $i = 0$ ), and no friction at the backface ( $\phi_1 = 0$ ), the value of  $(K_a)_c$  equals the Rankine value of  $K_a$  as already stated in Sec. 10:10. Assuming the angle of internal friction  $\phi = 32^\circ$ , the angle of friction of the earth material against the wall  $\phi_1 = \phi = 32^\circ$  (in reality,  $\phi_1 < \phi$ ), and the unit weight of earth material  $\gamma = 100$  lb. per cu. ft., the values of  $K_a$  and  $(K_a)_c$  are

$K_a = 31$  lb. per cu. ft.

$(K_a)_c = 28$  lb. per cu. ft.

Remembering that the weight of the equivalent fluid  $w$  is about 30 lb. per cu. ft. (Sec. 10:4) and that the horizontal component of the value  $(K_a)_c$  is less than 28 lb. per cu. ft., it should be concluded that under the given numerical conditions the Coulomb formula furnishes a more economical design whereas the Rankine formula and its modification—the method of equivalent fluid—are safer.

**10:13. General Wedge Theory.**—The “general wedge theory” as proposed by Terzaghi<sup>2</sup> is supposed to be a solution of a problem

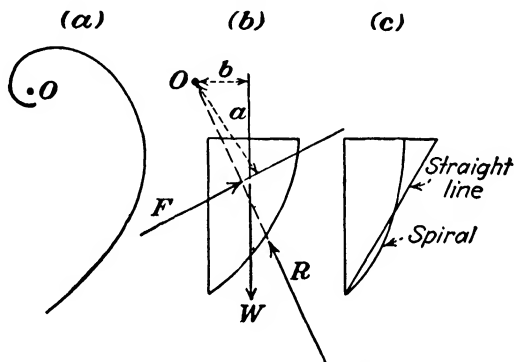


FIG. 10:8.—Logarithmic spiral-shaped wedge. (After Terzaghi.)

broader than Coulomb’s (Sec. 10:9). For a cohesionless backfill a surface of sliding (eventual failure line) is drawn with a vertical tangent at the earth surface (Figs. 10:8 and 10:9); the weight of the wedge  $W$  is computed; the thrust  $F$  is drawn under the angle  $\phi$ , that of internal friction, to the back face of the wall (see the beginning, Sec. 10:11); and the reaction of the mass  $R$ , which is the resultant of forces  $W$  and  $F$ , is drawn to make an angle  $\phi$  with a normal to the failure line (Fig. 10:8). If the failure line is a logarithmic spiral, reaction  $R$  passes through its origin  $O$ . The thrust  $F$  is found by taking moments of all forces about point  $O$ :

$$Fa = Wb \tag{10:27}$$

Since a logarithmic spiral may be very closely approximated by an arc of circle (Sec. 5:9), the designer of a retaining wall has to understand clearly whether or not in his case such a relatively complicated procedure as that described in this section is justified.

Particularly if the center of pressure on a retaining wall is at the third point, it is practically immaterial whether a curved or a plane wedge (as in the Coulomb formula) is considered, the difference in the results being about 6 per cent (Terzaghi<sup>2</sup>).

Von Kármán,<sup>9</sup> Jáky,<sup>10</sup> and Ohde<sup>11</sup> also made accurate computations of the true shape of the failure line and of the value of the earth pressure  $F$  and came to the conclusion that assuming a triangular wedge, the error involved is small. Figure 10:9 shows the true and the conventional shape of the wedge. According to

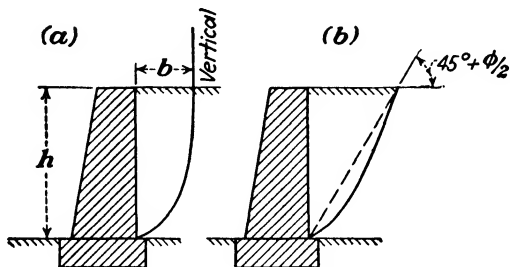


FIG. 10:9.—Two wedge types.

Peckworth,<sup>2</sup> the approximate ratio of the base  $b$  of the wedge (Fig. 10:9a) to its height  $h$  varies from 0.4 to 0.5.

### C. ANALYSIS OF NONFLEXIBLE WALLS

**10:14. Procedure.**—A nonflexible retaining wall, which is not expected to translate considerably, is dimensioned, and its dimensions and stability are analyzed. To analyze the dimensions of a wall, the full value of the thrust and its distribution along the height of the wall (lateral pressure diagram) should be known for computing moments and shears as in any other structure. This part of the analysis will not be considered here. So far as *stability* of a retaining wall is concerned, the wall is checked against (a) sliding (Sec. 10:15), (b) overturning (Sec. 10:16), and (c) overloading of the outer edge of the foundation due to the eccentricity of the resultant of the weight  $W$  of the wall and thrust  $F$ . The influence of such an eccentricity has been already discussed in Sec. 8:25.

**10:15. Sliding of a Retaining Wall.**—As the backfill is being erected by layers, the thrust is being built up. Consequently the wall moves, owing to the adjustment of the particles before the wall (black portions in Fig. 10:10). When the adjustment is

over, the wall is kept in place by the shearing resistance along a possible failure line (shearing surface)  $A'A''$ . Admittedly, another force preventing the wall from moving is friction at its base against the earth mass. The shearing strength of the material along line  $A'A''$  and friction are subject to variations due to weather conditions and should be kept as high as possible. Good drainage of the backfill must not be overlooked in this connection. Proper weep holes (weepers) are to be provided, and rock or gravel drainage is to be placed so as to prevent pressure of per-

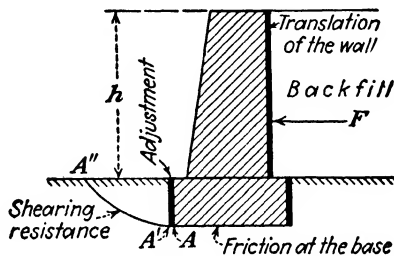


FIG. 10:10.—Sliding of a retaining wall.

colating rainstorm water from acting on the walls and thus decreasing their stability.

The condition of limit equilibrium of the wall with respect to sliding is, neglecting shear along line  $A'A''$ ,

$$F = Wf \tag{10:28}$$

where  $F$  = the horizontal component of the thrust.

$W$  = weight of the wall.

$f$  = the coefficient of friction of the base of the wall on underlying soil.

The average values of that coefficient of friction are as follows: masonry or concrete on gravel or coarse sand,  $f = 0.6$ ; masonry or concrete on soft clay,  $f = 0.3$ .

**10:16. Overturning of a Retaining Wall.**—Condition of limit equilibrium of a retaining wall with respect to overturning (Fig. 10:11) is

$$Fa = Wb \tag{10:29}$$

If there is a danger of overturning of the retaining wall together with the foundation, the corresponding checking should be done as in Sec. 9:11.

The expression "limit equilibrium" as used in Secs. 10:15 and

10:16 means that the value of  $F$  as computed in these sections is the possible maximum value of the thrust (safety factor = 1). If the actual design value of the thrust is introduced into Eqs. (10:28) and (10:29), corresponding safety factors may be computed.

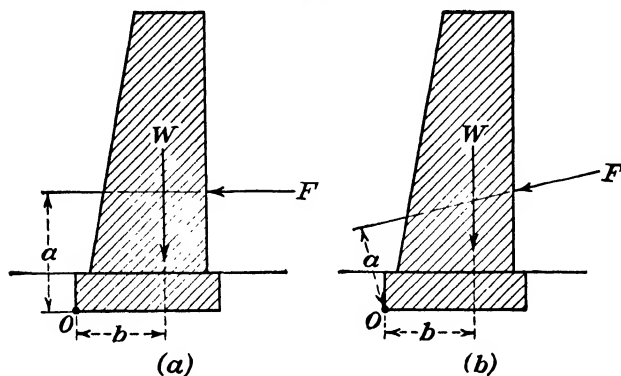


FIG. 10:11.—Overturning of a wall.

**10:17. Oblique Walls.**—Figure 10:12 represents schematically an oblique wall on a very exaggerated scale. In this case a part of the weight of the wall acts as a surcharge placed on the slope

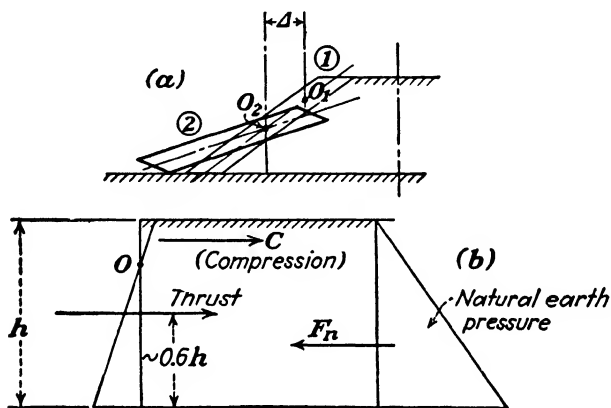


FIG. 10:12.—Tilting and sliding of an oblique wall.

of the fill. The wall passes from position 1 to position 2, and in this connection the upper part of the wall compresses the embankment (force  $C$ ). Ohde<sup>11</sup> found that in the case of the wall similar to that shown in Fig. 10:12, pressure is about 25 per cent higher

than that computed after Coulomb and that its point of application is rather high (about  $0.6h$  from the bottom). His findings seem reasonable and may be used in designing walls of the type shown in Fig. 10:12.

**10:18. Angle of Friction and Angle of Repose.**—In connection with the analysis of retaining walls it is convenient to emphasize the difference between the angle of internal friction  $\phi$  and the angle of repose  $\phi'$ . In many textbooks and handbooks used for determining the lateral pressure  $P$  the angle  $\phi$  is termed "angle of repose" instead of "angle of internal friction." The angle of internal friction  $\phi$  is somewhat larger than the angle of repose  $\phi'$ , and the difference between the two has been explained in Sec. 5:2. If, however, in a formula for lateral pressure containing a value of  $K_a$

$$K_a = \tan^2 \left( 45^\circ - \frac{\phi}{2} \right) \quad (5.5)$$

the value of  $\phi'$  instead of  $\phi$  is introduced, a somewhat larger lateral pressure would be obtained, and the result will be on the safe side. After all, the difference between the angle of internal friction and the angle of repose in the design and analysis of retaining walls is mostly a matter of terminology without serious practical significance. American engineers understood the difference between the angle of internal friction and the angle of repose many years ago. For instance, Paaswell in 1920 distinguished both of these angles.<sup>8</sup> There are also earlier statements to the same effect.

#### D. EXPERIMENTS WITH NONFLEXIBLE WALLS

**10:19. Terzaghi's Experiments with Retaining Walls.**—Terzaghi's large-scale experiments with retaining walls were made at the Massachusetts Institute of Technology<sup>12</sup> with a specially constructed bin, 14 by 14 ft. in ground plan and 7 ft. deep, which was closed at the front by a movable, exceedingly rigid metallic retaining wall, 14 ft. long and 7 ft. high. The experiments were carried on with different kinds of backfill. In the discussion that follows, the symbol  $h$  designates the height of the experimental wall.

*a. Backfill of Dry Sand.*—In this case uniform, medium, angular sand was used (effective size, 0.54 mm.; uniformity coefficient, 1.70). The value of the "coefficient of pressure at rest" (Sec. 4:25) was 0.4 in the case of loose sand and reached 0.6 to 0.7 in the case of compacted sand. The angle of repose of this material was  $34^\circ$ .

Apparently, compaction of the fill caused deflections of the wall, perhaps exceedingly small, and hence contact (passive) pressures. The outward motion of the wall was accompanied by its elastic recovery and considerable drop in contact pressure. Since the fill was compacted, only a relatively small number of sand grains followed the moving wall, hence exceedingly low values of  $K_a$  at the end of the experiment (about 0.1 or 0.2 instead of about 0.3, as could be expected). The point of application of the pres-

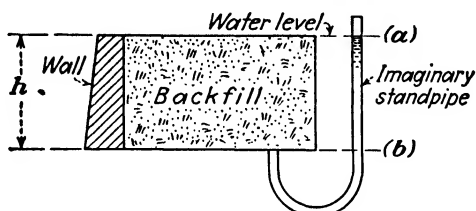


FIG. 10:13.—Submerged (a) and drained (b) backfill.

sure was above the third point in the beginning of the motion and close to it (even below) afterward. In the case of loose sands, the point of application of the lateral pressure was about the third point.

Terzaghi noticed that during intermissions there was a decrease of the coefficient of the wall friction (which was measured as the ratio of the vertical component of the pressure to its horizontal component), an increase in the Rankine active value  $K_a$ , and in general a slight rise of the point of application of the lateral pressure. These results have been obtained before by Feld (Sec. 10:20).

*b. Backfill of Saturated Sand.*—The sand material as described above was submerged and drained, and the horizontal pressure corresponding to these states was determined. When submerged, the sand contained 25 per cent of water by dry weight, and the moisture retained in the drained material amounted to 2.5 per cent by dry weight. The term “submerged” means that the water level in an imaginary piezometric standpipe connected with the sand coincides with the top of the backfill (Fig. 10:13), whereas it drops to the level of the bottom of the backfill if the latter is completely drained.

The presence of the sand behind the wall *has no influence whatsoever* on the intensity of the water pressure. This complete independence between the action of the water and the sand has

been demonstrated by Parsons<sup>13</sup> and confirmed by Terzaghi.<sup>12</sup> Furthermore, the presence of water has practically *no effect* on the coefficients of internal friction and wall friction.

The effects of drainage are as follows: For a position of the wall in the immediate vicinity of its initial position, the drainage of the fill produced a slight decrease of the Rankine active value  $K_a$  and an increase of the coefficient of wall friction  $\tan \phi_1$ . During a consequent intermission  $K_a$  increased and  $\tan \phi_1$  became smaller. In contrast, if the wall was at a distance  $1/1,000 h$  from the initial position, all the phenomena were completely reversed.

*c. Backfill of Fine-grained Sand.*—For coarse sands the tests of Parsons<sup>13</sup> have conclusively demonstrated that hydrostatic uplift in them is fully active. This statement, confirmed by Terzaghi, may be generalized as follows: *Any surface of a solid substance in intimate contact with submerged clay or with concrete is subject to the action of full hydrostatic uplift as if the adjoining porous material were not present.* Notice that this statement is very important in the design of masonry dams (compare Fig. 4:14b).

Terzaghi's experiments described in this section are quoted in order to clarify the actual behavior of the backfill under different conditions. Though only a few quantitative data are given, information obtained in these experiments may be illustrative to the designer in many practical cases.

**10:20. Other Experiments with Retaining Walls.**—Feld conducted experiments at the University of Cincinnati<sup>14</sup> using a wall 6 ft. 4 in. by 5 ft., the face of the wall against the backfill being interchangeable, either wooden, glass, or metallic. It was discovered that the thrust  $F$  acts under a certain angle to the horizon, that its horizontal component  $H_f$  does not depend on the material of the face referred to, but that the vertical component  $V_f$  does depend thereon. In other words, the vertical component of the thrust  $F$  depends on the angle of friction between the wall and the earth material. The point of application of the thrust lies between 0.33 and 0.40 of the height of the wall, computing from below. Some other interesting features of Feld's experiments are as follows: During the first two weeks after completion of the backfill, the value of the thrust  $F$  oscillates with a general tendency toward a decrease; the rise of temperature increases both components  $V_f$  and  $H_f$  of the thrust about 0.16 per cent per degree Fahrenheit.

Jenkin<sup>15</sup> noted a cyclical variation in the magnitude of the horizontal thrust: When a slip starts, the horizontal earth pressure has the maximum value. As soon as the plane of rupture forms and final slip occurs, the horizontal pressure first falls and then begins to rise again. The height of the center of pressure was in all cases greater than one-third of the height of the wall, except for large negative batters, when it tended toward one-fourth of that height. Jenkins also investigated L-shaped and T-type walls.

Whereas Feld and Jenkins used dry sand, Parsons investigated dry, saturated, and drained backfill. The pressure after drainage was found to be much greater than that of an originally dry material (compare Terzaghi's results, Sec. 10:18).

### E. REDISTRIBUTION OF THE LATERAL PRESSURE ON A WALL

If two bodies in contact tend to move with respect to each other, the force opposing the motion along their surface of contact is *friction*. If a part of a body or of a mass tends to move with respect to the other part of the same body or mass, the motion is opposed by *shearing stress*. In intermediate cases (for instance, in the case of stresses at the surface of piles or caissons driven into the ground) either term may be used.

Besides opposing motion of one part of the mass with respect to the other, shearing stresses transfer pressure from one part of the mass to the other. The transfer of pressure by shearing stresses is often termed "arching."

**10:21. Example of Transfer of Pressure.**—In Fig. 10:14 two cases of transfer of pressure are shown: (a) with formation of

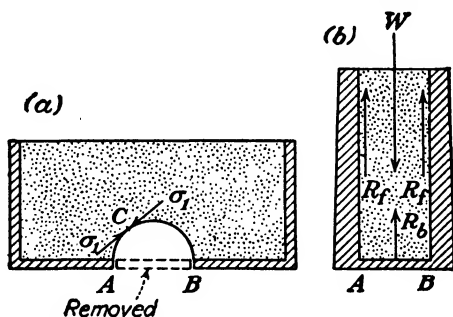


FIG. 10:14.—Redistribution (transfer) of pressure by shearing stresses.

actual arches and (b) without such a formation. If part *AB* of the bottom of a box filled with sand is removed, a part of the

material falls out, and the rest may form a convex surface  $ACB$  (Fig. 10:14a). In this case the weight of the material above the arch is fully transferred by shearing stresses to the adjacent parts of the bottom of the box, and there is only a compression stress  $\sigma$ , along curve  $ACB$ . In Fig. 10:14b a part of the weight of the material of a bin is transferred by shearing stresses  $R_f$  to the walls of the bin, whereas the rest of the weight is carried by the bottom of the bin (reaction  $R_b$ ).

**10:22. Pressure on Translating Rigid Walls and Flexible Walls.**—*a. Translating Rigid Walls.*—If a rigid wall slightly

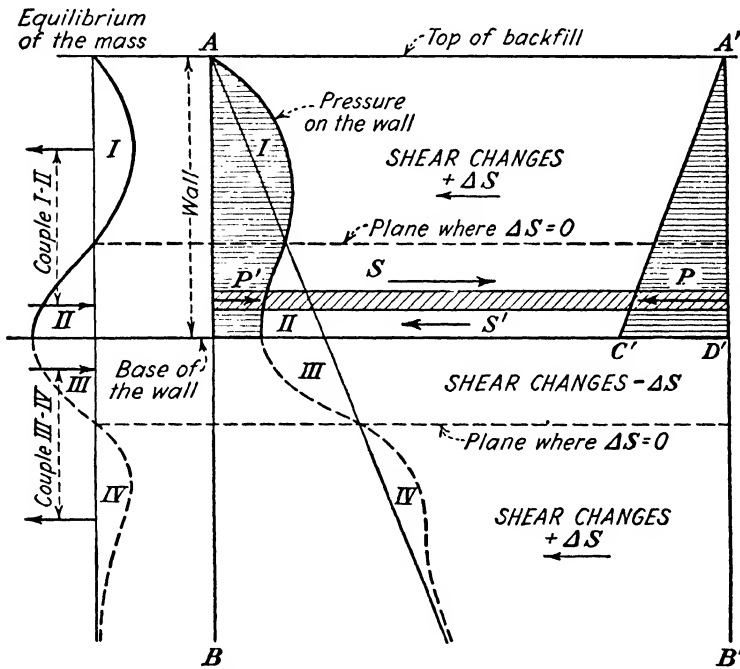


FIG. 10:15.—Lateral pressure on a translating rigid wall. ( $P$  is natural earth pressure.)

translates without formation of cracks in the backfill, the lower part of the latter pushed by larger horizontal pressure follows the moving wall rather closely. There are shearing forces at the top and bottom of each individual earth layer of the backfill (cross hatched in Fig. 10:15), and in the lower part of the backfill the shearing force  $S$  directed from the wall is larger than the shearing

force  $S'$  directed toward the wall. Thus for each individual layer in the lower part of the wall the "shear change"  $\Delta S$  or the difference  $S' - S$  is negative, *i.e.*, directed from the wall. At an infinite distance from the wall the natural lateral pressure  $F_n$  (Sec. 10:3) remains unchanged, however. In Fig. 10:15 this unchanged pressure is plotted from the vertical line  $A'B'$  and is expressed by the triangular area (cross hatched in Fig. 10:15)  $A'C'D'$ , its altitude  $A'D'$  being the height of the wall. Conditions of equilibrium require that the pressure from the wall on a given layer  $P'$  together with the shear change  $\Delta S$  balance the natural pressure  $P$  at that layer. In other words  $P' < P$ , and there is a decrease in pressure in the lower part of the wall. To compensate this decrease of pressure, there should be increase of

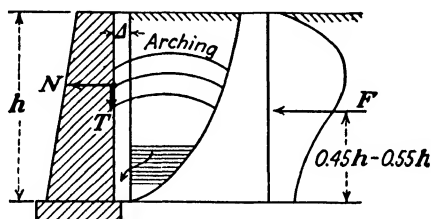


FIG. 10:16.—"Sand arching" in the case of translation of the wall. (After Terzaghi.)

pressure in the upper part of the wall (positive values of the shear change  $\Delta S$ ). The zones of positive and negative values of the shear change  $\Delta S$  are separated by a plane where  $\Delta S = 0$ . According to existing experiments (Sec. 10:23) this plane is located somewhat below the middle of the height of the wall.

Owing to redistribution of pressures, a counterclockwise acting couple is formed by the resultants of the pressures I and II (increase and decrease of pressure on the wall, Fig. 10:15, left). This couple tends to overturn the translating wall, but its action may be balanced by the resistance of the wall if the latter is heavy enough [compare Eq. (10:29)]. So far as the equilibrium of the earth mass is concerned, however, couple I-II should be balanced by another couple III-IV acting clockwise. Thus the triangular diagram of horizontal pressure in the mass is transformed into a wavy diagram, the sum area I + area IV being equal to the sum area II + area III. Figure 10:16 shows Terzaghi's explanation of the pressure redistribution in the case of a translating rigid wall; the lower part of the wedge falls down easily,

and the upper part arches. The point of application of the resultant of the redistributed pressure area lies perhaps between  $0.45h$  and  $0.55h$  above the base,  $h$  being the height of the wall.

*b. Flexible Walls.*—As follows from Fig. 10:15 a translating wall subdivides the whole earth mass into three horizontal zones, with alternate positive and negative “shear changes”  $\Delta S$ . The planes where the shear changes are zero are boundaries between those zones. The action of a flexible wall is essentially the same. Particularly, Fig. 10:17 refers to the pressure redistribution on the bracing of an excavation. It should be noticed that in the case

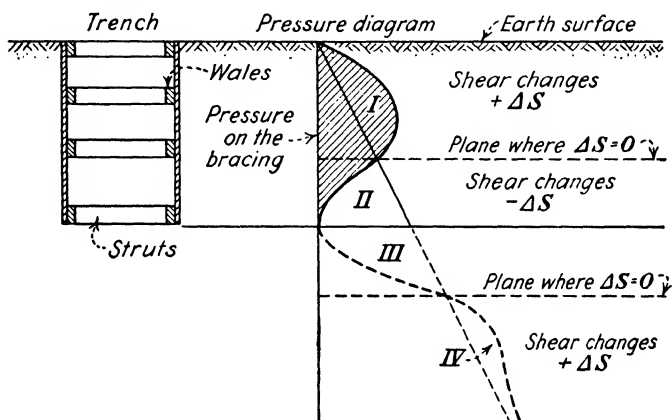


FIG. 10:17.—Lateral pressure on the bracing of an excavation.

of a translating rigid wall there is generally some unit pressure at the base of the wall (horizontal ordinate below  $P'$ , Fig. 10:15). This is because of insufficient flexibility of a rigid wall which does not permit shearing displacements in the backfill to be fully developed, and sufficient displacements are essential for the development of corresponding shearing stresses and hence pressures. In the case of a flexible wall there may or may not be unit pressure at the base of the wall according to the degree of flexibility of the latter (Figs. 10:19 and 10:17, respectively). Notice that designations I, II, III, and IV in Fig. 10:17 are analogous to those used in Fig. 10:15.

### 10:23. Equilibrium of Translating and Tilting Rigid Walls.—

Even a superficial inspection of existing nonflexible walls reveals that a great number of them are out of plumb but do not fall down. Hence the walls in question have reached a certain state

of equilibrium. The causes that may bring a moving or a tilting wall back into a state of equilibrium (but not to the original position) will be investigated hereafter.

a. *Translating Walls.*—If a rigid wall translates, pressure I (Fig. 10:15) is larger than pressure II. If the wall stops, both pressures

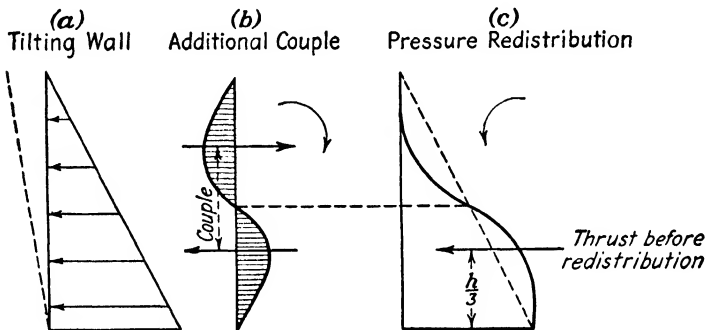


FIG. 10:18.—Pressure on a tilting wall brought to stop.

are equal, and the situation will be as in Sec. 10:22a. This may happen, for instance, owing to changes of the horizontal shears or the sliding resistance at the base of the wall (compare Sec. 10:15).

b. *Tilting Walls.*—In the case of a tilting wall there is practically a hinge at point *O* as in Fig. 10:11. If a wall starts to rotate about

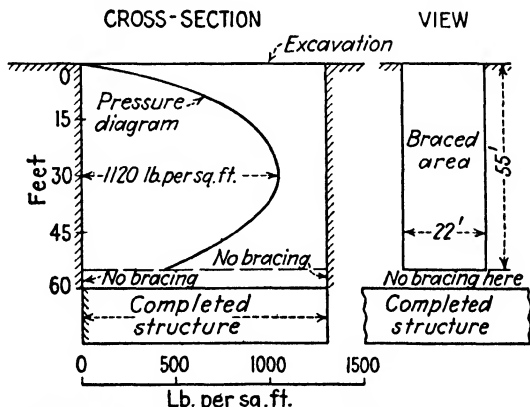


FIG. 10:19.—Pressures on sheeting and bracing, Flatbush Avenue, New York City. (After Moulton.)

point *O* under the action of an excessively large moment  $Fa$  (Fig. 10:11), it has to continue tilting until it falls down. This

is because the moment rotating the wall about point  $O$  can be balanced only by some other moment. If a tilting wall stops in

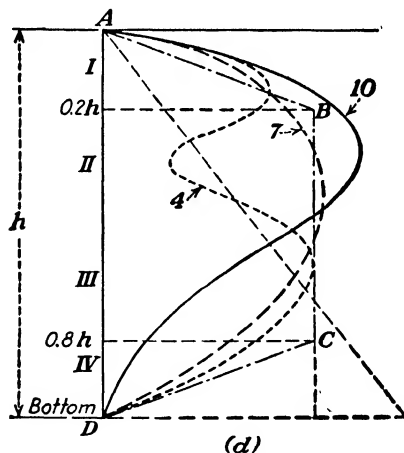
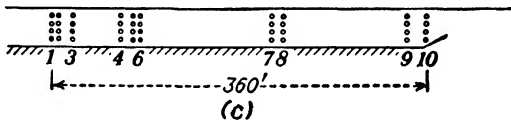
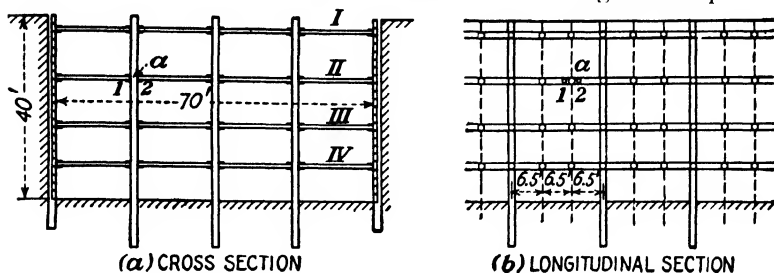


FIG. 10:20.—Terzaghi's experiments with flexible walls. (a) Cross section, (b) longitudinal section, (c) elevation showing places of measurements, (d) pressure curves. (From Proc. A.S.C.E., October, 1939.)

its motion, it means that some pressure redistribution took place in the backfill. Figure 10:18 is but a sketch giving an idea of a possible pressure redistribution in such a case.

**10:24. Examples of Pressure Redistribution.**—a. Figure 10:19 shows the results of pressure measurements made on Flatbush

Avenue, New York City, in 1916. According to Moulton,<sup>16</sup> the lateral pressure was computed from the deflections of rangers over a bank area measuring 22 ft. in a horizontal direction and 55 ft. in a vertical direction. A strip 5 ft. high was unbraced. Below a

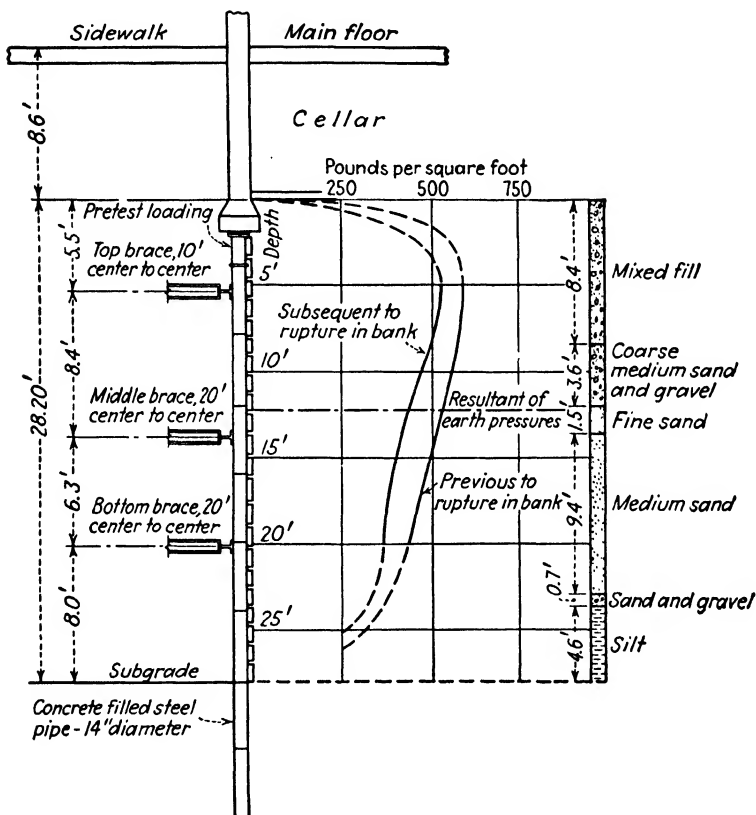


FIG. 10:21.—White and Paaswell's measurements in the Sixth Avenue Subway, New York City. (From *Trans., A.S.C.E.*, vol. 104.)

depth of 60 ft. the cut was occupied by the completed structure. The width of the cut was 85 ft., and the soil consisted of coarse sand mixed with 20 to 30 per cent of clay and some gravel.

b. The following results have been obtained by Terzaghi from his experimental work with the Siemens Bau Union, Berlin, Germany, in 1936.<sup>2</sup> Terzaghi measured the pressures in the struts of a 40-ft.-deep subway cut, the sides of the latter consist-

ing mostly of sand and gravel. Cross sections of this cut are shown in Fig. 10:20*a* and *b*. The length of the cut was 360 ft. (Fig. 10:20*c*). Finally, Fig. 10:20*d* represents some pressure diagrams, which are of a rather irregular shape. The centroid of the irregular areas shown in Fig. 10:20*d*, or the point of application of the earth pressure, is located between  $0.53h$  and  $0.60h$  above the bottom of the cut.

*c.* White and Paaswell<sup>18</sup> measured pressures exerted by a bank about 28 ft. high and 12 ft. long in a Sixth Avenue subway cut in New York City. The results of their measurements are shown in Fig. 10:21.

*d.* Peck<sup>32</sup> measured pressures on the bracing of excavations of the Chicago subway and obtained pressure diagrams of type 10 in Fig. 10:20. For design purposes Terzaghi<sup>2</sup> proposes using a conventional trapezoidal pressure distribution (*ABCD* in Fig. 10:20); Peck's trapezoid<sup>32</sup> differs a little from Terzaghi's.

*e.* Stroyer<sup>29</sup> conducted very elaborate experiments with models of flexible walls. His principal finding, that the Rankine formula cannot be used in similar cases, may be simply forecast.

### G. BULKHEADS AND COFFERDAMS

Before discussing the behavior of horizontally loaded sheet piling, it is convenient, for purposes of comparison, to consider the behavior of horizontally loaded isolated poles, posts, and piles.

**10:25. Action of a Vertical Pole Loaded Horizontally.**—If a rigid pole (height above the ground surface,  $h$ ; depth of penetration into earth,  $x$ ) as shown in Fig. 10:22*a* is loaded horizontally with a force  $P$ , it rotates about a "zero point" or "pivot"  $Z$ . The position of the zero point depends on (*a*) the material and stiffness of the pole, (*b*) the physical properties of the earth material, and finally (*c*) the arm  $h$  of the acting force.

Sometimes the opinion is advanced that a rigid pole loaded horizontally rotates about its tip (Fig. 10:22*b*). This opinion is *incorrect*, since it does not satisfy statics. The weight of the pile, which generally is insignificant in comparison with the lateral force  $P$ , may be neglected. Then the resultant  $R$  of earth reaction (Fig. 10:22*b*) will form an unbalanced couple with the acting force  $P$ , and this is incompatible with the conditions of equilibrium. Hence the existence of a zero point is a mechanical necessity, the acting force  $P$  and the reaction  $P_0$  of the earth at the bottom

part of the pile being balanced by the reaction  $P + P_0$  of the upper part (Fig. 10:22a). It should be remembered, however, that an end bearing pile reaching rock or other solid ground (Sec. 8:15) may rotate about its tip.

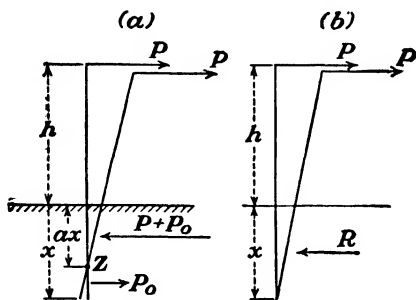


FIG. 10:22.—Action of a horizontal force on a rigid pole. (a) correct and (b) incorrect representation.

**10:26. Resistance of a Pole and of a Sheet-piling Wall Compared.**—If the lateral pulling force is gradually increased, the center of rotation (“pivot”  $Z$  in Fig. 10:23a) moves toward point  $Z'$  at the earth’s surface, and finally a conelike body is pushed out.

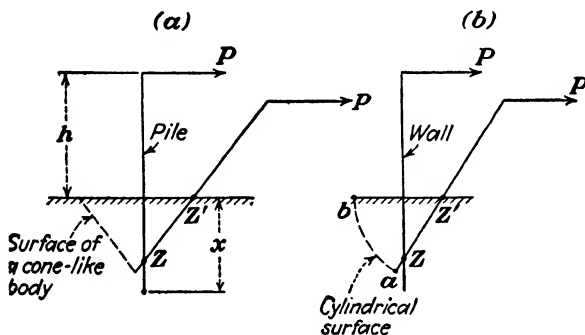


FIG. 10:23.—Comparative resistance to overturning of a pile and of a wall.

Experiments conducted at North Carolina State College, Raleigh, N.C., and by the State Highway Board of Georgia<sup>19</sup> have shown that the resistance of a pole to overturning is proportional to the square of the penetration depth ( $x$  in Fig. 10:23).

It should be borne in mind, however, that in the case of a sheet-piling wall, the resistance is proportional to  $x$  and not to  $x^2$ .

To push out a conelike body, as in the case of an isolated pole, it is necessary to break down the shearing resistance of the soil along the surface of that cone (Fig. 10:23a). In the case of a wall, the shearing resistance to be overcome is that along a cylindrical surface *ab* (Fig. 10:23b).

**10:27. Equilibrium of a Horizontally Loaded Pole, Pile, or Wall.**—A pole, a pile, or a sheet-piling wall cannot be permitted to assume an inclined position as shown in Fig. 10:23; the deviation from the vertical line should be insignificant. For this purpose the pile should be driven to a sufficient depth. In any case, it tends to rotate about a "pivot" and compresses the adjacent earth. To locate the corresponding zones in the case of an isolated pile, the following experiment was made: Wooden piles 3 to  $3\frac{1}{2}$  in.

in diameter, ranging in length from 6 to  $7\frac{1}{2}$  ft., were driven into a very uniform clay with 17 to 18 per cent of natural moisture. Then the piles were overturned by application of a horizontal force. A cross section through the center of the pile was excavated carefully with shovels, and the vertical surface was finished with a sharp knife. Figure 10:24 is a sketch made from a photograph of that cross section. The zero point *Z* located at a depth from

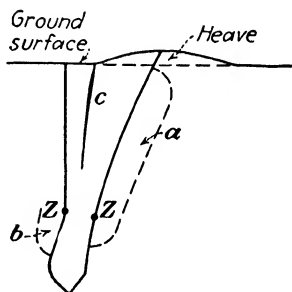


FIG. 10:24.—Action of a laterally pulled timber pile.

0.52*x* to 0.69*x*, is clearly seen. In the first phase of the overturning process, the pile rotates slightly about its zero point *Z*, being resisted by both the shearing resistance of the soil (compressed zones *a* and *b*) and also by its tensile strength (crack *c*). The second phase is characterized by the breaking down of the shearing resistance. A deeply driven weak pile breaks in this experiment.

German experiments quoted by Agatz<sup>23</sup> have shown the zero point rather close to the earth surface. It was located at 0.07*x* for strong wooden piles about 14 in. in diameter (*h* = 27 ft.; *x* = 21 ft.; designations of Fig. 10:22). Steel sheet piles have shown the zero point between 0.18*x* and 0.27*x* below the earth surface. Apparently owing to some inaccuracy in measurements, these figures are too small, and the actual zero point is located somewhat lower.

**10:28. Types of Bulkheads.**—Sheet-piling retaining walls (bulkheads) are applied mostly in harbors and to protect river banks. Though there are many wooden bulkheads in existence, steel sheet piles are mostly used for that type of structure at the present time. Figure 10:25 represents a cross section through a typical

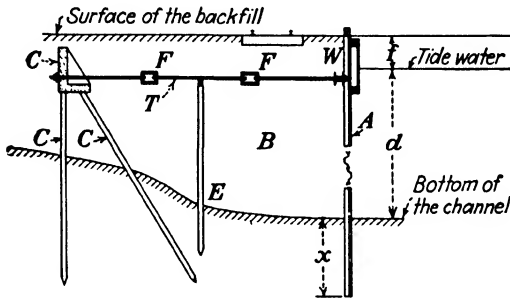


FIG. 10:25.—Cross section of a bulkhead.

steel bulkhead. The essential parts of a bulkhead are the sheet-piling wall *A*, which retains the backfill *B*; the anchor *C*; and the tie (anchor rod) *T*, which connects the sheet piling with the anchor. Small bulkheads are sometimes constructed without tie

and anchorage. These are *cantilever bulkheads*. The so-called “apron” arrangement of a bulkhead results from driving spaced master sheet piles *A* and short piles *B* (Fig. 10:26). The only purpose of the latter is to prevent the earth surface from falling down, whereas the master piles develop the resistance to overturning.

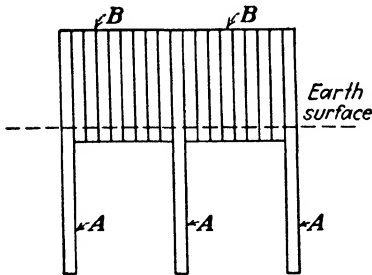


FIG. 10:26.—“Apron” arrangement of sheet piles.

When the load to be carried by the bulkhead is so considerable that available rolled sections of sheet piling cannot be used any longer, relieving platforms can be constructed, as shown in Fig. 10:27. The distribution of loads between the bulkhead proper and the relieving platform is a highly statically indeterminate problem. Piles supporting the relieving platform may be either steel or timber piles. The length *L* of the relieving platform is determined in practice by tracing a line *AB* from the bottom of

the channel *A* to intersect the tie at point *B*. Line *AB* makes an angle  $\phi$ , that of friction, with the horizon.

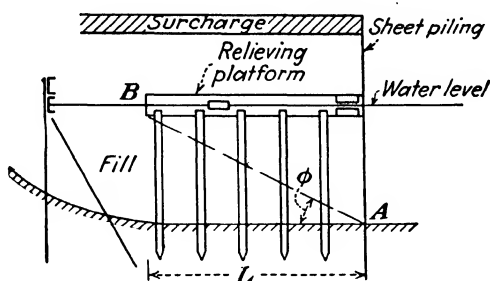


FIG. 10:27.—Bulkhead with a relieving platform.

**10:29. Principal Design and Analysis Features.**—Methods of bulkhead design have been thoroughly discussed in technical literature<sup>20</sup> and in the catalogues of steel companies.<sup>21</sup>

*a. Use of the Rankine Formula in the Analysis of a Bulkhead.*—The use of the Rankine formula for the determination of the active

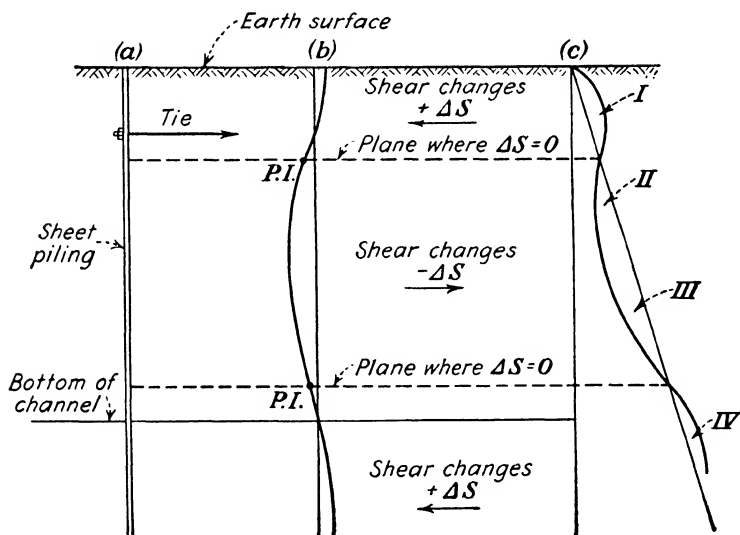


FIG. 10:28.—Possible final pressure distribution in the case of a bulkhead. (Compare Figs. 10:15 and 10:17.)

pressure on the bulkhead furnishes results that are on the safe side so far as the bending moment in the sheet piling is concerned. In fact, the hydraulically placed backfill acts in this case as a

liquid exactly as in the case of a rigid wall with a hydraulic backfill (Sec. 10:8). When, owing to the gradual motion of the bulkhead, the anchor tie and the passive resistance of the earth below the channel bottom become fully operative, the bulkhead stops tilting and possibly tends to be deflected as shown in Fig. 10:28*b*. The corresponding final pressure distribution is approximately shown in Fig. 10:28*c*, the symbols I, II, III, and IV having the same meaning as in Figs. 10:15 and 10:17. The planes where the "shear changes"  $\Delta S$  equal zero correspond to the points of inflec-

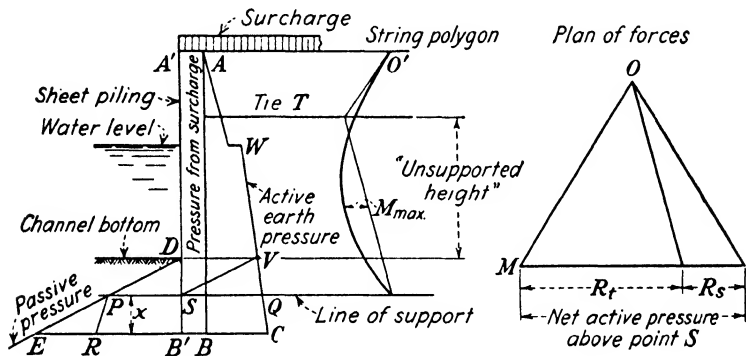


FIG. 10:29.—Analysis of a bulkhead.

tion of the sheet piling ( $P.I.$  in Fig. 10:28*b*). There is some decrease in the value of the maximum bending moment.

*b. Method of Equivalent Beam.*—In the so-called "method of equivalent beam" the analysis of a sheet-piling bulkhead consists essentially in the determination of (a) depth of driving, (b) tension in the tie, and (c) bending moment in the sheet piling.

The active pressure  $ABC$  and the passive pressure  $DB'E$  (Fig. 10:29) are computed using the Rankine formula. Line  $AC$  may be broken at point  $W$  (level of water in the channel) because of a difference between the values of the angle of internal friction  $\phi$  above and below water (usually  $30^\circ$  and  $25^\circ$ , respectively) and the apparent decrease in the weight of the earth material due to buoyancy. Line  $DE$  is sometimes drawn by doubling the Rankine passive value as determined by formulas (5:6) and (5:5) on the theory that similar results have been obtained by German professor Franzius.<sup>33</sup> Since Franzius's experiments were made in high narrow boxes and their results were distorted by friction against the walls, this increase in the value of the passive pressure

is hardly advisable. The influence of the surcharge is considered as in Sec. 10:5.

The bulkhead is visualized as a beam on two supports, one of which is the tie  $T$  and the other the so-called "line of support"  $S$ , the upper part of the bulkhead (above  $T$ ) being in cantilever. In order to visualize the bulkhead that way, the designer has to make points  $T$  and  $S$  as immovable as practicable. As far as the tie  $T$  is concerned, this is done by proper anchorage of the bulkhead (discussed in Sec. 10:31). The position of the line of support is found from the condition of equality of the unit active and the unit passive pressures ( $SQ = SP$ ). Further stability of point  $S$  is ensured by proper depth of driving below the line of support (designation  $x$  in Fig. 10:29).

*c. Tension in the Tie.*—Considering the active pressure as subdivided in a series of loads, the plan of forces and the string polygon are drawn in the usual way, and the reactions  $R_t$  (tension in the tie) and  $R_s$  (pressure at the line of support) are determined.

The tie is placed at the level of the water and usually not deeper than 18 in. below that level because of difficulties of deeper placing. The tie rods are usually spaced from six to eight widths of the sheet piles or, as an average, about 8 to 9 ft. center to center. The common diameter of the rods is between  $1\frac{1}{4}$  and 3 in., adding about  $\frac{1}{4}$  in. for corrosion.

*d. Depth of Driving.*—The reaction  $R_s$  applied at point  $S$  and the excess  $EPR$  of the passive pressure  $PSB'E$  over the active pressure  $SB'CQ$  (both below point  $S$ ) should be in equilibrium. Designate with  $K'_a$  and  $K'_p$  the active and passive Rankine values below water level and with  $\gamma'$  the weight of the earth material relieved by buoyancy. Notice that the force represented by area  $EPR$  equals

$$EPR = \frac{1}{2} E\bar{R} x = \frac{1}{2} (K'_p - K'_a) \gamma' x^2 \quad (10:30)$$

and that the arm of this force with respect to  $B'$  is  $x/3$ . Take moments of forces  $R_s$  and  $EPR$  with respect to point  $B'$ ;

$$x = \sqrt{\frac{6R_s}{(K'_p - K'_a) \gamma'}} \quad (10:31)$$

It is advisable to increase the *total theoretical depth* of driving thus found ( $DB'$  in Fig. 10:29) by 20 per cent. Practical values of the total depth of driving, as expressed in terms of the un-

supported height between the tie rod and the bottom of the channel, are (a) for unstable bottom soil and deep channel (25 to 35 ft.) the depth of driving may reach 75 per cent of the "unsupported height"; (b) for stable bottom and shallow water the depth of driving may be as low as 20 per cent of the "unsupported height." For cantilever walls (Sec. 10:28) the depth of driving approximately equals the height of the wall above the channel bottom.

e. *Maximum bending moment* in the sheet piles is found as the maximum ordinate of the closed string polygon (Fig. 10:29).

f. *Influence of High Tides.*—When a high tide is dropping, there is an additional pressure from the backfill due to the retarded

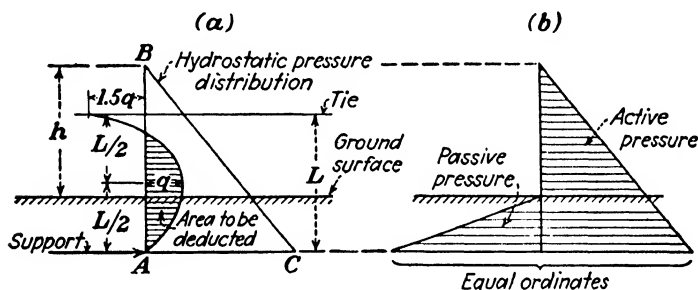


FIG. 10:30.—Danish method of designing bulkheads.

movement of water in the pores of the earth mass. If the height of the tide is insignificant (5 or 6 ft.), this pressure excess is either estimated, for instance, at 2 ft. of water pressure, or entirely neglected. In the case of very high tides this unbalanced pressure should be given due attention.

**10:30. Danish Method of Bulkhead Analysis.**—Danish engineers who have considerable practice in bulkheads reduce the value of the bending moment as caused by the Rankine pressure distribution in the following way: Let  $L$  be the span of the "equivalent beam" (distance between the tie and the line of support), the height of the wall above the ground surface being  $h$  (Fig. 10:30). The final bending moment  $M_f$  is

$$M_f = M - \frac{17}{10} q L^2 \quad (10:32)$$

where  $M$  is the bending moment of the beam loaded with the triangular load  $ABC$  (Fig. 10:30a). As to the value of  $q$ ,

$$q = k \left[ \frac{10(h/L) + 4}{10(h/L) + 5} \right] \times \left[ \frac{8M}{L^2} \right] \quad (10:33)$$

In turn the value of the coefficient  $k$  is variable, being from 0.7 to 0.85 for concrete piles. Admittedly, formulas (10:32) and (10:33) are given here merely as a matter of suggestion, not guidance. More data on this method may be found in refs. 22, 23, and 24.

**10:31. Anchorages.**—There are two types of anchorages for sheet piling: (a) brace piles as shown in Figs. 10:25 and 10:31a and (b) anchor walls or anchor plates (Fig. 10:31b and c). The anchor wall is continuous, whereas anchor plates are spaced. Any anchorage must be placed far enough from the wall so as to be beyond the region where a crack separating the wedge from the rest of the backfill is likely to be formed. Otherwise the tie would not accomplish its function of fixing the wall to an immovable object and thus preventing its motion away from the backfill. If the tie thus designed is too long, the weight of the earth resting on it may produce a sag of the tie, which in some cases may be very considerable (for instance, 1 ft. or more). To prevent such sagging of the tie, an intermediate support ( $E$  in Fig. 10:25) is made by driving short piles into the backfill under the middle of the length of the tie.

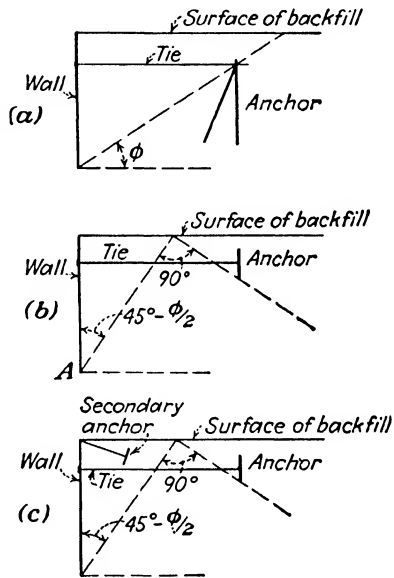


FIG. 10:31.—Locating anchorage.

Figure 10:31 shows the method of determining the distance of the anchorage from the wall: (a) as used by the Carnegie-Illinois Steel Company<sup>21</sup> and (b) and (c) as used by many German engineers and also sometimes in the United States. In the latter case the position of the anchorage is controlled by the position of the eventual failure lines. Point  $A$  in Fig. 10:31b is the lower end of the wall, though several engineers place it much higher, which, of course, is tantamount to a decrease of the distance of the anchorage from the wall. In Figure 10:31c is shown a small auxiliary

tie to keep the top of the wall in position. This auxiliary tie is neglected in stability computations.

If the anchorage consists of spaced pairs of brace piles, one of the piles is pulled and the other pushed and, in addition, both are bent. Each of the two brace piles, in being deformed, rotates about a zero point,  $Z_1$  or  $Z_2$ , respectively (Fig. 10:32).

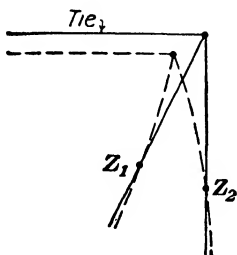


FIG. 10:32.—Action of brace piles in a bulkhead.

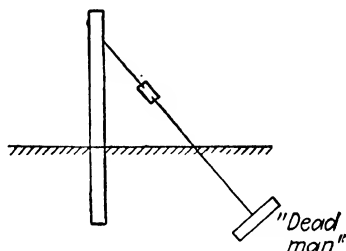


FIG. 10:33.—Sketch of a guardrail.

Each anchorage, whether it be of brace piles, anchor wall, anchor plates, or some other arrangement, works in the following way: In the first period, upon the application of the tension, soil near the anchorage is compressed (adjustment of the particles), and the tie thus becomes loose and must be adjusted by the turnbuckle ( $F$  in Fig. 10:25a), and in the second period the anchorage is held in place by the shearing resistance of the soil (compare

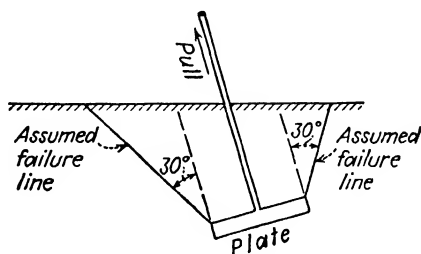


FIG. 10:34.—Simplified failure lines in the case of a "dead man."

Fig. 10:10). The latter is developed along the eventual failure lines radiating from the perimeter of the anchorage. This visualization of the action of an anchorage is true not only in the case of bulkheads but also generally for any anchorage. In Fig. 10:33 the well-known highway guardrail provided with a "dead man" is shown; it is obvious that it acts in the way described. The

eventual failure lines along which the shearing resistance of the earth mass is developed are curved, though in designing practice they are sometimes assumed to be plane, making a certain angle, for instance,  $30^\circ$ , with the rope (Fig. 10.34). If the tie is long and the plate is located at a shallow depth, the failure lines may develop toward the upper boundary of the earth mass as shown in Fig. 10.35. The latter represents the results of a laboratory experiment by Buchholtz.<sup>25</sup> Like in all cases of actual shear, failure lines develop toward the outer boundary of the given earth mass.

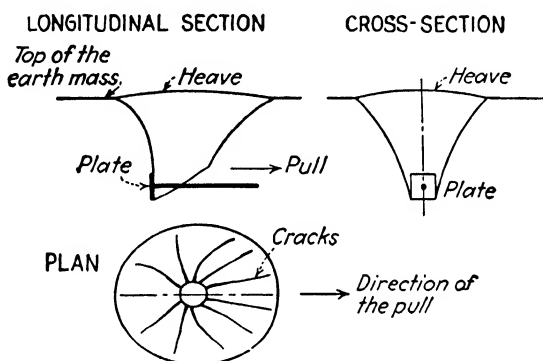


FIG. 10.35.—Pulling out an anchor plate. (After Buchholtz.)

**10:32. Deflections and Movements of Sheet-piling Walls.**—*a. Deflections.*—Rifaat<sup>26</sup> considered both rigid and elastic cantilever walls under the action of a concentrated force applied horizontally at the top of the wall; his results cannot be applied directly to sheet-piling walls sustaining earth pressure.

According to Baumann,<sup>27</sup> who made a comprehensive theoretical analysis of sheet-pile bulkheads, the movements of the wall against the earth mass at a given depth and the values of unit passive resistance are interconnected.

Theoretically speaking, it is possible to compute pressure on a flexible wall from its deflections (compare Sec. 10:24, Moulton's measurements). To avoid erratic results, however, such measurements should be made with extreme care and precision, which is not always feasible. Another difficulty is shown in Fig. 10.36. Formulas for determining bending moments and shears as used in mechanics presuppose a nonrigid load consisting of infinitely thin slices of a hypothetical material that possesses no physical

properties at all (Fig. 10:36a). In reality, a beam loaded with a pile of earth (Fig. 10:36b) does not deflect in the same way as the beam shown in Fig. 10:36a. To solve this contact problem, it is necessary to find numerical values of the modulus of elasticity  $E$  and of the Poisson ratio  $\mu$  of the earth mass, and, practically, this is an impossible problem.

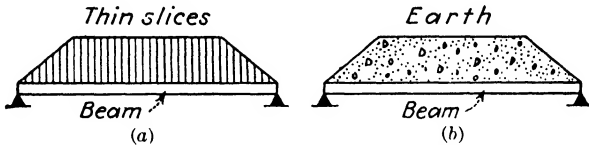


Fig. 10:36.—Theoretical load and earth pressure compared.

*b. Movements.*—Press<sup>28</sup> quotes several observations on the movement of sheet-piling walls in Germany. Generally with sandy soils, the wall moves slightly both vertically and horizontally. The first slip period is during the construction of the backfill. Both total vertical- and horizontal-movement components increase gradually upon the application of the live load and during and upon the first few fresh-water periods, after which the wall comes

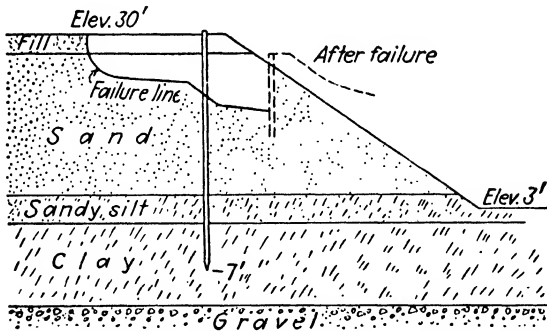


Fig. 10:37.—Failure of a sheet-piling wall by translation. (After Press.)

to rest. It may be concluded that in tidal regions a bulkhead should come to rest in the first days of its existence.

As observed by Press, the total movement of sheet-piling walls from 27 to 40 ft. high and driven from 9 to 15 ft. into the earth was 0.02 to 0.06 in. vertically and 0.03 to 0.04 in. horizontally. In an abnormal case, the vertical movement increased from 18 in. during the first fresh-water period to 34 in. after the third one. The respective figures for the horizontal movement were 2 and 23 in.

*c. Failures.*—Failures of bulkheads occur mostly during or very soon after construction. They are often caused by short anchor ties, as explained in Sec. 10:31. Failures by pure translation occur very seldom, though Press<sup>28</sup> quotes a case of failure of a vertical wall intended to reinforce the slope of an embankment (Fig. 10:37). The failure occurred after a heavy rainstorm and was probably due to stresses in percolating water and decrease in shearing resistance of the earth material.

**10:33. One-wall and Two-wall Cofferdams.**—There are one-wall and two-wall cofferdams built on or close to the bottom of a river

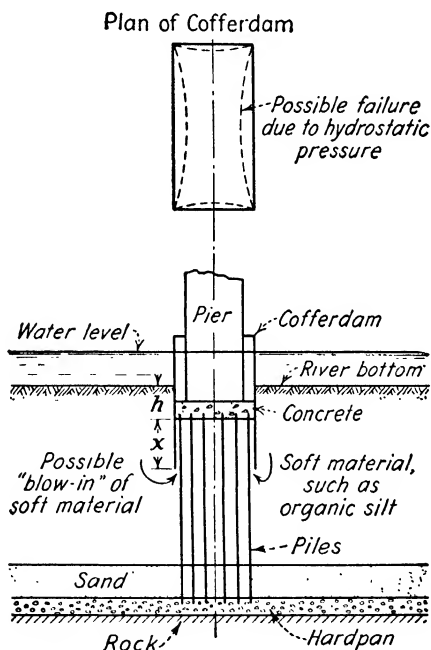


FIG. 10:38.—One-wall cofferdam for a bridge pier.

or a lake mostly to form a working space for building a structure. Different types of cofferdams have been comprehensively described by White and Prentis.<sup>34</sup> One example of a two-wall cofferdam has been given in Fig. 3:33 of this book.

Figure 10:38 shows schematically a one-wall cofferdam for the construction of a bridge pier to be founded on piles driven to a resistance layer such as hardpan or rock. To drive piles, a one-

wall sheet-piling cofferdam may be built, soft material (such as organic silt) excavated to a depth  $h$ , piles driven, tremie concrete placed on their heads, the cofferdam dewatered, and the body of the pier constructed. In excavating soft material from the cofferdam, there is a danger of a "blow in" of the adjacent soft material into the cofferdam. This can be prevented by sufficiently deep driving  $h + x$  of the sheet piles. The value of unit cohesion of organic silt in the deltas of some rivers flowing into the Atlantic (Hudson, Potomac, Thames, and others) is about  $c = 100$  lb. per

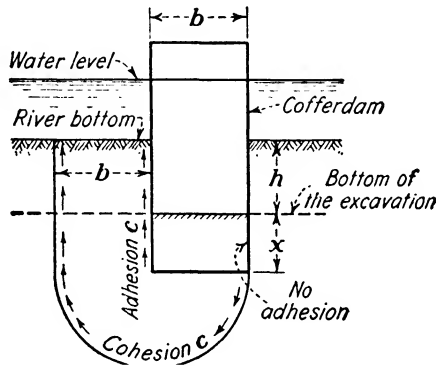


FIG. 10:39.—Checking a cofferdam against a "blow in."

sq. ft. A rough checking of the cofferdam can be done by assuming rotational flow of the soft material balanced by its cohesive resistance  $c$  (Fig. 10:39). The condition of limit equilibrium (safety factor = 1) in this case is

$$bh\gamma = [2(h + x) + \pi b]c \quad (10:34)$$

where  $\gamma$  is the unit weight of the soft material relieved by buoyancy. Other designations are shown on the drawing.

Cofferdams of this kind may also fail owing to hydrostatic pressure, and their bracing (struts, wales) should be duly designed.

**10:34. Cellular Cofferdams.**—Two principal types of cellular cofferdams, (a) circular type and (b) diaphragm type, are shown in Fig. 10:40. On the works of the Tennessee Valley Authority (TVA) a clover-leaf type (in plan) was also used occasionally.<sup>35</sup> As an example, the diameter of a circular cell of a TVA large Kentucky cofferdam is about 59 ft., whereas the width of a clover-leaf type cell is even over 100 ft. In a cellular cofferdam on rock

the width of the cell  $b$  is from 85 to 100 per cent of the height  $h$  of the cofferdam. For the designation  $b$  consult Fig. 10:40. To fill the cells, the hydraulic method is often used, the desirable material for the fill being sand and gravel. For cofferdams on sand, additional forces due to seepage and piping may affect stability of the structure and should be considered. Sheet piles should be driven into sand to about one-half of the height of the cofferdam above the ground.

The analysis of a cellular cofferdam is done in a conventional way. Stability against *sliding* and *overturning* by water is checked; *tension in locks* and *internal shear* are determined. The last two items are briefly discussed hereafter.

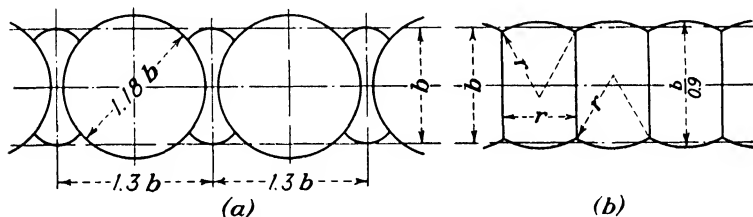


FIG. 10:40.—Cellular cofferdams (plan). (a) Circular type, and (b) diaphragm type.

*a. Tension in Locks.*—Unit lateral pressure exerted by the fill on the walls of a cell (radius  $r$ , height  $h$ ), is at a maximum at the bottom of the cofferdam and according to Rankine formula equals

$$p = K_a \gamma h \quad (10:35)$$

This pressure causes tension along the perimeter of the cell. The value of tension force from the condition of equilibrium is

$$t = pr \quad (10:36)$$

If  $p$  is expressed in pounds per square foot and  $r$  in feet,  $t$  will be expressed in pounds per linear foot of interlock. If expressed in pounds per linear inch of interlock, the value of  $t$  is

$$t = \frac{pr}{12} \quad (10:37)$$

The upper value of tension permissible in cofferdams is usually  $t = 6,000$  lb. per lin. in. of interlock.

*b. Internal Shear.*—Pennoyer<sup>20,35</sup> calls attention to the possibility of internal shear along the central plane  $gh$  of the cofferdam

(Fig. 10:41). Under the action of water pressure, the cofferdam tips, its deflection at the top ranging from insignificant values to 25 per cent of the height. If the deflection is too considerable,

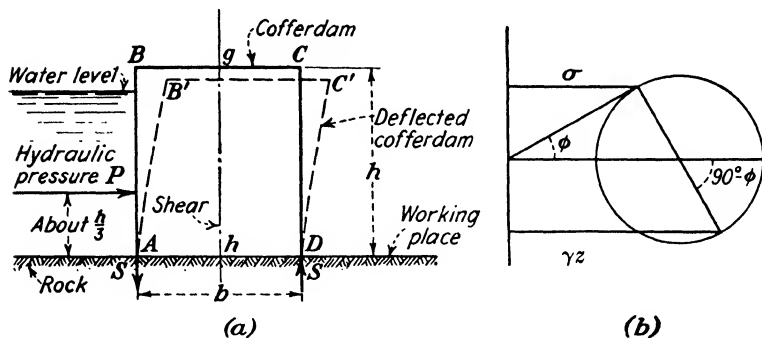


FIG. 10:41.—Internal shear in a cellular cofferdam.

the earth material inside the cofferdam starts to move. From the equation of moments about point  $D$ :

$$P \frac{h}{3} = Sb \quad (10:38)$$

where  $P$  = the hydrostatic pressure on the cofferdam (Fig. 10:41a).

$S$  = reaction of the rock at points  $A$  and  $D$ .

$b$  = the width of the cofferdam.

The value of the shear force  $S$  is constant along the width of the cofferdam if shear at the base caused by the weight of the cofferdam itself is neglected. The probability of shear failure along planes  $AB$  and  $CD$  is less than at the middle of the cofferdam. The central vertical plane  $gh$  is safe against shear failure if

$$F \tan \phi = S \quad (10:39)$$

where  $F$  is the total horizontal pressure on the plane  $gh$ . From the Mohr's circle (Fig. 10:41b), the horizontal pressure on any point of plane  $gh$  located  $z$  units below the top of the cofferdam is

$$\sigma = \gamma z \frac{\cos^2 \phi}{2 - \cos^2 \phi} = C \gamma z \quad (10:40)$$

where for the sake of brevity, the symbol  $C$  replaces the fraction  $\cos^2 \phi / (2 - \cos^2 \phi)$ . Hence Eq. (10:39) may be rewritten thus:

$$\frac{1}{2} \gamma h^2 C \tan \phi = S \quad (10:41)$$

A factor of safety (for instance, 2) should be introduced into Eq. (10:41).

It should be noticed that the value of  $C$

$$C = \frac{\cos^2 \phi}{2 - \cos^2 \phi} = \frac{1}{1 + 2 \tan^2 \phi} \quad (10:42)$$

will be used in the theory of tunnels (Sec. 11:8).

Terzaghi<sup>35</sup> advises to add a value of  $f = 0.3$  to  $\tan \phi$  in Eq. (10:41) to take care of the friction of steel on steel in the interlocks to be overcome at the moment of shear failure. This opinion is not shared by all cofferdam designers, however.

### Problems

1. Represent the Coulomb formula under the form (10:26)

$$F = (K_a)_c \left( \frac{\gamma h^2}{2} \right)$$

and compute the values of the ratio  $(K_a)_c$  for the value of the angle of friction  $\phi = 32^\circ$  and variable values of the angle  $i$ . Construct a graph in polar coordinates, considering  $i$  as the polar angle and  $(K_a)_c$  as the radius vector. Assume  $\phi = 90^\circ$  and  $\phi_1 = \phi$ .

2. A reinforced-concrete retaining wall 14 ft. high is to be constructed with no surcharge at the surface. The material available for the backfill is coarse sand; the foundation of the wall is clayey. Assume the necessary numerical characteristics of the soil and a cross section of the wall, and check these dimensions against sliding and overturning of the wall about the outer edge of the foundation.

3. A retaining wall is 50 ft. long and 14 ft. high. The surface of the backfill is uniformly loaded with stones. Assume a unit load of  $p$  tons per sq. ft. Estimate the horizontal pressure from this surcharge *only* at different points at the center line of the wall, using the following three methods:

- a. The usual office method, in which the unit lateral pressure is constant along the whole height of the wall and equals  $K_a p$ .
- b. The Rebhann method (Fig. 10:7).
- c. The elastic formula (4:23), replacing the surcharge with a concentrated load.

What value of lateral pressure do you recommend for the design of this wall?

4. Show that the value of the maximum horizontal pressure caused by a concentrated force  $P$  against a retaining wall at a given depth  $z$  below the surface of the backfill does not depend on the height of the wall. Use formulas (4:23).

5. The top of a harbor retaining wall is 10 ft. above the sea level, and the total height of the wall is 30 ft. The wall is backfilled hydraulically with local muddy silt. The characteristics of the backfill material are unit weight in the open air 90 lb. per cu. ft., porosity 68 per cent, angle of internal friction

under water  $10^\circ$ , cohesion 100 lb. per sq. ft. The surcharge consists of moving heavy cranes and may be estimated at 750 lb. per sq. ft. of the surface of the backfill. Assume the unit weight of sea water at 64 lb. per cu. ft., and determine the horizontal pressure on the wall and the height of the center of pressure above the base of the wall.

*Ans.* Pressure = 46,800 lb. per lin. ft. of the wall; applied 13.3 ft. above the base. Neglect cohesion and tides.

6. The Rankine active value for the case of a sloping backfill that makes angle  $i$  with the horizon may be determined by the following formula:<sup>7</sup>

$$(K_a)_i = \frac{\cos i - \sqrt{\cos^2 i - \cos^2 \phi}}{\cos i + \sqrt{\cos^2 i - \cos^2 \phi}}$$

The thrust  $F$  in this case is assumed parallel to the slope.

Use this formula for determining the thrust  $F$  against a wall 20 ft. high, the angle of friction  $\phi$  of the material of the backfill being  $34^\circ$ . Check your result with those furnished by other methods with which you are familiar. Use various values of  $i$ .

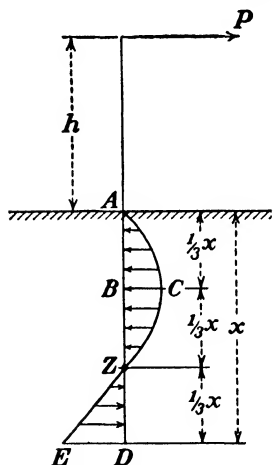


FIG. 10:42.—Parabolic distribution of pressure on sheet piling (an assumption).

For the sake of simplicity assume that the lower part of this parabola  $ZE$  is a straight line, and compute the ordinates  $\overline{BC}$  and  $\overline{DE}$ .

*Suggestion:* From statics: force expressed by area  $ACZ$  = force expressed by area  $EZD$  + force  $P$ . Besides this, area of parabolic segment

$$ACZ = \frac{2}{3} \overline{AZ} \times \overline{BC}.$$

9. Using formula (10:41), show that the danger of internal shear in a cellular cofferdam is the less

- The wider the cofferdam (*i.e.*, the larger the ratio  $b/h$ ).
  - The rougher the material of the backfill and the better it is packed, (*i.e.*, the larger the angle  $\phi$ ).
  - The heavier the material of the backfill (*i.e.*, the larger the ratio  $\gamma/\gamma_0$ ).
- Are there limitations of the statements  $a$ ,  $b$ ,  $c$ ?

7. Determine the depth of driving, the tie tension, and the value of the maximum bending moment of a sheet-piling wall. Its height above the water level is 10 ft., the depth of the channel being 12 ft. The tie is located 4 ft. 6 in. below the top of the wall. Assume the weight of dry earth to be 100 lb. per cu. ft. and its porosity at 30 per cent. The value of the surcharge is 700 lb. per sq. ft. The angle of internal friction is  $30^\circ$  above the water level and  $25^\circ$  below the water level.

*Ans.* 19 ft.; 8,450 lbs.; 490,000 in. lb.

8. Some writers on soil mechanics assume that in the case of a horizontally loaded sheet-piling wall (Fig. 10:42) the unit resistance of the driven part  $AD$  of the wall follows a parabolic law (curve  $ACZE$ ).

## References

1. CHARLES TERZAGHI: A Fundamental Fallacy in Earth Pressure Computations, *Jour. Boston Soc. Civil Eng.*, vol. 23, April, 1936.
2. CHARLES TERZAGHI: General Wedge Theory of Earth Pressure, *Proc. A.S.C.E.*, vol. 65, October, 1939.
3. C. D. COULOMB, ingénieur du Roi: Essai sur une application de règles de Maximis et Minimis à quelques problèmes de Statique, relatifs à l'Architecture, *Mém. math. phys.*, présentés à l'Académie Royale des Sciences (savants étrangers), 1773; published in 1776. Also "Théorie des machines simples," 2d ed., Bachelier, Paris, 1821.
4. BENJAMIN BAKER: The Actual Lateral Pressure of Earthwork, *Proc. Inst. Civil Eng. (London)*, vol. 65, part 3, 1880-1881.
5. G. REBHANN: "Theorie des Erddruckes und der Futtermauren," Gerold, Vienna, 1871; also OTTO MUND: "Der Rebhannsche Satz," Wilhelm Ernst und Sohn, Berlin, 1936.
6. J. V. PONCELET: "Sustaining Walls" (translated from French by D. P. Woodbury), 2d ed., Taylor and Maury, Washington, D. C., 1854. For the original paper, see *Mémorial de l'officier du génie*, 1840. (Compare footnote to Sec. 9:15.)
7. W. J. M. RANKINE: "A Manual of Applied Mechanics," 15th ed., Charles Griffin & Company, Ltd., London, 1898, p. 213. Rankine's original paper on this subject was published in *Phil. Trans. Roy. Soc. London*, vol. 147, p. 9, 1857.
8. GEORGE PAASWELL: "Retaining Walls; Their Design and Construction," McGraw-Hill Book Company, Inc., New York, 1920.
9. THEODORE VON KÁRMÁN: Über elastische Grenzzustände, *Proc. Second Intern. Cong. Applied Mech.*, 1926.
10. J. JÁKY: Classical Earth Pressure Theories (in Hungarian), *Északi Közlemények*, 1931; in German, 1937-1938.
11. JOHANN OHDE: Seven articles on earth pressure in *Die Bautechnik*, 1938.
12. CHARLES TERZAGHI: Large Retaining Walls Tests, five articles in *Eng. News-Record*, vol. 112, 1934.
13. H. DE B. PARSONS: Some Soil Pressure Tests, *Trans. A.S.C.E.*, vol. 100, 1935; also Hydrostatic Uplift in Pervious Soils, *ibid.*, vol. 93, 1929.
14. JACOB FELD: Lateral Earth Pressure, etc., *Trans. A.S.C.E.*, vol. 86, 1923.
15. C. F. JENKIN: The Pressure on Retaining Walls, *Proc. Inst. Civil Eng. (London)*, vol. 23, session 1931-1932.
16. H. G. MOULTON: Earth and Rock Pressure, *Trans. A.I.M.M.E.*, 1920.
17. J. C. MEEM: The Bracing of Trenches and Tunnels, etc., *Trans. A.S.C.E.*, vol. 60, 1908.
18. LAZARUS WHITE and GEORGE PAASWELL: Lateral Earth and Concrete Pressures, *Trans. A.S.C.E.*, vol. 104, 1939.
19. J. F. SEILER: Effect of Depth of Embedment on Pole Stability, *Wood Preserving News*, vol. 10, 1932.
20. RAYMOND P. PENNOYER: A series of articles in *Civil Eng.*, vol. 3, 1933; vol. 4, 1934; vol. 5, 1935. The last article was done in collaboration with GEORGE HOCKENSMITH. See also a letter by KENNETH L. DEBLOIS:

- ibid.*, vol. 4, 1934; also HERMANN BLUM: "Einspannungsverhältnisse bei Bohlwerken," Wilhelm Ernst und Sohn, Berlin, 1931.
21. Bending Moments as Developed by H. Blum and Earth Pressures Developed by H. Krey, *Carnegie Steel Sheet Piling Catalogue*, insert B, 1933.
  22. Provisional Rules Relating to the Calculation and Execution of Hydraulic Works in Reinforced Concrete, issued by the Association of Danish Engineers, *Perm. Intern. Assoc. Navigation Congr. Bull.*, vol. 4, No. 7, January, 1929.
  23. A. AGATZ: "Der Kampf des Ingenieurs gegen Erde und Wasser im Grundbau," Julius Springer, Berlin, 1936.
  24. G. SCHØNWELLER: Calcul des murs de quai, *Proc. World Eng. Congr. Tokyo, Japan, 1929*, vol. 11, Paper 17 (general number of order 416).
  25. WILHELM BUCHHOLTZ: "Erdwiderstand auf Ankerplatten," a reprint from *Jahrb. Hafenbautech. Ges.*, vol. 12, 1930-1931.
  26. I. RIFAAT: "Die Spundwand als Erddruckproblem," Institute of Structural Mechanics, Technische Hochschule in Zürich, *Pub.* 5, 1935.
  27. PAUL BAUMANN: Analysis of Sheet Pile Bulkheads, *Trans. A.S.C.E.* vol. 100, 1935.
  28. HEINRICH PRESS: Gemessene Bewegungen an geramnten Spundwänden, *Zentr. Bauverwaltung*, vol. 58, 1938.
  29. J. P. R. N. STROYER: Earth Pressure on Flexible Walls, also discussion, *Jour. Inst. Civil Eng. (London)*, vol. 1, 1935-1936. For a previous paper, see *Proc. Inst. Civil Eng. (London)*, vol. 226, 1927-1928.
  30. CHARLES TERZAGHI: Soil Mechanics—a New Chapter in Engineering Science, Forty-fifth James Forrest Lecture delivered at the Institute of Civil Engineers (London), session 1938-1939 (see also *Jour. Inst. Civil Eng.* of that year).
  31. H. MÜLLER-BRESLAU: "Erddruck auf Stützmauern," Alfred Kroener, Leipzig, 1906.
  32. RALPH B. PECK: Earth-Pressure Measurements in Open Cuts, Chicago Subway, *Trans. A.S.C.E.*, vol. 108, 1943.
  33. O. FRANZIUS: Versuche mit passivem Druck, *Der Bauingenieur*, vol. 5, 1924.
  34. LAZARUS WHITE and EDMUND A. PRENTIS: "Cofferdams," Columbia University Press, New York, 1940.
  35. KARL TERZAGHI: Stability and Stiffness of Cellular Cofferdam (paper and discussions), *Trans. A.S.C.E.*, vol. 110, 1945.

## CHAPTER XI

### PRESSURE ON TUNNELS AND CONDUITS

#### A. TUNNELS

**11:1. Terminology.**—The simplest way in which to construct a tunnel is by means of an *open trench* with subsequent back-filling. For instance, most of the London subway (“Underground”) was in shallow cuttings (“cut and cover”). Also a certain part of the Buenos Aires, Argentine Republic, subway was built in this manner.

Tunneling in *hard rock* is started by cutting out or blasting out rock in the headings. The muck or excavated material is removed, mostly longitudinally. A hard-rock tunnel may or may not require lining to support the weight of the overburden; obviously, *soft material* always requires lining for its support. Lining, if any, is of masonry or concrete, sometimes of cast iron. The sill of the cross section is often provided with an inverted arch (“invert”). Voids between rock and lining are packed with stone or concrete, also grouted under pressure.

Subaqueous tunnels (such as those below the bed of the Hudson River at New York City) are often constructed using the *shield method*, though this method may also be applied for tunneling in any soft-soil deposit (example: Chicago subway). A strong shield is pushed horizontally through the soil deposit, and excavating operations follow its path. A part of the earth material is taken into the heading and afterward removed, whereas the other part is pushed toward the top similarly to the action shown in Fig. 10:33.

**11:2. Statement of the Tunnel Problem.**—For the sake of simplicity, tunnels of circular and rectangular cross section only will be considered hereafter.

The following three questions are to be answered:

a. What are the conditions of stability of a circular or rectangular hole pierced through the mass at a depth  $z$  below the surface of the ground and standing safely without lining?

b. If lining is required for stability of the tunnel, what is the value of the pressure on that lining? Does the pressure on the lining depend on the magnitude of its deformations?

c. If the tunnel may hold without lining or, as occurs in many cases, the actual pressure on the lining is less than the weight of the overburden, which part of the mass carries the relieved weight? This question is closely connected with the possibility of transfer of pressure by shearing stresses (Sec. 10:22).

**11:3. Lateral-pressure Diagram.**—The diagram of the lateral pressure in a natural earth mass is triangular (Sec. 4:25). In reality this statement is no more than a possibility, since little is known about the ratio of the horizontal to the vertical pressure at a considerable depth. It will be assumed in this chapter that this ratio (designation  $K_a$ ) equals the well-known Rankine active value [Eq. (5:5)]

$$K_a = \frac{1 - \sin \phi}{1 + \sin \phi} = \tan^2 \left( 45^\circ - \frac{\phi}{2} \right) \quad (11:1)$$

The value of  $K_a$  as given by formula (11:2) is possibly slightly less than the actual ratio in question, because the Rankine formula corresponds to the state of plastic equilibrium (Sec. 5:3) and to reach this state the mass has to move somewhat. The horizontal shears that develop in this connection decrease the values of the lateral pressure existing in a natural earth mass.

**11:4. Circular Tunnel without Lining.**—Figure 11:1 represents conditions of equilibrium of the earth mass surrounding a tunnel without lining. Theoretically, the tunnel causes stress redistribution in the whole earth mass, and the triangular pressure diagram as defined by Eq. (11:1) holds only at infinity. In reality, at a rather short distance a tunnel has but a very limited influence on the stress distribution in the mass.

a. *Value of the Lateral Pressure.*—The diagram formed by the oblique line  $FD$  and the vertical  $FC$  (Fig. 11:1) is the lateral-pressure diagram at an infinite distance from the tunnel. The upper part of it  $FAB$  is balanced by the corresponding part of the symmetrical earth-pressure diagram (on the other side of the center line of the tunnel). In the same way all pressures below level  $CD$  are balanced. Trapezoid  $ABCD$  (cross hatched in Fig. 11:1) corresponds to the unbalanced earth pressure. The value of the latter is

$$P = (K_a \gamma h) (2r) = 2K_a \gamma hr \quad (11:2)$$



replaced by cuts, however; and if they are built, both pressures  $P_a$  and  $P_b$  are insignificant and their estimation is simply non-essential.

*c. Distribution of Additional Lateral Pressure along the Center Line of the Tunnel.*—The law of distribution of *additional* horizontal pressures  $P_a$  and  $P_b$  along faces  $EG$  and  $HI$  (Fig. 11:1) cannot be established from purely statical considerations. It seems quite logical, however, to admit that the influence of a tunnel on the stress redistribution in the mass is stronger close to the tunnel than far away from it. The planes tangent to the tunnel are the closest to it; hence the largest deviation from the stresses existing in a natural, or undisturbed, earth mass may be expected on or close to these planes. Purely for the sake of brevity this statement will be termed “basic” hereafter.

In Fig. 11:1 approximate diagrams of  $P_a$  and  $P_b$  are shown; the symbol  $a$  corresponds to the distance from the top of the tunnel to the resultant of the pressure  $P_a$ . The shape of the diagrams has been traced taking the “basic statement” into consideration. Hereafter, for approximate computations, the value of  $a$  will be estimated at  $a = \frac{3}{2} r$ .

*d. Planes Where  $\Delta S = 0$ .*—It should not be forgotten that the values of  $\Delta S$  are the *changes* of the total shearing forces when passing from one horizontal plane within the mass to another. Mathematically speaking, the value of  $\Delta S$  is the differential of the sum of all shearing stresses acting along a horizontal plane, computed from a given point on that plane to infinity. According to the “basic statement” the maximum horizontal shearing stresses are to be expected on the horizontal planes tangent to the tunnel. Hence their differentials (or shear changes) equal zero also on the same planes. In other words, there is no deviation from the values of the natural earth pressure on the horizontal planes tangent to the tunnel. Figure 11:1 right, shows the diagram of the lateral pressure on the vertical plane  $MN$  tangent to the tunnel. The pressure diagram is a curve intersecting the triangular diagram of the natural earth pressure at points  $Z$  and  $Z'$ . Crosshatched areas  $P'_a$  and  $P'_b$  are to be added to the diagram of the natural (triangular) earth pressure, whereas area  $P' = P'_a + P'_b$  is to be deducted therefrom. Presumably

$$P'_a < P_a; P'_b < P_b; \text{ and } P' < P$$

It may also be stated that at points *G* and *H* (top and bottom of the tunnel, respectively) there is no additional pressure. There is an analogy between the lateral pressure diagram in Fig. 11:1, right, and Figs. 10:15, 10:17, and 10:28.

*e. Transfer of the Weight of the Overburden.*—For deep tunnels the area of the tunnel itself as compared with the area of the over-

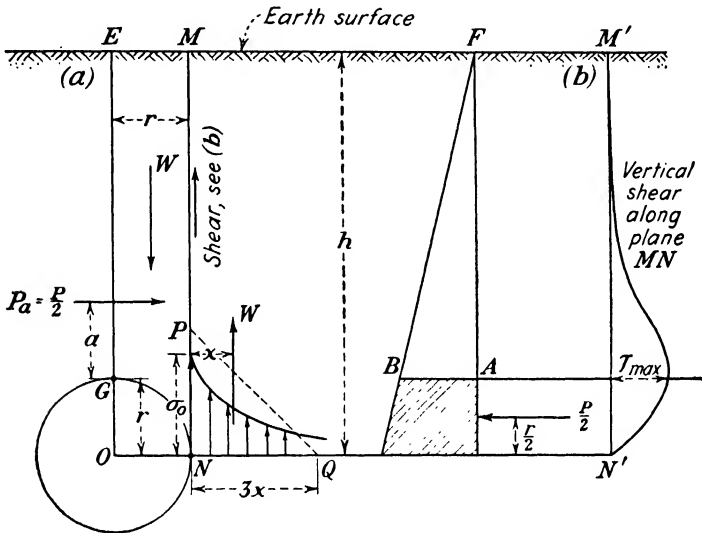


FIG. 11:2.—Transfer of the weight of the overburden located over the tunnel.

burden is negligible. Hence the weight  $2W$  of the overburden over a deep tunnel (Fig. 11:2) is

$$2W = 2\gamma hr \tag{11:3}$$

From comparison of Eqs. (11:2) and (11:3)

$$\frac{P}{2W} = K_a \tag{11:4}$$

Consider now that part of the mass cut out by a vertical and a horizontal plane passing through the center of the tunnel. Because of boundary conditions there are no stresses normal to the periphery of the tunnel, the only stress being compression along that periphery (compare Fig. 10:14). Consider the equilibrium of the two couples developed because of the presence of the tunnel, these couples being formed by the forces  $P/2$  and  $W$ . Designate with

$x$  an unknown distance from the side of the tunnel  $N$  to the resultant of the pressure distributed along plane  $ON'$  (shown with arrows in Fig. 11:2). This is the place to which the weight of the overburden  $W$  is transferred by shearing stresses. Taking moments of the forces acting on the part of the mass in question,

$$\frac{P}{2} \left( a + \frac{r}{2} \right) - W \left( x + \frac{r}{2} \right) = 0 \quad (11:5)$$

from which, remembering Eq. (11:4),

$$x = K_a \left( a + \frac{r}{2} \right) - \frac{r}{2} \quad (11:6)$$

Placing  $a = \frac{3}{2}r$  and remembering that for a perfectly cohesive mass ( $\phi = 0$ ), the value of  $K_a = 1$  [Eq. (11:1)], we have

$$x = \frac{3}{2}r \quad (11:7)$$

*f. Compressive Stresses around the Tunnel.*—If the pressure distribution along plane  $ON'$  were triangular (dotted line  $PQ$  in Fig. 11:2), the length  $NQ$  would equal  $3x$  and the value of the additional compressive stress as expressed by the ordinate  $PN$  would be

$$\overline{PN} = \frac{2W}{3x} = (2h\gamma r) \div \left( 3 \times \frac{3}{2} r \right) = \frac{4}{9} h\gamma \quad (11:8)$$

As seen from Fig. 11:2 the value of  $PN$  is probably exaggerated, and the actual value  $\sigma_0$  of the additional compressive stress equals about one-third of the compressive stress  $h\gamma$  that existed at point  $N$  (Fig. 11:2) before the construction of the tunnel.

As stated above, the compressive stress at point  $G$  (top of the tunnel) that existed in the earth mass prior to construction is not increased by the presence of the tunnel; hence the maximum compression stress  $\sigma_{\max}$  should be located above the top of the tunnel  $G$ . Its location can be found only in a very approximate way by tracing freehand a curve from point  $G'$  up (Fig. 11:3) to bound an area equal to  $P_a = P/2$ . A vertical tangent to this curve (point  $T$  in Fig. 11:3) defines the location of the maximum compression stress.

*g. Danger of Tension Failure.*—There is a possibility that the overhanging material located above the top of the tunnel without lining (point  $G$  in Figs. 11:1 and 11:3) might fall down. This may

occur if the sum of the absolute values of the *full* compression stress over the tunnel and the tension stress  $\gamma z_0$  (Fig. 11:3) is larger than approximately twice the shearing strength of the mass. The symbol  $z_0$  used here means the vertical distance computed from the top of the tunnel  $G$  up. The corresponding Mohr's circle for tension

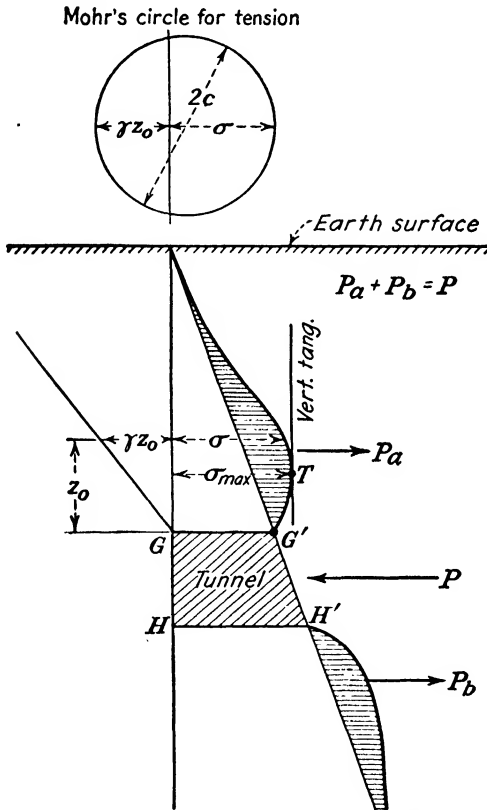


FIG. 11:3.—Compression stress above the tunnel: danger of tension failure.

plastic equilibrium of a perfectly cohesive material is shown in Fig. 11:3, top. After a tension failure occurs, another one may follow if the conditions of equilibrium are not satisfied.

**11:5. Determination of the Safe Diameter of a Circular Tunnel without Lining.**—Refer to Fig. 11:2, right, which shows the approximate distribution of vertical shearing stresses acting along the vertical plane  $NM$  to balance the weight of the overburden  $W$ .

The values of the vertical unit shears  $\tau$  are plotted as horizontal ordinates from the vertical line  $M'N'$ . Owing to boundary conditions the unit shearing stress  $\tau$  at point  $N$  (Fig. 11:2) is zero, and by virtue of the "basic statement" the maximum value of the unit shearing stress  $\tau_{\max}$  is located on or close to the horizontal plane tangent to the tunnel. The *average* value of the vertical shearing stress  $\tau$  along plane  $MN$  for a deep tunnel is

$$\tau = \frac{h\gamma r}{h} = \gamma r \quad (11:9)$$

In other words, the average value of  $\tau$  is practically independent from the depth of the tunnel. If the shear distribution along a vertical plane were triangular, the maximum unit shear would be twice the average unit shear. It will be assumed that when the shear distribution as in Fig. 11:2 (right) is curved, the maximum shear is also twice the average. In other words it will be assumed that

$$\tau_{\max} = 2\gamma r \quad (11:10)$$

For a perfectly cohesive material the value of the shearing strength equals the unit cohesion  $c$ , and the condition of plastic equilibrium is

$$2\gamma r = c \quad (11:11)$$

from which the radius of a tunnel built in a perfectly cohesive material and safe against plastic flow is

$$r = \frac{1}{2} \frac{c}{\gamma} \quad (11:12)$$

The points  $X$  (Fig. 11:1) where the danger of plastic flow is at a maximum are located at the intersection of the planes tangential to the tunnel. The four points  $X$  are located symmetrically with respect to the tunnel.

If plastic flow is acceptable, the radius of the tunnel without lining can be determined from the condition that the overburden should not fall down into the tunnel as a unit. In such a case the average shearing stress  $\tau$  along plane  $MN$  (Fig. 11:2) should not be larger than the value of the unit cohesion  $c$ . This condition furnishes a double value of the radius  $r$  of the tunnel as compared with that given by Eq. (11:12), namely,

$$r = \frac{c}{\gamma} \quad (11:13)$$

It should be remembered that the ratio  $c/\gamma$  is often used in the theory of stability of slopes (Chap. IX).

**11:6. Rectangular Tunnel without Lining.**—The preceding considerations (Secs. 11:3 and 11:4) are applicable also to tunnels of rectangular cross sections without lining. The danger of plastic flow in this case is at the four corners of the cross section. For the determination of the width of the tunnel  $b$  formulas (11:12) and (11:13) may be used by substituting

$b$  for  $2r$ . In both circular and rectangular tunnels without lining there are no shearing stresses at the center line due to symmetry. The horizontal pressure is then the major principal stress; and if a tension failure is caused by the weight of the overhanging material (Fig. 11:3), the failure lines form angles  $45^\circ - \phi/2$  with the horizontal. In the case of a flat roof, as in a rectangular tunnel without lining, these failure lines are very conspicuous (Fig. 11:4). To prevent the

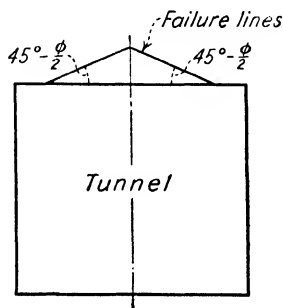


FIG. 11:4.—Failure of the flat roof of a tunnel without lining.

overhanging material from falling down, Terzaghi<sup>1</sup> advises shaping the roof of a rectangular tunnel without lining as a flat arch.

**11:7. Trap-door Experiment.**—In the trap-door experiment known to the engineers for over one hundred years, a box filled with sand (Fig. 11:5) is provided with a trap door (yielding strip) at the bottom. As the trap door moves down (small distance  $\Delta_1$ ), the pressure on the door first decreases; but as the motion proceeds (distance  $\Delta_2$ ), the pressure increases again. In Fig. 11:5 line  $AB$  represents the full weight of the overburden  $ABCD$ . When the trap door moves down through distance  $\Delta_1$ , the upward vertical shearing stresses are “mobilized” along vertical planes  $AB$  and  $CD$ . The larger the displacements of the overburden the larger the shearing stresses, until the latter reach their ultimate value (shearing strength of the material). At that time-moment portion  $AF$  of the weight of the overburden is carried by the shearing stresses, and portion  $BF$  by the trap door. Along all vertical planes of the mass in the box there are now upward-acting shearing forces, represented by the ordinates of the “total shear diagram.” Their differences, or changes  $\Delta S$ , act upward within the overburden

$ABCD$  (negative changes  $-\Delta S$ ) and downward outside. Further motion of the trap door causes the failure of the mass with or without formation of an arch (curved line above the trap door in Fig. 11:5). The sand mass tends to flow toward the trap door roughly following the slope of the angle of repose  $DI$ . The pressure on the trap door increases, and the pressure transferred to the bottom of the box  $AG$  decreases. Notice that distance  $HG$  is that portion of the weight of the overburden which may be carried by vertical walls of the box by friction if the box is not large enough.

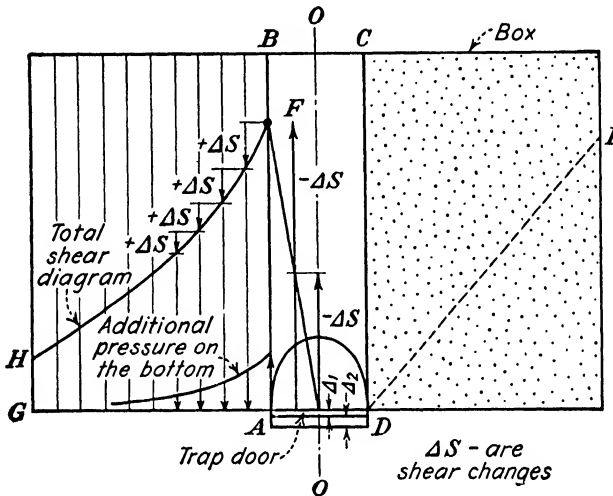


FIG. 11:5.—Trap-door experiment.

The conclusions to be drawn from this experiment are

a. If a tunnel is provided with a lining, the latter should be flexible enough to produce displacements in the overburden and mobilize possibly large upward-acting shearing stresses for balancing a possibly large portion of the weight of the overburden, thus relieving the pressure on the lining.

b. The lining should not be too flexible, however, since considerable displacements in the overburden may destroy the integrity of the mass and cause an increase of pressure on the lining.

Though these statements are theoretically clear and simple, it is quite difficult in practice to provide a tunnel with a satisfactory lining. The solution of the lining problem at the present time (1947) is mostly based on practice and engineering judgment.

**11:8. Vertical Pressure on the Roof of a Tunnel.**—Hereafter a few attempts to solve this problem as reported in the technical literature will be listed.

*a. Cellular Cofferdam Analogy.*—In considering tunnels through sand it is customary to assume that the failure lines are *vertical*. In such a case the situation becomes analogous to that discussed in Sec. 10:34 with regard to internal shear in cellular cofferdams. Referring to the designations in Fig. 11:6 and assuming that the pressure  $F$  on the roof of the tunnel is the difference between the weight of the overburden  $B\gamma h$  and the shearing force along the potential failure lines  $MN$ ,

$$F = B\gamma h - 2S \quad (11:14)$$

where the value of  $S$  may be determined using formulas (10:40) and (10:41). Such an approach was used, for instance, by Forchheimer<sup>2</sup> as early as in 1882. Formula (11:14) presumes that *full* friction is developed along the potential failure lines. This, however, cannot be proved.

*b. Bin Analogy.*—For both cohesionless and cohesive soils Terzaghi<sup>1</sup> assumes that the lining deflects in such a way that the mass on both sides of the tunnel is in the state of plastic equilibrium. Consequently, the sides (haunches) of the tunnel can be considered as retaining walls with the formation of wedges making angles  $45^\circ - \phi/2$  with the vertical. The corresponding failure lines are shown as dotted lines in Fig. 11:6.

Furthermore, Terzaghi uses the well-known bin formula and finds that the unit vertical pressure  $\sigma_z$  on the roof of a deep tunnel and on the top of the wedges at its sides is

$$\sigma_z = \frac{\gamma B_1}{K \tan \phi} \quad (11:15)$$

where  $B_1 = B/2 + H \tan (45^\circ - \phi/2)$  as in Fig. 11:6 and  $K$  is an empirical coefficient expressing the ratio between the horizontal and vertical pressures above the tunnel. According to Terzaghi, the value of this coefficient is approximately unity. In any event, the value of  $K$  is larger than  $K_a$ , since above a tunnel, at its center line, the horizontal pressure is larger and the vertical smaller than in an undisturbed earth mass in which the ratio of these two pressures approximately equals  $K_a$  (compare also Sec. 11:4f).

*c. Meem's Rule.*—Meem,<sup>3</sup> a well-known American foundation engineer,\* speaking of rectangular tunnels with lining, stated: "In a 20 ft. tunnel in normally dry soft ground, there is no greater pressure on the roof at a depth of 100-ft. than there is at 25-ft. depth."

According to Meem the average pressure on the roof of the tunnel of rectangular cross section may be estimated at 1,250 lb. per sq. ft.

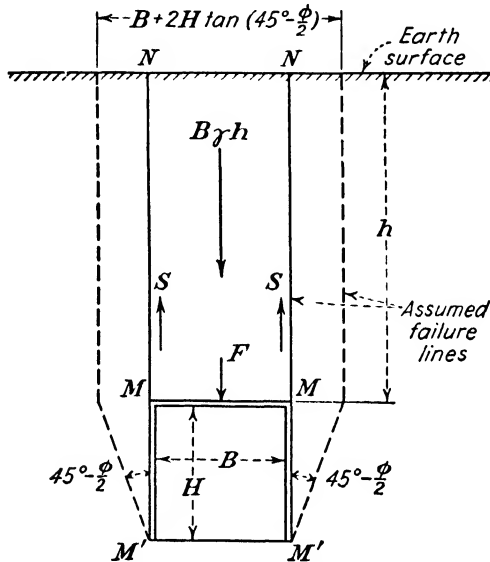


FIG. 11:6.—Vertical pressure on the lining of a tunnel through sand.

Of course, this numerical value may be used only for checking or comparison purposes.

**11:9. Systems of Forces Acting on a Tunnel.**—For checking the dimensions selected for a tunnel, forces acting on it are determined, after which the tunnel is analyzed as any other structure by determining moments and shears and correcting the chosen dimensions, if necessary.

Generally speaking, the forces acting on a tunnel are (a) vertical pressure at the top, (b) vertical reaction at the bottom, and (c) horizontal pressure at the sides. All pressures are referred to one lineal unit (lineal feet) of the tunnel. If the vertical pressure on the roof of the tunnel is determined as described in Sec. 11:8, then the

\* James Cowan Meem (1866–1936).

vertical reaction at the bottom equals the sum of the vertical pressure at the top and the weight of the tunnel. Sometimes it is assumed, however, that the mass around the tunnel acts as a fluid. In this case the vertical pressure on the roof is the total weight of the overburden, and the reaction at the bottom equals the hydrostatic pressure that a fluid of the unit weight  $\gamma$ , that of the given mass, would exert at the level of the bottom of the tunnel.

The horizontal pressure at the sides of the tunnel is generally assumed to be a certain portion of the vertical. This portion was assumed at between one-third and two-thirds in the design of the Chicago subway passing mostly through plastic blue clay and about one-half in the design of the tunnels in organic silt under the Hudson River, New York City. It is obvious that such a horizontal pressure distribution is the triangular pressure distribution of the Rankine formula. It should be clearly understood, however, that the actual horizontal pressures on the tunnel may or may not follow exactly this assumed triangular pressure distribution.

Undoubtedly in the case of a tunnel provided with lining the general equation of equilibrium (11:5) for a tunnel without lining also holds. In this case the weight of the overburden  $2W$  and the unbalanced lateral pressure in Eq. (11:5) should be decreased by some values  $2\Delta W$  and  $\Delta P$ , respectively, which represent the pressure on the top and one lateral side of the lining, respectively. These values of  $2\Delta W$  and  $\Delta P$  depend on the deflections of the lining (compare Sec. 11:6) and, generally speaking, cannot be determined theoretically, at least at the present time (1947).

Housel<sup>4</sup> measured pressures on the lining of a tunnel in plastic clay during and after the construction. According to his data, the stress distribution in the mass disturbed by the construction of the tunnel tends to return to the original stress distribution, *i.e.*, that which existed before the construction. This is tantamount to the gradual vanishing (extinguishing) of the shearing stresses along vertical and horizontal planes within the disturbed plastic mass. In tunnels *without lining*, however, the total vanishing of shearing stresses would contradict statics (Sec. 11:3) and hence cannot occur. So far (1947) there is no evidence of the possibility of gradual vanishing of shearing stresses in cohesionless sands, except by accidental causes such as vibrations. Additional field data along these lines are required, however.

**11:10. Shield Method.**—This type of circular tunnel has been mentioned already in Sec. 11:1. As shown in Fig. 11:7 there is a tendency for the earth in front of the advancing bulkhead to push forward. Since the shearing strength of the earth material is overcome, soil particles from the lower part of the mass move upward following curvilinear surfaces (failure lines) and enter the openings in the front face of the bulkhead. In the case of the Lincoln Tunnel, New York City, about 30 per cent of the excavated

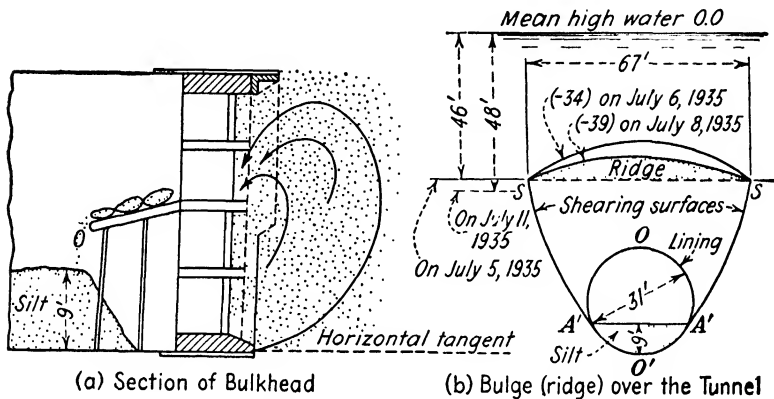


FIG. 11:7.—Shield method as used in the Lincoln Tunnel, Hudson River, New York.

silt entered the bulkhead. The particles from the upper portion of the disturbed mass push up the earth above them, creating a longitudinal bulge at the boundary of the earth mass similar to that shown in Fig. 10:33, right.

The soil material pushed upward forms curved shearing surfaces (failure lines). The upper part of the bulge is generally removed, by dredging or otherwise (Fig. 11:7), and the rest of it moves back and consolidates. Obviously, the vertical shearing stresses act downward at the very beginning of the process and upward when the mass tends to move down. Shearing stresses cannot be larger than the shearing strength of the corresponding material; hence in materials of low shearing strength the relief in the weight of the overburden cannot be considerable. In fact, in the case of the Lincoln Tunnel, built in organic silt (cohesion about 100 lb. per sq. ft.), the relief of the weight of the overburden as measured by special devices was less than 10 per cent of that weight.

Available field measurements are insufficient to judge concerning

the horizontal and upward vertical pressures on the tunnel of this type.

If the shield method is applied in plastic soils, such as organic silt or plastic clays, there is a decrease in horizontal diameter (and not in vertical diameter as is the case of tunnels through sands and similar materials and in the case of pipe culverts (Sec. 11:14*b*). In the case of the Lincoln Tunnel this decrease was  $1\frac{1}{2}$  in., the total diameter of the tube being 31 ft. During 6 months after construction the horizontal diameter of the Lincoln Tunnel tubes was gradually returning to its normal value. Apparently the decrease in question is caused by a considerable lateral pressure in the lower part of the lining during the initial stage of shoving, this action being combined with a simultaneous relief in vertical pressure due to the passage of the shield.

In the shield method and often in other methods as well the action of the stresses removed during the excavation is replaced by blowing compressed air into the tunnel. As in the case of pneumatic caissons, compressed air is used to keep water out during the construction of subaqueous tunnels in pervious soils.

An insufficiently loaded tunnel built by the shield method in soft soil under a river tends to float up. Shearing stresses mobilized in the earth mass in this connection act downward, *i.e.*, against the direction of the impending motion.

**11:11. General Remarks.**—*a. Changes in Seepage.*—Flow of moisture toward a new opening in the earth mass may influence the stress distribution in the earth mass (compare Sec. 13:17*b*).

*b. Quicksand.*—The presence of quicksand, *i.e.*, of sand, generally fine, which stands under pressure or hydraulic head (Sec. 3:1) handicaps excavation and increases the pressure on the tunnel. This is not because sand changes appreciably its angle of internal friction under water but because many grains in quicksand do not touch other grains at all. Drainage or freezing of quicksand may be helpful.

*c. Blowouts.*—A piece of rock may tear off by itself from an unprotected tunnel wall. Huge masses of rock or soil may separate from the tunnel wall and break the lining. The cause of such "blowouts" is traced to the action of shearing stresses.

*d. Measuring Pressures.*—Vertical deflections of the temporary lining used during construction of a tunnel have been measured on many occasions, and pressures estimated from them. In the

past 10 years (1936–1946) unprecedented measurements of pressures on the lining of circular tunnels using embedded plugs and cells have been made in the United States.<sup>4,5</sup> The “string method” of the Russian professor Davidenkov should be mentioned; it consists in estimating the stresses in a beam from the pitch difference of a string connected to the loaded and subsequently unloaded beam.

### B. CONDUITS

**11:12. Classification of Conduits.**—Conduits of liquids, water particularly, are pipes placed either in ditches with backfilling or under embankments. In the latter case they may be termed also “pipe culverts” or “culvert pipes.” Conduits of circular cross section only will be considered hereafter.

According to their rigidity conduits may be classified into rigid, semirigid, and flexible. For instance, concrete pipes are rigid; cast-iron pipes are semirigid; and pipes made of corrugated iron are flexible.

So far as bedding conditions of a conduit are concerned they vary through a wide range, from simple earth foundations in a ditch to concrete cradle beddings.

**11:13. Tunnels and Conduits Compared.**—Both tunnels and conduits are buried structures; but though in some respects they are similar, there is also a great difference between them. For instance, theories of stability of tunnels based on the homogeneity of the earth mass (Secs. 11:4–11:6) may be applied to conduits only with a certain reservation. In fact, in this case the structure is placed on one kind of material and covered with another, which may be earth in a loose state.

In most cases conduits are placed rather close to the earth surface. In this connection the problem arises of a minimum earth cover to protect the pipe from the impact and other hazards of the traffic. Because of shallow earth cover on a conduit, the action of the live load cannot be disregarded in this case. In the analysis of tunnels, however, such problems as the minimum cover or the live load action generally are not considered.

In compact, cohesive materials vertical shearing stresses may balance the weight of the overburden over a tunnel wholly (Sec. 11:3) or partly (Sec. 11:9). However, a conduit in the form of a hole pierced in the earth mass and left without reinforcement is an impossibility. As a rule, most of the weight of the overburden

over a conduit (including the live load) is transmitted to the bedding, and in some cases (Sec. 11:17a) the conduit carries a weight even exceeding that of the overburden, which never occurs in tunnels except perhaps tunnels built in open cuts (Sec. 11:1).

Since conduits are many and tunnels are few, the question of economical design is perhaps more important in the former case. Hence, the design of conduits requires careful determination of superimposed forces. This explains why a great number of tests and experiments have been made on conduits (Sec. 11:15) for obtaining empirical data on their behavior.

A factor that should be given serious consideration in the case of both conduits and tunnels is the possibility of changes of the superimposed loads as the time goes by due to the vanishing or extinguishing of the shearing stresses in the mass surrounding the culvert (compare Sec. 11:9).

**11:14. Existing Methods of Analysis of Pipe Culverts.**—The methods described in this section are those so far published (1947). Some peculiarities in the analysis of pipe culverts for airports are listed in Sec. 11:18.

a. For analyzing *rigid conduits*, Dean Marston's theory is often used. The following designations will be used in presenting the results given by this theory:

$W$  = the vertical external load on a closed conduit due to fill material (dead load), lb. per ft. of length.

$\gamma$  = unit weight of fill materials, lb. per cu. ft.

$B$  = greatest horizontal breadth of conduit, ft., or horizontal breadth of a ditch at top of conduit, ft.

$C$  = variable coefficient, abstract number.

Then

$$W = C\gamma B^2 \quad (11:16)$$

The designations for the case of live load will be

$W'$  = the average total vertical load on the conduit as caused by the live load, lb. per lin. ft.

$A$  = length of a section of a closed conduit, ft.

$I$  = impact coefficient (abstract number between 1.5 and 2).

$C'$  = variable coefficient, abstract number.

$T$  = a concentrated live load, lb.

Then

$$W' = \frac{1}{A} I C' T \quad (11:17)$$

In establishing his formulas, Marston used the bin theory (compare Sec. 11:8). For computation of the coefficients  $C$  and  $C'$  numerous tables and graphs are available.<sup>6,7,8</sup> The vertical reaction of the bedding equals the sum of the forces  $W$  and  $W'$  computed using formulas (11:16) and (11:17). The horizontal pressure at the side of the pipe is often computed as a fraction  $n$  of the vertical. According to A.R.E.A. data<sup>14</sup> the value of  $n$  may be estimated at  $\frac{1}{3}$ , a value that may be considered also as an average for highway pipe culverts. With these data the structural analysis of a conduit is possible (compare Sec. 11:9).

b. The method of analyzing *flexible pipe culverts* has been studied by Spangler,<sup>9</sup> of Iowa State College, which is also Marston's. A flexible pipe under an embankment load deforms from a circular to an ellipselike shape. Thus the vertical diameter is decreased, and the horizontal increased practically by the same value, which ordinarily equals a few per cent of the nominal diameter of the pipe. A deflection both ways of 5 per cent is sometimes used in the analysis and design of corrugated metal pipes. Owing to the law of equality of action and reaction, the embankment being pushed laterally by the deflecting pipe develops passive pressure (passive resistance, Sec. 5:5). Pressures are postulated to be proportional to displacements, and the passive pressures on each side of the pipe distributed parabolically over the middle 100° of the pipe. The maximum unit pressure  $\sigma_x$  which will occur at the ends of the horizontal diameter of the pipe (point A, Fig. 11:8) equals the product of the modulus of the passive resistance of the given soil  $e$  and one-half of the horizontal deflection  $\Delta/2$  of the pipe

$$\sigma_x = e \frac{\Delta}{2} \quad (11:18)$$

Spangler's "modulus of the passive resistance" of the given soil is that pressure (in pounds per square inch) which causes a one-way deflection of the pipe  $\Delta/2 = 1$  in. It may be expressed in pounds per square inch per inch (or in pounds per cubic inch). The value of  $e$  depends not only on the texture of a given soil but mostly on its compaction in the backfill as caused during construction and operation and, if the pipe is placed in a ditch, on the size of the latter. The average value of  $e$  is sometimes assumed at 15 lb. per sq. in. per in. The total vertical force acting at the top of the flexible

pipe and the vertical reaction at the bedding each equals  $W + W'$ , using designations of formulas (11:16) and (11:17). Both the vertical force at the top of the culvert and the vertical reaction at the bedding are assumed to be uniformly distributed on the horizontal projection of the culvert (BB' in Fig. 11:8).

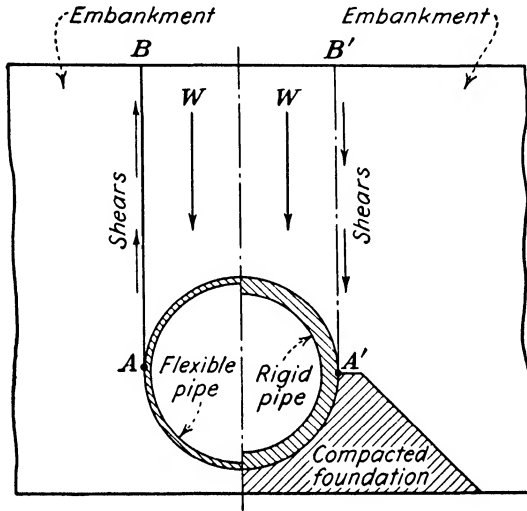


FIG. 11:8.—Shearing stresses may decrease or increase the vertical pressure on a pipe culvert.

**11:15. Modulus of Passive Resistance and Similar Concepts.**—Tunnel designers sometimes use the so-called “soil constant” or “soil compression constant.”<sup>10,11</sup> So far as tunnels are concerned, this is a concept analogous to the concept of the “modulus of passive resistance” as discussed in Sec. 11:14. To the same class of concepts belong

a. “Modulus of foundation” as discussed in Sec. 8:11. Cummings also used this concept in discussing buckling of piles (ref. 29, Chap. VIII).

b. “Modulus of subgrade,” as used in the design and analysis of pavements (Chap. XII).

Extreme care is needed in using these moduli, since repeated application of the load to the soil surface produces decreasing (and not constant) displacements or deflections. The moduli in question may be used, however, with fair approximation if the soil mass is well compacted, naturally or artificially. The physical

dimension of all moduli mentioned is pounds per square inch per inch (or pounds per cubic inch).

**11:16. Experiments with Pipe Culverts.**—Experiments with pipe culverts were carried on and the results published (*a*) at Iowa State College,<sup>12</sup> (*b*) at the University of North Carolina,<sup>13</sup> (*c*) at Farina, Ill., by the American Railroad Engineering Association<sup>14</sup> (A.R.E.A.), (*d*) in Switzerland,<sup>15</sup> and (*e*) in Russia.<sup>16</sup> At the present time (1947) much attention is being given to this item by the U. S. Army Engineers. Some conclusions from these experiments are

*a.* Pipes under embankments carry the weight of the vertical prism above it (overburden) plus some additional weight in the case of rigid pipes and minus some additional weight in the case of flexible pipes.

*b.* The vertical diameter of a loaded pipe decreases and the horizontal increases. According to measurements made at Chapel Hill<sup>13</sup> on pipes from 20 to 32 in. in diameter, the maximum one-way deflection  $\Delta/2$  [compare formula (11:18)] of a smooth iron pipe is not over 1.24 per cent of its diameter under the weight of a 12-ft.-high fill. Semirigid and rigid pipes furnished even smaller deflections.

*c.* Experiments at Iowa State College have shown that highway traffic has no appreciable load effects on pipe culverts when the height of the embankment exceeds 5 ft. In the case of a pipe buried in a ditch this height may be less.

**11:17. Shearing Stresses in the Embankment Covering a Pipe Culvert.**—In studying the action of shearing stresses in an embankment covering a pipe culvert, the following two essential features are to be considered:

*a. Increase or Decrease of the Pressure on the Pipe Culverts by Shearing Stresses.*—Figure 11:8, left, shows a flexible pipe placed under an embankment. Owing to flexibility of the pipe, the overburden (weight  $2W$ ) tends to move down with respect to the adjacent mass. Hence shearing stresses along the vertical plane  $AB$  tangent to the pipe act upward. They decrease the pressure on the pipe caused by the weight of the overburden  $2W$ . This phenomenon is analogous to the transfer of the weight of the overburden over a tunnel to the adjacent parts of the earth mass (Sec. 11:9).

The right side of Fig. 11:8 represents a rigid pipe placed on a

compacted foundation. In this case the shearing stresses act downward and increase the pressure on the culvert as caused by the weight of the overburden. This phenomenon is analogous to the "negative friction" in the case of piles driven through a consolidating medium (Fig. 8:16c).

The increase and decrease of the pressure on the pipe culvert as shown by Fig. 11:8 is in accordance with the results of the experiments as described in Sec. 11:16.

*b. Change in the Value of Shearing Stresses with Time.*—Apparently the shearing stresses along vertical and horizontal planes in a plastic mass vanish fully or partly as the time goes on (end, Sec. 11:9). Hence a pipe culvert designed to carry a limited overburden eventually may carry a much larger load. This increase in load takes place gradually, at a very slow rate. Apparently pipes placed in the field and subject to such gradually applied loads are able to stand stresses larger than those applied at an ordinary construction rate. This capacity, if any, of the pipes must be clarified by further research as an engineering problem that may be generalized to other materials.

Spangler<sup>9</sup> reports that corrugated-pipe culverts continue to deflect slowly for a period of time after the fill is completed ("deferred deflection"). Changes in shearing stresses may be an explanation thereof.

**11:18. Analysis and Design of Pipe Culverts for Airports.**—Even prior to the widespread construction of airports, the problem of transmission of static and impact loads was an object of theoretical and experimental investigations, mostly at Iowa State College.<sup>17,18</sup> At the present time (1947) the *vertical pressure* on a pipe is estimated mostly using a formula of the type  $C\sigma_z$ , where  $\sigma_z$  is the Boussinesq vertical pressure [formula (4:5)] and  $C$  is a coefficient that provides for uncertainties in the variables of subgrade, backfill, culvert, and pavement (or some other riding surface). The value of the coefficient  $C$  may be obtained through experimental data or merely estimated, its range being generally between 1.0 and 1.5, with an average of 1.25. Design loads produced by planes range between 30,000 and 300,000 lb. so far as the gross load of plane is concerned, with wheel loads from 15,000 to 150,000 lb. For purposes of design, the vertical unit stresses acting on the pipe culvert are converted into a vertical uniformly distributed load  $p$ . For concrete pipes the horizontal pressure is estimated

as a fraction  $np$  of the vertical pressure  $p$ , the value of  $n$  being zero at low values of the earth cover over the pipe (roughly up to 4 or 5 ft.) and a value of  $n = 0.1$  and not over  $n = 0.2$  for thicker covers. In comparison with highway or railroad pipe culverts (Sec. 11:14a) the value of  $n$  as used in the case of airports is rather small.

Numerical data of this section refer to military airports. The Army Engineers study experimentally the stress distribution on pipe culverts due to surface loads<sup>21</sup> and test pipe culverts to failure.<sup>22</sup> For the analysis of flexible pipe culverts, see Sec. 11:14.

It is obvious that the values of shearing forces acting along planes  $AB$  and  $A'B'$  (Fig. 11:8) are small in comparison with the heavy loads at the surface of the embankment, even if the latter is well compacted. Hence a larger portion of the load between points  $B$  and  $B'$  (Fig. 11:8) is carried by the pipe itself, without being transferred to other parts of the mass.

There is a tendency to consider the pavement, the subgrade, the backfill, and the pipe as a unit. According to Baron<sup>23</sup> possible loss of support under a concrete pavement due to settlement of backfill or an excessive deflection of the culvert would inevitably result in objectionable cracking of pavement. This would probably be less true for flexible pavements; however, possible pools of water or ice sheets which may form on such pavements should be considered. Given a pavement, its subgrade, a culvert, and the type of earth material for the backfill, the problem is to compute the thickness of the cover over the culvert for different weights of planes. According to Baron's computations, the thickness of the cover varies from 1.5 to 9 ft.

#### References

1. CHARLES TERZAGHI: "Theoretical Soil Mechanics," Chap. X, John Wiley & Sons, Inc., New York, 1943.
2. PH. FORCHHEIMER: Ueber Sanddruck und Bewegungerscheinungen im Inneren trockenen Sands, *Z. oesterr. Ing-und Arch. Ver.*, 1882.
3. J. C. MEEM: Tunnel Engineering, *Professional Engineer*, vol. 16, 1931; also The Bracing of Trenches and Tunnels, *Trans. A.S.C.E.*, vol. 60, 1908, and Pressure Resistance and Stability of Earth, *ibid.*, vol. 70, 1910.
4. Earth Pressure and Shearing Resistance of Plastic Clays; a Symposium. With respect to changing shearing stresses see the paper by W. S. Housel, *Trans. A.S.C.E.*, vol. 108, 1943.
5. G. M. RAPP and A. H. BAKER: "Lincoln Tunnel. The Field Measurements and Study of Stresses in Tunnel Lining" (lith.), Port of New York Authority, July, 1937.

6. ANSON MARSTON: The Theory of External Loads on Closed Conduits, *Iowa Eng. Exp. Sta. Bull.* 96, Ames, Iowa, 1930, and other publications.
7. W. J. SCHLICK: Structural Design of Rigid Pipe Sewers and Drains, *Bull. Assoc. (Iowa) Eng. Soc.*, vol. 6, 1931.
8. M. G. SPANGLER: The Supporting Strength of Rigid Pipe-culverts, *Iowa Eng. Exp. Sta. Bull.* 112, Ames, Iowa, 1933.
9. M. G. SPANGLER: The Structural Design of Flexible Pipe-Culverts, *Iowa Eng. Exp. Sta. Bull.* 153, Ames, Iowa, 1941.
10. M. A. DRUCKER: Determination of Lateral Passive Soil Pressure and Its Effects on Tunnel Stresses, *Jour. Franklin Inst.*, vol. 235, January-June, 1943.
11. ANDERS BULL: Stresses in the Linings of Shield-driven Tunnels, *Trans. A.S.C.E.*, vol. 111, 1946.
12. ANSON MARSTON: Report in the *Highway Mag.*, 1922; compare also ref. 6, 7, 8, and 9.
13. G. M. BRAUNE: Earth Pressures on Culvert Pipes, *Public Roads*, vol. 7, 1927; also *ibid.*, vol. 10, 1929.
14. Report of the Committee on Roadbed, *Proc. A.R.E.A.*, vol. 27, 1926; vol. 29, 1928; also *Eng. News-Record*, Mar. 19, 1925.
15. ADOLF VUELLMY: "Eingebettete Röhre," Gebr. Leemann & Company, Zürich and Leipzig, 1937.
16. G. I. POKROWSKI and J. G. KOUPTZOFF: Determination of Pressure on Pipes in Trenches (in Russian), official publication, Moscow, 1937.
17. Static and Impact Loads Transmitted to Culverts, Digest of Report of Experimental Determination at Iowa Experiment Station, *Public Roads*, August, 1927; also *Iowa Eng. Exp. Sta. Bull.* 31, 36, 47, 57, 76, 79, 96, 108, 112.
18. "Handbook of Culvert and Drainage Practice," Armco Culvert Manufacturers' Association, 1937.
19. "Concrete Culverts and Conduits," Portland Cement Association, 1940.
20. "Handbook of Water Control," New England Metal Culvert Company, 1936.
21. Investigation of Stress Distribution on Drain Pipe Due to Surface Load, U. S. Waterways Experimental Station, Vicksburg, Miss., Apr. 15, 1942.
22. Washington National Airport: Report on Field Tests on Non-reinforced Concrete Pipe, U. S. Engineering Office, April, 1940.
23. Professor Frank M. Baron, of Northwestern University, personal communication involving most of the data in Sec. 12:18.

## CHAPTER XII

### HIGHWAY AND RUNWAY SUBGRADES

Damage caused to a riding surface by the wheels of a vehicle (including airplanes) is essentially a change in shape rather than compression (ruts on earth roads, displacements under and next to pavements). Any change in shape, however, is due to the action of the shearing stresses which tend to overcome the shearing strength of the earth mass. Hence the two important preliminary items in both the design and construction of a pavement or other riding surface are (a) proper estimation of shearing stresses caused by moving vehicles (compare Chap. V) and, if necessary, (b) increase of the shearing strength of the surface of the mass where the given riding surface is located or *stabilization* of that part of the earth mass.

#### A. SOIL STABILIZATION

**12:1. Principles of Soil Stabilization.**—It is assumed in a conventional way (Sec. 5:1) that the shearing strength of an earth mass depends on its friction and cohesion. Hence soil stabilization should consist in increasing friction and cohesion combined with taking measures against factors that may decrease them.

*a. Increase of Frictional Resistance.*—By increasing the density of an artificial soil mixture, the value of its angle of friction  $\phi$  may be increased (Sec. 5:11). In its turn the density of a mass may be increased by proper grading and compaction already discussed in Chap. IX. Particularly, the important role of the optimum moisture content (Secs. 9:38 and 9:39) during the compaction cannot be overemphasized. Stability of densified soil mixtures can be checked by submitting them to drying, freezing, and capillary water action.<sup>1</sup> After being compacted, an unsatisfactory densified soil mixture may (1) shrink and crack owing to insufficient moisture content or (2) swell and expand owing to excessive moisture content. If excessive moisture in a soil mixture freezes, buckling, heaving, and even blowups may occur. If the excessive moisture

is in a liquid state, the corresponding mixture may lose its density and hence its bearing value.

*b. Increase of Cohesional Resistance.*—Cohesion may be increased by adding fine soil particles (“fines”) to an artificial soil mixture and by maintaining a proper moisture content. In natural soils cohesion may be increased by admixtures of *bituminous materials* or *Portland cement*.

Since an excess of moisture is harmful for the shearing strength of a mass and particularly for its cohesion, measures should be taken (1) against possible penetration of excessive moisture into the mass, which can be done, for instance, by creating *protective coats* outside (and also inside) the mass and (2) for elimination of excessive water, both from the surface of the mass and from inside of the mass, which can be done by *surface drainage* and *under-drainage*.

**12:2. Adding Fines; Using Deliquescents.**—The simplest example of addition of “fines” with the purpose to increase the cohesional resistance of the mass are sand-clay roads. Good examples present a sand content of 65 to 70 per cent and a clay content of 35 to 40 per cent. In a general way, the fines (the “binder”) added to a mixture must have a certain plasticity index (PI, Sec. 2:17), such as about 3 per cent for very wet areas, 4 to 8 per cent for average moisture conditions, and 9 to 15 per cent for dry or semiarid conditions. In fact, a clay supplies better bond at its plastic limit (PL); hence it is advisable to keep the plastic limit of the binder close to the natural moisture content of the given clay in a given locality. In wet localities the natural moisture content of a clay is presumably high and close to the liquid limit (LL). Hence, in designing a soil mixture for a wet locality the difference  $LL - PL = PI$  should be small in the binder. In dry areas the situation is reversed.

In order to enable the fines to perform their binding functions, there should be some amount of moisture in the mixture (compare Sec. 5:12). In order to attract moisture from air and maintain it at a certain minimum content within the mass, *deliquescents* are used (mostly calcium chloride, also sodium chloride or common salt). Calcium chloride<sup>2</sup> is often applied for stabilizing gravel roads (Vermont, New Hampshire, and other states) and also for airport runways and flight strips. Calcium chloride in the form of small white flakes is furnished in 100-lb. bags or 400-lb. drums.

It attracts moisture from the air and dissolves in the attracted moisture. Calcium chloride is mostly spread over the roadway, at a rate from  $\frac{3}{4}$  to  $1\frac{1}{2}$  lb. per sq. yd. Subsequent lighter applications depending on the dryness of the season, texture of the surface, and the amount of traffic may be needed. Sometimes materials for gravel roads stabilized with calcium chloride are premixed in a plant ("integral" method).

*Example.*—Proportion of a given soil mortar stabilized with calcium chloride is about 55 per cent of coarse aggregate (retained on No. 10 sieve), 33 per cent of fine aggregate (between No. 10 and No. 200 sieves), the rest, or 12 per cent, being the binder. The plasticity index of the binders is as explained above; the liquid limit of the binder is not over 35 per cent.

Notice that during heavy rains surfaces of gravel roads stabilized with calcium chloride are generally soft.

**12.3. Acid Soils; pH Value.**—Acid soils differ from alkaline soils by the content of ionized hydrogen which is larger in the former case. To measure the content ("concentration" or rather "activity") of ionized hydrogen, a conventional value of pH is used.\*

The value of pH is generally measured in the suspension of the given material. One of the methods consists in adding a chemical ("indicator") to a suspension of a few grams of tested material in several cubic centimeters of water and comparing the change in color thus produced with a standard color chart or a range of solutions with known values of pH. Various kinds of soil kits for determination of soil acidity are on the market. If a soil suspension made with 1 liter (1,000 cc. or grams) of water possesses a certain value of pH, it means by definition that it contains  $10^{-\text{pH}}$  g. of ionized hydrogen. The value of pH for pure water is 7. Values below 7 show acidity of the suspension.

The ionized hydrogen is replaceable or exchangeable; hence the more acid the soil the greater its base-exchange capacity and hence its detrimental influence on the chemicals used for stabilization. Metal pipes buried in acid soils are also subject to destruction by corrosion. The base-exchange capacity is measured in milliequivalents per 100 g. of soil (designation m. e. per 100 g.). A soil containing  $n$  g. of ionized hydrogen per kilogram (1,000 g.) has a base-exchange capacity of  $(100 n)$  m.e. per 100 g. For instance, the base-exchange capacity of a clay containing 0.82 g. of

\* pH means "puissance d'hydrogène" (French).

ionized hydrogen per kilogram of soil is 82.0 m.e. per 100 g. The larger the value of the silica-sesquioxide ratio of a soil (Sec. 1:8) the larger its base-exchange capacity (Winterkorn<sup>3</sup> and Baver<sup>3</sup>).

**12:4. Chemical Pretreatment of Soils to Be Stabilized.**—The acidity of a soil may be decreased by mixing it with a certain “neutralizer” such as limestone dust, or calcium carbonate,  $\text{CaCO}_3$ . To determine the amount of neutralizer to be used in “sweetening” of an acid soil the percentage of the ionized hydrogen in the soil should be multiplied by the equivalent weight of the neutralizer (about 50 for limestone dust). The product is the amount of neutralizer in per cent of the weight of the soil mass to be sweetened. In reality, much more neutralizer than described by that theoretical computation is needed. Calcium cations of the neutralizer displace the hydrogen cations of the soil and thus “correct” its acidity. Besides lime proper, hydrated lime, limestone dust and granulated slag may be used as neutralizers. At any event, the exchangeable hydrogen may be eliminated only if the neutralizer has the opportunity to percolate through the mass in solution and thus to wash all ionized hydrogen out.

A number of investigators report that soil properties, particularly consistency limits, depend on the nature of the exchangeable cations in the soil.<sup>4,5</sup> It should be noticed that the data immediately following are laboratory and not field information. Obviously, the applicability of laboratory-test results in the field depends on economical considerations. Apparently, the cation tends primarily to increase the plastic limit (PL) and decrease the plasticity index (PI). Admitting that in a general way a soil improves in structural quality with the decrease of the plasticity index (PI), the changes in consistency limits wrought by effective cations may be considered beneficial. According to Holmes<sup>6</sup> the plasticity index (PI) of a particular clay decreased from 21.1 in the test with water to 12.3 in a test with aluminum chloride, though a test using copper chloride furnished a value of  $\text{PI} = 21.7$ . As a rule anions increase the value of the plasticity index.<sup>6</sup> Acids may decrease or increase the consistency limits.

**12:5. Soil Stabilization with Bituminous Materials.**—*a. Oiling and Suboiling.*—Oiling at a rate of about 1 gal. per sq. yd. is the simplest way of waterproofing and dust prevention on an earth road. Suboiling is a variation of oiling, when oil is deposited at the

bottom of a scarified layer. This operation is followed by compaction, thus making the oil permeate downward.

*b. Use of Asphalt Cement and Cutbacks.*—Asphalt cement is a fluxed or unfluxed asphalt mostly refined from petroleum and specially prepared as to quality and consistency to be used in bituminous pavements. Cutback is asphalt cement rendered liquid by fluxing it with a light volatile petroleum distillate (kerosene, gasoline). To designate the bituminous products under discussion (item *b* of Sec. 12:5) the term “liquid asphalt” will be used.

A cohesionless earth mass (for instance, California sandy and desert soils) must be furnished both *waterproofness* and *cohesion*. In heavy cohesive soils (such as some heavy Midwestern clays) waterproofness only is needed. Hence, in the former case, liquid asphalt giving a residue of high cementing power should be used, whereas in the case of cohesive clays an application of road oil sometimes suffices. In a general way, in choosing a liquid asphalt for soil stabilization, the practical preference is for medium curing products.

Cutback asphalts used for road mixtures require heating to temperatures ranging from 100 to 175° F., but the emulsified asphalt (see item *d* following) can be applied at temperatures of 50 to 120° F.

With a few exceptions, direct mixing of the liquid asphalt with soil does not furnish satisfactory results. To ensure good spreading of the liquid asphalt throughout the mass, preaddition of water is needed, the amount of the latter being slightly above the optimum moisture content as determined by the Proctor plasticity needle (Sec. 9:39).

Water has more affinity (Sec. 2:10) to the soil surface than the liquid asphalt, and the latter, if used for stabilization purposes, should be chemically treated. The objective of the special chemical treatment is to increase the affinity of the asphalt to the soil and to decrease its surface tension which tends to maintain the liquid asphalt in spheroidal form. Otherwise water would take preference and leave the globules (small spheres) of the liquid asphalt scattered at the outside surface of the water film.

Figure 12:1 shows diagrammatically the distribution of liquid asphalt throughout the mass.<sup>7</sup> The latter is subdivided into groups of particles (cells) coated with asphalt, which prevents water from

entering into cells. In this way cohesion within the cell is preserved, and in the case of clay the latter cannot swell. Asphalt must not cover every particle, since overlubrication would cause loss of "stability" (division C, Chap. IX) and handicap compaction; hence excess of liquid asphalt is harmful.

The construction procedure in this case is as follows:

1. Additional aggregate, if any, is mixed with the soil by scarifying the subgrade to the specified depth and wetting with water (amount of water as specified above).

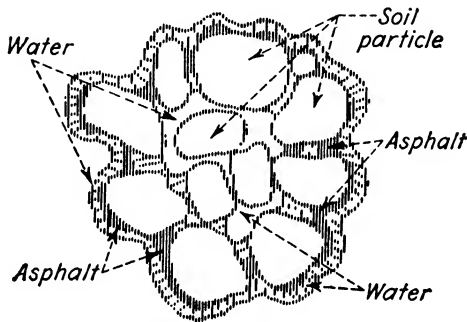


FIG. 12:1.—Distribution of liquid asphalt throughout stabilized soil.  
(After Endersby.)

2. Liquid asphalt is then added (0.5 gal. per sq. yd. or more per inch of stabilized depth at each application).

3. The soil is mixed with asphalt and compacted, mostly using sheepfoot rollers.

*c. Use of Tar.*—The role of tar used in soil stabilization is analogous to that of cutbacks (waterproofing and increase in cohesion). The amount of tar used is between  $\frac{1}{3}$  and  $\frac{1}{2}$  gal. per sq. yd. per in. of stabilized depth.

*d. Emulsified Asphalt.*—An emulsion is a dispersion of asphalt cement in fine droplets or globules in water containing a small amount of emulsifying agent such as soap. During the mixing process these globules become strongly attracted to soil colloids, so that only a small part of the asphalt used can be recovered by usual solvents. As in the case of liquid asphalt, excessive amount of emulsified asphalt will lubricate the mixture, and there will be no waterproofing with too little emulsified asphalt. Laboratory tests<sup>8</sup> show that the drying time of a wet mixture increases roughly as the square of the layer thickness. Hence, it appears advisable

in this case to construct the subgrade in several thin layers in preference to one thick one.

**12:6. Soil-cement Mixtures.**—A complete description of the working procedure used in this case may be found in special publications.<sup>9</sup> Briefly, the roadway is first scarified to a depth of about 6 in.; the soil pulverized; Portland cement spread; water added; the mixture compacted; and the surface finished. Prior to the construction, tests are run in order to answer the two basic questions (a) how much *water* should be added to a soil-cement mixture to make it as dense as possible; (b) how much *cement* should be added to make the mixture strong and resisting to weather changes.

*a. Moisture-density Test.*<sup>9,10</sup>—This test is similar to the Proctor plasticity needle test (Sec. 9:39), but it is run on soil mixed with approximately 8, 10, and 12 per cent by volume of cement and passed through No. 4 sieve (opening 0.185 in. or 4,760 microns).

*b. Wetting-and-drying Test;*<sup>9,10</sup> *Freezing-and-thawing Test.*<sup>9,10</sup>—For each cement addition (*i.e.*, 8, 10, and 12 per cent), four specimens are molded to the corresponding maximum densities, carefully measured, weighed, and placed in an atmosphere of high humidity at room temperature in which the cement is allowed to hydrate for 7 days. After that, two of those specimens are used in the wetting-and-drying test and the other two in the freezing-and-thawing test. Each test consists of 12 cycles and may last as long as about 24 days. At the end of each cycle one specimen is carefully measured and weighed, whereas the surface of the other is wire-brushed twice and its loss in weight recorded. For sandy soils the permissible total loss in weight is higher (for instance, 14 per cent) than for clayey soils (for instance, 7 per cent). Change in volume during the test should not be over 2 per cent, and the moisture content should never exceed that corresponding to the initial pore volume.

Elaborate laboratory studies on the influence of the base exchange and different admixtures on the soil-cement mixtures are being carried on<sup>11,12</sup> at the present time (1947).

**12:7. Deep Soil Stabilization.**—Strictly speaking, deep soil stabilization, *i.e.*, stabilization of the bottom of excavations for bridges, buildings, and similar structures, does not belong to this chapter. For convenience in reading, however, it is discussed here.

*a. Electrochemical Treatment.*—A method utilizing electricity for stabilization of clay has been proposed by Endell and Hoffmann.<sup>13</sup>

This method may be applied for both shallow and deep soil stabilization. Aluminum is used for the anode, and copper for the cathode. Direct current is allocated to pass between electrodes until the soil is hardened. Experiments were described in which a quite liquid clay (moisture content 80 per cent) became so hard after treatment that an iron rod about  $\frac{1}{4}$  sq. in. in cross section failed to penetrate it under a load exceeding 20 lb. Apparently immersion in water does not change the properties of this hardened clay.

More work along these lines has been done by Leo Casagrande and Bernatzik.<sup>14</sup> Among Leo Casagrande's various statements the following are to be noted: (1) The angle of friction of the soil increases (for instance, from  $23^\circ$  to  $33^\circ$ ); (2) water is eliminated from the pores of clay just as if it were squeezed out by pressure. The latter circumstance suggests that a clay layer which would settle under the action of an imposed load may be treated electrochemically before the erection of the structure. This practice, if successful, may diminish the settlement of the structure due to consolidation. The electrochemical treatment described (often termed "electro-osmosis") may be also used for drainage purposes.

The method was applied to a pile foundation of the bridge over the Pregel in Königsberg, Germany, where a 33-ft.-deep swamp was underlain by a stratum of very fine powdery sand containing 1 per cent of clay. The foundation for the bridge pier consisted of 90 wooden piles spaced 3 ft. center to center. The piles were 65 ft. long and had a diameter of about 16 in. at the top and 10 in. at the tip. Four piles were manted with a 30-gauge aluminum sheet to a height of about 25 ft., and the other four were not. Of the four manted piles, two were subjected to the electric current, the other two being used for comparison only. When the load, which was increasing, reached 90 tons per pile, the settlement of the untreated piles was from 0.27 to 0.95 in., whereas that of the treated piles fluctuated from 0.04 to 0.19 in.

*b. Principle of Deep Soil Stabilization by Means of Two Chemicals.*—The methods described below may be used to stabilize saturated fine sand masses which tend to flow away and cause settlement of the structure above them. A case of such flow is described in Sec. 13:13 (Example 3, settlement of a bridge pier).

Deep soil stabilization by means of two chemicals is accomplished in the following way. Two chemicals, termed chemical I and chemical II, are injected into the earth mass. Generally

they are injected separately (the Joosten method), though in the so-called K-L-M method they apparently are injected together. At a certain depth both chemicals come into contact and form a gel, or a jellylike colloidal mass, which upon hardening becomes impervious to water and possesses considerable shearing strength. Saturated fine sand is thus converted into a kind of sandstone. The nature of the chemicals used is not always disclosed.

*c. Joosten Method.*—A solution of hydrofluorosilicic acid or, depending upon the material, a solution of sodium silicate (chemical I), is first forced into the loose ground or the porous rock or concrete, and later a salt liquid (chemical II) is injected. In good siliceous material like ordinary gravel, the compressive strength of the solidified mass is about 1,200 lb. per sq. in., whereas in fine sand this value is about 300 lb. per sq. in. In clay this process does not work.

The general procedure is to drive the perforated pipe down into the material to be solidified, say 20 in., then to inject chemical I, drive the pipe another 20 in., inject chemical I, and so on, until the desired depth is reached. Chemical II is injected in 20-in. lifts as the pipe is pulled out. The distance of penetration from the injection pipe depends upon the size of the voids and is also directly proportional to the liquid pressure used.

*d. K-L-M Method.*—Soil stabilization with sodium silicate (water glass), with calcium chloride as chemical II, has been known for about a quarter of a century. It has been done as in the Joosten method, namely, by injecting chemicals II and I, one after the other. Before the Second World War Rodio, a successful Italian engineering contractor who has offices also in France, patented a solidification method known as K-L-M. Apparently, in this method both chemicals, water glass and the other (which is not disclosed), are injected *together* as a single mixture, and the time of the set of this mixture can be closely controlled. The injection can be modified in accordance with the chemical properties of the soil to be grouted. Spacing of grout holes may be estimated at 25 ft.<sup>15</sup>

In the method of two-chemical stabilization, it should be noted that a soil with low permeability is not capable of accepting the solution into its pores. It cracks, and chemicals follow the cracks instead of being uniformly distributed through the mass.<sup>16</sup>

*e. Examples of Two-chemical Soil Stabilization.*—Figure 12:2 shows the construction of a solid mat 6 ft. thick and 60 ft. long under the pile foundation of an apartment house in Berlin, Germany. Settlement was stopped by the mat.

In Fig. 12:3 it is shown how the flow of saturated fine sand under a bridge pier at Bremen, Germany, was prevented by confining

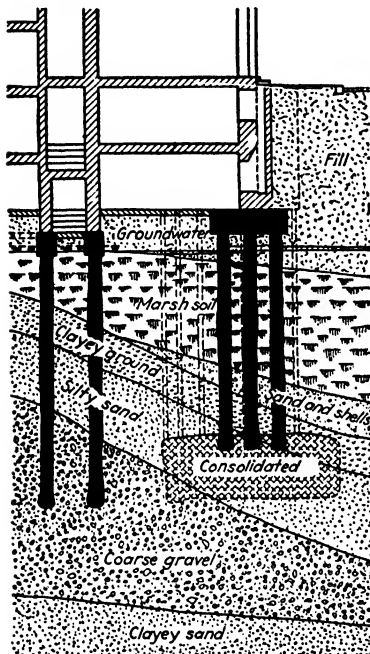


FIG. 12:2.

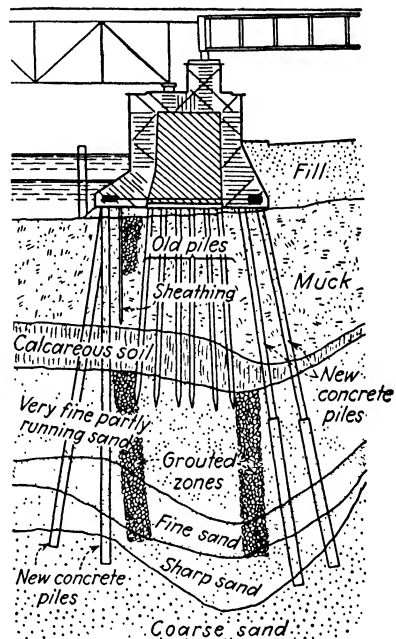


FIG. 12:3.

FIGS. 12:2 and 12:3.—Deep soil stabilization using two chemicals.

the sand mass in a box. The walls of this box are made of stabilized sand. Fewer additional piles were required.

More examples may be found in ref. 15. There are very interesting possibilities in the application of soil stabilization in tunnel construction instead of draining or freezing a fine sand mass running into the tunnel. Such a method was used during the construction of some parts of the London Subway ("Underground," Sec. 11:1).

### B. DESIGN OF A SUBGRADE

Pavements for highways and runways (Fig. 12:4) are subdivided into *rigid* (such as concrete slabs) and *flexible* (such as bituminous macadam, gravel, and others).

The objective of this book is not to discuss pavements as such but to discuss subgrades only. Since pavements and subgrades act as units, however, it is impossible to discuss the design and construction of a subgrade without referring to the corresponding pavement.

**12:8. Soil Classifications.**—Prior to the construction of a pavement, soil samples are taken and tests run. Most of these tests are described in this book. In choosing the type of pavement and subgrade, quick but proper identification of the nature of the soil, which may vary considerably at different points of the given line,

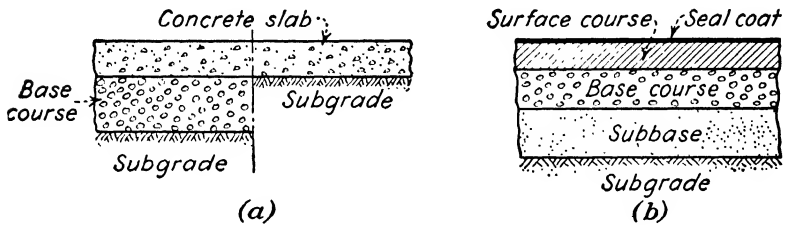


FIG. 12.4.—(a) Rigid pavement, and (b) flexible pavement.

is of importance, hence special interest among pavement engineers in the elaboration of an adequate soil classification. At the present time (1947), however, there is no soil classification accepted by all pavement engineers and builders. The highway engineers and some airport engineers accept the classification of the Public Roads Administration (Sec. 2:20 and ref. 17 of this chapter). The Army Engineers who build many airports use Casagrande's classification<sup>18</sup> which subdivides all soils into five groups:

- I. Gravels.
- II. Sands.
- III. Fine-grained soils (silts and clays) of low to medium compressibility.
- IV. Fine-grained soils of high compressibility.
- V. Peats. For very fine sand and rock flour the foreign term "Mo" is used. The groups are designated by the initial letters of their names (G, S, L, H combined with other letters, such as W, well graded; P, poorly graded).

The Civil Aeronautics Administration<sup>19</sup> uses a classification that falls into two groups. Granular soils (E-1 to E-4) belong to one group, whereas nongranular soils (E-5 to E-10) form the other.

The granular materials are subdivided into nonfrost-heave soils and soils subject to frost heave.

**12:9. Static Loads Used in the Design.**—*a. Highways.*—A gross load on four wheels of 32,000 lb. and a maximum wheel load of 9,000 lb. are considered in several states. A figure of 8,000 lb. per wheel is conservative for main highways, whereas on roads of less importance loads are from 3,000 to 5,000 lb. per wheel. The average impact coefficient for pneumatic tires and the pavement in use for several years is about 1.3 (compare Sec. 11:14*a*).

*b. Runways.*—Maximum loads used in design may reach figures as in Sec. 11:18. Actual military airports are subdivided into four classes,<sup>18</sup> the wheel loads being 60,000 lb. for Class I and 15,000 lb. for Class IV. Commercial airports are also subdivided into four classes.<sup>19</sup> Since a part of the weight of a plane is carried by its wings in landing, no impact is considered. The dynamic loading caused by vibrational stresses due to warming of engines is considered in designing aprons.

*c. Tire Prints and Contact Pressures.*—The prints of a tire are ellipselike. For design and analysis purposes of a highway slab they are considered circular. Assuming the diameter of a single tire print at 6 in. and a dual tire print at 8 in., the contact pressure computed on this basis would be about 300 lb. per sq. in., whereas the contact pressures of a plane tire are 55 to 75 lb. per sq. in. only. Runway designers sometimes replace ellipsoidal tire prints with rectangles.

*d. Frequency of loading* is larger on highways than on runways. This is mostly because of the considerable width of the runways, which in military airports may reach 500 ft., of which the center 100 or 150 ft. are paved, the shoulders being turfed or treated with dust preventatives. The width of runways is an insurance against too frequent repetition of loads. Taxiways in airports, however, are generally only about 50 ft. wide with 12½-ft. shoulders on each side.

**12:10. Difference between Rigid and Flexible Pavements.**—A rigid pavement is a structure in its own right. Under the action of static loads (Sec. 12:9) and the weight of the pavement, stresses and strains develop in the pavement, and the sum of all external forces applied to the pavement is carried by the subgrade. Thus the subgrade is a *support* to the pavement; the term “support” is used here in the same sense as when speaking of beam supports.

The distribution of pressure on the subgrade is far from being uniform and, in addition, cannot be determined using statics only. To simplify the analysis of a pavement slab, assumptions are made, as explained hereafter (Sec. 12:11).

In the case of a flexible pavement, external loads are carried by the earth mass. The pavement in this case is only a blanket covering the mass or a bag in which the mass is enclosed. Hence no particular strength is required from the pavement: it should be only strong enough to prevent its destruction by the traffic or unfavorable weather conditions. A flexible pavement is not expected to act as a beam as rigid pavements do; instead, it has to fit the subgrade "as a glove does the hand."<sup>20</sup> Discussion

It is to be remembered that after repeated loading and unloading earth mass acquires elasticity because of the gradual decrease of the pore volume and consequent densification of the mass (Sec. 6:1). This is precisely the case of a recently built subgrade under a flexible pavement which gradually becomes denser. Moreover, not only static loads but vibrations produced by engines of airplanes are also responsible for the densification of the subgrade, especially if the vibration stresses are superimposed on heavy static load stresses.<sup>20</sup> Important laboratory tests on the effect of vibrations on the bearing properties of soil were made at Princeton University for the Civil Aeronautics Administration.<sup>20</sup>

Because of the considerable difference in the very concepts of the rigid and flexible pavements, the design and analysis procedure is not the same in both cases.

**12:11. Design of Rigid Pavements and Their Subgrades.**—The design of highway and runway concrete slabs is based on the Westergaard formulas<sup>21</sup> which consider load at the middle of the surface of the slab and for highway loads also at the corners and the edges of the pavement. The formulas in question contain a constant  $k$ , termed "modulus of soil reaction" or "modulus of subgrade" (compare Sec. 11:15). The larger the value of  $k$  the smaller the tensile stress in the slab and the thinner the slab. The value of  $k$  may be defined as a conventional constant representing the load in pounds per square inch at the surface of the subgrade required to cause a vertical deformation (settlement) of 1 in. in the subgrade. The physical dimension of  $k$  is pounds per square inch per inch (or pounds per cubic inch). The average value of  $k$  for a natural soil subgrade is  $k = 100$ , its range being from 50 to 200.

By artificial means, as explained hereafter, the value of  $k$  may be considerably increased.

*a. Determination of the Modulus of Subgrade.*—At the present time (1947), the Army Engineers load the subgrade using bearing plates 30 in. in diameter. Either natural subgrade in cut, stripped of vegetation, and scarified to a depth of about 6 in., or a 30-in.-high fill is compacted at the optimum moisture content (compare Sec. 9:33). The load is applied to a bearing plate centrally, using hydraulic jacks. First the bearing plate is put firmly in

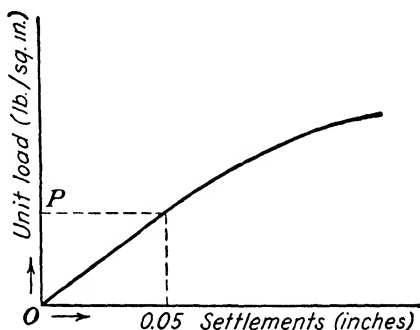


FIG. 12:5.—Determination of the modulus of subgrade.

place (“seated”) by a 5 lb. per sq. in. load, after which load increments of 5 lb. per sq. in. follow, allowing full settlement before another increment is applied. The test should be continued either beyond the yield point (“critical load,” Sec. 8:6 and Fig. 8:2) or up to a unit load 50 per cent higher than the contact pressure (Sec. 12:9) of the heaviest plane to be used. If settlements are plotted (in inches) against unit loads (in pounds per square inch), a load-deformation curve is obtained (Fig. 12:5). It is assumed that up to a settlement value of 0.05 in. the load deformation curve is a straight line. Designate the unit load causing this settlement with  $p$  lb. per sq. in. Then the value of the modulus of subgrade will be

$$k_u = p \div 0.05 = 20p \text{ lb. per sq. in. per in.} \quad (12:1)$$

In the case of clays and similar soils the value of  $k_u$  thus obtained should be corrected (reduced) for saturation. A rough way to do so is as follows: Two samples from the subgrade, one at the optimum moisture content and the other saturated, are placed into consolidation devices (Sec. 6:23) and subjected to unit loads

$p$  and  $p_s$ , respectively, to produce equal settlements. Obviously  $p_s < p$ , and the corrected value of the modulus of subgrade  $k$  is

$$k = \frac{p_s}{p} k_u \quad (12:2)$$

The correction for saturation is not necessary for sands, however, since in this case the value of  $k_u$  [formula (12:1)] is generally not reduced by saturation, and  $k = k_u$ .

*b. Base Course.*—Highway concrete slabs are usually 6 in. thick; and runway slabs are thicker. Generally speaking, thick pavement slabs are undesirable for the following reasons: (1) Vibrating of the concrete during the construction of a thick slab (over 8 in.) is difficult, and (2) the thicker the slab the larger the temperature difference between its top and bottom, especially during sunny days and hence a more pronounced warping of the slab (rising up at the middle) occurs. The thickness of the slab may be decreased by placing a *base course* between the pavement and the subgrade. This can be done either (1) by stabilizing the upper part of the natural subgrade or (2) by placing on the subgrade imported well-graded granular material with a low percentage of fines. Some cohesive material may be permitted close to the bottom of the base course. Figure 12:4*a* shows a concrete slab either resting directly on the subgrade (right part of the figure) or with an intermediary base course (left side). If the base course consists of granular material, it constitutes a drainage layer for the consolidating subgrade (as the pervious overburden in Fig. 6:4). A base course also prevents fine subgrade material from being pumped up into the pavement cracks. The highway practice shows that if the subgrade consists of frost-heaving soils, all of the frost-heaving soils should be replaced by the granular base course to the full depth of frost penetration (compare Sec. 3:23). Sometimes entire miles of highway pavements are provided with a base course 12 to 24 in. thick. There are cases when owing to frost danger it was necessary to place a granular base course even on a rock subgrade, the latter being in shallow cut with a shallow (*i.e.*, close to the earth surface) water table.

Theoretically speaking, that thickness of the base course should be used which furnishes the most economical design of pavement, base course, and subgrade. Various reasonable thicknesses of the base course are to be considered, and load tests made as described,

but bearing plates should be placed at the upper surface of the base course. As compared with the soft subgrade, the base course may be considered indeformable; hence the settlement (downward motion) of the experimental bearing plate may be ascribed to the deformation of the soft subgrade only. The pressure on the subgrade may be computed using the 2-to-1 method (Sec. 4:14*b*). Oftener the 1-to-1 method is used, which provides the pressure distribution within the subgrade under an angle of  $45^\circ$  to the vertical. Correction for saturation should be made for subgrade only. The presence of a base course may raise the average value of the modulus of soil reaction  $k = 100$  to several hundred pounds per square inch per inch. The thickness of the pavement decreases as the modulus of soil reaction increases, but at a considerably slower rate.

In the design and analysis of concrete pavements, as described above, strains caused by wheel loads are predominant factors to be considered in the design. Weather, although discussed, is often discounted or neglected as a factor in design. Differential settlements (compare Sec. 13:1) due to disturbance of the subgrade by a freeze or a thaw may be causes of objectionable cracking. Volumetric changes in the subgrade causing additional stresses in the pavement may be produced by changes in moisture content of the subgrade resulting from wetting, drying, or changes in ground-water conditions. The phenomenon of warping due to nonuniformity of temperature has been already mentioned. At the present time (1947) little is known quantitatively about the influence of all these additional factors on the design of pavements and subgrades. An interesting attempt at quantitative evaluation of uncertainties in the design of concrete pavements has been made by Baron.<sup>22</sup>

**12:12. Design of Flexible Pavements and Their Subgrades.**— Figure 12:4*b* represents the cross section of a flexible pavement. The surface course is basically a wearing course, mostly bituminous, from  $1\frac{1}{2}$  to 6 in. in thickness, provided with a protective bituminous seal coat. As a rule, the subgrade possesses but a limited shearing resistance; hence were the surface course placed directly on that weak subgrade, the shearing stress transmitted through the surface course to the subgrade would cause large displacements in the latter, accompanied with tearing or punching of the surface course. Since the shearing stress decreases from the point of application of

the load (a landing plane, a truck, etc.) in the downward direction, it is convenient to place layers of decreasing shearing resistance between the surface course and the subgrade, thus making the displacements in all of these layers more or less of the same order of magnitude. These layers are (Fig. 12:4) (a) base course of selected materials such as crushed stone, graded gravel, or soil cement and (b) subbase, the latter being either a stabilized (or simply well compacted) top layer of the subgrade or a layer of imported well-graded granular material placed on top of the subgrade. Sometimes both layers (a) and (b) are identified simply as "base."

*a. Deflections.*—A *deflection* is the lowering of a point of the loaded area of the pavement while the latter is still subjected to load. Upon removal of the load the deflection decreases, but a plastic (nonreversible) part of it remains. In other words, a deflection is the sum of the elastic and plastic deformations of the pavement and the underlying mass (compare Sec. 6:1).

Deflections of flexible pavements differ, however, from those of rigid pavements. In fact, owing to considerable thickness and stiffness of a well-built concrete slab, deflections in this case are small, and plastic settlements generally occur only during a short period after construction. Afterward there are elastic deflections only, and after each passage of the vehicle the slab returns to its position prior to that passage. Imagine now a point at the middle of a wide but rather thin flexible pavement. The mass under this point really behaves as if it were enclosed in a rubber bag or envelope, since during a brief time of application of the moving load, soil, water, and air particles cannot escape from that bag sidewise. Sudden application of the load causes neutral stresses in pore water (compare Sec. 4:19) and also compresses the air bubbles entrapped in the mass. In its turn the presence of neutral stresses decreases the shearing strength of the soil and hence increases the deflection [formula (5:11), in which the value of the normal stress  $\sigma$  should be decreased by the value of the neutral stress  $u$ ]. The compressed air bubbles push soil particles in all directions, thus causing additional pressures and shearing stresses. In simple terms, when a moving load hits the "bag" in question, the latter may burst owing to lateral displacements of its contents. Even if it does not burst at once, plastic deformations, being irreversible, are progressive, and as a result the surface of the pavement may become wavy and crack.

Still another cause that may produce the bursting of the "bag" in question is gradual saturation of the subgrade from below. As a result, swelling (expansion) of the mass and hence destruction of the pavement may occur.

Static loads using small bearing plates as in the case of rigid pavements (Sec. 12:11) cannot reproduce the deflections described chiefly because of expelling the surplus of water and air during the loading itself. A test therefore is needed that could determine (1) resistance to displacement of the mass under the pavement and (2) expansion properties of the mass from adsorption of moisture subsequent to construction. Such a test is briefly described hereafter.

*b. California Bearing Ratio Test.*—This test has been devised by O. J. Porter<sup>23</sup> of California Division of Highways and in a modified form was widely used for airports during the Second World War. The test consists in compacting about 8 lb. of material at optimum moisture content (Sec. 9:39) and expected field density in a cylindrical mold 6 in. in diameter and 7 in. high, soaking the sample, measuring its expansion, and testing for penetration of a 3 sq. in. piston in a testing machine. The unit loads required to produce certain penetrations are divided by some standard unit loads established for the same values of penetration. The smallest of several ratios (in per cent) thus obtained is the "California bearing ratio." The resulting bearing ratios for various materials available are substituted in special curves which have been drawn from California highway practice and extrapolated for runways. These curves furnish the total thickness of the pavement and its base and may indicate different possibilities of distribution in the base of materials available, after which the most economical solution is chosen.<sup>24</sup>

*c. Other Design Procedures.*—A flexible pavement may also be designed from building trial pavement sections on a given subgrade and incrementally loading them with predetermined loads; deflections recorded in this connection should be within a certain range.<sup>25, 26, 27</sup> There are also tables and curves for determining the thickness of flexible pavements and their bases from the type of the soil, carefully established, and the magnitude of the load.<sup>19, 29</sup> Sometimes formulas for the determination of that thickness are used.<sup>26, 28</sup> Important theoretical and experimental contributions have been made by some colleges.<sup>30</sup>

**12:13. Field Tests on and for Flexible Pavements.**—The objective of numerous field tests that have been carried on up to the present time (1947) is to obtain empirical data usable in the design of flexible pavements and their bases. In the past tests, both on highways and runways, emphasis has been placed on allowable deflection as related to the ultimate bearing capacity (compare Sec. 8:3) of the pavement. It is clearly understood at the present time that besides the absolute value of the deflection, the *curvature of the deflected pavement* is of great importance. In fact, from two pavements I and II (Fig. 12:6) made of the same material, being of equal thickness and showing equal deflections  $\Delta$  under load, pavement I with a smaller radius of curvature obviously will crack first if the load is gradually increased. In the load tests attention

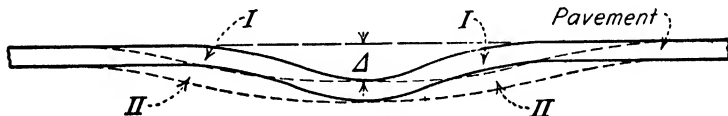


FIG. 12:6.—Danger of cracking as controlled by the curvature of the deflected pavement.

is also paid to the study of the behavior of the flexible pavement and its base within the yield point of the material.

The so-called “accelerated traffic tests” have been conducted by the Army Engineers in different parts of the country, either on special test sections or on existing runways.<sup>31</sup> The wheel loads used have ranged from 15,000 to 50,000 lb. The equipment consisted of rubber-tired earth-moving equipment, the number of “coverages” being about 5,000 in each case. The tests justified the application of the California bearing ratio test and the corresponding design curves (Sec. 12:12), though it has been felt that this test may sometime be refined or replaced. It has been concluded that high compaction of cohesionless subgrades and bases during the construction is essential. Particularly, compaction and drainage of subgrades of fine sand or silt prevent them from liquefaction under the action of a landing plane (the so-called “quick condition” of the subgrade; compare also Sec. 5:15).

### C. UNDERDRAINAGE OF THE SUBGRADE

No surface drainage problems as such will be considered hereafter, the discussion being limited to the moisture under an imper-

vious pavement and methods of the moisture removal from the subgrade.

**12:14. Moisture Content of a Subgrade.**—The moisture within a subgrade built at the optimum moisture content (Sec. 9:39), covered with the base course and the pavement, tends to reach equilibrium (a) with the water table and (b) with the atmosphere. Since the water table fluctuates, being in many localities at its highest position late in the spring and at its lowest position late

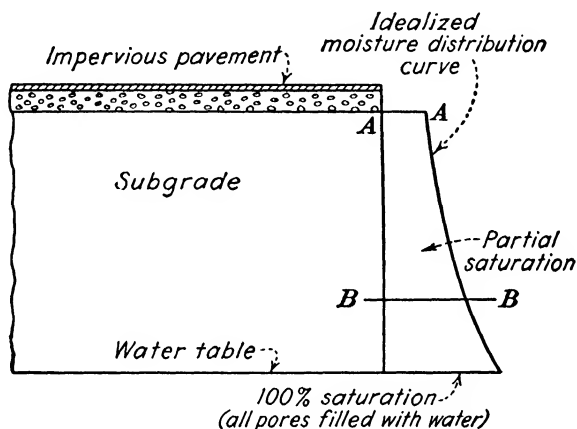


FIG. 12:7.—Moisture distribution in the subgrade. There may be condensation of vapor at the level AA.

in the fall, the moisture content in the subgrade may also fluctuate. Figure 12:7 shows an idealized moisture distribution curve of the subgrade. All soil pores next to the water table are filled with water (degree of saturation 100 per cent); and the degree of saturation decreases in the upward direction. The closer the top of the subgrade to the water table (level B-B instead of A-A, Fig. 12:7) the larger the degree of saturation of the subgrade. If the subgrade is built of a fine-grained soil capable of attracting more capillary moisture than its optimum moisture content and if the water table is shallow, the construction moisture content of the subgrade will possibly increase. Conversely, in the case of a sandy subgrade and a deep water table, the moisture content will possibly decrease. The capillary moisture that moves from the water table upward is accompanied by air bubbles and water vapor. In this connection a part of this air may be entrapped in the soil, and there may

\* Before reading Sec. 12:13 consult Secs. 2:9; 2:14; and 2:15.

be condensation of the vapor at the base of the pavement. In a humid climate both the amount of rainfall and the relative humidity of the air are high; hence the moisture content at the edges of the impervious pavement may be larger than at its middle. During periods of drought or in arid regions, the opposite phenomenon may take place.

There is an analysis of data concerning the moisture content in the highway and runway subgrades made by the Highway Research Board.<sup>32</sup> According to this analysis, the moisture content of clays generally exceeds their plastic limit; that of silts is close to the plastic limit; and that of sandy loams is generally (but not always) less than the plastic limit. A substantial proportion of the moisture values in all soil classes is in excess of the optimum moisture content. Generally speaking, the moisture content in the subgrades in humid regions is higher than in arid ones.

Theoretical attempts of solving the problem of the subgrade moisture content should be mentioned.<sup>33, 34</sup>

**12:15. Surface and Undersurface Drainage.**—In designing highways and runways, strict attention should be paid to the proper arrangement of the surface drainage. If the latter is well designed, water from the surface of a highway or an airport promptly runs off. A part of it, however, infiltrates into the soil and particularly into the subgrade (the so-called “roof leakage”). In a general case underdrainage is partial only and is designed if capillary moisture threatens to soften the subgrade. Airport engineers even state<sup>18</sup> that the usual conditions do not require underdrainage. Notice that both drainage and underdrainage are based on two different systems and that the terms “underdrainage,” “sub-surface drainage” and “undersurface drainage” are synonymous.

The terms “drain” and “underdrain,” which are usually interchanged, designate a deep narrow trench provided with a drainage pipe and backfilled with filter material. The so-called “French” or “blind” drains are trenches without pipes, but still with a back-fill of filter material.

In highways, spots where the pavement chronically suffers from frost heaves or is wavy owing to the softening of the subgrade are sometimes only gradually discovered during the operation; and to help the situation, underdrainage is often designed. On other occasions, such bad spots may be anticipated during the design. For instance, along the overpopulated Atlantic Coast practically

only low muddy places are available for airports with shallow (close to the earth surface) water tables. Again, on a transverse slope leading to a water basin (river, lake, or pond) there is generally a current of ground water, hence a possibility of softening of a subgrade built on that slope. In these two cases the locality itself suggests that at a given place underdrainage may be needed.

**12:16. Three Ways of Subsurface Drainage.**—These ways are as follows:

a. Before the ground-water flow (seepage zone, Fig. 12:8, also

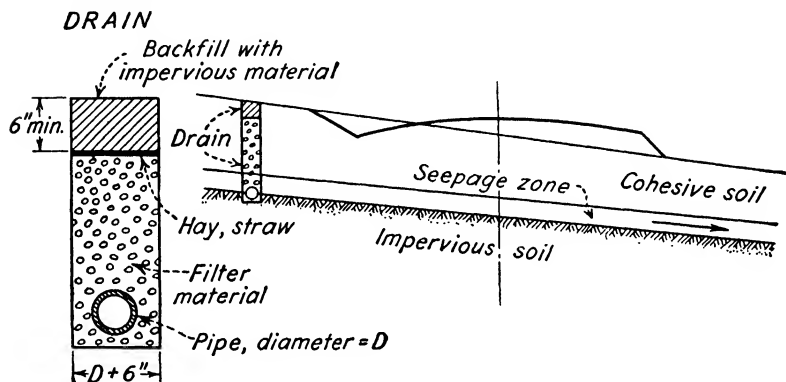


FIG. 12:8.—Interception of the ground-water flow.

Fig. 12:11) reaches the subgrade, it is *intercepted* by underdrains parallel to the way. The ground water flows to a few low points of the longitudinal profile and is removed by underdrains normal to the way. Notice that the seepage zone (Fig. 12:8) is accompanied from above by a zone of capillary moisture which would soften the subgrade if not intercepted.

b. The practically horizontal shallow water table is *lowered* (Fig. 12:9) with the use of open ditches or underdrains normal to the way. In difficult cases collecting sumps or pumping may be used. It is believed in practice that a water table located 5 or 6 ft. below the top of the subgrade is harmless; but if the water table cannot be kept deep enough, underdrainage is not helpful.

c. The *excess of moisture* is removed by underdrains placed in the subgrade itself. There are old highways with French drains at the center of the pavement. This type of underdrainage is seldom used at the present time (1947).

In all three cases discussed, both underdrains and ditches must

have adequate slopes and a good possibility of discharge to the outfalls.

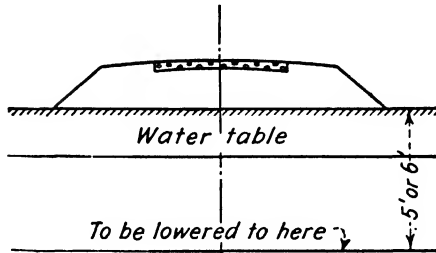


FIG. 12:9.—Lowering of the ground-water table.

**12:17. Direction of the Subsurface Flow.**—The design of an underdrainage system should start by establishing the direction of the underground flow. A rough way to do so is to assume that the ground-water levels at three borings *A*, *B*, *C* (Fig. 12:10) are located at an oblique plane, which is only approximately correct.

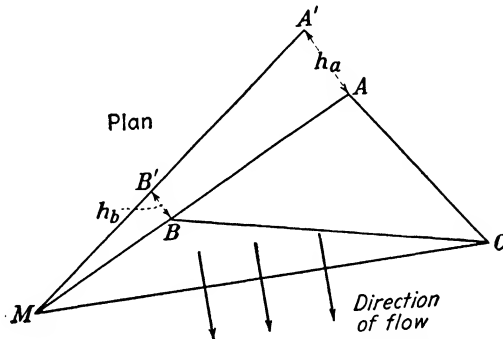


FIG. 12:10.—Direction of the subsurface flow.

Taking the lowest elevation of the three ground-water levels (for instance, at *C*) as a datum, designate the elevations at *A* and *B* with  $h_a$  and  $h_b$ , respectively. Plot  $AA' = h_a$  and  $BB' = h_b$ , and locate point *M*, that of intersection of lines *AB* and  $A'B'$ . The elevation of point *M* is zero, and the approximate direction of the ground-water flow is roughly perpendicular to line *MC*, this line being a contour line of the plane *ABC*. In complicated cases of the ground-water flow the help of a geologist may be needed.

**12:18. Removable Moisture.**—Moisture in the subgrade may be either capillary (or otherwise attracted) or gravitational. Gravitational

tional water may be removed by offering it an opportunity to flow along a slope of the underdrain. Attracted moisture, however, cannot be removed by the force of gravity only, but a part of it can be removed by evaporation. This may occur if the underdrain is fairly aerated and the rate of capillary flow toward the exposed surfaces ( $AE$ ,  $BC$ ,  $CE$  in Fig. 12:11) is less than the rate of evaporation from these surfaces.

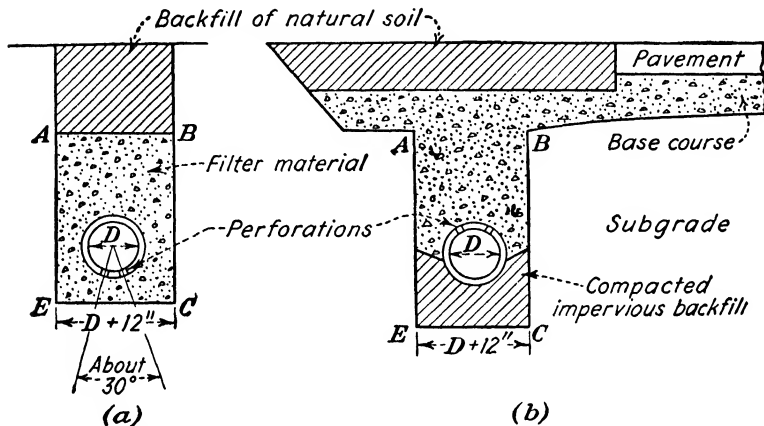


FIG. 12:11.—Drainage-pipe perforations. (a) "Down" and, (b) "up."

**12:19. Underdrainage Details.**—*a. Types of Pipes.*—For sub-surface drainage, the following types of pipes are used: vitrified clay pipes, concrete pipes (both laid with open joints), and perforated corrugated metal pipes. The minimum diameter should be about 6 in., though such diameters as 4 in. may be found in practice.

*b. Location of Pipes; Perforations "Up" and "Down."*—There are three ways of placing the pipe at the bottom of the drain trench (1) directly on the natural (undisturbed) soil if it has sufficient bearing capacity; (2) on pervious backfill, which is the common practice (Figs. 12:8 and 12:11a); and (3) on compacted impervious backfill (Fig. 12:11b). The third procedure is used when there is a danger of puncturing a thin impervious layer and losing the drained water into a deeper pervious layer, thus destroying the objective of the drainage. As to whether the perforations in the pipes should be "up" (Fig. 12:11b) or "down" (Fig. 12:11a), opinions divide. If the perforations are "down," the solids from

the backfill cannot enter the pipe; if they are "up," the danger of losing water is smaller. Apparently, the "down" location is more popular. The discharge end of the pipe must be approximately 6 in. above the bottom of the basin of discharge (outfall).

c. *Filter Material*.—The backfill material must be *fine enough* to keep the adjacent soil from entering the pipe and *coarse enough*

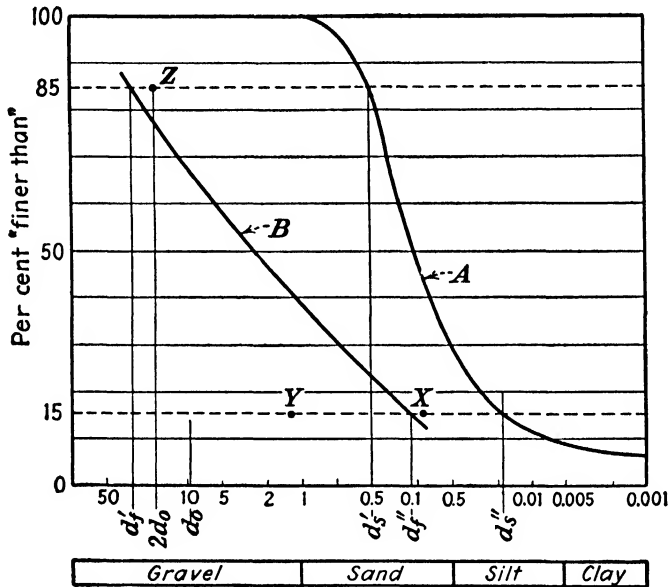


FIG. 12:12.—Size distribution of the filter material.

not to enter the pipe perforations or joints. Soil that might enter the drain would "silt" or "clog" it. Assuming the diameter of perforations at  $\frac{1}{4}$  to  $\frac{3}{8}$  in., the size of stone of  $\frac{3}{8}$  in. next to the pipe would be satisfactory. Proper grading of the filter material has been studied and discussed intensively.<sup>35,36,37,38</sup>

Generally speaking, the filter problem may be formulated thus: Given the size distribution curve of the subgrade A (Fig. 12:12), design the size distribution curve B of the filter material. The diameter of the perforations will be, say,  $d_0 = \frac{3}{8}$  in. Designate with  $d'$  and  $d''$  the diameters corresponding to 85 and 15 per cent "finer than" on a size distribution curve. Use subscripts  $f$  and  $s$  to designate "filter" and "soil," respectively. Thus, the symbol  $d'_f$  would mean, for instance, that 85 per cent of the filter material

is finer than  $d'_f$ . A solution of this problem from experience and laboratory experiments would be <sup>18</sup>

$$\frac{d''_f}{d'_s} \leq 5; \frac{d''_f}{d'_f} > 5; \frac{d'_f}{d'_s} > 2 \quad (12:3)$$

The limit values of  $d'_f$  and  $d''_f$  thus determined are shown in Fig. 12:12 with the letters X, Y, Z. Any curve B passing between points X and Y and to the left of (or through) point Z is satisfactory. To obtain more economical curves B, special tests are made.<sup>18,42</sup>

*d. Area Underdrainage.*—If an area in an airport has to be underdrained, the location of the subsurface drains may follow one of the patterns used in common land drainage. The larger the coefficient of horizontal permeability of the local soil the larger the distance between subsurface drains. In designing an area underdrainage, soil investigations to a depth of at least 6 ft. are essential.

#### References

1. W. H. CAMPEN and J. R. SMITH: Some Physical Properties of Densified Soils, *Proc. Highway Research Board*, vol. 22, 1942.
2. F. L. GUTHBERT: Use of Calcium Chloride in Granular Stabilization of Roads (lith.), a review of available literature, Highway Research Board, Washington, D. C., 1945. (Contains a bibliography of 145 items.)
3. H. F. WINTERKORN and L. D. BAVER: Sorption of Liquids by Soil Colloids, *Soil Sci.*, vol. 38, 1934; vol. 40, 1935.
4. L. D. BAVER: The Relation of Exchangeable Cations to the Physical Properties of Soil, *Jour. Am. Soc. Agr.*, vol. 20, 1928.
5. A. F. JOSEPH and H. B. OAKLEY: The Properties of Heavy Alkaline Soils, *Jour. Agr. Sci.*, vol. 19, 1929.
6. A. HOLMES and other members of the Standard Oil Development Company, Esso Laboratories: Factors Involved in Stabilizing Soils with Asphaltic Materials, *Proc. Highway Research Board*, vol. 23, 1943.
7. V. A. ENDERSBY: Fundamental Research in Bituminous Soil Stabilization, *Proc. Highway Research Board*, vol. 22, 1942.
8. C. L. MCKESSON: Recent Developments in the Design and Construction of Soil-emulsion Road Mixtures, *Proc. Highway Research Board*, vol. 20, 1940; also Emulsified Asphalt Treated Subbase, *ibid.*, vol. 24, 1944, with a comprehensive bibliography.
9. "Soil-cement Roads," 2d ed., Portland Cement Association, Chicago, 1941.
10. Procedures for Testing Soils, A.S.T.M., Pamphlet, Philadelphia, 1944.
11. H. F. WINTERKORN, H. J. GIBBS, and R. G. FEHRMAN: Surface Chemical Factors of Importance in the Hardening of Soils by Means of Portland Cement, *Proc. Highway Research Board*, vol. 22, 1942.

12. Papers by M. D. Catton of the Portland Cement Association, *Proc. Highway Research Board*, 1937-1944.
13. K. ENDELL and U. HOFFMANN: Electro-chemical Hardening of Clay Soils, *Proc. Intern. Conf. Soil Mech.*, vol. I, Paper M-3, 1936.
14. LEO CASAGRANDE: Grossversuch zur Erhöhung der Tragfähigkeit von schwebenden Pfahlgründungen durch electrochemische Behandlung, *Die Bautechnik*, vol. 15, 1937; vol. 17, 1939; also W. BERNATZIK: Electrochemical Consolidation of the Ground, *Second Congr. Intern. Assoc. for Bridge and Structural Eng. Final Rep.*, Berlin, 1936.
15. JOSEPH D. LEWIN: Grouting with Chemicals, *Eng. News-Record*, vol. 123, Aug. 17, 1939; also an article by E. Mast in *Der Bauingenieur*, vol. 15, 1934.
16. B. A. RZHANITZIN: "Chemical Soil Stabilization" (in Russian, official publication, Moscow, 1935).
17. C. A. HOGENTOGLER: "Engineering Properties of Soil," McGraw-Hill Book Company, Inc., New York, 1937 (for Public Roads Administration classification see pp. 241-243).
18. "Engineering Manual," Chaps. XX and XXI, War Department, Office of the Chief Engineer (these two chapters, including Casagrande's classification, are reprinted on pp. 154-173 of *Proc. Highway Research Board*, vol. 22, 1942).
19. "Airport Design Information," Civil Aeronautics Administration, Washington, D. C., 1941.
20. G. P. TSHEBOTARIOFF: Effect of Vibrations on the Bearing Properties of Soil, *Proc. Highway Research Board*, vol. 24, 1944 (discussion by L. A. Palmer).
21. H. M. WESTERGAARD: Stresses in Concrete Pavements Computed by Theoretical Analysis, *Public Roads*, April, 1926; Stresses in Concrete Runways of Airports, *Proc. Highway Research Board*, vol. 19, 1939.
22. F. M. BARON: Uncertainties in Design of Concrete Pavements Due to Differential Settlements and Volumetric Changes, *Proc. Highway Research Board*, vol. 23, 1943; also vol. 24, 1944.
23. O. J. PORTER: Foundations for Flexible Pavements, *Proc. Highway Research Board*, vol. 22, 1942.
24. For a full description of the California bearing ratio test and a design example, see *Proc. Highway Research Board*, vol. 22, 1942, pp. 124-129 and 162-165, respectively; see also ref. 18 and T. A. MIDDLEBROOKS: Design of Flexible Pavement Foundations, *Roads and Streets*, vol. 86, 1943.
25. "Procedure for Determination of Thickness of Flexible Type Pavements," U.S. Navy Department, Bureau of Yards and Docks, 1943.
26. Report of Committee on Flexible Pavement Design, *Proc. Highway Research Board*, vol. 23, 1943.
27. Certain Requirements for Flexible Pavement Design for B-29 Planes, (lith.), U. S. Waterways Experiment Station, Vicksburg, Miss., War Department, 1945.
28. Asphalt: Pocket Reference for Highway Engineers, Asphalt Institute, New York, 1942.

29. "War-time Problems," Issue No. 8, Highway Research Board, Washington, D. C., 1943.
30. M. G. SPANGLER (of the Iowa State College): The Structural Design of Flexible Pavements, *Proc. Highway Research Board*, vol. 22, 1942.
31. T. A. MIDDLEBROOKS and R. M. HAINES: Results of Accelerated Traffic Tests on Runway Pavements, *Proc. Highway Research Board*, vol. 23, 1943; also papers on the same subject in vol. 24, 1944.
32. M. S. KERSTEN: Survey of Subgrade Moisture Conditions, *Proc. Highway Research Board*, vol. 24, 1944; also vol. 25, 1945.
33. M. G. SPANGLER: Some Problems in Subgrade Moisture Control, *Proc. Highway Research Board*, vol. 25, 1945.
34. H. F. WINTERKORN and H. EYRING: Theoretical Aspects of Water Accumulation in Cohesive Subgrade Soils, *Proc. Highway Research Board*, vol. 25, 1945.
35. "Investigations of Filter Requirements for Underdrains" (lith.), U. S. Waterways Experiment Station, Vicksburg, Miss., War Department, 1941.
36. "Filter Design" (lith.), Soils and Paving Laboratory, U. S. Engineer Office, Providence, R. I., 1942.
37. PHILIP KEENE: Underdrain Practice in the Connecticut State Highway Department, *Proc. Highway Research Board*, vol. 24, 1944.
38. H. E. COTTON: Mistakes in Drainage, *Highway Mag.*, September-December, 1945.

## CHAPTER XIII

### SETTLEMENT OF STRUCTURES

#### A. GENERAL

**13:1. Definitions.**—The term “settlement” means the *vertical* displacement of the base of a structure that may result in displacements or deteriorations of portions of that structure. When referring to pavements the term “deflection” (Chap. XII) is usually substituted for the term “settlement.” The term “differential settlement” means that one or more parts of a structure settle

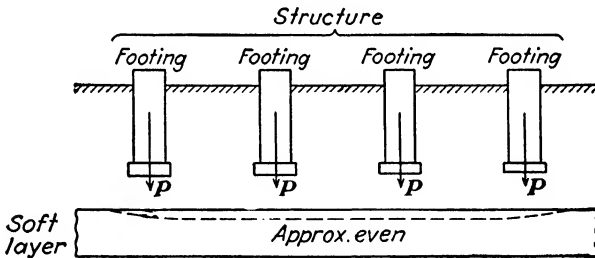


FIG. 13:1.—Practically even settlement.

more than the rest of the structure. In its turn the differential settlement results in a curvature of the base of the foundation. The smaller the radius of curvature the more serious the crack danger (compare Fig. 12:6). Strictly speaking, there is no ideal uniform settlement. A certain approximation to such a settlement is the settlement under the central part of a uniformly loaded large area as shown in Fig. 13:1.

Besides the vertical settlement, there may be a *horizontal* displacement of the structure. For instance, some ancient cathedrals move both vertically and horizontally. There are sometimes horizontal movements of large masonry and concrete arches. The concept “seat of settlement,” introduced by Terzaghi, corresponds to that part of the earth mass which is responsible for about 75 per cent of the settlement observed. This concept is clarified in the following sections.

**13:2. Causes of Settlement.**—A structure may move, as explained in Sec. 13:1, because of either the action of static forces or that of dynamic forces. For action of static forces the sketch (Fig. 7:2) is fully applicable. Settlement or movement in a vertical direction occurs when forces  $W$  and  $R$  in that sketch do not balance each other; and yield of the lateral support  $P_L$  causes horizontal motion which, of course, is necessarily combined with some vertical subsidence.

Static forces are

*a. Static loads proper, i.e.,* dead load and live load. Live loads may influence settlement, but generally their effect is negligible, except in such cases as highway pavements, silos, and sometimes bridge supports.

*b.* Change in *ground-water* level, since this change is tantamount to decrease or increase of the weight of the overburden and of the structure.

*c.* Undermining due to *subterranean activities* such as mining operations or tunnel construction. Sometimes simple excavation in the neighborhood of a structure may cause its settlement or horizontal displacement or both. Undermining may be caused also by erosion.

Very close to these static forces are some dynamic forces, such as (*d*) *landslides* or other natural movements of surface ground and also changes in volume in deeper strata (for instance, in gypsum) and (*e*) *frost action* (compare Chap. III). Settlement of structures on ever-frozen soils, very important in some parts of Russia and China, and also in Alaska, will not be considered here.

Dynamic forces which may cause considerable settlements are due to *vibrations* and *earthquakes* (Sec. 13:22).

## B. SETTLEMENT CAUSED BY STATIC LOADS

**13:3. Contact Settlement.**—Static loads transmitted by the structure to its base cause displacements within the earth mass that are, respectively, (*a*) contact settlement due to stresses close to the base of the structure (Fig. 13:2*a*) and (*b*) settlement in deeper strata due to the presence of a soft compressible layer at greater depth (Fig. 13:2*b*). In the first case, if the earth mass is more or less homogeneous, stresses and consequently strains decrease from the base downward; hence the seat of settlement is close to the



Then the settlement of a nonrigid disk of diameter  $D$ , loaded with a uniformly distributed load  $p$ , is

$$\Delta = \frac{p}{C} D \quad (13:2)$$

The settlement underneath the edge of the disk is about two-thirds of the settlement at the center (Fig. 13:4a).

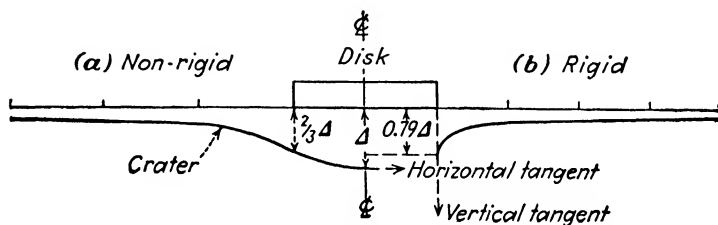


FIG. 13:4.—Elastic settlements under a circular disk.

If the disk is rigid, all points of its base settle uniformly (Fig. 13:4b). The settlement in this case is approximately (but not exactly) equal to the average settlement for a nonrigid disk:

$$\Delta = \frac{\pi p}{4C} D = 0.79 \frac{p}{C} D \quad (13:3)$$

Formulas (13:2) and (13:3) show that the theoretical settlement of a circular disk is proportional to its diameter.

In Fig. 13:4a a crater is found under the nonrigid disk, which in its settlement follows exactly the shape of the crater. The term "crater" is also applied to depressions (hollows) under and around buildings and even entire cities.

Elastic formulas furnish information on the elastic part of the settlement only. As is well known (Chap. VI) in the case of sands there are elastic (reversible) and nonelastic (irreversible) deformations. If the latter are small, as with very compact sands and gravels, elastic formulas may be of a certain value; and this is the reason why they are given here.

*c. Use of the Results of a Confined Compression Test.*—A particular case of settlement of a rigid bridge pier (unit load  $p$ ) on a very deep sand foundation will be discussed (Fig. 13:5). It will be shown what kind of research work should be done in order to make settlement estimates in such cases possible, since at the present time they are impossible. Fortunately this case is not of great practical importance.

Undisturbed samples of sand from various depths should be taken, and confined compression tests made. This can be done in the consolidation apparatus (Sec. 6:24). A stress-strain diagram is shown in Fig. 13:5*b* for a sample 1 in. thick. Loading and unloading furnish the value of  $(\Delta_e)_0$ , the elastic part of the settlement, and  $(\Delta_i)_0$ , the nonelastic (irreversible) part. In reality the pier is loaded *only once*, and the value of  $(\Delta_e)_0$ , corresponding to one

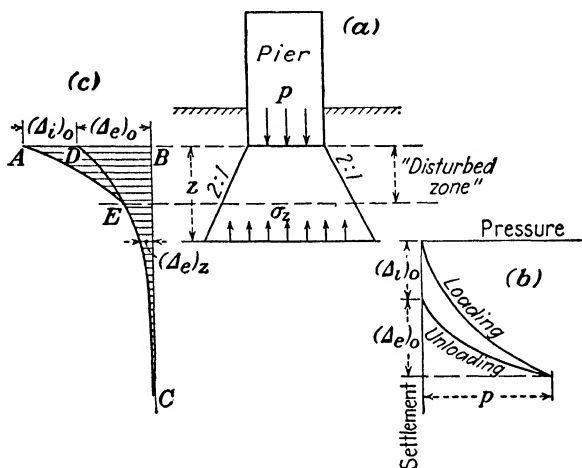


FIG. 13:5.—Estimating settlement of a bridge pier on deep sand foundation.

loading-unloading cycle in the consolidation apparatus, is a fair approximation. Notice that  $(\Delta_i)_0$  and  $(\Delta_e)_0$  in Fig. 13:5*b* are fractions of an inch, and in Fig. 13:5*c* they are fractions of a unit. Vertical pressures may be computed by the 2-to-1 method (Sec. 4:15*b*), and strains  $(\Delta_e)_z$  at different depths  $z$  may be determined from the loading curve. By plotting them, curve  $AEC$  is obtained. The settlement equals area  $ADBCE$  (in square inches) divided by the product  $ab$  of the vertical and horizontal scales. Vertically 1 in. represents  $a$  ft., and horizontally 1 in. represents  $b$  units. Point  $C$  should be taken reasonably deep. Another approach would be to assume that below the bottom of a "disturbed zone" there are no irreversible settlements and to trace the curve of elastic settlements  $DEC$ .

There are two main handicaps in the use of this method: (1) as will be explained in Chap. XIV, it has not been possible so far to obtain undisturbed sand samples, and (2) the depth of the dis-

turbed zone is not known. For preliminary purposes, the latter may be estimated, for example, at 10 ft. It may be seen from Fig. 13:5c that the seat of settlement in this case is in the disturbed zone, as may be expected. There is no doubt that *friction of a deep caisson* against sand decreases the settlement, and it is very difficult to estimate this decrease.

*Soft Layers.*—If there is a soft layer at the surface, settlement is to be determined as consisting of two parts: (a) settlement before consolidation starts and (b) settlement due to consolidation. Part (a) may be computed considering the structure as a disk of equivalent area. For this purpose formulas (13:2) and (13:3) may be used, placing in them the value of  $E$  from a nonconfined compression test (Sec. 6:4) and  $\mu = \frac{1}{2}$  as for incompressible masses. Part (b) of the settlement may be found as explained in Sec. 13:5 for deep soft layers. To apply the theory of consolidation, soil must be saturated. If the soil under the structure consists of porous non-saturated material (such as wet loam or moist clay) there is no approach to the solution of the problem. Relatively fair results could be obtained by using the theory of elasticity and assuming that these soils follow Hooke's law—which, however, is not the case.

### 13:5. Settlement in Deeper Strata.

—The problem is to compute the settlement at an arbitrary point  $B$  of the ground surface caused by a structure represented by a concentrated force  $P$  acting at point  $A$ . All deformations in the overburden, *i.e.*, above the soft layer which is bounded by the horizontal planes  $ab$  and  $a'b'$ , are disregarded (Fig. 13:6). Vertical pressures  $\sigma_z$  are determined at all points of the vertical  $Bm'n'$  passing through the given point  $B$ , and the "pressure area"  $A_p = \text{area } m'p'q'n'$  is computed. To simplify operations, often only one average value of  $\sigma_z$  is computed; upon being multiplied by the thickness of the layer, this value furnishes the "pressure area"  $A_p$ .

In Fig. 13:6 the structure is replaced by the concentrated force  $P$ . Such a procedure is more or less accurate if the soft layer where

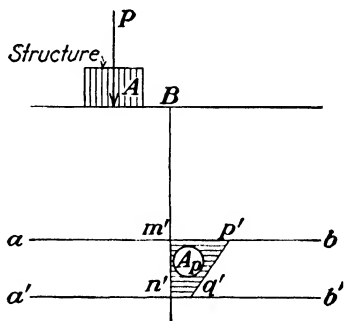


FIG. 13:6.—Estimating settlement due to consolidation in deeper strata.

the seat of settlement is located is deep enough. Otherwise pressures  $\sigma_z$  are to be determined by one of the methods for computing stresses as caused by distributed load. It should not be forgotten that if an area is loaded with a uniformly distributed nonrigid load of  $p$  tons per sq. ft., at no point of the earth mass can the vertical pressure  $\sigma_z$  be greater than  $p$ .

Simultaneously with the office operations described, undisturbed samples are extracted from the soft layer in question and tested in the laboratory. Two questions are to be answered by the laboratory (Sec. 6:23): (a) What is the value of the total settlement of the layer, or in other words what are the values of the voids ratios in the soil before construction and after complete consolidation? (b) What is the value of the coefficient of consolidation,  $c_v = (k/\gamma_0)[(1 + e)/a]$ ? For this purpose, consolidation tests are run in the laboratory. The value of total settlement is defined as the product of the pressure area and the reciprocal of the "modulus of elasticity" of the soil  $E_2$  [compare Eq. (6:5) and (6:8)]:

$$\Delta H = A_p \frac{a}{1 + e}$$

The distribution of settlement in time (trend of settlement) may be determined either by tracing isochrones, or using graphs of the time factor (Chap. VI). In both cases the coefficient of consolidation is used.

### 13:6. Lines of Equal Settlement.—

If the values of the expected settlements at different points of the ground surface are available, isolines connecting points with equal values of settlement may be drawn. This is done in the same way that contour lines are traced in surveying. Besides theoretical lines of equal settlement, there may be actual lines based on observations of settlement after the erection of the structure.

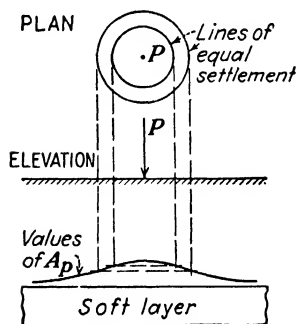


FIG. 13:7.—Lines of equal settlement under a concentrated load.

Assume a homogeneous soft layer of a thickness  $H$ . Then the settlements at a point of the ground surface are proportional to the pressure area  $A_p$  or, in other words, to the average vertical pressure as determined from the condition  $(\sigma_z)_{av.} = A_p/H$ .

According to Saint-Venant's principle (Sec. 4:11), stresses in a deep layer caused by a structure may be approximately replaced by those caused by a concentrated force. It is obvious that lines of equal settlement in this case are concentric circles. Hence the deeper seat of settlement the closer observed lines of equal settlement should approach circles (Fig. 13:7).

**13:7. Influence of the Rigidity of the Structure on Its Settlement.**—The following three cases will be considered:

a. The seat of settlement is at a deep soft layer, and the effect of a structure placed on or close to the ground surface may be re-

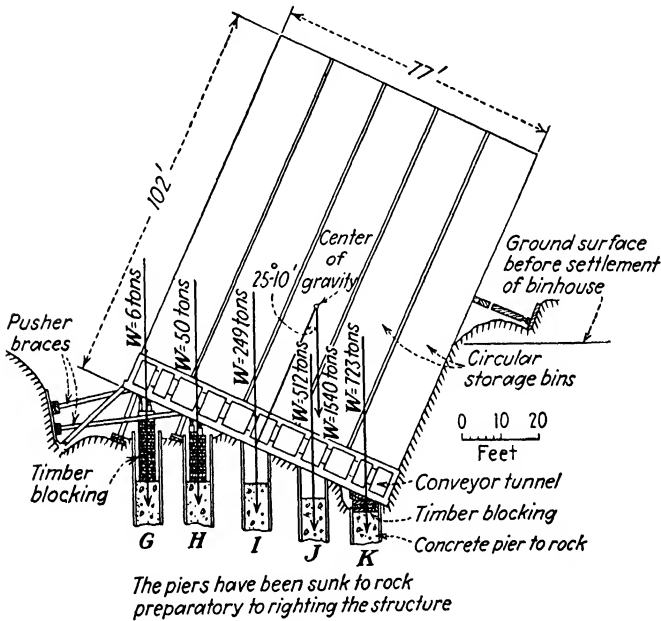


FIG. 13:8.—Tipping of the Transcona Grain Elevator (underpinned by the Foundation Company, New York City).

placed by that of a concentrated force. The values of the pressures within the soft layer are then controlled merely by the total weight of the entire structure (assuming, of course, that this weight is the same in the case of both rigid and nonrigid structures).

b. The seat of settlement is in a shallow compact layer (sand, gravel). Settlements are very small, and, practically, there is no difference between rigid and nonrigid structures.

c. The seat of settlement is in a shallow, compressible layer

possessing weak shearing resistance. If the structure is wide, there will be more differential settlement with a nonrigid structure than with a rigid structure (compare, for instance, Fig. 4:22). If the structure is narrow and rigid, it will work as a punch and destroy the earth mass by shear. If actual failure does not happen, considerable settlement may take place. The failure in such cases is mostly one-sided (tipping).

Figure 13:8 shows the failure of the Transcona Grain Elevator, Winnipeg, Canada, in 1914.<sup>5</sup> The building was founded on a mat foundation on saturated clay, the unit load on the foundation being about 3.3 tons per sq. ft. When the bins were first filled, the bin

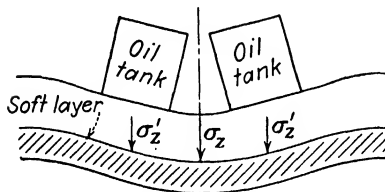


Fig. 13:9.—Tipping of oil tanks due to consolidation in deeper strata.

house started to settle and to tip, and at the end of 24 hr. the east side of the mat foundation was 5 ft. above its original grade and the west side 29 ft. below the original grade. The structure was underpinned and righted by installing concrete piers *G, H, I, J, K* down to rock at a depth of

54 ft. In this, as in some other similar cases, the tipped structure was gradually rotated back to the vertical position.

The Transcona failure and other similar cases as well were due to the action of the shearing stress. In some rare cases consolidation is instrumental in the tipping. For instance, Fig. 13:9 shows on an exaggerated scale two oil tanks inclined toward each other; vertical pressure  $\sigma_z$  between the tanks is greater than under each of them ( $\sigma'_z$ ) and causes a depression in a deep clay layer.

From the point of view of the sketch (Fig. 7:2) the failure of the Transcona Elevator (Fig. 13:8) was due to the weakening of the lateral support  $P_L$ , whereas the phenomenon shown in Fig. 13:9 is caused by the insufficiency of the vertical reaction  $R$ , as in all cases of consolidation in deeper strata.

### 13:8. Secondary Stresses in the Structure Due to Settlement.—

*a. Reinforced Concrete and Masonry.*—Owing to differential settlement of a reinforced-concrete structure resting on the earth's surface, there are secondary stresses in the structure. Since the value of the stress in a beam is proportional to the deflection and the depth (thickness in the plane of bending) of the beam, the value of a secondary stress may be computed from the measurements of

the settlement. In many cases the values of secondary stresses computed in this way, added to primary stresses, furnish values close to the ultimate strength. Sometimes open cracks appear, and the structure produces the impression of having suffered serious damage. Cases of collapse are very rare, however.

Terzaghi's observations<sup>1</sup> have shown that brick walls have a considerable strength to bridge weak points of the earth surface and can stand considerable angular deflection (or small radii of curvature) before cracking. Straight brick walls with few openings are more stable than the irregular ones with numerous openings.\*

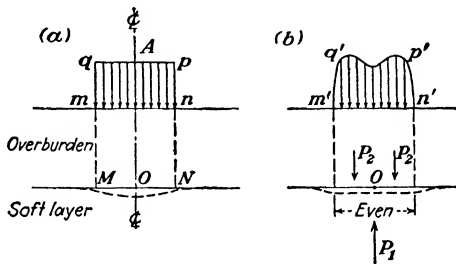


FIG. 13:10.—Influence of even settlement on the stresses in a structure. (After Taylor.)

*b. Stresses in a Structure in the Case of Even Settlement.*—The general opinion is that secondary stresses due to settlement may develop in a structure if settlement is uneven (differential) and that if a structure settles evenly, there are no such secondary stresses. It may be argued thus,<sup>3</sup> however (Fig. 13:10): A structure *A* produces larger pressures underneath its center than underneath its edges. Hence point *O* at the top of the soft layer tends to settle more than point *M* or *N*. Since the structure is rigid and the settlement even, there should be an additional system of forces,  $P_1$  acting upward and  $P_2$  acting downward. It is obvious that  $P_1 = P_2 + P_2$ . These forces produce secondary stresses in the structure *A*. The secondary stresses upon being superimposed on the primary stresses (area  $mnpq$ ) furnish an area  $m'n'p'q' = mnpq$ . No numerical data with respect to the value of the forces  $P_1$  and  $P_2$  can be given so far.

**13:9. Influence of the Size of a Structure on Its Settlement.**—Returning to Fig. 13:4 and the accompanying text, we see that the theoretical elastic settlement for both rigid and nonrigid disks is

\* More information on the influence of the settlement on the stresses in a structure should be sought in the works on the analysis and design of structures.

proportional to their diameters. This means approximately that settlements of the two structures are proportional to the square roots of their areas. Hence if one structure has an area of  $A$  sq. ft. and another that of  $a$  sq. ft., the ratio of their maximum settle-

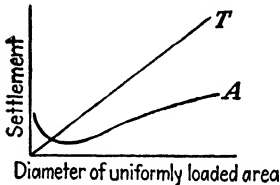


FIG. 13:11.—Relationship between the loaded area and the settlement ( $T$ , theoretical;  $A$ , actual).

ments should be  $\sqrt{A/a}$  (compare also Sec. 8:6). In reality, all circumstances being equal, the larger structure would settle more than the smaller, but its settlement would be less than the theoretical. This fact is represented graphically in Fig. 13:11, where the straight line  $T$  shows the theoretical proportionality between the size of a structure and its settlement, and curve  $A$  roughly represents that relationship as actually observed.

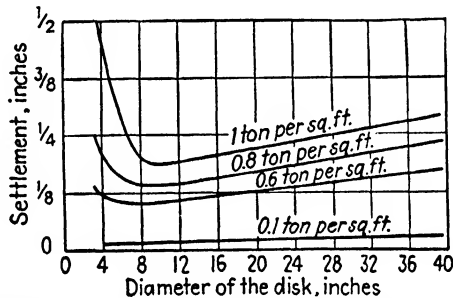


FIG. 13:12.—Experimental relationship between settlement and diameter of the disk. (After Kögler and Scheidig.)

Figure 13:12 shows the results of small-scale experiments in Kögler's laboratory.<sup>2</sup> The settlement of the loaded plate increases with its area but not, as the theory of elasticity states, exactly in direct proportion with its diameter. When the area is very small, the settlement increases again—a fact that is explained by Kögler by the "pile action" of the loaded plate.

The settlement of a structure is *greater* than that obtained in a loading test, though there is no direct proportionality. This rule and exceptions from it have already been mentioned in Sec. 8:7.

**13:10. Field Time-settlement Curves.**—Theoretical time-settlement curves have been discussed in Chap. VI. They are constructed by plotting theoretical values of settlement against time.

In the same way, by plotting actually observed values of settlement against time, field time-settlement curves may be obtained.

Various types of such curves are shown in Fig. 13:13. The upper diagram in this figure represents the increase of the acting load during the construction period (about one year), after which the acting load remains constant. If the structure is constructed on sand (curve *a*), there is settlement only during the construction period, after which, as a rule, the structure remains stable. In the case of a clay foundation (curve *b*), the field time-settlement

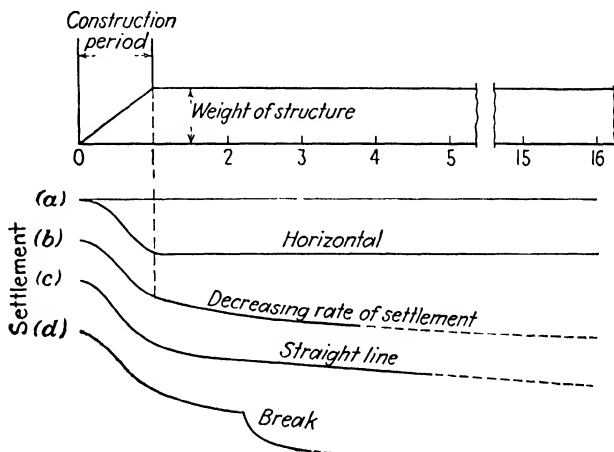


FIG. 13:13.—Field time-settlement curves (numerals 0, 1, 2 . . . are years).  
(After Terzaghi.)

curve is quite similar to theoretical curves as discussed in the theory of consolidation (compare Fig. 6:8). In both curves *a* and *b* and in the other curves of Fig. 13:13 also, the part of the time-settlement curve corresponding to the construction period has a peculiar shape corresponding to the action of an increasing load (compare Fig. 6:12).

Curve *c* in Fig. 13:13 shows the case of the so-called “straight-line settlement.” The rate of settlement in this case does not decrease as in the case of curve *b*. The straight-line settlement is attributed to the *plastic flow* (leakage) of soil from underneath the foundation. It is to be remembered that overloaded plastic materials flow at a constant rate. The seat of settlement may even be far away from the structure (for instance, leakage at point *A*, Fig. 13:14).

Curve *d* represents a *spontaneous settlement*. Upon construction, the structure settles in a regular way, following curve *b*, for instance. At a certain stage of the settlement some change occurs in the soil condition. This change may be an increase in acting stresses or a decrease in resistance due to excessive moisture or

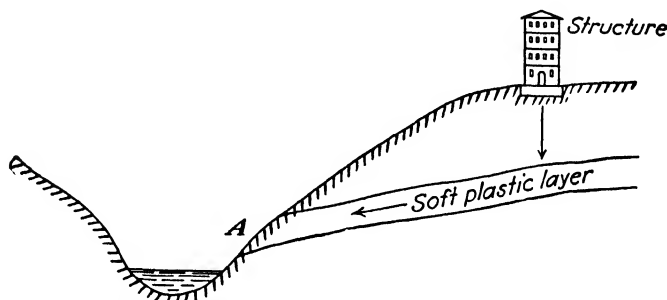


FIG. 13:14.—A hypothetical case of straight-line settlement.

both. Figure 13:15 shows the case of spontaneous settlement of a building due to the filling of a near-by canal. The weight of the fill produced an additional vertical pressure  $\sigma'_z$  under the structure. This additional vertical pressure  $\sigma'_z$ , added to the existing stress  $\sigma_z$ , caused the break shown in the time-settlement curve *d* in Fig. 13:13.

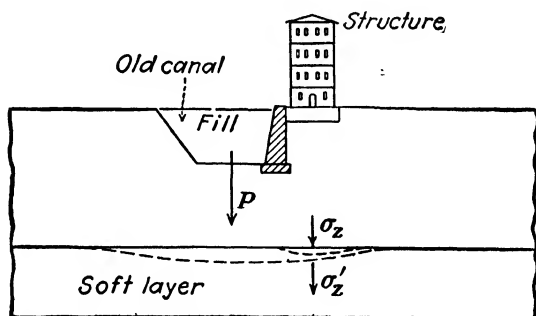


FIG. 13:15.—A hypothetical case of spontaneous settlement.

**13:11. Examples of Contact Settlement.**—Homogeneous earth masses are exceedingly rare; hence cases of contact settlement discussed here will refer only incidentally to such masses and will be concerned mostly with homogeneous or nonhomogeneous shallow, soft layers underlain by a more rigid mass.

*Tanks.*—The structure most similar to a nonrigid disk (Fig. 13:16a) is an oil or water tank. Sometimes tanks possess very rigid bases, such as reinforced-concrete circular mats resting on piles. As proposed by Terzaghi,<sup>4</sup> an experimental tank was placed directly upon the ground, the rim resting within a circular ring of reinforced concrete, as shown in Fig. 13:16. If in the design of the tank adequate provision for its settlement has been made, such an arrangement may be quite advisable.

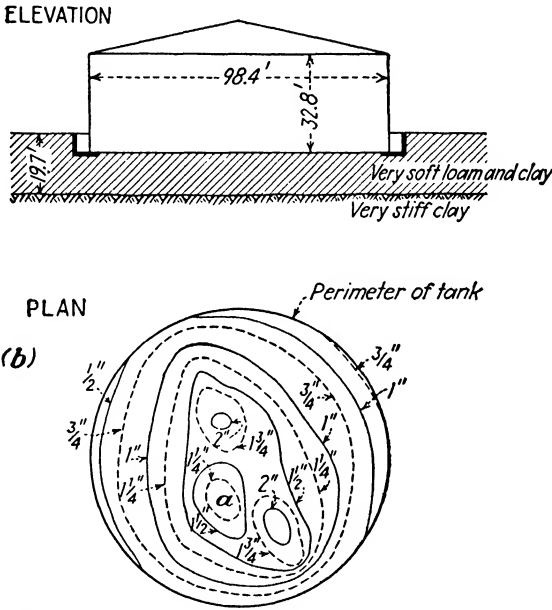


FIG. 13:16.—Settlement of a tank. (After Terzaghi, *Proc. A.S.C.E.*, May, 1933.)

Curves of equal settlement shown in Fig. 13:16b correspond to a stage when the experimental tank referred to was almost filled with water. This corresponded to a uniformly distributed pressure somewhat less than 1 ton per sq. ft. of the base. Owing to the nonhomogeneity of the earth mass, there was some confinement of the material. This is shown by the hill *a* and the irregular shape of some of the curves. Otherwise, for symmetry, lines of equal settlement should be concentric circles.

This example may be used to clarify further the difference between a homogeneous elastically isotropic body and a natural earth mass. In the former theoretical case, matter becomes compressed

and is assumed to move in a slightly oblique downward direction; in the latter actual case there was apparently also lateral movement from the center of the tank toward its perimeter.

Another example of tank settlement is shown in Fig. 13:17. These are metallic oil containers, 98.4 ft. in diameter, in Hamburg, Germany.<sup>2</sup> The time-settlement curves show very clearly that

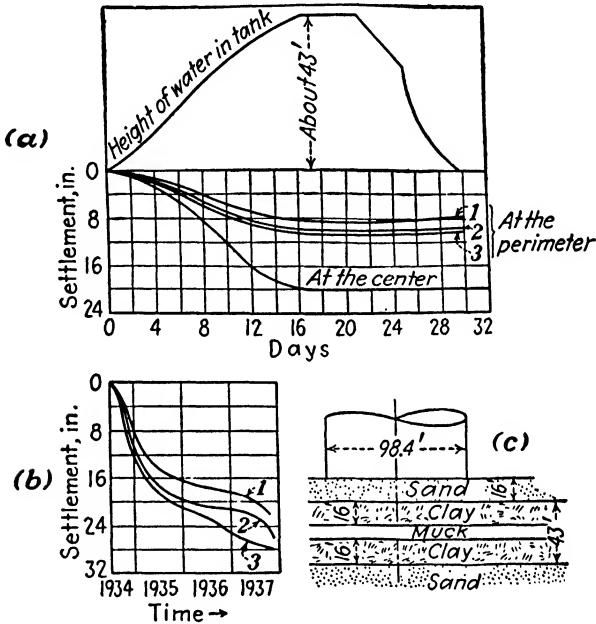


FIG. 13:17.—Settlement of tanks. (After Kögler and Scheidig.)

during the initial loading both elastic and nonelastic (irreversible) displacements took place; and afterward, during the unloading, there was a small elastic rebound, as shown by the upward direction at the end of curves 1, 2, 3 in Fig. 13:17a. The settlement at the center of the tank was twice the settlement at its perimeter. It is to be remembered that this ratio is  $1\frac{1}{2}$  in the case of a nonrigid disk placed on top of a homogeneous elastically isotropic body (Fig. 13:4a). The soil consisted of about 40 ft. of clay and muck, sandwiched between the upper sand layer (16 ft. thick) and the underlying sand mass (Fig. 13:17c). During the first 30 days the tank behaved practically as a nonrigid disk on top of an elastic continuum. Afterward, consolidation of the two clay layers in

somewhat more than three years caused a settlement of between 22 and 28 in. (curves 1, 2, 3 in Fig. 13:17b). Irregular down-bent ends of the time-settlement curves show that the settlement was not yet over in 1937.\*

*Buildings on Weak Soil Approaching Elastic Continuum.*—Buildings may be more rigid than the oil and water tanks just discussed, without being, however, perfectly rigid. If placed on top of a weak

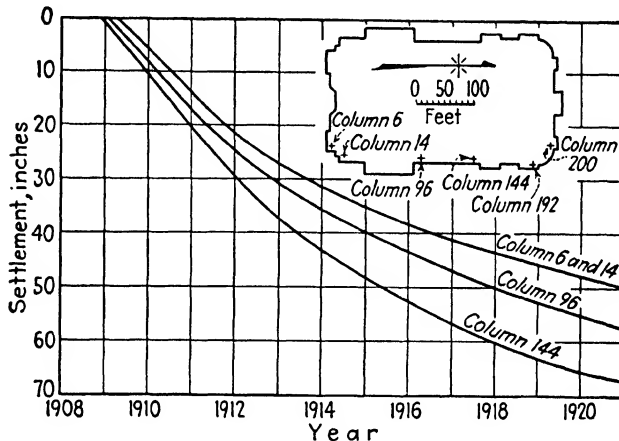


FIG. 13:18.—Settlement of the National Theatre in Mexico City. (From Proc., A.S.C.E., May, 1933.)

earth mass approaching an elastic continuum, they will reveal considerable settlement at or close to the center of the structure.

One of the most treacherous soils in the world is the soil in Mexico City, Mexico (compare end of Sec. 1:2). This city is located at the bottom of a large lake bed filled with volcanic ash. This ash, under the action of weathering agents, formed a highly saturated plastic soil. Mexico City represents a characteristic example of the "crater" mentioned in Sec. 13:4, since the city is sinking down as a whole with secondary craters appearing around large heavy buildings. As an example, the School of Engineering in that city is located in a 300-year-old building, the front wall of which has sagged 4 ft. in the middle. There are no visible cracks in the wall in question, and this shows that the masonry has adapted itself to the settlement (compare Sec. 13:8 on the rigidity of masonry).

\* See Fig. 13:9 for another case of settlement of tanks.

Figure 13:18 represents time-settlement curves of the National Theater in Mexico City. Its construction took many years, and the building settled at a surprising rate. On the front of the building, for instance, columns settled as much as 4 or 5 ft.; the settlement at the rear was much smaller.

Obviously, these examples of settlement from Mexico City represent an exception. As stated before, homogeneous masses

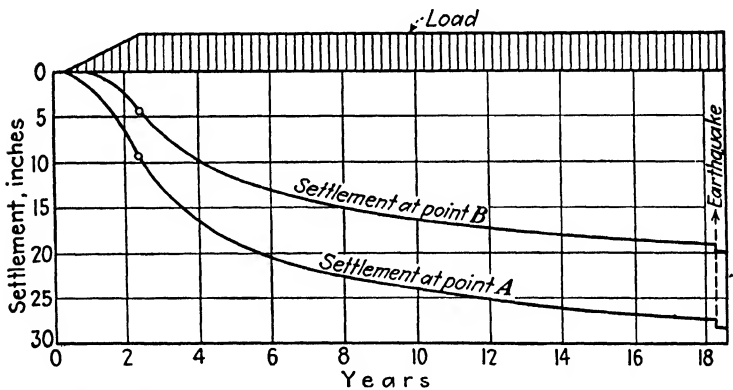
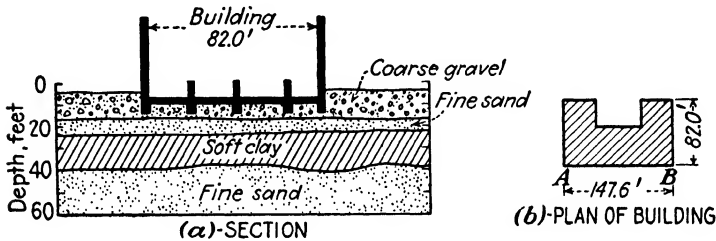


FIG. 13:19.—Settlement of a post office building in Germany. (From Proc., A.S.C.E., May, 1933.)

serving as bases for buildings generally are firm and compact, and actual settlement rarely exceeds 2 in. Larger settlements may arouse misgivings as to the safety of the structure.

*Buildings on Weak Soil Approaching an Idealized Fragmental Mass.*—As stated, the maximum settlement of a structure constructed on weak soil approaching an elastic continuum is at or near the middle of the structure. If, in contrast, the earth mass approaches an idealized fragmental mass (for instance, sand) and the structure is not rigid enough, there may be settlement at the edges of the structure. This is in accordance with the experiment

represented graphically in Fig. 4:22. Scheidig reported in the German periodical *Die Bautechnik* (1931) the settlement of new brick apartment houses in Moscow, Russia. Apparently, owing to hasty work, the mortar had no time to set, and the building was not rigid enough. As a result, edge settlement also occurred.

*Buildings on Shallow Soft Layers.*—Several examples of settlement due to consolidation of a homogeneous or nonhomogeneous soft layer between the structure and an underlying rigid mass are given here.

*Example 1.*—The post-office building in Bregenz, Germany, was constructed in 1894. Geological conditions are shown in Fig. 13:19. Settlement started immediately after construction. In 1911 measures were taken to decrease the acting unit load, which was from 3 to 6 tons per sq. ft., to a smaller figure of 1.3 tons per sq. ft., of the foundation. The bearing area was increased by adding cantilevers; a rigid reinforced-concrete floor in the basement was arranged to carry a part of the total load. Settlement continued as before, however. This fact suggests that what matters in some cases of settlement due to consolidation *in deeper strata* is the *total weight* of the structure and not its distribution over the foundation.

Time-settlement curves in Fig. 13:19 show the settlement only during the first 18 years of the existence of the building. Settlement, however, is still continuing.

*Example 2.*—The cathedral at Königsberg, Germany, the construction of which probably started in 1333 (Fig. 13:20), rests on a 30-ft.-thick, weak layer of peat and fine sand, followed by a thick marl layer. The latter may be considered rather incompressible, so that consolidation takes place between the base of the cathedral

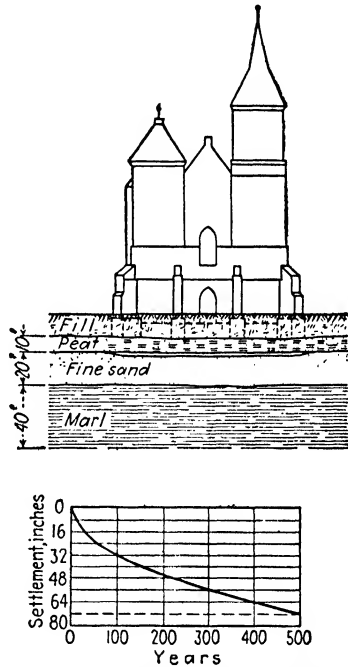


FIG. 13:20.—Settlement of the cathedral in Königsberg, Germany.

and the top of the marl layer. There are five floors, placed on top

of each other, and the original threshold was discovered 5 ft. below the present entrance. Owing to the fact that the lower part of the cathedral has disappeared from view, the building loses much from an architectural point of view.

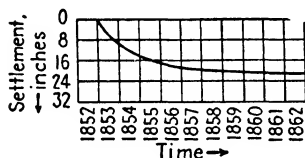
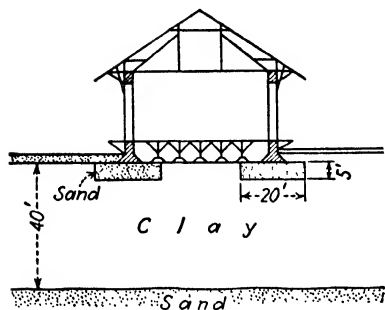


FIG. 13:21.—Settlement of a freight shed in Germany. (After Kögler and Scheidig.)

This example shows that even such an insignificant unit load as that of

*Example 3.*—Settlement of a freight shed at the railroad station at Emden, Germany,<sup>2</sup> is shown in Fig. 13:21. A very careful record of the settlement of this old structure during the period 1852–1862 permits the drawing of a time-settlement curve. Settlement was due to consolidation of a shallow, 35-ft.-thick clay layer underlain by sand. The shed is placed on

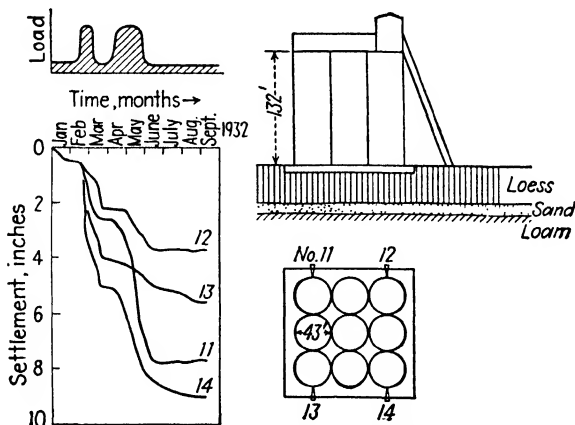


FIG. 13:22.—Settlement of a coal elevator in Siberia.

a railroad freight shed can cause a considerable settlement, which in the given case reached 20 in. in 10 years.

*Example 4.*—Coal silos of Kusnetzstroy, Siberia, shown in Fig. 13:22, are constructed on loess, the thickness of the loess layer being between 12 and 30 ft. The time-settlement curves are of irregular shape, according to the filling and emptying of the silos (see the load diagram, at the left, top). Owing to considerable permeability of the loess, the consolidation process was very rapid.

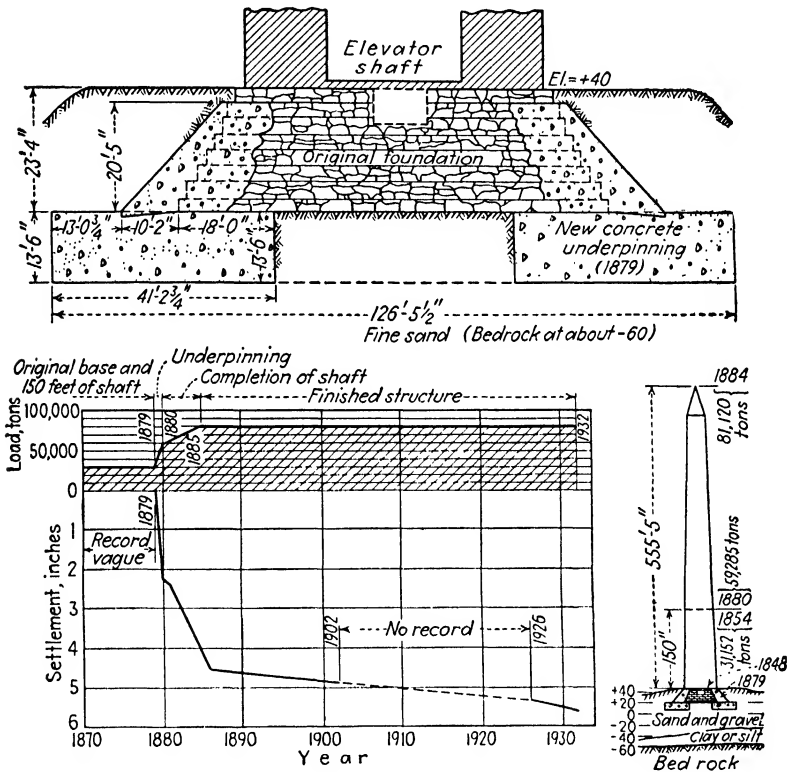


FIG. 13:23.—Settlement of the Washington Monument. (From Proc., A. S. C. E., May, 1933.)

**13:12. Examples of Settlements in Deeper Strata; Settlement of Pile Foundations.**—Only one example of settlement due to consolidation in deeper strata will be discussed, and the remainder of this section will be dedicated to the settlement of pile foundations.

*Example 1.*—The original foundation of the Washington Monument in Washington, D. C., was only 80 ft. square, and when work ceased in 1854, the height of the structure was 150 ft. and its weight

31,152 tons—a unit load of about 5 tons per sq. ft. In 1879 underpinning of the Monument was begun, apparently because of settlements. The work was done by U. S. Engineers under the supervision of General Casey. The old foundations were underpinned to an area 126 ft. 5½ in. square; the present height of the monument, 555 ft. 5 in., was reached in 1884. When the unit load was increased, the monument settled 4½ in. and after 1885 another inch; a very slow settlement probably is still continuing (Fig. 13:23).

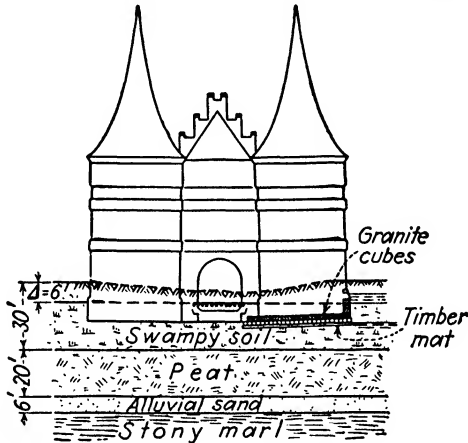


FIG. 13:24.—Settlement of the Holsten Gate, Lübeck, Germany. (After Kögler and Scheidig.)

Reliable borings were not made until 1931, when an irregular bed of compressible clay 10 to 40 ft. thick, overlying the rock, was disclosed. Hard rock is about 100 ft. deep at that place. This particular clay layer is apparently the seat of settlement of the monument, which, however, seems to be a perfectly safe structure.

*Example 2.*—The monument shown in Fig. 13:24 is Holsten Gate (Holstentor) at Lübeck, Germany, constructed between 1464 and 1478. The monument represents two towers with a passage between them and is founded on a layer of peat and muck, underlain by good sand and marl. The settlement in the past 550 years has reached 6 ft.; both towers are slightly inclined toward each other. In this connection Fig. 13:9 is to be remembered. The monument is still settling, but at a very slight rate.

This monument affords an excellent opportunity to discuss the value of pile foundations. Suppose that the builder of the monument, who was conscious of the poor properties of the local soil,

had placed the structure on short piles, making them work as friction piles. Such piles would have been *worthless*, because they would have been unable to stop consolidation and would have sunk down with the consolidating peat. Longer piles reaching the compact sand probably would have prevented the settlement.

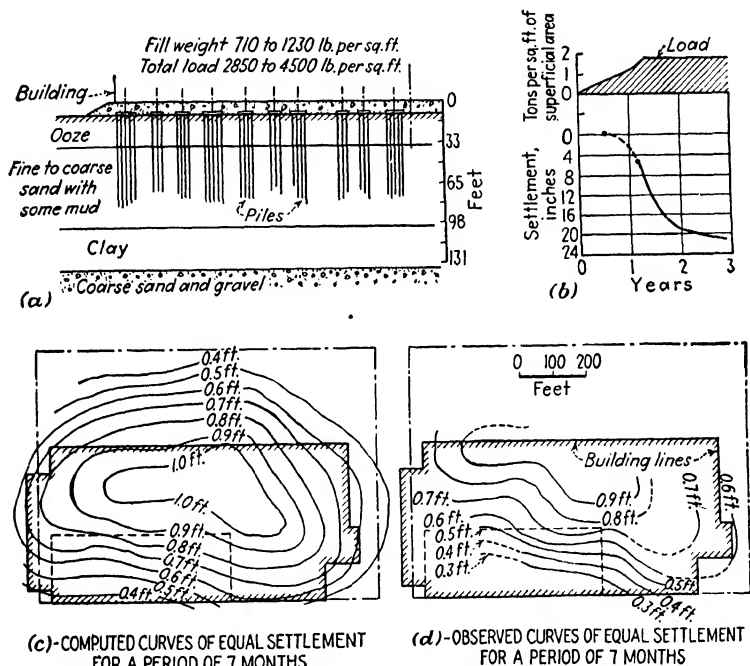


FIG. 13:25.—Settlement of a pile foundation. (From Proc. A.S.C.E., May, 1933.)

It is not exactly known, however, whether or not there are piles under this particular structure. Borings and deep soil investigations generally are *not permitted* in the proximity of ancient valuable structures in a dangerous condition, for fear that their ultimate failure might be caused accidentally. Thus many features can only be guessed at in such cases.

*Example 3.*—The factory building in Fig. 13:25 is another example of the settling of a pile foundation due to consolidation of a deep soft layer below the points of the piles.<sup>4</sup> The dimensions of the building are approximately 500 by 460 ft., the structure being carried on isolated piers with piles varying in length from 65 to

75 ft. The surface unit load was from  $1\frac{1}{2}$  to  $2\frac{1}{4}$  tons per sq. ft. Hard material (course sand and gravel) was present at a depth of about 130 ft., so that the pile tips did not reach it. As usual, the piles were driven to satisfactory penetration, but settlement started at once owing to consolidation of the compressible layer, which included a bed of stiff clay over 30 ft. thick.

*Example 4.*—An analogous case of settlement took place in the 20-story Charity Hospital in New Orleans. The building, constructed in 1937 and 1938, started to settle at once. Investigation made in 1939 showed that, as in the preceding case, the settlement is due to the gradual consolidation of beds of clay located at a considerable depth beneath the points of the piles.

Apparently *scores of buildings in every country* have settled in the same fashion. The designer and the construction engineer must be perfectly acquainted with local geological conditions to avoid surprises of this sort.

**13:13. Settlement of Structures Combined with Horizontal Motion.**—In this section a few cases will be discussed in which the vertical settlement of a structure is complicated by the presence of a considerable horizontal component.

*Example 1.*—The Leaning Tower of Pisa, as shown in Fig. 13:26*a* and *b*, was constructed gradually between 1174 and 1350. Its height is 177 ft., and the full weight about 15,000 tons (about 9 tons per sq. ft. of the base). Tipping was observed when about 35 ft. of masonry was laid, but it apparently stopped in 1186. Vertical settlement proceeded, however, though very slowly. In 1838 it was reported that the tower came to equilibrium. A ditch dug around the tower and lined with masonry contains ground water in motion. There are three hypotheses concerning the instability of the tower: (*a*) the erosion hypothesis; (*b*) the static hypothesis, ascribing the instability to the low bearing power of the sand layer; and (*c*) the consolidation hypothesis, explaining the settlement by the gradual consolidation of deeper clay strata. Apparently the static hypothesis prevails in Italian official circles, because since 1932 more than 1,000 tons of high-strength cement in the form of grout has been injected into the soil through 361 holes, 2 in. in diameter.

More or less trustworthy observations of the settlement have been made in the past 100 years, and it has been thought that the tower is inclining southward. More detailed study with a special

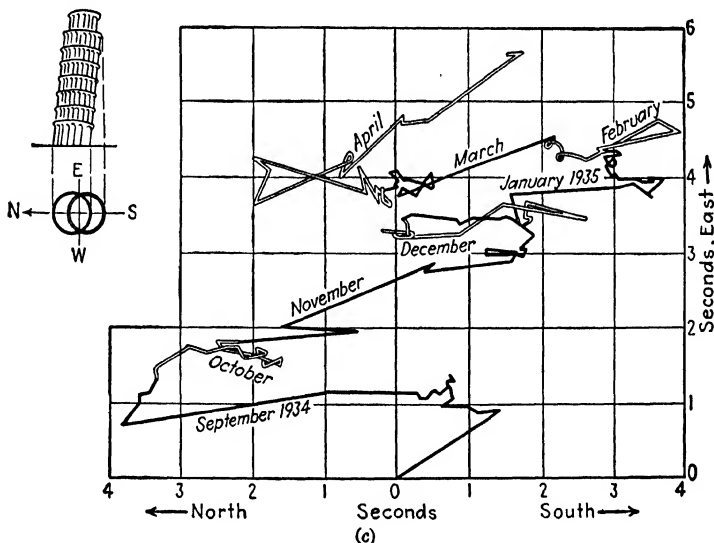
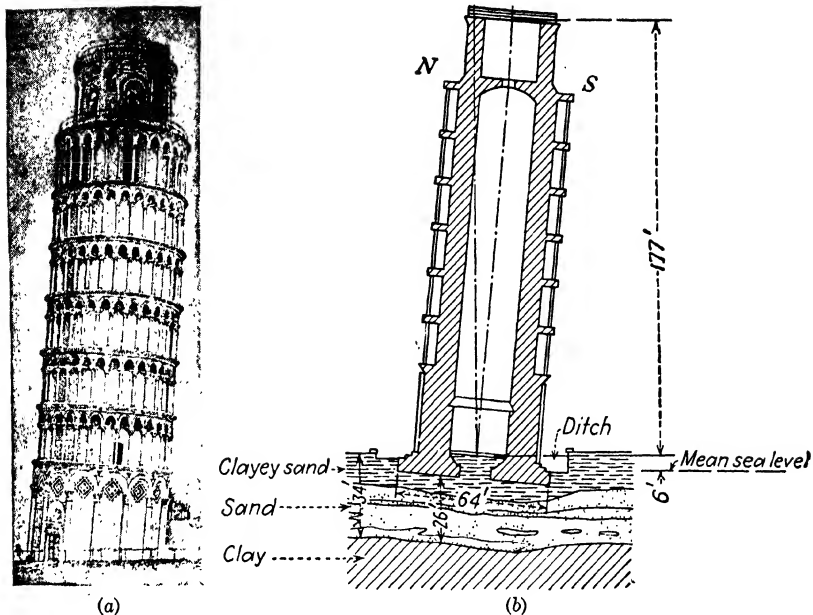


FIG. 13:26.—(a) View of the tower of Pisa; (b) cross section and probable soil conditions; (c) movement observed using precise instrument.

inclinometer has shown that the tower not only has a north-south cyclic and recuperative tendency but also moves persistently eastward. At least, it did so during the period of observations (Fig. 13:26c).

*Example 2.*—The former cathedral of St. Isaac at St. Petersburg, Russia—at present known as Godless Museum, Leningrad, U.S.S.R.—was constructed in the first part of the nineteenth century on very weak swampy ground and is steadily settling. The structure rests on a spread foundation in the form of a masonry mat 22 ft. thick, supported by wooden piles about 19 ft. long. Apparently the earth mass under the cathedral is consolidating, and the short piles referred to are useless in the same way as in the Holsten Gate at Lübeck, Germany (Sec. 13:12). A precise leveling of the floor of the cathedral suggested that the masonry mat had possibly cracked and that there is differential settlement of the cathedral. There are two explanations of this cracking: (a) The cathedral is constructed at the site of an old church, which in turn was supported on piles that never have been extracted; thus at the present time these piles exert a punching effect on the masonry mat in question. (b) The loads are nonuniformly distributed around the mat. Apparently, both causes act together. Information about the total settlement and its rate is very scarce.

A very important conclusion to be drawn from this example is that *the remnants of a smaller old structure should be completely removed* before construction of a larger new one is begun at the same place. This is especially true where weak soils are present.

*Example 3.*—Fine sand masses *if confined* represent a good foundation material, but a saturated fine sand mass if permitted to move laterally may flow along with the structure that it supports. Several cases of bridge-pier failures due to this cause are known. In most of these cases the bridge piers are founded on piles driven into saturated fine sand deposits. The bridge shown in Fig. 13:27 is a double-leaf bascule, with a span 96 ft. center to center of trunnions. Each of the two supports of this span consists of two masonry piers, *N* (north) and *S* (south), connected by a reinforced-concrete tie. Settlement of the western support will be considered (left support in Fig. 13:27a).

The piers are based on piles, 25 ft. long, driven into a fine sand deposit, the load being 27 tons per pile. The bridge was constructed about 1918, and settlement started at once. The piers

tended to tip in opposite directions; hence tension in the tie resulted. Settlement proceeded at a reasonable rate until 1932, when the tie finally broke, causing a spontaneous settlement of the piers (compare Fig. 13:13d). The time-settlement curve in Fig. 13:27c corresponds to pier S. It is to be noted that owing to the tipping there was in this case both upward and downward vertical movement and also considerable horizontal movement toward the sea.

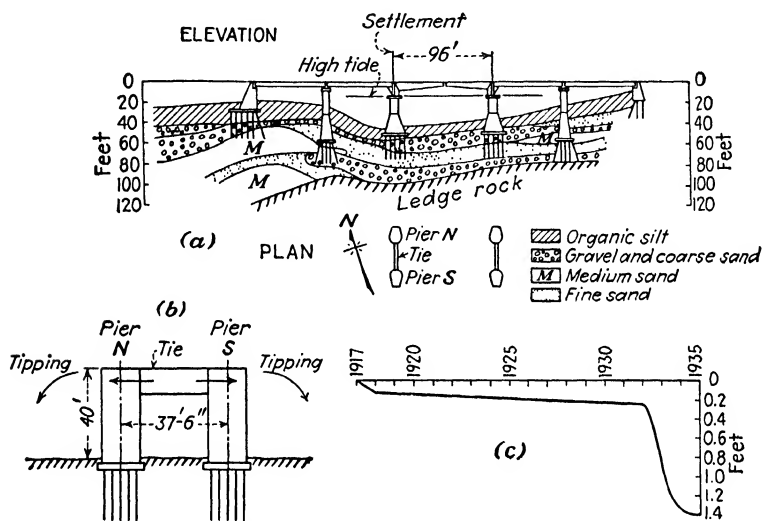


FIG. 13:27.—Settlement of a bridge pier at Bridgeport, Conn.

Soil samples extracted at the site of the bridge after the spontaneous settlement started were obtained by simple wash borings (see Chap. XIV) and did not show any colloids or clay particles in the fine sand. Since in wash borings fine colloidal and clay particles may be washed out from the samples, it was believed that this may have happened and that in reality fine colloidal and clay particles were responsible for the flow. Soon it was learned, however, that a couple of failures of bridge piers on fine sand occurred also in Germany, where settlement was stopped by stabilization of the soil (see also Sec. 13:31e).

Conclusions from this example are that (a) bridge piers on piles to be driven into saturated fine sand deposits merit the special attention of the designer and (b) for extracting soil samples from

a certain depth, improved methods and not wash borings should be employed (Chap. XIV).

*Example 4.*—Settlements combined with horizontal motion may be caused by *landslides*. Specifically, there are examples of such combined settlement in harbors (compare Figs. 9:12 and 10:37). The horizontal motion may be even more considerable than the vertical.

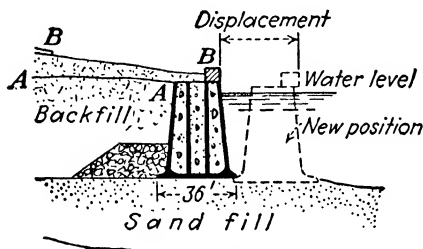


FIG. 13:28.—Unusual movement of a harbor wall. (After Loos.)

The following example is taken from Loos's experience in Java and Celebes.<sup>7</sup> A harbor retaining wall in Sverabaya was begun, and the backfill was made up to line *AA*. The work was interrupted and was resumed several months later. When sand which was being filled in hydraulically reached line *BB*, the wall moved outward considerably and sank down about  $1\frac{1}{2}$  ft. (Fig. 13:28). The factor of safety against sliding assumed by the designers was only 1.2; and subsequent borings revealed the existence of a slippery

clay layer about 3 ft. below the base of the wall (not shown in Fig. 13:28). These two circumstances combined apparently caused the failure.

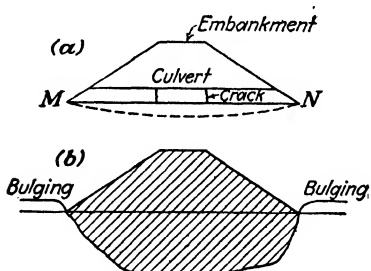


FIG. 13:29.—Settlement of embankments (compare with Figs. 9:27 and 9:28).

### 13:14. Settlement of Embankments and Structures Connected with Them.—*a. Embankments.*

—It should be remembered that an embankment may settle in a twofold manner: (1) as a non-rigid strip load (Fig. 13:29b) or (2) as shown in Figs. 9:27 and 9:28, with two depressions and a relatively high section (dome) in the middle. The first kind of settlement corresponds to the case when the foundation of the

embankment (local earth mass) approaches an elastically isotropic body. This happens in clay, loam, and even silt foundations. It cannot be definitely stated when the second kind of settlement takes place. It occurs often if the base of the embankment is wide and the local soil is saturated fine sand. Under the action of horizontal pressure (minor principal stress  $\sigma_{111}$ ), this sand becomes rather dry and compact and may form a dome. Other developments are also possible.

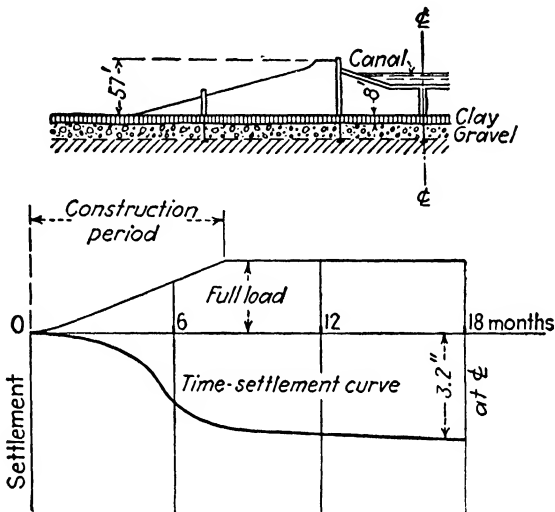


FIG. 13:30.—Settlement of an embankment for a canal at Magdeburg, Germany.

If there is a culvert under the embankment (Fig. 13:29a), it should follow the deflection line of the base of the embankment. To avoid cracks in the central part as shown in the figure, the culvert should be constructed in sections with vertical joints completely separating one section from another. The central part of the culvert is generally cambered to take care of the eventual settlement. Figure 13:29b shows an exaggerated settlement in which the earth material sinks into a swamp and the ground surface bulges.

Load diagrams and time-settlement curves may be traced for embankments in the same way as for buildings. Figure 13:30 shows the time-settlement curve of an embankment for the Mittelland-Kanal in Germany<sup>8</sup> which came to rest soon after its completion (compare curves *a* and *b* in Fig. 13:13).

*b. Influence of the Approaches to a Bridge on the Settlement of the Supports.*—Each of the supports of the bridge in Fig. 13:31 may be considered as a concentrated force transmitted by the piles to the top  $MN$  of a sand layer. At a certain depth  $z$  below the plane  $MN$ , these concentrated forces produce vertical pressures  $\sigma_z$ , represented in the form of curves (plane  $M'N'$ ) which in reality overlap. If the spans are large enough, ordinates of the overlapping sections are very small and can be neglected. In turn, the embankment produces pressures  $\sigma'_z$ , which become smaller and smaller

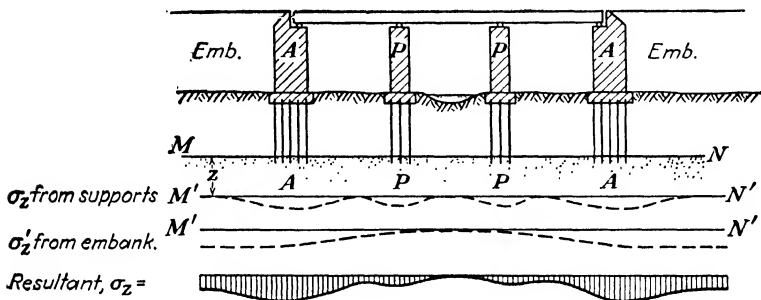


FIG. 13:31.—Influence of the approach embankment on the settlement of a bridge.

toward the center of the bridge. If both kinds of vertical pressure are superimposed, the final diagram (dashed, at the bottom of Fig. 13:31) is obtained. Specifically, abutments are affected by the weight of the embankment much more than the piers. In any event, pressure distribution caused by a bridge is *nonuniform*.

Geological conditions shown in Fig. 13:32a are somewhat different. Consider the settlement of both the left abutment and the left pier. These supports are founded on short piles that in the case of the abutment, are useless, since they are driven into a compressible layer of plastic clay. (Compare settlement of both the Holsten Gate and the Cathedral of St. Isaac.) The points of the pier piles stand on gravel; hence the settlement of the pier should be smaller than that of the abutment. Besides, the pier is but very little influenced by the approach embankment, which adds considerably to the vertical pressure under the abutment.

Time-settlement curves shown in Fig. 13:32b justify these statements. The abutment sank much more than the pier. Moreover, the embankment side of the abutment sank 16 in. as an average, while a part of the span side sank a few inches and a part rose

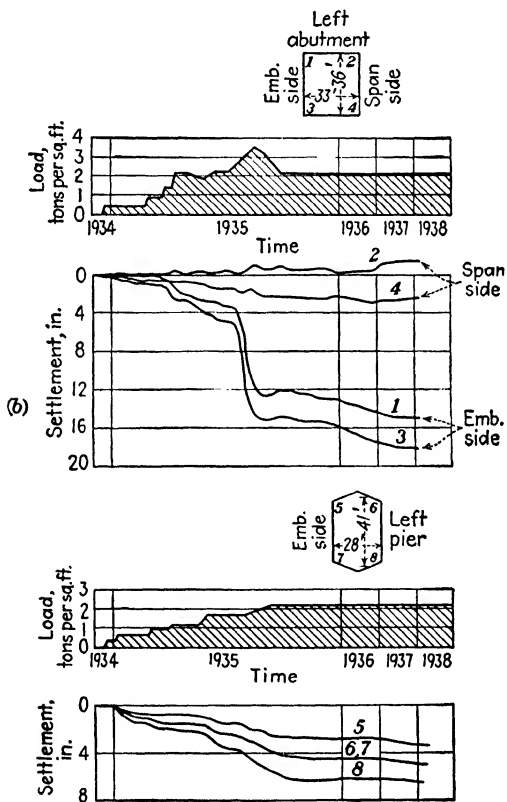
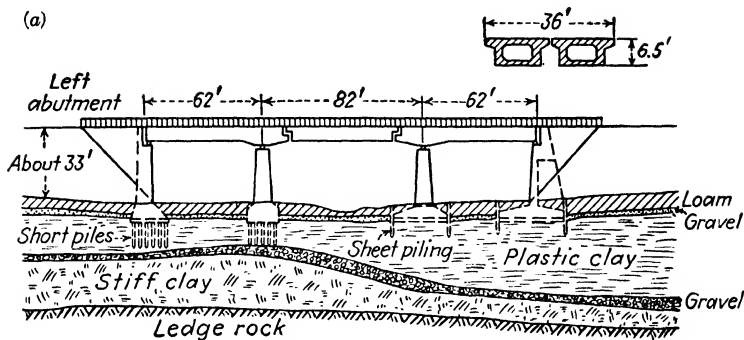


FIG. 13:32.—Settlement of a bridge at Niederoderwitz, Germany. (After Kögler and Scheidig.)

above the original horizontal plane. Such a phenomenon of upward movement of a bridge support has already been discussed (settlement of a pier in Bridgeport, Conn., Fig. 13:27). Spontaneous increase in settlement of the abutment (Fig. 13:32*b*) took place about the middle of 1935 because of a temporary increase in unit load. It is to be noticed that the settlement of the pier was also

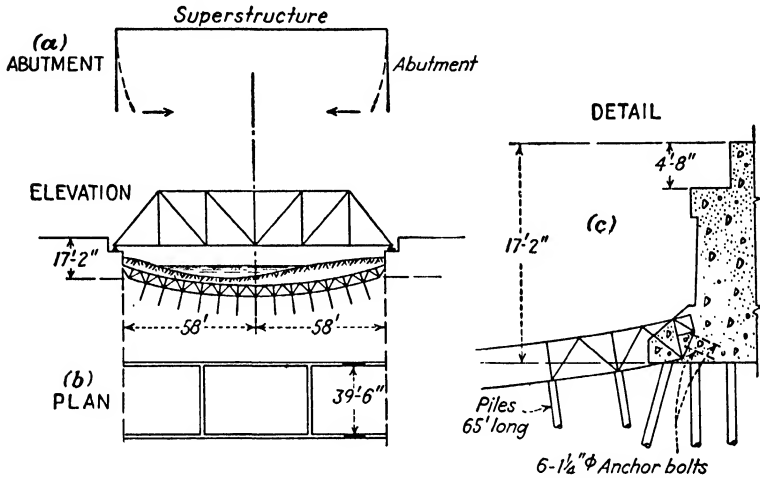


FIG. 13:33.—Arch truss to stop movement of bridge abutments at Westbrook, Conn. (After Nord.)

differential (curves 6 and 8 on the span side are lower than curves 5 and 7 on the embankment side). This fact may be explained by the increasing thickness of the plastic layer from left to right in Fig. 13:32*a* and possible flow of plastic matter in that direction.

It may be concluded from Figs. 13:31 and 13:32 that *construction of the embankment should precede that of the bridge* if considerable settlement is expected. In practice, just the opposite is generally done. However, if the embankment is constructed first and the earth mass is given time to consolidate, the masonry will settle only under the weight of the bridge. Thus its downward movement will be decreased, and hence the danger of cracking or uneven settlement reduced.

*c. Horizontal Motion of Bridge Supports.*—A pier is prevented from longitudinal motion along the axis of the bridge by the superstructure, but it is relatively free to move transversely. Actually,

it may do so if there is lateral motion of the local earth mass (compare the settlement in Bridgeport, Conn., Fig. 13:27).

So far as one-span bridges are concerned, the superstructure may be visualized as a strut between the abutments. The latter (Fig. 13:33a) are capable, however, of an inside horizontal motion due to earth pressure even if founded on piles. An extraordinary case of abutment motion has been described by Nord.<sup>9</sup> The abutments of a bridge in Westbrook, Conn., moved back and forth according to whether the fill behind the abutments was in place or removed. This movement was stopped by installing a metallic arch to keep the abutments in place (Fig. 13:33b and c).

**13:15. Settlement Due to Fluctuations of the Water Level.—**

*a. Fluctuations of the Ground-water Table.*—The weight of both the overburden and the structure is decreased by the uplift caused by the ground water, if any. In terms of the sketch, (Fig. 7:2) ground water furnishes a part of the upward reaction  $R$ . If ground water is being heavily and steadily pumped, this part vanishes fully or partly, and settlement of an otherwise stable structure may start. Should ground water be removed from underneath a structure that is still settling, this fact may cause its spontaneous settlement (Fig. 13:13*l*) or, at any rate, modify its rate of settlement. Admittedly, such a modification may be not a sudden but a gradual process.

It is obvious that the rise of the ground-water table decreases the acting weight of the structure and retards its settlement, if any.

*b. Fluctuations of Water Level in Rivers; Influence of Tides.*—Suppose that at a point of the mass the vertical pressure due to the weight of a bridge is  $\sigma_z$ . Owing to uplift during the fresh-water period, there is some loss in this pressure (designation  $\Delta\sigma_z$ ). At the same time the whole bottom of the river is additionally loaded with the weight of fresh water  $\sigma'_z$ , which creates an additional vertical pressure  $\sigma'_z$  at the given point of the earth mass. If  $\Delta\sigma_z > \sigma'_z$ , the given point of the mass will move up, and it will settle in the opposite case. In particular cases this simple pattern of acting stresses may be more complicated.

It is obvious that a tide at the delta of a river would produce an analogous effect. When the water retires, the value of the stress returns to  $\sigma_z$ . In terms of strains this is an elastic rebound. In the case of an old pier, this action is generally purely elastic; because of a great number of subsequent loadings and unloadings

of the mass, there are no irreversible deformations at all (Sec. 6:2). To avoid change in level of the bench marks, the latter must be placed far enough from the zone under observation.

*Example 1.*—Figure 13:34 represents a part of the soil profile of the Huey P. Long Bridge over the Mississippi River.<sup>5a</sup> Piers 1 to 5 are located within the permanent river bed, and pier A is beyond

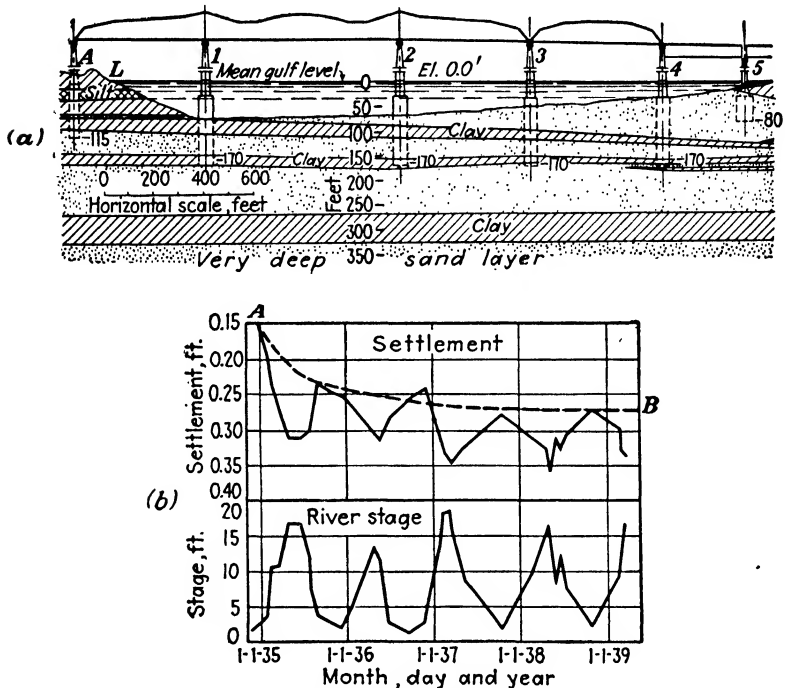


FIG. 13:34.—Huey P. Long Bridge over the Mississippi River. (a) Part of the longitudinal section; (b) settlement of pier 1. (After Kimball; from *Civil Eng.*, March, 1940.)

the water level  $L$ . All these piers are of reinforced concrete, the caissons of four of them being put down through sand islands. These piers are underlain by strata of sand and strata of clay. It may be approximately assumed that sand under the lower clay level extends perhaps to a depth of about 2,000 ft. below the datum (mean gulf level).

Time-settlement curves of pier 1 are shown in Fig. 13:34b. The simplest explanation of the movement of pier 1 may be obtained by joining the highest points of the time-settlement line (curve

*AB*). Thus the settlement would be broken into two parts: that depending on the consolidation of the deep clay layers (typical time-settlement curve *AB*) and that depending on the surcharge.\*

*Example 2.*—The Pennsylvania Railroad tunnel under the Hudson River at New York City undergoes an average settlement of 0.008 ft., coinciding with an average rise of the tide of 4.38 ft. with an equal rise of the tunnel as the tide falls.<sup>b</sup> This phenomenon probably also takes place in other tunnels under the Hudson River.

*Example 3.*—The Transatlantic Terminal, Le Havre, France, settled owing to consolidation in deeper strata, and in this connection it was observed that there is an additional daily up-and-down movement of about  $\frac{1}{4}$  in., corresponding to the fall and the rise of the tide.<sup>c</sup> Figure 13:35 shows fluctuations in level of this structure during 14 hr. of observation.

Impervious soil in this example is exposed during the fall of the tide. Hence the increase in settlement during the falling tide, whereas in Examples 1 and 2 the contrary takes place.

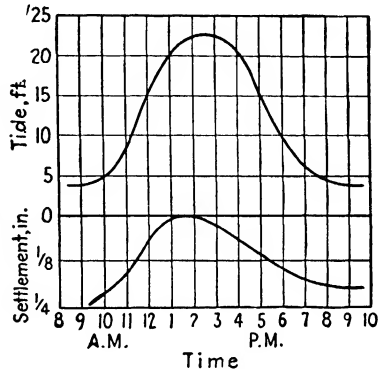


FIG. 13:35.—Movement of a structure due to tide action at Le Havre, France.

### C. SUBSIDENCES DUE TO EXCAVATIONS AND TUNNELS

**13:16. Causes of Settlement Close to Openings within an Earth Mass.**—An earth mass in equilibrium is under the action of a certain system of stresses which cause corresponding strains. The strains in such a mass are completed, and assuming that pore moisture is also in equilibrium, there is no movement at all in that mass. As soon as an opening is made, be it an open excavation or a tunnel, the earth mass becomes unsupported, laterally or vertically or both. This fact causes additional strains, which must take place in order to bring the mass into a new state of equilibrium. As a rule, these strains correspond to downward displacements or settlements of the ground surface, but in particular instances there

\* For other explanations of this settlement, see ref. 5a.

may be upward displacements (compare Fig. 11:7*b* and the explanatory text).

An opening may not produce any settlement whatsoever at the earth surface. This case is that of a deep tunnel when there may be local displacements around the tunnel, which do not exert any influence on the shape of the ground surface above the tunnel.

**13:17. Openings in Soils Approaching an Elastic Continuum.**—  
*a. Open Excavation in an Elastic Continuum.*—Consider Fig. 13:36*a* in which an open excavation dug close to a building is represented.

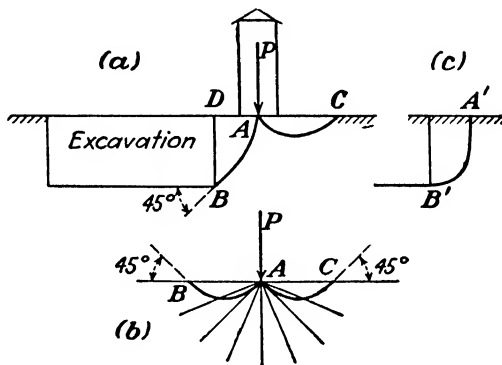


FIG. 13:36.—Effect on a near-by excavation on the settlement.

The fact that the slopes of the excavation are vertical suggests that the soil is cohesive, for instance, stiff clay. It will be considered as an elastic continuum. The weight of the building will be replaced by a concentrated force  $P$ . If there were no excavation at the site under consideration, eventual failure lines under the building would be logarithmic spirals intersecting the lines of principal stresses at a  $45^\circ$  angle. This may be obtained from Fig. 5:7 by making the value of the angle of friction  $\phi$  equal to zero. It is to be remembered that the lines of major principal stress,  $\sigma_1$  in the case of Fig. 13:36*b*, are straight lines radiating from the point  $A$ , that of application of force  $P$ . Assuming approximately that the major principal stress at point  $B$  in Fig. 13:36*a* is vertical, the failure line  $AB$  must make a  $45^\circ$  angle with it. In reality, the failure line probably has a shape between  $AB$  in Fig. 13:36*a* and  $A'B'$  in Fig. 13:36*c*. Of the two failure lines  $AB$  and  $AC$ , as shown in Fig. 13:36*a*, the former is that of least resistance; and if failure happens, this will be approximately along the

curve  $AB$ . Rendulic<sup>13</sup> suggested that this curve is a logarithmic spiral but gave no mathematical proof.

It is known that the actual shear failure is preceded by a rather large strain. Hence, before actual failure occurs, the building under consideration would settle, and it may tilt in this case. Furthermore, should the clay mass be saturated, there would be a great number of menisci formed along the slope  $DB$ . This circumstance would cause the flow of moisture toward that slope, as explained in Sec. 2:11. Consequently, because of the removal of some moisture from the pores of the earth mass under the building, the latter may settle additionally.

*b. Shallow Tunnel in an Elastic Continuum.*—If a shallow tunnel is constructed in rock, there are elastic deformations around it. Deformations of the ground surface in this case are very small and may be disregarded. The same is true of nonsaturated stiff clay.

If a shallow tunnel is built in saturated stiff clay, there are menisci formed along its perimeter, and hence flow of moisture occurs in the same way as described in Secs. 2:11 and 11:11a. Because of worse ventilation and less favorable evaporation conditions, this flow apparently should be less intensive in a tunnel than in an open excavation. No observations or other field data along these lines are available.

**13:18. Pumping from a Clay Excavation.**—It has been shown in Sec. 13:15 that pumping of the ground water may increase the weight of a structure and thus contribute to its settlement. Pumping from a clay excavation may also contribute to the settlement of the ground surface around that excavation. Actually, if water is at the level  $AB$  in the excavation shown in Fig. 13:37, the slope  $BC$  is in

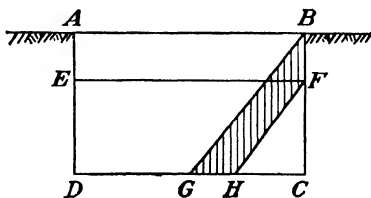


FIG. 13:37.—Effect of pumping from an excavation on the settlement of near-by structures.

equilibrium, the force acting on it from the left being the water pressure as expressed by the triangle  $BCG$ . As soon as water is pumped out from the excavation down to the level  $EF$ , the total water pressure becomes equal to triangle  $FCH$ . The decrease in pressure is expressed by the dashed area  $BFHG$ . This means that plane  $BC$  is not in the state of equilibrium any longer. Water flows from the upper part  $BF$  into the excavation, and addi-

tional stresses are being created in the mass. Thus clay may creep into the excavation and may later cause settlement. This phenomenon is quite analogous to the case of sudden drawdown as discussed in Chap. IX.

Terzaghi\* first called attention to the danger of unreasonable pumping from wells under construction. As soon as the exposed part of the well exceeds a certain limit, clay starts to creep into the well, and the surrounding locality settles.

**13:19. Open Excavation in a Fragmental Mass.**—As known from Chap. X, lateral earth pressure in this case is not triangular (hydrostatic) but follows a curvilinear distribution. If bracing yields too much, a crack may be formed within the mass. This

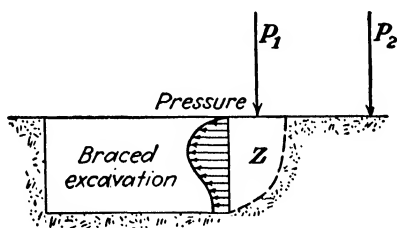


FIG. 13:38.—Effect of braced excavation on the settlement of near-by structures.

crack separates a wedge or a “zone of discontinuity,” located close to the bracing, from the rest of the mass. Now it is to be remembered that this “zone of discontinuity” corresponds to an earth mass under the action of its weight only. If there is a concentrated load  $P_1$  acting at the ground surface, the shape of the crack may be different. Practice shows, however, that loads applied at the ground surface outside the “zone of discontinuity,” corresponding to the weight of the mass only, have practically no influence on the pressure against the bracing. Thus if  $Z$  in Fig. 13:38 is the zone of discontinuity, load  $P_2$  does not affect the value of the pressure on the bracing, which is controlled by the weight of zone  $Z$  and the value of load  $P_1$ .

**13:20. Plastic Flow toward an Opening.**—In the example (Fig. 13:36), clay was assumed to be stiff. Such a clay possesses a rather rigid skeleton acting as a frame for the mass. If clay particles were more movable with respect to each other, clay would be soft and subject to flow plastically under the action of a relatively weak shearing stress. Plastic flow (creep) may cause settlement of a

\* Communication in a public lecture.

remote structure *A* as shown in Fig. 13:39*a*, whereas the neighboring structures *B*, *C* may remain safe. A simple explanation of this fact is shown in Fig. 13:39*b*. As may be concluded from the discussion of different cases of settlement (settlement of bridge piers in Connecticut and at Berlin, Germany), phenomena as shown in Fig. 13:39*a* may occur in both soft plastic clay and saturated fine sand.

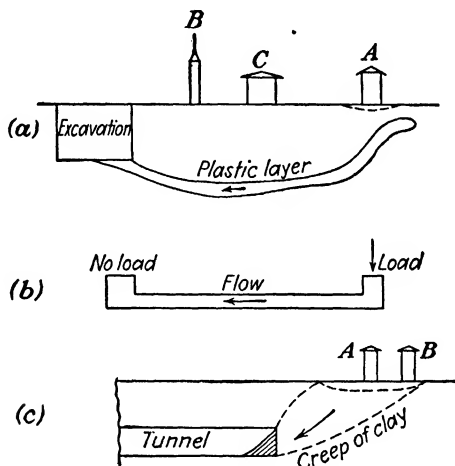


FIG. 13:39.—Plastic flow toward openings (compare with Fig. 13:14).

Creep of clay into a tunnel that is being constructed with an open front (Fig. 13:39*c*) has two unfavorable consequences: (1) The volume of clay actually removed from the tunnel is greater than the geometric volume of the tube, owing to the creep from outside: (2) there is settlement of structures before the tunnel (*A*, *B* in Fig. 13:39*c*). In the case of a subway tunnel, such a settlement may be very harmful to entire blocks of buildings. The situation may be helped by abandoning the method of tunneling mentioned above and passing to the more expensive shield method (Sec. 11:10).

**13:21. Settlements Due to Mining Operations.**—There is a vast literature on settlements in mining districts both in Europe and in the United States (for instance, refs. 13, 14, 15, 16, 17 and 18). Many mining engineers visualize the situation caused by a shaft as shown in Fig. 13:40, the sinking mass being subdivided into “main break” and “afterbreak.” Notice analogy with the trap-door experiment (Sec. 11:7).

Consider Fig. 13:41, which shows a wide strip of coal that has been mined out. If the earth mass above that strip is able to resist tensile stresses, it acts as an elastic slab. Tension and compression in this slab are shown with signs "minus" and "plus," respectively. Thus in the central part of the subsidence (marked I) there is, close to the earth's surface, a compression that may

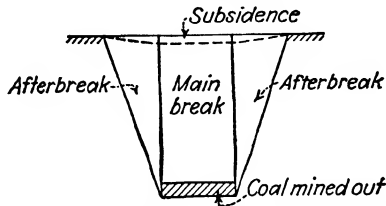


FIG. 13:40.—Wedgelike subsidence due to mining.

break pipes and culverts or warp roads and sidewalks. Buildings in this zone simply settle down. In the outside zone (III) there are tensile stresses at the top of the mass. These may cause cracks in the earth mass and also vertical cracks in the buildings. These cracks obviously appear first at the weakest parts of the building; namely, close to doors and windows. The case of the intermediate

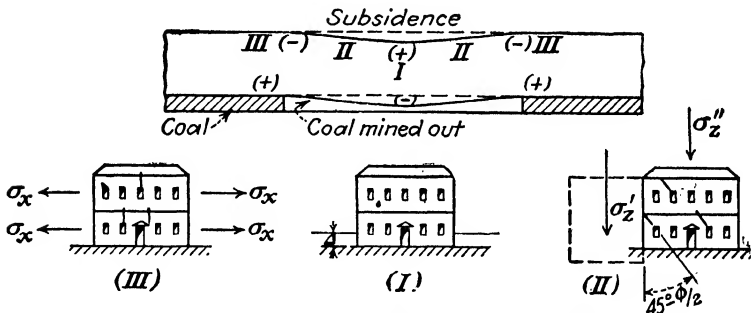


FIG. 13:41.—Slablike subsidence due to mining.

zone II is very similar to that of the differential settlement (compare Sec. 13:28).

Subsidences due to mining operations caused many troubles in coal districts of the State of Illinois.<sup>14, 15, 16</sup>

**13:22. Settlements Due to Vibrations and Earthquakes.**—Behavior of soil masses subject to vibrations has been studied on the laboratory scale on several occasions (Sec. 14:21); field data, however, especially quantitative, are exceedingly scarce. It may

be stated that sands are more responsive to settlement due to vibrations than clays. For instance, the best way to compact a sand in the laboratory is not to compress the material but to shake the container. It has been reported on many occasions that vibration is most easily transmitted through sand saturated with ground water.<sup>24</sup> In the case of adjacent buildings resting on wet sand, vibration in one building is readily transmitted to the other. It has been observed in railroad work that vibration through wet soil may be damped by dry cinder embankment. The 20-story Pennsylvania Railroad building in Philadelphia is directly over the subway, and as a precaution against vibration the ground-water level was lowered to a point below the footings.<sup>24</sup>

From observations<sup>25</sup> in the St. Louis, Mo., area on engine vibrations in a gas compressor plant, it may be concluded that pressure grouting of the sand foundation of the engine reduces the vibration effect.

Many cases of earthquake damage, particularly in California, are discussed in ref. 26. In the Santa Barbara earthquake of 1929, buildings on swampy ground or sand, regardless of type, suffered more than those on a hard, firm clay bed or other solid ground. Besides, buildings with deep foundations suffered less than those with shallow foundations. It should be noticed also, as a general remark, that tunnels practically do not suffer at all from earthquakes.

Observations on settlement of highway embankments and other structures were made during the New Zealand earthquakes of 1929 and 1931. Among other things, the case was reported of the settlement of a 22-ft.-high, six-year-old embankment which sank as much as 3 ft. It is interesting to notice that in this particular instance the vegetation covering the slopes of the embankment was not visibly disrupted.<sup>27</sup>

#### D. OBSERVATIONS; MEASURES; DAMAGE

**13:23. Settlement Observations.**—Settlement observations may be made in the following three cases: (a) when the structure is damaged by settlement in such a way that it becomes a threat to life and property, (b) when the structure is steadily settling without giving signs of immediate danger, (c) when it is decided to study the relative behavior of one or more safe structures which apparently are not in a dangerous condition at all. If analogies from

medicine are considered, case (a) corresponds to a gravely sick patient who seeks the help of a specialist, case (b) is that of a patient with a chronic ailment treated by a family doctor, and, finally, case (c) corresponds to study and observations of both healthy and sick persons carried on by research workers. Under the present conditions of foundation engineering case (a) is the most characteristic and will be discussed in some detail.

**13:24. Emergency Procedure.**—The procedure followed by a consulting engineer retained to study a serious case of settlement strongly suggests the procedure of a physician summoned to the bed of a dangerously ill patient with whom the physician is unfamiliar. He first makes general inquiries concerning the age, family conditions, and previous life of the patient. In an analogous way the consulting engineer examines the plans and the specifications and inquires when the structure was built, who built it, and of what materials it was constructed. If borings were made, their results are examined; otherwise new borings are ordered, and samples are tested.

The next step of the physician is to determine the history of the illness. In the same way the consulting engineer wants to know when symptoms of failure appeared, what they were, and how the damage to the structure developed. If there are previous settlement observations and other measurements, he examines them.

Then comes the next and the most important step—diagnosis. In obvious cases the cause of the sickness may be established immediately; otherwise the patient must be put under observation. In the case of a structure, this procedure corresponds to more or less prolonged observations of settlement, after which the final decision is made. The consulting engineer generally prepares a preliminary report on the situation. After a period of study and observation a final report is submitted. The object of the diagnosis is to determine whether or not foundations are to be blamed for the failure. In many cases the failure is caused by defects in the design of the superstructure or poor quality of the materials used. If the cause of settlement is traced to a poor foundation, the seat of settlement should be definitely established.

The final step in the procedure of the consulting engineer, as in that of an examining physician, is prescription. The consulting engineer may recommend underpinning, removal or redistribution of unit load, or additional pile driving to solid strata to support

the settling structure, under the condition, however, that vibrations do not harm the rest of the structure. For instance, if a narrow pile foundation settles owing to consolidation of a rather shallow layer under the points of the piles, additional piles to rock may be driven around the structure, and the latter may be anchored to them. If there is bulging around a structure, additional load around the structure would balance the acting shearing stress wholly or partly. In some cases, the consulting engineer sees that the cause of the settlement is reaching its natural end. This may happen, for instance, when progressing consolidation has reached a high percentage, say  $U = 80$  per cent. Nothing should be advised in this case except a general repair of the structure, taking into account the eventual small settlement.

**13:25. Continuous Observations.**—As soon as a resident engineer notices that a structure is settling, even without presenting signs of danger, he must organize observations of the settlement. All the observations should be plotted on the plan and the longitudinal and transverse profiles. Two intersecting base lines should be traced in the proximity of the structure, and these lines should be oriented on remote objects so that they can be retraced at any time. Horizontal motion, if any, is to be tied to these axes. Good bench marks should be established at a distance such that the settlement of the structure will not disturb them (in most cases 200 ft. is enough). The bench marks themselves must be very substantial, since cases of their settlement also have been observed. Borings should be organized, samples tested, and the corresponding results plotted on the profiles. Efforts should be made to understand the cause of the settlement; and if local authorities are not sufficiently trained, help of a specialist must be asked for.

When continuous observations are made, it should be realized that they may last 15 or 20 years or more and that it is very possible that the work will be finished by another person. Hence all the documentation should be in exceedingly good order.

**13:26. Research Settlement Observations.**—Settlement of all new structures of a certain size should be recorded and compared with theoretical computations made by designers. In turn, the design of any foundation should be accompanied by an estimate of its probable settlement. In addition to settlement observations, pressure-measuring cells (such as Goldbeck cells) should be embedded under new structures in all cases where interesting

results concerning the interaction between the structure and the earth mass may be expected. In this way, the stress-strain relationship under actual structures may be studied.

**13:27. Technique of Settlement Observations.**—The simplest type of reference point within a building is a bolt embedded in

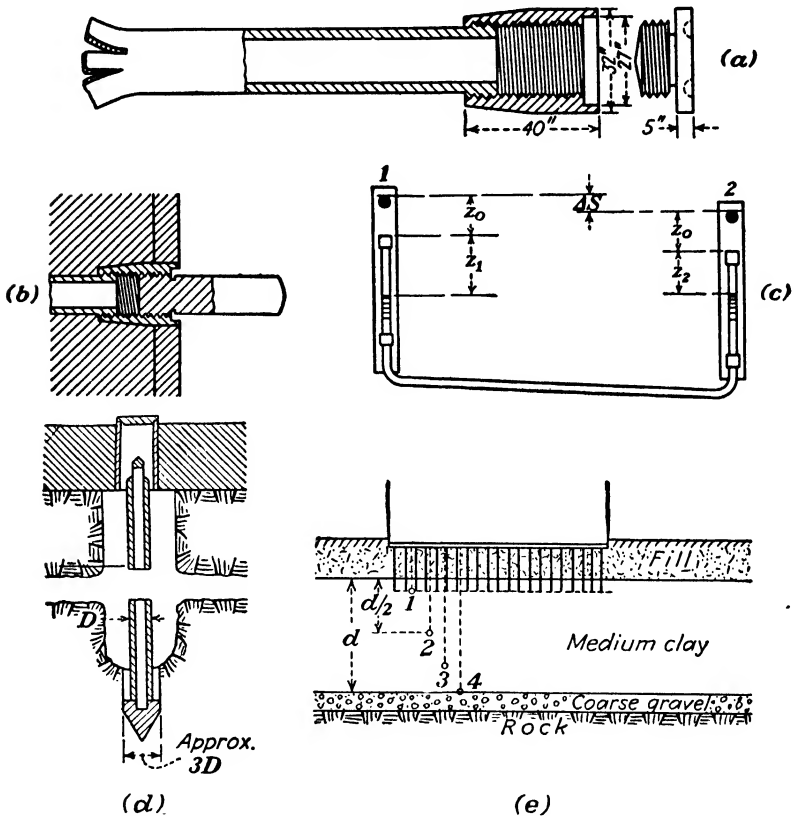


FIG. 13:42.—Accurate measurement of settlement. (After Terzaghi, *Trans. A.S.C.E.*, vol. 103.)

masonry. Such reference points readily disappear during or after construction. An improved type (suggested by Terzaghi<sup>10</sup>) consists of a short pipe embedded in the masonry. Its opening is closed by a brass plug which can be unscrewed and replaced by a horizontal metallic cylinder (Fig. 13:42a and b; also black circles 1 and 2 in Fig. 13:42c). Instead of a level, the device shown in Fig. 13:42c may be used for determining elevations. To find the

difference between the levels  $\Delta S$  of the reference points 1 and 2, the device is hung on the corresponding cylinders and the two glass tubes, which are connected with a rubber hose, are filled with water. Distances  $z_0$  from the top of the glass tube to the top of the metallic cylinder 1 or 2 are constant, and the distances  $z_1$  and  $z_2$  from the top of the tube to the level of water in each tube are measured with a micrometer. The results of such a measurement are supposed to be very accurate (within the range of 0.002 in.).

A simple underground bench mark is shown in Fig. 13:42*d*. It consists of a metallic rod with asphalt coating wrapped in oil-soaked waste. The base of the rod rests in the layer under study, and the elevation of the top can easily be measured from the surface

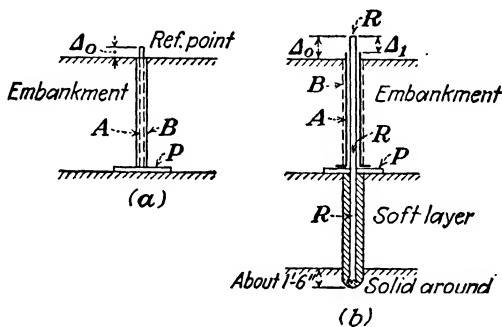


FIG. 13:43.—Measuring settlement of an embankment.

of the floor. Several bench marks placed at different levels may be seen in Fig. 13:42*e*.

A reference point to measure settlements of embankments and their foundations is shown in Fig. 13:43*a*. A metallic plate  $P$  is simply placed on the surface of the natural ground. A pipe  $A$  connected with that plate protrudes over the surface of the embankment and serves as a reference point for taking levels. Pipe  $A$  is protected against friction and corrosion by an outside pipe  $B$ . Symbol  $\Delta_0$  in Fig. 13:43*a* and *b* shows the difference between the levels of the reference point and the top of the embankment.

The device in Fig. 13:43*b* precludes the use of the level in the measurement of the settlement of an embankment. If at a certain depth under the proposed embankment there is a solid soil layer, a boring is made, and a standing rod  $R$  is fixed in that boring. The latter is backfilled, and a plate  $P$  with a hole for the rod  $R$  is placed on the surface of the natural ground. A pipe  $A$  is connected with

the plate and inserted in a protection pipe *B*, in the same way as in Fig. 13:43*a*. Differences of levels are measured:  $\Delta_1$  before the construction starts and  $\Delta_0$  when the construction of the fill is just finished. Subsequent periodical measurements of the values of both  $\Delta_1$  and  $\Delta_0$  furnish data for tracing time-settlement curves for the embankment and for its foundation separately, the same as in the case of Fig. 13:43*a*.

**13:28. Damage Caused by Settlement.**—Damage caused to a structure by settlement ranges in masonry from thin fissures to

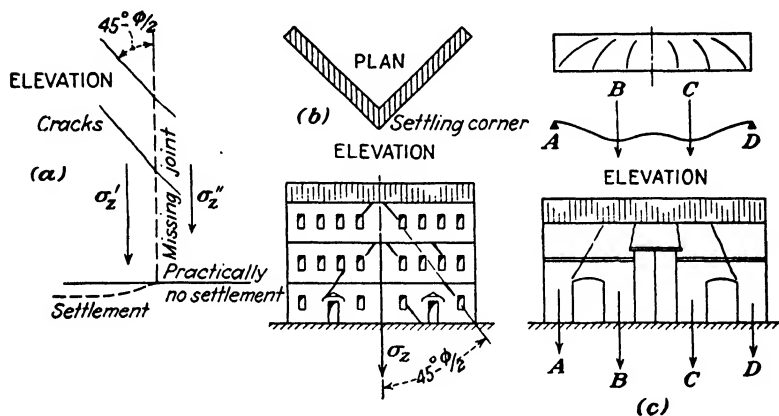


FIG. 13:44.—Cracks in buildings due to settlement.

open cracks. If reinforced concrete disintegrates, reinforcement rods may be broken by tension. The metallic superstructure of a bridge may be so bent and twisted as to prevent passage of traffic. An earth structure may decrease in height, crack, and disintegrate.

If there is differential settlement at a point of a nonuniformly loaded foundation (Fig. 13:44*a*), cracks making angles somewhat less than  $45^\circ$  with the vertical appear in the settling part. Apparently the major principal stress in this case is vertical, and cracks make an angle of about  $45^\circ - (\phi/2)$  with the direction of this stress. In Fig. 13:44*b* a corner is overloaded. The earth mass fails and sinks, and the nonrigid masonry follows it.

Cracks in zone II (Fig. 13:41) are analogous to those shown in Fig. 13:44*a*, the latter cracks being due to differential settlement.

A somewhat different situation is represented in Fig. 13:44*c*, where settlement is due to overloading of the piers *B* and *C* in

comparison with piers *A* and *D*. The whole building acts as a beam on two supports located at *A* and *D*. The beam is loaded with two loads applied at *B* and *C*. Cracks in this case follow approximately the trajectories of maximum shearing stress, as may be seen at the top of Fig. 13:44c.

Angle  $\phi$  as used in this section is some average of the angles of friction of the earth material and of the masonry. By no means should the expression  $45^\circ - (\phi/2)$  as used here be interpreted as a value that can be accurately computed.

Obviously, cracks may serve only for the approximate establishment of the seat of settlement. As soon as a crack appears in the wall, the latter represents two or more bodies to be considered instead of one. If a crack forms approximately an angle of  $45^\circ - (\phi/2)$  with the vertical, a subsequent crack may deviate from this direction because of the change in direction of the principal stresses due to cracking. Furthermore, appearance, direction, and width of the cracks depend very much on the temperature. The nonuniformity of the foundation soil is tantamount to non-uniform loading and may be the cause of cracks.

Sometimes cracks appear in transverse walls close to the perimeter of a uniformly loaded large building on fairly uniform soil. In this connection, Fig. 4:22 and Scheidig's experience in Moscow (Sec. 13:11) should be remembered.

**13:29. Measures against Settlements.**—There will be practically no settlement if the base of the structure reaches rock. In all other cases settlement is unavoidable; but it may be partly prevented (*a*) by proper design of a structure, (*b*) by proper construction, and finally (*c*) by improving soil properties, which is done by soil stabilization. In this section both design and construction measures will be discussed.

*Decrease in Stress.*—It is very difficult to decrease the value of the acting stress if the seat of settlement is somewhere in a deeper stratum. As is well known, the stress controlling the situation in such a case is the vertical pressure  $\sigma_z$ , and it acts practically as if it were produced by a concentrated force *P*. The only way to decrease the stress is to decrease the load *P*. This can be done by designing a deep basement under a building. The weight of the excavated earth would then somewhat relieve the load *P*. An example of such a procedure is the Telephone Building in Albany,

N. Y. Another example of similar design is the new office building of the New England Mutual Life Insurance Company, Boston, Mass. (compare Sec. 8:14). When the former building was under construction, settlement started when the weight of the structure was approximately equal to the weight of the excavation. Such phenomena may happen, however, if the excavation is rather sandy or consists of a clay that for some reason does not expand or swell if unloaded. Otherwise, the slightest load on the bottom of the excavation should produce a settlement.

If the layer under consolidation is not very deep, increase of the area of the structure's base may be of assistance. In such a case the structure no longer acts as a concentrated load, and the value of the vertical pressure  $\sigma_z$  decreases along with the decrease of the unit load on the base of the structure.

The same is true if the seat of settlement is quite close to the earth surface, and shear is likely to produce a failure.

*Use of Statically Determinate Structures.*—If heavy differential settlement is expected, the support reactions of a structure should be statically determinate. Uneven settlement of bridge piers may cause heavy secondary stresses in the superstructure.

*Use of Separation Joints.*—Parts of a structure loaded with different unit loads or resting on different soils must be separated from each other by vertical joints from top to bottom of the structure.

*Construction Measures.*—A few construction measures having for their object the decrease in settlement have been discussed already in different sections of this book and should be remembered. For instance, it is advisable to construct the approach embankments to the bridge first and afterward the bridge itself (Sec. 13:14). The principle of pretesting a structure, used for the pile foundations, may be generalized. According to Cuevas,<sup>11</sup> the bottom of the excavation for the National Lottery Building in Mexico City, Mexico, was loaded with gravel, which afterward was removed. Thus a part of the irreversible deformations took place prior to construction, and not after it.

As a rule, uniform distribution of loads around the base of a structure under construction is recommended.

To accelerate the settlement of an embankment due to consolidation, borings on both sides of the embankment and under it may

be made and filled with pervious material. Admittedly, these borings should reach somewhat into the consolidating soft layer. This idea originated by California highway engineers (hence the term "California wells") has been applied to embankments of various types. Sometimes wells form in plan a pattern of equilateral triangles, for instance 20 ft. in side, the diameter of the wells being from 6 to 18 in. Very like this kind of wells are relief wells in dams and levees that are sometimes used to relieve harmful uplift caused by a foundation more pervious than the earth dam itself.<sup>29</sup>

It was stated in Chap. IX, in reference to dam construction, that dams should be constructed slowly so that the shearing resistance of the foundation, if the latter consolidates, will increase. In this way, the eventual settlement of the dam may be decreased.

**13:30. Importance of Soil Stabilization for the Structural Engineer.**—Since there is a seat of each settlement, this seat should be *stabilized* or deprived of its capacity to produce harmful motion of the structure. The changing of properties of an earth mass in order to increase its resistance is a practice worth attention. Good progress in this field may modify the use of soil-mechanics theories in some cases. This is the reason why a foundation engineer must follow with great care new developments in the province of soil stabilization, both deep and shallow.

Particularly, both existing methods of deep soil stabilization (Sec. 12:7) tend to *petrify* the earth mass. Solutions have been reached in special cases, but the most important cause of settlement—consolidation in deeper strata—practically has not yet been attacked, and this is the most important problem of deep soil stabilization.

In this respect foundation engineering is in the same position as medicine with respect to cancer. Cancer has been very widely studied, but there is no certain remedy for it. Likewise there is an excellent theory of consolidation; but if a consolidation process at deeper strata starts, there is no way to stop it until it finishes by itself. Hence, one of the most outstanding problems of foundation engineering is to try, together with specialists in physical chemistry, to stabilize deeper strata under consolidation. If and when this is done, a new page in the practice of foundation engineering will be opened.

## References

1. KARL VON TERZAGHI: Soil Mechanics—A New Chapter in Engineering Science, *Jour. Inst. Civil Eng. (London)*, session 1938–1939.
2. KÖGLER-SCHIEDIG: "Baugrund und Bauwerk," Wilhelm Ernst und Sohn, Berlin, 1938.
3. DONALD W. TAYLOR: "Notes on Soil Mechanics" (lith.), Massachusetts Institute of Technology, Cambridge, Mass., 1938.
4. Progress Report of the Special Committee on Earths and Foundations, *Proc. A.S.C.E.*, May, 1933.
- 5a. WILLIAM P. KIMBALL: Settlement Studies of Huey P. Long Bridge, *Civil Eng.*, vol. 10, March, 1940; discussions by Gilboy, Terzaghi, and Creager.
- 5b. CHARLES M. JACOBS: The New York Tunnel Extension of the Pennsylvania Railroad, *Trans. A.S.C.E.*, vol. 68, 1910.
- 5c. Les affaissements de la gare transatlantique du Havre, Centre d'Études et de Recherches Géotechniques (Paris, France), *Bull.* 3, 1935.
6. WILLIAM SELIM HANNA and GREGORY P. TSCHEBOTAREFF: Settlement Observations of Buildings in Egypt, *Proc. Intern. Conf. Soil Mech.*, vol. I, Paper F-1, 1936.
7. W. LOOS: "Praktische Anwendung der Baugrunduntersuchungen," 1st ed., Julius Springer, Berlin, 1935.
8. E. TODE: Spülkipfverfahren und Toneinbau bei der 17 m hohen Dammstrecke des Mittellandkanals nördlich Magdeburg, *Die Bautechnik*, vol. 10, 1932.
9. C. L. NORD: A Case of Bridge Abutment Movement, *Proc. Intern. Conf. Soil Mech.*, vol. 1, Paper F-5, 1936.
10. CHARLES TERZAGHI: Settlement of Structures in Europe, *Trans. A.S.C.E.*, vol. 103, 1938.
11. JOSÉ A. CUEVAS: The Floating Foundation of the New Building for the National Lottery in Mexico, *Proc. Intern. Conf. Soil Mech.*, vol. 1, Paper N-5, 1936.
12. L. RENDULIC: Ein Beitrag zur Bestimmung der Gleitsicherheit, *Der Bauingenieur*, vol. 16, 1935.
13. REDLICH, TERZAGHI, and KAMPE: "Ingenieurgeologie," 1st ed., Julius Springer, Vienna and Berlin, 1929, particularly Chap. XI, B.
14. L. E. YOUNG and H. H. STOCK: Subsidence Resulting from Mining, *Univ. Ill. Eng. Exp. Sta. Bull.* 91, 1916.
15. GEORGE S. RICE: Some Problems in Ground Movement and Subsidence, *Trans. A. I. M. M. E.*, vol. 69, 1923.
16. C. A. HERBERT and J. J. RUTLEDGE: Subsidence Due to Coal Mining in Illinois, *U. S. Dept. Commerce Bull.* 238, 1927.
17. MAX ROLOFF: Die Einwirkung des Bergbaues auf die Eisenbahn, *Die Bautechnik*, vol. 13, 1935.
18. CARP: Baugrundfragen in Bergbaugebieten, *Der Bauingenieur*, vol. 18, 1937.
19. K. ENDELL and U. HOFFMANN: Electro-chemical Hardening of Clay Soils, *Proc. Intern. Conf. Soil Mech.*, vol. I, Paper M-3, 1936.

20. LEO CASAGRANDE: Grossversuch zur Erhöhung der Tragfähigkeit von schwebenden Pfahlgründungen durch electrochemische Behandlung, *Die Bautechnik*, vol. 15, 1937 and vol. 17, 1939; also W. BERNATZIK: Electrochemical Consolidation of the Ground, *Second Congr. Intern. Assoc. for Bridge and Structural Eng., Final Rept.*, Berlin, 1936.
21. JOSEPH D. LEWIN: Grouting with Chemicals, *Eng. News-Record*, vol. 123, Aug. 17, 1939; also an article by E. MAST in *Der Bauingenieur*, vol. 15, 1934.
22. B. A. RZHANITZIN: "Chemical Soil Stabilization" (in Russian), official publication, Moscow, 1935.
23. C. C. WILLIAMS: Small Earth Vibrations Affect Foundations, *Civil Eng.*, vol. 2, 1932.
24. S. E. SLOCUM: "Noise and Vibration Engineering," D. Van Nostrand Company, Inc., New York, 1931.
25. WILLIAM C. E. BECKER, Consulting Engineer, St. Louis, Mo. (by letter).
26. J. R. FREEMAN: "Earthquake Damage and Earthquake Insurance," McGraw-Hill Book Company, Inc., New York, 1932.
27. F. W. FURKERT: The Effect of Earthquakes on Engineering Structures, *Proc. Inst. Civil Eng. (London)*, vol. 23, 1932.
28. JACOB FELD: Trade Practice in the Heavy Construction Industry, *Proc. Purdue Conf. Soil Mech. and Its Applications*, Lafayette, Ind., 1940.
29. T. A. MIDDLEBROOKS and WILLIAM H. JERVIS: Relief Wells for Dams and Levees, *Proc. A.S.C.E.*, June, 1946; discussion, *ibid.*, October, 1946.

## CHAPTER XIV

### SOIL SAMPLING AND FIELD SOIL TESTING

#### A. GENERAL

Prior to preparation of plans for a structure of importance, field soil investigations should be made. These investigations consist (1) in taking soil samples and (2) in making field tests. Soil samples are sent to a soil laboratory for study, as discussed in Parts One and Two. Very often a complete set of samples is preserved for future reference, for instance, in case of eventual extension of the structure. As to field tests, these are not always made, and some of them are met with serious theoretical objections, to be discussed in division C of this chapter.

**14:1. Necessity and Character of Field Investigations.**—Field investigations are not made if soil conditions at a given locality are already perfectly known, as is the case with most city buildings. For heavy and expensive city structures it is advisable, however, to perform these investigations in order to be perfectly sure of the nature of the local soil. As a matter of fact, in some particular cases information from neighboring structures may not be sufficient. As an example, two buildings distant about 200 ft. and based on dolomite rock may be perfectly safe, whereas rock between them may be filled with caverns.

Another instance in which field investigations should not be made is that in which their cost is prohibitive, *i.e.*, when the cost of field investigations is unreasonably high as against the possible damage that might result from lack of investigations. Such are, for instance, secondary earth roads and structures on them. It is also very questionable if field soil investigations should be made in the case of mass construction of small structures spread over an area or a distance, as, for instance, canal locks in a vast irrigation system or small culverts in the construction of a new railroad or a highway. In such cases soil conditions may be assumed on the basis of restricted soil investigations. It is to be borne in mind that detailed field investigations require not only money but also time, and on

many occasions it is better, if necessary, to stop construction and to change plans for a few such spread structures than to spend time and money investigating soil conditions *under all of them*.

It is obvious that in the case of emergency structures, such as ways of communication built close to the war theater, field soil investigations are but superficially made if at all. But military structures built in peacetime are generally very carefully studied from all points of view.

**14:2. Classification of Field Investigations.**—Field soil investigations may be roughly subdivided into three classes:

*a. Foundation investigations*, to determine whether or not the soil at a given point will support a given structure.

*b. Earthwork investigations*, to explore the material to be excavated from an eventual borrow pit, also to examine sites of eventual cuts and embankments in the planning of railroads, highways, and canals. These tests, which often form part of a general soil survey along the whole proposed line or a portion of it, may be either (1) lineal soil surveys covering a relatively narrow strip of land where the communication line may eventually be constructed or (2) area soil surveys where a large tract of land is to be irrigated, drained, or protected from erosion.

*c. Failure investigations*, to determine the cause of a construction failure if there is reason to believe that the failure may be ascribed to soil factors. Such failures and failure investigations have been already treated in Chap. XIII.

Sometimes soil tests are made not only before construction but also as the job progresses, in order to determine the suitability of the material used.

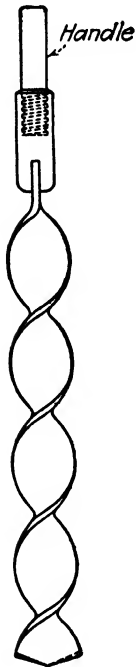
## B. SAMPLING

**14:3. Kinds of Soil Samples.**—Soil samples may be either *disturbed* or *undisturbed*. A perfectly undisturbed sample should keep all the properties of the earth mass of which it is a representative, namely, (*a*) stresses both in moisture and in the skeleton; (*b*) structure, texture, and voids ratio; (*c*) moisture content.

The original stressed condition (average stress, at least) is better preserved in clays than in sands and also better in shallow samples of any soil than in deep ones, because stresses close to the ground surface are insignificant.

The structure of a cohesive soil is disturbed in sampling, owing

to the wall action of the sampling cylinder. In this connection horizontal layers become distorted; also, different soil layers may be mixed up.



If a sample is exposed, there may be loss of moisture due to evaporation. If there are clay and sand layers in the sample, moisture may flow ("migrate") from the former to the latter.

Samples of organic soils are sometimes subject to swelling due to liberation and expansion of gases.

The texture of a soil sample may be disturbed because of the washing out of fine particles, which happens oftener with sand samples than with clays.

Soil samples kept for a long time may change color. For instance, red sands often turn yellow. As a rule, all samples become lighter in drying out. For instance, organic silt in the deltas of rivers, quite dark in nature, turns light gray when dry.

**14.4. Shallow Sampling.**—*a. Shallow Sampling in Cohesive Soils.*—The simplest method of shallow sampling is to use a soil auger (Fig. 14:1), which obviously furnishes samples with a disturbed structure. The auger is first driven into the soil, by hand or with a hammer, then rapidly turned about its vertical axis, and pulled out.

FIG. 14:1.— Auger. A sample of cohesive soil may be taken from the earth's surface or from a shallow depth also by

using a galvanized iron cylinder which is gently worked down by hand (Fig. 14:2). Earth around the sampler is removed, and the sample is cut off from the rest of the mass. It is then dipped into or covered with hot paraffin and sealed in a slightly larger container.

Should cohesive soil contain gravel and pebbles, a sample may be obtained by placing a box (top and bottom removed) around a column of soil that has been carefully cut out from the earth mass (Fig. 14:3a). Empty

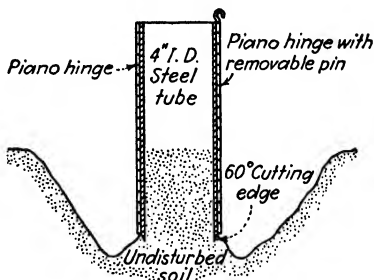


FIG. 14:2.—Shallow sampling in cohesive soil without gravel or pebbles. (After Taylor.)

space between the sample and the walls of the box is packed with damp sand; the top is screwed into place; and the sample is cut

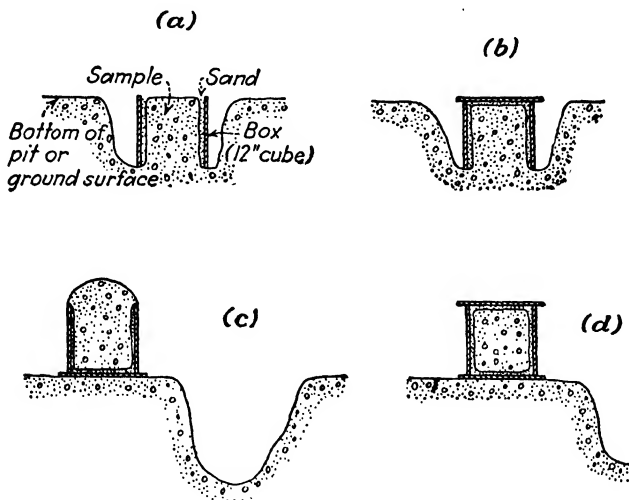


FIG. 14:3.—Shallow sampling in cohesive soils with gravel or pebbles. (After Gilboj and Taylor.)

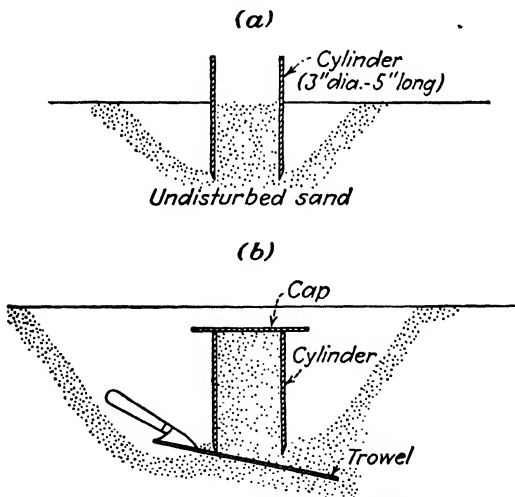


FIG. 14:4.—Shallow sampling in sand.

off from the rest of the mass with a spade (Fig. 14:3b). The box is turned over (Fig. 14:3c), and the surplus soil is removed. Empty

spaces, if any, are again filled with damp sand, and the missing side of the box is screwed into place.

*b. Shallow Sampling in Sand.*—Figure 14:4*a* represents a brass cylinder driven into sand in a way analogous to that shown in Fig. 14:2. The excess sand at the top is leveled off flush, and a cap is put on (Fig. 14:4*b*). One hand is placed on the sampler, and the other on a trowel introduced below the sampler, the latter being taken out and reversed. The excess sand having been again leveled, the operation may be considered finished. Since the volume of the container is known, porosity  $n$  or the voids ratio  $e$  of the given sand in the natural state is easily found (compare problem 1, Chap. I).

**14:5. Methods of Deep Sampling.**—*a. Trenches and Pits.*—The most efficient but also the most expensive method of deep sampling is to excavate trenches or test pits. The strata found in such excavations should be described, and samples of them about 4 by 4 by 3 in. should be carefully cut from various points to be marked on a plan. In important cases large soil monoliths, say, 40 by 10 by 4 in., may be cut out from the soil mass.

Figure 14:5 shows a pit provided with sheathing and bracing to prevent caving in. Obviously, other efficient methods of supporting the walls of a pit are available, such as the driving of metallic sheet piles.

*b. Open Holes.*—Machines for making holes in the ground, such as are used by telephone companies for planting poles, may find application in foundation testing for lighter structures such as small culverts on railroads and highways. The diameter of a hole is usually from 10 to 20 in., the depth up to 10 ft. In soft soils the hole is made in a few minutes. More complicated machines drill very deep holes up to 3 ft. in diameter.

*c. Borings.*—Before starting borings, a *datum* should be established, also bench marks and base lines to fix the position of the borings in the plan. In all methods of boring, casing (sections of metallic pipe) is used. The purpose of the casing is to provide an opening through which the actual boring operation may be carried on. When the boring is finished, the casing is pulled out.

Generally the work is done by special contractors who possess necessary equipment and experience. The foreman or inspector on the job submits daily reports to the resident engineer and to the laboratory in charge of the testing. Such a report contains infor-

mation on (1) depths of the top and the bottom of each stratum, (2) identification of the soil in different strata (whether sand, clay, hardpan, etc.; whether hard or soft; and color), (3) depth of the water table, (4) lost wash water, (5) obstacles (boulders etc.), and also data specified in Secs. 14:6 and 14:9.

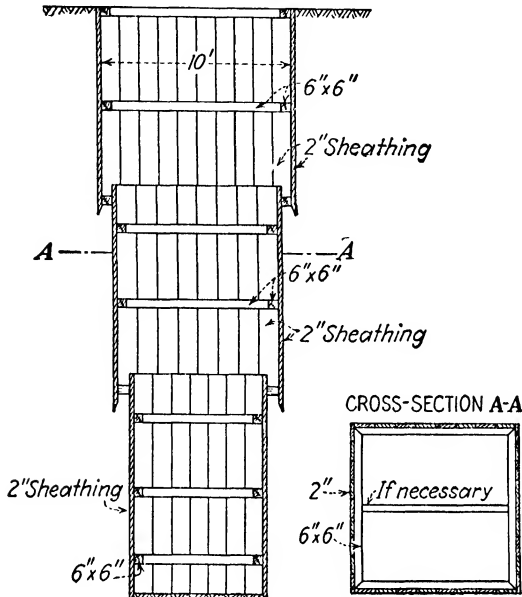


FIG. 14:5.—Test pit.

On the *log of the boring* (a narrow vertical rectangle subdivided to scale into horizontal sections showing strata) the foreman's data properly corrected by the laboratory are shown converting depths into elevations. Since the water table fluctuates, the month and year when the borings were taken should be specified on a sheet of logs.

The results of several borings plotted on the transverse profile of a locality form a *soil profile*. Sometimes the term "geological section" is also used, especially if the borings go deep into rock.

Borings should be supervised by a responsible technician who determines when the work has to be discontinued. Generally the depth of the borings is not less than one and one-half maximum width of the structure. Obviously this rule cannot be generalized to heavy narrow structures such as towers or stacks. Within the

depth mentioned above, any bed of clay with a water content above the plastic limit (which can be easily established in the field by rolling material from the boring between the palms of the hand into very thin threads) is a potential source of harmful settlement and has to be carefully sampled.

**14:6. Driving Casing.**—A *rig*, or set of machinery and devices for driving casing and boring, consists first of a four-legged derrick (Fig. 14:6) with a block at its top which is centered over the given point. A rope is fastened to the drive weight. To start a boring, a section of casing is set and driven. The length of such a section

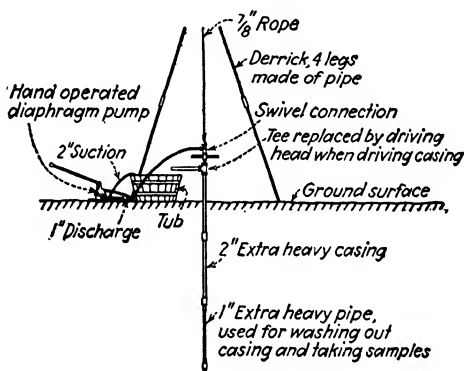


FIG. 14:6.—“Wash” and “dry” sampling. (After Mohr.)

is usually between 5 and 10 ft.; its diameter is  $2\frac{1}{2}$  in. or more—seldom less. As soon as the casing section is cleaned out in the way described, another section is added and driven. Connections between sections must be made as tight as possible by using large wrenches. Recess couplings of different systems are also used.

Casing is provided at the bottom with a drive shoe if passage of very hard layers is expected and with a drivehead at the top. If a boulder is met during the sinking of the casing, it should be drilled through and blasted out of the way with dynamite. To avoid damage, the casing must be pulled back 8 or 10 ft. before the blasting.

The foreman or the inspector on the job keeps track of the following data: (a) diameter and weight of the casing per linear foot; (b) whether or not the casing sinks into soft soil owing to its own weight, and if so, through what vertical distance; (c) weight of the hammer, average height of fall, and number of blows required to

force the casing through each linear foot (compare Sec. 14:5). To record blows, it is advisable to make 1-ft. marks on pipes with chalk and to use a common hand counter. The usual weight of a hand hammer is about 150 or 200 lb., the height of fall being about 2 or 2½ ft. For power operations, hammers weighing up to 800 lb. are used. The plotting of field data referred to on a boring profile may furnish useful information on the resistance of different layers. Admittedly, in the study of such a graph, changes, if any, in the weight of hammer and the casing, should not be overlooked.

**14:7. Wash Borings.**—Wash borings<sup>1</sup> are made by sinking a casing about 2½ in. in diameter. The casing encloses a wash pipe 1 in. in diameter. The wash pipe projects a jet of water at its lower end, and wash water erodes the soil mass next to the tip of the casing and returns between the casing and the wash pipe, bringing soil in suspension.

To wash material from a driven section of casing, the drivehead is replaced by a tee, and a tub or simply a pail is placed under the horizontal pipe to receive the suspension (Fig. 14:6). The wash pipe, connected to a swivel, is set, and the swivel is connected to a pump. The pump shown in Fig. 14:6 is a hand pump, and its suction occurs in the tub or the pail just mentioned. Such an installation is rather objectionable and perhaps may be used if borings are made for a structure that is far from water. If the structure is close to a river or a lake, it is preferable to pump water directly. Apparently<sup>1</sup> a pump that will furnish from 20 to 60 gal. per min. under a pressure of 50 lb. per sq. in. may be considered quite satisfactory in any material.

The wash pipe is provided with a chopping bit at the bottom. Water ports in the walls of the chopping bit permit wash water to be forced into the soil. To facilitate erosion of the material, the wash pipe is churned up and down and also twisted.

Samples are simply recovered from the suspension in the tub or in the pail or scraped out from the bottom of the tube. These samples do not indicate the character of the soil texture correctly, however, since fine particles are generally washed out. It is obvious that the structure of the earth mass and its resisting properties cannot be established by wash borings either. Wash borings have been generally abandoned, though in some particular cases they may be of real service. Such is the case when it is

known that rather shallow rock underlies a certain locality and the exact depth of the rock is to be considered in the design. Wash borings may also be useful in the preliminary exploration of a locality before expensive deep undisturbed sampling starts (compare also Sec. 14:8).

Washing out of soft material, such as clay or organic silt, can be done to a depth of about 60 or 70 ft. by the use of a restricted length of casing (for instance, 15 ft.) at the top of the layer.

**14:8. Dry Sampling.**—To obtain a “dry sample” during the washing process described in Sec. 14:7, the wash pipe is lifted, and the chopping bit is replaced with a section of plain pipe or spoon and forced again into the bottom of the hole. “Dry sample,” or perhaps more correctly “drive sample,” is a conventional term. Dry samples preserve the soil texture better than wash samples.

A further step in this direction has been proposed by Mohr,<sup>1</sup> using Shelby steel tubes\* fixed to a drilling pipe forced to a depth of about 30 in. below the bottom of the casing. In this way long samples are obtained that, upon being cut in the laboratory into short sections and examined, furnish information on the elevations at which eventual undisturbed samples should be taken. Such preliminary investigation is preferable to the procedure generally used when undisturbed samples are automatically taken, for instance, every 10 ft. or at changes in material established in the field by visual inspection. In many practical cases information furnished by 2 ft. long Shelby samples, 3 in. or more in diameter, is quite sufficient for designing purposes.

Wash borings may cost from \$0.50 to \$1.25 per foot, with an addition of about 50 per cent for dry samples according to the intervals where samples are to be taken.

**14:9. Deep Undisturbed Sampling in Cohesive Soils.**—To obtain a deep undisturbed sample, casing is sunk in the usual way, and earth material from it is removed—for instance, by washing out. The wash pipe is then taken out, and the sampler, which represents an open cylinder, is connected to its tip or to the tip of a drilling rod or otherwise and is lowered slowly to the bottom of the hole. Forcing of the sampler into earth is made by loading or jacking or sometimes by driving with a hammer. Data to be recorded in this connection are

\* Shelby tube is the trade name for a seamless steel tubing. In boring operations a No. 16, 18, or 20 gauge is used.

*a.* In the former case both the value of the acting load and the time required for the sampler to be forced through 1 ft. below the bottom of the casing.

*b.* In the latter case the weight of the hammer, height of fall, number of blows, distance of driving (compare Sec. 14:5).

When the sampler is full, it is carefully lifted up and split. The soil sample within the sampler is received into the brass lining (or "liner"); and, upon the splitting of the sampler, the soil is squared off at each end of the brass lining, which is 12 in. or more long, and the ends of the liner are sealed with paraffin and covered with metal caps. After the latter are firmly secured, the ends of the tube are sealed either with adhesive tape or with shellac, and the tubes are weighed. The samples come to the testing laboratory in the form of brass cylinders, which are reweighed before testing, and correction for loss of moisture is introduced. To extract a sample from the brass cylinder, the latter is sawed into transversal sections, preferably by hack saws, since circular saws moved by a motor produce vibrations that may alter the sample. Samples of soft clays and organic silts may sometimes be gently shaken out from an open end of the brass cylinder. As a rule, the opening of samples should be done in a humid room to prevent evaporation.

Undisturbed sampling may cost from \$5 to \$8 per foot, being somewhat less expensive than core drilling in rock, which may cost up to \$10 per foot.

**14:10. Composite Samplers.**—There are two classes of samplers for cohesive soils; these will be termed "composite samplers" and "piston-type samplers." The former only will be described in this section. Piston-type samplers are described in Sec. 14:11.

*a. Moran and Proctor Soil Sampler.*—This sampler was designed by Moran\* and Proctor, consulting engineers, New York City. It was developed for securing samples of plastic soils, such as clays or silts, and is not adapted for recovering samples of sand, gravel, or other granular materials. The sampling tube proper is split to facilitate the removal of the brass liner, as already explained. It is held by the sampler shoe at the bottom and by a short section of heavy pipe at the top (marked "connecting sleeve" in Fig. 14:7). A ball check valve at the head of the sampler permits water to pass

\* Daniel E. Moran (1864–1937) dedicated his whole life to foundation engineering. The foundations for the San Francisco-Oakland Bridge were made feasible by the "domed" type of caisson devised by Moran.

up and prevents it from returning to the sample. The connecting sleeve serves also as a deposit for the material just at the bottom of the hole, which may be somewhat disturbed. This poor material is cut off when the sample is squared as explained above. Copies of these samplers are manufactured by Sprague and Henwood

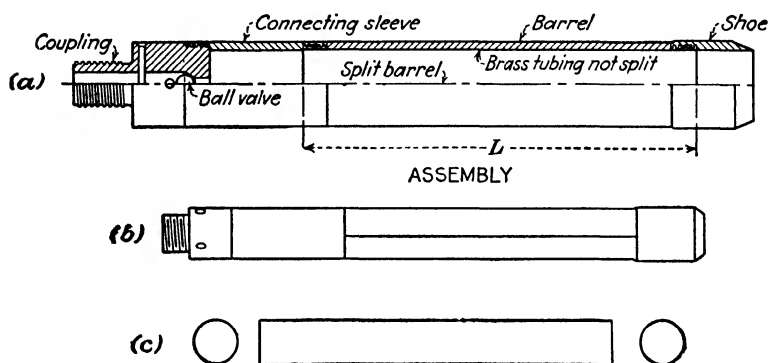


FIG. 14.7.—Moran and Proctor sampler. (a) Section; (b) view; (c) brass tube and caps.

(abbreviation "S. & H.") and by the American Instrument Company.<sup>3, 4</sup> The commercial-size samplers furnish samples  $1\frac{1}{2}$  in. in diameter, 12 in. long, and 3 in. in diameter, 16 in. long. Over-all

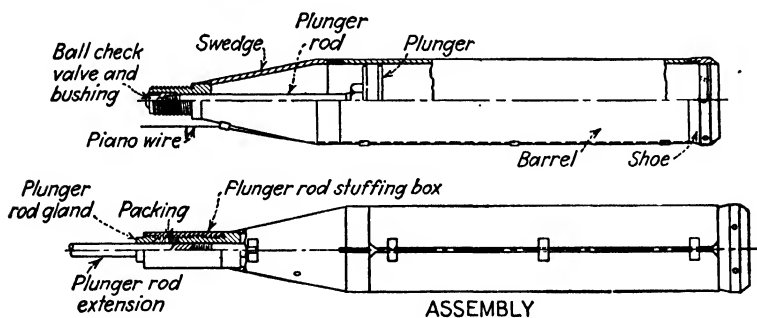


FIG. 14.8.—M.I.T. sampler.

length of this sampler for the latter diameter is 27 in., its net weight being 27 lb.

b. *M.I.T. Soil Sampler*.—This sampler is adapted for securing samples about 2 ft. long and 5 in. in diameter. It was designed by members of the Massachusetts Institute of Technology (Gilboy and Buchanan<sup>5</sup>) with the help of A. Casagrande. A similar type

of sampler had been constructed before by Beatty.<sup>6</sup> Figure 14:8 shows the M.I.T. soil sampler as modified by Sprague and Henwood,<sup>3</sup> who added a plunger to facilitate the removal of the sample. Compressed air also may be used to force the sample out. A special feature of this sampler is the piano-wire arrangement for cutting

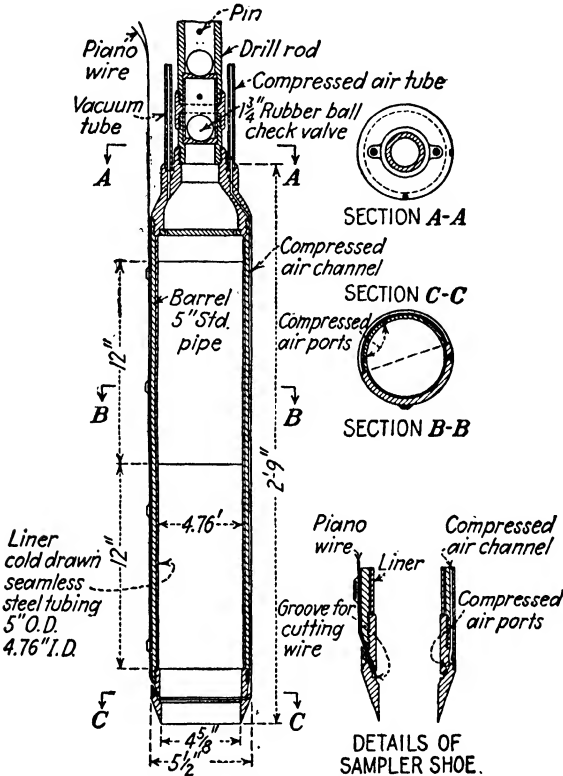


FIG. 14:9.—Casagrande-Mohr-Rutledge sampler.

the sample at the bottom to separate it from the rest of the earth mass. It is placed in a groove in the shoe and controlled from above. The wire thus remains in the shoe during the withdrawal and may damage the sample if the latter starts to slide out. No liner is shown in Fig. 14:8, though samplers with liners may also be obtained. The over-all length of this sampler is 40 in., the net weight being 52 lb.

The two samplers described are sold commercially, whereas other samplers described here are to be built by the interested persons.

*c. Casagrande-Mohr-Rulledge Soil Sampler.*—Figure 14:9 represents this sampler, which furnishes samples 2 ft. long and 4.76 in. in diameter. It has been much improved in comparison with its prototype, the M.I.T. sampler. There are two air-hose connections at the top of the sampler—one to maintain vacuum over the sample during the withdrawal and the other to convey compressed air to the bottom of the sample. The cutting wire is pulled free of the sampler during the withdrawal and cannot damage the sample as in the M.I.T. sampler. The sampler is provided with a check valve and is lined.<sup>1</sup>

*d. Missouri Division Soil Sampler, Corps of Engineers, U.S. Army.*—Among several samplers designed by the members of the

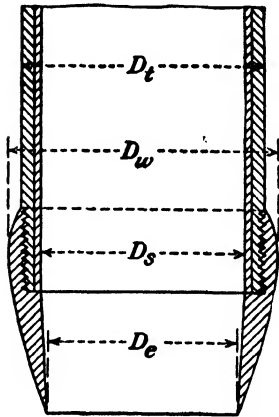


FIG. 14:10.—Different diameters of a sampler. (After Hvorslev.)

U.S. Engineer's Office, the Missouri sampler will be described.<sup>2</sup> It furnishes samples 2 ft. long and 6 in. in diameter. The sampler is forced into the soil by means of a hydraulic ram which can develop a total pressure up to 50 tons. It was found that the following loads were required to force the sampler into the soil: saturated silty clay loam, 3 tons; medium clay, 8 tons; compacted roll fill of silty loam, 11 tons; damp medium sand, 24 tons. Dry medium sand refused penetration under a load of 35 tons.

*e. Clearances and "Area Ratio."*—It follows from the preceding descriptions that a composite soil sampler is a cylinder of slightly variable diameter provided with a cutting edge (shoe) and consisting of a thick-walled outer and a thin-walled inner container. Figure 14:10 shows the bottom of a composite sampler. There are four different diameters:  $D_t$ ,  $D_w$ ,  $D_s$ ,  $D_e$ . The inside clearance is the difference between  $D_s$  and  $D_e$ , expressed in per cent of  $D_s$ , and the outside clearance is the difference between  $D_w$  and  $D_t$ , expressed in per cent of  $D_t$ . For instance, the M.I.T. sampler has an inside clearance of 2.5 per cent and an outside clearance of 2.2

per cent, whereas the Moran and Proctor sampler has an outside clearance only (3.6 per cent).

The object of the inside clearance is to permit the entering, heavily stressed sample to expand elastically without change in water content. The outside clearance diminishes the outside wall friction. It should be remembered that these statements refer to cohesive nonswelling soils only and may be untrue otherwise.<sup>2</sup>

The total volume of the earth material affected by the sampling operation is the volume of the cylinder with the outer (maximum) diameter  $D_w$ , whereas the effective volume of the sample is controlled by the inner (minimum) diameter  $D_e$ . The difference between these two volumes is the amount of displaced soil. This difference, if expressed in per cent of the effective volume of the sample, is sometimes termed the "area ratio" of the sampler:

$$\text{Area ratio} = \frac{D_w^2 - D_e^2}{D_e^2} \times 100 \quad (14:1)$$

The larger the area ratio the more considerable is the disturbance of the sample. A value of that ratio of about 40 per cent is satisfactory. Greater values, especially when combined with heavy blows of the hammer to drive the sampler, may render the sample completely useless. The term "area ratio" will not be used hereafter.

**14:11. Piston-type Samplers for Cohesive Soils.**—Figure 14:11 shows a piston-type sampler used by the Fort Peck Division, Corps of Engineers, U.S. Army,<sup>2,7</sup> for sampling in slightly cohesive materials. The principle of this sampler and of other samplers of the same type is to lower the sampler with the piston flush to the bottom of the sampler, then to use the inner rods to fix the piston steady in this position, and finally to force the sampler into the bottom of the hole, as is done in obtaining dry

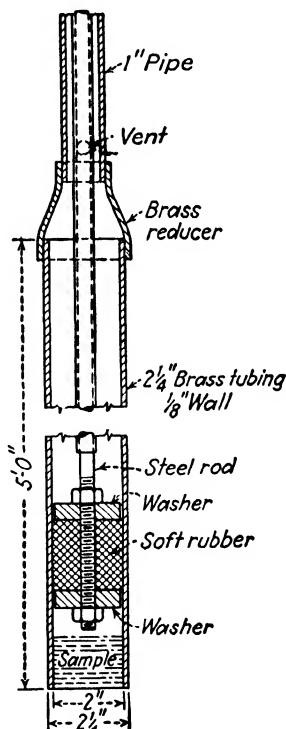


FIG. 14:11.—Fort Peck sampler.

samples (Sec. 14:8). Long samples of different diameters (up to 6 in.) may be obtained by this device.

Figure 14:12 represents in a diagrammatic form the well-known "California sampler," designed by California state highway engineers.<sup>8</sup> This sampler may be used practically without casing.

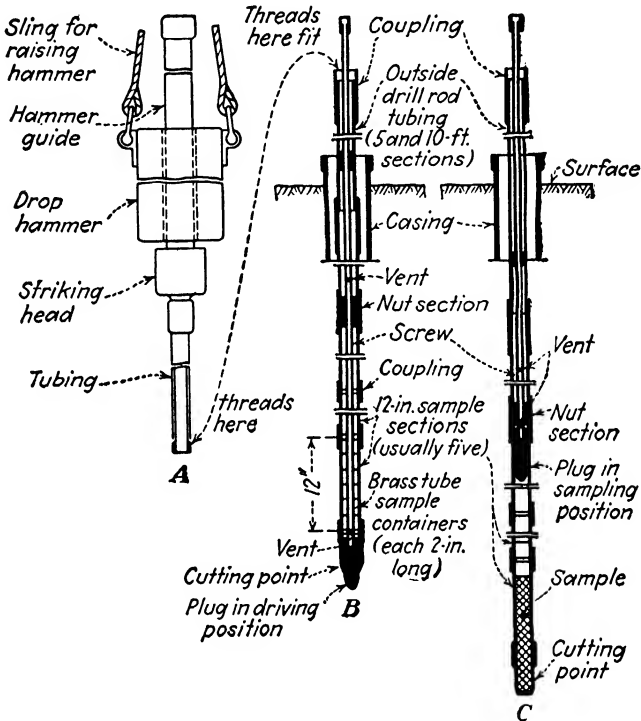


FIG. 14:12.—California sampler. (a) Drop-hammer assembly; (b) plug in driving position; (c) plug withdrawn, sample within the tube.

Its cutting edge is provided with a plug, which can be raised upward. The essential operations are (a) forcing the sampler as a plugged tube to the desired depth, (b) retracting the plug and forcing the open sampler into undisturbed material, (c) raising the plug farther to produce an airtight seal above the sample. Thereupon the entire device is withdrawn to the earth surface. Samples 2 in. in diameter and 3 or 4 ft. long are obtained in one sampling operation.

It is quite obvious that the M.I.T. sampler is not a piston-type device, though it possesses a piston.

**14:12. Deep Sampling in Cohesionless Soils.**—A sand or gravel sample has no cohesion and, as a rule, cannot stay unsupported within the sampler. To extract deep undisturbed samples from cohesionless material, it is necessary either to prevent the sample

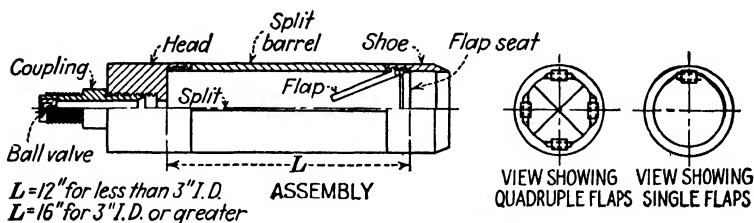


FIG. 14:13.—Sampler for cohesionless soils.

from falling out of the sampler or to stabilize the material before extracting samples therefrom. Neither of these two problems has been satisfactorily solved, so that, strictly speaking, deep undisturbed samples of cohesionless material cannot be obtained at the present time.

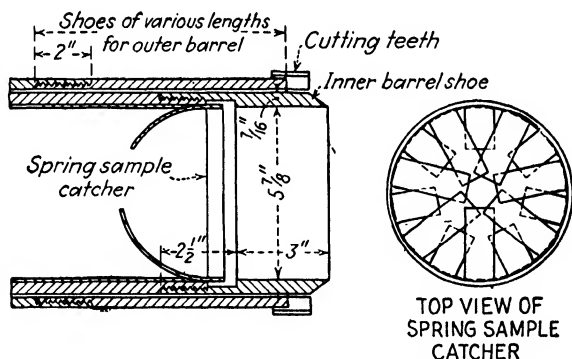


FIG. 14:14.—Bottom of the Johnson and Young sampler.

*a. Direct Sample Taking.*—Figure 14:13 shows the Sprague and Henwood (S. & H.) “Main”-type sampler commercially sold.<sup>3,4</sup> The sand is kept within the sampler by the “flaps” or flap doors. The inconvenience of this type consists in the disturbance of the sand sample when it passes the flap doors in entering, in the loss of a part of the sample, and possibly in washing out of the fines

when the flap doors are being closed. This sampler furnishes samples from  $3\frac{1}{2}$  to 5 in. in diameter and nominally 16 in. long.

Johnson<sup>9</sup> describes a 6-in. double barrel which has been used in taking samples, mostly from cohesionless soils, during the investigations for the Denison Dam in Texas. Casing was used only in the upper part of the hole, the rest being filled with thick, jellylike drilling mud which prevented the walls of the boring from caving in. Figure 14:14 represents the bottom of this sampler, provided with special spring sample catcher. Johnson reports that the poorest recovery in this sampling was 41 per cent, the best 92 per cent, and the average 70 per cent. The best results were obtained in materials above the water table and in all kinds of clays. Fine sands below the water table were the most difficult to sample, whereas undisturbed gravel samples were an impossibility.

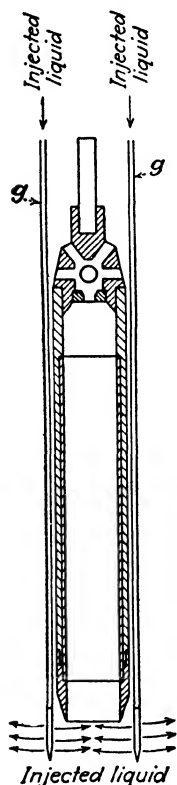


FIG. 14:15.—Injection of chemicals into sand to stabilize it.

Mohr<sup>1</sup> developed a sampler provided with four curved flap valves in the sampler shoe. The closing of the valves is started by the operator by means of a special wire that, at the same time, serves to cut the sample free from below. Once started, the closing of the valves is completed automatically by the sinking of the sample itself.

*b. Preliminary Stabilization of the Sand.*—Some procedures mostly used in Europe are briefly described here.

A way to take undisturbed samples in sand is to inject bituminous emulsion into the sand and to extract the sample when hardened. The bituminous emulsion is then removed from the sample by evaporation. Some change of structure, however, is involved in this procedure.<sup>2</sup>

A sampler of this kind is shown schematically in Fig. 14:15. Injected liquid is carried to the bottom of the boring by pipes *g*. Instead of chemicals, clay suspension may be injected. Use of sodium silicate and calcium chloride (compare Sec. 12:4) also has been recommended.

On some occasions the freezing of fine sand has been practiced in the same way as in tunneling. Such procedure has been tried in this country by Fahlquist.<sup>2</sup> In the case described by Kollbrunner and Langer,<sup>11</sup> five 2½-in pipes were driven around a casing to a desired depth so that they were located at a circumference (radius 2 ft.). The pipes were filled with a cold mixture at a temperature between -112 and -130°F., and this mixture was renewed every 2 hr. At the end of 12 hr., quicksand acquired consistency of soft clay, so that samples could be extracted. It is interesting to note that porosity of quicksand as determined in this test was  $n = 47.3$  per cent, whereas maximum possible porosity amounts to  $n = 47.6$  per cent (compare Sec. 1:10).

It is obvious that stabilization by both injections and freezing disturbs somewhat the natural soil structure and, from this point of view, is objectionable.

**14:13. Other Samplers.**—Some rough devices for preliminary soil investigations are sold commercially, and their description may be found in catalogues.<sup>3, 4</sup> A complete description of various types of American and foreign samplers has been prepared by Hvorslev.<sup>2</sup> Interesting details on sampling in Germany are contained in ref. 11.

**14:14. Lost Wash Water.**—Sometimes wash water is lost during the boring process and does not return to the earth's surface. This circumstance is of great importance and should be specially reported, with the estimated amount of water lost being indicated. The meaning of lost wash water is twofold: At a certain depth either there is porous material with empty voids, or there is a downward hydraulic gradient which pushes the wash water downward together with other water moving in that direction. The first case is not dangerous, but the latter may cause serious trouble during the construction and perhaps afterward. As a matter of fact, this would mean that when the excavation reaches the given depth, it will be difficult or impossible to remove water by pumping.

Other signs of possible trouble during the construction appear when (a) the water level in the boring cannot be lowered by bailing and (b) there is a rise of fine saturated sand left in the boring. For instance, as in Fig. 14:16, saturated fine sand reduced to the level *B* by the boring may return to its original level *A* if left alone. Both cases (a) and (b) mean that the given stratum is in communication

with a large water basin. Case (b) may also be indicative of the possibility of high hydrostatic pressure.

**14:15. Rock Exploration.**—A boring must be carried on to hard bottom (“resistance”). Usually this is ledge rock. In order not to confuse ledge rock with boulders which may be met in driving casing, it is necessary to drill resistance found through to a certain depth, for instance, 10 ft. Sometimes 5 ft. is considered satisfactory. A boulder or boulders may be blasted out of the way with dynamite. To avoid damage, the casing must be pulled back 8 to 10 ft. before blasting.

Among the different ways of taking rock samples or core borings,

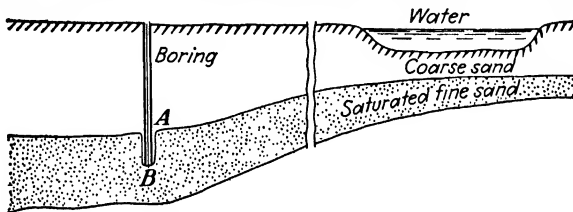


FIG. 14:16.—Fluctuations of saturated fine sand in a boring.

the most advisable is diamond drilling. This and other methods of rock exploration are thoroughly described in technical literature, for instance, in ref. 1. The sample is a cylinder cut out of rock by wearing action. The smallest core made is of  $\frac{7}{8}$ -in. diameter; very common is the core  $1\frac{3}{4}$  in. in diameter. It is advisable to record the partial lengths of core recovered at different depths and not the average of the whole drilling operation. Recovery is expressed in per cent of the length drilled and is plotted on the profile at the corresponding depth. Sound rock furnishes high recovery; seamy rock may furnish low recovery and cores broken into pieces. Seams are fissures in the sound rock or boundaries between two materials of different origin. They are mostly filled with sand and also with breccias, agglomerates, and other formations.

With such rock as dolomite and limestone, borings should not be very distant from the proposed site of the structure, since in such cases considerable cavities may be found. If there is some doubt regarding the behavior of the given rock (as with some slates or shales) under the action of water, a simple field test, consisting of plunging a piece of rock in water, should be made.

If there are highway or railroad cuts through the rock outcrops

close to the place under study, it is advisable to examine them very carefully. In some occasions such an examination may furnish very useful analogies.

Loss of wash water during the drilling of rock is to be reported in the same way as for simple earth borings. In the case of water barriers this may furnish useful information on possible loss of water through fissures in the rock. In the case of bridge piers and similar heavy structures loss of wash water should be also carefully examined and explained to avoid troubles such as unexpected settlement.

It goes without saying that in complicated and doubtful cases of rock exploration, help of an experienced geologist should be sought.

**14:16. Preservation of Soil Samples.**—All soil samples must be numbered and labeled. If a set of samples is sent to the laboratory, it should be accompanied by a list containing the following data: numbers of the samples, date of sampling, description of the tare (whether a bag, a paraffined lump, a brass cylinder, etc.), depth, whether from the excavation or from a borrow pit, sketch or other data required to place the sample on a plan or a map and to determine its elevation.

A shallow sample or a wash sample may be placed in a container, often a 1 pt. jar, sometimes a bag or a box, and transported to the laboratory. Large wooden boxes containing all the samples pertaining to a given boring are sometimes used. Undisturbed samples in brass cylinders are sometimes placed in individual boxes. Transportation over short distances is effected in cars or light trucks, as carefully as possible, and all measures to prevent disturbance, specifically by vibrations, should be taken if samples are sent a long distance.

In the laboratory, samples to be studied should be placed in a moist and cool place to avoid evaporation. More details on preservation of soil samples may be found in ref. 2.

### C. FIELD TESTS

Field tests may be subdivided into

- a. Tests for determining physical properties of the soil, such as unit weight or permeability in the field.
- b. Tests for determining resistance of the soil to the action of loads. These tests may be either static or dynamic.

**14:17. Determining Some Physical Properties of the Soil in the Field.**—*a. Unit Weight.*—The earth surface is evened, and a sample of arbitrary shape taken, for instance by a spade (Fig. 14:17*a*). The sample is weighed promptly (weight,  $W$ ) and the volume  $V$  of the hole is determined. For this purpose the hole is filled flush with the earth's surface with dry sand or heavy oil from a calibrated bottle. The unit weight of soil obviously equals  $W/V$ .

As an alternative (Fig. 14:17*b*), a rubber bag  $A$  with a flat metallic cover  $B$  may be introduced into the hole and filled with

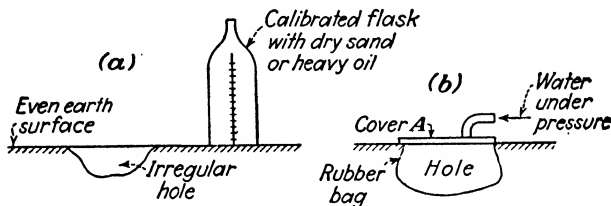


FIG. 14:17.—Determining unit weight of soil in the field.

water under pressure by a small hand pump. If the net weight of water filling the bag is  $W_0$ , the apparent specific gravity of the soil is  $W/W_0$ , and its unit weight in pounds per cubic foot is  $62.4 \times W/W_0$ .

*b. Permeability.*—It was shown in Sec. 3:17 how to determine the coefficient of permeability of a soil in the field. Still another method would be to extract undisturbed samples at different points of a cross section, to test them in the laboratory, and to take an average of their coefficients of permeability. This average value should be again checked in the field by a visual inspection of the cross section after the laboratory results have been learned.

**14:18. Coefficient of Permeability Determined from a Geological Section.**—In Fig. 14:18 a stratum (total thickness  $h$ ) consists of several layers. Their thicknesses and laboratory coefficients of permeability are  $d_1$  and  $k_1$ ,  $d_2$  and  $k_2$ ,  $d_3$  and  $k_3$ , etc. The coefficient of permeability of the whole stratum in the horizontal direction  $k_h$  is the weighted average of the values  $k_1$ ,  $k_2$ ,  $k_3$ , . . . The latter are plotted horizontally as shown in the figure, and their weighted average  $k_h$  is controlled by vertical line  $AB$ . The latter is traced so as to equalize dashed areas at the right and at the left of it; after a little practice this can be easily done by eye.

To determine the value of the coefficient of permeability of the whole stratum in the vertical direction  $k_v$ , consider the downward flow of water from the top of the stratum to its bottom through a vertical column of soil with the cross-section area equal to unity. If the flow starts at the top of the column without velocity, the loss in head to reach the bottom is  $h$  in a distance  $h$ . The corresponding hydraulic gradient is  $i = h/h = 1$ . By the Darcy formula (3:4), the discharge during a unit of time equals  $k_v$ . The

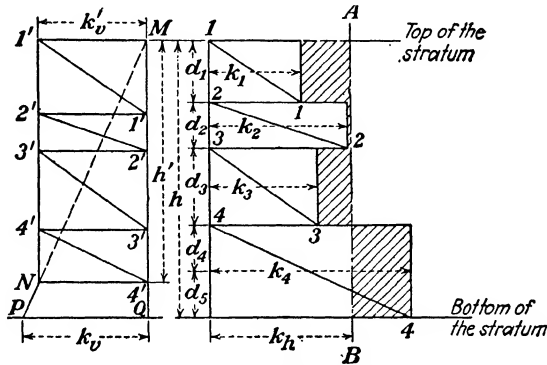


FIG. 14:18.—Vertical and horizontal coefficients of permeability determined graphically.

discharge in a unit of time through a portion of the vertical column referred to—for instance, from the top to the bottom of the uppermost layer (thickness,  $d_1$ )—obviously equals  $k_v$ . Designating by  $h_1$  the unknown loss of head in passing that portion and applying the Darcy formula (3:4)

$$k_v = k_1 \frac{h_1}{d_1} \tag{14:2}$$

It follows from formula (14:2) that the loss of head  $h_1$  is

$$h_1 = \frac{d_1}{k_1}$$

Since the sum of the values  $h_1, h_2, h_3, \dots$  equals  $h$ , it may be stated that

$$h = k_v \left[ \frac{d_1}{k_1} + \frac{d_2}{k_2} + \frac{d_3}{k_3} + \dots \right] \tag{14:3}$$

The value of  $k_v$  can be found by assuming first an arbitrary value

$k'_v$  for the coefficient of permeability  $k_v$ . Plot  $M1' = k'_v$ , and trace  $1'1'$  parallel to  $11$ , to intersect the vertical  $MQ$ . If this operation is repeated for other layers, the total value of head lost will be  $M4' = h'$  instead of  $MQ = h$ . The assumed value  $k'_v$  is corrected by tracing diagonal  $MN$  and continuing it to intersect the bottom of the stratum at point  $P$ . Then  $PQ = k_v$ . Obviously  $k_v < k_h$ .

Figure 14:18 represents the graphical solution of a problem analytically solved by Terzaghi.<sup>10</sup>

**14:19. Field Static Tests.**—These tests are (a) sounding to “resistance,” (b) penetration tests, and (c) the load test.

*a. Sounding.*—A steel rod or pipe about  $\frac{3}{4}$  or 1 in. in diameter is driven into the earth mass until “resistance” is reached. The rod or pipe consists of sections 4 or 5 ft. long. If it does not sink when driven by hand, a sledge hammer or a drop weight is used, and the number of blows is recorded just as in the driving of casing (Sec. 14:6). Sounding may be useful in preliminary investigations, for instance, in determining the depth of a swamp. Sounding is not sampling, since no samples are extracted.

*b. Penetration Tests.*—A shallow-penetration test as recommended by the Swedish Geotechnical Committee<sup>12</sup> consists in forcing into the earth mass or dropping from a certain height a standard metallic cone. The value of penetration is recorded. Like all shallow tests (compare Sec. 8:7), this test is open to criticism.

An example of a deep-penetration test is the jacking soil investigation by Paaswell, made in 1929 for the extension of the New York subway.<sup>13</sup> A conical metallic shoe about  $2\frac{3}{4}$  in. in diameter, attached to an extra heavy pipe, was jacked down through a casing. Pressure required for jacking at different elevations was recorded and plotted against penetration. The “penetration-resistance curve” thus obtained is shown in Fig. 14:19. The curve in question clearly shows that the earth resistance fluctuates from point to point. Probably it depends also on the time rate of driving. Hence, in analyzing the results of a similar test, some reasonable *average value* of the resistance should be adopted.

*c. Load Tests.*—As explained in Sec. 8:7, load tests (termed also “area tests” or “platform tests”) may or may not give a correct idea of the so-called “bearing power” or “bearing value” of a soil. This circumstance should never be overlooked.

In a load test an open excavation is made, and a round, polyg-

onal, or square plate of practically undeformable material, such as steel, concrete, or hardwood, is placed at its bottom and gradually loaded. The usual dimensions of a square plate are 1 by 1 ft. or 2 by 2 ft. The load may consist of pig iron, stones, or other

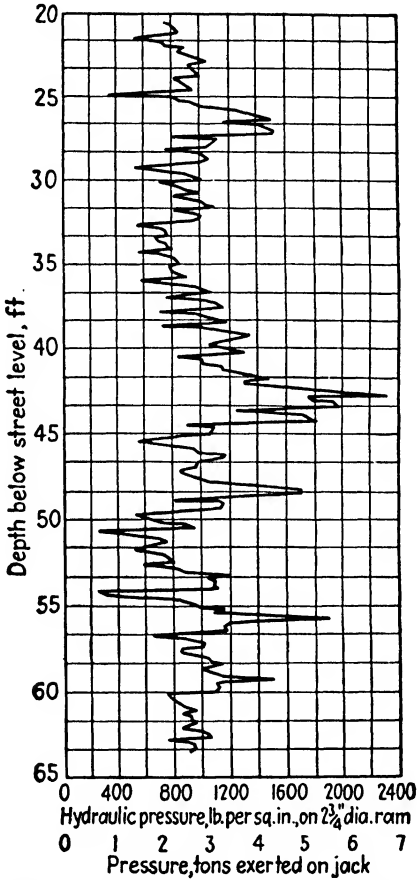


FIG. 14:19.—Deep-penetration test. (After Paaswell.)

materials; it should be built carefully and evenly. As a rule, a bench mark is established, and settlement is observed periodically with a level or a transit.

Sometimes a vertical wooden post is planted close to the loaded plate, and a horizontal lever, fixed at one end to the load or to the plate and carrying a pencil at its other end, traces the supposed

progress of the settlement of the post. Such an arrangement is not very advisable, however, since the ground level around the

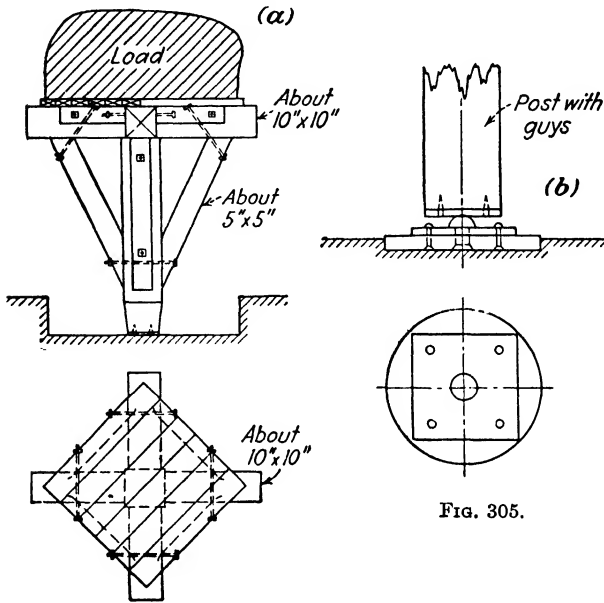
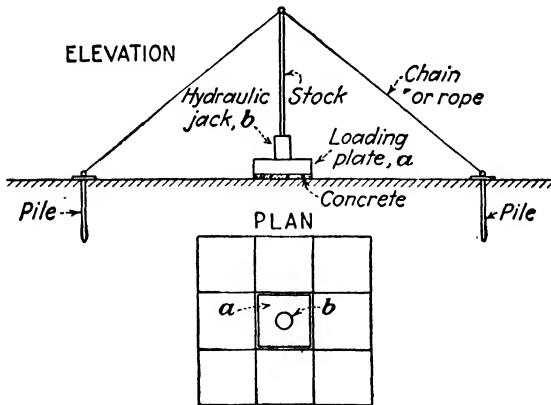


FIG. 305.



Figs. 14:20 and 14:21.—Examples of simple load test.

loaded plate is subject to fluctuations caused by the load.

The following precautions are to be taken during a loading test:

1. Keep the plate or post even by guys with turnbuckles or by

other means. The guys are not supposed to be stretched, yet are ready to take care of a deviation at any time.

2. Protect the entire setup from rain or other unfavorable weather conditions.

The site of the test is sometimes sheltered and drained from surface water. Load tests generally are not made during heavy frosts.

Figure 14:20a shows a simple load-test installation. The foot of the vertical post, which transmits the load to the earth's surface, is provided with a metallic plate, which in the case of soft ground may be omitted. Figure 14:20b shows a post bearing upon a

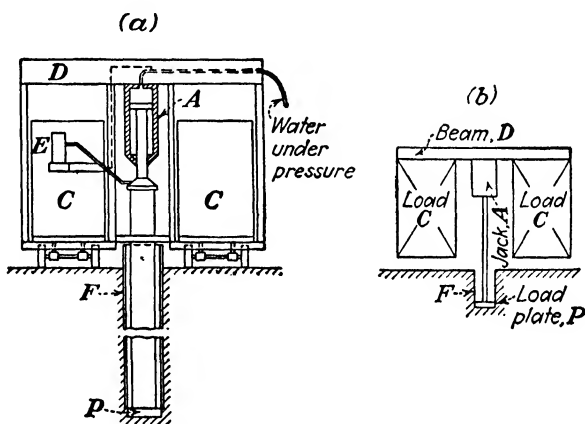


FIG. 14:22.—A loading test in Germany (Wolfsholz or Siemens-Bau Union).

metallic plate through a cup-headed pin, the post itself being fitted with a metallic plate.<sup>14</sup>

A self-explanatory sketch of a load test is given in Fig. 14:21. Interesting features of this sketch are eight plates surrounding the basic loading plate *a*. Tests shown in Figs. 14:20 and 14:21 are very different from the mechanical point of view. Stress is applied in the former, and corresponding deformation (settlement) is measured. In the latter test deformation is produced by the jack, and stress required to maintain this deformation is measured.

In Fig. 14:22a a method of making load tests, known as the "Wolfsholz method" or "Siemens-Bau Union method," is shown.<sup>15</sup> Figure 14:22b is merely a simplified sketch of the method. The symbol *A* marks a hydraulic jack; *P* is a round test plate about 1 ft. in diameter; *D* is a strong metallic beam fixed to the containers *C*, which are movable and may be loaded with water or sand; *E* is a

recording drum on which the time-settlement curve is traced automatically. Casing *F* protects the walls of the experimental pit from caving in.

**14:20. Geophysical Methods of Soil Exploration.**—There are two geophysical methods of soil exploration, namely, the resistivity method and the seismic method,<sup>18,19</sup> which are discussed here.

*a. Resistivity or Potential Method.*—The principle involved in this method is shown in Fig. 14:23*a*. An electric current is caused to flow through the earth mass between the electrodes  $C_1$  and  $C_2$ .

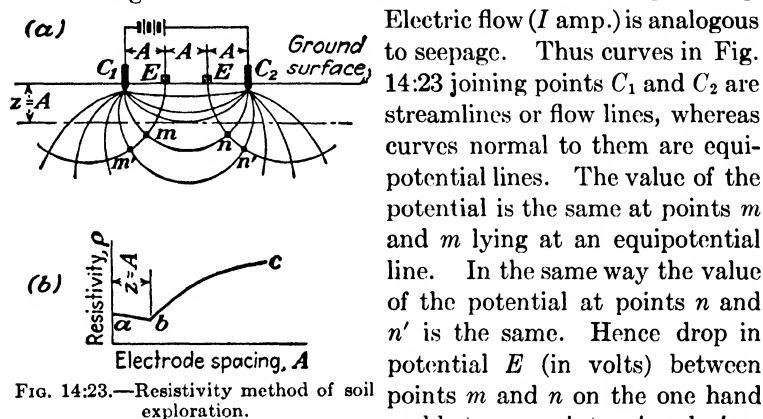


FIG. 14:23.—Resistivity method of soil exploration.

Electric flow ( $I$  amp.) is analogous to seepage. Thus curves in Fig. 14:23 joining points  $C_1$  and  $C_2$  are streamlines or flow lines, whereas curves normal to them are equipotential lines. The value of the potential is the same at points  $m$  and  $m'$  lying at an equipotential line. In the same way the value of the potential at points  $n$  and  $n'$  is the same. Hence drop in potential  $E$  (in volts) between points  $m$  and  $n$  on the one hand and between points  $m'$  and  $n'$  on the other is the same and can be measured at the intermediate electrodes  $E, E'$ . Electrode spacings  $C_1E = EE' = E'C_2$  are made equal. They are designated by the letter  $A$  and expressed in centimeters. The specific resistivity of the soil  $\rho$ , expressed in ohm-centimeters, is the resistance in ohms between parallel faces of a centimeter cube of the earth material:

$$\rho = 2\pi \frac{AE}{I} \quad (14:4)$$

or if the electrode spacing is expressed in feet,

$$\rho = 191 \frac{AE}{I} \quad (14:5)$$

When the electrode spacing  $A$  is varied, different values of the specific resistivity  $\rho$  of the earth material are obtained and plotted against the electrode spacing  $A$ . A typical resistivity curve is shown in Fig. 14:23*b*. A rather flat or even descending distance

*ab* of the curve shows that down to a certain depth  $z$  equal to electrode spacing  $A$ , there is soft earth mass (sand, loam, clay, etc.). At a depth  $z = A$  there is another material of high resistivity such as rock, and this circumstance is shown by the ascending branch *bc* of the resistivity curve.

*b. Seismic Method.*—Sound waves travel in soft earth materials such as sand, clay, or loam with velocities from 1,000 to 6,000 ft.

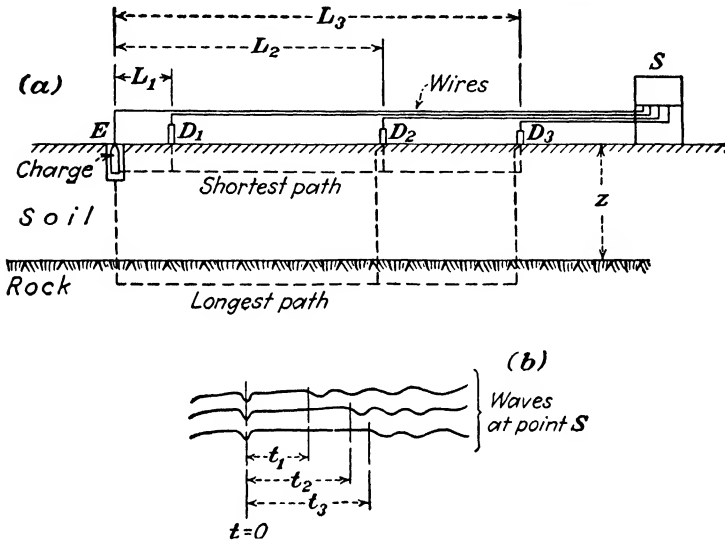


FIG. 14:24.—Seismic method of soil exploration.

per sec. Rocks or crystalline matter transmit such waves at 16,000 to 20,000 ft. per sec.

Of the two methods of seismic soil exploration, that of refraction shooting is used for engineering purposes. The other method, that of reflection shooting in which waves reflected from different strata are considered, is not well adapted for shallow investigations.

In the case of refraction shooting, a blasting cap or small charge of dynamite is exploded at point *E* (Fig. 14:24*a*). This point then becomes the center of a wave disturbance. Waves from center *E* propagate through soil and through rock in all directions, from which only those toward the seismograph *S* are shown. Detectors *D*<sub>1</sub>, *D*<sub>2</sub>, *D*<sub>3</sub> pick up this disturbance and carry the impulses to three galvanometers, which record them on a moving photographic film (Fig. 14:24*b*). In the same way the

time moment of explosion ( $t = 0$  in Fig. 14:24*b*) is also recorded on that film through a wire wound around the blasting cap. As soon as the disturbance reaches a detector—for instance,  $D_2$ —it is recorded on the film referred to. (In this case the time moment  $t_2$  is recorded.) The disturbance may come first through the earth and afterward through the rock, or vice versa; in any case, only the earlier of these two events may be clearly located at the film. In the case of a detector located very close to the center of wave disturbance, such as  $D_1$ , distant  $L_1$  from the center  $E$ , the disturbance comes first through the soil, and this serves to determine the speed  $V_s$  of the wave propagation in soil:

$$V_s = \frac{L_1}{t_1} \quad (14:6)$$

To reach detector  $D_3$  through the rock, the wave has to go down and again up in the soil, passing a total distance  $z + z = 2z$ , the corresponding velocity being  $V_s$  [formula (14:6)]. Besides, the horizontal distance  $L_3$  through the rock also has to be passed (velocity  $V_r$ ). From these considerations

$$t_3 = \frac{2z}{V_s} + \frac{L_3}{V_r} \quad (14:7)$$

from which the depth  $z$  of the rock is easily determined.

The problem may be solved if there are at least three detectors, as shown in Fig. 14:24. More than two detectors permit checking of the result, since there will be more than one linear equation for determining one unknown  $z$  which is the depth of the rock. It may happen that a certain detector is reached simultaneously by two waves, that coming through the soil and that passing rock. The distance of this detector from the center  $E$  is termed "critical shooting distance,"  $L_{cr}$ . A fairly close approximation is

$$z = 0.45L_{cr} \quad (14:8)$$

According to the classification of field tests given in the beginning of division C of this chapter, the resistivity method is a static test of physical properties of the soil, whereas the seismic method is a dynamic test. Other examples of dynamic tests are vibration tests, described in the following section.

**14:21. Vibration Tests.**—*a. Exciting and Measuring Vibrations.* The general idea of a vibration soil test consists in loading the

earth surface at various places by gradually changing forces that follow the sine law. Frequency and size of these forces can be measured. The earth mass vibrates with forced and damped oscillations.

A simple oscillator consists of two eccentrically supported disks which revolve in opposite directions. For this purpose a small electric motor of 1 to 2 hp. may be used. Eccentricity of the disks

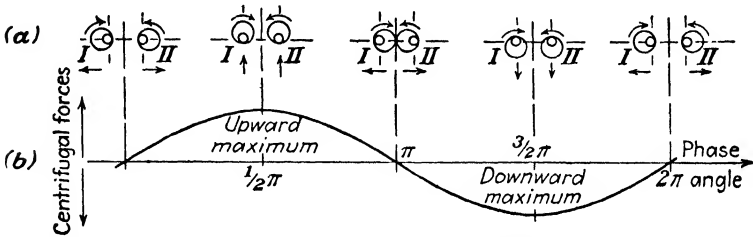


FIG. 14:25.—Exciting vibrations. (a) Two revolving masses; (b) centrifugal forces in a sine form. (After Bernhard.<sup>23</sup>)

and the motor input may be changed, and this modifies the value of the centrifugal force and the speed of revolution and hence the frequency of the exciting forces. Since the disks referred to rotate in opposite directions, horizontal forces are balanced, and vertical forces are superimposed in the form of a sine curve (Fig. 14:25). Vibrations may be excited in two ways: (1) beginning with low

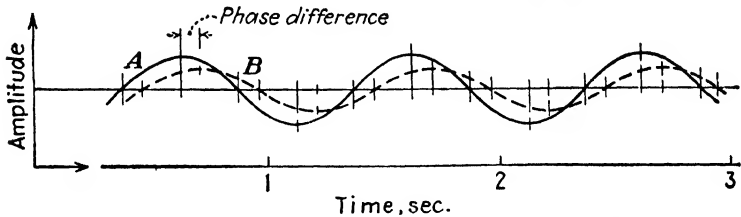


FIG. 14:26.—Amplitude-time curves. (After Bernhard.<sup>23</sup>)

frequencies and gradually increasing them or (2) working with constant frequency.

To measure the amplitude of the excited vibrations at different points of the earth mass, standard seismographs are used. They may be connected with an oscillograph which permits combining on one diagram up to 24 seismographic readings at different points. In Fig. 14:26 amplitude-time curves A and B, recorded by two seismographs at two different points I and II, are shown. The

phase difference of both curves indicates the time required by the wave to cover the distance between the two points in question. The phase speed is indicative so far as the probable "bearing value"

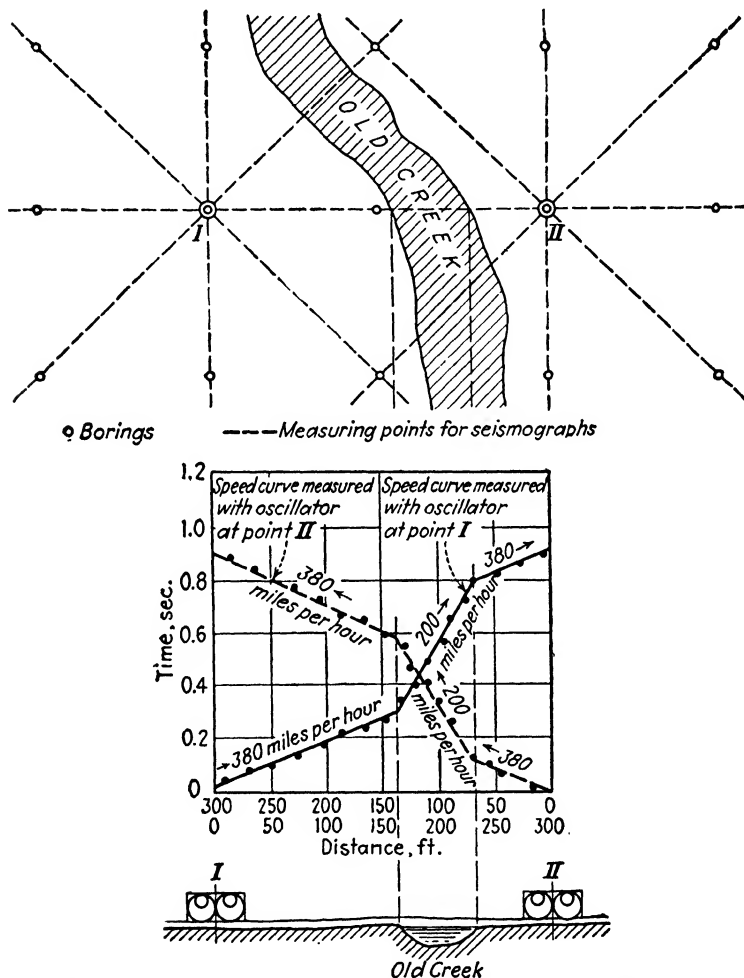


Fig. 14:27.—Vibration-test data and boring data compared. (After Bernhard.<sup>11</sup>)

(Sec. 8:3) is concerned. Loose sand has a low phase speed (250 to 350 m.p.h., frequency 20 to 25 cycles per sec.), whereas the phase speed in sandstone is about 1,450 m.p.h. Again, the phase

speed in clay is about 400 m.p.h. and close to 1,000 m.p.h. in dense gravel.

When vibrations are excited with increasing frequency, for each frequency the amplitude and the settling of the oscillator or the power input of the driving motor can be measured, and the so-called resonance curve can be plotted (frequency against amplitude, settling, or power). The natural frequency of the oscillator on the given soil being determined, *i.e.*, its resonance point, some idea of the "bearing power" of the soil also may be formed, since higher frequency corresponds to a higher bearing power. For instance, the natural frequency for clay is about 23 cycles per sec. and about 30 cycles for gravel.

*b. Examples.*—In Fig. 14:27 marshy land is shown with a covered old creek which has not been disclosed by the borings.

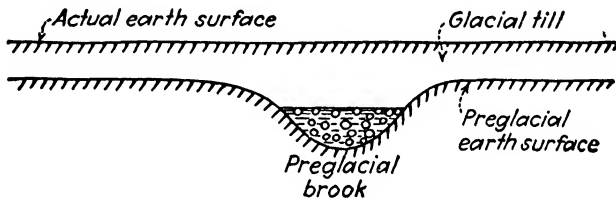


FIG. 14:28.—A subsurface gorge.

The latter are shown with circles in the figure, and symbols I and II indicate positions of the oscillator. Amplitude-time curves having been constructed as in Fig. 14:26, it is possible to plot the time required by the wave to reach a point against the distance of that point from the oscillator. Specifically, curves at the bottom of Fig. 14:27 have been plotted in this way, and the change in speed from 380 to 200 m.p.h. indicates the change in soil profile. Similar problems are to be solved in preliminary soil investigations for earth dams when subsurface gorges are sought (Fig. 14:28). An invisible preglacial creek with a gravel bed may be covered by glacial till, and this is very dangerous for the dam, which may be undermined by it. As a rule, such subsurface gorges are located at the present time by digging trenches (Sec. 14:5).

*c. Literature.*—Thorough research along these lines is being done by the German Research Society for Soil Mechanics ("Degebo"<sup>20</sup>). A comprehensive report of this society has been translated into English by the Public Roads Administration.<sup>21</sup> There are also pam-

phlets<sup>22</sup> and papers in technical journals.<sup>23</sup> Tschebotarioff's contribution as discussed in Chap. XII (ref. 20) should be remembered.

**14:22. Dynamics of Earth Masses.**—Vibration soil tests represent only one item in the study of the behavior of vibrating earth masses. Obviously, there is a voluminous literature on earthquakes and the discussion of elastic waves in the theory of elasticity, which could furnish comprehensive data along these lines. What is required, however, is a thorough experimental study of the behavior of a vibrating earth mass and systematization and integration of all existing data. This study would be of great importance for airports, railroads, and highways and also for factory design and would constitute what may be termed *dynamics of earth masses*.

#### References

1. H. A. MOHR: "Exploration of Soil Conditions and Sampling Operations," 3d ed., publication of the Harvard School of Engineering, Cambridge, Mass., 1943.
2. M. JUUL HVORSLEV: "The Present Status of the Art of Obtaining Undisturbed Samples of Soil," a preliminary report of the Committee on Sampling and Testing, Soil Mechanics and Foundation Division, A.S.C.E., Cambridge, Mass., 1940.
3. Sprague and Henwood, Inc., Scranton, Pa.: Sampling and Sampling Devices, *Bull.* 36-A, 1937.
4. American Instrument Co., Silver Spring, Md.: *Catalog* 15, 1939, pp. 39-80.
5. GLENNON GILBOY and SPENCER J. BUCHANAN: Earths and Foundations, committee report, *Proc. A.S.C.E.*, vol. 59, May, 1933.
6. J. L. BEATTY: *Eng. News-Record*, vol. 108, 1932.
7. Fort Peck Division, Corps of Engineers, U. S. Army: "Notes and Principles and Applications of Soil Mechanics," Fort Peck, 1939.
8. New Soil Sampler for Deep Tests, *Eng. News-Record*, vol. 116, 1936.
9. H. L. JOHNSON: Improved Sampler and Sampling Technique for Cohesionless Materials, *Civil Eng.*, vol. 10, June, 1940.
10. KARL TERZAGH: abstract of his lectures, *Third Tex. Conf. on Soil Mech. and Foundation Eng.*, Feb. 23 and 24, 1940 (published by the University of Texas).
11. CURT F. KOLLBRUNNER and CHARLES LANGER: "Probebelastungen und Probebohrungen," Privat-Gesellschaft für Bodenforschung und Erdbaumechanik, Zürich, 1939.
12. Statens Järnvägers Geotechniska Kommission: "Slutbetänkande," official publication, Stockholm, 1922.
13. GEORGE PAASWELL: *Eng. News-Record*, vol. 106, Apr. 2, 1931.
14. W. SIMPSON: "Foundations," Constable & Company, Ltd., London, 1928.
15. A. SCHOKLITCH: "Der Grundbau," Verlag Julius Springer, Berlin, 1932.
16. W. S. HOUSEL: A Practical Method of the Selection of Foundations, *Univ. Mich. Dep. Eng. Research, Eng. Research Bull.* 13, 1929.

17. W. S. HOUSEL: *Eng. News-Record*, vol. 110, Feb. 23, 1933.
18. E. R. SHEPARD: Subsurface Explorations Made by Resistivity and Seismic Methods, *Public Roads*, vol. 16, June, 1935.
19. KARL SUNDBERG: Determination of Depth to Bedrock, *Trans. Second Congr. on Large Dams*, vol. 4, Paper D-46, 1938.
20. *Veröffentlich. Inst. der deut. Forschungsgesellschaft für Bodenmechanik* ("Degebo"), Technische Hochschule, Berlin, Heft 1, 1933; Heft 4, 1936.
21. A. C. BENKELMAN (trans.): "Application of the Dynamic Method of Soil Testing in Practices" (mimeographed), publication of Degebo.
22. FRANZ MEISTER: "Die dynamischen Eigenschaften von Strassen," Martin Boerner, Halle (Saale). Contains comprehensive bibliography. There is an English translation (mimeographed), also by A. C. Benkelman.
23. RUDOLPH K. BERNHARD: *Civil Eng.*, April, 1937; *Proc., Sixteenth Annual Meeting of the Highway Research Board*, November, 1936; *A. I. M. M. E. Tech. Pub.* 834, 1938; *Penn. State College Bull.* 49, 1939.



## APPENDIXES



## APPENDIX A

### WET MECHANICAL ANALYSIS OF SOILS

**A: 1. Theory and Practice of the Hydrometer Test.**—The following discussion refers to the streamlined hydrometer (Fig. 1:3).

*a. Sample.*—Only that portion of a soil sample which passes through a No. 10 sieve (or some other fine sieve) is used in the hydrometer test, and admittedly its percentage with respect to the whole sample is also determined. Hygroscopic moisture content is found and deducted from the weight of the part of the sample that passes through the sieve referred to. Let  $W_0$  equal the net weight of the sample computed in this way. The value of  $W_0$  is usually about 20 to 50 g. in the case of clays and about 50 to 100 g. in that of sands.

*b. Pretreatment.*—The Public Roads Administration recommends the following pretreatment of samples: (1) If the plasticity index of the given soil is less than 20, the sample is placed in a beaker with 200 cc. of water and allowed to stand for 18 hr.; (2) if the plasticity index is greater than 20, the sample is slowly mixed with 100 cc. of 6 per cent hydrogen peroxide, ( $H_2O_2$ ), and placed in an oven at  $110^\circ C.$  for 1 hr., after which 100 cc. of water are added and the mixture is allowed to stand for at least 18 hr. Hydrogen peroxide pretreatment is supposed to remove organic matter that may cement soil particles and hence interfere with the separation of the material into grade sizes.

*c. Mixing and Shaking.*—After pretreatment the sample should be thoroughly mixed in the cup of an electric rotary drink mixer. Deflocculating agents such as a normal solution of sodium silicate (or sodium oxalate) are introduced into the cup before the mixing or into the beaker during the pretreatment period. Sodium salts are used on this occasion to transform the given clay into a Na-clay easily dispersed (compare the concept of "base exchange," Sec. 1:8). The amount of the deflocculating agent is from 5 to 10 cc., though some investigators use only about  $\frac{1}{2}$  cc. Correction in the hydrometer reading for a deflocculating agent may be found as the difference in readings in clean water and in water with the given amount of the deflocculating agent. The contents of the cup are then placed in a graduate carrying a mark corresponding to 1 liter (1,000 cc.) and filled with water up to that mark. Distilled water is preferable, but clean colloidless water may also be used. To avoid recording fluctuations of the temperature during the first 15 min. of the test, it is advisable to keep a reasonable supply of water in the room before the test. The filled graduate is thoroughly shaken for at least 1 min., the mouth being covered with the palm of the hand or with a rubber pad, and is placed on the table.

*d. Reading and Recording.*—As soon as the graduate is placed on the table, a stop watch is started, a hydrometer is introduced into the suspension, and

readings are taken at different times after the start—for example,  $\frac{1}{2}$ , 1, 5, 15, 45 min., 2, 5, 24 hr., etc. Water, as it comes into contact with the stem of the hydrometer, rises owing to capillary action, and a meniscus is formed. Readings are made *at the top of this meniscus*. The hydrometer reading may be represented in the form  $1 + R/1,000$ . For instance, if the reading is 1.0215, the value of  $R$  equals 21.5, and it is advisable to read and to record this value only.

The hydrometer remains in the suspension for the first 2 min.; afterward it is taken out, rinsed, and dried with a clean cloth. For subsequent readings the hydrometer is introduced into the suspension slowly to reach an expected position and to avoid as much fluctuation as possible. After each reading the hydrometer is removed and cleaned as specified; sometimes between two readings it is left to float in clean water. The temperature is measured once during the first 15 min. and *after each reading* subsequently. The thermometer readings are made generally within  $\frac{1}{2}^{\circ}$  C., sometimes within  $0.1^{\circ}$  C. The five first columns of the following table are test records, and figures in the rest of the table are computed according to the theory developed here. Strictly speaking, in making computations one should use the data of column 3 in the table (see below) for estimating the *average temperature* from the beginning of the test *up to the given reading*. These average temperatures are to be used in computations.

HYDROMETER TEST RECORD

1	2	3	4	5	6	7	8	9	10
Date	Hour	Tem- pera- ture	Time since start	Readings		Equiv. diam., $d$	Cor- rected reading, $R + m_T$	Per cent "finer than"	No. of the hy- drom- eter
				$R'$	$R = R' + c_m$				
Jan. 15, 1940	2:15 P.M.	23.0°C.	15 min.	11.8	12.2	0.013	12.7	87.3	A 8934

*e. Meniscus Correction.*—The height of the meniscus, or "meniscus correction"  $c_m$ , is determined experimentally once for all by taking readings at the top of the meniscus and at its bottom (reading "through water"). Since the divisions of a hydrometer increase downward, the meniscus correction  $c_m$  is always positive and is to be added to the hydrometer reading. The value of this correction depends on the length of a division of a hydrometer and for common types fluctuates between 0.3 and 1.0. In order to have the meniscus well developed, it is necessary to keep the stem clean—to wash it with soap or alcohol before the test.

*f. Determination of the Equivalent Diameter.*—Each hydrometer reading furnishes a point on the size distribution curve. It will be first shown how to determine the abscissa of this point.

Since at the start of the hydrometer test the suspension is thoroughly mixed there are, at each horizontal section of the graduate, particles of all the sizes present in the given sample in their natural concentration. As sedimentation proceeds, all grains of a given diameter settle with equal velocity; hence their concentration at all horizontal sections of the graduate is the same. Owing to the limited supply of particles from above, coarser particles gradually fall down, however. Thus at a given time moment there are, at a given horizontal section of the graduate, particles *finer than* a given diameter only, though in their natural concentration. The horizontal section of the hydrometer passing at the given time moment through the middle of the hydrometer bulb will be considered. This is practically the center of buoyancy of the hydrometer. The distance from a given hydrometer reading  $H$  cm. to the middle of the bulb can be *measured directly* once for all. Hence if the reading is made at a time moment  $t$  min. after the start of the test, the velocity of fall is  $H/t$  cm. per min. or  $H/60t$  cm. per sec. Using the Stokes formula [(1:1), Sec. 1:3 of the text], the diameter of the coarsest particle (in millimeters) at the center of the bulb may be determined,  $v = H/60t$  being placed in formula (1:1),  $s_0 = 1$  being assumed, and the diameter of a particle being considered as  $d$  cm. =  $2r$  cm. =  $20r$  mm.

$$d = \sqrt{\frac{30\eta H}{g(s-1)t}} \quad (\text{A:1})$$

It is to be borne in mind that  $d$  is the *equivalent diameter*, i.e., the diameter of an ideal spherical particle made of the same material as the actual soil particle and sinking down with the same velocity.

#### VISCOSITY OF WATER AND TEMPERATURE CORRECTION

Temperature		Viscosity of water, c.g.s. units		Temperature correction, $m_T$
Deg. C.	Deg. F.	$\eta$	$\sqrt{\eta}$	
16	60.8	0.011,111	0.105	-0.7
18	64.4	0.010,559	0.103	-0.4
20	68.0	0.010,050	0.100	0.0
22	71.6	0.009,579	0.098	0.4
24	75.2	0.009,142	0.096	0.8
26	78.8	0.008,737	0.093	1.2
28	82.4	0.008,360	0.091	1.8
30	86.0	0.008,007	0.090	2.3

As soon as the value of  $d$  is known, its logarithm is plotted as the abscissa of a point of the size distribution curve.

Thus in any one test the variables are  $H$ ,  $t$ , and  $\eta$ , the latter value depending on the temperature.

Formula (A:1) may be rewritten thus:

$$d = k_1 \sqrt{\eta \frac{H}{t}} \quad (\text{A:1a})$$

where  $k_1 = \sqrt{\frac{30}{981(s-1)}}$  is a constant to be used in computing the values in column 7 of the table on page 476.

*g. Correction for the Finite Size of the Graduate.*—When measuring distances  $H$ , one has to remember that formula (A:1) corresponds to an infinitely wide graduate. Designating the cross section of the experimental graduate by  $A$  and the volume of the bulb by  $V$  and neglecting the influence of the stem, we have a correction  $c_g = \frac{1}{2}(V/A)$  to be subtracted from each value of  $H$  directly measured (Fig. A:1). The hydrometer is held by hand, and its

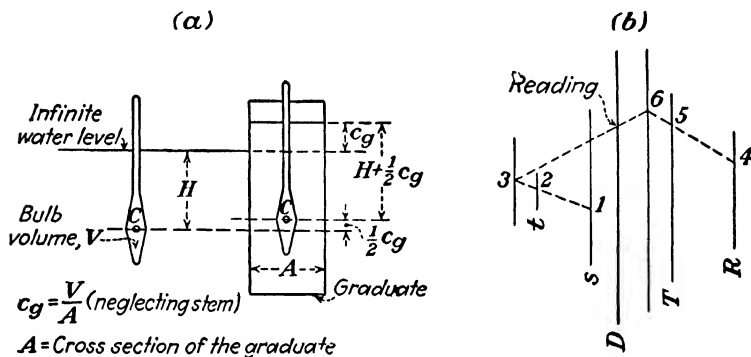


FIG. A:1.—Hydrometer test. (a) Correction for finite size of the graduate; (b) Casagrande's nomograms in a sketchy representation.

bulb only is immersed in water, placed in the *given* experimental graduate. The water level in the graduate will then rise to a distance  $V/A$ .

*h. Temperature Correction.*—There is a notice on the hydrometer showing its calibration temperature, for instance,  $20^\circ/20^\circ\text{C}$ . The latter notice means that at a temperature  $T_c = 20^\circ\text{C}$ . the hydrometer shows the ratio of the density of the suspension to that of distilled water at that temperature,  $(s_0)_c$ . Hence, if the hydrometer placed in a suspension at the calibration temperature shows  $1 + R/1,000$ , the true density of that suspension is  $[1 + (R/1,000)]: [(s_0)_c]$ . The value of  $(s_0)_c$  at  $68^\circ\text{F}$ . (or about  $20^\circ\text{C}$ .) is 0.998203.

At a temperature  $T$  higher than that of calibration  $T_c$ , the reading is different for two reasons: (1) The density of the water decreases, and (2) the bulb expands. The expansion of the bulb causes an increase in buoyancy, which is accompanied by the upward shifting of the hydrometer and hence by an increase in reading. Owing to an increase in temperature from  $T_c$  to  $T$ , the water rarefies, the hydrometer shifts down, and the reading decreases. Hence, if the hydrometer reading is taken at a temperature different from the calibration temperature, the temperature correction should be considered.

A reading of the hydrometer is composed of two parts: (1) that part due

to the density of the water and (2) that part due to the presence of suspended soil particles. The latter part may be assumed to be independent of the temperature. This means that the temperature correction does not depend on the amount of suspended soil particles in the suspension and, if determined for the case of distilled water, would be the same for any suspension.

The hydrometer placed in distilled water at the calibration temperature  $T_c$  shows unity, and, if placed in distilled water at the temperature  $T$ , shows  $(s_0)_T/(s_0)_c$ , where  $(s_0)_T$  is the density of distilled water at that temperature. To bring this reading back to the true reading "unity" a correction  $c'$  is needed:

$$c' = 1 - \frac{(s_0)_T}{(s_0)_c} = \frac{(s_0)_c - (s_0)_T}{(s_0)_c} \quad (\text{A:2})$$

or simply

$$c' = (s_0)_c - (s_0)_T \quad (\text{A:3})$$

since the value of  $(s_0)_c$  in the denominator of formula (A:2) is close to unity.

Designate the volume of the bulb of the hydrometer conventionally as "unity." Then at a temperature  $T$  this volume would be  $1 + \epsilon(T - T_c)$ . The symbol  $\epsilon$  designates the coefficient of expansion of glass which may be estimated at 0.000025 per degree centigrade. If, instead of calibrating the given hydrometer with a "unity" bulb, a hydrometer with a bulb volume  $1 + \epsilon(T - T_c)$  were calibrated, the reading at the temperature  $T_c$  instead of being unity would be  $1 + \epsilon(T - T_c)$  on the assumption that the readings of two hydrometers taken simultaneously in a suspension are proportional to the volumes of their bulbs. Hence the correction for the expanded bulb is

$$c'' = -\epsilon(T - T_c) \quad (\text{A:4})$$

The total temperature correction would be

$$c' + c'' = (s_0)_c - (s_0)_T - \epsilon(T - T_c) \quad (\text{A:5})$$

This correction refers to the total hydrometer reading  $1 + R/1,000$ . If referred to the reading  $R$  only, the temperature correction (to be designated with  $m_T$ ) is

$$m_T = 1,000 [(s_0)_c - (s_0)_T - \epsilon(T - T_c)] \quad (\text{A:5a})$$

Since in reality the bulb expands in a rarefied and not in the original suspension, there is a small error in the preceding computations which is quite negligible, however.

It is obvious that the trend of derivation of formula (A:5a) does not change if  $T < T_c$ . The values of  $m_T$  computed by formula (A:5a) are given in the last column of the table on page 477. At temperatures higher than the calibration temperature ( $T > T_c$ ), the correction  $m_T$  is positive; at lower temperatures ( $T < T_c$ ), the correction is negative.

*i. Determination of the Percentage "Finer than."*—If the graduate were filled with a uniform suspension containing soil particles in exactly the same proportion as at the center of buoyancy of the hydrometer floating in the given nonuniform suspension, the hydrometer reading would be the same in either case. Also, the coarsest particles in both suspensions would be of the same

size [diameter  $d$ , as determined by formula (A:1)]. For further considerations, this hypothetical uniform suspension will be substituted for the actual non-uniform suspension. Designate by  $x$  the weight of particles "finer than" the diameter  $d$  contained in the graduate filled with that hypothetical suspension. Their volume will be then  $x/s$ , where  $s$  is the specific gravity of the particles. Remembering that the total volume of the graduate is 1,000 cc. and assuming approximately that 1 cc. of water weighs 1 g. at any laboratory temperature,

$$1,000 - \frac{x}{s} + x = 1,000 \left( 1 + \frac{R + mT}{1,000} \right) \quad (\text{A:6})$$

from which

$$x = (R + mT) \frac{s}{s - 1} \quad (\text{A:7})$$

The percentage of particles "finer than" the given diameter  $d$  is, then,

$$\text{Percentage} = 100 \frac{x}{W_0} = 100 \frac{R + mT}{W_0} \frac{s}{s - 1} \quad (\text{A:8})$$

The latter formula may be written in the form

$$\text{Percentage} = k_2(R + mT) \quad (\text{A:8a})$$

where  $k_2$  is a constant to be used in computing the values in column 9 of the table on page 476. Formulas (A:1a) and (A:8a) furnish a complete solution of the given problem.

When the hydrometer test is finished, the contents of the graduate are washed through a fine sieve, for instance, No. 325. The material retained on No. 325 sieve is dried out and separated into grades by means of coarser sieves.

*j. Nomograms.*—Instead of applying formula (A:1) to determine the diameter of particles  $d$ , nomograms traced according to a proposal by A. Casagrande<sup>2</sup> are in use. The hydrometer is measured as described above, and readings are correlated to the heights of fall by plotting both on different sides of the vertical line  $R$  of the nomogram (Fig. A:1b). Point 3 is found by joining points 1 and 2, corresponding to the specific gravity  $s$  of the particles and the temperature  $t$ . Point 6 lies on the continuation of the line, passing through points 4 (height of fall) and 5 (time of fall). The diameter is read at the intersection of line 3-6 with line  $D$ . There are also special slide rules.

**A:2. Other Methods of Wet Analysis.**—Other methods of wet analysis sometimes used by engineers are the *pipette method* and the *elutriation method*.<sup>3,4,5</sup> The pipette method is based on the principle already discussed in the development of formula (A:1) namely, that at a certain time  $t$  after the beginning of the experiment and at a level  $H$  below the surface of the suspension, the latter will contain the full concentration of the material "finer than" that corresponding to the speed of fall  $H/t$ . Using a pipette, a sample, 10 or 20 cc., is taken at a given level  $H$  at various intervals and is dried out. If  $W$  and  $X$  are the weights of solid particles in the given sample at a time  $t$  and at the beginning of the experiment ( $t = 0$ ), respectively, the percentage of particles "finer than" that corresponding to the velocity of fall  $H/t$  is  $100X/W$  [compare formula (A:8)]. Temperature variations admittedly influence this result.

As an example of an elutriation installation, the apparatus used in the studies for Cobble Mountain Dam (Springfield, Mass.) may be described.<sup>4</sup> There were three glass cones of different diameters, each provided with an inlet tube running to the bottom and an outlet tube running to the next cone. The material to be tested was first placed in a special funnel, from which it was carried successively to the three cones referred to and afterward to a large glass jar. There was a rising column of water in each cone, and sedimentation proceeded against the direction of movement of the water. The largest particles were deposited in the narrowest cone (the first), and the smaller were carried over into the next cone (medium diameter) and afterward to the widest. In each cone the particles settled according to their diameter. The test was continued until the overflow discharge became practically clean; the tested sample was thus separated into four fractions.

#### References

1. A. CASAGRANDE: "Die Aräometer-Methode zur Bestimmung der Kornverteilung der Böden und anderen Materialien," Julius Springer, Berlin, 1934.
2. Nomograms published by Julius Springer, Berlin, W-9.
3. U. S. Dept. Agr. Tech. Bull. 170, January, 1930.
4. HARRY H. HATCH: *Trans. A.S.C.E.*, vol. 99, 1934.
5. W. C. KRUMBEIN: *Jour. Sedimentary Petrology*, vol. 2, 1932; vol. 3, 1933; vol. 5, 1935; also W. C. KRUMBEIN and FRANCIS PETTLOHN: "Handbook of Sedimentary Petrology," D. Appleton-Century Company, Inc., New York, 1938.
6. Different methods of wet mechanical analysis are fully described in Chap. II of BERNARD A. KEEN: "The Physical Properties of Soil," Longmans, Green and Company, London, 1931. For a historical review, see W. C. KRUMBEIN: *Jour. Sedimentary Petrology*, vol. 2, 1932.

## APPENDIX B

### VERTICAL PRESSURE FROM A DISTRIBUTED LOAD

**B:1. General Principle.**—Vertical pressure from a unit load  $p$  uniformly distributed around an area  $A$  is computed by subdividing the given area into small elements  $dA$  and assuming that the load acting on an element  $p \cdot dA$ , may be considered as a concentrated load. Applying formula (4:5) the elementary vertical pressure  $d\sigma_z$ , corresponding to that element, is

$$d\sigma_z = k \frac{p \cdot dA}{z^2}$$

The sum of all elementary pressures expressed by the foregoing formula is the vertical pressure  $\sigma_z$  at the given point. The best way to compute this sum

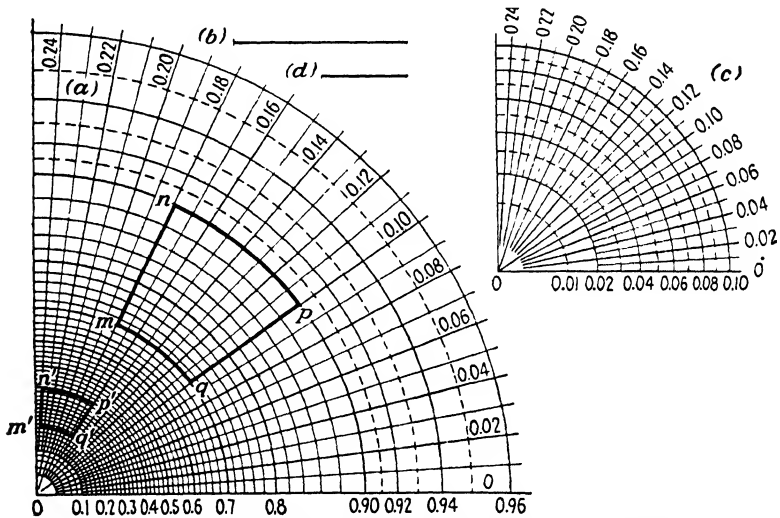


FIG. B:1.—Newmark's method of determining vertical pressure.

is to employ *graphical integration*. Several methods of such integration and many references may be found in *Trans. A.S.C.E.*, vol. 103, 1938.

**B:2. Newmark's Chart.**—Newmark's chart for determining vertical pressure is shown in Fig. B:1. The problem is to determine vertical pressure at point  $O$  (see the left lower corner of the chart). The foundation plan is drawn up to the same scale as the chart. For this purpose the distance shown under  $b$  in Fig. B:1 is considered to be equal to the depth  $z$  at point  $O$ , where the

vertical pressure  $\sigma_z$  is to be determined. The plan in question, drawn up on tracing paper or tracing cloth, is laid on the chart so that the point under which the pressure is desired falls on point  $O$ . A "large rectangle" on the chart bounded by two circular arcs (such as marked 0.7 and 0.8 or 0.2 and 0.3, and so on) and two radii (such as 0.20 and 0.22 or 0.02 and 0.04, and so on) has a value of 0.002. Each "large rectangle" is subdivided into ten small ones. The vertical pressure  $\sigma_z$  is then estimated by counting the large rectangles covered by the foundation plan. For example, assume that area  $mnpq$ , bounded by curves  $mq$  and  $np$ , and straight lines  $mn$  and  $pq$ , is the plan of a building loaded with 5 tons per sq. ft. Area  $mnpq$  occupies eight rectangles in question; hence vertical pressure at point  $O$  and at a depth  $z$  equals

$$\sigma_z = 8 \times 0.002 \times 5 = 0.08 \text{ ton per sq. ft.}$$

If point  $O$  falls within the plan, the procedure must be carried through four times. Fractions of rectangles are estimated. Numerals shown on the chart are not needed in practical applications. Figure B:1c is the increased portion of the graph close to point  $O$ . In this case, distance shown in Fig. B:1d equals one-tenth of the depth  $z$ . It is obvious that areas  $mnpq$  and  $m'n'p'q'$ , loaded with the same unit load, produce the same vertical pressure at point  $O$  for occupying equal numbers of rectangles on the diagram (Fig. B:1a).

#### Reference

NATHAN M. NEWMARK: Graphical Procedure for Computing Vertical Pressures, *Univ. Ill. Eng. Exp. Sta. Circ. 24*, 1935; also "Graphical Procedure for Computing Vertical Pressures" (mimeographed), University of Illinois, Urbana, Ill., 1937.

## APPENDIX C

### SHEARING TESTS

**C:1. Direct Shearing Test.**—Apparently, the device for direct shearing test in sands was first constructed by Leygue in France and by Krey<sup>1</sup> in Germany and introduced in the United States by the late Prof. Cain of the University of North Carolina.<sup>2</sup> Subsequently, this device was improved by both Terzaghi and A. Casagrande and their collaborators.

There are two methods of shear application. In one of these methods the pulling force is built up at a predetermined rate (“controlled stresses”). In the other the displacement of a shearing box with respect to the other proceeds at a predetermined rate (“controlled strains”). Both types of machines and other types of shear devices are being steadily improved.<sup>3,4,5,6</sup>

A shearing machine is generally provided with two dials, a vertical one to check the thickness of the sample and a horizontal one to measure displacements. In performance of the shearing test on sands, several complications arise: (a) it is difficult to keep sand grains away from the surfaces of contact of the boxes themselves; (b) a part of the normal force  $N$  is transmitted to the walls of the boxes owing to friction; (c) the shear surface tends to bulge up. To avoid this latter inconvenience and to keep the shearing surface straight, the sand sample is placed between metallic plates provided with thin but stiff metallic ribs.

**C:2.—Triaxial Compression Test.**—The *triaxial compression test*, termed also the *cylinder test*, has been applied in Europe for many years, particularly by the late Prof. Keverling Buisman of Delft, Netherlands. In the United States it was introduced in 1937 by the Army Engineers as advised by A. Casagrande. It was preceded by a series of lectures by Terzaghi in 1936.

A soil specimen enclosed in a rubber membrane is set up within a lucite compression chamber (cylinder), the latter being enclosed between a head and a base (Fig. C:1). In its turn the sample is enclosed between two porous stones. The sample is acted upon by the vertical load which is transmitted by a piston rod passing through the head of the compression cylinder; this load contributes to the formation of the major principal stress  $\sigma$ , in the sample. The minor principal stress  $\sigma_{111}$  and the intermediate principal stress  $\sigma_{11}$  are formed by the liquid (glycerin or water) pumped in from the pressure reservoir. To build up pressure in the cylinder, bellows may be also used. The values  $\sigma_{11}$  and  $\sigma_{111}$  are equal and constant throughout a given test, whereas the value of  $\sigma$ , which at the beginning of the test equals  $\sigma_{11}$  and  $\sigma_{111}$ , is gradually increased until the failure occurs. The vertical deformation of the sample is measured by a dial.

In the case of sand volume changes of the sample are recorded. The sample

is completely saturated before the test, so that its volume changes can be read on the vertical pipette connected with the sample. Before starting saturation, vacuum is applied to the top of the sample. The Harvard Soil Mechanics Laboratory subjects the sample to a vacuum of about 72 to 74 mm. of mercury for 5 min., after which the vacuum is reduced to 60 to 65 mm. in the case of coarse sand or completely discontinued in the case of fine sand. Then

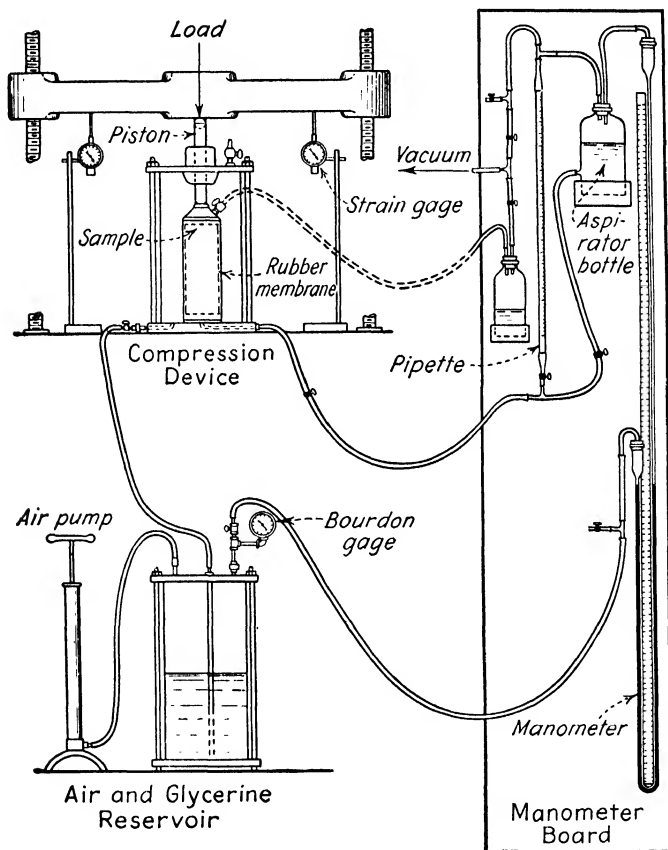


FIG. C:1.—Triaxial Compression Test [from *Trans. A.S.C.E.*, vol. 109 (1944), see ref. 7].

water is permitted to saturate the sample from the bottom. It should be noticed that the preparation of the sand sample is done using special forming jackets which stay on the sample until saturation is completed. Next the height and the average cross section of the sample are carefully measured; the cylinder placed into position; liquid forced into the compression chamber; and the vertical load applied. Load increments are added every minute on the minute, and the volume changes are recorded every minute on the half

minute. The load increments are so chosen that the time required to reach the ultimate strength will be 20 to 30 min.

**C:3. Types of Failure in a Compression Test; Cause of Cracks.**—There are two principal types of failure in a nonconfined or triaxial compression test made on different materials, including concrete which in many respects approaches cohesive fragmental soil masses. If the material is brittle, it fails by sliding on one or two planes as shown in Fig. C:2a, whereas plastic material “bulges” and fails by sliding on many planes throughout the sample (Fig. C:2b). This fact is a further proof of the necessity of a subdivision of soils into two groups: those approaching an idealized fragmental mass and those approaching an elastic continuum, according to the views developed in Chap. IV. Specifically, Fig. C:2a shows that the Rankine conditions of failure are applicable to soils approaching idealized fragmental masses. The Mohr’s envelope in this instance is a straight line. Should a soil mass approach an elastic continuum, made of a perfect homogeneous material (such as a glue-like

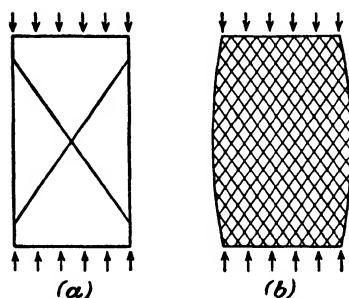


FIG. C:2.—Two types of failure in a nonconfined compression test.

moisture attracted by the particles), it probably would fail by plastic flow in a lateral direction, in which it bulges. Since there are inclusions of small fragmental masses throughout the sample, these inclusions fail according to Rankine’s conditions of failure, which create the picture shown in Fig. C:2b. The envelope in this case is not a straight line.

The subdivision of soils into two groups as specified should be done rather carefully. Not all sands behave as fragmental materials, and not all clays fail by bulging. Particularly, if a clay has a relatively rigid skeleton of mineral grains, it may fail as a brittle material (Fig. C:2a); but if remolded, it acts as a plastic body (Fig. C:2b). In a triaxial test, a dense sand may fail as brittle material (Fig. C:2a), whereas it may bulge if its voids ratio is considerable.

Referring to the work done at the University of Illinois (Sec. C:2), Brandtzaeg assumed a material made up of elements of varying strength. Some of these elements yield plastically before others, through lamellar sliding action in the direction of least resistance. According to Brandtzaeg, “The lateral compression developed in an element in the plastic stage must be balanced by lateral tension in the surrounding elements; this may be characterized as a “wedging” action against which the material is kept from a splitting failure only by the action of its stronger elastic elements which form lateral ties. As plasticity spreads throughout the material with increasing loads, it is evident that the critical lateral tensile stress or strain will be reached at which splitting failure of certain elements will occur. These many small fractures may be expected to combine into continuous cracks running parallel to the direction of the principal compressive stress.”

This view may be generalized in the form of the following statement: All

Condition of failure according to Coulomb may be obtained by combining Eqs. (5:11) and (5:12):

$$\tau = s = \sigma \tan \phi + p_i \tan \phi \quad (C:1)$$

Several investigators attempted to correct this formula. They replaced  $\tan \phi$  in the first member of Eq. (C:1) by a frictional coefficient  $f$  and the second member by a cohesional coefficient  $f_c$ , and tried to find a pressure to be used in formula (C:1) instead of internal pressure  $p_i$ . Thus the Krey-Tiedemann condition of failure was proposed:

$$\tau = f\sigma + f_c p_0 \quad (C:2)$$

where  $\sigma$  is the normal pressure at the failure line when plastic flow starts and  $p_0$  is the preconsolidation pressure. Hvorslev did not find this formula satisfactory either. He studied clays in the state of either natural consolidation

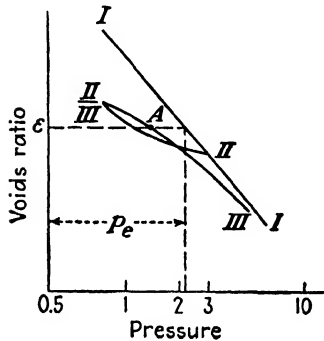


FIG. C:4.—Equivalent pressure.  
(After Hvorslev.)

ratio  $e$  in the plane of and at the moment of failure, and this function is independent of the "stress history of the sample." Dividing both sides of Eq. (C:3) by  $p_e$

$$\frac{\tau}{p_e} = f \frac{\sigma}{p_e} + f_c \quad (C:4)$$

which, if plotted, furnishes practically a straight line. The angle of friction  $\phi = \tan^{-1} f$  determined from Eq. (C:4) closely checks with the value of  $\phi$  from a nonconfined compression test.

A comparison of the results of slow and quick shearing tests led Hvorslev to the conclusion that in the case of rapid shearing tests, the viscosity of the soil may cause an apparent increase of shearing resistance (10 to 20 per cent). If the test is discontinued when plastic flow starts but the ultimate shearing value has not yet been reached, there may be a recovery of shearing resistance due to thixotropic phenomena.

#### References

1. WILLIAM CAIN: Experiments on Retaining Walls and Pressure in Tunnels, *Trans. A.S.C.E.*, vol. 72, 1911; for Leygue's article, see *Ann. ponts chaussées*, November, 1885.

2. H. KREY and I. EHRENBURG: "Erddruck, Erdwiderstand und Tragfähigkeit des Baugrundes," 3d ed., Wilhelm Ernst und Sohn, Berlin, 1932.
3. HARRY H. HATCH: Tests for Hydraulic-fill Dams, *Trans. A.S.C.E.*, vol. 99, 1934.
4. C. R. YOUNG: A Soil Shear Dynamometer, *Eng. News-Record*, vol. 123, 1939 (also discussion).
5. TRENT R. DAMES: Practical Shear Tests for Foundation Design, *Civil Eng.*, vol. 10, 1940.
6. FRED BURGGRAF: Field Tests on Shearing Resistance, *Proc. Sixteenth Ann. Meeting, Highway Research Board*, vol. 19, 1939.
7. P. C. RUTLEDGE: Relation of Undisturbed Sampling to Laboratory Testing, *Trans. A.S.C.E.*, vol. 109, 1944.
8. T. E. STANTON and F. N. HVEEM: Role of the Laboratory in the Preliminary Investigation, etc., *Proc. Fourteenth Ann. Meeting, Highway Research Board*, vol. 15, 1935.
9. F. E. RICHART, ANTON BRANDTZAEG, and R. L. BROWN: A Study of the Failure under Combined Compressive Stresses, *Univ. Ill. Eng. Exp. Sta. Bull.* 185, 1928.
10. L. JÜRGENSON: The Shearing Resistance of Soils, *Jour. Boston Soc. Civil Eng.*, vol. 21, 1934.
11. M. J. HVORSLEV: "Über die Festigkeitseigenschaften gestörter bindiger Böden" (with an abstract in English), Danmarks Naturvidenskabelige Sæfundersøgelse, Copenhagen, 1937; also *Proc. Soils and Foundation Conf., Corps of Engineers, U. S. Army, Boston, Mass.*, 1938.
12. KARL TERZAGHI: The Static Rigidity of Clays, *Jour. Rheology*, vol. 2, 1931.

## APPENDIX D

### THEORY OF CONSOLIDATION: CONSOLIDATION TEST

**D:1. Mathematical Theory of Consolidation.**—In Chap. VI the theory of consolidation was discussed in an elementary way. This theory has been originally developed using more complicated mathematics.<sup>1,2</sup>

The pore water is squeezed out from the voids of a soil with a velocity  $ki$ , where  $k$  is a coefficient of permeability, assumed to be constant during the consolidation process, and  $i$  the hydraulic gradient. By definition, the latter is the ratio of hydraulic head loss to distance on which it is lost. Its value is  $-dh/dz$ , where  $h$  is the hydraulic head and  $z$  vertical coordinate. The minus sign denotes flow in the negative direction of the  $z$ -axis. During the consolidation process, the hydraulic head  $h$ , the hydrostatic excess pressure  $u$ , and the intergranular pressure  $p$  are interconnected thus:

$$-\gamma \Delta h = -\Delta u = \Delta p \quad (\text{D:1})$$

from which the value of the hydraulic gradient  $i$

$$i = -\frac{1}{\gamma} \cdot \frac{\partial u}{\partial z} \quad (\text{D:2})$$

Consider a horizontal plane at a depth  $z$  below the top of the layer. The discharge through 1 square unit of this plane:

$$q = -\frac{k}{\gamma} \cdot \frac{\partial u}{\partial z} \quad (\text{D:3})$$

Consider another horizontal plane displaced  $dz$  upward. The discharge through that plane is

$$q + dq = -\frac{k}{\gamma} \left( \frac{\partial u}{\partial z} + \frac{\partial}{\partial z} \frac{\partial u}{\partial z} \cdot dz \right) \quad (\text{D:4})$$

In other words, the increment of flow between the two horizontal planes considered, is

$$dq = -\frac{k}{\gamma} \cdot \frac{\partial}{\partial z} \frac{\partial u}{\partial z} \cdot dz \quad (\text{D:5})$$

The rate at which moisture is squeezed from the pores, per unit of volume, is

$$\frac{dq}{dz} = -\frac{k}{\gamma} \cdot \frac{\partial^2 u}{\partial z^2} \quad (\text{D:6})$$

Since the rate must equal the rate of decrease in volume, it can be written, taking into account that the voids ratio  $e$  decreases as the time  $t$  increases:

$$-\frac{k}{\gamma} \cdot \frac{\partial^2 u}{\partial z^2} = -\frac{1}{1+e} \cdot \frac{\partial e}{\partial t} \quad (\text{D:7})$$

To establish the relationship between the voids ratio  $e$  and the intergranular pressure  $p$ , it is assumed that at a given range of pressures  $p_1 - p_2$ , the slope of the  $e-p$  curve is constant:

$$a = \frac{e_1 - e_2}{p_1 - p_2} = - \frac{\Delta e}{\Delta p} = \frac{\Delta e}{\Delta u}; \quad \partial e = a \cdot \partial u \quad (\text{D:8})$$

where  $a$  is the coefficient of compressibility. Combining Eqs. (D:7) and (D:8)'

$$\left[ \frac{k(1+e)}{a\gamma} \right] \cdot \frac{\partial^2 u}{\partial z^2} = \frac{\partial u}{\partial t} \quad (\text{D:9})$$

The expression in brackets [Eq. (D:9)] is the coefficient of consolidation  $c_v$ . Hence

$$c_v \frac{\partial^2 u}{\partial z^2} = \frac{\partial u}{\partial t} \quad (\text{D:10})$$

Equation (D:10) expresses the so-called "thermodynamic analogy of consolidation." A similar equation is applied in the study of transmission of heat through an isotropic plate bounded from above and from below by two parallel planes. The hydrostatic excess  $u$  is then analogous to temperature.

To solve the differential equation (D:10) it is necessary to find such a function  $u$

$$u = f(z, t)$$

that upon being differentiated twice with respect to  $z$  and once with respect to  $t$  would furnish derivatives  $\partial^2 u / \partial z^2$  and  $\partial u / \partial t$  to satisfy Eq. (D:10). There are a great number of such functions, and the true one should satisfy the boundary (or limit) conditions. At the top of the layer, where moisture pours freely into the pervious material, there is no hydrostatic excess; hence  $u = 0$  when  $z = 0$ . On the other hand, there is no motion of moisture at the bottom of the layer; hence the velocity and the hydraulic gradient there equal zero. This means that  $\partial u / \partial z = 0$  when  $z = H$ . If the soft layer is sandwiched between two pervious ones, the boundary conditions must be changed accordingly. As soon as these boundary conditions are established, the differential Equation (D:10) may be solved using the Fourier series. For a load uniformly distributed at the horizontal boundary of a semi-infinite mass

$$u = \frac{4}{\pi} \sigma_z \sum_{N=0}^{N=\infty} \frac{1}{2N+1} \sin \left[ \frac{(2N+1)\pi z}{2H} \right] e^{-(2N+1)^2 \frac{\pi^2 T}{4}} \quad (\text{D:11})$$

where  $e$  is the base of natural logarithms and

$$T = \frac{c_v}{H^2} t \quad (\text{D:12})$$

where  $T$  is an abstract time-factor. The symbol  $\sigma_z$  is explained hereafter.

The percentage (degree) of consolidation may be computed as follows: At the time moment of application of the load ( $t = 0$ ) the excess hydrostatic pressure is  $\sigma_z$ , the latter value being the vertical pressure at the given point

as caused by the given load. At any time  $t$ , the average value  $u = u_0$  of the function (D:11) throughout the layer  $H$  thick is

$$u_0 = \frac{1}{H} \int_0^H u dz \quad (D:13)$$

and the corresponding value of the percentage consolidation

$$U = 1 - \frac{u_0}{\sigma_z} \quad (D:14)$$

Solutions for other kinds of loadings may be obtained, and  $U-T$  graphs as in Fig. 6:11 traced.

Data for constructing  $U-T$  graphs for three different shapes of pressure area have been first computed analytically by Terzaghi, Gilboy,<sup>3</sup> and Kimball.<sup>3</sup> Besides this "one-dimensional" consolidation (flow in a vertical direction), two- and three-dimensional cases have been studied, mostly by Biot.<sup>4,5,6</sup>

**D:2. Preconsolidation Unit Load in the Laboratory.**—Figure D:1 has to be considered together with Figs. 6:5 and 6:14. To find a conventional value of the preconsolidation unit load in the laboratory,<sup>7</sup> the position of the virgin branch I is established from several loadings and unloadings. At a point  $T$  which corresponds to the smallest radius of the compression curve ( $\rho_{min}$ ) a horizontal  $Th$  and a tangent  $Tt$  are drawn. The point  $C$  of intersection of the bisector of the angle formed by these lines with the virgin branch I determines the value of the preconsolidation unit load  $p_c$ .

**D:3. Experimental Time Curve.**—Time curves are generally constructed upon application of each load increment (Sec. 6:24). Settlements as measured by the dial are plotted vertically, and the logarithms of corresponding times horizontally.

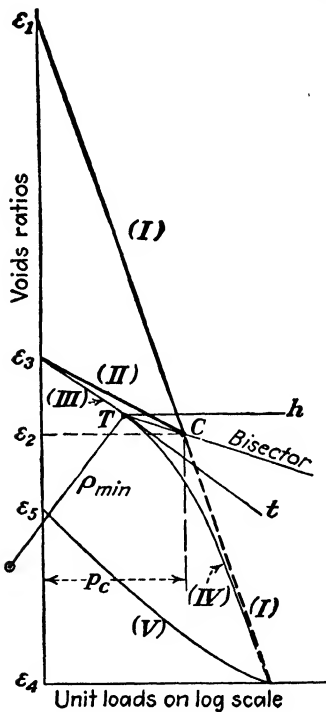


FIG. D:1.—Preconsolidation load.  
(After A. Casagrande.)

tally. Convenient time moments for recording settlements are 0.1, 0.5, 2, 4, 8, 16, and 32 min. and afterward at arbitrary time intervals. Since the experimental time curve shows the three stages of deformation (a), (b), and (c) as specified in Sec. 6:3, the upper and the lower part of it should be eliminated, and only the middle part of it, which obeys the theory of consolidation, is to be considered. This elimination is known as "fitting the time curve."

a. *Fitting the Time Curve.*—The fitting of the experimental time-settlement

curve is a purely empirical procedure and can be done in different ways. The method shown in Fig. D:2 is applied by A. Casagrande.<sup>7,8</sup> (1) The practically straight line  $AB$  at the end of the empirical time-settlement curve is prolonged to intersect the tangent  $CD$  to the time-settlement curve at its point of inflection  $C$ . The point  $E$ , that of intersection of the lines  $AB$  and  $CD$ , corresponds to theoretical 100 per cent. The fitted time-settlement curve lies over the horizontal line passing through point  $E$ . (2) Consider a point  $F$  of the time-settlement curve above the 50 per cent theoretical curve. This point corresponds to a time moment  $t$ . Now find a point  $G$  corresponding to the time moment  $\frac{1}{4}t$ . The difference between the vertical ordinates of points  $F$  and  $G$  being simple  $a$ , the "theoretical zero point" is located  $2a$  above the point  $F$  and  $a$  above point  $G$  (dotted line in Fig. D:2). This is due to the fact that the upper part of a time curve (on arithmetic scale) closely approaches a parabola.

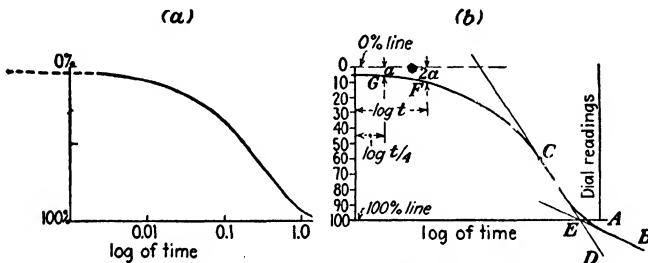


FIG. D:2.—Time-settlement curve and its "fitting." (After A. Casagrande.)

b. *Determination of the Coefficient of Consolidation.*—Let  $t_{50}$  be the time on the time-settlement curve required to reach 50 per cent consolidation (Fig. D:2). The pressure area of the sample in a consolidation device is a rectangle with drainage up and downward. The time factor  $T$ , for this case and 50 per cent consolidation, is 0.2 (Fig. 6:11). The thickness of the sample at 50 per cent consolidation will be designated with  $2h_{50}$ . From formula (6:23)

$$c_v = \frac{0.2h_{50}^2}{t_{50}} \quad (\text{D:15})$$

Sometimes 90 per cent consolidation only is considered. In this case the value of the time factor  $T$  is 0.848, and formula (D:15) is to be modified accordingly.

Since the determination of both the theoretical zero point and the theoretical 100 per cent point is subject to errors, it is believed that the 50 per cent point is least affected by these errors and that its use is preferable to the use of the 90 per cent point.

c. *Use of the Experimental Time Curve for Tracing Voids-ratio-pressure Curves.*—A load increment applied to the sample stays generally for 24 hr. before the next load increment is applied. In any case, the straight line representing the secondary compression must be clearly defined on each time curve before the test is discontinued.

To construct a voids-ratio-pressure curve such as curve III, IV in Fig.

D:1 it is necessary to know the value of the voids-ratio corresponding to each load increment. This voids ratio is determined either (a) by selecting a time moment such that the dial readings for each time curve corresponding to that time moment are close to and beyond the end of the primary compression<sup>7</sup> or (b) from the dial readings immediately before the application of the next load increment.

**D:4. Coefficients of Compressibility and Permeability from a Consolidation Test.**—Instead of determining the coefficient of consolidation  $c_v$  directly from the time curve (Sec. D:3), both coefficients of compressibility  $a$  and permeability  $k$  may be first determined and used in formula (6:17).

*a. Coefficient of Compressibility.*—When the unit pressure on the piston is increased from some value  $p$  to some other value  $p + \Delta p$ , the voids ratio decreases by a value  $\Delta e$ . Assuming that during this process the Hooke's law holds, it can be written

$$a = \frac{\Delta e}{\Delta p} \quad (\text{D:16})$$

In other words, the coefficient of compressibility  $a$  is the average slope of the laboratory voids-ratio-pressure curve for a given pressure increment  $\Delta p$ . Obviously, the value of  $a$ , which is assumed to be constant for a given load increment  $\Delta p$ , in general is variable.

The value of the coefficient of compressibility  $a$  may be determined from two points of the virgin compression line (Fig. D:1), corresponding to the increase of pressure from a certain value  $p$  to  $p + \Delta p$ . The value of the coefficient of compressibility thus determined is sometimes designated by  $a_p$ .<sup>7</sup>

*b. Coefficient of Permeability.*—Using again formulas (6:17) for the coefficient of consolidation and formula (6:23) for the time factor, it can be written.

$$k = \frac{0.2a\gamma_w t_{50}}{(1 + e)t_{50}} \quad (\text{D:17})$$

The values of the coefficient of compressibility  $a$  and of the voids ratio  $e$  are average values for a given load increment.

The coefficient of permeability  $k$  found by this method may be checked against the result of a direct permeability test.

As a rule, the consolidation device is combined with a tube of water that may percolate through the sample in the upward direction (Fig. 6:13). In such a case the tube in question works as a permeameter with a falling hydraulic head (Sec. 3:4). To simplify computations, it is generally assumed that if water in the tube drops from the mark  $H_2$  to the mark  $H_1$  above the sample, the average hydraulic head under which it has percolated through the sample is  $(H_1 + H_2)/2$ . Thereupon the Darcy formula is simply applied.

**D:5. Compressibility of the Apparatus.**—The influence of the compressibility of the apparatus itself, of its base, and of the loading table, can be estimated by comparing the results of two tests, namely, with and without the sample and the enclosing ring. Comparison should be made for a range of loads, from which a calibration curve can be traced. For very compressible

soils the compressibility of the apparatus itself has but little influence on the results of a consolidation test.

#### References

1. CHARLES TERZAGHI: "Erdbaumechanik," Franz Deuticke, Leipzig and Vienna, 1925.
2. CHARLES TERZAGHI: "Theoretical Soil Mechanics," John Wiley & Sons, Inc., New York, 1943.
3. Earth and Foundations, Progress Report of special committee, *Proc. A.S.C.E.*, vol. 59, 1933, pp. 777-820; for W. P. Kimball's discussion, see *ibid.*, August, 1938.
4. M. A. BIOT: General Theory of Three-dimensional Consolidation, *Jour. Applied Phys.*, vol. 12, 1941.
5. M. A. BIOT: Consolidation Settlement under a Rectangular Load Distribution, *Jour. Applied Phys.*, vol. 12, 1941.
6. M. A. BIOT and F. M. CLINGAN: Consolidation Settlement with an Impervious Top Surface, *Jour. Applied Phys.*, vol. 12, 1941.
7. A. CASAGRANDE and R. E. FADUM: "Notes on Soil Testing for Engineering Purposes" (lith.), Graduate School of Engineering, Harvard University, 1940.
8. D. W. TAYLOR: "Notes on Soil Mechanics" (lith.), Massachusetts Institute of Technology, Cambridge, Mass., 1938.



## AUTHOR INDEX

### A

Agatz, A., 234, 319, 336  
 Atterberg, A., 44, 50

### B

Baker, A. H., 358  
 Baker, B., 290, 335  
 Barber, E. S., 50  
 Baron, F. M., 358, 359, 386  
 Baumann, P., 327, 336  
 Bayer, L. D., 50, 385  
 Beatty, J. L., 449, 470  
 Becker, W. C. E., 471  
 Beckman, H. O., 27  
 Bendell, L., 234  
 Benkelman, A. C., 471  
 Bernatzik, W., 367, 386,  
 Bernhard, R. K., 467, 468, 471  
 Bescow, G., 38, 79, 82, 87  
 Beugler, E. J., 96  
 Biot, M. A., 109, 130, 495  
 Blank, E., 50  
 Blum, H., 336  
 Boussinesq, J. V., 96, 129  
     *(See also Subject Index)*  
 Bouyoucos, G. J., 21, 79  
 Brahtz, J. H. A., 264, 265, 288  
 Brandtzaeg, A., 486, 489  
 Braune, G. M., 359  
 Brown, R. L., 489  
 Buchanan, S. J., 288, 448, 470  
 Buchholtz, W., 327, 336  
 Buckman, H. O., 28  
 Bucky, P. B., 289  
 Buisman, K. *(see Keverling Buisman)*  
 Bull, A., 359  
 Burggraf, F., 489  
 Burmister, D. M., 129, 240, 272,  
     289

### C

Cain, W., 488  
 Campbell, F. B., 86  
 Campen, W. H., 385  
 Caquot, A., 209, 233  
 Carothers, S. D., 109, 130, 287  
 Carp, 436  
 Casagrande, A., 24, 43, 44, 48, 50, 60,  
     67, 68, 79, 81, 83, 86, 87, 149, 155,  
     156, 179, 184, 215, 233, 370, 448-  
     450, 478-481, 485, 493, 495  
 Casagrande, L., 74, 367, 386, 437  
 Casey, T. L., 407  
 Catton, M. D., 386  
 Chambers, R. H., 190  
 Chellis, R. D., 233  
 Clingan, F. M., 495  
 Collingwood, F., 183, 184, 206  
 Cooling, I. F., 87, 289  
 Cornwell, F. E., 265, 289  
 Cotton, H. E., 387  
 Coulomb, de, C. A., 4, 137, 290, 295,  
     335  
     *(See also Subject Index)*  
 Creager, W. P., 264, 268, 269, 273,  
     289  
 Cross, H., 101, 129  
 Cuevas, J. A., 434, 436  
 Culmann, K., 251, 288  
 Cummings, A. E., 109, 130, 156, 223,  
     233, 234, 355

### D

Dachler, R., 87  
 Dames, T. R., 489  
 Darcy, H. P. G., 53  
     *(See also Subject Index)*  
 Davidenkov, N. N., 352  
 Davies, W. W., 199  
 Davis, R. P., 234

Dean, A. C., 233  
 DeBlois, K. L., 335  
 Dokouchaev, V. V., 12  
 Dore, S. M., 50, 271, 289  
 Drucker, M. A., 359

## E

Ehrenberg, I., 233  
 Endell, K., 365, 436  
 Endersby, V. A., 365, 385  
 Enger, M. L., 115, 121, 129  
 Eyring, H., 387

## F

Faber, O., 117, 130  
 Fadum, R. E., 156, 184, 233, 495  
 Fahlquist, F. E., 50, 455  
 Fehrman, R. G., 385  
 Feld, J., 290, 308-310, 335, 437  
 Fellenius, W., 241, 248, 288  
 Fields, K. E., 289  
 Flint, R., 27  
 Forchheimer, P., 69  
 Fox, E. N., 234  
 Français, 251, 295  
 Franzius, O., 322, 336  
 Fraux, C., 233  
 Freeman, J. R., 471  
 Fröhlich, O. K., 172, 176, 233  
 Frontard, M., 288  
 Furkert, F. W., 471

## G

Galloway, J. D., 288  
 Gerber, E., 115, 130  
 Gersevanoff, N. M., 129, 185  
 Gibbs, H. J., 385  
 Giesecke, F. E., 124, 130  
 Gilboy, G., 58, 260, 266, 267, 288, 441,  
 448, 470, 492  
 Glanville, W. H., 234  
 Glinka, S. F., 12  
 Glover, R. I., 265, 289  
 Goldbeck, A. T., 115, 129  
 (See also Subject Index)

Golder, H. W., 289  
 Grime, G., 234  
 Guthbert, F. L., 385

## H

Haines, R. M., 387  
 Hanna, W. S., 436  
 Hatch, H. H., 481, 489  
 Hazen, A., 183  
 Hencky, H., 266, 289  
 Hennes, R. G., 251, 289  
 Herbert, C. A., 436  
 Hiley, A., 233  
 Hinds, J., 264, 273, 289  
 Hockensmith, G., 335  
 Hoffman, U., 365, 436  
 Hogentogler, C. A., Jr., 50, 386  
 Hogentogler, C. A., Sr., 50, 386  
 Hooke, R., 101  
 (See also Subject Index)  
 Hough, B. K., 289  
 Housel, W. S., 144, 156, 233, 470, 471  
 Hugli, H., 115  
 Hveem, F. N., 487, 489  
 Hvorslev, M. J., 156, 455, 470, 487,  
 489

## J

Jacobs, C. M., 275, 436  
 Jacoby, H. S., 199  
 Jáky, J., 251, 288, 335  
 Jenkin, C. F., 290, 310, 335  
 Jervis, W. H., 437  
 Johnson, H. L., 453, 454, 470  
 Johnston, C. M., 50, 87  
 Joseph, A. F., 385  
 Jürgenson, L., 487, 489  
 Justin, J. D., 264, 273, 288, 289

## K

Kampe, R., 436  
 Kármán, von, Th., 304, 335  
 Keen, B., 50  
 Keene, P., 387  
 Kenerson, W. J., 50

Kersten, M. S., 387  
 Keverling Buisman, 485  
 Kick, 115  
 Kimball, W. P., 420, 436, 492  
 Knappen, T. T., 50, 288  
 Knopf, A., 27  
 Kögler, F., 115, 117, 121, 122, 129,  
 398, 402, 417, 436  
 Kollbrunner, C. F., 455, 470  
 Kouptzoff, J. G., 359  
 Kozeny, J., 66, 87  
 Krey, H., 208, 233, 336, 484, 489  
 (See also Subject Index)  
 Krumbein, W. C., 481

## L

Ladd, G. E., 288  
 Lane, E. W., 86  
 Lane, K. S., 50  
 Langer, C., 455, 470  
 Lederer, E. L., 183  
 Lee, C. H., 273, 275, 276, 289  
 Leggett, R. F., 27  
 Lewin, J. D., 386, 437  
 Leygue, L., 484, 488  
 Longwell, C., 27  
 Loss, W., 289, 414, 436  
 Lyon, T. L., 28

## M

MacDonald, R. F., 288  
 McKesson, C. L., 385  
 Marston, A., 352-354, 359  
 May, D. R., 288  
 Meem, J. C., 335, 348, 358  
 Meinzer, O. E., 49  
 Meister, F., 471  
 Merchant, W., 181, 185  
 Middlebrooks, T. A., 386, 387, 437  
 Miller, R. W., 233  
 Mindlin, R. D., 234  
 Mohr, H. A., 444, 446, 449, 450, 470  
 Mohr, O., 99  
 (See also Subject Index)  
 Moran, D. E., 447, 448  
 Moulton, H. G., 314, 316, 327, 335

Moyer, J. A., 129  
 Müller-Breslau, H., 336  
 Muskat, M., 86

## N

Nádai, A., 120, 156  
 Newmark, N. M., 129, 482, 483  
 Nord, C. L., 418, 419, 436

## O

Oakley, H. B., 385  
 Ohde, I., 306, 335

## P

Paaswell, G., 307, 317, 335, 460, 461,  
 470  
 Palmer, L. A., 386  
 Parsons, H. de B., 290, 309, 335  
 Paul, C., 259, 288  
 Peck, R. B., 39, 50, 317, 336  
 Peckworth, H. F., 304  
 Pennoyer, R. P., 331, 335  
 Pettersson, K. E., 237  
 Pettijohn, F., 481  
 Phillippe, R. R., 50  
 Poisson, S. D., 102  
 (See also Subject Index)  
 Pokrowski, G. I., 269, 359  
 Poncelet, J. G., 290, 302, 335  
 Porter, O. J., 377, 386  
 Prandtl, L., 207, 208, 233  
 Prentis, E. A., 86, 234, 336  
 Press, H., 328, 329, 336  
 Price, W. H., 86  
 Proctor, C. S., 448  
 Proctor, R. R., 277, 279, 289

## R

Rankine, W. J. M., 4, 134, 290, 335  
 (See also Subject Index)  
 Rapp, G. M., 358  
 Rebhann, G., 302, 335  
 Redlich, A., 436  
 Relton, F. E., 234

Rendulic, L., 263, 288, 423, 436  
 Résal, J., 251, 288  
 Reynolds, O., 149, 150  
 Rice, G. S., 436  
 Richart, F. E., 489  
 Ries, H., 27  
 Rifaat, I., 327, 336  
 Robinson, G. W., 28  
 Rodio, G. D., 368  
 Roloff, M., 436  
 Russell, H. L., 87  
 Russell, M. B., 50  
 Rutledge, J. J., 436  
 Rutledge, P. C., 449, 450, 489  
 Rzhantzin, B. A., 386, 437

## S

Saint-Venant, A. B., 101, 147  
 Samsioe, F. A., 71, 108  
 Scheidig, A., 27, 28, 115, 117, 121,  
 122, 129, 398, 402, 417, 433, 436  
 Schleicher, F., 130  
 Schlick, W. J., 359  
 Schoklitch, A., 470  
 Schönweller, G., 336  
 Seiler, J. F., 335  
 Sharpe, C. F. S., 288  
 Shepard, E. R., 471  
 Simpson, W., 470  
 Slichter, C. S., 77  
 Slocum, S. W., 471  
 Smith, J. R., 385  
 Sooy Smith, W., 183, 185, 224  
 Sooy Smith, C., 224  
 Soumgin, M. I., 87  
 Spangler, M. G., 127, 128, 130, 354,  
 357, 359, 387  
 Sprague and Henwood, 448, 449, 453,  
 470  
 Stanton, R. B., 96  
 Stanton, T. E., 489  
 Steiner, F., 115  
 Stevens, O., 87  
 Stock, H. H., 436  
 Stokes, Sir George G., 13, 21  
 (See also Subject Index)  
 Strohschneider, O., 129

Stroyer, J. P. R. N., 317, 336  
 Sundberg, K., 471

## T

Taber, S., 79-81, 85, 87  
 Talbot, A., 275  
 Taylor, D. W., 86, 181, 185, 244-246,  
 248, 250, 288, 436, 440, 441, 495  
 Terzaghi, C., 4, 7, 56, 57, 72, 75, 77, 87,  
 129, 156, 172, 176, 181, 182, 184,  
 212, 213, 233-235, 244, 290, 303,  
 309, 310, 315-317, 333, 335, 336,  
 345, 347, 358, 390, 397, 399, 401,  
 424, 430, 436, 470, 485, 489, 492,  
 495  
 Terzaghi, von Karl (see Terzaghi, C.)  
 Tiedemann, B., 488  
 Tode, E., 436  
 Tschebotareff (see Tschebotarioff)  
 Tschebotarioff, G. P., 386, 436, 470  
 Turneure, F. E., 87  
 Tyndall, J., 183

## V

Valle-Rodas, R., 50  
 Vetter, C. P., 232, 234  
 Vreedenburgh, C. G. L., 87  
 Vuellmy, A., 359

## W

Ward, W. H., 87  
 Washburn, D. E., 50  
 Watson, T. L., 27  
 Wedernikow, V. V., 87  
 Wellington, A. M., 222  
 Wells, W. L., 289  
 Wenzel, L. K., 49  
 Westergaard, H. M., 232, 234, 386  
 Weston, C. M., 289  
 White, L., 86, 234, 317, 335, 336  
 Williams, C. C., 437  
 Winn, H. F., 87  
 Winterkorn, H. F., 385  
 Wolf, K., 130

Wolfsholz, A., 463  
Woodbury, D. P., 335

Young, I. E., 436  
Young, R. A., 453

**Y**

Young, C. R., 489

**Z**

Zinn, A. S., 288



## SUBJECT INDEX

### A

- Accelerated traffic tests, 378
- Acid soils, pH value for, 362
- Adobe, 19
- Affinity to water, 20, 34, 47, 364
- Air, entrapped, 29
- Analogies, elastic, 65, 188
  - electric, 62, 63
  - between formulas, 188
  - thermodynamic, 188, 491
- Analysis of soils, mechanical, 21-23, 475-481
- Angle, of (internal) friction (*see* Friction)
  - of obliquity, 95, 261
  - of repose, 133, 253, 307
  - of rupture, 134, 151, 152
  - of visibility, 106
- Anions, 363
- Arching, 310, 312
- Asphalt, emulsified, 365
- Asphalt cement, 364

### B

- Base course, 374
- Base exchange, 20, 362
- Base failure, 246
- Beach deposit, 16
- Beach of a dam, 74, 256
- Bearing power (*see* Bearing value)
- Bearing value, 201
  - from field experiments, 204
  - theoretical determination of, 207
  - ultimate, 201, 213
- Bedrock, 11, 12
- Blankets, impervious, 72, 272, 273
- Boiling of a soil, 51, 71, 72
- Borrow pit, yield of, 279-280
- Boundary conditions, 97, 151, 491

- Boussinesq formula, 103, 110
- Bridges, Bridgeport Conn., 412, 413
  - Huey P. Long Mississippi River, 420
  - Oder River, Germany, 416-418
  - Rhine River, Germany, 123
  - San Francisco-Oakland, Calif., 448
  - Westbrook, Conn., 418.
- Bridging effect, 109
- Buildings, Charity Hospital, New Orleans, La., 409
- Chicago Auditorium, 177
- Egyptian, 436
- National Lottery, Mexico City, 434, 436
- National Theatre, Mexico City, 403
- New England Mutual Life Insurance, Boston, Mass., 215, 434
- Standard Oil Company, San Francisco, Calif., 206
- Texas Agricultural and Mechanical College, 124
- Bulkheads, anchorages and ties, 320, 325-327
  - deflections and movements of, 327-328
  - design and analysis of, 321-324
    - Danish method for, 324
    - with relieving platforms, 320-321
  - types of, 320

### C

- Caliche, 19
- California bearing ratio, test, 377
- Canals, Mittelland (Germany), 415
  - Panama, 251, 288
  - Volga-Don (Russia), 76
- Capillarimeters, 37-38
  - Beskow, 38
- Capillarity, horizontal, 60

- Caquot formula, 208  
 Cathedrals (*see* Monuments)  
 Cations, 20, 363  
 Centrifuge tests, for moisture equivalent, 46-47  
   stability of an embankment, 269  
 Chemistry, role of, 3  
 Classification, soil, 17, 47, 48, 370  
 Clays, 17, 18, 19-21  
   thixotropic, 18, 149, 488  
   varved, 25  
 Coagulation, 15  
 Coal mines, Illinois, 426  
   Kuznetzkstroy, Siberia, 407  
 Coefficient, of compressibility, 164, 491, 494  
   of consolidation, 168, 394, 491-493  
   of permeability, 55, 60, 76, 77, 494  
 Cofferdams, cellular, 330-332  
   one wall, 329  
   two wall, 329  
 Cohesion, 92, 131, 145  
   apparent, 145  
   true, 145  
 Colloids, 17  
 Compaction of earth material, 276  
 Compression, elastic, 157-159  
   nonelastic, 157-159  
   secondary, 177  
 Compression tests, confined, 160  
   nonconfined, 151, 152, 159-160  
   triaxial, 151-154, 485, 486  
 Conduits, 352  
 Consistency limits, determination of, 42-44  
   liquid, 42-44  
   plastic, 42-44  
   shrinkage, 42, 45  
 Consolidation, 157  
   coefficient of, 168, 394, 491-493  
   differential equation of, 491  
   history of, 183  
   under increasing load, 176  
   percentage (degree of), 168, 169, 492  
   test of, 177-180, 490-492  
   theory of, 160-177, 183, 490-492,  
   time of, 168-171, 182  
 Continuity, in an elastic body, 92, 186  
   in seepage, 54, 55, 187  
   of strains, 100, 141, 187  
 Coulomb formula, 137, 188  
 Cracks, cause of, 486  
   due to settlement, 426  
   on slopes, 250  
 Curve, moisture-pressure (*see* Isochrones)  
   size distribution, 21-23, 271, 275  
   time-settlement, experimental, 180, 492-493  
   field, 399  
   under increasing load, 176  
   tracing of, 170  
   voids-ratio-pressure, 179, 493  
 Cutbacks, 364  
 Cuts, 235-251  
   Cucuracha, 251  
   Culebra, 251, 288  
 Cylinder test (*see* Triaxial compression test)
- D
- Dams (*see* Earth dams)  
 Darcy formula, 52, 167, 188  
 Degebo, 5, 469, 471  
 Density, absolute, 26  
   bulk, 26  
   critical, 155  
   relative, 23  
   (*See also* Specific gravity)  
 Diameter, equivalent, 18, 476, 477  
   statistical, 34  
 Dike, Connecticut River Front, 285, 289  
   Quabbin, 271, 289  
 Discontinuity, 139, 186  
 Disturbed samples, 60, 439  
 Disturbed zone, 118, 119  
 Drawdown, sudden, 249  
 Dunes, 16
- E
- Earth dams, examples of, Alexander, 25, 285, 287

- Earth dams, examples of Belle  
     Fourche, 284, 286  
     Calaveras, 252, 283  
     El Capitan, 252  
     Cobble Mountain, 252, 481  
     Denison, 454  
     Dix, 256  
     Fort Peck, 252, 283  
     Marshall Creek, 287  
     Miami, Conservancy District,  
         259, 288  
     Muskingum River (Tappan), 264  
     Oneanta, 257  
     Pickwick Landing, 289  
     Salt Spring, 256  
     San Gabriel, 284, 287  
 failures of, 282  
 general features of, 252-257  
     cross section, 252-254  
     spillway, 255  
 hydraulic fill, 255  
     construction of, 255  
     core consolidation of, 258  
     selection of materials for, 270-  
         272  
     stability of core of, 260  
 rock-fill, 255, 256  
 rolled-filled, 255  
     compaction of material of, 276-  
         277  
     selection of materials for, 272-  
         276  
 semihydraulic fill, 255  
 stability, of the body of, 257-265  
     of the foundation of, 265-270  
     stresses in, 264  
 Elastic constants, 102  
 Elastic continuum, 92, 93  
 Elastic limit, 159  
 Elastic rebound, 157  
 Elasticity, modulus of, conception of,  
     102, 159  
     from confined compression, 160  
     from nonconfined compression, 159  
 Electrolytes, 15  
 Embankments, 235-287, 356, 414-418  
 Entrapped air, 29  
 Ever-frozen soils (permafrost), 78, 85  
 Experiments, loading, 113-123  
     disturbed zone in, 119  
     trend of, 113, 114  
     Reynold's 149, 150  
  

F

 Factor, climatic, 12  
     concentration, 121  
     safety, 238, 240, 245, 269  
     time, 173  
 Failure, base, 246  
     conditions of, 132  
     definition of, 131  
     flow, 148  
     Mohr's theory (hypothesis) of, 131  
     progressive, 146  
     toe circle, 248  
 Failure lines, 140-145  
 Fetch, 253  
 Field tests, geophysical, 464-466,  
     loading, 203-206, 460-463  
     penetration, 461  
     permeability, 76  
     unit weight, 458  
     vibration, 466  
 Filter, graded, in a dam, 73  
 Filter material, 384  
 Flocculation, 15  
 Flow, through aeolotropic masses, 70  
     under a dam, 64  
     parabolic, 65-67  
     plastic, 51, 147-148, 188  
     viscous, 51  
 Flow failure, 148  
 Flow lines, 62  
 Flow net, 61  
 Footings, 199, 215, 216  
 Formula, Boussinesq, 103, 110  
     Caquot, 208  
     Coulomb, 137, 188  
     Darcy, 52, 167, 188  
     elastic, limitations of, 110  
     pile driving, 221-223  
     Prandtl, 207  
     Rankine, 133  
     Résal, 251

- Formula, Stokes, 13  
   straight line, 187, 188  
   theoretical, validity of, 193
- Foundations, 199-232  
   depth of, 199  
   eccentrically loaded, 229-232  
   mat, 199  
   modulus of, 213  
   pile, 216-229  
   raft, 199  
   spread, 199-216  
   width of, 199
- Fractions, soil, 17
- Fragmental masses, idealized, 92, 93
- Freehand drawing, 191
- Freezing point of soil moisture, 79
- Friction, angle of (internal), 132, 145, 250, 307  
   negative, 220  
   piles, 217  
   in samplers, 451  
   skin, of piles, 219
- Frost action, controlling factors of, 80-82  
   crystallization at, 82  
   depth of, 78  
   kinds of, 78  
   lifting of stones by, 85  
   permafrost, 78, 85  
   technical measures against, 83
- Frost heaves, 78, 80-82, 83
- G
- Gel, 17
- Geophysical tests (*see* Field tests)
- Gley, 13
- Goldbeck cells, 113, 114
- Gumbo, 19
- H
- Harbors, Göteborg, failure of, 247, 248  
   Le Havre, Transatlantic Terminal at, 421  
   Sverabaya, failure of, 414
- Hardpan, 13, 19
- Highway subgrade, 360-385
- Hooke's law, 101, 188
- Humus, 12
- Hydraulic gradient, 53, 167
- Hydrogen, ionized, 362, 363
- Hydrometer method, 22, 475-480
- Hydrostatic excess, 161  
   uplift, 111
- Hygroscopic coefficient, 32
- Hysteresis loop, 158
- I
- Idealized masses, 91-93  
   elastic, 92  
   fragmental, 92
- Ignition, 18
- Illite, 20
- Index, flow, 49  
   plasticity, 44  
   shrinkage, 49  
   toughness, 49
- Infiltration, 21
- Isochrones, 165  
   tracing of, 173  
   types of, 172
- Isotropy, statistical, 93
- K
- Kaolinite, 19
- Krey method, 208, 209
- L
- Landslides, 235
- Lateral support, 134, 194
- Laterite, 12, 13
- Levee, Chingford, England, 286  
   Mississippi River, 257, 288  
   Pendleton, Ark., 286, 287, 289
- Limit equilibrium, 132, 189, 259, 305, 306
- Limits of consistency (*see* Consistency limits)
- Line, equipotential, 62  
   failure, 140-145  
   flow (stream), 62

- Line, phreatic, 66  
 saturation, 66
- Load, concentrated (point), 93  
 distributed, 93  
 increasing, 176  
 line, 93  
 strip, 93  
 superimposed, 93  
 (loading) tests, 203-206, 460-463
- Loam, 18
- Loess, 16
- M**
- Marl, 19
- Mass, 11, 61  
 aeolotropic, 70  
 anisotropic, 70  
 elastically isotropic, 61  
 heterogeneous, 111  
 homogeneous, 61  
 idealized, 91-93  
 isotropic, 61
- Mechanical analysis of soils, 21-23,  
 475-481
- Meniscus, 34  
 lifting force of, 34, 35  
 shape of, 34
- Method, centrifuge, of checking sta-  
 bility of embankment, 269  
 elutriation, 22, 480, 481  
 hydrometer, 21, 22, 475-480  
 Krey, 208, 209  
 pipette, 22, 481  
 Siemens Bau Union, 463  
 Swedish, 238, 239
- Models, 191, 192  
 of flexible walls, 317  
 in the theory of consolidation, 161
- Modulus, of elasticity (*see* Elasticity,  
 modulus of)  
 of foundation, 213
- Mohr's circle, applications of, 134,  
 138, 152, 332, 343  
 construction of, 97-99
- Mohr's envelope, 153
- Mohr's theory (hypothesis) of failure,  
 153
- Moisture in soils, capillary, 33  
 equivalent, 46, 47  
 hygroscopic, 32  
 natural, 39  
 pore, 111-113, 192  
 removable, 382  
 varieties of, 32
- Moisture content, 30
- Montmorillonite, 19, 25
- Monuments (including cathedrals),  
 Holsten Gate, Germany, 408, 409  
 Königsberg Cathedral, Germany,  
 405, 406  
 Pisa, Leaning Tower of, 410, 411  
 St. Isaac's Cathedral, Russia, 412  
 Washington Monument, 407, 408
- Movement, capillary, length (height)  
 of, 37
- Muck, 19
- Mud, 19
- Muskeg, 19
- N**
- Neutralizer, 362
- O**
- Oiling, 363
- Orientation of particles, 25
- P**
- Particles (*see* Soil particles)
- Path of percolation, 73
- Pavements, flexible, 370-372, 375-  
 378  
 rigid, 371, 372
- Peat, 19
- Perimeter shear, 205
- Permafrost, 78, 85
- Permeability, coefficient of, 55, 494  
 average values of, 56  
 field determination of, 76, 77  
 laboratory determination of, 55-  
 60
- Permeameters, constant head, 56, 57  
 falling head, 57-59

- pH value, for acid soils, 362  
 Photoelasticity, 192, 266, 267  
 Picnometers, 26  
 Pile driving, purpose of, 216, 217  
   formulas, 221-223  
 Piles, friction, 217  
   groups of, 223-224  
   length of, 228  
   loading tests of, 224-225  
   pretested, 226  
   resistance of (*see* Resistance)  
 Pipe culverts, 353  
   for airports, 357  
 Pipe perforations, 383-384  
 Piping, 71  
   measures against, 71-73  
 Plastic equilibrium (*see* Limit equilibrium)  
 Plastic flow, 51, 147-148, 188  
 Plastic number (*see* Plasticity index)  
 Plasticity of a soil, controlling factors  
   of, 46  
   index, 44  
   needle, Proctor's, 277-279  
 Podzol, 12  
 Poisson's ratio, 102, 126, 148  
 Pole, vertical, 317-319  
 Pore moisture (*see* Moisture in soils)  
 Porosity, 23  
 Potential, 62  
 Prandtl formula, 207  
 Precipitation, 15  
 Preconsolidation load, 162, 179, 492  
 Pressure, active, 135, 291  
   capillary, 36  
   equivalent, 488  
   internal, 138  
   lateral, 125-127  
   passive, 135  
   of pore moisture, 111  
   redistribution of (examples), 315  
   under structures, 123-125  
   transfer of, 310  
   vertical, 103-106, 108, 109, 482-483  
 Pressure area, 164, 165  
   in computing settlement, 165  
   conception of, 164  
   types of, 172-174  
 Principle, Saint-Venant's, 100, 101  
   of superposition, 100
- Q
- Quicksand, 51
- R
- Railroads, Canadian Pacific, 195  
   Emden, Germany, 406  
 Rankine formula, 133  
   active, 134  
   passive, 136  
   value, 134  
 Ratio, area, 450  
   perimeter-area, 205  
   Poisson's, 102, 126, 148  
   silica sesquioxide, 20  
   voids, 23, 31, 32, 162-164, 179, 180  
   water plasticity, 49  
 Résal formula, 251  
 Resistance, bond, 487  
   cohesion, 137  
   dynamic, of piles, 218  
   frictional, 137  
   passive, 137, 213, 354, 355  
   point, of piles, 218  
   skin, of piles, 219  
   static, of piles, 218  
 Retaining walls, 290-332  
   Coulomb formula applied to, 298  
   equivalent fluid method applied to,  
   292  
   experiments with nonflexible, 307-  
   310  
   flexible, 313  
   general wedge theory applied to, 303  
   irregularly surfaced backfill, 300  
   lateral pressure on, from cohesive  
   backfill, 294-296  
   from submerged backfill, 297-298  
   from surcharge, 293  
   oblique, 306  
   overturning of, 305  
   Rankine formula applied to, 292  
   Rebhann's theorem applied to, 301  
   shape of the wedge for, 304  
   sliding of, 304-305

- Retaining walls, tilting of, 313  
 translating of, 311
- Rise, capillary (*see* Movement, capillary)
- Rock-fill dams, 256
- Runways, 360-385
- S
- Safety factor, 240
- Samplers, 447-455
- Samples of soil, kinds and preservation of, 439, 457  
 undisturbed, 439, 447
- Sampling, casing in, 444  
 deep, 442  
 in cohesionless soils, 453-455  
 in cohesive soils, 446-477  
 dry, 446  
 lost wash water, importance in, 455  
 rock exploration in, 456  
 shallow, 440-442  
 wash borings, use of in, 445
- Sand, angular, 18  
 rounded, 18  
 subangular, 18
- Saturation line, 66
- Secondary stress, 396
- Secondary time effect, 159, 177
- Sedimentation, 14
- Seepage, 61-76  
 from canals, 75  
 in an earth dam, 66-68  
 effect of slopes on, 75  
 elastic analogies of, 63-65  
 electric analogy of, 62  
 line of, 66
- Settlement of structures, causes of, 389  
 combined with horizontal motion, 388, 409  
 contact, 389  
 damage from, 432  
 in deeper strata, 393  
 due to excavations and tunnels, 422-425  
 due to fluctuations of water level, 419
- Settlement of embankments, 414, 427  
 influence, of the rigidity on, 395  
 of the size of structure on, 397, 398  
 lines of equal, 394  
 measures against, 433  
 observations of, 427-432  
 seat of, 388  
 secondary stresses due to, 396
- Shear, as cause of failure, 131  
 (*see also* Stress)
- Shear danger, 200
- Shearing test, direct, 151-154, 484  
 triaxial (cylinder), 151-154, 485-486
- Sheet piling, 317-333
- Shell, of a dam, 74, 260
- Shoulder, of a dam, 74
- Silt, organic, 18, 19
- Size, effective, 23, 24  
 of particles, 17
- Slides, Panama Canal, 251
- Slopes, base failure of, 246-249  
 checking stability of, circle method, 241-243  
 Swedish method, 238, 239  
 in cohesive soils, 237  
 cracks on, 250  
 critical height of, 243  
 design of, 237  
 in noncohesive soils, 236  
 safety factor of, 238, 240, 245  
 sudden drawdown, 249
- Slow flowage, 235
- Sluice, 255
- Soil, acid, 362  
 definition of, 11  
 perennially frozen, 78, 85  
 stabilization of, 360-369  
 with bituminous materials, 363  
 with cement, 366  
 chemical pretreatment, 363  
 deep, 366
- Soil air, 29
- Soil classification, 17, 47, 48, 370
- Soil formation, 12
- Soil fractions, 17
- Soil horizons, 12

- Soil mechanics, history of, 4-5  
 basic problem of, 91  
 present work in, 5-6  
 trend of, 6
- Soil moisture, 29-48  
 capillary, 32-39  
 solidified, 40  
 free, 32  
 gravitational, 32  
 hygroscopic, 32
- Soil particles, adjustment of, 149, 150, 158  
 equivalent diameter of, 18, 476, 477  
 orientation of, 25  
 shape of, 17  
 size of, 17  
 specific gravity of, 25
- Soil physics, 2
- Soil samples (*see* Samples of soil; Sampling)
- Soil science, 3
- Soil suspensions, 13
- Sol, 17
- Solifluction, 235
- Solutions, infinite, 189  
 soil, 13
- Sorption, 21
- Specific gravity, apparent, 25  
 mass, 25  
 of particles, 25
- Squeezing test, 487
- Stability number, 244
- Stabilization (*see* Soil, stabilization of)
- Stabilometer, 487
- Sticky point, 45, 46
- Stokes formula, 13
- Strain, 99
- Stress, compression, 95  
 normal, 94  
 in and around a pile, 226-228  
 plane, 95  
 principal, 64, 96  
 intermediate, 97  
 trajectories of, 64  
 secondary, 396  
 shearing, 95
- Stress, shearing, at the base of embankment, 262-264  
 in elastically isotropic foundation, 265, 266  
 maximum, 106-108  
 at the rigid boundary, 287  
 sign of, 95  
 tangential, 95
- Stress distribution, three-dimensional, 94  
 two-dimensional, 94
- Stress-strain relationship, 101
- Subgrade, 358  
 design of, 369-378  
 static loads in, 371  
 for flexible pavement, 375  
 for rigid pavement, 372
- Suboiling, 363
- Subsidence, 235, 288  
 Freeport, Tex., 195, 196
- Subsoil, 11
- Substratum, 11
- Subsurface, drainage (*see* Under-drainage)  
 flow (direction), 382
- Subways, Buenos Aires, 337  
 London, 337  
 New York City, 317, 460
- Sudden drawdown, 249
- Surface, internal, of a soil, 25
- Surface tension, 34, 35
- Swedish break, (base failure), 246

## T

- Tanks, 396, 401, 402
- Tensiometers 38-39
- Texture of soil, 18  
 heavy, 18  
 light, 18
- Thixotropic clay, 18, 149, 488
- Time effect (secondary), 159, 177
- Time element, 190
- Time factor, 173
- Time-settlement curve (*see* Curve)
- Toe-circle failure, 248
- Topsoil, 11

- Toughness index, 49  
 Transporting agents, 13  
 Trap-door experiment, 345  
 Triaxial compression test, 151-154,  
 485, 486  
 Tunnel problem, 337-338  
 Tunnels, circular, without lining,  
 338-343  
     creep of clay into, 425  
     forces acting on, 348  
     safe diameter of, 344  
     settlement due to, 425  
     tension failure above, 342  
     vertical pressure on the roof of, 347
- U
- Underdrainage, 378-385
- Undersurface drainage (*see* Under-  
 drainage)  
 Uplift, hydrostatic, 111, 309
- V
- Vibrations, 228, 372, 426, 427, 466  
 Voids ratio, 23, 31, 32, 162-164, 179,  
 180  
 Volcanic action, 13
- W
- Water table, 29  
 Water-holding capacity, 46  
 Wedge, 139  
 Wedge theory, general, 303  
 Wind action, 16



